



TEXTEH X
INTERNATIONAL CONFERENCE
ON TEXTILES AND CONNECTED R&D DOMAINS

Proceedings of the 10th
International Conference TEXTEH

October 21-22, 2021

Online event



NATIONAL RESEARCH DEVELOPMENT
INSTITUTE FOR TEXTILES AND LEATHER

Description of the National Library of Romania

TEXTEH X INTERNATIONAL CONFERENCE PROCEEDINGS

Coordinator: Alexandra Ene

Cover and design: Florin Prisecaru

DOIs Crossref indexed

Under evaluation for indexing: CrossRef, SCOPUS, EBSCO, ProQuest, Index Copernicus etc.



© Certex Publishing House 16 Lucretiu Patrascanu Street
Bucharest, 030508 Romania

Phone: +040213404200

Fax: +040213405515

e-mail: office@incdtp.ro

10th TEXTEH INTERNATIONAL CONFERENCE PROCEEDINGS
BUCHAREST, ROMANIA, OCTOBER 21 - 22, 2021

Sabina Olaru
EDITOR

TEXTEH X INTERNATIONAL CONFERENCE
PROCEEDINGS

21 - 22, OCTOBER 2021
National Research Development Institute for Textiles and Leather

ISSN 2068-9101, Vol. 10

TEXTEH X INTERNATIONAL CONFERENCE

SCIENTIFIC COMMITTEE

Carmen Ghițuleasa, General Manager INCDTP, Romania
Alina Popescu, Scientific Director INCDTP, Romania
Alexandra Ene, President of Scientific Council INCDTP, Romania
Sabina Olaru, Editor in Chief of Industria Textila journal, INCDTP, Romania
Lucian-Ionel Cioca, Lucian Blaga University of Sibiu, Romania
Bahar Basim, University of Florida, USA
Braz Costa, General Manager CITEVE, Portugal
Xianyi Zeng, Ecole Nationale Supérieure des Arts et Industries Textiles (ENSAIT), France
Luis Almeida, University of Minho, Portugal
Zoran Stjepanović, University of Maribor, Slovenia
Alexandra De Raeve, HOGENT University of Applied Science and Arts, Belgium
Lubos Hes, Technical University of Liberec, Czech Republic
Aminoddin Haji, Yazd University, Yazd, Iran
Simona Di Gregorio, University of Pisa, Italy
Enrique Montiel Parreño, Vesica Piscis Footwear, Spain
Dimosthenis Papakonstantinou, CRE.THI.DEV, Greece
Adnan Mazari, Technical University of Liberec, Czech Republic
António Dinis, University of Minho - TecMinho, Portugal
Miguel Ângelo Carvalho, University of Minho - TecMinho, Portugal
Anton Ficai, "Politehnica" University of Bucharest, Romania
Carmen Loghin, Pro-rector, Faculty of Industrial Design and Business Management, Technical University "Gh. Asachi", Iasi, Romania
Mariana Ursache, Dean, Faculty of Industrial Design and Business Management, Technical University "Gh. Asachi", Iasi, Romania
Daniela Stelescu, INCDTP-ICPI, Romania
Maria Sönmez, INCDTP-ICPI, Romania

ORGANIZING COMMITTEE

Carmen Ghițuleasa, General Manager INCDTP, Romania
Alina Popescu, Scientific Director INCDTP, Romania
Alexandra Ene, President of Scientific Council INCDTP, Romania
Sabina Olaru, Editor in Chief Industria Textila journal, Romania
Andreja Rudolf, University of Maribor, Slovenia
Simona Vasile, HOGENT University of Applied Science and Arts, Belgium
Ana Dias, University of Minho - TecMinho, Portugal
Mohammad Khajeh Mehrizi, Textile Engineering Department, Yazd University, Iran
Mădălin Ioniță, Magurele Science Park, Romania
Carmen Mihai, INCDTP, Romania
Cristina Grosu, INCDTP, Romania
Adrian Săliștean, INCDTP, Romania
Constantin Dragomir, Site Administrator INCDTP, Romania
Florin Prisecaru, Graphic Designer INCDTP, Romania
Cosmina Prisecaru, INCDTP, Romania

Organizers



**INCDTP The National R&D Institute
for Textiles and Leather - Bucharest,
Romania**

[INCDTP](#)



ITA-Texconf Business Incubator

[ITA-Texconf](#)

Co-Organizers



**HOGENT University of Applied
Sciences and Arts, Belgium**

[HOGENT](#)



**University of Maribor, Faculty of
Mechanical Engineering, Slovenia**

[Maribor](#)



**University of Minho - TecMinho,
Portugal**

[TecMinho](#)



**Yazd University, The Textile
Engineering Department, Iran**

[Yazd University](#)



Magurele Science Park, Romania

[Magurele
Science Park](#)

TABLE OF CONTENT

KEYNOTE SESSION

- Design of garments using adaptable digital body models 9
A. Rudolf, Z. Stjepanović, A. Cupar

PLENARY SESSIONS

- Development and characterisation of stitch-based sensors 18
S.A. Odhiambo, S. Vasile, J. Sarrazyn, I. Rottiers, A. De Raeve
- Development of multilayer textile structures for filtering applications – A new surgical mask approach26
R.V. Costa, C. Silva, T. Sousa, J. Bessa, F. Cunha, J. Belino, R. Figueiro
- Development of multifunctional yarn from the functionalization of organic raw cotton fibers with zinc nanoparticles 35
S. Ferreira, P. Silva, J., Bessa, F. Cunha, C. Castro, A. Aguilar, R. Figueiro
- The effect of plasma treatment on the printability of polyester fabric using cochineal natural dye 45
M. Khajeh Mehrizi, A. Haji, Z. Shahi, M. Golshan
- Behaviour assessment of tridimensional multilayer fibrous structures as respiratory protection substrates 50
C. Silva, T. Sousa, J. Bessa, F. Cunha, M. Costa, A. Roças, R. Figueiro
- A sustainability approach: integration of a microencapsulated phase change material to a recycled PES nonwoven fabric to develop a heat storing recycled material58
E.G. Saraç, E. Öner, M.V. Kahraman
- Recycled textiles: evolving design practices for changing the circular future of fashion sector 65
E. D'Itria, C. Colombi
- Water repellent breathable PET/wool fabric via plasma polymerisation technology 74
A. Haji, M.K. Mehrizi, M.A. Tavanai, M. Gohari
- Development of ecological denim bleaching methods 81
İ. İvedî, K. Yağcı, E. Tağaç
- A new approach for classification of different woven fabric patterns and thread densities with convolutional neural networks 88
E. Gültekin, H.İ. Çelik, H.K. Kaynak
- Research regarding new sustainable methods of garment pattern drafting 94
I.E. Marin
- Carbon fibre alignment for reinforced composites using embroidery technology 102
J. Domenech-Pastor, P. Diaz-Garcia, D. Garcia
- Selective deposition of nanofibers net on textile structures 109
D. Minguez, E. Bou-Belda, I. Montava, P. Díaz-García, M. Bonet-Aracil, J. Gisbert-Payá
- Effects of aramid sewing yarn type and fabric compositions on some seam properties of high performance fire retardant fabrics 116
S. Kara

Aqueous solutions of chitosan: viscometric and flocculation properties	123
C.-E. Brunchi, L. Ghimici	
A research on the breathability property of baby diaper backsheet	131
H.K. Kaynak, M. Alsayed	
Degradation of nonwoven fabrics suitable for wet wipes buried in soil	137
V. Sülar, B. Keçeci	
A case study for water footprint assessment of a denim product	142
V. Sülar, B. Soy, K. Yağci	
Encapsulation lavender oil by spray drying for sportswear	148
G. Erkan, G.C. Türkoğlu, S.Y. Karavana, A.M. Sarişik, B. Ütebay, A.Ç. Bakadur, A. Popescu	
Growing materials: exploring new design practices towards a sustainable fashion sector	155
E. D'Itria, P. Bolzan, F. Papile	
Two-step crosslinking of PVP/gel nanofibers	164
H.K. Güler, F.C. Çallıoğlu	
Electrospinning of St. John's wort oil loaded microcapsules based PVA nanofibers	171
H.K. Güler, F.C. Çallıoğlu, İ.Y. Mol, M. Geysoglu	
Solvent optimization of electrospun poly(acrylic acid) nanofibers	178
M. Geysoglu, F.C. Çallıoğlu	
Electrospinning of antibacterial polyurethane/ZnO nanofibers	185
İ.Y. Mol, F.C. Çallıoğlu	
Emulsion electrospinning of polyvinylpyrrolidone (PVP)/paracetamol nanofibers	193
M. Geysoglu, H.K. Güler, F.C. Çallıoğlu, İ.Y. Mol	
Paracetamol drug loaded microcapsule based nanofiber production	200
İ.Y. Mol, F.C. Çallıoğlu, H.K. Güler, M. Geysoglu	
Performance properties of knitted fabrics produced from r-PET and cotton/r-PET blended vortex and ring yarns	208
A. Oruç, Y. Arıkan, E. İlanbey, K. Özşahin	
Optimization of some weaving machine parts design. Theoretical approach	215
A. Mostafa, W. Hashima, M. Hassan, S. El-Gholmy, A. Eloufy	
Interaction of clothing in thermoregulation in the case of preterm infants	222
V. Danila, A. Curteza, S. Balan	
Active principles applied on biomaterials for the curative therapy of inflammatory skin diseases - a review	229
A. Țigău, G. Vasile, L. Chirilă, A. Popescu, S. Olaru	
Theoretical considerations regarding virtual methods to obtain the garment prototype (2D/3D and 3D/2D)	238
M. Avadanei, A. Talpa, A. Curteza, D. Viziteu, I. Dulgheriu	
Analysis of the physico-mechanical properties of different woven structures with potential applications in the healthcare and hygiene sector	247
C.E. Stroe, T. Sârbu	

Clothes development based on methods of handling of premature babies in the intensive care unit	256
V. Danila, A. Curteza, S. Balan	
Characterization of airborne particles in mechanical textile yarns processing	263
E. Visileanu, C. Mihai, A. Ene, C. Grosu, R. Scarlat, A. Vladu	
Development of textile-rubber composite materials using recycled rubber and textiles with applications in industry	272
F.St.C. Mustata, A. Curteza	
An integrated solution for the online marketing of custom-made garments that incorporates a virtual fitting room	279
M. Avadanei, A. Matasel, I. Ionescu, E. Loghin, D. Ionesi	
Analysis of the mechanical properties of some high-tech yarns with different functions	287
T. Sârbu, C.E. Stroe	
Virtual 3D kinematic human model prototype	293
D.-R. Viziteu, A. Curteza, M. Avadanei	
Correlative and covariance analysis of the electroconductive fabrics	300
R.M. Aileni, L. Chiriac	
Integration of magnetic materials with actuator role on textile supports	308
C. Grosu, R.M. Aileni, S. Olaru	
Role of the e-learning courses for capacity building in the field of advanced materials development..	314
R.M. Aileni, L. Chiriac	
Review on different types of clay and their use as antimicrobial agents for textiles treatment	321
M.C. Lite, E.C. Tănăsescu, L.O. Secăreanu, I.M. Săndulache, O. Iordache, E. Perdum	
Accessibility and usability of the learning tools to accelerate innovation in the field of smart materials development	328
R.M. Aileni, L. Chiriac	
Development of jacket patterns for teenagers using Optitex flattening module	334
G. Popescu, S. Olaru, C. Grosu, I. Badea	
Overview of the knitted materials with vibrations damping capacity	342
C. Grosu, M. Blaga	
The gain in shielding effectiveness achieved by superposition of stainless-steel plasma coated woven fabrics	348
I.R. Radulescu, L. Surdu, E. Visileanu, I. Sandulache, C. Morari, B. Mitu	
Predictive mathematical model for absorbant substrate achievement, through electrospinning process	355
C. Mihai, A.G. Ene, R.-G. Hertzog, D. Popescu, A.F. Vladu	
Floating tank for transporting oil and hydrocarbons following a maritime disaster	363
M. Jomir, D. Zamfirache, A. Ene, C. Mihai	

Training of textile creatives in the field of e-textiles design software	371
I.R. Radulescu, R.M. Aileni, A. Salistean, S. Olaru, C. Grosu, R. Scarlat, I. Sandulache	
A study on enhancing the flame retardancy of polypropylene yarn with boron compounds	378
E. Eskiyyapar, Hatice K. Kaynak, Halil İ. Çelik, E. Sarıoğlu	
Antimicrobial properties of rabbit collagen glue-chitosan biomaterial loaded with cymbopogon flexuosus essential oil	385
M. Râpă, M.D. Berechet, C. Gaidău, R.R. Constantinescu, A. Moşuţiu	
Antimicrobial activity of FIR functionalized textile materials	391
O. Iordache, E.C. Tanasescu, I. Sandulache, C. Lite, L.-O. Secareanu, E. Perdum	



DESIGN OF GARMENTS USING ADAPTABLE DIGITAL BODY MODELS

DOI: 10.35530/TT.2021.09

A. Rudolf^{1*}, Z. Stjepanović¹, A. Cupar²

¹Institute of Engineering Materials and Design, Faculty of Mechanical Engineering, University of Maribor, Slovenia

(E-mail: andreja.rudolf@um.si, zoran.stjepanovic@um.si)

²Mechanical Engineering Research Institute, Faculty of Mechanical Engineering, University of Maribor, Slovenia

(E-mail: andrej.cupar@um.si)

Abstract: *In recent years, the 3D design software has been mostly used to improve the garment design process by generating virtual 3D garment prototypes. Many researchers have been working on the development of 3D virtual garment prototypes using 3D body models and involving the 3D human body scanning in different postures. The focus of research in this field today relies on generating a kinematic 3D body model for the purposes of developing the individualized garments, the exploration of which is presented in this paper. The discussed area is also implemented in the Erasmus+ project OptimTex - Software tools for textile creatives, which is fully aligned with the new trends propelled by the digitization of the whole textile sector. The Slovenian module focuses on presenting the needs of digitization for the development of individualized garments by using different software tools: 3D Sense, PotPlayer, Meshroom, MeshLab, Blender and OptiTex. The module provides four examples: 3D human body scanning using 3D photogrammetry, 3D human body modelling and reconstruction, construction of a kinematic 3D body model and 3D virtual prototyping of individualized smart garments, and thus displays the entire process for the needs of 3D virtual prototyping of individualized garments. In the OptimTex project, the 3D software Blender was used to demonstrate and teach students how to construct the "armature" of the human body as an object for rigging or the virtual skeleton for a 3D kinematic body model, using the knee as an example.*

Keywords: *3D body model, 3D scanning, kinematic 3D body model, virtual prototyping of garments*

1. INTRODUCTION

Digital transformation can be stated as the ultimate challenge for the fashion industry. In response to the pressure for growth and cost efficiency, many brands have started a series of initiatives to improve their speed to market and to implement sustainable innovation in their core product design, manufacturing, and supply chain processes. The role of the consumer has shifted from one of passive observance to enabled dominance. The vast majority of consumers use digital channels before, during or after making their purchases [1]. The fourth industrial revolution brings a lot of potentials, but also challenges. So, companies in the apparel industry are already facing a major transformation, greatly aided by effective digitalization. Virtual prototyping of garments can be termed as one of the most important parts of digitalization of the entire process. The purpose of 3D virtual prototyping is to create a virtual garment model instead of developing a real clothing product. For this, we have to

develop and employ digital body models. These topics are being investigated by some universities and research institutions that are collaborating in different research programmes, one of these being the EC Erasmus+ programme.

Goals and objectives of the new Erasmus+ project *OptimTex – Software tools for textile creatives* are fully aligned with the new trends propelled by the digitalisation of the whole textiles sector. OptimTex is already the fourth in the row of the successful projects devoted to e-learning in the wider scope of textiles. The projects are carried out by the consortium, consisting of the Universities and Institutes from different European countries [2].

OptimTex is a higher education project with underlined multidisciplinary concept. Connections between modern software applications and textiles are being investigated and explored. The main outputs of the project are: (1) Course of software applications for textiles, (2): Instruments for applying software solutions within textile enterprises, (3) E-learning tool and courses organization. The Slovenian Team has developed its module on Design and modelling of garments by 3D scanning software and CAD/PDS software. The contribution is focused on design of garments using adaptable digital body models, a contemporary topic, which is fully described in the module.

2. DIGITAL BODY MODELS

In today's digital age, the development of garments is increasingly taking place with the help of advanced technologies for 3D scanning of the human body and 3D CAD systems for the design, simulation, and visualization of clothing on virtual 3D body models. Their breakthrough is geared towards supporting the development of new advanced personalized products, such as garments for physically impaired persons, persons with physical deformities, the elderly or, for example, athletes, workers etc. who in carrying out various activities occupy specific postures, as well as for every individual who wants custom made garments. 3D body models provided by commercial 3D CAD systems for simulating and visualizing garments on virtual 3D body models are still a problem in this area. By using them we can adjust the body dimensions, muscles and postures to a certain extent. The studies showed that the use of advanced technologies is of paramount importance for the development of garments in terms of ergonomic and functional needs of the individual in order the garment properly fits the body [3-11].

3D body models of individuals can be obtained by 3D scanning of persons in the standard posture or in many other postures, which can be imported into 3D CAD systems for the development of personalized garments. Alternatively, the scanned digital record of the individual can be upgraded to a kinematic 3D body model, of which the body postures can be adjusted according to the needs during development and prototyping of garments for individuals.

The beginnings of the development of a kinematic 3D body model for virtual clothing prototyping go back years and coincide with the development of computer graphics in the field of human body kinematics and the animation of virtual garments, where from the very beginning rigged human body models also emerged [12,13] to improve deformable virtual humans [14].

A kinematic human body model intended for 3D garments development was presented by Leipner A. and Krzywinski S. [15], which consists of the anatomical structure of the human body or skeleton, muscles and skin, Figure 1. Modeling and animation of 3D body model was carried out using the Autodesk Maya 2012 software and Maya plug-in MuscleCreator. An inverse kinematics animation was created to study the proper deformation of the leg surface during the movement of the leg (figure 1). In the study by Kozar et al [16],

Blender software was used to design an adaptable 3D body model intended for the development of clothing for people with limited physical abilities (figure 2). This study shows the importance of using different tools to achieve smooth 3D mesh deformation and the influence they have on the body perimeters.

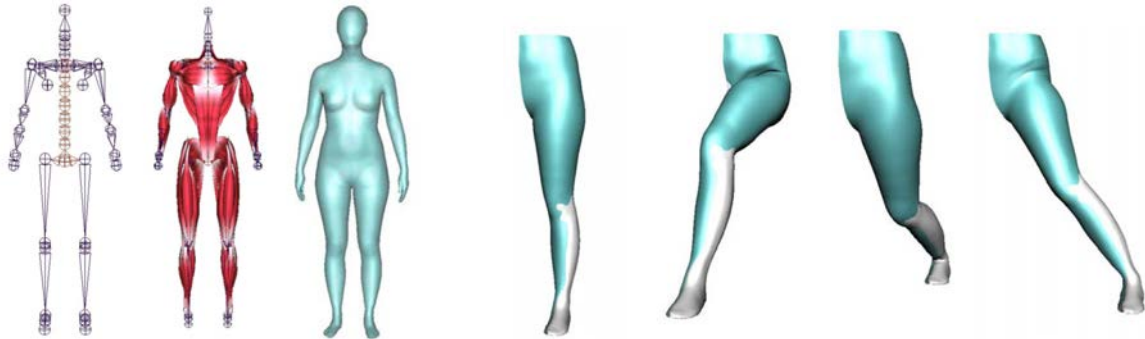


Figure 1. Kinematic 3D human body model construction: skeleton, muscles, skin (left) and animation of leg movement (right) [15].



Figure 2. Designing a 3D kinematic body model and fitting it to a wheelchair racing athlete [16].

Other research has also shown that there is currently no 3D kinematic human body model that represents realistic body deformations during movement, particularly in the elbow, knee and hip joints [17,18]. Examined were four methods, linear blend skinning in the simulation software Clo3d, auto-rigging of 3D scans on the online service Maximo, skinned multi-person linear human model and anatomical simulation using the plugin Ziva Dynamics, which also indicated improper deformation of the body mesh during bending in the elbow, knee, and hip joint regions. As an example of working with Clo3d a 3D human body scan conversion into an avatar adapted the body shape is shown on figure 3.

A new process for construction of a kinematic 3D body model using Blender 3D software can be found in the research by Klepser A. and Pirch K. [19]. There, a comparison between the three-dimensionally software-provided avatars and 4D scans of real test persons was carried out. Figure 4 shows that despite carefully performed 3D human body scanning of the tested person and mesh processing during kinematic 3D body model generation, difficulties remained due to incorrect mesh deformations during posture adjustments. In addition, 4D scans of the tested person's movements were taken as a starting point for the creation of a new kinematic 3D body model, the accuracy of which was improved.

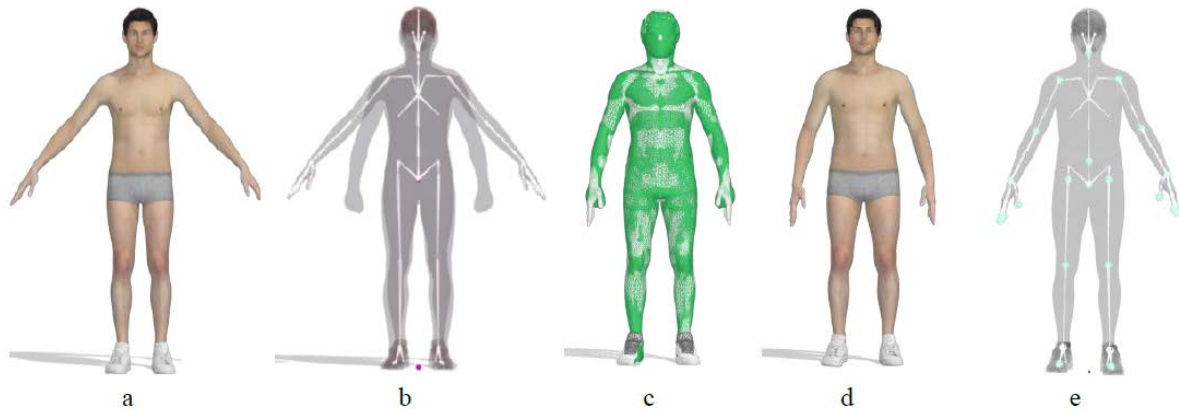


Figure 3. Converting a 3D body scan to an avatar: a - Clo avatar; b - aligned 3D body scan and Clo avatar; c - aligned avatar joints; d - converted avatar; e - 3D body scan with joints [17,18].

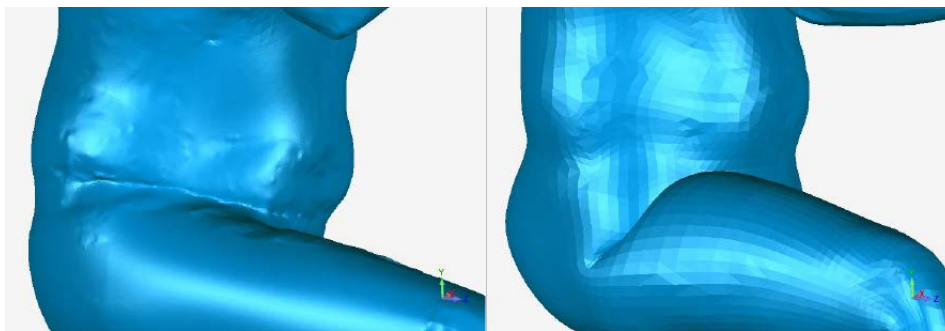


Figure 4. Leg's flexion pose of a scanned 3D body model (left) and generated kinematic 3D body model (right) [19].

Research trends in the development of a kinematic 3D body model for the purpose of virtual prototyping of individualized garments have been transferred to the OptimTex Erasmus+ project with the aim of providing students with the full range of new digital skills and knowledge for virtual development of individualized garments.

2.1 OptimTex Module 3 - Design and modelling of garments by 3D scanning software and CAD/PDS software

The module focuses on presenting the needs of digitization for the development of personalized clothing by using different software tools: 3D Sense, PotPlayer, Meshroom, MeshLab, Blender and OptiTex.

The module provides four examples:

1. 3D human body scanning using the 3D photogrammetry,
2. 3D human body modelling and reconstruction,
3. Construction of a kinematic 3D body model and
4. 3D virtual prototyping of personalized smart garments

and thus displays the entire process for the needs of 3D virtual prototyping of individualized garments.

Each example consists of the related theory, the application of software tools and some multiple-choice questions for self-assessment of the acquired knowledge.

The example of constructing a 3D kinematic body model from a 3D body model obtained by scanning and reconstructing a digitized body shows its creation through the acquisition of basic knowledge about:

1. the human body joint types divided according to their mechanics: pivot, hinge, ball-and-socket, condyloid, saddle and plane joints, which are important for skeleton generation and joints movements,
2. Blender 3D software which was used to demonstrate and teach students how to design the human body skeleton as an object for rigging or as a virtual skeleton for a kinematic body model, using the leg and flexion/positioning of the knee as examples.

The students will learn how to design a kinematic 3D model of leg's lower part and its skeleton as two bones, positioned within a 3D mesh of the leg as a junction in the knee joint (hinge joint; move in the Y axis), which enables manipulation and deformation of a mesh by moving bones in the knee joint, Figure 5.

The prepared course contains study material richly supported by video content that helps students in their creative work with software.

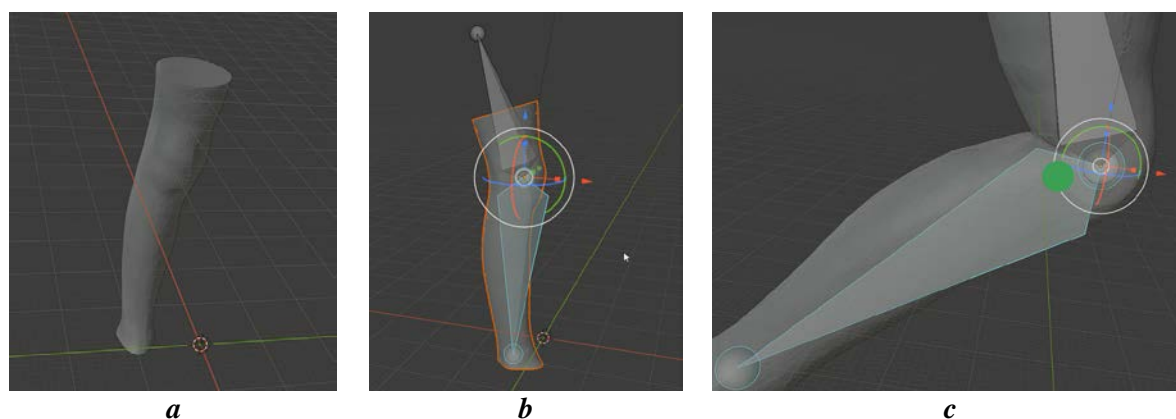


Figure 5. Designing of a kinematic 3D leg model: a -scanned 3D leg model; b – skeleton; c - kinematics of the rigged 3D model

3. DESIGN OF GARMENTS USING KINEMATIC 3D BODY MODELS

Recognitions that scanned 3D human body models in standard scan posture are not always suitable for the development of individualized garments, such as sports, medical and protective clothing, indicate the needs to use kinematic 3D body models. Indeed, garments that fit a standard scan posture can be very uncomfortable when performing daily tasks including walking, sitting, or reaching, and even more when performing sports or work activities. A garment design in a standard scanning posture is shown in figure 6, a, while the developed pattern designs for speed-skating trousers and rowing dress using a kinematic 3D body model is shown in figure 6, b and c [15].

In the OptimTex Erasmus+ project the last example of the module - *Design and modelling of garments by 3D scanning software and CAD/PDS software* - the development of individualized smart garment for a sitting posture of people with immobile lower extremities was presented, figure 7. Using the OptiTex PDS 3D software, the development of the pants'

pattern design on the kinematic 3D body model is shown from the point of view of correct positioning of heating elements, temperature sensors and conductive paths for acquisition and regulation of data when measuring pants' microclimate temperature and regulating the microclimate to the desired temperature.

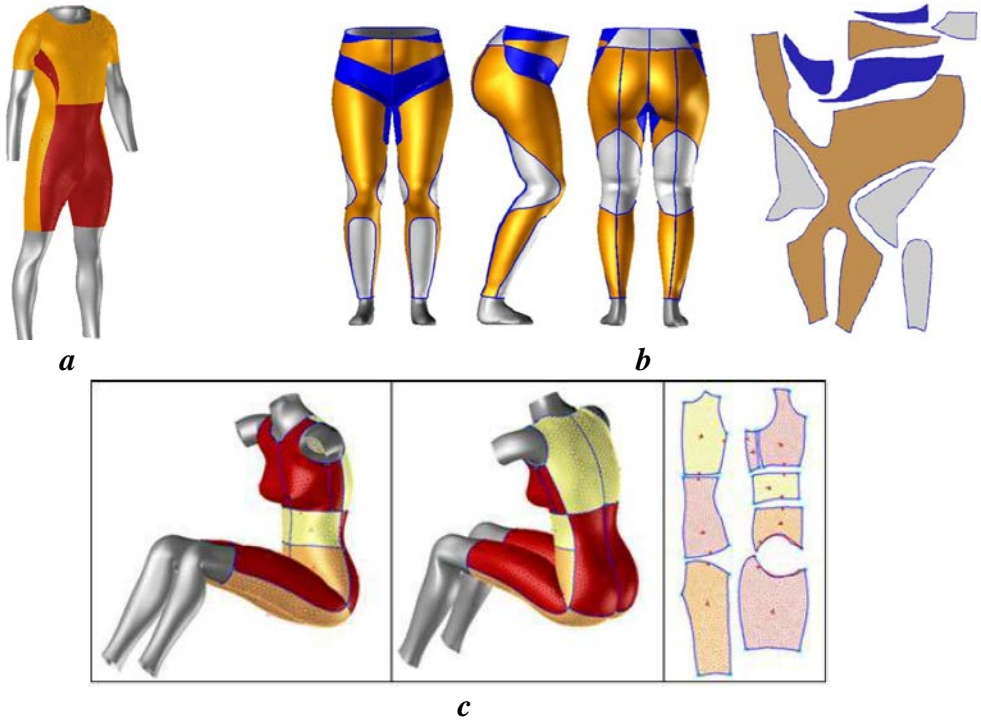


Figure 6. Garment pattern design in standard scanning posture: a - development of pattern pieces for speed-skating trousers; b - rowing dress; c - on a kinematic 3D body model [15]



Figure 7. Virtual prototypes of trousers: a – regular; b - heated [20]

Because the quality of garment fit depends besides the accurate 3D body model also on the realistic fabric draping, within the theoretical part of the module the low-stress mechanical properties for fabric drape simulation in OptiTex PDS 3D software were

presented. Measurement of fabrics' low-stress mechanical properties including tensile, shear, bending, surface and compression properties with FAST measuring system was presented, as well as their use for calculation of simulation of a physical model of a fabric and fabric behaviour during virtual prototyping.

The individual steps necessary for the creation of a garment virtual prototype using the 2D/3D Optitex PDS software are shown in the study material and supported in more detail with five videos (figure 8).

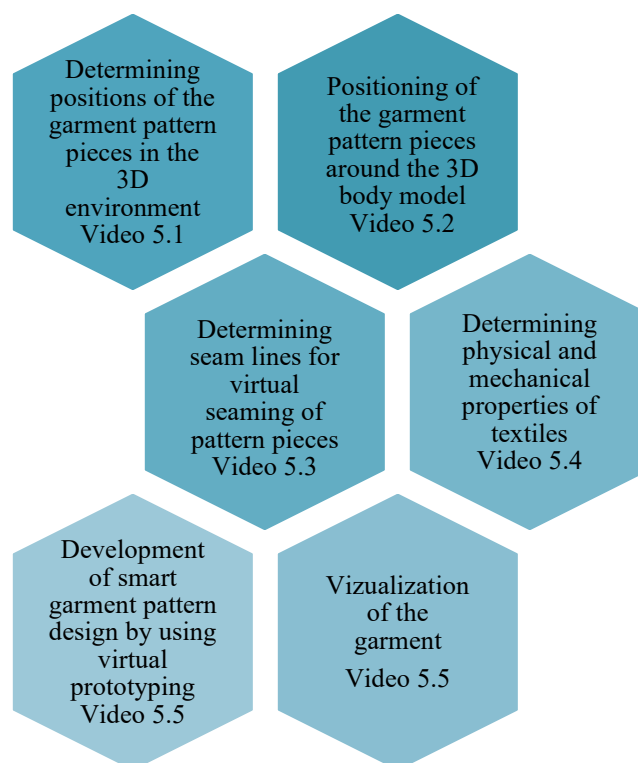


Figure 8. Steps for creation of a garment virtual prototype using 2D/3D Optitex PDS software

4. CONCLUSIONS

With the growing demand for customized products, e-commerce, and advances in virtual reality applications, virtual garment development is now in high demand to streamline the design and development processes of the apparel industry. Virtual garment prototyping has great potential in the fashion industry, especially by using adaptable digital body models to develop personalized garments for sports, medical and protective clothing. This contribution presents the development of kinematic 3D body models and their use for designing garments for different body postures. It also presents the topics of the module for the Erasmus+ project OptimTex, which is fully aligned with the new trends of digitalization.

ACKNOWLEDGMENT

The authors would like to acknowledge the support of the EC Programme Erasmus+, Project n° 2020-1-RO01-KA203-079823 “Software tools for textile creatives”, acronym OptimTex. This project has been funded with support of the European Commission. This

publication reflects the views only of the author, and the Commission cannot be held responsible for any use which may be made of the information contained therein.

REFERENCES

- [1] Lay, R., *Digital transformation - the ultimate challenge for the fashion industry*, In: Perspectives, Available at: <https://www2.deloitte.com/> [Accessed 10.7.2021]
- [2] *OptimTex project Application form*, Erasmus+ KA2 – Strategic Partnership for Higher Education, Call 2020
- [3] Stjepanović, Z., Rudolf, A., Jevšnik, S., Cupar, A., Pogačar, V., Geršak, J., *3D virtual prototyping of a ski jumpsuit based on a reconstructed body scan model*, In: Buletinul Institutului Politehnic din Iași. Secția Textile, Pielarie, 2011, 57, 17-30
- [4] Jevšnik, S., Pilar, T., Stjepanović, Z., Rudolf, A., *Virtual prototyping of garments and their fit to the body*, In: DAAAM International scientific book 2012, DAAAM International Publishing, Vienna, 2012, 601-618
- [5] Rudolf, A., Cupar, A., Kozar, T., Stjepanović, Z., *Study regarding the virtual prototyping of garments for paraplegics*, In: Fibers Polym., 2015, 16, 1177–1192
- [6] Bruniaux P, Cichocka A, Frydrych I., *3D Digital Methods of Clothing Creation for Disabled People*, In: Fibres & Textiles in Eastern Europe, 2016, 24, 5, 119, 125-131
- [7] Naglič, M.M., Petrak, S., Stjepanović, Z., *Analysis of 3D construction of tight fit clothing based on parametric and scanned body models*, In: Proc. of 7th Int. Conf. on 3D Body Scanning Technologies, Lugano, Switzerland, 2016, 302-313
- [8] Rudolf, A., Görlichová, L., Kirbiš, J., Repnik, J., Salobir, A., Selimović, I., Drstvenšek, I., *New technologies in the development of ergonomic garments for wheelchair users in a virtual environment*, In: Industria Textila, 2017, 68, 2, 83–94, <https://doi.org/10.35530/IT.068.02.1371>
- [9] Bogović, S., Stjepanović, Z., Cupar, A., Jevšnik, S., Rogina-Car, B., Rudolf, A., *The Use of New Technologies for the Development of Protective Clothing: Comparative Analysis of Body Dimensions of Static and Dynamic Postures and its Application*, In: Autex Research Journal, 2019, 19, 301-311
- [10] Cupar, A., Stjepanović, Z., Olaru, S., Popescu, G., Salistean, A., Rudolf, A., *CASP methodology applied in adapted garments for adults and teenagers with spine deformity*, In: Industria Textila, 2019, 70, 5, 435-446, <http://doi.org/10.35530/IT.070.05.1619>
- [11] Olaru, S., Popescu, G., Anastasiu, A., Mihăilă, G., Săliștean, A., *Innovative concept for personalized pattern design of safety equipment*, In: Industria Textila, 2020, 71, 1, 50–54, <http://doi.org/10.35530/IT.071.01.1620>
- [12] Boulic, R., Magnenat-Thalmann, N., Thalmann, D., *A global human walking model with real-time kinematic personification*, In: The Visual Computer: International Journal of Computer Graphics. 1990, 6, 344-358
- [13] Jung, M., Badler, N.I., Noma, T., *Animated Human Agents with Motion Planning Capability for 3D-Space Postural Goals*, In: Journal of Visualization and Computer Animation, 1994, 5, 225-246
- [14] Kalra, P., Magnenat-Thalmann, N., Moccozet, L., Sannier, G., Aubel, A., Thalmann, D., *Real-time animation of realistic virtual humans*, In: IEEE Computer Graphics and Applications, 1998, 18, 42-56
- [15] Leipner, A., Krzywinski, S., *3D Product Development Based on Kinematic Human Models*, In: Proceedings of the 4th International Conference on 3D Body Scanning Technologies, Long Beach CA, USA, 19-20 November 2013; Editor: Hometrica Consulting, Switzerland; Publisher: Hometrica Consulting, Switzerland, 310-316
- [16] Kozar, T., Rudolf, A., Cupar, A., Jevšnik, S., Stjepanović, Z., *Designing an adaptive 3D body model suitable for people with limited body abilities*, In: Journal of Textile Science & Engineering, 2014, 4, 5, 1–13
- [17] Zhang, D., Krzywinski, S., *Development of a Kinematic Human Model for Clothing and High Performance Garments*, In Proc. of 3DBODY.TECH 2019 - 10th Int. Conf. and Exh. on 3D Body Scanning and Processing Technologies, Lugano, Switzerland, 22-23 Oct. 2019, 68-73

- [18] Zhang, D., Krzywinski, S., *Development of a Kinematic Human Model for Clothing Design / simulation*, AUTEK2019 – 19th World Textile Conference on Textiles at the Crossroads, 11-15 June 2019, Ghent, Belgium
- [19] Klepser, A., Pirch, C., *Is this real? Avatar Generation for 3D Garment Simulation*, In: Journal of Textile & Apparel Technology & Management (JTATM), 2021, Special Issue, 12, 1-11
- [20] Rudolf, A., Štampfer, J., Sadek, J., Surla-Pavlović, B., Hudournik, M., Kolanovič, V., Novak, J., Borovec, M., Belšak, R., Gotlih, K., *Designing a smart heating trousers to improve wheelchair users legs thermal comfort* (paper in review).



DEVELOPMENT AND CHARACTERIZATION OF STITCH-BASED SENSORS

DOI: 10.35530/TT.2021.08

S.A. Odhiambo*, S. Vasile, J. Sarrazyn, I. Rottiers, A. De Raeve

FTI Lab⁺, HOGENT University of Applied Sciences & Arts, Belgium
(E-mail: sheilla.odhiambo@hogent.be, simona.vasile@hogent.be, ingeborg.rotters@hogent.be, jochen.sarrazyn@hogent.be, alexandra.deraeve@hogent.be)

Abstract: Strain sensing seams have been developed by integrating conductive sewing threads in different types of seam designs on a fabric typical for sports clothing using sewing technology. The aim was to obtain a simply integrated stitch-based sensor that can be applied on sports clothing to monitor the movements of the upper body parts of the user during exercising. Stitch types 304; 406; 602 and 605 were produced. The seams were made on a knitted fabric composed of 80% polyamide 6.6 and 20% elastane. The seams underwent stretch cycling for 10 cycles and up to 44 cycles following EN ISO 14704-1:2005 (modified), using an INSTRON tensile tester machine. The changes in the resistance of the seams with time were recorded simultaneously using Agilent meter U1273A. Sensing functionality among which is sensor gauge factor (GF), stability, drift, and reproducibility were evaluated on the promising sensor seams. The type of base fabric used, stitch type, stitch formation process (friction and dynamic forces during sewing), integrated EC thread length, and positioning of thread(s) in the fabric have a significant influence on the performance of the seams. Sensor seam 406-001 comprising 2 EC yarns (Madeira HC12) and Sensor seam 304-010 comprising 1 EC yarn (Madeira HC40) turned out to be very promising and others shall be improved (sensor 602-006 with Madeira HC 40 and sensor 605-002 with a Muriel yarn).

Keywords: electro-conductive sewing thread, sensing seams, sewing technology, stitch structure, electrical resistance

1. INTRODUCTION

The recent rise of personalized wearable devices that can monitor body parameters while sporting has made it increasingly important to have flexible textile-based sensor alternatives that can be comfortably worn [1-3]. Textile strain sensors offer a new generation of devices that combine strain sensing functionality with wearability and high stretchability [4-7]. Previously, sensors have been integrated into the textile structure before garment production, through printing [5], coating [8-10], weaving [11], or knitting [4]. These high levels of sensor integration mostly face challenges related to sensor connection with other parts of the smart systems [12] and also make potential garment repairing or disassembling for recycling purposes at the end of life difficult.

Stitch-based strain sensors are easily embedded in the garment and connected with other parts of the smart system such as the processing and communicating unit. Moreover, their integration into the garments towards the end of the production process offers definite advantages in terms of flexibility and production costs. Tangsirinaruenart & Stylios [13] employed sewing technology to develop strain sensors based on two specific

conductive sewing threads and several stitch types. Also, Gioberto et al. [14] confirm that most common sewing machines (the cover stitch and overlock machines) can produce reliable, repeatable, sensitive sensors. Each sewing machine produces sensors with slightly different characteristics and parameters. The tension of the conductive yarn during lock-stitching is an important factor to control the sensitivity of the strain sensor [15].

Despite the potential of this technology, the number of studies investigating stitch-based sensors is rather limited. Therefore this research aims to investigate some commercially available electro-conductive (EC) sewing threads, assess their properties, sewability and characterize the performance of their various stitch-based sensor configurations.

2. MATERIALS AND METHODS

2.1 Electro-conductive (EC) sewing threads and their characterization

Commercial EC threads with various compositions were selected and their properties were assessed: linear density (ISO 2060: 1994), linear electrical resistance (EN 16812:2016), tensile strain, and load at break (ISO 2062: 2009). A knitted fabric typically used in sports clothing, (80/20 PA/ EL) was used as the substrate for the strain sensor seams. The fabric was characterized to determine its weight per unit area (ISO 3801: 1977), thickness (ISO 5084: 1996), and elasticity (EN ISO 14704-1: 2005). We informally evaluated the suitability of sewing the selected EC yarns on conventional sewing machines and used in some cases silicone oil to smoothen the sewing process.

2.2 Seams and stitch-based sensors characterization

In the production of the sensing seams, EC threads were mostly used as bobbin threads aiming at low friction and low thread tension, in some cases the EC thread could be used as a needle thread too. Stitch types 304, 406, 602, and 605 were produced and the successfully stitched sensors were characterized using an experimental set-up similar to [13], using a tensile tester Instron and an Agilent meter U1273A. Rectangular fabric strips of 5x20 cm containing the sensor seam were fixed between the machine clamps at a gauge of 100 mm. The resistance response of the sensors according to the applied strain force was recorded upon several stretch cycles performed to a maximum load of 35 N with a speed of 500 mm/ min (EN ISO 14704-1: 2005). Several specimens were tested to assess potential variations within the same type of sensor configuration and to assess the reproducibility of the sensors. The sensors underwent 10 cycles to assess their sensitivity and 44 cycles to assess their stability i.e. 44 cycles is the maximum number of cycles for the tensile tester Instron machine. The average time per cycle (loading and offloading) was 12 seconds. The initial sensor seam electrical resistance (R_0) was noted for each sensor just before the onset of cycling. The changes in resistance and strain were recorded continuously throughout the stretch cycling. The sensor gauge factor (GF) was determined at the 2nd, 10th, and 44th cycles. The GF represents the sensitivity of the sensor and was calculated as the ratio of changes in resistance at any given cycle relative to R_0 , to the relative strains. The drift of the GF between the 2nd and 44th cycles was also determined. These parameters indicate the sensor's sensitivity, stability, and reproducibility.

3. RESULTS AND DISCUSSIONS

The linear density (count) of the EC threads ranged between 260-2000 dtex, their resistance between 82- 2000 ohm/m, and they had an elongation (strain at break) between

18 - 36 % (table 1). The knitted fabric (substrate) had a mass per unit area of $276 \pm 5 \text{ g/m}^2$, a thickness of 0.46 mm, and exhibited a tensile strain of $132.4 \pm 3.1 \%$ and $150 \pm 6.6\%$ in the wales and course direction respectively.

In some cases, the **sewability** of EC threads was challenging, adjustments of the machine speed and use of silicon oil were necessary to avoid irregular stitches. The density of the base fabric affected the precision of the stitches, doubling the fabric in some cases enabled more accurate and neat stitches but affected the stretchability of the seam. For uniformity purposes, all characterized seams presented hereafter were produced on a single fabric without a backing.

The descriptions of the sensors seams produced are shown in figure 1, the type of the respective EC yarn and the conventional yarns used in each seam, the stitch dimensions, and the images of the front and the back of the seams. Visual inspection of the seams after cycling shows that the main fabric is elongating as well as narrowing during cycling. This means that any portion of the EC thread in the direction of the stretch is also elongated.

Table 1. Properties of selected EC threads

EC thread reference (company)	EC thread composition	Count (dtex)	Resistance (Ω/m)	Strain at break (%)
Silvertech 120 (Amann)	Silver coated PA/PES hybrid thread (spun)	260	530	17
Madeira HC 40	Silver plated PA (spun)	300	< 300*	20
Madeira HC 12	Silver plated PA (spun)	630	< 100*	25
Soieries Elite Elinox 3x(PESHT140dtex2VN35)	(Twisted PES/ 2 SS filaments) x 3 doubled	900	134	14
Soieries Elite Elinox 5x(PESHT140dtex2VN35)	(Twisted PES/2 SS filaments) x 5 doubled	1980	82	15
Soieries Elite Elinox PESHT140dtex2VN35	Twisted PES/ SS filaments	1780	100	16
Soieries Elite Elinox PESHT280dtexVN35PES20dtex	Twisted PES/ SS filaments	430	865	17
Lemur Muriel sensor yarn 70Sh	Elastic conductive silicone monofilament	2000*	2000*	300*

*Asterisk shows manufacturers specifications: PES - polyester; PA - Polyamide; SS - filaments stainless steel VN35 (Bekintex)

The strain sensor performance depended on the resistance per meter (ohm/meter) of the EC yarn(s) used/employed (mainly 1 EC yarn), the length of the EC yarn in the seam length of 100 mm, the number of contact points within the seam length, the seam stretchability, and the base fabric stretchability. The initial resistance of the seam just before loading depended on the total yarn length in the seam concerning the effective current path. Thus complexly configured seams with many flexible loops tend to comprise more EC yarn length with more flexible contact points thus unpredictable behavior of the strain sensor. The variation in sensitivity could also be due to irregularities in the stitches during production or the EC yarn imperfection at microscopic levels.

The gauge factor (GF) is the most important performance parameter which is a dimensionless value that determines the sensitivity of a sensor. The gauge factor of the strain sensors at the 2nd, 10th, and 44th cycles was calculated by equation 1:

$$GF = \frac{\Delta R/R_0}{\epsilon} = \frac{\Delta R/R_0}{\Delta L/L_0} \quad (1)$$

where R_0 and L_0 are the unstretched resistances and length respectively; ΔR and ΔL are the changes in resistances and length due to stretching respectively; ϵ is the strain. Higher initial resistance means that for a given gauge factor changes in strain would produce larger changes in resistance. However high resistance sensors also tend to have a much lower gauge factor so offsetting this advantage.

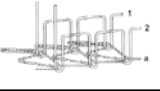
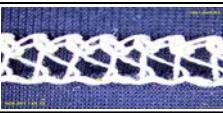


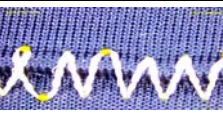

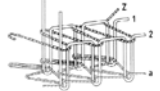



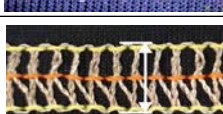
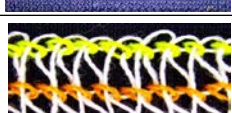


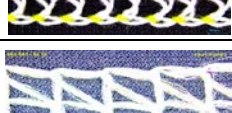
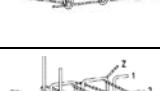
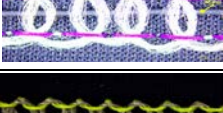

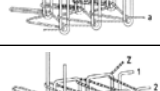
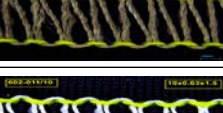
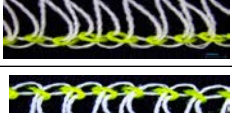
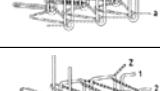
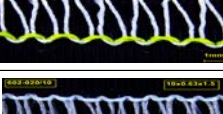
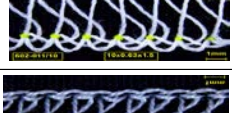
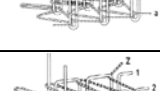
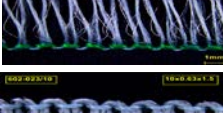
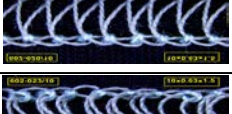
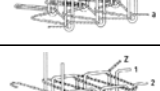
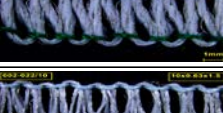
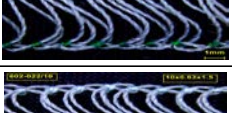
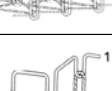
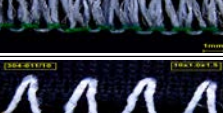

Test Sample nr.	EC Threads	Stitch-type	Stitch structure	Description	Stitch length	Stitch width	Close-up stitch front	Close-up stitch back
406-001	Madeira HC12 (410SMP)	406		Needle thread 1/2: Madeira HC 12 a: looper thread, 100% PES 120 dtex	2 mm	6 mm		
304-010	Madeira HC40 (410SMP)	304		Needle thread 1 Madeira HC 40, a- bobbin thread 100% PES 75 dtex	1 mm	4 mm		
602-006	Madeira HC40 (410SMP)	602		Needle 1 & 2, a looper thread 100% PES, z cover thread Madeira HC 40	2 mm	4 mm		
S605-005	Madeira HC40 (410SMP)	605		Needle 1, 2, 3 and a looper thread 100% PES 120 dtex, z- cover thread Madeira HC40	3,6 mm	7 mm		
605-002	Muriel sensor yarn 70 sh	605		z/1/2/3/a PES sewing threads; Muriel sensor yarn is in laid (see close-up stitch front)	3,6 mm	7 mm		
602-012	Amann Silvertex +100 Tex33	602		Needle 1, 2 and a- looper 100% PES 120 dtex, z- cover thread AmannSilvertex+ 100 tex 33	1,5 mm	2 mm		
602-011	Soiree Elite Elinox PES HT VN35 280 Dtex + PES 20 Dtex 1000t S/Z	602		Needles 1, 2 and a -looper 100% PES 120 dtex, z- cover thread PES HT 140 VN35 280 dtex (with silicone)	1 mm	4 mm		
602-020	Soiree Elite Elinox 1x (PES HT 140 dtex VN35), bobbin thread 100% PES 75dtex	602		Needles 1, 2 and a-looper 100% PES 120 dtex, z-cover thread PES HT 140 dtexVN35 200T S/Z	1 mm	4 mm		
602-023	Soiree Elite Elinox 5x (PES HT 140 dtex2 VN35), bobbin thread 100% PES 75dtex	602		Needle 1, 2 and a- looper 100% PES 120 dtex, z-cover thread 5x (PES HT 140 dtexVN35)	1 mm	4 mm		
602-022	Soiree Elite Elinox 3 x (PES HT 140 dtex2 VN35)	602		Needle 1, 2 and a- looper 100% PES 120 dtex, z-cover thread 3 x (PES HT 140 dtexVN35)	1,5 mm	4 mm		
304-011	Soiree Elite Elinox 3 x (PES HT 140 dtex2 VN35)	304		Needle thread 1 Elinox 3 x (PES HT 140 dtex2 VN35), a-bobbin thread PES 75dtex	1 mm	4 mm		

Figure 1. Configurations of the produced sensor seams

Linearity between seam resistance and absolute strain during loading and offloading in the cycling process, repeatability of the loading-offloading patterns for the consequent cycles (up to 44), and reproducibility of the strain sensor seams were key aspects in selecting the performing sensors. The selected sensors presented in this paper exhibited

these properties, however, each sensor could hardly return to its exact previous state during cycling, hence slight drifts were observed in the consecutive cycles. The **drift** was calculated as the differences in the change in resistance at the peak of the second cycle and the peaks of the respective cycles (the 10th, or the 44th cycles). The summary of the GF values and Drifts at the respective cycles is shown in table 2.

Not all seams produced real strain sensors, some seams could barely show any response during stretch cycling. Seams with a low response (i.e. low changes of resistance upon stretching) were discarded. Therefore after screening only the most promising sensors have been selected for presentation.

Table 2. Summary of G.F values and drifts of the presented sensors

EC yarn	Madeira HC 40	Madeira HC 12	Muriel sensor yarn 70sh	Madeira HC 40
Stitch number	304-010	406-001	605-002	602-006
R0 (Ohm)	245.38	250.5	607.92	159.63
L0 (nm)	100	100	100	-
Strain (%) cycle 2	116.33	72	84.67	63.8
Strain (%) cycle 10	121	74	101.92	1.3
Strain (%) cycle 44	124	75	-	-
$\Delta R2/R2$ (%)	11.1	32.47	149.77	0.53
$\Delta R10/R0$ (%)	11.5	38.46	197.75	1.41
$\Delta R44/R0$ (%)	17.87	50.07	-	-
GF cycle 2	cycle 2	0.45	1.77	0.41
GF cycle 10	0.10	0.52	1.94	1.08
GF cycle 44	0.14	0.67	-	-
GF drift cycle 10	-0.0004	0.0688	0.1714	0.6769
GF drift cycle 44	0.049	0.217	-	-
GF drift (%) cycle 10	-0.04	6.88	17.14	67.69
GF drift (%) cycle 44	4.90	21.66	-	-

The sensor performance varied depending on stitch type to EC-thread combination. For instance, **sensor seam 406-001** (comprising two EC threads Madeira HC12) had a good performance. This sensor seam showed linearity during cycling (the proportional changes in resistances during loading and offloading to the changes in the strain) and stability in consequent cycles (the same cycle pattern was observed throughout the cycling). Three different samples of the same were compared and the results showed consistency. The sensor seam is reproducible and showed low variation among the three specimens, its resistance varied relatively narrowly between 300-350 ohm (figure 2, a). This seam reached an elongation of 80 % during stretch cycling (figure 2, b) at a maximum load of 35 N and its GF was 0.52 at the 10th cycle and 0.67 at the 44th cycle, with a drift of 21% at the 44th cycle.

Sensor Seam 304-010 (comprising one EC yarn Madeira HC40) was very elastic with maximum elongation of 120%, at 35 N (figure 3, b), and could withstand 44 cycles with only 4.8% drift in GF at the 44th cycle. A sample of this sensor seam was very stable and had a very low variation of the sensing response between cycles 1-44. However, its GF was low (about 0.1). Figure 3, a shows that its resistance varied narrowly (250-270 Ohm) and that it exhibited low variation between the three similar specimens tested hence shows good reproducibility. Figure 3, b shows that this sensor is stable up to 44 cycles.

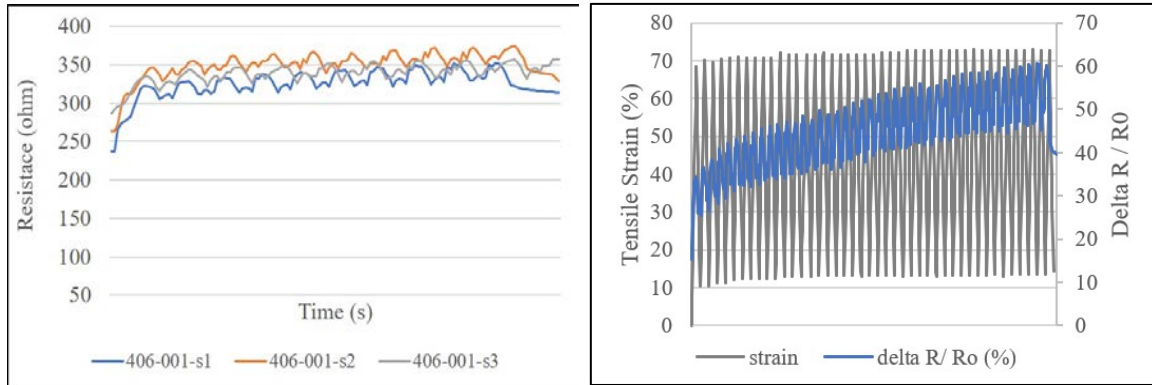


Figure 2. Seam 406-001 performance for the three specimens: a - comparison of s1, s2, and s3 changes in electrical resistance in time of cycling among samples (reproducibility); B - sensor seam stability up to 44 cycles

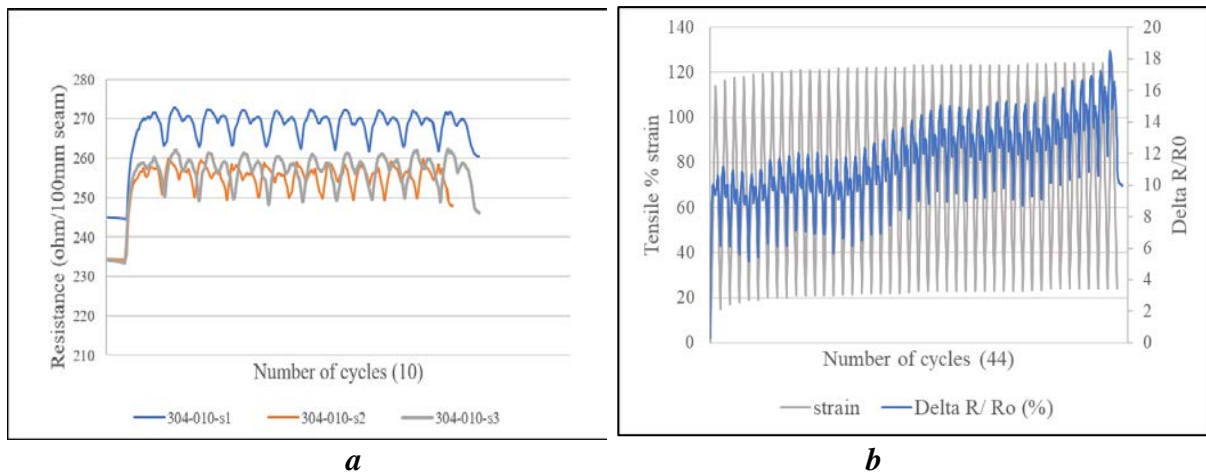


Figure 3. Seam 304-010 performance for the three specimens: a - comparison of s1, s2, and s3 changes in electrical resistance in time of cycling among samples (reproducibility); b - sensor seam stability up to 44 cycles

Sensor seam 602-006 (comprising one EC-yarn Madeira HC 40) was less elastic (around 60% at 35 N) and its resistance varied very narrowly (160-170 ohm) within the 10 cycles as shown in figure 4. The sensor GF was 0.41 at the 2nd cycle and 1.08 at the 10th cycle) with a high drift of 68%, at the 10th cycle (it can be seen in figure 4, b that the peak of the strain or delta R/R0 shifts with an increase in the number of cycles). However, this sensor had good reproducibility (figure 4, a).

Sensor seam 605-002 (comprising one Muriel yarn, laid in the seam, on the fabric surface) exhibited very high sensitivity. Controlling the yarn tension during sewing was very difficult and this resulted in large variation among identical samples as can be seen in figure 5, a. Nevertheless, the sensitivity pattern of the first 10 cycles was similar for both samples with large strains. These seam sensors could easily stretch up to 100% of the original length at the given load of 35N and exhibited very high variation in delta R/R0 after 10 cycles. The sensor GF was 1.77 at the 2nd cycle and 1.94 at the 10th cycle with a high drift of 17%, at the 10th cycle.

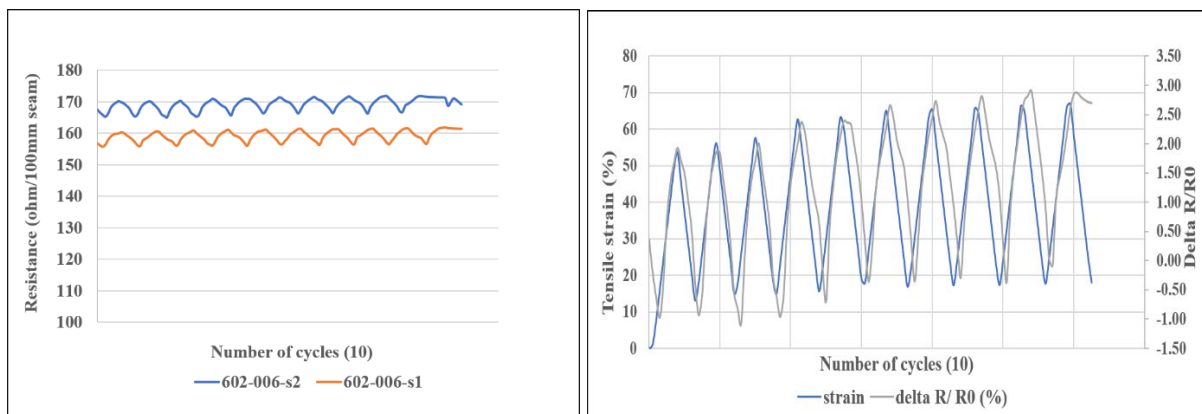


Figure 4. Seam 602-006 performance for the two specimens: a - comparison of s1 and s2 changes in electrical resistance in time of cycling among samples (reproducibility); b - drift in the gauge factor with the increase in the number of cycles within sample 2

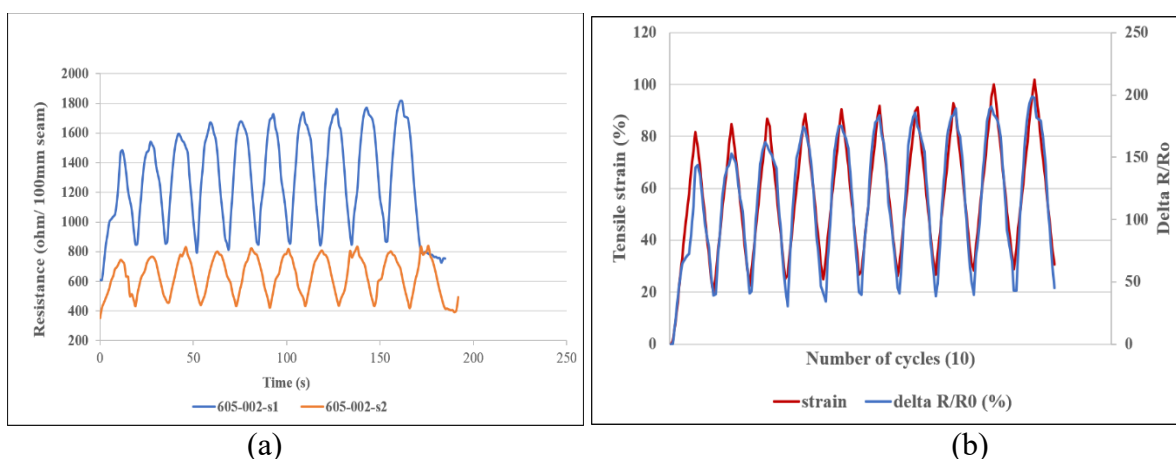


Figure 5. Seam 605-002 performance for the two specimens; a - comparison of s1 and s2 changes in electrical resistance in time of cycling among samples (reproducibility); b - drift in the gauge factor with the increase in the number of cycles within sample 2

The sensing mechanism is as a result of the alteration of the electromechanical properties of the seams under stress/strain deformation. Therefore the type of base fabric used, stitch type, stitch formation process (friction and dynamic forces during sewing), integrated EC thread length, and positioning of thread(s) in the fabric have significant influence on the performance of the seams during cycling hence an influence on the sensitivity stability and reproducibility of the strain sensor seams.

4. CONCLUSION

Different types of EC threads were used to produce various seam types on a fabric substrate typically used for sportswear. The EC yarns were used mostly as bobbin threads to sew them with as little tension and friction as possible.

Sensor seam 406-001 comprising 2 EC yarns (Madeira HC12) and Sensor seam 304-010 comprising 1 EC yarn (Madeira HC40) turned out to be very promising and others shall be improved (sensor 602-006 with Madeira HC 40 and sensor 605-002 with a Muriel yarn). Such strain sensors can be potentially used for monitoring body movement

in sportswear. Further research is needed to optimize configuration EC yarns-fabric-stitch for monitoring movements with the desired stretch, to integrate the sensor, to foresee appropriate connections, and actual assessment of sensor performance and reliability in time and upon garment washing among others.

ACKNOWLEDGMENT

The authors would like to express appreciation for the financial support of the sponsors VLAIO TETRA programme (B) & AiF (German federation of Industrial research association) [Project nr. HBC.2019.2679 (478) (CORNET)].

REFERENCES

- [1] Cherenack, K., Pieterse, L.V., *Smart textiles: Challenges and opportunities*, In: Journal of Applied Physics, 2012, 112, <https://doi.org/10.1063/1.4742728>
- [2] Derojeda, K., *Smart Textiles for Sports; Report on promising KETs-based products*, 2021, Available at: https://ec.europa.eu/growth/tools-databases/kets-tools/sites/default/files/documents/analytical_report_nr1_smart_textiles_for_sports_final.pdf. [Accessed on June 2021]
- [3] Research, T.M., *Smart Textile Market - Global Industry Analysis, Size, Share, Growth, Trends and Forecast 2015 - 2023: TMR*, 2016, 9/29/2016
- [4] Zhang, Q., et al., *Textile-Only Capacitive Sensors for Facile Fabric Integration without Compromise of Wearability*, In: Advanced Materials Technologies, 2019, 4, 10
- [5] Agcayazi, T., et al., *Fully-Textile Seam-Line Sensors for Facile Textile Integration and Tunable Multi-Modal Sensing of Pressure, Humidity, and Wetness*, In: Advanced Materials Technologies, 2020, 5, 8
- [6] Islam, G.M.N., Ali, A., Collie, S., *Textile sensors for wearable applications: a comprehensive review*, In: Cellulose, 2020, 27, 11, 6103-6131
- [7] Guo, L., et al., *Improvement of electro-mechanical properties of strain sensors made of elastic-conductive hybrid yarns*, In: Textile Research Journal, 2012, 82, 19, 1937-1947
- [8] Takamatsu, S., et al., *Fabric pressure sensor array fabricated with die-coating and weaving techniques*, In: Sensors and Actuators a-Physical, 2012, 184, 57-63
- [9] Chatterjee, K., et al., *Electrically Conductive Coatings for Fiber-Based E-Textiles*, In: Fibers, 2019, 7, 6
- [10] Chedid M., Belov, I., Leisner, P., *Experimental analysis and modelling of textile transmission line for wearable applications*, In: International Journal of Clothing Science and Technology, 2007, 19, 1-2, 59-71
- [11] Vasile, S. et al., *Study of the contact resistance of interlaced stainless steel yarns embedded in hybrid woven fabrics*, In: Autex Research Journal, 2017, 17, 2, 170-176
- [12] Matsouka, D., et al., *Electrical connection issues on wearable electronics*, In: IOP Conference Series-Materials Science and Engineering, 2018
- [13] Tangsirinaruenart, O., Stylios, G., *A Novel textile stitch-based strain sensor for wearable end users*, In: Materials, 2019, 12, 9, 1469
- [14] Gioberto, G., et al., *Machine-Stitched E-textile Stretch Sensors*, In: Sensors & Transducers, 2016, 202, 7, 25-37
- [15] Park, J., et al., *Wearable Strain Sensor Using Conductive Yarn Sewed on Clothing for Human Respiratory Monitoring*, In: IEEE Sensors Journal, 2020, 20, 21



DEVELOPMENT OF MULTILAYER TEXTILE STRUCTURES FOR FILTERING APPLICATIONS – A NEW SURGICAL MASK APPROACH

DOI: 10.35530/TT.2021.05

R.V. Costa^{1*}, C. Silva¹, T. Sousa², J. Bessa¹, F. Cunha¹, J. Belino³, G. Paixão³, R. Figueiro^{1,4}

¹Center for Textile Science and Technology (2C2T), University of Minho, Braga, Portugal
(E-mail: ritacosta@fibrenamics.com, cristinasilva@fibrenamics.com)

²Pixartidea, Praça Conde de Agrolongo, Braga, Portugal
(E-mail: tiagosousa@pixartidea.com)

³Borgstena Textile Portugal, Unipessoal Lda, Nelas, Viseu, Portugal
(E-mail: joao.belino@borgstena.com)

⁴Department of Mechanical Engineering, University of Minho, Guimarães, Portugal

Abstract: *Universal mask use has emerged as one of the main strategies for reducing community transmission of the SARS-COV-2 virus. Due to the scarcity of material to produce disposable surgical masks, the governmental strategy was oriented to the community masks, even though performance levels were still not the same.*

This study intended to develop a new generation of surgical masks with different warp knit structures, evaluating the potential of multilayer gradient performance. The assembling methodology was also considered by modifying flat-bed calendaring process parameters and manipulating final structures into a new origami design concept, and the overall mask filtration performance was reviewed.

The overlapping of monolayers increased the substrate resistance to air and water vapour permeability, also influencing the water molecule's adhesion. The introduction of the web allowed a better layer assembling during the flat-bed process. Moreover, the breathability and water vapour diffusion are compromised since the adhesive web with temperature tends to merge and occupy the empty spaces between the layers. Moving forward, calendared structures without a web proved to be the best approach, meeting the certification criteria for surgical masks level I and II.

Keywords: *calendaring, filtration, mask design, multilayer, warp knit*

1. INTRODUCTION

The Covid-19 pandemic virus is transmitted mainly through air droplets generated when infected individuals cough, sneezes, talk or exhale. These droplets are too heavy to be suspended in the air and quickly settle on surfaces [1-3]. Transmission occurs through inhalation of the virus or contact with contaminated surfaces crossed with the touch of the eyes, nose, or mouth. For that reason, universal mask use has emerged as one and primary strategy for reducing community transmission of the virus [4]. The study of Chan et al. [5], confirmed that wearing a surgical mask prevents and reduces the transmission of the virus between the infected patient and the unexposed person [5].

Until the Covid-19 pandemic, production of most of the masks was relatively cheap, so advanced economies left their production aside. In this context, for several years, Asia has responded to the market's needs in terms of melt-blown nonwoven manufacturing. However, due to the nonwoven immediate and uncontrolled need, the response capacity was no longer

efficient, and the rest of the world depended on a single source [6].

This pandemic caused the purchase of personal protective equipment (PPE) to increase rapidly, and promote the global shortage of equipment, especially face masks. Surgical masks are the most common type of face masks used to prevent respiratory infections. Surgical masks are composed of three layers, composed of synthetic nonwoven materials, and one of them, the middle layer, is the filtration layer. In Europe, properties and performance levels are governed by the EN 14683: 2019 standard, which encompasses three types of surgical masks (Type I, Type II, and Type IIR) [1]. Due to the scarcity of material to produce disposable surgical masks, the governmental strategy was oriented to the community masks, even though performances were still not the same [2].

Respirator masks have a higher level of protection against smaller particles (aerosols, gases, and vapours), however surgical masks are most comfortable. Violante concluded that the respirator masks are the most difficult to breathe, creating one obstacle for continuous use [7]. The frictional forces caused by using medical devices distort skin cells and tissues, which leads to damage. The loss of the integrity of the facial skin creates a portal for the penetration of pathogens. These damages in the skin are caused by the materials used in the construction of the masks, which have a high coefficient of friction with the skin, do not release efficiently the moisture created, which in turn increase the coefficient of friction even more. This problem can be solved through a more efficient choice of raw materials, with a lower friction coefficient [8].

To assembly the different layers that compound the masks, several processing technologies can be considered. Between them, calendering is a thermal bonding process where thermoplastic fibres melt and are bonded with the base material. Several variables in the calendering process change the properties of the final product, such as temperature, applied pressure, speed, and contact time. For application in nonwovens, it is necessary to be especially careful with the temperature, since the excessive increase may lead to the degradation of the raw material and a decrease in porosity, promoting the decrease in permeability [9].

According to Çinçik and Günaydin [9], the calendering process affects the structural properties and the mechanical performance (abrasion resistance), and the moisture management properties (permeability) of the final products. According to the results obtained, the thickness of the samples decreased with increasing temperature, which caused a decrease in porosity, an increase in density, and, consequently, makes the structure more compact. This more compact structure presents worse mechanical performance and permeability since a larger area is melted [9].

In this context, the main goal of this work consists of the study of the influence of different types of materials and calendaring processing conditions in the development of multilayer textile structures for filtering applications.

2. MATERIALS AND METHODS

This study is divided into two phases, namely:

- Phase I – Development of Fibrous Structures;
- Phase II – Development of Multilayer Filtration Fibrous Structures.

In Phase I, five knits and a nonwoven are analysed individually, to select the most efficient monolayers for the development of the multilayer that will be analysed and evaluated in Phase II.

2.1 Phase I: Development of Fibrous Structures

To develop fibrous structures for filtration was applied a multilayer concept, composed of three layers of knitted structures with different functions – comfort, filtration, and protection. The comfort layer (inner layer) should promote thermoregulation and moisture management as well as should be ergonomic and adaptable to the face. A filtration layer (intermediate layer) acts as diffusion and electrostatic filter for particles and microorganisms. The protective layer (outer layer) should be hydrophobic and behave as a semi-permeable barrier.

Therefore, it is crucial to choose materials based on the individual performance of specific functional tests. A performance study was realized with six different monolayers, comparing different knitted structures, shown in table 1 and figure 1.

Table 1: Fabric properties used in the experimental procedure

Sample code	Production method	Composition	Areal weight (g/m ²)	Substrate thickness (mm)
A	Warp knitting 2-bar	Polyester	117 ± 8.50	0.41
B	Warp knitting 2-bar	Polyester	115 ± 10.00	0.41
C	Warp knitting 3-bar	Polyester	155 ± 15.00	0.69
D	Warp knitting 3-bar	Polyester	92 ± 5.00	0.48
E	Warp knitting 3-bar	Polyester	89 ± 5.00	0.47
F	Melt-blown Nonwoven	Polypropylene	25 ± 0.01	0.17

Samples A and B were produced with the 2-bar warp knit structure, samples C, D, and E were produced with the 3-bar system, and sample F is a melt-blown nonwoven polypropylene meant to be placed in the filtration layer because it captures the unwanted particles [10].

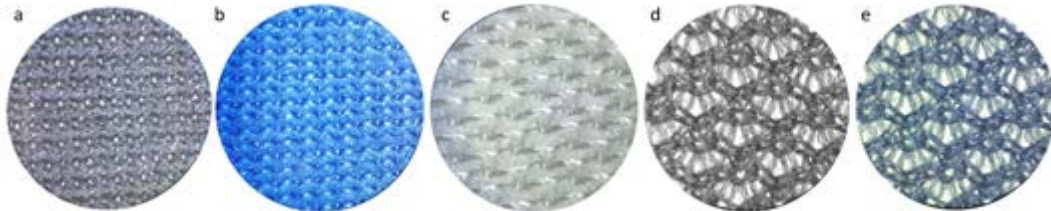


Figure 1: Knitted Structures: a - Sample A; b - Sample B; c - Sample C; d - Sample D; e - Sample E.

The sample's performance was evaluated through the moisture management properties - water vapour, and air permeability.

The air permeability of the substrates was performed by the rate of airflow passing perpendicularly through a 20 cm² area of fabric measured at a given pressure over 1 minute. The air permeability properties of the materials were measured using TEXTEST FX 3300 air permeability instrument according to the NP EN ISO 9237 – 2005 standard. The evaluation of this property was evaluated using three different air pressures: 40 Pa as required for mask characterization, 100 Pa for personal protective equipment, and 200 Pa for knitted structure evaluation. The water vapour permeability test determines the amount of water dissipation in the form of steam using Shirley Water Vapour Permeability Tester - SDL International. The "Control dish method" was used by the tissues and following the BS 7209: 1990 standard under isothermal conditions to perform this test. A Contact Angle System OCA 20

goniometer was used to measure the samples' top layer's hydrophobicity through droplet contact angle parameters. The water was injected slowly onto the surface by a syringe, repeated for ten droplets with the 5 μ l volume. The experiments were performed under similar conditioned laboratory environments. The surface is considered hydrophobic when the contact angle is superior to 90° or super hydrophobic if higher than 150°.

2.2 Phase II: Development of Multilayer Filtration Fibrous Structures

The multilayer fibrous structures used in this study have three distinct layers, namely: the chosen comfort layer was sample B due to its good moisture release capacity and water vapour permeability. The protective layer chosen was sample D, due to demonstrated liquid repellence and semi-permeable barrier effect. The diffusion layer was composed of polypropylene TNT produced through a melt-blown process (sample F). Thus, with the same fibrous structure, 9 different samples were developed, as can be seen in table 2.

To promote better adhesion between the layers and form a multilayer fibrous structure, a calendaring process was carried out. A Flatbed KFK- EL, Meyer® was the calendar used in this study, where the influence of pressure, temperature, speed, and level variable parameters were studied. As a result, nine different multilayers were produced, based on the variation of temperature and pressure, as well as the addition of an adhesive copolyester web (ZK8 from Protechnic).

Sample NC refers to multilayer without calendaring process, being composed by the overlapping of structures B, D and F. The four samples with code M refer to calendared structures without adhesive web, while the remaining four samples coded as MW refer to samples calendared with adhesive web addition. Numbers 1 to 4 present throughout the sample codes are related to the conditions used during the calendaring process. Number 1 refers to 110°C and 7 N/m²; number 2 - 110°C at 10 N/m²; number 3 - 120°C at 7 N/m², and number 4 - 120°C at 10 N/m². In addition, the performance of multilayer samples was compared to a marketed surgical mask level II, with the sample code SM. As described in Table 2.

Table 2: Sample production calendaring parameters

Sample code	Fibrous structure	Calendar Parameter				Adhesive web
		Temperature (°C)	Pressure (N/m ²)	Level (mm)	Speed (m/min)	
SM	Multilayer Melt-blown	Calendared				Without
NC	Multilayer B+D+F	Non-calendared				
M1		110	7	0	5	
M2		110	10			
M3		120	7			
M4		120	10			
MW1		110	7			
MW2		110	10			
MW3		120	7			
MW4	120	10	With			

After the calendaring process, the samples' performance was evaluated through the moisture management properties - hydrophobicity, water vapour, and air permeability.

3. RESULTS AND DISCUSSION

In this chapter, the results of the two studies presented above will be presented and discussed.

3.1 Phase I: Development of Fibrous Structures

The air permeability behaviour of monolayers was shown in table 3.

Table 3: Air permeability behaviour of monolayers

		A	B	C	D	E	F
Air permeability (L/min)	40 Pa	32.40 ± 4.50	37.56 ± 2.50	38.16 ± 4.50	148.80 ± 15.00	140.40 ± 15.00	9.76 ± 0.80
	100 Pa	76.80 ± 7.00	86.40 ± 19.50	90.36 ± 21.50	290.40 ± 15.00	280.80 ± 0.00	23.04 ± 7.00
	200 Pa	140.40 ± 5.00	158.40 ± 5.00	170.40 ± 5.00	474.00 ± 5.00	454.80 ± 5.00	50.40 ± 8.00
Water vapour permeability (%)		96.10 ± 0.02	96.79 ± 0.12	92.60 ± 0.06	99.11 ± 0.02	94.26 ± 0.02	-

The knits produced with warp knitting 2-bar (A and B) and the knit produced with warp knitting 3-bar (C) have very similar behaviour and a lower air permeability than presented by the knits produced with warp knitting 3-bar (D and E). The sample F used in the development of surgical masks, acting as a filter, as expected, has the lowest air permeability of the samples, due to its more closed structure, with small pores. Therefore, it is considered suitable for the filtration layer.

As verified in figure 1, similar fibrous structures translate into similar breathability, as seen from samples A/B, and D/E. The structure of sample C is very different from the rest but has behaviour identical to samples A/B. The structures of the D/E knits are more open and less dense than the rest knits (table 1), so it is normal to have higher air permeability than the other samples, as these two parameters significantly influence the permeability. These results are according to the study by Rodriguez-Palacios et al., 2020, in which more porous structures are more permeable and thus more susceptible to the passage of microbial agents, therefore less efficient in the retention of these agents [3]. It is important to note that these samples are all made of polyester and that in this case, the type of fibre used is not a differentiable factor. However, the fibrous structure has a significant effect on the breathability of the different textile samples.

The increase in pressure promoted the increase of air permeability. The increase from 40 to 100 Pa caused more than double the increase in air permeability. This correlation no longer happens in the increase from 100 to 200 Pa. All samples met the requirement of allowing the passage of airflow of 8 l/min.

The water vapour permeability of monolayers is illustrated in Table 4. Based on the requirements, all samples must allow water vapour permeability higher than 80%. It appears that all samples comply with the condition, exceeding it by a considerable margin. Sample D has water vapour permeability very close to 100%, like the behaviour of the standard fabric. Therefore, this sample has suitable properties to be applied in the outer layer once it translates into a decrease in the moisture accumulated inside the mask, and therefore greater comfort during use.

As verified with air permeability, identical structures were expected to exhibit similar water vapour permeability. However, this does not happen between D and E samples. It would also be expected that the samples with the highest air permeability would be the same as the water vapour permeability, being valid for sample D, but not for E. This could be

explained by the saturation of the samples due to the hygroscopic capacity of the fibres. For the validation of this perspective, further tests should be carried out.

On the other hand, sample C did not behave identically to A and B samples. It was evident that the structure of sample C is more closed than the structures of samples A and B, due to the higher number of bars used in the production. Thus, although these three samples (A, B, and C) are denser and have a more closed structure, they present higher water vapour permeability, which correlates with the samples' hydrophilicity.

In this sense, it was concluded that the best combination of monolayers is with B-D-F samples. Sample B is suitable for the inner layer of the mask to promote comfort, being the sample that showed the best results regarding water vapour permeability, turning it suitable for the human face can diffuse the moisture created inside the mask and not damage the skin. Sample D is one that best fits the function of the protective layer. It stood out with good levels of air permeability and good repellency on its surface, characteristics that allow ideal protection. The nonwoven sample F fulfils the requirements to perform the filtration function, not allowing the passage of pathogens. It presented low air permeability and the necessary hydrophobicity for this function.

3.2 Phase II: Development of Multilayer Filtration Fibrous Structures

The air permeability behaviour of multilayer fibrous structures is shown in table 5.

Table 5: Air permeability behaviour of multilayers

		SM	NC	M1	M2	M3	M4	MW1	MW2	MW3	MW4
Air permeability (l/min)	40 Pa	5.02 ± 0.96	7.96 ± 1.88	2.17 ± 0.32	2.80 ± 0.81	2.62 ± 0.84	2.28 ± 1.24	1.46 ± 0.56	1.51 ± 0.34	1.44 ± 0.91	1.91 ± 1.16
	100 Pa	12.96 ± 3.67	19.68 ± 3.89	5.92 ± 1.71	6.76 ± 2.53	6.38 ± 1.01	5.50 ± 2.57	3.92 ± 1.39	3.91 ± 0.61	3.94 ± 2.11	5.11 ± 1.07
	200 Pa	26.28 ± 6.78	39.72 ± 6.33	10.72 ± 4.62	13.32 ± 4.00	11.88 ± 3.83	10.22 ± 2.87	7.09 ± 3.30	7.62 ± 1.77	7.38 ± 5.17	9.78 ± 2.61

The increase of the number of layers, as well as the combination of different structures, increases the density, which consequently increases the resistance to airflow [3]. In addition to the permeability decreasing with the increase of layers, it also decreases with the calendaring process because the applied temperature and pressure reduce the pore size of the knit. The calendaring process promotes the decrease of air permeability around 69% at 40 and 100Pa, and 71% at 200Pa, compromising the capacity to allow air to diffuse, compared to the non-calendared sample (NC). The addition of the web in the calendaring process further decreases the air permeability, as it is another layer and an adhesion layer. The addition of the web (samples MW1, MW2, MW3, and MW4) causes the decrease of air permeability around 36% at 40Pa, and 31% at 100 and 200Pa, compared to the without web samples (samples M1, M2, M3, and M4). Thus, it appears that the addition of layers and processes decreases the permeability to air.

The multilayer NC has greater air permeability than the SM, which may be associated with the fact that the NC does not have its three layers united and has no process that changes its structure. The multilayer fibrous structures developed have lower air permeability than the commercialized multilayer (SM), which may be due to the structures of the knits as suggested by Lu et al. [11].

The water vapour permeability of multilayer fibrous structures is presented in table 6.

Table 6: Water vapour permeability behaviour of multilayer fibrous structures

	NC	M1	M2	M3	M4	MW1	MW2	MW3	MW4
Water vapour permeability (%)	98.93 ± 0.01	91.86 ± 0.00	90.80 ± 0.02	90.47 ± 0.03	97.68 ± 0.02	91.17 ± 0.01	86.35 ± 0.05	90.47 ± 0.03	92.03 ± 0.00

All samples have excellent water vapour permeability, higher than 80%, where NC and M4 samples have permeability close to 100%. The increase in density due to the increase in the number of layers contributes to a decrease in permeability compared to monolayers. Following Rodriguez-Palacios et al., 2020, in which the addition of several layers contributed to the decrease in permeability and manages to avoid the ejection of large macro-drops [3]. The calendaring process and the introduction of the web decrease the water vapour permeability. It is possible to deduce that higher temperatures and pressures promote greater permeability (samples M4 and MW4) and that the introduction of the web naturally promotes a slight decrease in permeability (MW4 vs M4).

The study of the contact angle is shown in figure 2.

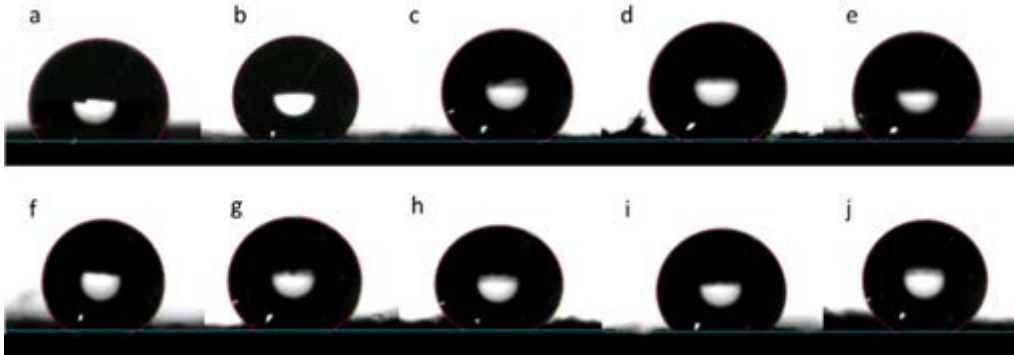


Figure 2: Contact Angle: a - Sample SM, 163.1°; b - Sample NC, 144.4°; c - Sample M1, 148.0°; d - Sample M2, 159.4°; e - Sample M3, 147.3°; f - Sample M4, 150.2°; g - Sample MW1, 161.0°; h - Sample MW2, 167.5°; i - Sample MW3, 159.2°; j - Sample MW4, 156.0°

As it can be observed in the calendaring process, the increase in pressure and the web introduction tend to increase the substrate hydrophobicity, except for the MW4 sample. The adhesion between the layers produces a multilayer with greater repellence, which does not allow the molecules adhesion on its surface. The sample MW2 has a more hydrophobic surface than the SM. The SM, M2, M4, MW1, MW2, MW3, and MW4 samples are super hydrophobic, having a contact angle over 150°C.

According to the DSC analysis, the melting temperature of polyester knits, samples B and D is approximately 255°C, while the melting temperature of sample F (polypropylene nonwoven) is 165°C. The calendaring process did not reach these temperatures, causing the assembly process to fail, not creating adhesion between the layers. However, in the temperature range of 110-120°C, polypropylene already begins the melting phase transition, shrinking its pores, thus creating higher air and water vapour permeability resistance.

In this context, it can be concluded that the introduction of the web intensifies the effects caused by the calendaring process. Furthermore, the breathability and water vapour diffusion are affected since the adhesive web with temperature tends to merge and occupy the empty spaces between the layers. However, the adhesion of the layers becomes advantageous

at the mechanical performance, allowing that the nonwoven improves its resistance, comfort, adaptability to the skin, and the surface repellence of the multilayer fibrous structure.

4. CONCLUSIONS

Through this work, was intended to study the influence of different types of materials and calendaring processing conditions in the development of multilayer textile structures for filtering applications. In this context, it can be concluded that the materials that best fit the desired purpose were a multilayer fibrous structure composed of the monolayers B, D, and F. Regarding the processing parameters in the calendaring process, it can be concluded that the pressure has more influence than temperature, and 10 N of pressure reveals as the best condition to obtain better results in air and water vapour diffusions, and a super hydrophobic surface, making the samples perform better with the imposed needs.

Through a decision matrix, where all tests have the same degree of importance, it was concluded that the sample that has the best performance is MW3. It stands out mainly for its comfort and the super hydrophobicity of its surface.

ACKNOWLEDGMENTS

The authors gratefully acknowledge the funding by P2020, under Individual Project SI I&DT POCI-01-02B7-FEDER-053071, entitled “MultigradeMask – Development of a surgical mask with gradient properties, according to EN 14 683”.

REFERENCES

- [1] World Health Organization, *Coronavirus disease (COVID-19): Masks*, Available at: <https://www.who.int/emergencies/diseases/novel-coronavirus-2019/question-and-answers-hub/q-a-detail/coronavirus-disease-covid-19-masks> [Accessed on April 26, 2021]
- [2] Bhattacharjee, S., Bahl, P., Chugthai, A.A., Macintyre, C.R., *Last-resort strategies during mask shortages: optimal design features of cloth masks and decontamination of disposable masks during the COVID-19 pandemic*, In: *BMJ Open Respir. Res.*, 2020, 7, 1-10, Available at: <https://bmjopenrespres.bmj.com/content/bmjresp/7/1/e000698.full.pdf> [Accessed on May 20, 2021]
- [3] Rodriguez-Palacios, A., Cominelli, F., Basson, A.R., Pizarro, T.T., Ilic, S., *Textile Masks and Surface Covers - A Spray Simulation Method and a ‘Universal Droplet Reduction Model’ Against Respiratory Pandemics*, In: *Front. Med.*, 2020, 7, May, 1–11, <https://doi.org/10.3389/fmed.2020.00260>
- [4] World Health Organization, *Coronavirus disease (COVID-19)*, Available at: <https://www.who.int/emergencies/diseases/novel-coronavirus-2019> [Accessed April 21, 2021]
- [5] Chan, J.F.-W., et al., *Surgical Mask Partition Reduces the Risk of Noncontact Transmission in a Golden Syrian Hamster Model for Coronavirus Disease 2019 (COVID-19)*, In: *Clin. Infect. Dis.*, 2020, 71, 16, 2139-2149, <https://doi.org/10.1093/cid/ciaa644>
- [6] Allan, D., *Nonwovens technology plays key role in the world’s response to COVID-19*, In: *Fastmarkets RISI*, 2020, Available at: <https://insights.risiinfo.com/-nonwovens-technology-plays-key-role-in-the-world-response-to-covid-19-/index.html> [Accessed on May 20, 2021]
- [7] Violante, T., Violante, F.S., *Surgical masks vs filtering facepiece respirators for the protection against coronavirus infection: current state of the art*, In: *Med Lav*, 2020, 111, 365-371, <https://doi.org/10.23749/mdl.v111i5.9692>
- [8] Gefen, A., *Skin Tears, Medical Face Masks, and Coronavirus*, In: *Wound Manag. Prev.*, 2020, 66, 4, 6

- [9] Çinçik, E., Günaydin, E., *The influence of calendaring parameters on performance properties of needle-punched nonwoven cleaning materials including r-PET fiber*, In: J. Text. Inst., 2017, 108, 2, 216-225, <https://doi.org/10.1080/00405000.2016.1161694>
- [10] O'dowd, K., et al., *Face Masks and Respirators in the Fight Against the COVID-19 Pandemic: A Review of Current Materials, Advances and Future Perspectives*, In: Materials (Basel), 2020, 13, 3363, 1-27
- [11] Lu, H., Yao, D., Yip, J., Kan, C.-W., Guo, H., *Addressing COVID-19 Spread: Development of Reliable Testing System for Mask Reuse*, 2020, 20, 2309-2317, <https://doi.org/10.4209/aaqr.2020.06.0275>



DEVELOPMENT OF MULTIFUNCTIONAL YARN FROM THE FUNCTIONALIZATION OF ORGANIC RAW COTTON FIBERS WITH ZINC NANOPARTICLES

DOI: 10.35530/TT.2021.20

S. Ferreira^{1*}, P. Silva¹, J. Bessa¹, F. Cunha¹, C. Castro², A. Aguilar², R. Figueiro³

¹Center for Textile Science and Technology (2C2T), University of Minho, Guimarães, Portugal
(E-mail: silviaferreira@fibrenamics.com, joabessa@fibrenamics.com)

²TEARFIL Textile Yarns, Av. Comendador Joaquim de Almeida Freitas 3, 4815-270 Moreira de Cónegos, Portugal

(E-mail: cristina.castro@tearfil.pt)

³Department of Mechanical Engineering, University of Minho, Guimarães, Portugal

Abstract: *The emergence of increasingly contagious diseases in these days, such as COVID-19, increased the need to develop more effective personal protection equipment's (PPEs). Therefore, the goal is to create textile materials capable to act against bacteria, virus or fungi, with a long-lasting performance but, at the same time, that could be comfortable and safe for their users. In this sense, based on the advantages of nanotechnology, the aim of this work was to functionalize organic raw cotton fibers with zinc nanoparticles (NPs) and previously treated with NaOH, for the further production of multifunctional yarns with antimicrobial activity. Thereby, the fibers functionalization was tested using 1% w/w and 2% w/w of zinc NPs aqueous dispersion, being subsequently evaluated their distribution, chemical nature and zinc concentration by SEM/EDS and Atomic Absorption Spectroscopy, respectively. Subsequently, using the functionalized fibers, a yarn was spun and their structural, mechanical and moisture management properties determined. Also, to assess the influence of the produced yarn on the properties of a fibrous structure, a single jersey knit sample was further produced and evaluated regarding their mechanical, moisture management and antibacterial properties. Based on the methodology used it was possible to develop a yarn with a tenacity 24% higher and a knit sample 28% more breathable and with a water evaporating ratio 37% higher than the one without any treatment or functionalization, but mainly with a strong antibacterial activity against both gram-negative (*Klebsiella Pneumoniae*) and gram-positive (*Staphylococcus Aureus*) bacteria, presenting therefore potential to be used in the production of effective PPEs.*

Keywords: *antimicrobial activity, exhaustion, multifunctional yarn, organic cotton, Zinc nanoparticles*

1. INTRODUCTION

The outbreak of the COVID-19 pandemic, which appeared at the end of 2019, has had a tremendous impact on the entire world, both in terms of health, economics and the environment. Being a highly infectious disease that is transmitted by droplets released when an infected person coughs, sneezes, or exhales and that quickly contaminate the surrounding environment, COVID-19 pandemic has triggered an urgent need for effective personal protective equipment's (PPEs), capable to protect, control and prevent the spread of this potentially fatal virus [1]. Hence, in the field of textile materials directed to this issue, the challenge has been to design and develop suitable textile structures that encompass multiple functionalities, namely, long-lasting resistance to the attack of dangerous microorganisms,

such as bacteria, virus or fungi, but without compromising their comfort properties and safety standards [2,3].

For this purpose, the application of nanotechnology has opened a new frontier in the area of textile finishing of imparting various functional properties to the textile materials. A variety of metal and metal oxide nanoparticles (NPs), such as silver, gold, zinc, zinc oxide, titanium oxide, or copper oxide are now applied as an effective way to provide textiles with antimicrobial properties due to their high specific surface area, which allows to react with multiple microorganisms [3-6]. In particular, zinc-based NPs have been extensively used for textile finishing, since they have proven to be a viable solution for fighting a broad spectrum of bacteria, both gram-positive and gram-negative, fungi and even viruses [7]. The mechanisms pointed out as the main responsible for the antimicrobial activity of this nanomaterial are the release of antimicrobial ions, such as Zn^{2+} , the interaction between the nanoparticles with microorganisms cell wall and the formation of reactive oxygen species (ROS), which ultimately destabilize or damage the cellular structure of the microorganisms, killing and/or inhibiting their growth [8].

In order to apply this type of nanomaterials into textile structures, the most common ways are their incorporation into the polymer bulk during the processing of synthetic fibers or the application of a surface finishing, such as coating, or modification as a chemical or physical finishing treatment in natural and synthetic textiles. Among these methods, the application at the textile finishing stage is a more common and popular choice, being done mostly via traditional pad-dry-cure or exhaust techniques [3,6,9-12]. However, the application of antimicrobial agents during textile finishing stage could have some disadvantages associated like disappearance of the functionalizing layer from the textile surface over time or the low incorporation of antimicrobial agents, which ultimately results in an ineffective and short-lasting antimicrobial activity.

Therefore, in the present work, it is proposed a new approach, namely the functionalization of a very common natural fiber – organic cotton fiber, with zinc nanoparticles (NPs), by exhaustion method, for the development of a multifunctional yarn with antimicrobial properties. The goal with this new multifunctional yarn is to produce any organic cotton-based fibrous structure, homogeneously composed by zinc NPs and consequently resistant against a broad spectrum of dangerous microorganisms, being therefore able to be used in the development of PPEs.

2. MATERIALS AND METHODS

2.1 Materials

Organic raw cotton fibers, supplied by TEARFIL Textile Yarns, were used in this study. The zinc NPs (130 nm) applied for the functionalization of organic raw cotton fibers were purchased from *IoLiTec-Ionic Liquids Technologies GmbH*.

2.2 Alkaline pretreatment of raw cotton fibers

Prior the functionalization with zinc NPs, organic raw cotton fibers were subjected to an alkaline pretreatment where organic cotton fibers were treated with an aqueous solution of 10 g/l NaOH, 2 g/l Kieralon OLB New and 1 g/l Calgon T at 98°C, keeping a material to liquor ratio of 1:40. After 60 minutes, the temperature was dropped to 50°C and the fibers were washed with abundant distilled cold water until it reached a neutral pH. Finally, the pretreated fibers were dried in an oven at 65°C, for 24 hours.

2.3 Functionalization of organic cotton fibers with zinc nanoparticles

The functionalization of pretreated organic cotton fibers was performed by exhaustion method applying a zinc NPs aqueous suspension. For the preparation of the aqueous suspension, 1% w/w and 2% w/w of zinc NPs, were diluted in distilled water, under vigorous stirring, until complete homogenization, and then sonicated for 5 minutes at room temperature. Subsequently, the pretreated cotton fibers were submerged into the zinc NPs suspension with a material to liquor ratio of 1:40 and placed in AHIBA SPECTRADYE datacolor® equipment. The functionalization proceeded at 100°C, 40 rpm, for 60 minutes. At the end of the process, the temperature was dropped to 50°C and the functionalized cotton fibers were rinsed thoroughly with cold distilled water and dried at 65°C, for 24 hours.

2.4 Yarns and jersey knit samples production

From organic cotton fibers subjected to an alkaline pretreatment followed by zinc NPs functionalization and from organic raw cotton fibers with no treatment applied, two yarns, CO_Zn and CO_0, respectively, were spun by ring spinning at Tearfil with a Ne 24/1. These yarns were further used to produce two jersey knit samples with a loop length of 0.38 cm using a laboratorial single jersey circular knitting machine.

2.5 Characterization methods

In order to evaluate the effectiveness of the methodology used to incorporate zinc NPs into organic cotton fibers and its influence on the properties of the yarns and jersey knit samples subsequently produced, a set of characterization methods and normative tests were performed.

The incorporation of zinc NPs into organic cotton fibers was evaluated by Scanning Electron Microscopy (SEM), Energy-dispersive X-ray spectroscopy (EDS) and quantified by Atomic Absorption Spectroscopy (AAS). By SEM/EDS it was observed the presence and distribution of zinc NPs and analyzed the elemental composition of the surface cotton fibers. This analysis was performed using a NOVA 200 Nano SEM equipped with an EDS integrated system from FEI Company (Hillsboro, OR, USA). The determination of zinc concentration in functionalized cotton fibers was carried out with a novAA 350 atomic absorption spectrophotometer from Analytik Jena GmbH using an acid digestion method. Therefore, approximately 1 g of functionalized cotton fibers was dissolved in a hot mixture of concentrated nitric acid and sulphuric acid (1:3). After cooling, the solution was diluted to 25 mL using distilled water and the concentration of zinc, in parts-per-million (ppm), was determined.

Regarding the yarns under study, it was evaluated their structural properties (linear density and twist), mechanical properties (tensile strength and loop tensile strength) and moisture management properties (vertical wicking behavior and static water absorption capacity). The linear density and twist of yarns were determined in accordance with NP ISO 2060:1995 and NP ISO 2061:2015, respectively. The yarns tensile strength was determined according to NP EN 2062 and loop tensile strength was determined according to ASTM D3217, NP EN 2062 and ASTM D7269. In both tests, ten specimens from each yarn, without and with a loop, were pulled at a constant speed rate of 500 mm/min until its break. The length between grips was 500 mm and the pre-tension applied was 0.5 cN/Tex. These tests allowed to determine the breaking force, maximum elongation and tenacity of the yarns under study. To evaluate the yarns capillarity, a vertical wicking testing was performed. The vertical wicking test followed the method described in Fangueiro, 2010 [13], where ten specimens with 200 mm of length were analyzed. Each specimen was placed in an upright position and the lower end was immersed 30 mm into stained water

where the water displacement was subsequently measured every minute until 10 minutes. To measure the static water absorption of yarns, the Bureau Veritas Consumer Product services BV S1008 internal testing method was carried out. In this test, five specimens of each yarn were conditioned and their mass evaluated. The samples were then kept in water for five minutes at room temperature. After that, the samples were hanged for three minutes to remove the excess of water and then the mass of the wet samples was measured. The amount of water absorbed by the yarn samples were calculated by taking the difference between the wet (m_w) and the dry mass (m_d). The percentage of water absorption (S_w) was calculated according to equation 1:

$$S_w = \frac{(m_w - m_d)}{m_d} \times 100 \quad (1)$$

The jersey knit samples performance was evaluated through the mechanical properties (tensile and friction tests), moisture management properties (air permeability and drying rate capacity) and antibacterial activity. The breaking strength and elongation of jersey knit samples were determined by applying the grab test method specified in ASTM D5034, where ten specimens (five in wale direction and five in course direction) from each knitted structure were cut, with dimensions of 200 x 100 mm, and pulled at a constant speed rate of 100 mm/min until its break, using a length between grips of 100 mm. To measure the surface friction of the knit samples, a frictional feel analysis was performed using the equipment protected by Portuguese Patent No. 102790. The working principle of this equipment is based on a rotary movement and, therefore, on the measurement of a friction reaction torque. Friction coefficient (μ) is computed from the friction reaction torque measured by the torque sensor and is used to infer about the friction of the knits with the human skin [14]. The air permeability of the knit samples was evaluated by measuring the rate of airflow passing perpendicularly through a 20 cm² area of five specimens from each knit sample, at 200 Pa, for 1 minute. For this purpose, a TEXTTEST FX 3300 air permeability equipment was used according to NP EN ISO 9237 – 2005 standard. Drying capacity was evaluated by calculating the drying rate of the knit samples, according to the method described in Fangueiro, 2010 [13]. Briefly, five specimens from each jersey knit sample, previously conditioned, were cut as 200 x 200 mm square, put on the plat of the balance and the drying weight was recorded as w_f (g). After that, 30% of the dry sample weight, on water, was added to each specimen and the resultant weight was recorded as w_0 (g). The wet specimens were then put in an oven at $33 \pm 2^\circ\text{C}$ and their weight (w_i) was recorded at regular intervals, for 30 minutes. The “Water Evaporating Rate (WER)”, which expresses the percentage of water that evaporated from the sample, was then calculated according to equation 2:

$$WER = \frac{(w_0 - w_i)}{(w_0 - w_f)} \times 100 \quad (2)$$

Antibacterial activity of the jersey knit samples against *Staphylococcus Aureus* (ATCC 6538) and *Klebsiella Pneumoniae* (ATCC 4352) was evaluated by the absorption method in accordance with ISO 20743:2013 standard. In order to evaluate the commercialization potential of this new yarn, the obtained results were compared to a jersey knit sample produced from a commercial antibacterial fiber incorporating also zinc NPs, *SmartcelTM Sensitive*. Therefore, a bacterial suspension was directly inoculated on the jersey knit samples and the antibacterial activity value (A) was calculated according to equation 3:

$$A = F - G = (\log C_t - \log C_0) - (\log T_t - \log T_0) \quad (3)$$

where F and G are the growth values on the reference sample and on the jersey knit samples under study, respectively. C_0 , C_t , T_0 and T_t are the average of the number of bacteria (Colony Forming Units per milliliter) obtained from three reference samples (C) or three knit samples (T), immediately after inoculation (C_0 and T_0) and after 24 h incubation (C_t and T_t). Based on the A value, the efficacy of the antibacterial properties of the jersey knit samples can be considered as null, if $A < 2$, significant, if $2 \leq A < 3$, or strong, if $A \geq 3$.

3. RESULTS AND DISCUSSION

Knowing in advance that the organic cotton fibers are composed by cellulosic molecular chains that in a neutral aqueous solution became negatively charge, it is expected an easy adsorption of positively charged ions, such as Zn^{2+} on the organic cotton fibers surface without the application of additional chemical reagents [15]. Moreover, based on literature, the application of elevated temperatures during the exhaustion process supplies a higher kinetic energy to the functionalizing NPs, which strikes cotton fibers with more frequency and greater force, becoming entrapped in surface pores more easily [5]. Therefore, based on these inputs it was proposed the functionalization of organic raw cotton fibers with 1% and 2% of zinc NPs, applying only a simple zinc NPs aqueous suspension at high temperature using the exhaustion method which, based on the characterization performed, proved to be effective in incorporating zinc NPs into organic cotton fibers. As can be seen in figure 1, b and c, it is observed the presence of NPs distributed homogeneously through the surface of cotton fibers that are not present in the organic cotton fibers without functionalization, as observed in figure 1, a, which indicates an effective incorporation of the zinc NPs. In order to confirm the chemical nature of these NPs, the samples were further analyzed by EDS. In the case of organic cotton fibers without functionalization the only chemical elements detected were carbon (C) and oxygen (O), as observed in the spectrum of figure 1, d, which are the main chemical elements that compose the cellulosic chains of cotton fibers [16]. However, in the case of organic cotton fibers functionalized with 1% and 2% of zinc NPs, another chemical element was detected by EDS, zinc, as observed in figure 1, e and f, which unmistakably proves the presence of zinc NPs on the organic cotton fibers and therefore the success of the functionalization process used.

Despite the SEM analysis of cotton fibers functionalized with zinc NPs already suggest a greater incorporation of NPs in the fibers functionalized with 2% of zinc NPs (figure 1, c), a quantitative analysis of these fibers was also performed in order to determine the real zinc concentration. By AAS, it was determined that the concentration of zinc in cotton fibers functionalized with 1% and 2% of zinc NPs suspension was, respectively, 4300 ppm and 6200 ppm, which confirms the qualitative analysis previously performed through SEM images.

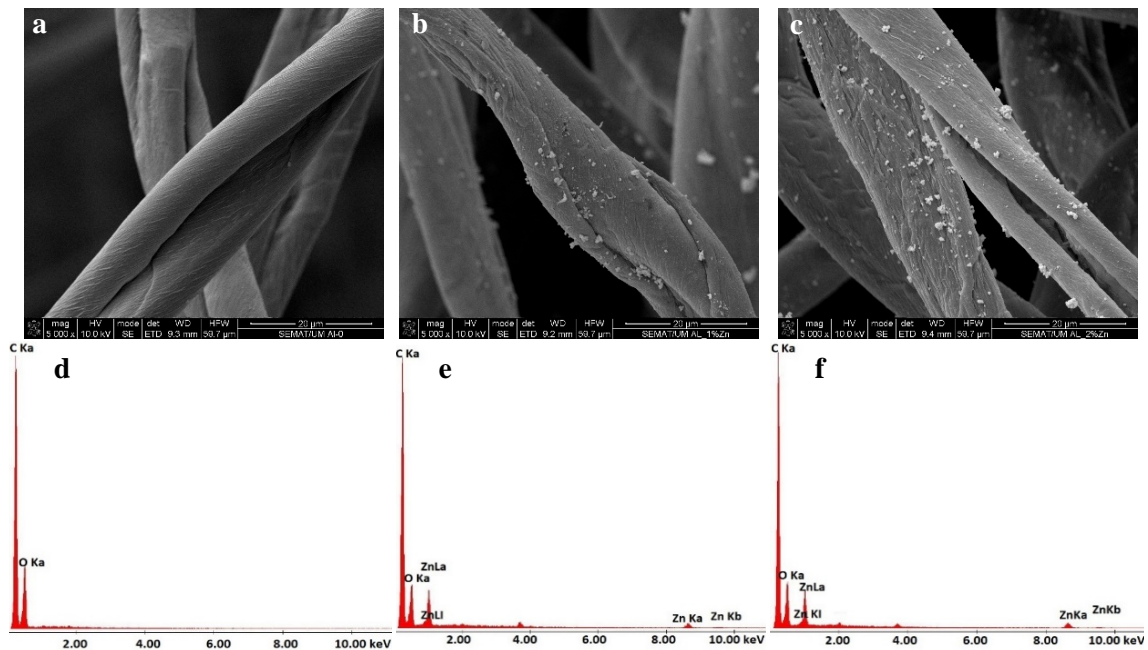


Figure 1. SEM images and EDS spectra of organic cotton fibers: a, d - without functionalization; b, e - functionalized with 1% of zinc NPs suspension; c, f - functionalized with 2% of zinc NPs suspension

Following these results, from organic cotton fibers functionalized with 2% of zinc NPs suspension, a yarn was spun (CO_Zn) and their properties compared with an equal, but without the alkaline pretreatment and the functionalization with zinc NPs (CO_0). As presented in table 1, regarding the structural properties, both yarns under study showed a similar linear density and twist, which sustains any comparison in further analysis. Thus, comparing the mechanical properties of the two yarns, where it was evaluated the tensile strength and the tensile loop strength of the yarns, some differences in the obtained values were verified. Based on the tenacity and maximum elongation values obtained in both tests, which were the same, it was observed an increase of these values in 24% and 10%, respectively, from CO_0 yarn to CO_Zn yarn. This increase observed mainly in the tenacity value could be related with the methodology applied on cotton fibers, namely the alkaline pretreatment and the zinc NPs incorporation. Based on the literature, it is proved that the alkaline pretreatment of cotton fibers allows to improve, among other properties, the tensile strength of the fibers since the waxes and pectins are removed, increasing the inter-fiber friction and therefore, their tensile strength [17,18]. In addition, the incorporation of zinc NPs and their interaction with cellulose chains of cotton fibers could also be related with an increase in fibers cohesion contributing too for the production of a mechanically stronger cotton-based yarn.

Regarding the moisture management properties of the yarns under study, it was observed a similar vertical wicking behavior for both yarns but, in terms of water retention capacity (S_w) it was observed a decrease of 35% from CO_0 yarn to CO_Zn yarn. This reduction in water retention capacity could be related mainly with the interaction between zinc NPs and the hydroxyl groups present in cellulose chains of cotton fibers, which later leads to a decrease in the hydroxyl groups available to interact with other molecules, such as water molecules. Since water molecules have fewer hydroxyl groups to bond, less amount of water will be retained in the cotton fibers and therefore the S_w will be lower.

Thereby, the alkaline pretreatment of organic cotton fibers followed by their functionalization with zinc NPs allowed to develop a yarn (CO_Zn) with higher tensile properties and better moisture management properties, such as a lower water retention capacity and similar vertical wicking behavior, when compared to yarn CO_0.

Table 1. Structural, mechanical and moisture management properties of organic cotton yarns without (CO_0) and with zinc NPs (CO_Zn).

Samples	Linear density (tex)	Twist (turns/m)	Tenacity (N/tex)	Max. Elongation (mm)	Vertical wicking (cm)	S_w (%)
CO_0	25 (± 0.2)	868 (± 14)	0.13 (± 0.005)	29.0 (± 1.0)	10 (± 0.3)	725
CO_Zn	26 (± 0.5)	765 (± 37)	0.17 (± 0.01)	32.3 (± 1.2)	11 (± 1.8)	471

Using the yarns under study, two single jersey knit samples, with a loop length of 0.38 cm and a mass per unit area of 160 g/m², were further produced and their mechanical, moisture management and antibacterial properties were also evaluated, being summarized in table 2 and table 3, respectively.

Table 2. Mechanical and moisture management properties of jersey knit samples produced from the CO_0 and CO_Zn yarn.

Samples	Breaking force (N)		Elongation (mm)		Friction coefficient		Air permeability (L/m ² /s)	WER (%)
	Wale direction	Course direction	Wale direction	Course direction	μ static	μ kinetic		
CO_0	219.4 (± 9.7)	147.4 (± 3.5)	90.9 (± 1.8)	149.0 (± 13.2)	0.27 (± 0.01)	0.23 (± 0.01)	1002 (± 70)	36
CO_Zn	203.9 (± 2.7)	170.8 (± 2.6)	76.0 (± 13.8)	137.7 (± 7.1)	0.28 (± 0.02)	0.23 (± 0.01)	1393 (± 5)	57

Table 3. Antibacterial activity values of jersey knit samples produced from CO_0, CO_Zn and SmartcelTM Sensitive yarns against *Staphylococcus Aureus* and *Klebsiella Pneumoniae*.

Samples	Antibacterial activity value (A)	
	<i>Staphylococcus Aureus</i> (ATCC 6538)	<i>Klebsiella Pneumoniae</i> (ATCC 4352)
CO_0	-0.604	0.075
CO_Zn	3.882	6.290
Smartcel TM Sensitive	4.065	5.668

Regarding the tensile properties of the two knit samples under study, presented in table 2, it was observed, in both cases, that the breaking force was higher in wale direction and the elongation was higher in the course direction, being this behavior characteristic of a single jersey [19]. In general, the yarn used for the production of both knit samples had no significant influence on their final tensile properties, having only been observed a slight increase of the breaking force in course direction in 13%, when CO_Zn yarn was used. Another mechanical property evaluated was the friction coefficient, both static and kinetic, an important property to assess when the goal is to use the textiles under study in direct contact with human skin. Based on the obtained values, it was observed that the static and kinetic friction coefficient was the same for both knit samples under study, which suggests that the methodology applied on cotton fibers to incorporate zinc NPs didn't change the friction coefficient of the knitted structure. Therefore, the friction on the human skin will be the same using a single jersey produced from a simple organic cotton yarn or an organic cotton yarn functionalized with zinc NPs, using the methodology presented in this work.

Contrarily to the mechanical properties, in the case of the moisture management properties it was observed an influence of the type of yarn used on the air permeability and

water evaporating rate (*WER*) values obtained for the knit samples under study. Thus, the single jersey produced from yarn CO_Zn, presented an air permeability and a water evaporating ratio, 28% and 37% higher than the single jersey produced from the yarn CO_0. This result shows that the use of CO_Zn yarn allows to produce a more comfortable single jersey than the one produced from CO_0, and that not only is more breathable, but also has the capacity to evaporate moisture more rapidly, being these results in agreement with the properties obtained for the respective yarns. Since the methodology applied to incorporate zinc NPs into cotton fibers has led to a decrease in water retention capacity of the resultant yarn, it is expected that the knit sample shows more greater ease in releasing water as there are fewer hydroxyl groups available to retain water molecules. This makes water to evaporate more quickly, which translates in a higher *WER* value and a higher drying capacity by the knit sample, giving a dry feeling to the user.

Since the main goal with the incorporation of zinc NPs into cotton fibers is to produce an antimicrobial yarn to be further used for the production of antimicrobial fibrous structures, following this work, the antibacterial activity of the two jersey knit samples, produced from CO_0 and CO_Zn yarns was assessed against a gram-positive (*Staphylococcus Aureus*) and gram-negative (*Klebsiella Pneumoniae*) bacteria according to ISO 20743:2013 standard, being the results compared to the ones from a jersey knit sample produced from a commercially antibacterial fiber, *Smartcell™ Sensitive*.

The antibacterial activity values presented in table 3 showed that the jersey knit sample produced from CO_0 yarn, presented a null antibacterial activity for both bacteria, since the *A* value is lower than 2. However, in the case of the jersey knit sample produced from Co_Zn yarn, the *A* value is, respectively, 3.882 and 6.290, for both *Staphylococcus Aureus* and *Klebsiella Pneumoniae*. Based on the classification system of ISO 20743:2013 standard, this jersey knit sample is classified as having strong antibacterial activity for both gram-positive and gram-negative bacteria, revealing the excellent antibacterial properties of zinc NPs. In this case, the antibacterial activity of the single jersey produced from CO_Zn yarn, despite strong for both bacteria, was more pronounced on the gram-negative bacteria instead of the gram-positive bacteria, being the difference between the *A* values around 38%. Furthermore, when compared with the *A* values obtained for *Smartcell™ Sensitive* knit sample, it was concluded that the antibacterial activity for both bacteria were the same in both cases, have been recorded a difference between the *A* value of 5% and 10% for *Staphylococcus Aureus* and *Klebsiella Pneumoniae*, respectively, which indicates that the CO_Zn yarn as a great commercialization potential in terms of antibacterial properties.

In this context, based on the results obtained in this study it is possible to conclude that the methodology applied to incorporate zinc NPs into organic cotton fibers, allowed to develop a mechanically stronger yarn with lower water retention capacity, which ultimately led to the production of a single jersey knit sample with mechanical properties similar to the conventional organic cotton single jersey, but more breathable, with a greater dry feeling and above all with strong antibacterial activity against both gram-negative and gram-positive bacteria. In order to assess the durability of the properties obtained, as future work, the main goal is to determine the washing resistance of the zinc-functionalized jersey knit sample.

5. CONCLUSIONS

In this work, it was proposed the functionalization of organic raw cotton fibers with zinc NPs, previously treated with NaOH solution, by exhaustion method for the production of a multifunctional cotton-based yarn. The applied method allowed a homogeneous distribution of NPs into organic cotton fibers incorporating 6200 ppm of zinc, which were

further used to spin a yarn and consequently to produce a single jersey knit sample. Based on the properties obtained for both yarn and single jersey knit sample incorporating zinc NPs, it was concluded that the methodology used improved the mechanical and moisture management properties, achieving a yarn tenacity 24% higher and a water retention capacity 35% lower than the yarn without any pretreatment or functionalization, and subsequently a knit sample 28% more breathable and with a water evaporating ratio 37%. Moreover, the incorporation of zinc NPs into organic cotton fibers also allowed to produce a jersey knit sample with an antibacterial activity value of 3.882 and 6.290 against both *Staphylococcus Aureus* and *Klebsiella Pneumoniae*, being therefore classified as a knit sample with strong antibacterial activity, the same antibacterial behavior as *SmartcelTM Sensitive*, a commercially antibacterial fiber.

In this sense, the development of this new cotton-based yarn pretreated with NaOH and incorporating zinc NPs allowed the production of multifunctional fibrous structures with strong antibacterial activity without comprising their mechanical and comfort properties, presenting therefore potentiality to be used for the production of effective PPEs.

ACKNOWLEDGEMENTS

The authors gratefully acknowledge the funding by P2020, under Individual Project SI I&DT POCI-01-02B7-FEDER-057041, entitled as “COV_YARN – Development of active PPE based on multifunctional yarns”.

REFERENCES

- [1] Shirvanimoghaddam, K., Akbari, M.K., Yadav, R., Al-Tamimi, A.K., Naebe, M., *Fight against COVID-19: The case of antiviral surfaces*, In: APL Mater., 2021, 9, 3, 1-14
- [2] Militky, J., et al., *A review of impact of textile research on protective face masks*, In: Materials (Basel), 2021, 14, 8, 1-16, <https://doi.org/10.3390/ma14081937>
- [3] Karim, N., et al., *Sustainable personal protective clothing for healthcare applications: A review*, In: ACS Nano, 2020, 14, 10, 12313-12340
- [4] Shadpour Mallakpour, C.M.H., et al., *The latest strategies in the fight against the COVID-19 pandemic: the role of metal and metal oxide nanoparticles*, In: New J. Chem., 2021, 45, 14, 6167-6179
- [5] Arputharaj, A., Prasad, V., Saxena, S., Nadanathangam, V., Shukla, S.R., *Ionic liquid mediated application of nano zinc oxide on cotton fabric for multi-functional properties*, In: J. Text. Inst., 2017, 108, 7, 1189-1197, <https://doi.org/10.1080/00405000.2016.1222984>
- [6] Hardin, I.R., Kim, Y., *Nanotechnology for antimicrobial textiles*, Elsevier Ltd, 2016
- [7] Borda D'Água, R., et al., *Efficient coverage of ZnO nanoparticles on cotton fibres for antibacterial finishing using a rapid and low cost: In situ synthesis*, In: New J. Chem., 2018, 42, 2, 1052-1060
- [8] da Silva, B.L., et al., *Relationship between structure and antimicrobial activity of zinc oxide nanoparticles: An overview*, In: Int. J. Nanomedicine, 2019, 14, 9395-9410
- [9] Zhou, J., Hu, Z., Zabihi, F., Chen, Z., Zhu, M., *Progress and Perspective of Antiviral Protective Material*, In: Adv. Fiber Mater., 2020, 2, 3, 123-139
- [10] Kokol, V., Vivod, V., Peršin, Z., Čolić, M., Kolar, M., *Antimicrobial properties of viscose yarns ring-spun with integrated amino-functionalized nanocellulose*, In: Cellulose, 2021, 28, 10, 6545-6565
- [11] Granados, A., Pleixats, R., Vallribera, A., *Recent advances on antimicrobial and anti-inflammatory cotton fabrics containing nanostructures*, In: Molecules, 2021
- [12] Emam, H.E., *Generic strategies for functionalization of cellulosic textiles with metal salts*, In: Cellulose, 2019, 26, 3, 1431-1447
- [13] Fangueiro, R., Filgueiras, A., Soutinho, F., Meidi, X., *Wicking Behavior and Drying Capability of Functional Knitted Fabrics*, In: Text. Res. J., 2010, 80, 15, 1522-1530, <https://doi.org/>

10.1177/0040517510361796

[14] Silva, L.F., Lima, M., Seabra, E., Vasconcelos, R., Martins, D., *Study, Design and Development of a New Add-on Function for the FRICTORQ® – Friction Test Instrument*

[15] Grancarić, A.M., Ristić, N., Tarbuk, A., Ristić, I., *Electrokinetic phenomena of cationised cotton and its dyeability with reactive dyes*, In: *Fibres Text. East. Eur.*, 2013, 21, 6, 106-110

[16] Ibrahim, N.A., Eid, B.M., El-Aziz, E.A., Abou Elmaaty, T.M., Ramadan, S.M., *Multifunctional cellulose-containing fabrics using modified finishing formulations*, In: *RSC Adv.*, 2017, 7, 53, 33219-33230

[17] Jordanov, I., Mangovska, B., Tavčer, P.F., *Mechanical and structural properties of mercerized cotton yarns, bio-scoured with pectinases*, In: *Tekstil*, 2010, 59, 10, 439-455

[18] Rippon, J.A., Evans, D.J., *Improving the properties of natural fibres by chemical treatments*, Woodhead Publishing Limited, 2012

[19] Sitotaw, D.B., Adamu, B.F., *Tensile Properties of Single Jersey and 1×1 Rib Knitted Fabrics Made from 100% Cotton and Cotton/Lycra Yarns*, In: *J. Eng. (United Kingdom)*, 2017



THE EFFECT OF PLASMA TREATMENT ON THE PRINTABILITY OF POLYESTER FABRIC USING COCHINEAL NATURAL DYE

DOI: 10.35530/TT.2021.49

M. Khajeh Mehrizi*, A. Haji, Z. Shahi, M. Golshan

Department of Textile Engineering, Yazd University, Yazd, Iran
(E-mail: mkhajeh@yazd.ac.ir, ahaji@yazd.ac.ir, zahrashahi6284@yahoo.com, mrs.golshan82@gmail.com)

Abstract: Use of synthetic dyes for dyeing of textile fabrics is most problematic environmental concerned for textile industry. The demand of natural colourants for the dyeing of textile fabrics has been increasing. Thus, sustainable novel technologies for textile dyeing are needed that utilize improved colour strength and enhanced performance characteristics of the fabric. This study attempts to highlight the possibility of using cochineal natural dye in the printing of polyester fabrics after surface modification by O₂/Ar plasma treatment. The colour strength, air permeability, crease recovery angle of printed fabrics, colour fastness to rubbing, washing and light, were also studied. The surfaces of untreated and plasma-treated polyester fabrics were analysed by SEM to compare the morphological changes. Surface roughness and cracks were indicated after the plasma pre-treatment. The results indicated that plasma treatment could improve the printability of polyester fabric compared with untreated samples, with enhanced the adhesion and penetration of printing paste to the surface. The air permeability of printed fabrics has decreased, while the angle of crease recovery has increased. The fastness properties of printed samples were found suitable to very good.

Keywords: cochineal, colour fastness, plasma treatment, polyester fabric, printing

1. INTRODUCTION

Natural dyes or colourants are non-toxic and bio-degradable materials and are actually safe for applications in several scopes. Revitalized attention in the use of natural dyes in textile colouration has been increasing [1]. Nowadays, it is known that metal mordants may impose hazards to human beings, animals and the environment. So, various studies have been completed to reduce the use of metal mordants in natural dyeing procedures or replace them with more ecologically friendly choices.

Cochineal is a type of natural dye which is obtained from an insect of the same name that is mostly found in cacti of Mexico and South America. It is scraped off, dried and crushed to make the cochineal extract that produces red or purple colour dyes. Screen printing gained popularity because it is economical and easy to apply. Also, it uses less dye and achieves the same product appeal for a lower cost than weaving a design [2].

Plasma is described as the fourth condition of a substance having the highest energy. Furthermore, plasma is an ionized gas that contains electrons, ions, neutral atoms or molecules. In the textile industry, cold plasma is used for the modification of textile materials. In addition, plasma treatment is considered a dry, environmental and eco-friendly process in the textile industry so as not to require water and chemicals. Plasma treatment causes physical

and chemical modification in textile materials. In the textile dyeing industry, the use of water, energy and chemical at considerable rate creates problems for the environment. It has been widely used in many applications of textile area for targeted surface modifications, mainly include the improving of dyeability, printability, wettability, antimicrobial properties, etc [3-8].

In this paper, we have studied and compared the effect of plasma on the printing of polyester fabrics with cochineal natural dyes. Colour yields, colour fastness values, wrinkle-resistance properties, air permeability and surface topographies of printed samples was investigated.

2. EXPERIMENTAL

2.1. Materials

100% weave polyester fabrics was used for screen printing. Also, cochineal was used as natural dyes. Polyester fabrics were soaped with 5g/l non-ionic detergent and L:R= 1:40 for 30 min at 40°C. Pre-treatment of the sample was used with copper sulphate (5%) as a mordant for 30 min at 80°C.

2.2. Plasma treatment

The fabrics were prepared for O₂/Ar vacuum plasma treatments (Plasma DEJ Model BF60) under powers of 100 W for a time of 15 min.

2.3. Preparation of the printing paste

After the treatment with plasma, the fabric was printed according to table 1.

Table 1. Composition of the printing paste

Consumable materials	Amount of consumable materials (g)
Natural dye	50
Sodium alginate	600
Lodigol	60
Chitosan	100
Sodium carbonate	50
Urea	100
Softener	40
Balance	x
Total	1000

After treatment of printed fabric, samples were dried at 100° C for 5 min and fixation of all samples were done by steaming for 180°C for 5 min. The effect of plasma treatment time (5, 10 and 15 minutes), concentrations of copper sulphate (1%, 3% and 5%) and fixation temperatures (160, 170 and 180°C) analysed and optimized by using Response Surface Methodology (RSM).

A spectrophotometer (X-rite SP 62) was utilized to measure the colour components of the printed specimens under a D65 light source and 10° observer angle. The surface morphology of the printed polyester fabrics was studied under a scanning electron microscope (SEM Phenom ProX). In order to analyse the air permeability, the BS9237-1995 standard was used. The rubbing fastness was measured by the AATCC-116 standard. The light and wash fastness were also evaluated by BS EN 20105 and ISO105 C02 1994 (E), respectively. The wrinkle-recovery angle was tested according to the AATCC test method IS 4681-1968.

3. RESULTS AND DISCUSSION

3.1. Colour strength and fastness properties of printed samples

The colour fastness of the printed samples is in table 2. It can be seen from the K/S values that; plasma treatment has been improved the printability of fabrics. Plasma treatment increases the wettability of fabric which raises penetration of any material containing in printing paste [9].

The critical parameter for the evaluation of natural dyes used in printing is the fastness of prints [10]. Colour fastness showed higher values when compared with untreated which can be due to the higher K/S values of plasma treated fabrics.

Table 2. Colour strength and colour fastness of printed samples

Sample		Colour strength (K/S)	Wash Fastness		Light Fastness	Rubbing Fastness	
			Staining on cotton	Colour change		Dry	Wet
Untreated		0.23	3	3	5	3-4	3
Plasma-treated and printed treated	K/S_{max} : 15 min plasma, 5% copper sulphate, 180° C fixation	1.54	5	4	7	5	4-5
	K/S_{min} : 5 min plasma, 5% copper sulphate, 180° C fixation	0.61	5	3-4	5-6	4	4

3.2. Air permeability of printed samples

As shown in table 3, the air permeability of the printed samples decreased. The printing process reduce the amount voids and pores on the surface of fabrics, which led to a decrease in the air permeability [11]. Also, the fabric thickness has a significant effect on air permeability. The plasma treatment and create roughness on the fibre surface, increases the fabric thickness and decreases the air permeability of the printed samples [12].

Table 3. Air permeability of printed samples

Sample	Air permeability values (mm/s)	
Untreated	65	
Plasma-treated	56	
Plasma-treated and printed	K/S_{max}	41
	K/S_{min}	50

3.3. Crease recovery of the printed samples

According to table 4, the printed samples have a greater crease recovery angle and greater resistance of against bending compared to the raw samples. After printing, the crease recovery angle increased due to the structure relaxation, which the most strained segments of the molecules disappear and turn into moderately strained segments [13]. Also, plasma pre-treatment improved the wrinkle resistance of the cotton fabrics.

Table 4. Crease recovery angle of printed samples

Sample	Crease recovery angle (°)
Untreated	97
Plasma-treated	108

Plasma-treated and printed	K/S_{max}	125
	K/S_{min}	115

3.4. Surface morphology

As can be seen from figure 1, plasma treatments had an etching effect on the fibre surface. Surface roughness, cracks and voids were showed after the plasma pre-treatment due to the bombardment of the surface of the fibres with ions and free radicals [14]. Printing on fabrics formed thin homogeneous and relatively well dispersed films on the surface and between the fibre edges containing the natural dye and other material in printing paste [15].

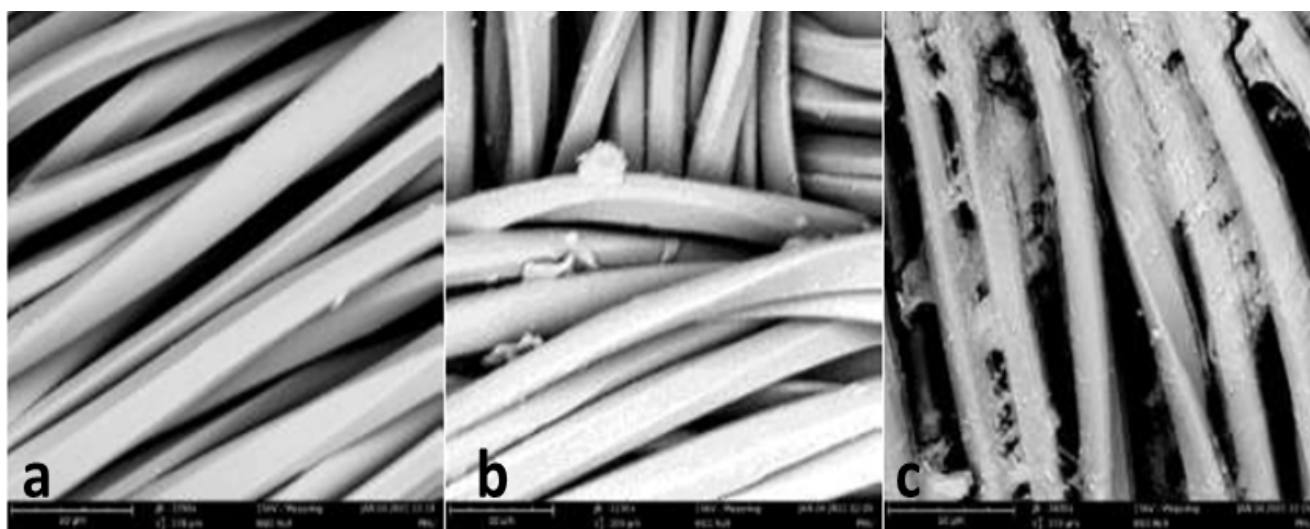


Figure 1. SEM images of: a – untreated; b - plasma-treated fabric; c - plasma-treated and printed fabric

4. CONCLUSIONS

It is evident from the results that polyester fabric can be successfully screen printed with cochineal natural dye. Plasma pre-treatment for the modification of polyester fabrics, which is an environmentally friendly dry process, has high industrial application potential. Plasma treatment had a positive effect on the printability of polyester fabrics and is an effective method for improving the colour fastness properties and wrinkle-resistance.

REFERENCES

- [1] Ashrafi, N., Gharanjig, K., Hosseinnezhad, M., Khajeh Mehrizi, M., Imani, H., Razani, N., *Dyeing Properties and Colour Fabrics Using Natural Dye and Mordant*, In: Prog. Colour Colourants Coat., 2018, 11, 79-83.
- [2] Dasgupta, S., Ghosh, S., *Evaluation of screen printing using cochineal natural dye*, In: Trends. Text. Eng. Fashion Tech., 2, 5, 2018, 217-222
- [3] Molakarimi, M., Khajeh Mehrizi, M., Haji, A., *Effect of plasma treatment and grafting of β -cyclodextrin on colour properties of wool fabric dyed with Shrimp shell extract*, In: J Tex Ins., 2016, 107, 1314-1321
- [4] Zhang, Ch., Fang, K., *Surface modification of polyester fabrics for inkjet printing with atmospheric-pressure air/Ar plasma*, In: Surface. Coat. Tech., 2009, 203, 2058-2063
- [5] Sajed, T., Haji, A., Khajeh Mehrizi, M., Boroumand, M.N., *Modification of wool protein fiber with plasma and dendrimer: Effects on dyeing with cochineal*, In: Inter. J. Bio. Macro., 2018, 107, 642-653

- [6] Labay, C., Canal, J.M., Canal, C., *Relevance of surface modification of polyamide 6.6 fibers by air plasma treatment on the release of caffeine*, In: Plasma Proc. Polym., 2012, 9, 2, 165-173
- [7] Canbolata, S., Kilinca, M., Kutb, D., *The Investigation of the Effects of Plasma Treatment on the Dyeing*, In: Procedia - Social and Behavioral Sci., 2015, 195, 2143-2151
- [8] Haji, A., Khajeh Mehrizi, M., Sharifzadeh, J., *Dyeing of wool with aqueous extract of cotton pods improved by plasma treatment and chitosan: optimization using response surface methodology*, In: Fib. Poly., 2016, 17, 9, 1480-1488
- [9] Özdoğan, E., Demir, A., Aylin karahan, H., Ayhan, H., Seventekin, N., *Effects of atmospheric plasma on the printability of wool fabrics*, In: Tekstil Ve Konfeksiyon., 2009, 19, 2, 123-127
- [10] Babel, S., Gupta, R., Mogra, D., *Eco friendly screen printing using natural and indigenous thickener- mango kernel and cassia tora gum*, In: J. Env. Sci. Computer Eng. Tech., 2015, 4, 2, 417-423
- [11] Abdelslam, Sh.H., Saleh, S.M., El-Thalouth, J.I.A., Isail, E.E., *Ultraviolet Protection of Cotton Fabrics and Their Blends Using Natural Plant Extracts by Printing Style*, In: Egyptian. J. Chem., 2020, 63, 9, 3481-3489
- [12] Prakash, C., Ramakrishnan, G., Chinnadurai, S., Vignesh, S., Senthilkumar, M., *Effect of plasma treatment on air and water-vapor permeability of bamboo knitted fabric*, In: Int J Thermophys, 2013, 34, 2173-2182
- [13] Arora, Sh., *Effect of printing on physical properties of muga silk fabric with reactive and acid dyes*, In: Int. J. Home. Sci., 2016, 2, 3, 20-23
- [14] Elnagar, Kh., Abou elmaaty, T., Raouf, S., *Dyeing of polyester and polyamide synthetic fabrics with natural dyes using ecofriendly technique*, In: J. Tex., 2014, 1-8.
- [15] Jafari, H., Khajeh Mehrizi, M., Fattahi, S., *The effect of Inorganic Nanoparticles on Camouflage Properties of Cotton/Polyester Fabrics*, In: Prog. Colour Colourants Coat., 2016, 9, 29-40



BEHAVIOUR ASSESSMENT OF TRIDIMENSIONAL MULTILAYER FIBROUS STRUCTURES AS RESPIRATORY PROTECTION SUBSTRATES

DOI: 10.35530/TT.2021.39

C. Silva^{1*}, T. Sousa², J. Bessa¹, F. Cunha¹, M. Costa³, A. Roças³, R. Figueiro⁴

¹Center for Textile Science and Technology (2C2T), University of Minho, Braga, Portugal (E-mail: cristinasilva@fibrenamics.com, joãobessa@fibrenamics.com)

²Pixartidea, Praça Conde de Agrolongo, Braga, Portugal (E-mail: tiagosousa@pixartidea.com)

³LMA - Leandro Manuel Araújo, S.A., Rebordões - Santo Tirso, Porto, Portugal (E-mail: marta.costa@lma.pt, ana.rocas@lma.pt)

⁴Department of Mechanical Engineering, University of Minho, Guimarães, Portugal (E-mail: rfigueiro@dem.uminho.pt)

Abstract: Despite the growing appearance of new solutions for social masks, there are still few aimed for the use by professionals in frequent contact with the public, since depending on the of the functions they perform, still have special needs regarding thermophysiological comfort, high protection level and reusability, such as firefighters and police officers. Aiming at the development of a multilayer filtration system combining three-dimensional and planar fibrous structures, the present study intends to verify the feasibility of applying warp-knit spacers as diffuser filters for nano and micro particles. Therefore, three different spacer structures performance was studied, and then combined with planar knit structures to enhance the comfort characteristics and its bacterial filtration efficiency (BFE). The diffusion filtration performance of the samples, due to the particle size, it was found a direct relation between the outer layer density and porosity with its filtration capacity of microparticles. Moreover, the increase in the spacer thickness revealed more problems diffusing water vapor molecules. To achieve the standard requirements, the samples Techno_1 and 2 were developed and tested. The addition of a new fibrous structure increased substantially the filtration efficiency without damaging the comfort characteristics of the Spacers. Considering the BFE standard tests for facemask certification, despite it was possible to achieve filtration rates above 70% for the samples Techno_1 and 2. In addition, its washability and performance durability were tested and stated as viable to be applied as a social facemask with level III of protection for at least 25 washing cycles, despite having noticed a decrease in the filtration efficiency, in both samples, in the order of 10%, due to the unbalance of mechanical properties of the fibrous structures in the multilayer systems.

Keywords: breathability, filtration efficiency, mask design, multilayer structures, three-dimensional knitting

1. INTRODUCTION

The COVID-19 pandemic has led to the creation and adoption of a set of preventive measures to contain the spread of the disease. The mandatory use of masks emerges as an indispensable measure for the mitigation of community transmission. Considering that the size of these droplets alters the method of infection, droplets with more than 20 μm will fall onto objects easier than smaller droplets due to gravity, while droplets with 5 to 10 μm will evaporate mid-air allowing for airborne transmission [1].

A study by Eunice Y.C. Shiu et al. revealed that droplets of 1 μm were capable of staying in the airborne for more than 12 h with strong coughs or sneezes capable of sending these particles over 6 meters [2]. Therefore, the effectiveness of a face mask or a respirator is fundamental by two significant factors, namely the filtration efficiency that measures the microparticles filtering performance, as well as the fit that measures how well the mask or respirator prevents the leakage around the facepiece [3].

There are many kinds of medical textiles, such as woven, non-woven textiles, braided or knitted textiles, that may be applied on air filtration systems being disposable most of the times [4]. Knitted fabrics form a small part of the medical textiles, but are greatly applied in high-tech medical textiles, ensuring good structural stability, comfort, and easy maintenance. These structures are also popular due to their loose and flexible structure, higher porosity, and better forming technology [5]. Despite the microscale structure, by manipulating the composition and structure of wires, it is already possible to ensure required filtration percentages for protection levels 2 and 3, greater than 90% and 70%, respectively. The major mechanisms involved in particle removal by fibrous materials include gravity settling, inertial impaction, diffusion and electrostatic attraction [6].

Considering the low weight of the biological agents and aerosols, gravity settling is not possible to be applied, and inertial impaction would not be an efficient approach due to the imbalance between the size of fibres and molecules that it is intended to filter, otherwise a much denser fibrous structure would be needed to perform the filtration [7]. Therefore, for the intended application, it would be necessary to consider the diffusion patterns in the textile structures and looking for fibrous materials that would be able to create electrostatic charges to attract the micro and nanoparticles dispersed on the air that is breathed. Diffusion in fibrous materials media can be only found for very small particles such as viruses, being that those particles move randomly within the air stream due to Brownian molecular motion. Accordingly, to the study of K. Ardon-Dryer et al. [8], the lower the airflow between the filter structure, the better the filtration efficiency it has, once the particle size velocity reduces, than the rate of diffusion becomes more noticeable. Through this concept, the particle residence period is increased once the probability of collision between particle and filter media increases as well. Thus, the development of fibrous textile patterns capable of retaining particles larger than 1 μm in diameter, and decreasing the air flow between layers, are important to ensure greater filtering capacity [8].

To create a complex fibrous structure to form a barrier capable of creating an air flow slowdown zone, promoting the filtration of small particles by diffusion concepts, and without increasing the density of the structure, emerges the development of a spacer fibrous structures. Spacer fabrics are an advanced three-dimensional textile structure consisting of two separate outer fibrous layers that are joined together but kept apart by spacer yarns. These fibrous structures can be achieved by warp knitting, weft knitting, weaving, non-woven or even braiding technologies, reaching different outputs. However, knitted spacer structures made of monofilaments have been studied and applied in medical care and apparel as an outer layer due to its air permeability and appropriate compressibility. It has been found and stated in the work of Y. Liu et al. [9], that the air resistance of such structures increases with the increase in the spacer yarn distance. It was also observed that structures with higher loop densities on the outer layer resulted in a poor air permeability of the three-dimensional structures [9,10]. In this sense, considering the available literature and taking advantage of the manipulation of knits and their characteristics, combining them with three-dimensional spacer fibrous structures and their properties of permeability and air diffusion, with the choice of advanced technical materials, this study is intended to develop a new generation of filtering fibrous

systems. The main goal in this development consists in the use of them to produce protective masks with improved comfort and evaluating the potential of multilayer gradient performance. The overall multi-layered masks moisture management, breathability, and filtration performance were reviewed, and compared with the required parameters standardized by ISO 14683:2020.

2. MATERIALS AND METHODS

The performance study was carried out with 5 different multilayer three-dimensional knitted structures, shown in table 1. The samples coded as Acti_1, 2, and 3 refer to the study of the pattern of the three-dimensional warp-knit spacer, in terms of porosity and areal weight, as shown in figure 1. All these spacer structures vary in yarn density on the outer layer in ascending order from Acti_1 to Acti_3. Consequently, the thickness of the spacers varied slightly in the set of samples presented, namely: 2.2 mm for the Acti_1; 2.4 mm for Acti_2; and 1.7 mm for Acti_3 sample. The variation of parameters intends to analyse the balance of resistance to the passage of air, and the diffusion capacity of the structure. This balance may allow a fibrous structure to be able to filter particles of different sizes effectively, as described on the literature [7,9].



Figure 1. Representative images of the warp-knit spacer surface and connection structures

On the other hand, the structures coded as Techno 1 and 2 have the combination of a denser circular knit structure with comfort jersey layer, being added the spacer of Acti_3 for the Techno_1 Mask. The layers of each sample fibrous system were sewed together and then evaluated its properties.

The samples performance was evaluated through the structural and moisture management properties with water vapor permeability, air permeability, bacterial filtration efficiency (BFE), and friction coefficient, according to the following tests:

- Water Vapor Permeability (WVP) - This test was carried out following the BS 7209: 1990 standard under isothermal conditions, aiming to determine the water dissipation in the form of steam using Shirley Water Vapor Permeability Tester - SDL International [11];
- Air Permeability - The permeability of the fibrous structures was performed by quantification of the rate of airflow through a 20 cm² area passage at a given pressures of 40, 100, and 200 Pa for over 1 minute, using TEXTTEST FX 3300 air permeability instrument according to the NP EN ISO 9237 – 2003 standard [12];
- Moisture Release - This experimental procedure is based on the methodology presented in R. Fangueiro et al. [13], where it is intended to evaluate the ability to release moisture from structures that will be in open space, thus considering a

temperature of $20\pm 1^\circ\text{C}$. This method consists of releasing 30% of water in relation to the weight of the dry sample and evaluating the loss mass after 30 minutes. Once this study was focused on the development of a new fibrous filtration system for respiratory social masks, the air temperature applied to the sample was fixed at $34\pm 1^\circ\text{C}$, being more approximated to the temperature of exhaled air during respirations. During the test the maximum relative humidity inside the thermal chamber was 80%;

- Friction Coefficient - This analysis was performed based on the work by Lima, M et al. [14], consisting of place a sample on the base of the equipment. After, a sensor, which is placed on the sample, performs rotational movement on itself, to assess the friction that exists between the sensor and the sample, thus calculating the friction coefficient between samples [14];
- Bacterial Filtration Efficiency (BFE) - This test is used to measure the BFE of materials for respiratory protection devices, using *Staphylococcus aureus* as a bacterial aerosol, which is applied to the surface of the sample, measuring the residual concentration on the sample. This is a quantitative method that allows the determination of filtration efficiency up to a maximum of 99.9% [12].

Table 1. Sample description summary of structural composition

Sample Code		Acti_1	Acti_2	Acti_3	Techno_1	Techno_2
Layer_1	Composition	100%PES	100%PES	100%PES	100%PES	94%PES+6%EA
	Structure	3D warp knit	3D warp knit	3D warp knit	3D warp knit	Circular knit
	Areal Weight (g/m^2)	$150\pm 5\%$	$255\pm 5\%$	$300\pm 5\%$	$300\pm 5\%$	$300\pm 5\%$
Layer_2	Composition	58%PES+42%PP	58%PES+42%PP	58%PES+42%PP	94%PES+6% EA	58%PES+42% PP
	Structure	Circular knit	Circular knit	Circular knit	Circular knit	Circular knit
	Areal Weight (g/m^2)	$130\pm 5\%$	$130\pm 5\%$	$130\pm 5\%$	$300\pm 5\%$	$130\pm 5\%$
Layer_3	Composition				58%PES+42%PP	
	Structure				Circular knit	
	Areal Weight (g/m^2)				$130\pm 5\%$	

The results, described in table 2, were then analysed according to EN 14683:2019 requirements. Subsequently, the samples with better performance regarding comfort and filtration properties, were also characterized between 25 domestic washing and drying cycles accordingly to the methodology of ISO 6330:2012 [15], and evaluated the bacterial filtration efficiency before and after washes. Also, the air permeability was measured according to the differential pressure methodology for respiratory protection devices, described in EN 14683:2020[16], to establish a direct comparison of performance and overall breathability comfort of the face masks materials with protection level II and III, identified in table 3 as SM Level II and SM Level III, respectively.

Table 2. Comfort and filtration efficiency tests result for warp-knit spacers multilayer

Sample code	COF		Air permeability (L/min)			Moisture release (%)	WVP (%)	BFE (%)
	μ static	μ kinetic	40 Pa	100 Pa	200 Pa			
Acti_1	0.25	0.19	16.48	27.80	72.0	84.0	96.0	22.0
Acti_2	0.20	0.15	16.72	28.96	73.0	68.0	93.0	23.0
Acti_3	0.25	0.19	12.70	24.60	70.3	83.0	93.0	30.0

3. RESULTS AND DISCUSSIONS

The study of the tridimensional multilayer performance results is shown in table 2. Analyzing the results, it is possible to observe that all the structures revealed similar friction behavior as expected since the physical comfort layer was the same throughout the multilayer systems, being noticed that the spacer structure does not influence this property. The Acti_2 sample obtained a lower relative friction coefficient in both categories; this may be due to its greater compressibility relative to its greater thickness.

Regarding the air permeability properties, all samples reached values greater than 8l/min at 40 Pa, the lower limit established by the NP EN ISO 9237 – 2003 standard. However, the structures with the spacers with lower density obtained an air flow 2 times higher than the stated minimum, at the same pressure, which may indicate a deficiency on the barrier effect of the outer layer spacer structure. Though this test in the subsequent differential pressures of 100 and 200 Pa, applied in technical textiles, it is possible to note an increase in permeability in all samples. It was not possible to detect any atypical phenomena such as the formation of a vacuum effect, due to unbalance between the densities of the outer layers, as well as the independent spacer meshes that form the multilayer systems. These characteristics are interesting considering the application of these structures in respiratory protection equipment to be utilized in high demand physical stress environments.

On the other hand, regarding water vapor permeability, all the samples reached values greater than 80%, which represents a standard parameter for sport technical textiles, due to the need to act in response to demanding moisture saturation conditions that have been stated to happen in respiratory masks after several hours of use [17]. Consequently, to better understand the moisture management behaviour and drying capability of these complex structures, a moisture release teste was performed. In this test, for technical textiles, it is expected that after 30 minutes, 70% of the absorbed water have evaporated, which was stated for all samples except for Acti_2. It is possible to infer that a spacer with greater thickness have more difficulty in diffusing water molecules. The samples with higher density (Acti_2 and Acti_3), have matched the standard requirements, not showing a direct and clear relation between density and moisture management behaviour as found in traditional knit structures. This characteristic may be due to the air layer formed between the layers, acting as a heat accumulator on the surface of the comfort meshes used, or can be related with the filament composition of spacers, whose materials have low hygroscopicity and hydrophilicity.

Regarding the BFE test, the results fell short especially for the Acti samples. Even though those were samples with high air permeability as referred before, it was expected that the air layer formed by the spacer yarns would have greater influence in reducing the rate of penetration of bacterial aerosol particles, based on the diffusion filtration principles.

Considering these preliminary results and the test parameters considered, it was possible to conclude that, even though the structures were developed considering viruses particles of Covid-19, which particle size varies between 0.02 μ m and 0.5 μ m, the standard

test uses bacterial aerosol droplets with a diameter between 1.0 and 5.0 μm . Therefore, for those particle sizes, the filtration by diffusion is not possible to apply, as seen in figure 3, once the filtration efficiency is a function of the size of the particles and is not dependent on whether they are bioaerosols or inert particles.

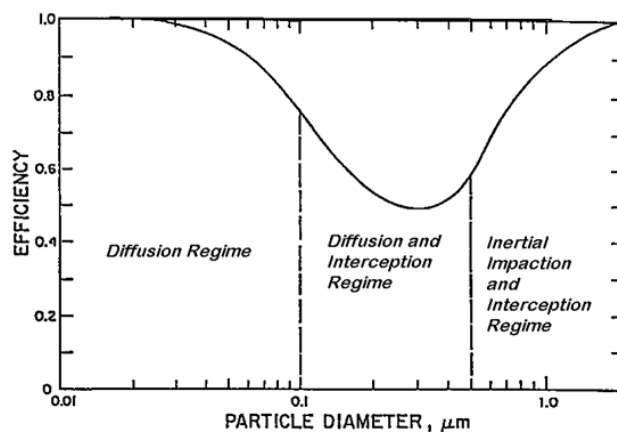


Figure 2. Face mask filter efficiency versus particle diameter

In this sense, regarding the test parameters, the more efficient filtration mechanism is through gravity settling or inertial impaction of the particles with the fibrous structures. These filtration mechanisms are characterized for semipermeable surfaces, high density textiles or fibrous structures with small pores and low porosity. Those characteristics are very difficult to achieve with warp-knit spacers. For that reason, it was decided to use a new filter fibrous layer produced by a circular knit technical polyester and elastane, to reinforce the performance of the sample Acti_3, that achieved the higher bacterial filtration efficiency, thus creating the multilayer system and sample Techno_1. The sample Techno_2 was studied to assess the influence of the warp-knit spacer structure within the multilayer system, whose performance results are presented in table 3.

By the analysis of the friction coefficient, it is possible to verify that the presence of the three-dimensional fibrous structure increases the CoF value, due to the surface irregularities, implied by the high static CoF, relative to the beginning of the rotational movement, which substantially decreases under dynamic conditions. Moreover, the variation for the Techno_2 sample between the two states, is considerably smaller the samples with a spacer layer.

Comparing the air permeability results, at 40 Pa with the ones achieved by the sample Acti_3, it is possible to verify that the introduction of a third layer promotes a subsequential decrease in the air flow for all tested pressures. However, the moisture management properties were maintained stable with the introduction of the third layer, considering the small decrease of the moisture release and water vapour permeability of Techno_1 sample. On the other hand, comparing the influence of the use of 3D warp knit (samples Techno_1 and Techno_2), as expected, with the removal of the spacer structure the multilayer system had a worst performance on moisture diffusion, and more slightly a decrease in the drying capacity.

The new circular planar knit structure developed for Techno sample has lower porosity than the spacer structures, reaching by itself an air permeability of approximately 12 L/min at 40 Pa, and a hydrophobic surface with a water drop contact angle higher than 130°. Once its characteristics cover the empirical requirements for inertial impaction, it was observed, as expected, a substantially increase on the bacterial filtration efficiency on its samples. It's also

possible to conclude that the spacer has an influence on the filtration performance boosting it in almost 5%, without impairing breathability.

Table 3. Comfort and filtration efficiency tests results for advanced multilayer system, with and without warp-knit spacer structure.

Sample code	CoF		Air permeability (l/min)			Moisture release (%)	WVP (%)	BFE (%)
	μ static	μ kinetic	40 Pa	100 Pa	200 Pa			
Techno_1	0.25	0.19	10.80	35.00	88.4	80.7	90.2	88.4
Techno_2	0.19	0.16	12.60	32.70	83.9	78.9	87.8	83.9

After that, it was also performed a washing resistance test for 25 washing and drying cycles to the samples Techno_1 and Techno_2, being analysed the variation on the behavior in the standard social facemask tests (differential pressure and BFE), table 4. In addition to analyse the influence of the washing and drying cycles in the breathability and filtering capacity of the samples, it is also possible to infer problems related to the structural stability of the fibrous structures that make up the multilayer systems.

Regarding breathability, inferred by the differential pressure results in table 4, there aren't observed significant variation on the sample behaviour, both reaching a differential pressure below 40 Pa/cm² for 8l/min, before and after de washing and drying cycles. In contrast, it is noticeable a decrease in filtration efficiency for both samples after the washing cycles, a loss of approximately 12%. Therefore, is possible to assess that one of the common fibrous structures are being affected by the durability test and putting at risk the viability and durability of systems. Still, both samples can be certified and marketed as level III social face masks.

Table 4. Respiratory protection performance evaluation

Sample code	Differential pressure (Pa/cm ²)		BFE (%)	
	0 washing cycles	25 washing cycles	0 washing cycles	25 washing cycles
SM Level II	< 40		> 90.0	
SM Level III	< 40		> 70.0	
Techno_1	< 20.0 ± 1.2	< 20.0 ± 1.2	88.4	78.0
Techno_2	< 20.0 ± 1.2	21.9 ± 1.3	83.9	74.2

4. CONCLUSION

The main objective of this work was to study the behaviour of three-dimensional multilayer fibrous structures as respiratory protection substrates. In this sense, three-dimensional structures were developed. The three-dimensional structures revealed a good performance regarding the breathability within the multilayer structures. The interconnecting yarn layer creates a diffusion layer for air and water vapour, creating a greater distribution of fresh air throughout its extension.

The development of a new compact planar knit revealed capable to enhance bacterial filtration without impairing the breathability of the multilayer fabric. Achieving moisture release above 70% and water vapour permeability closer to the 90% level, a similar performance to sport technical textiles, and still ensuring a BFE considerably higher than 70% for both samples. Therefore, it was concluded that it is possible to obtain the same performance close to a social mask level III, without harming the individual's lung capacity or putting the same at risk of

infection by viruses, bacteria and/or fungi.

ACKNOWLEDGMENT

The authors gratefully acknowledge the funding by P2020, under Individual Project SI I&DT POCI-01-02B7-FEDER-053071, entitled “ActiFiber – Development of reusable level II protective masks”.

REFERENCES

- [1] Jarosińska, A., Walicka, A., Jarosińska, D., Miecznikowska, D., Cuchí, P., *Operational considerations for case management of COVID-19 in health facility and community*, In: *Pediatr. i Med. Rodz.*, 2020, 16, 27-32
- [2] Milton, D.K., Cowling, B.J., Leung, N.H.L., Chu D.K.W., Shiu, E.Y.C, Chan, K-H., Mcdevitt, J.J., Hau, B.J.P., Yen, H.-L., Li, Y., Ip, D.K.M., Peiris, J.S.M., Seto, W-H., Leung, G.M., Cowling, B.H., *Brief Communication Respiratory virus shedding in exhaled breath and efficacy of face masks*, In: *Nat. Med.* 26 (2020) 676-680
- [3] Liao, M., Liu, H., Wang, X., Hu, X., Huang, Y., Liu, X., Brenan, K., Mecha, J., Nirmalan, M., Lu, J.R., *A technical review of face mask wearing in preventing respiratory COVID-19 transmission*, In: *Curr. Opin. Colloid Interface Sci*, 2021, 52, 101417
- [4] O’Dowd, K., Nair, K.M., Forouzandeh, P., Mathew, S., Grant, J., Moran, E., Bartlett, J., Bird, J., Pillai, S.C., *Face Masks and Respirators in the Fight Against the COVID-19 Pandemic: A review of Current Materials*, In: *Advances and Future Perspectives, Materials*, 2020, 13
- [5] Rebelo, R., Guise, C., Rosado, K., Figueiro, R., *Aplicações de Materiais Fibrosos na Área Médica*, In: *Int. Conf. Eng. UBI2011*, 2011.
- [6] Ferreira, D., Figueiro, R., Silva, C., Silva, P., Navarro, M., *Máscaras de Proteção*, 2020
- [7] Tcharkhtchi, A., Abbasnezhad, N., Seydani, M.Z., Zirak, ., Farzaneh, S., Shirinbayan, M., *An overview of filtration efficiency through the masks: Mechanisms of the aerosols penetration*, In: *Bioact. Mater.* 2021, 6, 106-122
- [8] Ardon-Dryer, K., Warzywoda, J., Tekin, R., Biroş, J., Almodovar, S., Weeks, B.L., Hope-Weeks, L.J., Sacco, A.J., *Mask Material Filtration Efficiency and Mask Fitting at the Crossroads: Implications during Pandemic Times*, In: *Aerosol Air Qual. Res.*, 2021, 21, 200571
- [9] Liu, Y., Hu, H., *Compression property and air permeability of weft-knitted spacer fabrics*, In: *J. Text. Inst.*, 2011, 102, 366-372
- [10] Onal, L., Yildirim, M., *Comfort properties of functional three-dimensional knitted spacer fabrics for home-textile applications*, In: *Text. Res. J.*, 2012, 82, 1751-1764
- [11] British Standards, *BS 7209:1990 - Specification for water vapour permeable apparel fabrics*, 1990, 1-12
- [12] Figueiro, R., Ferreira, D., Silva, C., Silva, P. Navarro, M., *Máscaras de Proteção*, 2020
- [13] Figueiro, R., Filgueiras, A., Soutinho, F., Meidi, X., *Wicking Behavior and Drying Capability of Functional Knitted Fabrics*, *Text. Res. J.*, 2010, 80, 1522-1530
- [14] Lima, M., Silva, L.F., Vasconcelos, R., Martins, J., Hes, L., FRICTORQ, *Tribómetro para Avaliação Objectiva de Superfícies Têxteis*, In: *IBERTRIB*, 2005, 1-11
- [15] ISO 6330:2012 (en), *Textiles — Domestic washing and drying procedures for textile testing*, 2012
- [16] CEN, *EN 14683:2019+AC:2019 - Medical face masks - Requirements and test methods*, 2019
- [17] Scarano, A., Inchingolo, F., Lorusso, F., *Facial Skin Temperature and Discomfort When Wearing Protective Face Masks: Thermal Infrared Imaging Evaluation and Hands Moving the Mask*, In: *2International Journal Environmetak Res. Publi Heal.*, 2020, 17



A SUSTAINABILITY APPROACH: INTEGRATION OF A MICROENCAPSULATED PHASE CHANGE MATERIAL TO A RECYCLED PES NONWOVEN FABRIC TO DEVELOP A HEAT STORING RECYCLED MATERIAL

DOI: 10.35530/TT.2021.01

E.G. Saraç^{1*}, E. Öner¹, M.V. Kahraman²

¹Department of Textile Engineering, Faculty of Technology, Marmara University, Turkey
(E-mail: egsarac@gmail.com, eoner@marmara.edu.tr)

²Department of Chemistry, Faculty of Arts and Sciences, Marmara University, Turkey
(E-mail: mvezir@marmara.edu.tr)

Abstract: Phase change materials (PCMs) are thermal energy storing materials which are adopted in various industries including textiles. They provide temperature regulation by absorbing the heat from the ambient or releasing the latent heat that they store. PCMs are widely integrated into textiles in microencapsulated form where the core PCM is covered by the microcapsule shell and protected during phase change. This form also provides a higher thermal conductivity. In this work, a blend of organic coconut oil and n-octadecane were used as phase change material in core, and melamine formaldehyde was used as shell material to develop microencapsulated PCM for heat storage. The microcapsules were produced by using in situ polymerization method. The developed microcapsules (MPCMs) were integrated to a recycled PES (polyester) nonwoven fabric, generated from PET (polyethylene terephthalate) fibres, and manufactured by combing and needle punching technique. The MPCMs were implemented to the fabric by coating method. The core PCM, MPCM, and the coated nonwoven fabric were assessed by Differential Scanning Calorimetry (DSC), Scanning Electron Microscopy (SEM) and Fourier Transform Infrared Spectroscopy (FT-IR). SEM results indicated that spherical and uniform microcapsules were obtained with a particle size of 3-9 μm . DSC results revealed that MPCM and the MPCM coated nonwoven fabric possessed a remarkable melting enthalpy of 111 J/g and 30.9 J/g, respectively at peak melting temperatures of 28.1°C and 27.4°C.

Keywords: coconut oil, heat storage, microencapsulation, phase change material, sustainability

1. INTRODUCTION

The use of thermo-regulative textiles has been growing in several areas such as home textiles, bedding, protective textiles, and active wear. Phase change materials (PCMs) provide thermal regulation property by storing or releasing the heat at a specific temperature range where the phase change takes place. Microencapsulation is a way of packaging the PCM which prevents the leakage of the core substance on textile material in liquid state during phase change, and ensures chemical durability as well as increased area of heat transfer. PCMs are usually incorporated to fibre or fabric in microencapsulated form [1]. PCMs which

are used to be incorporated in textiles are linear long chain hydrocarbons, polyethylene glycols, fatty acids and their blends [1,2]. PCMs with melting points between 15°C and 35°C are suggested as the most effective PCMs for cooling in textile and clothing [1]. Recent studies focused on to generate novel encapsulated PCMs [5-7] and to develop new design PCM-incorporated textiles with a high thermo-regulating performance. Lin et al. studied in thermo-regulating glove design as a protective wear by integrating microencapsulated PCMs to a fabric layer of the glove by coating application [8]. Borreguero et al. worked on the use of PCMs in footwear by doping the microcapsules with carbon nanofibers (CNFs) on various fabric surfaces, formed composites, and analysed the thermal energy storage and the thermal insulation properties of the developed composites [9]. Saraç et al. applied the microencapsulated PCMs to a medical textile by coating on to a nonwoven fabric layer and then confining the material within the layers of the textile to create a thermo-regulation property [10].

In this study, novel microcapsules containing a blend of organic coconut oil and n-octadecane in core were synthesized by in situ polymerization method [3,5] and then applied on a recycled PES nonwoven fabric by coating to obtain a sustainable thermo-regulating heat storing material which can be used as a textile substrate in geotextiles, medical textiles, or automotive textiles [11]. Thermal performance of the core PCM, MPCM and the treated fabric were tested and assessed.

2. GENERAL INFORMATION

2.1 Materials

100% Organic Coconut Oil (Sri Lanka origin, supplied by LifeCo Company) and crystalline mass/melt n-octadecane (%98, Alfa Aesar) were used as PCM core materials. Melamine (99% pure) from Aldrich, formaldehyde (37% aqueous solution, Merck) were used as shell materials. Sodium dodecyl sulphate (SDS, Fluka Chemika) was used as emulsifier, Melateks 700 containing methylol was used as crosslinker for the melamine formaldehyde shell, and ammonium chloride (extra pure, Riedel-de Haen) was used as nucleating agent in encapsulation reactions. Triethanolamine (99%, Merck) was used to adjust the pH in reactions. For coating treatment, chemicals from Organik Kimya (Turkey) were used in the coating solution. Dispersant K 850 was used as an anionic dispersing agent, Antifoam S6010 was used to prevent foaming in the coating solution, polyurethane based Orgaresin PN 50 was used as binder and Orgafix DX New was used as the fixator in the coating treatment. Recycled PES nonwoven fabric, which was made of 100% recycled PET fibers and manufactured by combing- needle punching technique, was supplied by Hassan Tekstil A.S., Turkey.

2.2. Methods

A blend of organic coconut oil and n-octadecane (30% organic coconut oil and 70% n-octadecane by weight) was microencapsulated in melamine formaldehyde shell by using in situ polymerization method [5]. The encapsulation process comprised preparation of pre-polymer solution of melamine and formaldehyde, preparation of oil in water emulsion, and the synthesis of microcapsules [3,5]. The pre-polymer solution was prepared by dissolving 6 g of melamine and 30 mL of formaldehyde in 30 mL of distilled water with magnetic stirring at

750 rpm at 70 °C. The pH of the solution was adjusted to 9 by the addition of triethanolamine. As the solution became clear, 1 g of melamine and 10 ml distilled water were added and dissolved. For the emulsion preparation, 12 g of organic coconut oil and 28 g of n-octadecane were emulsified in 300 mL distilled water by the addition of 4 g SDS as an emulsifier and 1.5 g Melateks 700 as a cross-linker. The emulsion was mechanically stirred at the rate of 2700 rpm at 50 °C for 3 h. The pH of the emulsion solution was adjusted to 4 by the addition of acetic acid dropwise. Then, the pre-polymer solution was added dropwise to the emulsion solution while stirring at 600 rpm. 1 g of ammonium chloride was added to the solution as nucleating agent. The encapsulation reaction was carried out at 60 °C for 100 min. The reaction was terminated by adjusting the pH to 8.5. The microcapsules were filtered and then washed repeatedly by 30% ethanol solution, then dried at 50 °C for 24 h.

The fabricated microcapsules were integrated to recycled PES nonwoven fabric by coating application (figure 1). The coating solution was prepared according to the recipe given in table 1. The coating paste was applied on the nonwoven surface. Following that, the coated fabric was dried for 15 min at 110°C and cured for 5 min at 160°C.



Figure 1. Images of: a - untreated fabric; b - treated fabric

Table 1. Coating recipe of MPCM

Name of the contents	Weight (g)	% in total wt.
MPCM	8	16.7
Dispersant K 850	0.25	0.5
Antifoam S 6010	0.25	0.5
Orgaresin PN 50	16	33.3
Orgafix DX New	1.6	3.3
Distilled water	19	39.6
Orgal M 420	2.9	6.0
Total	48	100

The chemical composition of the core PCM and the MPCM were characterized by FT-IR (figure 2). The surface morphology of the MPCM and the treated fabric were examined by SEM analysis (figure 3). The heat storage performances of the core PCM, the MPCM and the coated nonwoven fabric were assessed by DSC measurements (figures 4 and 5). The encapsulation ratio (R%), which indicates the core content of the MPCM,

was calculated by equation 1 and the coating add-on% was calculated by equation 2.

$$R (\%) = (\Delta H_{m,MPCM} / \Delta H_{m,PCM}) \times 100 \quad (1)$$

$$\text{Add-on} (\%) = [(\text{Dry fabric weight after coating} - \text{Dry fabric weight before coating}) / \text{Dry fabric weight before coating}] \times 100 \quad (2)$$

The coated and the uncoated fabric thicknesses were also tested. Thermographic temperatures of the untreated and the treated fabrics were measured at the ambient temperature of 28.5°C, on a temperature-controlled oven at 50-70°C (table 2) during heating and cooling processes.

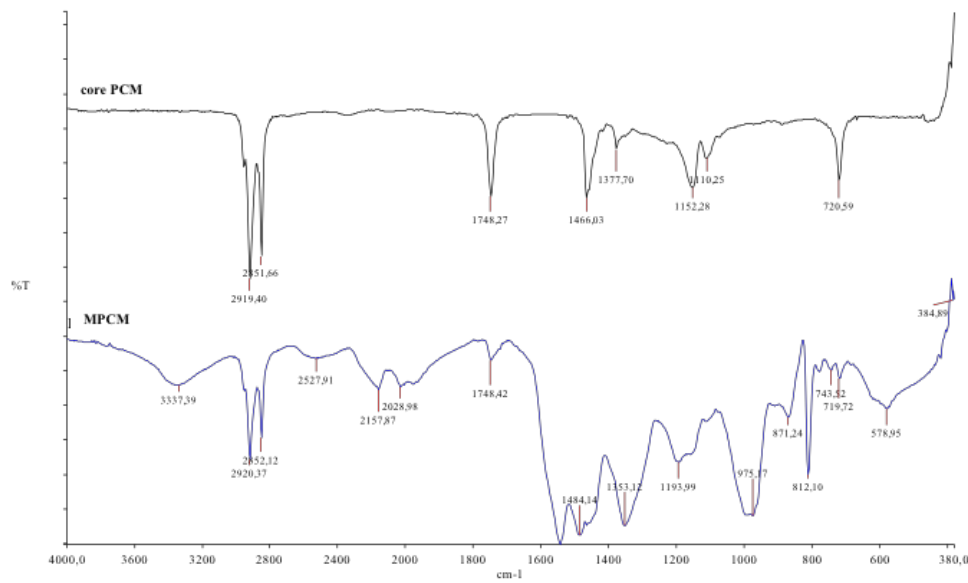


Figure 2. FT-IR Spectra of the core PCM and the MPCM

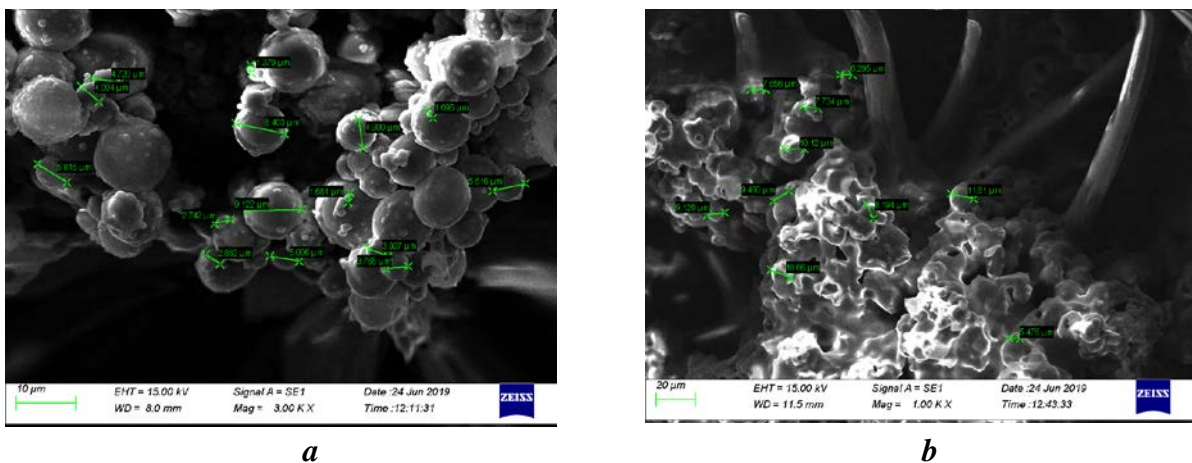


Figure 3. SEM images of: a – MPCM; b - MPCM coated fabric

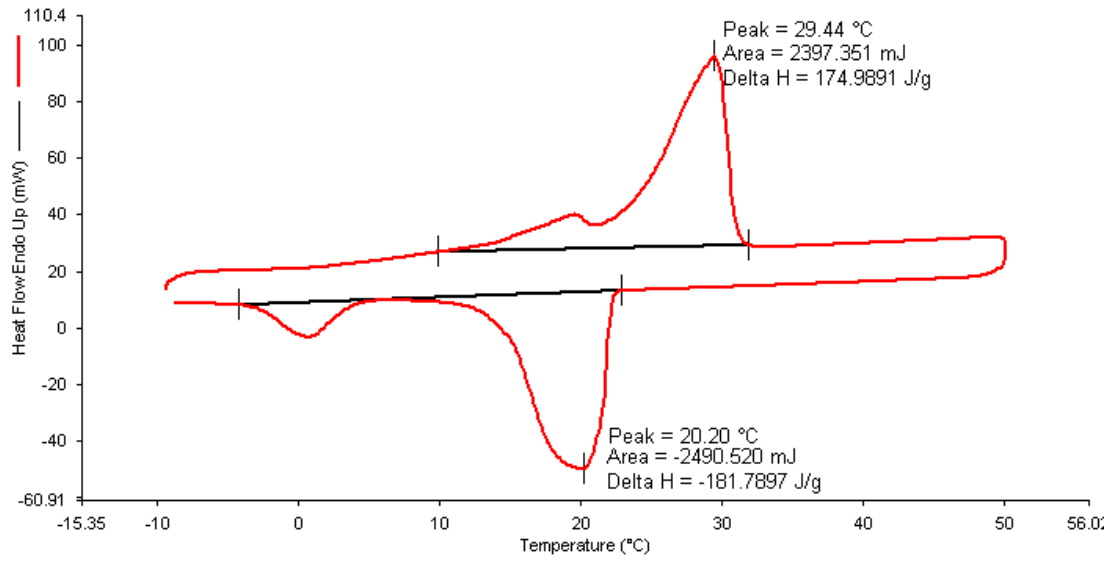


Figure 4. DSC curve of the core PCM

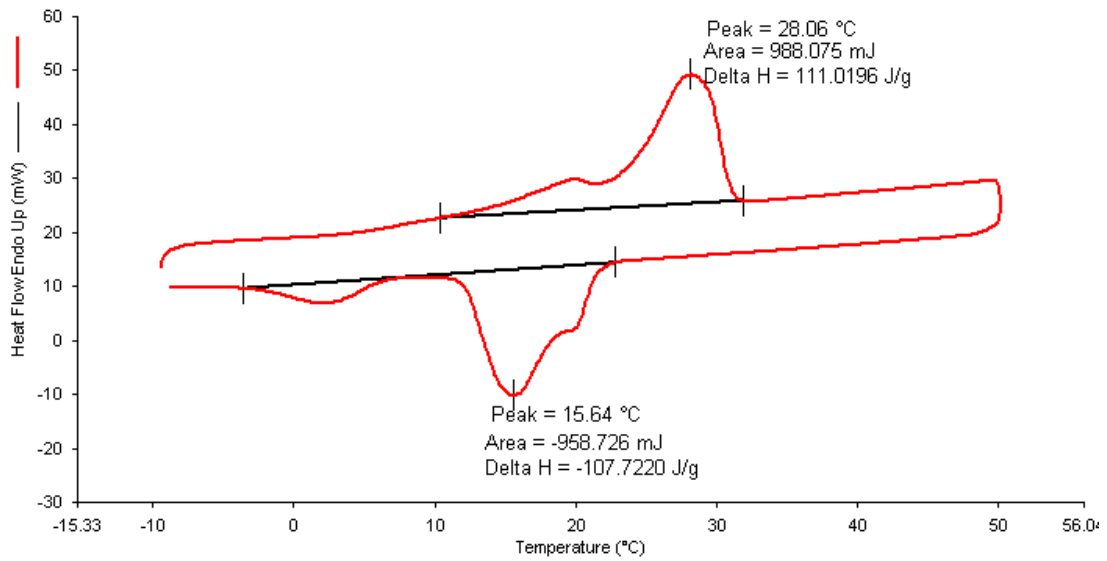
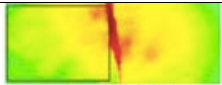
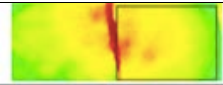
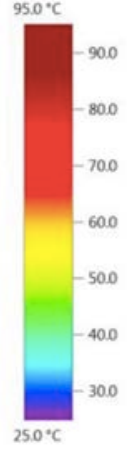
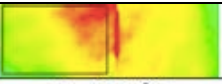
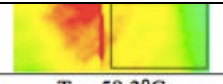
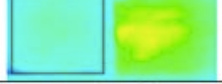







Figure 5. DSC curve of the MPCM

Table 2. Thermographic images of untreated and treated fabric samples

Time	Untreated Sample	Treated Sample	Temperature Colour Scale
Heating 0 s	 $T_r = 55.7^\circ\text{C}$	 $T_i = 55.6^\circ\text{C}$	
Heating 5 min	 $T_r = 59.1^\circ\text{C}$	 $T_i = 58.3^\circ\text{C}$	
Cooling 0 s	 $T_r = 39.5^\circ\text{C}$	 $T_i = 48.6^\circ\text{C}$	
Cooling 60 s	 $T_r = 31.1^\circ\text{C}$	 $T_i = 34.1^\circ\text{C}$	
Cooling 120 s	 $T_r = 30.3^\circ\text{C}$	 $T_i = 31.7^\circ\text{C}$	

5. CONCLUSIONS

The MPCMs, which contain a blend of coconut oil and n-octadecane in core and melamine formaldehyde in shell, were produced by in situ polymerization successfully. The MPCMs were integrated to the recycled PES nonwoven fabric by coating application.

FT-IR spectra of the core PCM and the MPCM was given in figure 2. The absorption peak at 3333 cm^{-1} was attributed to O-H bending vibration of the melamine formaldehyde microcapsule crosslinked with the cross-linker containing methylol. The peaks placed at 2920 cm^{-1} and 2852 cm^{-1} were assigned to C-H bond stretching vibrations. The absorption peak at 1748 cm^{-1} was attributed to C=O stretching vibration of the microcapsule and the fatty acid. The peaks placed at approximately 1540 cm^{-1} and 1490 cm^{-1} were assigned to C=N and C-N stretching vibrations of melamine formaldehyde [3,5]. FT-IR results confirmed that the melamine formaldehyde microcapsule was formed successfully. SEM images (figure 3) revealed that spherical and uniform microcapsules were obtained with a particle size of 3-9 μm . The SEM image of the treated fabric illustrated that the microcapsules were densely and uniformly distributed on the fabric surface with the coating binder. The DSC analyses (figures 4 and 5) showed that the core PCM and the MPCM had significantly high melting enthalpies of 175 J/g and 111 J/g at peak melting temperatures of 29.4°C and 28.1°C , respectively. The encapsulation ratio of the MPCM was calculated as 63.4% (equation 1). The DSC results revealed that the MPCM treated fabric possessed a 30.9 J/g latent heat of fusion at the peak temperature of 27.4°C which is close to human skin comfort temperature [12]. The latent heat storage performance was found to be remarkably high comparing to literature [3-5]. The coating add-on was calculated as 171% due to the light weight structure of the nonwoven fabric. The thickness of the untreated and the MPCM treated fabric were measured as 1.84 mm and 2.22 mm, respectively. Thermographic images (table 2) of the untreated and the treated fabrics indicated that, the

MPCM treated fabric absorbed and stored the heat more in the heating process due to its PCM content, and the treated fabric temperature decreased more slowly comparing to the untreated one.

This experimental work advanced that the recycle PES nonwoven fabric gained a significant latent heat of fusion capacity after MPCM treatment, which is a reusable energy to regulate the temperature. The study suggests a novel application for nonwoven fabrics which can be used to develop a thermo-regulative filling material for bedding, geotextiles, home textiles, or automotive textiles. It also contributes to the sustainability of textiles by upcycling a recycled PES nonwoven fabric to a heat storing material. It is possible to carry out this study to an industrial scale.

ACKNOWLEDGEMENTS

The authors gratefully acknowledge the Grant FEN-C-DRP-200318-0117 by the Scientific Research Project Unit (BAPKO) of Marmara University.

REFERENCES

- [1] Mondal, S., *Phase change materials for smart textiles-an overview*, In: Appl Therm Eng, 2008, 28, 1536-1550
- [2] Sarier, N., Önder, E., *Organic phase change materials and their textile applications-an overview*, In: Thermochim Acta, 2012, 540, 7-60
- [3] Saraç, E.G., Öner, E., Kahraman, M.V., *Microencapsulated organic coconut oil as a natural phase change material for thermo-regulating cellulosic fabrics*, In: Cellulose, 2019, 26, 8939-8950
- [4] Karthikeyan, M., Ramachandran, T., Sundaram, O.L.S., *Synthesis, characterization, and development of thermally enhanced cotton fabric using nanoencapsulated phase change materials containing paraffin wax*, In: J Text Inst, 2014, 105, 1279-1286
- [5] Saraç, E.G., *Development of thermo-regulating smart textiles and investigation of their performance properties*, Doctoral Thesis, 2020
- [6] Ruiz-Calleja, T., Bonet-Aracil, M., Gispert-Paya, J., Bou-Belda, E., *Analysis of the influence of graphene and phase change microcapsules on thermal behavior of cellulosic fabrics*, In: Materials Today Communications, 2020, 25, 101557
- [7] Skurkyte-Papieviene, V., Abraitiene, A., Sakauskaitė, A., Rubeziene, V., Baltusnikaite-Guzaitiene, J., *Enhancement of the thermal performance of the paraffin-based microcapsules intended for textile applications*, In: Polymers, 2021, 13, 1120
- [8] Lin, S.H., Chang, C.P., Lynn, M., Ashdown, S.P., *Exploring phase change materials in gloves to regulate body temperature*, Conference paper, ICDHS Taipei, 2016. 214-217
- [9] Borreguero, A.M., Talavera, B., Rodriguez, J.F., Valverde, J.L., Gonzales, J.L., Carmona, M., *Enhancing the thermal comfort of fabrics for the footwear industry*, In: Textile Research Journal, 2013, 83, 16, 1754-1763
- [10] Saraç, E.G., Öner, E., Kahraman M.V., *Developing a thermo-regulative system for nonwoven textiles using microencapsulated organic coconut oil*, In: Journal of Industrial Textiles, 2020, <https://doi.org/10.1177/1528083720921490>
- [11] Iqbal, K., Khan, A., Sun, D., Ashraf, M., Rehman, A., Safdar, F., Basit, A., Maqsood, H.S., *Phase change materials, their synthesis and application, in textiles- a review*, In: Journal of the Textile Institute, 2019, 110, 1, 1-14
- [12] Erkan, G., *Enhancing the thermal properties of textiles with phase change materials*, In: Research Journal of Textile and Apparel, 2004, 8, 2



RECYCLED TEXTILES: EVOLVING DESIGN-DRIVEN PRACTICES FOR CHANGING THE CIRCULAR FUTURE OF THE FASHION SECTOR

DOI: 10.35530/TT.2021.02

E. D'Itria*, C. Colombi

Design Department, Politecnico di Milano, Italy
(E-mail: erminia.ditria@polimi.it, chiara.colombi@polimi.it)

Abstract: *In recent times, waste materials such as deadstock or used clothing have captured the fashion industry's attention. These materials have been the subject of studies to design sustainable production systems and new manufacturing techniques, intending to approach a circular economy model. In this context, the fashion industry has implemented strategic, design-led actions to prevent waste and promote recycling and recovery actions. Recycled textiles are fertile ground for fashion experimentation that, starting from the circular economy concept, can involve the entire textile supply chain: all the different actors working together proactively to encourage the establishment of industrial symbiosis systems between the districts. An excursion among the ideas and techniques applied to this field can show the possibilities of sustainable material-led approaches that can make a more positive future thrive.*

Keywords: *circularity, fashion design, industrial transformation, sustainability, recycling*

1. INTRODUCTION

Today, the production and consumption actions are starting to involve a systemic approach guided by design and follow a defined pattern that supports industries in meeting the needs of today, preserving the future ones [1]. This systemic approach is particularly evident in the fashion sector and represents the intersection between fashion, design, and sustainability [2]. Fashion Design for Sustainability (FDfS) is the branch that investigates this specific point of intersection. This study of fashion, design and sustainability began in the early 2000s informed by several scholars [3-8]. They built the framework focusing on the environmental and social implications of the fashion sector, offering new examples and approaches. Prof. Fletcher's work "Design Journeys" marked a turning point expanding the sector boundaries and going beyond the simple interest in the material or technical characteristics but enhancing the physical and emotional well-being of people, as well as contributing to the use of resources ethically and responsibly without destroying social and ecological balance [9]. The fashion industry is now translating these concepts into tangible actions by developing greener design concepts, paying attention to materials choice, performing greener processes, involving ethical change, and empowering communities [2].

Therefore, the sustainable dimension of fashion contemplates the whole product lifecycle pattern the items might create from the design phase to the end of life.

Fashion is investing intending to green the industrial machine processes to repair social and business practices and create a new way of viewing and living fashion [10].

According to those mentioned above, how can fashion move forward to achieve the objectives set?

The fashion industry is implementing different circularity practices which aim at incrementally reducing the harm of the current linear model considering waste alternatives: Repairing, reusing, remaking, and composting [11].

In the last few years, waste of industrial production and consumption, such as deadstock or used clothes, both of textile matrix and coupled with plastics, has been studied. These studies aimed to design sustainable production systems and new manufacturing techniques to approach a circular economy model [12-14].

These strategic actions, guided by design, are intended to prevent waste and promote recycling. These efforts are coherent with the necessity to positively impact People and the Planet, stressing the importance of rethinking research and design (R&D) strategies and converting the old linear supply chain model into a new circular one [15].

Recycled textiles are a fertile ground for fashion experimentation that, starting from the concept of circular economy, encompasses the entire textile supply chain, involving the different actors along the supply chain in a proactive way to encourage the establishment of a system of industrial symbiosis between the districts.

A plethora of fashion and textiles companies are currently working on disruptive and ecological innovations to produce regenerated materials with high sustainable performative characteristics [16]. An excursus among ideas and techniques - that have been applied to this field of research - can show the possibilities enabled by the design-led approaches which hack the present to create the conditions of the future [17].

The proposed paper investigates, with a view to the materials recovery, the valorisation of waste. At the base of the sourcing activity, there is the collection by companies of unsold, deadstock, and processing waste of some, which are circularly recovered into yarns, clothes, and accessories. The presented shift to circularity is consistent with the times as the global fashion industry needs to consider the scarcity of essential and finite resources. Resource-dependent enterprises need to seek alternative ways that allow for sustainable and continuous sources. The linear production that characterizes modern business models is unsustainable and requires a system of industrial symbiosis along the supply chain [17]. It is not just a technical issue. There is a need for a design, management, and optimization of material-driven activities to promote new strategic practices that can prevent waste production and, through materials recycling, drive the fashion sector's passage to a positive model of consumption.

Starting from the presented state of the art in Fashion Design for Sustainability, the paper investigates the evolution of production practices in fashion and textile recycling. Particular attention is paid to the design-driven transition of the textile industry from a linear to a circular model. A design-driven change explores the potential positive impact of design on competitive advantage, addressing new product meanings. De Goye et al. [18] states that this development is guided by new knowledge on different contexts including,

2. MATERIALS AND METHODS

The paper aims to present the result of research conducted into how fashion and textiles companies, particularly those working in the European area, are focusing on implementing their recycling practices and performances through the adoption of the technological medium.

Methodologically, the approach consisted of four main stages to co-construct new knowledge: the first phase of desk-based research of the current recycling practices in the fashion industry; the second phase mapped company and designers who are working on disruptive and ecological innovations for the production of regenerated materials with high sustainable performative characteristics identifying the best practices; the third phase of in-depth analysis of the recognized best practices; and the last phase integrated all the collected

data to define the evolving design practices which are changing the circular future of fashion sector.

The initial desk research phase made it possible to identify a varied and fragmented panorama of SMEs carrying out virtuous practices on the Continent.

The further phase of mapping led to the identification of 202 companies located in 23 nations worldwide, which have distinguished themselves for having reached a mature level within their production practices concerning the theme of sustainability (figure 1). All the identified practices were operating in the fashion or textile field, enhancing sustainable and responsible practices which considered both People and the Planet.

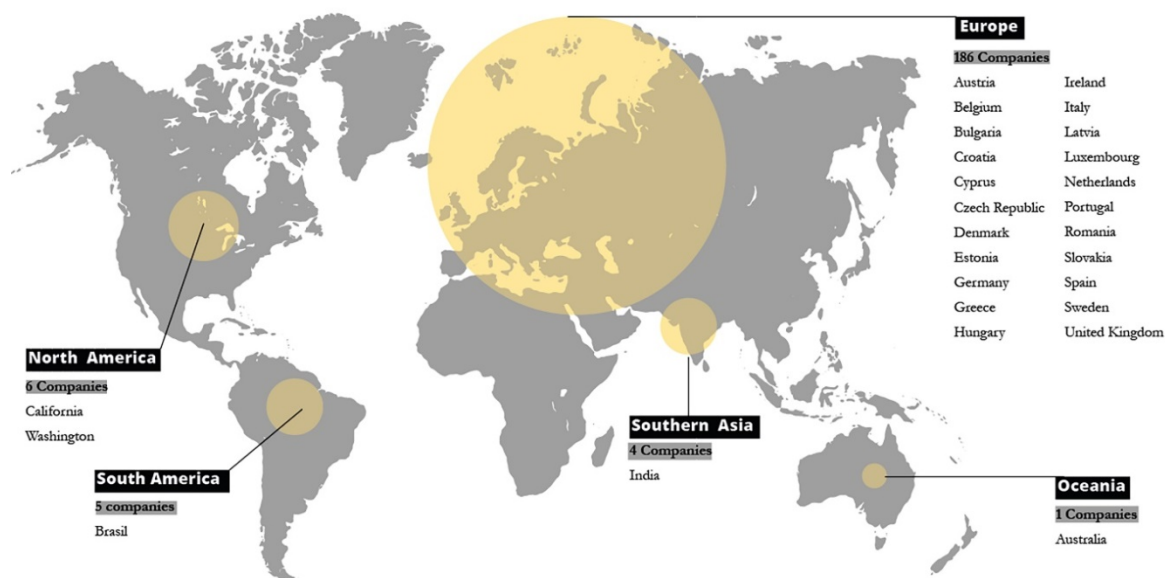


Figure 1. Map of the sustainable company analysed

The composition of the companies was heterogeneous. They were players implementing sustainability in their action, not only in the design field but also in the management and technology/engineering. Of the 188 companies mapped, 35 were selected as case studies. The case studies aimed to narrow down a vast field of research into easily researchable topics. They were chosen according to several criteria:

- Level of maturity to understand who was moving from greenwashing to become feasible and strategic.
- Dimension, since the study was intended to be as representative as possible, the authors wanted to have cases from all ranges of companies (from micro to big);
- Textile recycling technology selects representatives of the different methods and technologies for textile waste recycling to understand the state of the art (figure 2).

All these enterprises are today relevant for the methods they pursue implementations of sustainable practices within their system, often adopting a technological transformation approach as support.

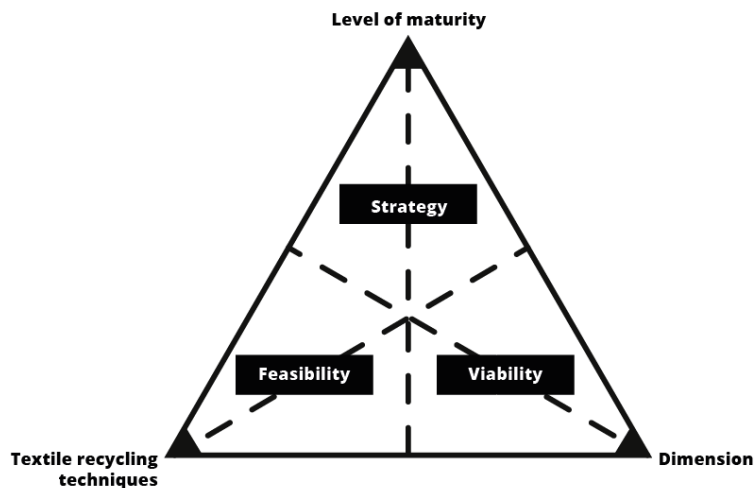


Figure 2. Case studies criteria selection

The following phase consists of a further analysis through 5 selected face-to-face interviews with representatives from 5 companies that had previously distinguished themselves as best sustainable practices.

The interviewed were selected according to:

- their background;
- company history and reputation;
- their tangible outcomes;
- sustainable initiatives that efficiently improved their performances (reports, stakeholders' evaluations, certifications), and communication.

All these case studies showed a desire to evolve and respond to the new needs of the surrounding environment, evidenced by their path towards circularity through recovering practices.

The next phase interpreted the collected data exploring how a positive transformation in the fashion system is possible by implementing specific design-driven aspects. This step allowed the authors to understand which criteria a company working on design-led recycling practices must meet. These aspects are today related to materials, and they lead towards circularity by imagining and implementing processes with high sustainable performative characteristics in two particular areas: recycling, converting waste into new materials by destroying it and then giving it a new life; and regenerating, reusing scraps and waste, without destroying them, to create products that have more value [20].

3. RESULTS AND DISCUSSIONS

From the research emerged a clear overview of current recycling practices. To date, there are two methods of textile recycling: mechanical and chemical. Mechanical recycling is the recycling of textiles into fibres without the use of chemicals. During this process, the used garment is shredded and carded to extract the fibres from the fabric. This fibre can then be spun to make yarn for fabric or knit. Chemical textile recycling adopts a series of chemical processes to depolymerize/dissolve the thread to make a monomer/solvent, create a new fibre compound, or extract a combination from a mix. These processes' end products are often of the same quality as their virgin counterparts, with no loss of physical properties through the recycling process. Both these practices are carried out to achieve the goal of a circular economy. This goal is consistent with what the European Union has established: By 2025, end-of-life textiles must be collected separately and recycled so that new fibrous

material with properties similar to virgin material can be produced [19]. This goal is already technically feasible for selected mono-material waste textiles of a single fibre type, the problem is multi-material textiles. To date, there are no technologies that can allow a sustainable transformation of these materials. While, in cases where textile blending is necessary, it will be mandatory to design new forms of recycling capable of separating different fibre materials directly or through selective processing of individual fibre materials into useful chemicals. Furthermore, as Piribauer and Bart [20] reported, since any recycling process to be implemented by a private company must be profitable, a bonus-malus system based on extended producer responsibility should be considered.

In addition, design can play a crucial role in enabling easier and more effective recycling methods. Below is a list of the significant design actions highlighted by the research:

- Design for recycling, avoid mixing to allow materials to return to their cycle.
- Design for mono materials, use sewing threads with the same composition as the garment material.
- Consider sustainable colours, dyes, finishes, and prints and avoid toxic chemicals.
- Design for sustainable systems; since the selection process is still manual, consider switching to an automated process.
- Design for people, educate consumers.

The presented results address how design drives solutions that lead towards circularity. A new paradigm by imagining and implementing processes with high sustainable performative characteristics. This move towards circular models is happening in two specific areas:

1. Recycling means converting waste into a new material by destroying it and then giving it a new life.
2. Regenerating means reusing scraps and waste without destroying them to create valuable products [21].

Recycling responds to the new pace of consumption in the Western world which follows fast and unsustainable patterns. This unsustainable path has led to an increase in disposed of clothing and textiles rather than being reused or recycled. According to data, 85% of clothing and textiles end up in landfills, even though 95% can be reused and recycled [22]. Once in landfills, there are two possible scenarios. First, natural fibres can take a few weeks and/or a few years to decompose, releasing methane and CO₂ gas into the atmosphere [23]. In the second scenario, synthetic textiles are designed not to deteriorate and may release toxic substances into groundwater and surrounding soil [24]. According to the processed data, textile recycling can be a solution to these issues and offer both environmental and socio-economic benefits: decreasing the need for landfill space, bearing in mind that synthetic fibre products do not decompose and that natural fibres can release greenhouse gases; avoiding the use of virgin fibres; reducing energy and water consumption; impacting on the pollution of land and resources while preserving the health of people and workers [25]. Regenerating addresses the fact that today the textile industry is a vast and high-impact industry. Fibres are the primary raw material for textiles, and their manufacture produces tremendous environmental and social impact, which is necessary to find sustainable alternatives [26]. In this context, the case of cotton is emblematic. Cotton is the most widespread profitable non-food crop in the world. Its production provides income to more than 250 million people worldwide and employs nearly 7% of all labour in developing countries. About half of all textiles are made from cotton. Hence, cotton's global reach is vast, but current cotton production methods are environmentally unsustainable, undermining the industry's ability to maintain future production [27]. In the presented scenario, textile

manufacturing industries need to design new resources, technologies, and environmentally and socially adequate processes.

From the collected data emerged how regenerated fibres may represent a solution. In recent years, they proved to be a viable alternative that has overcome the limits linked to the environmental and social dimensions. Regenerated fibres address the chemical issues in two ways:

- using innovative solutions that make it possible to beat impacts and produce in a way that is compatible with both people and the environment [28];
- rediscovering historical techniques whose application can be a positive and sustainable added value for companies and their production [2]. These productive practices support an industrial shift to circularity which is consistent with the times.

The global fashion industry needs to consider the scarcity of essential and finite resources. Resource-dependent industries need to seek alternatives. As previously stated (see Section 1), the linear production that characterizes modern business models is unsustainable and requires a system of industrial symbiosis along the supply chain. The introduced discussion will be enhanced by presenting two case studies selected among the best practices identified by the research. According to the strategies mentioned above, companies are operating to innovate their production practices and waste management to improve their circular performances and develop new sustainable alternatives. The following sections will enhance the discussion introduced above by presenting two case studies selected among the best practices identified by the research. The purpose of using case studies is to focus on one case but simultaneously consider their entire context. Thus, their illustration will include many variables and qualities sufficient to delineate the research field and offer actual data [29].

3.1. Destroying materials for giving new life: The Ecoalf case

Ecoalf is a Spanish apparel label committed to creating an alternative business model to preserving the Planet. Ecoalf uses a high proportion of eco-friendly materials concentrating their R&D strategies on recycled materials limiting the number of chemicals, water, and wastewater used in their production. Their garments are made from recycled materials, such as plastic bottles from the bottom of the ocean, recycled nylon, cotton, and wool, and recycled used tires. Also, they are an example of industrial synergy as their products are made through partnerships in different countries such as Spain, Portugal, Taiwan, or Japan, among others. The aim is to create products that promote sustainability among consumers seeking design and quality [30]. Their sources characterize the materials: Ecoalf uses the recycled plastic trash collected from the oceans. The company has been interrogated specifically on their initiative "Upcycling the Oceans". This initiative – co-founded by EU Commission- allow them to recycle over 70,000,000 plastic bottles and 60 tonnes of fishing nets: with 70 plastic bottles and 135 grams of nets, the company can create one meter of fabric [31]. The project started in 2015 on the initiative of the Ecoalf Foundation together with the HAP Foundation. They aimed to help remove marine debris from the bottom of the oceans thanks to the support of anglers: recuperating the plastic trash that is damaging the sea and transforming it into top-quality yarn to produce their garments.

The company has come a long way in the last six years, mainly concerned with the quality of the final materials. The main issue was the low and inconsistent quality of the debris recovered by the fishermen. They overcame these complex barriers thanks to crucial investments in R&D. Their work focused on recycling PET plastic bottles - which now constitute the primary raw material of Ecoalf. Their innovative process transforms old plastic bottles into flakes and pellets to obtain a high-quality, 100%

polyester recycled filament. This technology offers a successful alternative to the use of the Planet's natural and finite resources. Using recycled materials, the brand saved over 20% in water, 50% in energy, over 60% in greenhouse emissions, and holds 27% in terms of natural resources [32]. Ecoalf is now meeting the challenge of recycling ocean plastic waste, transforming it into a sustainable and profitable resource. They have been selected and introduced in this paper as sustainability pioneers. Their practices succeeded in creating the first generation of recycled products with the same quality and design as the best non-recycled ones. This achievement results from a design-driven innovation that started from the company's culture and their vision of doing things. They explore how values and aspirations could evolve. This culture and vision do not come from *the market but creates new markets; they do not push new technologies but give rise to new meanings* [33]. Ecoalf's winning practice, which is today replicable, is an example of the industry's positive conversion. This conversion is based on the company's purpose of starting recycling practices that could convert waste into a new material giving it a new life. Ecoalf proves that companies can manage this process to redefine dominant meanings and thus bring long-term competitive advantage [34].

3.2. Preserving materials for giving new value: The Evrnu case

Evrnu® is an American textile innovations company creating a circular ecosystem. The company became famous in the international textile scene thanks to its partnership with Levi Strauss & Co. This collaboration aimed to develop the world's first jeans made from discarded cotton. The company develops a patented technology to create engineered fibres characterized by high performance and minimal environmental impact made from discarded clothing. Evrnu® primary objective was regenerating cotton waste - post-consumer (worn and used garments) cotton waste - to create premium fibres. Today, the fashion industry is estimated to create 92 million tons of textile waste annually, and landfilled waste produces methane over 20 times more harmful than CO₂ [32]. For these reasons, the company aims at contributing to minimize textile waste and address natural resource vulnerability. To reach this goal, the company researched and developed an innovative technology that purifies cotton garment waste, converts it to a pulp, and extrudes it as a new fibre to create premium textiles.

Furthermore, they build a closed-loop system that creates positive synergies between pivotal actors along the supply chain as producers, retailers, and consumers. Evrnu's mission focuses on the idea that taking waste and turning it into something else is meaningless if that something else has a fate that ends up in a landfill or incinerator: companies just created a delay to the inevitable waste [33]. What characterizes the process developed by Evrnu is its creation of minimal negative environmental impact. Their technology uses 98% less water than is required to produce virgin cotton. In addition, Evrnu eliminates 80% of the polluting emissions typical of manufacturing these products and can be remanufactured multiple times [34]. Evrnu has been selected as a case study for their environment-sparing alternative for the world's highest-demand fibres such as cotton, polyester, and rayon. From a design-driven perspective, their work gives new meaning to waste. They can meet latent needs and desires and explore new markets, developing innovative products differently from the past and showing a new future [19]. Their practices are laying the foundations for closing the loop on fashion overproduction/waste.

4. CONCLUSIONS AND FUTURE RESEARCH

This paper discussed the current scenario of the recycling textiles dimension in the fashion and textile sectors. Here are reported innovators, in the two identified categories, through the use of case studies. The discussion informs directions towards a

circular paradigm enabled by the adoption of design-led practices in the European fashion industry. The main methods highlighted how design is crucial in driving a continuing evolution to a more sustainable context. The paper suggests that the link between circularity and innovation-driven innovation in the fashion field is related to systemic practices. Such practices nurture an industrial symbiosis along the supply chain that considers actions carried out to extend product time in the system, transforming them or assigning them to another loop or sector. These practices are now contributing to the circular passage thanks to their role in preserving non-renewable resources and eliminating waste.

Future points of reflection stimulated by this work may concern possible directions for the evolution of recycling technologies and the exploration of the role of design in developing systems to improve collection and recycling of used textiles to follow up amounts and quality levels of collected, used materials.

REFERENCES

- [1] World Commission on Environment and Development (WCED), *Our Common Future*, Oxford: Oxford University Pre, 1987
- [2] Williams, D., Stevenson, N., Crew, J., Bonnelame, N., Vacca, F., Colombi, C., D'Itria, E., Aus, R., Pupart, P., Moora, H., Valle-Noronha, J., Riisberg, V., Ræbild, U., Hasling, K.M., *Fashion Design for Sustainability in Higher Education in Europe: Benchmarking Report*, In study - Fashion SEEDS – Fashion Societal, Economic & Environmental Design-led Sustainability, EU funded Erasmus + Strategic Partnership, 2019
- [3] Black, S. ed., *Eco- Chic, the Fashion Paradox*, Blackdog Publishing, 2008
- [4] Fletcher, K., *Sustainable Fashion and Textiles - Design Journeys*, London: Earthscan, 2008
- [5] Riisberg, V., *Teaching Sustainable Design to Textile and Fashion Students – from a micro and macro perspective*, In: Sustainable Fashion – Issues to be addressed, Design School Kolding, 2010
- [6] Salcedo, E., *Moda ética para um futuro sustentável*, Barcelona: Editorial Gustavo Gili, 2014
- [7] Von Busch, O., *Post-script to Fashion-able, or a methodological appendix to activist design research*, 2009
- [8] Williams, D., Baldwin, N., Fletcher, K., *Volume 3.0: Centre for Sustainable Fashion: tactics for change*, London: Centre for Sustainable Fashion, 2009
- [9] Fletcher, K., *Sustainable Fashion and Textiles*, London: Routledge, 2014
- [10] Rinaldi, F., *Fashion Industry 2030*, Milano: Egea, 2019
- [11] *Vision of a circular economy for fashion*, Available at: <https://www.ellenmacarthurfoundation.org/assets/downloads/Vision-of-a-circular-economy-for-fashion.pdf> [Accessed on February 2021]
- [12] Circle Economy, *Circle textiles programme*, 2021, Available at: [circle-economy.com/programmes/textiles](https://www.circle-economy.com/programmes/textiles) [Accessed on March 2021]
- [13] European Commission, *Circular economy action plan*, 2021, Available at: ec.europa.eu/environment/strategy/circular-economy-action-plan_en [Accessed on March 2021]
- [14] PACE, *Circular Economy Action Agenda*, 2021, Available at: [circle-economy.com/programmes/textiles](https://www.circle-economy.com/programmes/textiles) [Accessed on March 2021]
- [15] *A New Textiles Economy: Redesigning Fashion's Future*, Available at: https://www.ellenmacarthurfoundation.org/assets/downloads/publications/A-New-Textiles-Economy_Full-Report_Updated_1-12-17.pdf [Accessed on August 2021]
- [16] *Bof-Mckinsey, State of Fashion 2020*, Available at: <https://www.mckinsey.com/~media/McKinsey/Industries/Retail/Our%20Insights/The%20state%20of%20fashion%202020%20Navigating%20uncertainty/The-State-of-Fashion-2020-final.aspx> [Accessed on August 2021]
- [17] *Textiles in Europe's circular economy*, Available at: <https://www.eea.europa.eu/publications/textiles-in-europes-circular-economy> [Accessed on August 2021]
- [18] De Goey, H., Hilletoft, P., Eriksson, L., *Design-driven innovation: a systematic literature review*, In: European Business Review, 2019, 31, 1, 92-114, <https://doi.org/10.1108/EBR-09-2017->

- [19] Verganti, R., Dell'Era, C., *Design-driven innovation: meaning as a source of innovation*, In: Dodgson, M., Gann, D.M., Phillips, N. (Eds), *The Oxford Handbook of Innovation Management*, Oxford University Press, Oxford, 2014, 139-162
- [20] Piribauer, B., Bartl, A., *Textile recycling processes, state of the art and current developments: A mini review*, In: *Waste Management & Research*, 2019, 37, 2, 112-119
- [21] *Riciclare & Rigenerare*, Available at: <https://rifo-lab.com/blogs/blog-di-rifo/riciclare-rigenerare-ifferenza#:~:text=Riciclare%20significa%20convertire%20un%20rifiuto,successivamente%20dargli%20una%20nuova%20vita> [Accessed on August 2021]
- [22] *Secondary Materials and Recycled Textiles Association*, Available at: <https://www.smartasn.org/resources/frequently-asked-questions/> [Accessed on August 2021]
- [23] *Strategies for End of Life: Biodegrade Organic Textile*, Available at: <https://www.close-the-loop.be/en/phase/3/end-of-life#tab-26> [Accessed on August 2021]
- [24] *A Peek inside a Landfill*, Available at: <https://www.planetaid.org/blog/the-gas-from-your-clothes> [Accessed on August 2021]
- [25] Leal Filho, W., Ellams, D., Han, S., Tyler, D., Boiten, V.J., Paço, A., Moora, H., Balogun, A. L., *A review of the socio-economic advantages of textile recycling*, In: *Journal of Cleaner Production*, 2019, 218, 10-20, <https://doi.org/10.1016/j.jclepro.2019.01.210>
- [26] Periyasamy, A.P., Militky, J., *Sustainability in Regenerated Textile Fibers*, In: *Sustainable Textiles: Production, Processing, Manufacturing & Chemistry*, 202, 63-95, https://doi.org/10.1007/978-3-030-38013-7_4
- [27] *Cotton*, Available at: <https://www.worldwildlife.org/industries/cotton> [Accessed on August 2021]
- [28] Sayyed, A.J., Deshmukh, N.A., Pinjari, D.V., *A critical review of manufacturing processes used in regenerated cellulosic fibres: viscose, cellulose acetate, cuprammonium, LiCl/DMAc, ionic liquids, and NMMO based lyocell*, In: *Cellulose*, 2019, 26, 5, 2913-2940, <https://doi.org/10.1007/s10570-019-02318-y>
- [29] Johansson, R., *On Case Study Methodology*, In: *Open House International*, 2007, 32, 3, 48-54, <https://doi.org/10.1108/OHI-03-2007-B0006>
- [30] Núñez-Barriopedro, E., Llombart Tárrega, M.D., *New Trends in Marketing Aimed at the Fourth Sector in the Fashion Industry*, In: Sánchez-Hernández, M.I., Carvalho, L., Rego, C., Lucas, M.R., Noronha, A. (eds), *Entrepreneurship in the Fourth Sector. Studies on Entrepreneurship, Structural Change and Industrial Dynamics*, Springer, Cham., 2021, https://doi.org/10.1007/978-3-030-68390-0_12
- [31] *Ecoalf*, Available at: <https://ourgoodbrands.com/ecoalf-100-recycled-plastic-fashion-oceans/> [Accessed on August 2021]
- [32] *Upcycling the Oceans*, Available at: <https://ecoalf.com/en/p/upcycling-the-oceans-15> [Accessed on August 2021]
- [33] Rathinamoorthy, R., *Sustainable Apparel Production from Recycled Fabric Waste*, In: Muthu, S. (eds), *Sustainable Innovations in Recycled Textiles, Textile Science and Clothing Technology*. Springer, Singapore, 2018, https://doi.org/10.1007/978-981-10-8515-4_2
- [34] Verganti, R., *Design driven innovation: changing the rules of competition by radically innovating what things mean*, Harvard Business Press, 2009



WATER REPELLENT BREATHABLE PET/WOOL FABRIC VIA PLASMA POLYMERISATION TECHNOLOGY

DOI: 10.35530/TT.2021.50

A. Haji^{1*}, M. Khajeh Mehrizi¹, M. Ali Tavana², M. Gohari¹

¹Textile Engineering Department, Yazd University, Yazd, Iran
(E-mail: ahaji@yazd.ac.ir, mkhajeh@yazd.ac.ir, mgrock72@yahoo.com)

²Textile Engineering Department, Amirkabir University of Technology, Tehran, Iran
(E-mail: tavanaie@aut.ac.ir)

Abstract: Water-repellent textiles are usually prepared by application of hydrophobic polymers such as fluorocarbons on fabrics using padding or spraying methods followed by drying and curing steps. These procedures impart hydrophobicity to the fabric, but harm the physical and handle properties of the fabric. In this study, low-pressure plasma was employed for the polymerization of 1H,1H,2H,2H-Perfluorooctyl acrylate on PET/Wool fabric for obtaining water-repellent properties with minimum effect on other desirable properties. To compare the results with the conventional industrial processes, a sample was treated with a commercial water-repellent agent using pad-dry-cure method. The water contact angle, bending length, tensile strength, air permeability, and surface morphology of the samples were compared. The plasma-treated sample showed similar water contact angle and higher fastness properties compared with the sample prepared by the conventional method. The tensile strength of the samples was similar, while the air permeability of the plasma-treated sample was higher and the coating was more uniform compared with the sample prepared by the pad-dry-cure method.

Keywords: fluorocarbon, plasma, polyester, water repellent, wool

1. INTRODUCTION

Water-repellent textiles are highly demanded especially for outdoor use, such as tents and outdoor clothing. Silicon or fluorine compounds are usually employed for hydrophobic finishing of textiles and are usually applied by padding, coating or spraying processes. It is important that the fabric retain its physical properties such as tensile strength, tearing strength, handle, and air permeability after being treated with a water repellent finishing agent [1,2].

Pad-dry-cure is the most commonly used method for water-repellent finishing of textiles. The application of high amounts of water repellent agent at elevated temperature usually causes severe damage on the textile fibres. It also consumes a lot of energy and is not environmentally-friendly. Plasma technology is one of the alternative methods for application and polymerization of water repellent monomers on textiles with minimum effect on their physical properties. Plasma treatment also improves the adhesion between the water repellent film and the textile fibres, which improves the fastness properties of the finished goods [3,4].

Plasma treatment can be employed in water repellent finishing of textiles in two ways. Pre-treatment of the textile surface with oxygen, air, or nitrogen plasma can enhance the adhesion of conventional water repellent finishing agents on the fibres. Also, it is possible to polymerise and graft some gases such as CF₄, C₂F₆, SF₆, SiH₄, etc. on textile fibres using

plasma. In this case, the plasma discharge must occur in the fluorine or silicone containing gas [3,5,6]. By the aim of plasma enhanced chemical vapor deposition method, thin inert fluorocarbon coatings can be deposited uniformly on the surface of any type of textile material in a single stage process with the minimum use of chemicals, water, and energy. In this process, the composition, uniformity, morphology, and thickness of the coating can be easily controlled and water repellent, oil repellent, and anti-fouling properties can be obtained by the proper choose of the precursors [7].

Zanini et al. employed an atmospheric pressure plasma pre-treatment to improve the hydro- and oleo-repellent finishing of cashmere and wool/nylon fabrics coated with a commercial fluorocarbon resin by a pad-dry process. Dielectric barrier discharge plasma treatment using air/water vapour mixture as the processing gas improved the uniformity of coverage and enhanced the hydro- and the oleo-repellent properties of the finished fabrics [8].

Ramamoorthy et al. grafted a C₆ fluorocarbon (2-(perfluorohexyl) ethyl acrylate) on cotton fabric using atmospheric pressure plasma. The monomer was evaporated and injected in the glow discharge region of the plasma treatment reactor. Argon was used as the carrier gas. Cotton fabric was slowly moved through this region and a thin film of the fluoro-polymer was deposited on the surface of the cotton fibres. The resulting fabric showed water, alcohol, and oil repellent properties comparable with the samples prepared by the conventional pad-dry-cure process. The water repellent property was durable against soxhlet extraction, which confirms the good adhesion between the coating and cotton fibres [9].

In this study, PET/Wool fabric was treated with a commercial water repellent agent by a pad-dry-cure process and compared with another sample prepared by direct polymerization of 1H,1H,2H,2H-Perfluorooctyl acrylate using low-pressure plasma.

2. EXPERIMENTAL

2.1 Materials

1H,1H,2H,2H-Perfluorooctyl acrylate (figure 1) was purchased from Sigma-Aldrich (USA). Repellan EPF (Fluorocarbon based water repellent agent) was obtained from Pulcra chemicals GmbH (Germany). Twill weave 55% polyester/45% wool fabric with a weight of 237 g/m² and Nm (yarn count) = 44 (two ply) was obtained from Motahari spinning and weaving company, Qazvin, Iran. Non-ionic detergent (Ultravon GPN) was obtained from Huntsman (Switzerland).

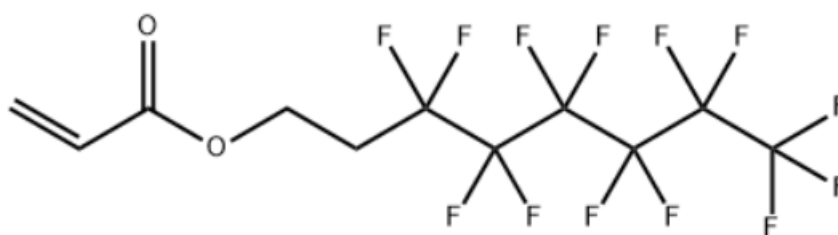


Figure 1. The chemical structure of 1H,1H,2H,2H-Perfluorooctyl acrylate

2.2 Methods

To remove any impurities, the fabric samples were scoured using a solution containing 2 g/l non-ionic detergent and 2 ml/l ammonia (L:G = 30:1) at 60°C for 45 min, then rinsed with distilled water and dried at ambient temperature.

Plasma treatment was done using a low-pressure equipment made by BasaFan company, Iran (Plasma DEJ BF60). Before introduction of the vapour of the fluorocarbon monomer to the plasma treatment chamber, the surface of the fabric was activated by

oxygen/argon plasma for 2 minutes at power of 100 W. The flow rate of oxygen and argon was 50 Sccm. 1H,1H,2H,2H-Perfluorooctyl acrylate was heated in a bottle to 50°C and the vapour was introduced to the chamber with a flow rate of 300 Sccm. Argon gas with a flow rate of 20 Sccm was also used as the carrier gas. Plasma was ignited for 10 minutes at power of 100 W. Finally, the sample was removed and used for further characterizations.

For commercial water repellent finishing, the fabric was padded with 40 g/l Repellan EPF at pH=5.5. The pick-up was 60%. The sample was dried at 110°C and cured at 150°C for 2 minutes.



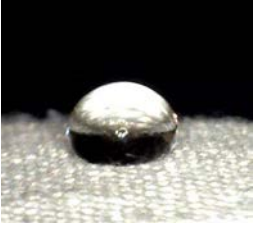
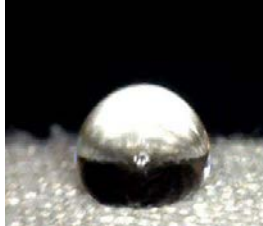
The surface morphology of the samples was investigated using SEM images taken on a Vega3 scanning electron microscope (Tescan, Czech Republic). FTIR spectra was obtained using a Vertex 70 (Brucker, Germany) spectrometer in the range of 400-4000 cm⁻¹. The bending length, air permeability, and tensile strength of the samples were measured according to BS-3356, BS-5636, and ASTM D5035 standards, respectively. Washing fastness was evaluated according to the ISO 105-C03: 1994 standard. The contact angle of the fabrics was measured according to the method described in the literature [10,11].



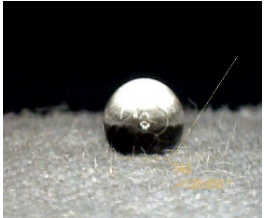
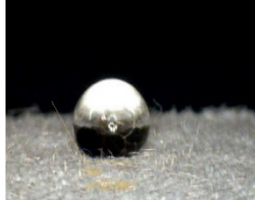


3. RESULTS AND DISCUSSION

3.1. Contact angle

Table 1 shows the contact angle (CA) of water droplets on raw fabric as well as the samples prepared by plasma treatment and commercial method at time of zero and after 30 seconds. The samples have been washed according to ISO 105-C03: 1994 standard and the CA of the washed samples is reported as well. It can be seen that the raw sample has the lowest contact angle at the beginning and it is decreased drastically after 30 s. The contact angle of water droplet on the plasma-treated sample is much higher than the raw sample and lower than the commercially prepared sample at time of zero and after 30 s. But comparing the contact angles of the washed samples, the plasma-treated sample showed a higher contact angle even after 30 s of contact with the fabric. This confirms the better fastness of the water repellence imparted to the fabric by plasma polymerization. It is due to the grafting of the water repellent film to the surface of the fibres and higher crosslinking of the plasma polymerized film.

Table 1. Contact angles of the samples prepared by plasma and commercial methods

CA at t= 30 s	CA at t= 0 s	t= 30 s	t= 0	Sample
79.02	100.32			Raw
107.25	107.53			Plasma-treated

107.22	107.85			Plasma-treated-washed
125.65	128.99			Commercially prepared
99.7	101.72			Commercially prepared-washed

3.2. Surface morphology

Figure 2 shows the SEM images of raw fabric as well as the samples prepared by plasma treatment and commercial method. It can be seen that the fibres have been coated more uniformly using the plasma polymerization compared with the conventional pad-dry-cure method.

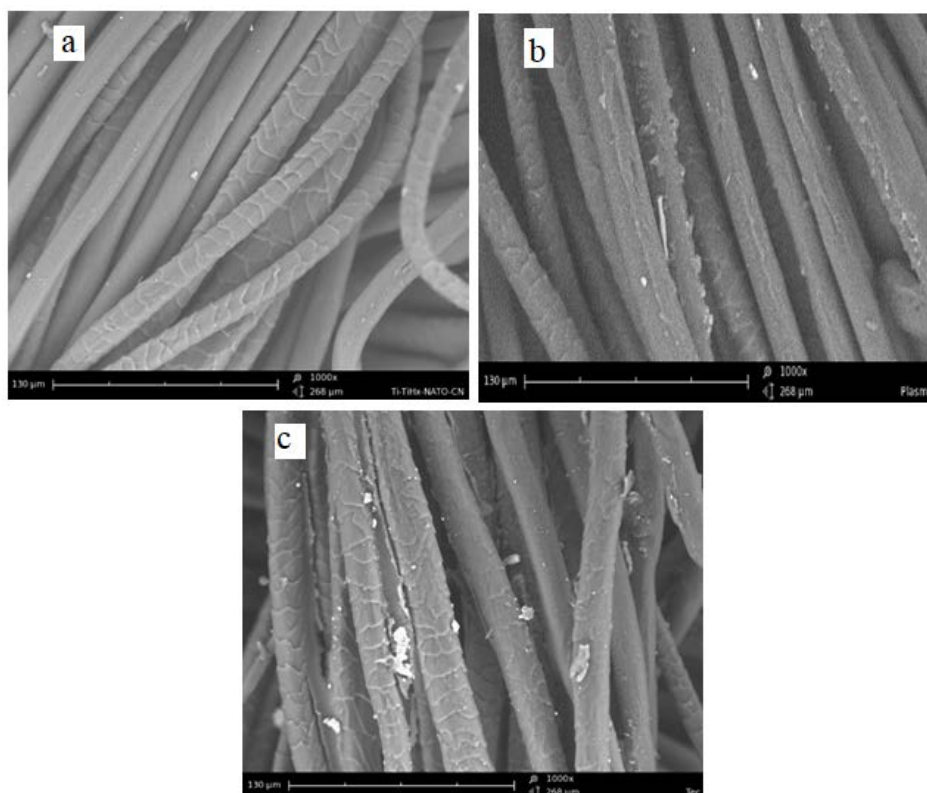


Figure 2. SEM images of: a – raw; b - plasma-treated; c - commercially treated samples

Also, it can be seen that the spaces between the fibres have been filled with the water repellent resin and the fibres have been stucked together which can affect the handle and breathability of the fabric.

3.3. FTIR spectroscopy

The FTIR spectra of the raw, plasma-treated and commercially treated samples are shown in figure 3. The FTIR spectra shows no significant difference between the raw and plasma-treated samples, which may be due to the thinness of the coating. The peak at 1620 cm^{-1} which corresponds to the carbonyl groups of wool and PET fibres has been diminished in the spectrum of the commercially-treated sample which means the coating of the surface of the fibres with a comparably thick layer of the hydrophobic coating. Figure 4 shows a schematic presentation of the grafting and polymerization of 1H,1H,2H,2H-Perfluorooctyl acrylate on wool and PET fibres in the presence of plasma. Ar/O₂ plasma etches and activates the surface and subsequently a thin film of crosslinked fluoropolymer is grafted on the activated fibres in the next stage.

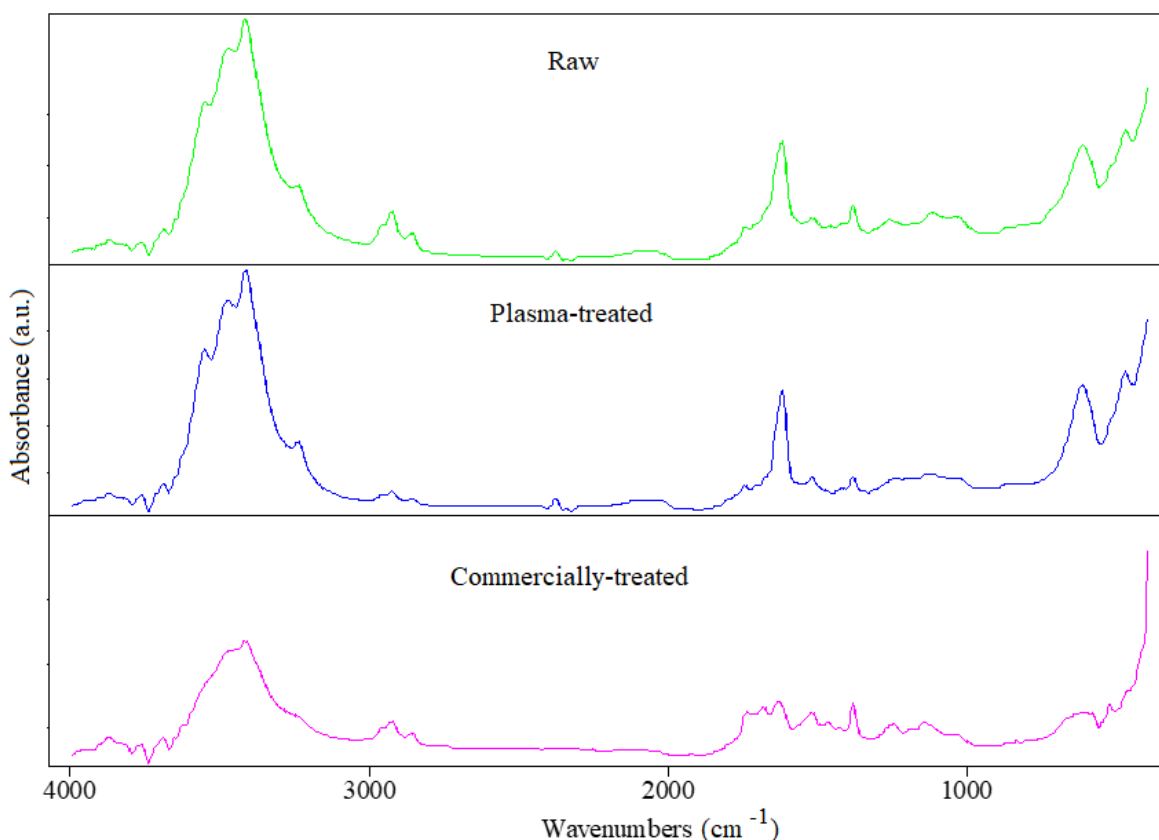


Figure 3. FTIR spectra of raw, plasma-treated, and commercially-treated samples

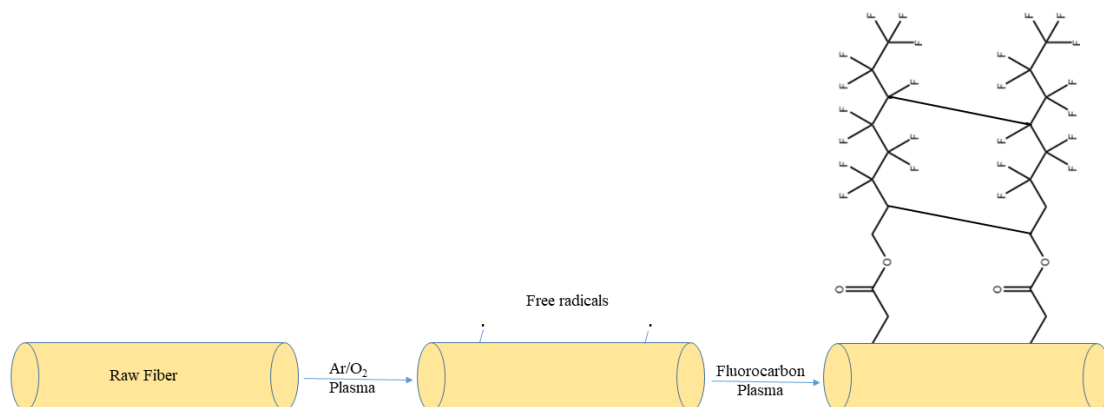


Figure 4. The schematic presentation of plasma polymerization of 1H,1H,2H,2H-Perfluorooctyl acrylate of the fabric surface [12]

3.4. Physical properties

Table 2 shows the bending lengths of different samples. It can be seen that both water repellent samples showed higher bending lengths compared with the raw sample, which means an increase in the stiffness of the fabric. However, the bending length of the sample prepared by plasma coating is lower than the commercially prepared sample. This means that a better handle can be obtained when plasma technology is used for water repellent finishing of PET/Wool fabric.

The air permeability values of the samples are shown in table 3. It can be seen that the air permeability of the plasma-treated sample is near to the raw sample which confirms that a thin film of the fluorocarbon polymer has been deposited on the surface of the fibres which does block the air passing between the fibres and does not affect the air permeability and breathability of the fabric. As can be seen, the commercial process highly affected the air permeability due to binding the fibres with the high amount of the resin.

Table 2. bending lengths of different samples

Sample	Bending length (cm)	CV%
Raw	1.76	0.152
Plasma-treated	2.23	0.152
Commercially prepared	2.83	0.254

Table 3. Air permeability values of different samples

Sample	Air permeability (cc/s.cm ²)
Raw	100
Plasma-treated	95
Commercially prepared	64.5

Table 4 shows the breaking force and extension at breaking point. Both treated samples showed higher breaking force and extension compared with the raw sample. It seems that the presence of the fluoropolymer film on the surface of the fabrics increased their strength. Also, the absence of bonding between the fibres and yarns in the plasma-treated sample let the fibres to slip more easily, causing higher extension for this sample.

Table 4. Breaking force and extension at breaking point of different samples

Sample	Extension at break (%)	CV %	Force (N)	CV %
Raw	36.15	4.81	325	6.78
Plasma-treated	38.33	2.31	339	5.60
Commercially prepared	36.40	5.81	347	8.12

4. CONCLUSIONS

PET/Wool fabric was subjected to water repellent finishing by two different methods including a conventional pad-dry-cure procedure by a commercial water repellent agent and plasma polymerization of 1H,1H,2H,2H-Perfluorooctyl acrylate as a new method. The results showed that the plasma treatment method results comparable results in term of water contact angle with the conventional method. However, the wash fastness of the plasma-treated sample was higher compared with the sample prepared by the conventional method.

The coating of the plasma-treated sample was more uniform and the produced film was thin and the fibres were not stucked together. This resulted in better handle and higher air permeability and extension at break for this sample. The breaking force of both samples was higher than the raw sample. The breaking force of the commercially prepared sample was a little higher than the plasma-treated sample.

The results of this study show the great potential of plasma technology for eco-friendly, uniform and long-lasting water repellent finishing of PET/Wool fabrics with minimum effect on their desirable properties.

REFERENCES

- [1] Williams, J.T., *Waterproof and Water Repellent Textiles and Clothing*, Woodhead Publishing, Kidlington, UK, 2018
- [2] Rabia, S., Muhammad, M., Naveed, R., Waqas, A.S., Qutab, H.G., *Development of free fluorine and formaldehyde oil and water repellent finishes for cotton fabrics through polymerization of bio-based stearic acid with carboxylic acids*, In: *Industria Textila*, 2020, 71, 2, 145–155, <http://doi.org/10.35530/IT.071.02.1731>
- [3] Leroux, F., Campagne, C., Perwuelz, A., Gengembre, L., *Fluorocarbon nano-coating of polyester fabrics by atmospheric air plasma with aerosol*, In: *Appl. Surf. Sci.*, 2008, 254, 3902-3908
- [4] Malshe, P., Mazloumpour, M., El-Shafei, A., Hauser, P., *Multi-functional military textile: Plasma-induced graft polymerization of a C6 fluorocarbon for repellent treatment on nylon–cotton blend fabric*, In: *Surf. Coat. Technol.*, 2013, 217, 112-118
- [5] Ceria, A., Hauser, P.J., *Atmospheric plasma treatment to improve durability of a water and oil repellent finishing for acrylic fabrics*, In: *Surf. Coat. Technol.*, 2010, 204, 1535-1541
- [6] Bae, G.Y., Min, B.G., Jeong, Y.G., Lee, S.C., Jang, J.H., Koo, G.H., *Superhydrophobicity of cotton fabrics treated with silica nanoparticles and water-repellent agent*, In: *J. Colloid Interface Sci.*, 200, 337, 170-175
- [7] Kumar, V., Pulpytel, J., Arefi-Khonsari, F., *Fluorocarbon Coatings Via Plasma Enhanced Chemical Vapor Deposition of 1H,1H,2H,2H-perfluorodecyl Acrylate-1, Spectroscopic Characterization by FT-IR and XPS*, In: *Plasma Processes Polym.*, 2010, 7, 939-950
- [8] Zanini, S., Freti, S., Citterio, A., Riccardi, C., *Characterization of hydro- and oleo-repellent pure cashmere and wool/nylon textiles obtained by atmospheric pressure plasma pre-treatment and coating with a fluorocarbon resin*, In: *Surf. Coat. Technol.*, 2016, 292, 155-160
- [9] Ramamoorthy, A., El-Shafei, A., Hauser, P., *Plasma induced graft polymerization of C6 fluorocarbons on cotton fabrics for sustainable finishing applications*, In: *Plasma Processes Polym.*, 2013, 10, 430-443
- [10] Wiener, J., Dejlová, P., *Wicking and wetting in textiles*, In: *Autex Res. J.*, 2003, 3, 64-71
- [11] Rani, K.V., Chandwani, N., Kikani, P., Nema, S.K., Sarma, A.K., Sarma, B., *Optimization and surface modification of silk fabric using DBD air plasma for improving wicking properties*, In: *J. Text. Inst.*, 2018, 109, 368-375
- [12] Bhatt, S., Pulpytel, J., Arefi-Khonsari, F., *Low and atmospheric plasma polymerisation of nanocoatings for bio-applications*, In: *Surface Innovations*, 2015, 3, 63-83



DEVELOPMENT OF ECOLOGICAL DENIM BLEACHING METHODS

DOI: 10.35530/TT.2021.07

İ. İvedi^{1*}, K. Yağcı², E. Tağaç²

¹R&D Department, Roteks Tekstil İhr. San. Ve Tic. A.Ş., Turkey
(E-mail: ismailivedi@roteks.com.tr)

²Washing Department, Roteks Tekstil İhr. San. Ve Tic. A.Ş., Turkey
(E-mail: korhanyagci@roteks.com.tr, edaozgen@roteks.com.tr)

Abstract: Although the textile industry has many products to offer to humanity, it consumes a lot of energy and indirectly causes greenhouse gas emissions. With increasing environmental awareness, parameters such as the cost and performance of each industrial activity to society, as well as the use of natural resources and the possibility of causing global environmental problems to have become more frequently considered factors. In the denim bleaching process, the desired effect is usually obtained with the help of sodium hypochlorite. Sodium metabisulfite is then used for the neutralization process. Since these processes are carried out at high liquor ratios, the waste load resulting from the consumption of necessary chemicals and water is also high. In this study, ecological bleaching methods have been developed as an alternative to the conventional sodium hypochlorite bleaching method by reducing the use of water and chemicals with low liquor and spraying bleaching methods. Denim garments subjected to bleaching with low liquor and spraying methods were compared with denim garments applied to sodium hypochlorite bleaching in industrial washing machines according to exhaustion method. In the spraying method, the mixture coming out of the narrow nozzle is mixed with the compressed air by means of a specially designed spray gun and sprayed in very small droplets. Thus, a good atomization is ensured, and a low liquor ratio water cloud is created. The results between conventional and ecological bleaching processes were compared according to processes cost, water and chemical consumption, aging effect, tear strength, elasticity, and recovery analyses.

Keywords: bleaching, denim, low-liquor ratio, sustainability, spraying

1. INTRODUCTION

The concepts of sustainability, product life cycle and ecological production have become more and more important considering the dangers that may affect the entire ecosystem, such as global warming. Therefore, companies and consumers become more conscious day by day. According to a report published by the World Bank, the textile and fashion industry is the second most polluting world and responsible for 20% of the water consumed on our planet [1].

With the increase in greenhouse gas emissions and the risk of lack of water, many countries, companies, and organizations around the world have started to implement innovative initiatives and technologies in order to re-evaluate their activities and produce their products both using less water and causing low carbon emissions [2].

Textile is one of the basic human needs and almost all the textile fabrics are colored. Unfortunately, the extensive amounts of clean water, petrochemical based dyes, and chemicals are used for textile dyeing. After dyeing, these substances are discharged as pollutants. The disposal of this discharge is a serious issue which pollutes the natural

environment. Therefore, there is a dire need to develop the novel dyeing processes with extremely low consumptions of water, dyes and chemicals [5].

Denim clothing has been deeply in people's favorite due to its easy and simple style. Along with the evolution of denim clothing, the self-characterized washing technique, for its production impose, has antique appearance and comfortable texture, which becomes the essential element leading to fashion [3]. In the production of denim garments, in order to create the desired aged effect on the products, whisker, laser, stone washing, spray, bleaching, etc. processes are implemented which are called dry and wet processes [4]. Among various methods, sodium hypochlorite oxidation method (chlorine bleaching), with its supreme efficiency, apply into the further area in industrial production [3].

In denim bleaching process a strong oxidative bleaching agent such as sodium hypochlorite or potassium permanganate added during the washing with or without stone addition. Discoloration produced is usually more apparent depending on strength of the bleach liquor quantity, temperature and treatment time. It is preferable to have strong bleach with short treatment time. Neutralization process should be taken for the bleached goods so that they should be adequately antichlored or after washed with peroxide to minimize yellowing [6]. The effect of enzyme wash using cellulase enzyme on the properties of denim garments to develop novel design and fashion. Three parameters in enzyme washing namely concentration of enzyme, washing temperature and time at pH 5.5 were considered. They were chosed indigo dyed cotton denim garments (trousers) to investigate the optimum washing condition and processed by enzyme with the concentration of 0.5% to 3.5%, temperature 40°C to 70°C and time 20 min to 60 min for the achievement with desired worn and aged effect. The effect of each parameter was discussed, and denim garments properties like tensile strength, elongation at break, weight loss, stiffness, water absorption, shrinkage, color fading and morphological values by SEM were evaluated. The optimized washing condition for the best value was found, 2% enzyme concentration at 55°C for 40 min [7].

The influences of the ultrasonic power, the processing time, temperature and sodium hypochlorite concentration on the bleaching-washing effect were analyzed based on the surface K/S value of denim fabric during the ultrasonic-assisted chlorine bleaching washing the denim. They were found that the ultrasonic collaborative sodium hypochlorite washing the denim with a better bleaching effect could save more energy than traditional stirring way. The optimum process followed as the ultrasonic power 400 w, the ultrasonic total times 20 min, the bleaching temperature 25°C and the solution concentration 5% [8].

Jie Xu et al., were investigated the optimization methodology by combining ensemble of surrogates (ESs) with particle swarm optimization (PSO) to optimize production cost of chlorine bleaching for denim were proposed. The methodology starts from the data collections by conducting a Taguchi L25 (56) orthogonal experiment with the process variables and metrics for evaluating bleaching performances. Based on the data, they were separately constructed the quantitative relationships by using RBFNN, SVR, RF and ensemble of them. Then, accuracies of the surrogates were evaluated, and it was proved that the ESs outperforms the others. The ESs PSO approach shows great capability of optimizing production cost of sodium hypochlorite bleaching washing for denim [9].

In one article, the researchers studied nano bubble dyeing of cotton with 11 different reactive dyes. The fabric dyeing performance properties of shade depth, dry rubbing fastness, wet rubbing fastness, and washing fastness were assessed for the liquor ratio of 1:1. The performance of 1:1 dyeing was compared with the conventional dyeing having liquor ratios of 1:5 and 1:10 for the same dyes. All the 11 reactive dyes, dyed at liquor ratio of 1:1 exhibited the uniform dyeing, acceptable fastness properties, and superior air permeability along with zero liquid discharge in the main dyeing cycle [5].

2. MATERIALS AND METHODS

Indigo dyed denim fabric was purchased from Matesa Denim AŞ., Turkey. Weight of the fabric is 12 oz/yd². It has a 3/1 Z twill weave structure, 99/1% - CO/EL mixture and 24% elasticity. The amylase enzyme and dispersing agent for the desizing process were supplied from Dystar, Singapore. Sodium hypochlorite for bleaching process was purchased from Rubin Kimya AŞ., Turkey. Pumice stone for stonewash process was purchased from Kastone LTD., Turkey. Stonewash enzyme was purchased from Dystar, Singapore. Sodium metabisulfite used for neutralization was purchased from Akkim Kimya A.Ş., Turkey. Tolkar's 1326 liter model industrial washing machines were used for the conventional method and Yılmaz's 5000 liter Rainforest model was used for low liquor bleaching processes. The spraying machine was supplied from Method Makine, Turkey. The experimental scheme of the bleaching processes is shown in table 1. The flow chart of each process is shown in figure 1.

Table 1. The experimental scheme of the bleaching processes

Method	Sample quantity (pants)	Liquor ratio (kg/lit)	Water (L)	Temperature (°C)	Chemical amount (g/lit)
Conventional Exhaustion	50	1:10 (Bleach) 1:7 (Neutralization) 1:7 (Washing) 1:7 (Washing)	250 (Bleach) 175 (Neutralization) 175 (Washing) 175 (Washing)	50 Cold Cold Cold	12 (NaOCl) 4 (Na ₂ S ₂ O ₅) - -
Low Liquor Washing	50	1:5 (Bleaching) 1:3 (Neutralization) 1:3 (Washing) 1:3 (Washing)	125 (Bleaching) 75 (Neutralization) 75 (Washing) 75 (Washing)	50 Cold Cold Cold	24 (NaOCl) 13 (Na ₂ S ₂ O ₅) -
Spraying	50	1:0.24 (Bleaching) 1:3 (Neutralization) 1:3 (Washing) 1:3 (Washing)	6 (Bleaching) 75 (Neutralization) 75 (Washing) 75 (Washing)	Cold Cold Cold Cold	334 (NaOCl) 3 (Na ₂ S ₂ O ₅) - -

Firstly, denim pants were produced after cutting-sewing processes. Then, they were subjected to washing processes according to the experimental plan shown in Table 1. In order to evaluate the differences between the application methods, the following tests were applied to the products:

- Elasticity and recovery analyses according to ASTM D3107-07 standard.
- Tear strength analysis according to ISO 13937-2:2000 standard.
- Light cabinet analysis to evaluate the aging effect according to ISO 3664:2009 standard.
- Wasteload of bleaching methods analysed and compared each other.

Wastewater analyzes of ecological and conventional processes carried out in Çevtest Ölçüm Laboratuvarı Tic. Ltd., a laboratory accredited by TÜRKAK according to AB-0091-T and TS EN ISO/IEC 17025:2017 standard. Only conventional and low liquor methods have been analyzed since almost no wastewater is generated in the spraying method. In addition to these analyses, process cost, water and chemical consumption were calculated and compared each other. Table 2 includes wastewater measurement parameters and standards.

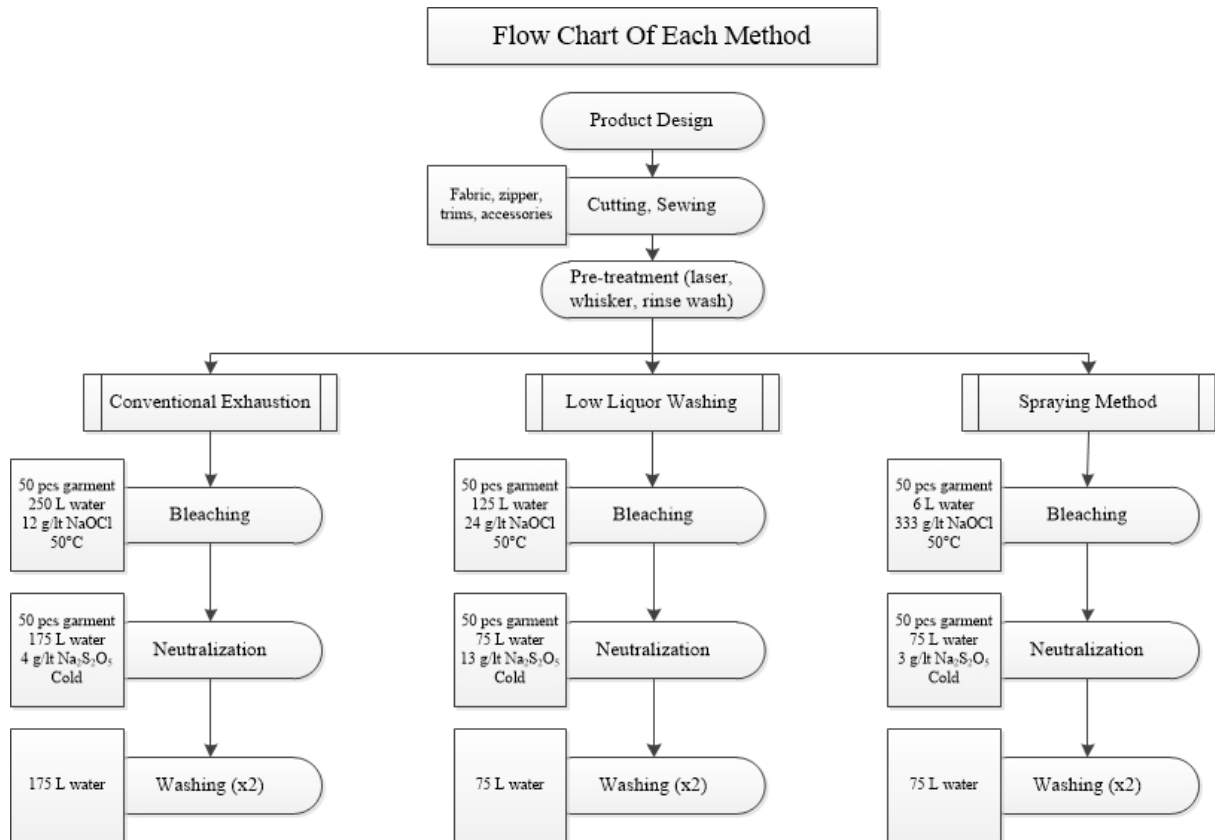


Figure 1. Flow chart of each process

Table 2. Wastewater measurement parameters and standards

Parameter	Unit	Standard
Chemical Oxygen Demand (COD)	mg/lt	SM 5520-B
Free Chlorine	mg/lt	SM 4500-CI G
Biochemical Oxygen Demand (BOD)	mg/lt	SM 5210 B
Ammonium Nitrogen	mg/lt	SM 4500-NH ₃ B, F
Suspended Solids	mg/lt	SM 2540 D
Conductivity	μS/cm	SM 2520 B
pH	-	SM 4500 H B

3. RESULTS AND DISCUSSIONS

When the results are examined, for the aging effect, although less water is used in the low liquor process compared to the conventional method, a similar effect was obtained in a shorter time. In addition, the homogeneity between the products is within acceptable limits. As it can be seen in figure 2, more vivid and moire effects were obtained in the spraying method. Table 3 shows the elasticity and tear strength analysis results of the conventional methods with alternative ecological bleaching processes.



Figure 2. Bleaching methods

Table 3. Tear strength, elasticity and recovery analyse results

Bleaching Method	Tear strength (N)		Elasticity (%)	Recovery (%)
	Warp	Weft		
Raw Samples (non-bleached)	35.74	41.84	18.44	4
Conventional Exhaustion	29.16	29.46	21.94	12
Low Liquor Ratio	22.58	30.23	18.57	6
Spraying	23.45	26.49	19.92	9

No statistically significant difference was observed between the results of elasticity and tear strength analysis. All samples have tear strength above the limits (15 N) determined according to the ISO 13937-2:2000 standard. Exposure of fabrics to chemical, heat and mechanical forces caused a loss of strength as expected. Considering the results of the elastic recovery analysis, it was measured as raw samples, low liquor, spraying and conventional method, in descending order. The highest water consumption is realized in the conventional method with the amount of 31 liters/kg of product. The least water consumption was achieved in the spraying method with 9 liters/kg of product. Chemical usage per product was occurred as spraying method, conventional and low liquor ratio, in ascending order, respectively. Although the waste load seems to have been realized at the least in the conventional method, the reason for this seems to have decreased proportionally as more water is used in the conventional method. Figure 3 shows the comparison of water, chemical and waste loads.

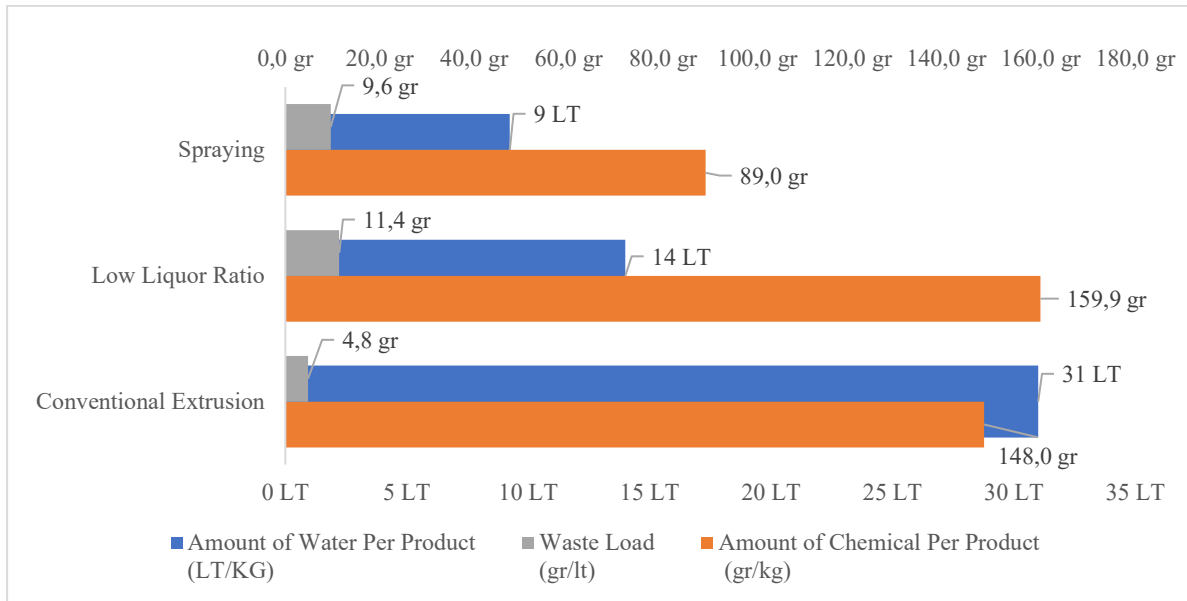


Figure 3. Amount of water, chemical and waste load

When the process costs are compared, it is seen that the spraying method is 30% lower and the low liquor method is 20% lower than the conventional method. Wastewater analysis results are shown in table 4.

Table 4. Wastewater analysis results

Parameter	Low liquor method	Conventional exhaustion	Low liquor method	Conventional exhaustion	Standard
	Value (total)		Value (per kg.product)		
Chemical Oxygen Demand (COD)	323.80 mg/lt	294.70 mg/lt	2.89 mg/lt	5.36 mg/lt	TS 2789
Free Chlorine	28.10 mg/lt	1.87 mg/lt	0.25 mg/lt	0.03 mg/lt	SM 4500-Cl G
Biochemical Oxygen Demand (BOD)	64.40 mg/lt	56.40 mg/lt	0.58 mg/lt	1.03 mg/lt	SM 5210 B
Ammonium Nitrogen	0.81 mg/lt	15.67 mg/lt	0.01 mg/lt	0.28 mg/lt	SM 4500-NH ₃ B, F
Suspended Solids	1951.00 mg/lt	5334.00 mg/lt	17.42 mg/lt	96.98 mg/lt	SM 2540 D
Conductivity	2900 µS/cm	6780 µS/cm	25.89 mg/lt	123.27 mg/lt	SM 2520 B
pH	8.57 / 23.2°C	7.96 / 23.2°C	8.57 / 23.2°C	7.96 / 23.2°C	SM 4500 H+ B

When the results are examined, although the pH difference is not much, the difference can be explained by the amount of sodium hypochlorite used in the boiler with the same liquor ratio. When the sodium hypochlorite usage rates of low liquor ratio and conventional exhaustion processes are examined, it is seen that more sodium hypochlorite per liter is used in conventional exhaustion. COD-BOD ratios appear slightly higher in the low liquor trial. However, per kg, it is seen that low liquor method has more advantageous. The difference in conductivity - suspended solids - ammonium nitrogen is due to the high amount of sodium hypochlorite given per liter. Therefore, these values were higher in conventional exhaustion method.

4. CONCLUSIONS

In this study, denim fabrics with 3/1 twill weave structure containing 99/1% cotton/elastane were carried out in bleaching processes by conventional, low liquor and spraying methods after cutting-making processes. The results were compared in terms of aging effect, physical properties of the fabric such as elasticity, tear strength etc., waste load, water and chemical consumption, and process cost.

When the results were examined, the aging effect closest to the conventional method was obtained with the low liquor method. No statistically significant difference was observed between the results of elasticity and tear strength analysis. All samples have tear strength above the limits (15 N) determined according to the ISO 13937-2:2000 standard. Considering the results of the elastic recovery analysis, it was measured as low liquor, spraying and conventional method, in descending order. A similar effect has been developed in a shorter time compared to the conventional method, without affecting the physical properties of the product, with a 20% lower cost.

The highest water consumption is realized in the conventional method with the amount of 31 liters/kg of product. Compared to the conventional method, the water consumption was reduced by 69.3% and chemical consumption by 39.8% with the spraying method. Thus, approximately 88 million liters of water and 5.92 million kg of chemicals were saved for a company that produces an average of 8 million denim pants per year.

ACKNOWLEDGEMENTS

The authors would like to express appreciation for the support of the The Scientific and Technological Research Council of Turkey [Project Number = 3180537].

REFERENCES

- [1] Kant, R., *Textile Dyeing Industry an Environmental Hazard*, In: Natural Science, 2012, 4, 1
- [2] Pekin, M., Sorousbay, C., *Greenhouse Gas Emissions Produced By Transportation Sector*, In: Thesis (M.Sc.), İstanbul Technical University, Institute of Science and Technology, 2006
- [3] Li, S., et al., *Optimization of Chlorine Bleaching Parameters for Indigo Denim Textile Based on the Model of Response Surface Model and Genetic Algorithm*, In: Journal of Physics: Conference Series, IOP Publishing, 2020, 012026
- [4] Arjun, D., et al., *Technology of industrial denim washing*, In: International Journal of Industrial Engineering & Technology, 2013, 3, 4, 25-34
- [5] Mohsin, M., et al., *Novel, sustainable and water efficient nano bubble dyeing of cotton fabric*, Cellulose, 2020, 27, 10, 6055-6064
- [6] Arjun, D., Hiranmayee, J., Farheen, M.N., *Technology of industrial denim washing*, International Journal of Industrial Engineering & Technology, 2013, 3, 4, 25-34
- [7] Haq, U.N., Khan, M.M.R., *Investigation of the bulk, surface and transfer properties of chlorine bleached denim apparel at different condition*, European Scientific Journal, 2015, 11, 12
- [8] Shi, W.Q., et al., *Study on chlorine bleaching-washing of denim fabric under ultrasonic conditions*, In: Key Engineering Materials. Trans Tech Publications Ltd, 2016, 202-209
- [9] Xu, J., et al., *Cost optimization of sodium hypochlorite bleaching washing for denim by combining ensemble of surrogates with particle swarm optimization*, Journal of Engineered Fibers and Fabrics, 2021, 16, 15589250211022331



A NEW APPROACH FOR CLASSIFICATION OF DIFFERENT WOVEN FABRIC PATTERNS AND THREAD DENSITIES WITH CONVOLUTIONAL NEURAL NETWORKS

DOI: 10.35530/TT.2021.10

E. Gültekin*, H.İ. Çelik, H.K. Kaynak

Gaziantep University, Faculty of Engineering, Textile Engineering Department, Gaziantep, Turkey
(E-mail: elfgultekin30@gmail.com, hcelik@gantep.edu.tr, tuluze@gantep.edu.tr)

Abstract: Fabrics produced from microfilaments are superior to conventional fiber fabrics, due to their properties such as light weight, durability, waterproofness, windproofness, breathability and drapeability. Tightly woven fabrics produced from microfilament yarns have a very compact structure due to small pore dimensions between the fibers inside the yarns and between yarns themselves. It is almost very difficult to distinguish the structures of densely woven fabrics with the visual evaluation. Therefore, it is very important to automatically determine the differences in the texture properties of such fabrics. Thanks to the developments in image acquisition technology and image processing methods, the texture classification of fabrics can be estimated more quickly and reliably than visual inspection. In this study, the classification of high-density microfilament woven fabrics according to different texture types and thread density was achieved by using the ResNet-50 algorithm. The obtained results were evaluated in a confusion matrix form. The classification accuracy of the CNN algorithm was measured as 0.95 on average.

Keywords: CNN, fabric density, fabric pattern classification, ResNet-50, transfer learning, deep learning

1. INTRODUCTION

Deep learning is being utilized in a number of artificial intelligence applications, such as facial recognition, image processing, natural language processing, and etc. Deep learning is a sub-branch of machine learning. The interest in artificial intelligence has progressively grown from the beginning of machine learning to the present, leading to the development of deep learning architectures, which are currently most widely used artificial intelligence algorithms today. It develops intelligent solutions in a variety of sectors, including industry, medicine, robotics, image processing, computer vision, object identification, sound processing-recognition, translation, future forecasting, and finance. In the subject of textile engineering, deep learning may be used in a variety of ways. Fabric pattern is visible from the surface view of the fabric and acts as a very important aesthetic item. Fabric pattern and thread density (yarns/cm) are determined by textile technologists in order to gather information for reverse engineering. The process is done by identifying the yarn interlacements pattern and counting the number of yarns in unit length via a special magnifying lens by human effort. The mentioned process is very difficult, prone to mistakes and time-consuming.

Fabric pattern (texture) identification has received a lot of attention in recent years and has made significant progress. Texture-based statistical approaches and database/model-

based methods are the two most common types of weave pattern identification methods. Pre-processed images are commonly used in the texture-based statistical approach. To get information on fabric structure from multiple directions, Li et al. [1] presented a technique based on photometric differential analysis, utilizing histogram equalization and an adaptive wiener filter. Then, to acquire gray-scale characteristics, an adaptive mesh model was utilized to split pictures into sub-images. Even though the approach proved effective for extracting interlacing points in the weaving structure, the study was confined to just basic woven textiles.

The database/model-based recognition approach identifies and matches weave patterns using a recognition or classification algorithm. Backpropagation (BP) neural networks were assessed by Kuo et al. [2] and Pan et al. [3–5] for the classification of a pre-recognized weave pattern stored in a database of weave patterns based on a white-black co-occurrence matrix. To extract texture characteristics, Kuo and Kao [6] utilized a co-occurrence matrix and the CIE-Lab color model, followed by a self-organizing map (SOM) network to categorize the fabric weave patterns. The recognition accuracy and performance of these techniques, on the other hand, were reliant on the database size. Guo et al. [7] proposed a local feature similarity (LFS) approach for recognizing weave pattern repeat size based on seven weave pattern features. For the identification of woven fabric pattern, Xiao et al. [8] applied Transform Invariant Low-rank Textures (TILT) and Histogram of Oriented Gradients (HOG), as well as Fuzzy C-means Clustering (FCM) to detect the warp and weft cross points. However, these investigations were limited by the inability to recognize double-yarn weave patterns, as well as the fabric's significant rotational fluctuations. Khan [9] proposed a biologically based approach for recognizing fabric weave and color that was resilient even when the yarn color and appearance were altered. Liu et al. [10] developed a fabric defect detection approach for complex textures that combined an improved convolutional neural network (CNN) with a visualization methodology. They chose to explore with a small number of images in a relatively confined setting.

The woven fabric pattern recognition has various limitations. The texture features extraction during image acquisition was directly impacted by the rotational changes in fabric. Image texture may be distorted as a result of poor illumination. Since the deep learning architecture is trained by means of a data set that comprise rotated and scaled image forms, the restriction of traditional Neural Network (NN) method is overcome. In this study, weave type classification of high-density microfilament woven fabrics was carried out depending on the fabric density. In this way, it is very difficult to distinguish the weave type of high-density woven fabrics visually. Thanks to the developments in image acquisition technology and image processing methods, the texture classification of fabrics can be estimated more quickly and reliably than visual inspection.

2. MATERIALS AND METHODS

2.1 Material

This paper describes a novel approach for recognizing the basic microfiber woven fabric patterns (Plain, Twill, and Satin) with different fabric densities from fabric images (figure 1). Fabric manufacturing was done with polyester microfilament textured yarns of 110 dtex with 0.33, 0.57, and 0.76 dtex filament linear densities, as well as standard polyester textured yarns of 110 dtex with 1.14 and 3.05 dtex filament linear densities. These yarns were used in weft direction. For warp yarn 83 dtex polyester yarns with 1.14 dtex filament linear density was used. Three different weave types namely, 1/1 Plain, 3/2 Twill and 4/1 Satin were constructed for this study. For every weave type four different weft sett values were applied considering the weavability limitations (table 1).

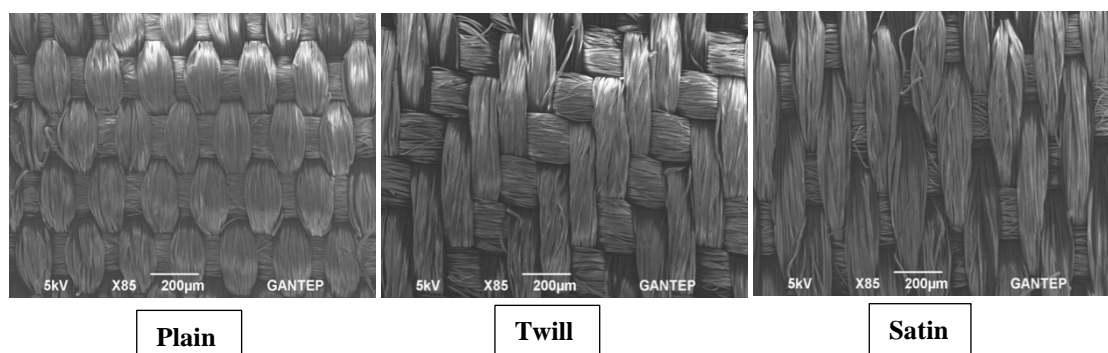


Figure 1. Fabric images taken under SEM

Table 1. Structural properties of sample fabrics

Weft yarn filament linear density (dtex)	Weft sett (weft/cm)		
	Plain	Twill	Satin
0.33	30	41	43
0.57	30	41	43
0.76	30	41	43
1.14	30	41	43
3.05	30	41	43
0.33	32	43	45
0.57	32	43	45
0.76	32	43	45
1.14	32	43	45
3.05	32	43	45
0.33	34	45	47
0.57	34	45	47
0.76	34	45	47
1.14	34	45	47
3.05	34	45	47
0.33	36	47	49
0.57	36	47	49
0.76	36	47	49
1.14	36	47	49
3.05	36	47	49

2.2 Convolution Neural Networks-CNN

A CNN is a type of neural network that is a subset of the neural network. As in a normal neural network, a CNN consists of one or more convolutional layers, frequently with a subsampling layer, followed by one or more fully connected layers (figure 2). The discovery of a visual process in the brain, the visual cortex, inspired the creation of a CNN. Many cells in the visual cortex are responsible for detecting light in receptive fields, which are tiny, overlapping sub-regions of the visual field. The more sophisticated cells have bigger receptive fields, acting as local filters across the input space. A CNN's convolution layer mimics the operation of visual cortex cells [11]. Image and pattern identification, speech recognition, natural language processing, and video analysis are all domains where CNNs are employed. Convolutional neural networks are gaining popularity for a variety of reasons. Feature extractors are handcrafted in traditional pattern recognition models. During

the training phase, the weights of the convolutional layer used for feature extraction and the fully connected layer used for classification are calculated in CNNs. A hand-designed feature extractor extracts essential information from the input and removes unnecessary variabilities in the traditional approach of pattern/image recognition. Following the extractor is a trainable classifier, which is a conventional neural network that divides feature vectors into classes. Convolution layer's function plays as feature extractors in CNNs. However, they are not handcrafted. Kernel weights for convolution filters are determined during the training phase. Because the receptive fields of the hidden layers are restricted to be local, convolutional layers are able to extract local characteristics.

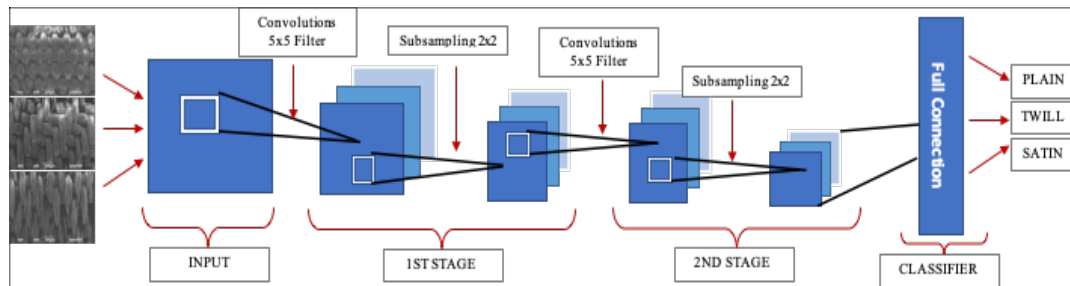


Figure 2. CNN's block diagram

For implementation, a convolutional neural network (CNN) architecture which is capable of effectively extracting image features is considered to be useful. For this aim, before training, a total of 480 images were captured from microscope camera and manually labelled according to the fabric structure. So, 3 pattern classes were created for each fabric type separately. Each fabric classes: plain, twill and satin were divided into 4 subclasses regarding to thread density. For this approach, it was decided to use Resnet-50 model which is one of the most frequently used architectures as transfer learning. Training of ResNet-50 architecture was carried out to discriminate plain, satin and twill fabric classes. Captured fabric images were applied into ResNet-50 to extract features from the images. The images that were categorized into subclasses according to their fabric densities were classified by using the same network training.

In this study, the system consists of image acquisition hardware and pattern recognition software. Image Acquisition Toolbox and Deep Learning Toolbox have studied in Matlab®. Total 480 images, 40 image frames for each of the 3 different weave types with 4 different thread densities, were compiled for using in CNNs. While training networks; 70% of data base is utilized for training and remaining is for (30%) validation. The information obtained from the literature, it was observed that the most frequently changed parameters during transfer learning applications were “Learning Rate”, “Mini Batch Size” and “Number of Epoch”. Meanwhile, many different values were applied for these parameters during training network and the best network training result was obtained.

3. RESULTS AND DISCUSSIONS

The fully connected “fc” (fully connected) that is the last layer in the ResNet-50 network has been changed to arrange our own data. The parameters selected for the training network are; Learning Rate=0.01, Mini Batch Size=32 and Number of Epoch=50. The success percentage of the CNN trained with the entered parameters was obtained as 73.61% for thread density and weave type (figure 3).

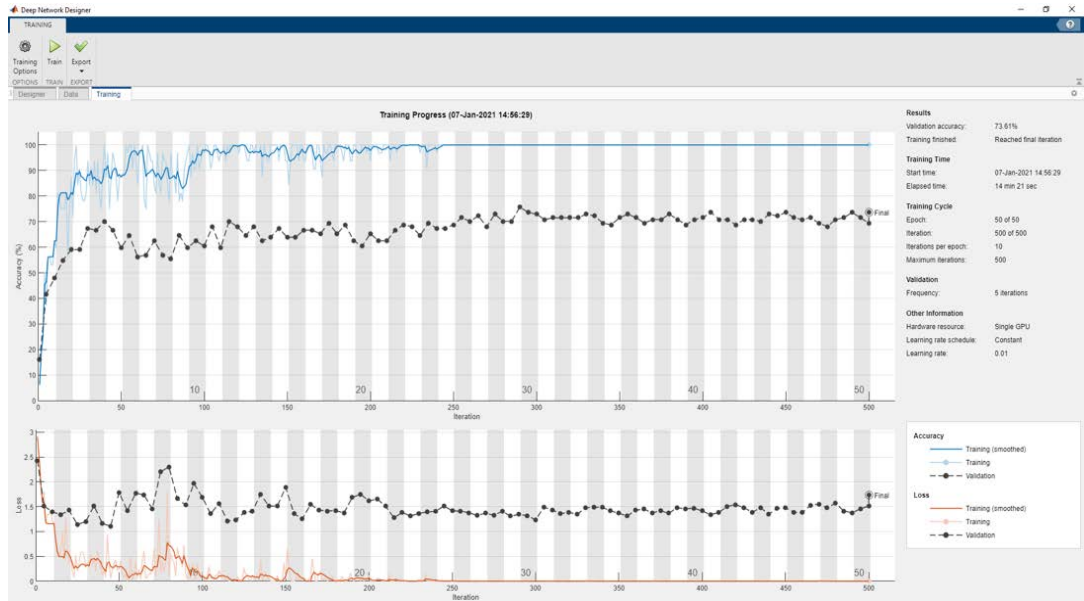


Figure 3. ResNet-50 network training chart

The success statistics of the obtained results from the newly trained networks were analysed as a confusion matrix. A confusion matrix, often known as an error matrix, is a table arrangement that provides for the display of an algorithm's performance [12]. When the results were examined, 7 of the 12 classes in the data set were predicted with 100% accuracy (figure 4). Among the remaining classes, the lowest success rate 84.6% was obtained. The average success of the CNN algorithm was measured as 0.95. This ratio is considered to be a very good result for determining the classes of with high density woven fabrics.

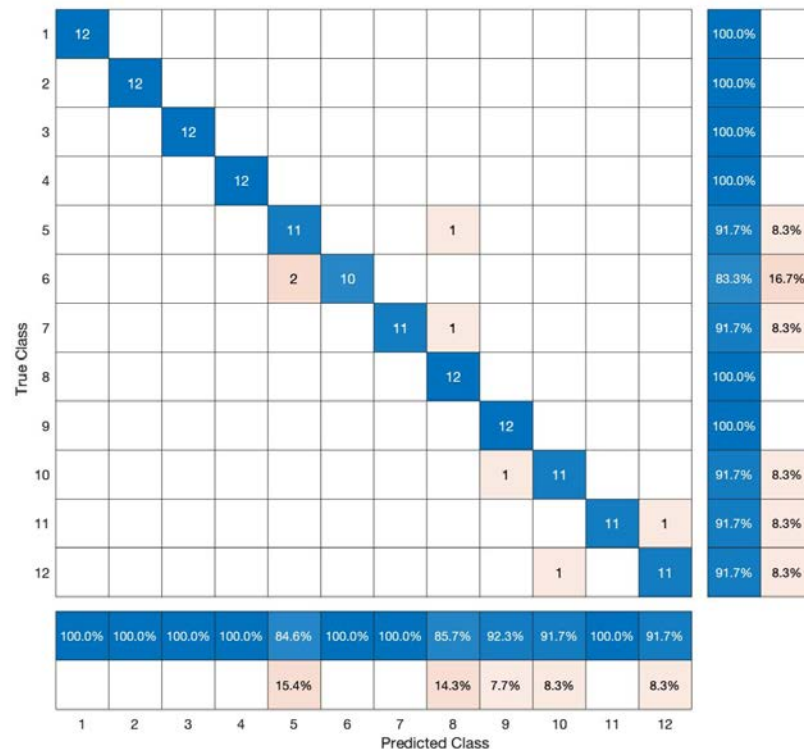


Figure 4. Confusion matrix of weave type classification according to thread density

5. CONCLUSIONS

Textile industries attach importance to technologies and developments that will provide speed and flexibility in production, reduce costs, improve product quality, and improve their functions. The most important contribution of this study is that the weave type and fabric density of the textile sample can be detected automatically via using image processing and artificial intelligence techniques, by eliminating human error and manual tests. The proposed technique outperformed the current research, according to the experimental data. When factors like yarn thickness, rotational direction, and uneven lighting are taken into account, the model holds up well. When training, the suggested CNN model employs less parameters. As a result, the approach is computationally efficient and hence has potential in the textile and fashion industries. A tailored deep learning model for recognizing and classifying high-density microfilament woven fabrics was suggested in this work. The proposed deep learning model is based on residual network (ResNet-50) architecture. The high-level texture features were extracted and then classified based on the types of woven fabric with different thread density. The performance of trained CNN was evaluated via confusion matrix. The accuracy of the CNN was calculated as 0.95.

REFERENCES

- [1] Li, J., Wang, W., Deng, N., Xin, B., *A novel digital method for weave pattern recognition based on photometric differential analysis*, In: Measurement, 2020, 152, 107336
- [2] Kuo, C.F.J., Shih, C.Y., Ho, C.E., Peng, K.C., *Application of computer vision in the automatic identification and classification of woven fabric weave patterns*, In: Text. Res. J., 2010, 80, 2144-2157
- [3] Pan, R., Gao, W., Liu, J., Wang, H., *Automatic recognition of woven fabric patterns based on pattern database*, In: Fibers Polym., 2010, 11, 303-308
- [4] Pan, R., Gao, W., Liu, J., Wang, H., Zhang, X., *Automatic detection of structure parameters of yarn-dyed fabric*, In: Text. Res. J., 2010, 80, 1819-1832
- [5] Pan, R., Gao, W., Liu, J., Wang, H., *Automatic recognition of woven fabric pattern based on image processing and BP neural network*, In: J. Text. Inst., 2011, 102, 19-30
- [6] Xiao, Z., Nie, X., Zhang, F., Geng, L., Wu, J., Li, Y., *Automatic recognition for striped woven fabric pattern*, In: J. Text. Inst., 2015, 106, 409-416
- [7] Xiao, Z., Guo, Y., Geng, L., Wu, J., Zhang, F., Wang, W., Liu, Y., *Automatic Recognition of Woven Fabric Pattern Based on TILT*, In: Math. Probl. Eng., 2018, 11, 1-12
- [8] Khan, B., Han, F., Wang, Z., Masood, R.J., *Bio-inspired approach to invariant recognition and classification of fabric weave patterns and yarn color*, In: Assem. Autom., 2016, 36, 152-158
- [9] Liu, Z., Zhang, C., Li, C., Ding, S., Dong, Y., Huang, Y., *Fabric defect recognition using optimized neural networks*, In: J. Eng. Fibers Fabr., 2019, 14
- [10] *Convolutional neural network*, Available at: https://en.wikipedia.org/wiki/Convolutional_neural_network [Accessed on June 2021]
- [11] *Confusion matrix*, Available at: https://en.wikipedia.org/wiki/Confusion_matrix [Accessed on June 2021]



RESEARCH REGARDING NEW SUSTAINABLE METHODS OF GARMENT PATTERN DRAFTING

DOI: 10.35530/TT.2021.11

I.E. Marin

Doctoral School at the “Gheorghe Asachi” Technical University of Iași, Romania
(E-mail: irina.marin13@yahoo.com)

***Abstract:** Based on the present need for change in the garment industry, multiple solutions for waste reducing have been established. It has become common to associate fashion with pollution, and this association has its roots in the statistical data that constantly raise red flags regarding the negative impact that our everyday textiles have over the planet. The following paper has been developed under the strict rules that the zero waste pattern drafting has, keeping in mind the design and product finishing matters. Further possible issues have been taken into account whilst defining and shaping the pattern pieces, aiming to obtain a product that is framed by proper aesthetics, fit, zero waste drafting technique and quality finishing. The way in which the waste management can be kept under control from the pattern drafting step is the key to gaining a sustainable clothing item. Apart from the fabric scraps, the time and energy needed for sampling can also be optimized, by using the virtual prototyping opportunity. These two crucial elements, combined, led to garments that can last in time. The nexus of the garment manufacturing techniques that have increased in popularity lately has been elaborated in the following paper, following the process accordingly, shaping into a number of digital clothing items. The method used can be successfully implemented by clothing manufacturers that wish to adopt a healthy and non pollutive process.*

***Keywords:** Consumer's behaviour; efficient cutting; sewing patterns; sustainability; waste management*

1. INTRODUCTION

Driven by the increasing numbers that point out the negative impact that fashion has over the environment, searching for sustainable approaches within production has become the main concern of the experts working in the field. So far, the consumers were delighted by fashion's colourful and mesmerizing aesthetics, without acknowledging the harm that's being inflicted on the environment for catwalks and mass production to be possible.

It has become widely known that the fashion industry is one of the most pollutive industries in the world, based on the fabric scraps that end up in the landfill, carbon footprint that's generated by production and water poisoning caused by poor waste management. The effects have been publicized enough to catch the public eye and turn consumer's awareness to the disaster that's happening behind the deceitful splendour of fashion.

However, apart from acknowledgement, consumers must be informed, encouraged, directed and advised in regards of taking proper care of their garments, and thus ensure their clothing items can get a growth in longevity. And by doing so, the fast fashion trend will be drastically reduced, from the customer's behalf. By informing the consumers about the damage that they unknowingly and unwillingly make may bring their awareness over the habitual clothing disposal. By encouraging them, the process will have a much greater rate of success. By directing the buyer, one will know and be able to dispose and care for its clothing items accordingly. Last but not least, by advising the consumer in regard to the correct

methods of caring for its garments leads to a win-win situation: longer lasting clothes contribute to diminishing the chaotic disposal, and thus landfill pollution.

Some producers have also adopted more sustainable methods and kept their mind open when implementing the new approaches within the factories. New sustainable fabrics have been developed, along with sewing threads and natural dyes, which contribute to decreasing the negative impacts of the garment industry over the planet.

Within the designing sphere, the Zero Waste method started to flourish for the past decade. Approaching an ancient manufacturing technique and using creative fabric manipulation methods, it has led to a series of solutions that reduce the fabric scraps, in most cases, completely [1].

This new way of approaching the pattern drafting has been introduced within the 21st century [2], but it dates back in the ancient times, if we were to consider the traditional Kimono – for manufacturing this type of clothing, a rectangular fabric was needed, using it completely and thus, avoiding fabric waste.

Moreover, virtual prototyping software have been developed and launched for use in the past years. These programs aim to assist in sustainable methods, by displaying the final product on the screen. This enables to have a better view of the fitting, pattern accuracy or fabric drape, without having the physical sample manufactured. Important resources such as time and energy are reduced when digitally assembling a clothing item.

This study has been made by analysing the information gathered, a series of testing and simulating the final virtual prototypes developed along the process.

2. MATERIALS AND METHODS

2.1 Materials

For the present paper, digital resources have been mostly used to display the consumer's perception of what is known as sustainable fashion, its behaviour regarding garment disposal, as well as testing the pattern drafting method and simulating the end result within the 3D space.

Consumers have been addressed by an online survey, which contained a series of key questions, meant to bring to light the consumer's way of thinking and awareness regarding everyday life textiles.

The patterns have been drafted using the dedicated software Gemini Pattern Editor and garments were simulated by using the CLO 3D virtual fashion software.

The paper has been developed as a result of researching the already existing techniques, analysing the results and spotting the downsides of each experimentation. Theoretical information has been collected from studying current literature, complemented by notes gathered from personal practice.

2.2 Methods

2.2.1. Analysing the consumer's behaviour

When asked, a number of participants have claimed that they have heard of sustainability within the fashion field. More than a half of them are somewhat familiar to the term, which gives a clue regarding the consumer's information. However, despite being informed, most of them do not hold the proper knowledge of what does sustainability stand for.

The following question gave much clearer information regarding the comprehension of this term: most of them associated sustainable clothing items to high prices. This stands for the fact that quality and price are reliable. Most consumers aim to purchase good quality items

on lower prices, and that's because they are not informed regarding the costs of manufacturing and producing the fabric, the thread and the garment itself, which also includes labour and shipping. This conclusion stands from the following simple analysis: 60% of the consumers have heard of "sustainability" before, but only 47% of them knew what it stands for. Thus, a quantum of 13% of them is not properly informed nor do they hold the correct pieces of information regarding this matter.

The participants have been asked about the way they dispose of their unwanted garments. This question is meant to offer a clear image of their behaviour. Over 50% of them hand their clothing to others in need, by donating them to charity or younger family members, friends, acquaintances (figure 1). This gives a clue regarding the way the consumer cares for its garments, assuming that their donated items are still in good condition. This way of disposing seems more comfortable and efficient, but only when it comes to a certain category of garment. Ideally, the clothes that are worn out, torn or have any sort of damage should be disposed at local collecting bins that specialize in sorting and recycling. However, unfortunately that's not the case, since 5% of the consumers questioned have claimed that they simply throw away their unwanted clothing. This highlights the poor level of information, education of the consumers, as well as the poor fabric waste management.

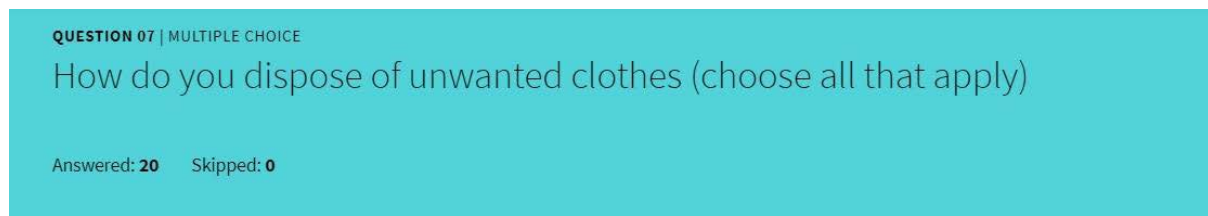


Figure 1. Data collected from the consumer regarding their clothing disposal habits

2.1.2. Drafting the Zero Waste patterns

This Zero Waste pattern drafting method consists of altering the pattern shapes of an already existing pattern set. Thus, there's been a transition from a regular fit to a looser fit. This method approaches in a different way the Zero Waste pattern drafting: rather than starting from a simple rectangle that would represent the lay plan, the patterns have been amended in order to fit within and form a lay plan [3]. The pieces have been modified and reshaped, starting from a classic form and obtaining a geometrical configuration. This procedure allowed the direct and evident observations of the differences between classic and zero waste patterns, based on fabric consumption, lay plan efficiency and body fit. Moreover, the final design of each style has been established during the process, in accordance to the pieces' permeability. The process consists in a series of consecutive systematic steps, that can't be skipped nor replaced.

Simplifying the pattern's geometry consisted in reducing the French curves as much as possible, keeping in mind the intention of creating a clothing item that's more than a square and less than a typical garment piece. In some cases, the already existing curves have been kept in order to serve to a better pattern interpolation and were used as joining edges for other pattern pieces that were further used for practical or aesthetic purposes.

The most crucial step was to define the seam allowances value – pattern nesting is highly influenced by the cutting perimeter. A method studied has revealed the solution of using variable values for seam allowances [4]. However, given the poor aesthetic on the inside of the garment resulted by using such technique, this doesn't stand for unlined garments. Moreover, the sewing technology is being limited to a simple stitch, with possible serged edges. Considering these possible results, all seam allowances that were to be assembled have been defined with constant values.

It's important to mention the fact that in order to avoid having an exaggerated fit, some garments designed have been modelled on the important areas of the body (for example, on the waistline) by using rows of elastic thread. This solution also allowed for the specific pattern pieces to be as wide as it needed to fit and match for an efficient lay plan, acknowledging that they will shape the body by later on. Other shape manipulation techniques have been used, such as pleats on the shoulder line, elasticated cuffs and shirring rows sewn on the waistline, as shown in the figure 2.



Figure 2. Example of an accurate fitting obtained by using shape manipulation solutions: pleats on the shoulder line, to maintain a regular shoulder length and shape, elastic thread close the sleeve hem, for aesthetic and practical purposes and elastic threads on the waistline

3. RESULTS AND DISCUSSIONS

This Zero Waste pattern drafting method has been applied to several clothing items, adapted to the garment's functionality and design. Given the example of a woollen coat, the classic basic patterns have been drafted from scratch. The geometrical patterns have been further developed, in order to gain the required jigsaw placement, and thus result in two different, yet similar pattern sets which have been used for further analysis. The final shapes are shown in figures 3 and 4.

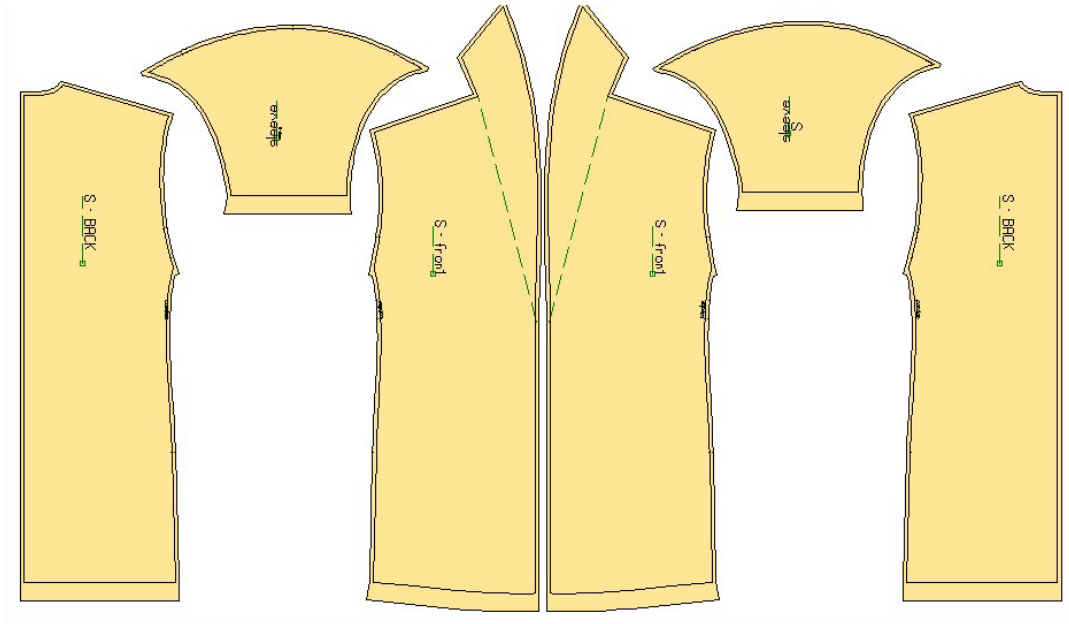


Figure 3. Basic patterns for the classic woollen coat

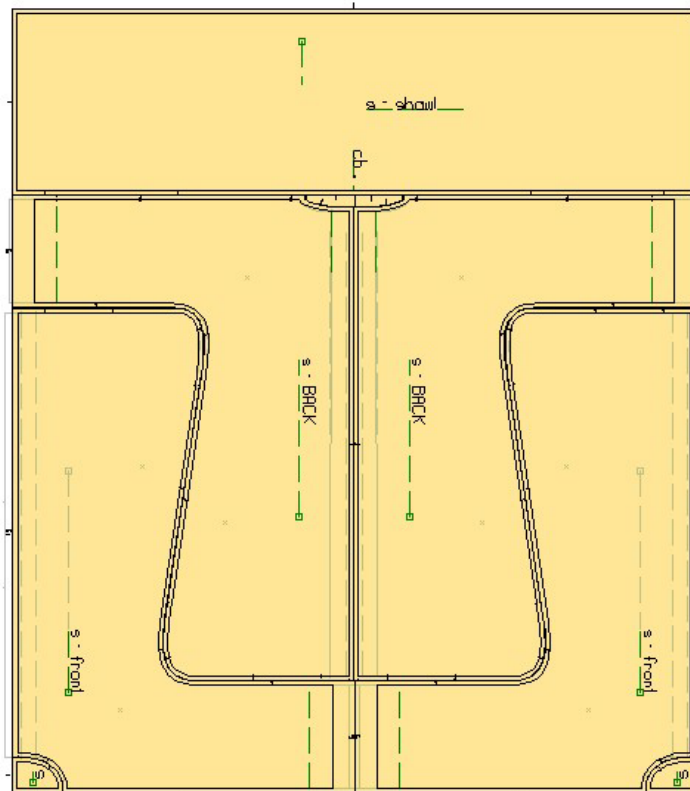


Figure 4. Zero waste patterns for the woollen coat

Once the patterns were defined for both cuts, the next step was to generate individual lay plans, and thus gather the first pieces of information that highlighted the differences in fabric consumption and nesting efficiency. The values obtained have been summed in the table 1.

Table 1. Differences between two types of patterns for the same clothing item

Woolen Coat	Classic cut efficiency [%]	Zero waste cut efficiency [%]	Classic cut fabric rating [m]	Zero waste cut fabric rating [m]
	68.05	95.2	2.7	1.75

Analysing these results brings a clear insight regarding how much the fabric waste can be reduced when approaching different drafting methods.

By examining the efficiency values, it is clear to see that the overall fabric consumption when using zero waste patterns increased by 71,4%, which signifies that the pattern pieces have been joined and placed together with little space between them.

In the same time, the fabric consumption has decreased by 64.8%, meaning that it takes less fabric to cut the zero waste patterns, hence their jigsaw placement. It's important to mention that both pattern sets have been nested on the same fabric width, figures 5 and 6.

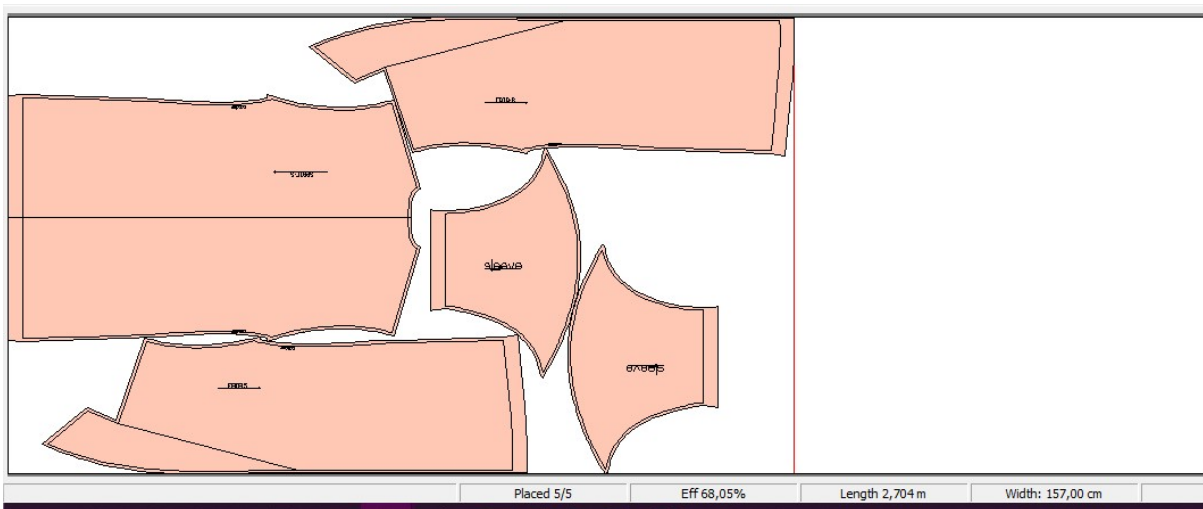


Figure 5. Lay plan for the classic coat patterns

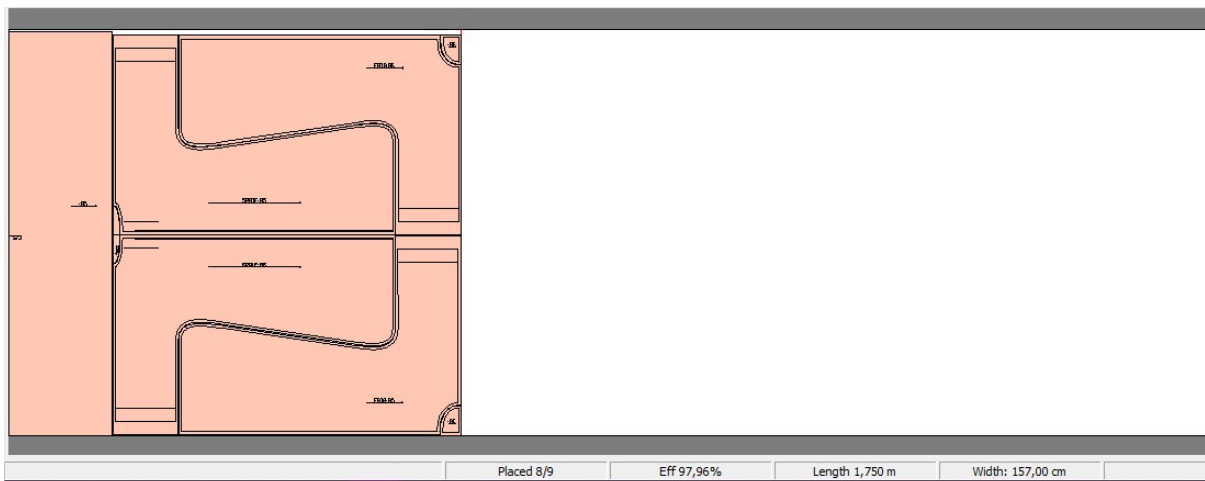


Figure 6. Lay plan for the zero waste coat patterns

Once the data have been collected, the second part of the process was approached: aesthetics. The garment has been digitally assembled, fitted and finished by using the virtual prototyping software. The avatar's measurements correspond to the Alvanon size 36 EU. The patterns have been drafted for size S (36 EU).



Figure 7. Simulated virtual sample for the woollen coat: classic fit to the left and zero waste fit to the right

5. CONCLUSIONS

It takes both creativity and know-how to develop zero waste pattern sets for almost any type of garment item. Apart from establishing the final design during the pattern drafting process, the finishing and manufacturing technology must also be kept in mind. Each step is framed into a series of future possibilities; therefore, the technological and design matters are co-dependent and complementing each other.

The results haven't been regarded as virtual prototypes, but as real physical samples that can be worn, and thus must have clean finishing and true practical purposes, above all. Edges finishing, assembling and hem edges – all of these matters have been taken into account during the drafting process and whilst defining the seam allowances.

Applying this method has proven to be an efficient solution for reducing fabric waste and, also, designing unique clothing that hold the possibility to refresh the fashion market across the world.

REFERENCES

[1] Gwilt, A., *Zero Waste Fashion Design: Approaches and strategies to reduce textile waste*, Sheffield Halam University, UK, 2016

- [2] Jalil, M., Hosseini, S., *Quest for the fashion market: Zero Waste skirt design as a solution toward sustainable pattern making*, In: The Chitrolekha Journal on Art and Design, 2020, 4, 2, 2, <https://dx.doi.org/10.21659/cjad.41.v4n205>
- [3] Rissanen, T., McQuillan, H., *Zero waste fashion design (Vol. 57)*, In: Bloomsbury Publishing, 2016
- [4] Ejeimi, S., *Grading zero waste design using digital and virtual methods*, Kansas State University, USA, 2020



CARBON FIBRE ALIGNMENT FOR REINFORCED COMPOSITES USING EMBROIDERY TECHNOLOGY

DOI: 10.35530/TT.2021.14

J. Domenech-Pastor^{1*}, P. Diaz-Garcia², D. Garcia³

¹Smart Textiles and Digitalization, Asociación de Investigación de la Industria Textil - AITEX, Spain

(E-mail: jdomenech@aitex.es)

²Ingeniería Textil y Papelera (DITEXPA), Escuela Politécnica Superior de Alcoy, Universitat Politècnica de València (UPV), Spain

(E-mail: pdiazga@txp.upv.es)

³Instituto de Tecnología de Materiales (ITM), Escuela Politécnica Superior de Alcoy, Universitat Politècnica de València (UPV), Spain

(E-mail: dagarga4@epsa.upv.es)

Abstract: Composites are materials formed by the combination of two or more components that acquire better properties than the ones obtained by each component on its own. Composites have been widely used in the industry due to its light weight and good mechanical properties. To improve these properties several layers of reinforced material (e.g., carbon fibre) are overlapped which produce an increase in the fibre consumption. In this sense Tailored Fibre Placement (TFP) embroidery can offer good opportunity to reduce the consumption of reinforced fibre while improving the mechanical properties due to the alignment of the fibres in the effort direction. This study analyzes the performance of carbon fibre reinforced composites with Polyester resin made with TFP embroidery technology against flexural strength efforts and without using plain woven fabrics to demonstrate that the use of reinforcement fabrics in composites can be optimized by a curved alignment of the fibers. Two different structures were embroidered with TFP technology, one simulating a woven fabric with straight unidirectional alignment of fibres in horizontal and vertical direction, and a second structure made with curvilinear alignment of carbon fibers. After the study of the flexural mechanical properties an improvement of 18% was obtained in maximum flexural strength.

Keywords: composites, embroidery, resin transfer moulding, tailored fibre placement, textile

1. INTRODUCTION

Composites have been used from centuries ago when first humans combined mud and straw to make adobe bricks that were used in the construction of houses. It was not until the twentieth century, when the first polymeric composite materials appeared that began to be used in automotive and aeronautical applications. Over the years, the use of these composite materials has become widespread, as they allow, with equal volume and lower density, to obtain lighter pieces with similar characteristics and in some cases with better mechanical properties than with other materials such as steel.

Glass and carbon fibers are generally the most widely used reinforcement fibres used in the composites industry due to their high strength/weight ratio [1]. In general, they include high tensile strength, good compressive strength, high tensile modulus, low density,

good thermal resistance, low thermal expansion, good electrical and thermal conductivity, and chemical resistance [2,3].

Composites reinforced with textile fibres are used in the industry due to its good properties of high strength and light weight [4]. Textile reinforcement fibers are aligned in one single direction, for this reason it is needed to combine different layers of textile fibers aligned in different directions to improve the isotropy of the composite material and its strength in the desired directions. This reinforcement textiles are limited in terms of fiber alignment due to the plain weaving technology used and the only possibility to vary the orientation and alignment of the fibers is using axial fabrics which allow to place the fiber in different angles, but all of them unidirectional in straight line, without any curve [5,6].

To obtain composites with good mechanical properties it is necessary to combine and overlap different layers of reinforcement fibers in different directions. This overlapping increases the time for processing the composite and it depends on the know-how and experience of the worker to place the fiber and reinforcement fabric all over the surface of the mould. This is a critical process as composites have better properties in the direction in which the reinforcement fabrics are aligned [7]. In this sense, Tailored Fiber Placement technology (TFP) allows the placement of the reinforcement fibers that permit to produce composites with a variable axial geometry, obtaining laminar structures with fibers aligned in multiple directions to increase the mechanical performance [8]. Tailored Fiber Placement technology is capable of manufacturing embroidered textiles with a variable axial fiber pattern by using adapted embroidery machines. This presents a novel concept for the simulation and optimization of curvilinear fiber-reinforced composites, where the novelty is based on the local optimization of both the fiber angle and the intrinsic thickness accumulation concomitantly. This is also known as Direct Fiber Path Optimization (DFPO) which is based on Tailored Fibre Placement. The key results show a clear improvement compared to the current frequently used approach where principal stress trajectories are applied for a variable axial reinforcement pattern [9]. This article confirms that in the case of structural parts that do not suffer tension stresses with conventional main trajectories (eg. tensile stress at 90°), it is necessary to arrange the reinforcing fibers in curvilinear trajectories (variable axial) in order to improve their mechanical properties.

2. OBJECTIVES

TFP embroidery technology can place the reinforcement fibres in the location where material is going to suffer more efforts and can adapt to the shape of the final object. In contrast, in the traditional composites manufacturing, the excess of fibre must be manually cut to adapt it to the shape of the desired object. This traditional manufacturing process is not very efficient in terms of fibre consumption and amount on manual tasks as it cannot be automated.

This study has the objective to evaluate the performance against flexural strength efforts of carbon fiber reinforced composites using TFP technology and without using plain woven fabrics and to demonstrate that the consumption of reinforcement fabrics (carbon, glass fibers, etc.) can be optimized by a curved alignment of fibers. Two textile structures were embroidered with TFP technology. First structure named as S-TFP (Straight TFP), simulating a woven fabric combining carbon fibers with straight unidirectional alignment in horizontal and vertical direction. The second structure named as C-TFP (Curvilinear TFP), was made with curvilinear alignment of carbon fibers, replacing the straight unidirectional fibers in horizontal direction (weft direction) by curvilinear fibers (figure 1).

3. MATERIALS AND METHODS

3.1 Materials

The carbon fiber used to develop the composites was 880TEX continuous 12K multifilament, embroidered on a 0.25 mm thick 30 g/m² polypropylene (PP) non-woven substrate. The resulting S-TFP embroidered textile had a weight of 646.79 g/m² and the C-TFP 524.15 g/m².

As matrix of the composite, a polyester (PES) resin DCPD (DiCicloPentadiene Resin) was used, to avoid contact with VOC (volatile organic compounds).

Vacuum-assisted RTM (Resin Transfer Moulding) equipment and the embroidery machine of the manufacturer ZSK were used for the formation of the composite. To cut the samples according to UNE-EN ISO 527-1:2019 a CNC machine (Control Computerized Numeric).

Finally, for the flexural strength test, the universal testing machine was used. For the flexural tests, the samples had a section of 10 x 1.2 mm.

3.2 Composites manufacturing process

First step consisted of embroider the carbon fibre on the PP substrate according to the designs defined S-TFP and C-TFP (figure 1). Once the fibre is embroidered, it is necessary to cut the excess of PP substrate to introduce the embroidered textile in the mould to proceed with the injection of the PES resin (figure 2).

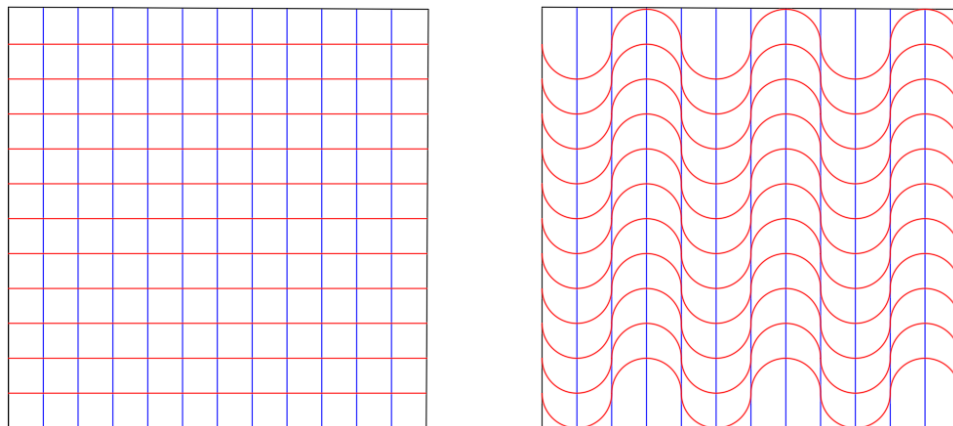


Figure 1. Designs S-TFP (left side) and C-TFP (right side); weft direction in red colour and warp direction in blue colour

Then, when the resin is injected, obtaining the final composite with the shape of the mould, in this case of study a square shape. Later, it is necessary to cut the samples according to the standard UNE-EN ISO 178:2020 for flexural effort with the 200 W Mini CNC 3040 machine (figure 3).

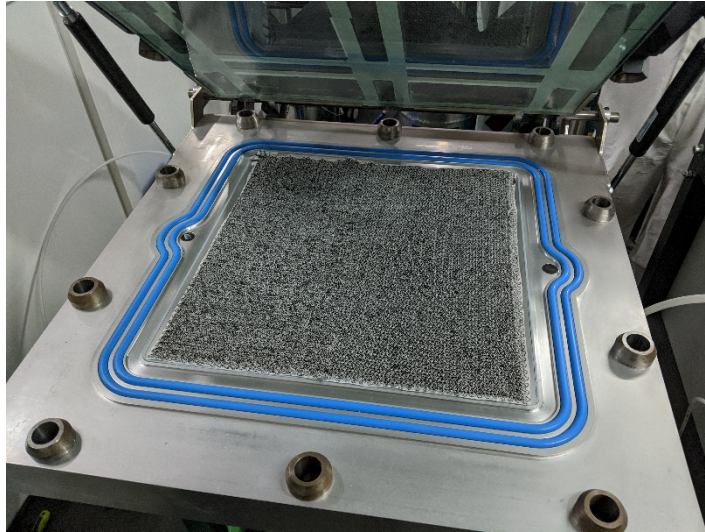


Figure 2. Non-woven PP substrate with embroidered carbon fibre in the RTM machine

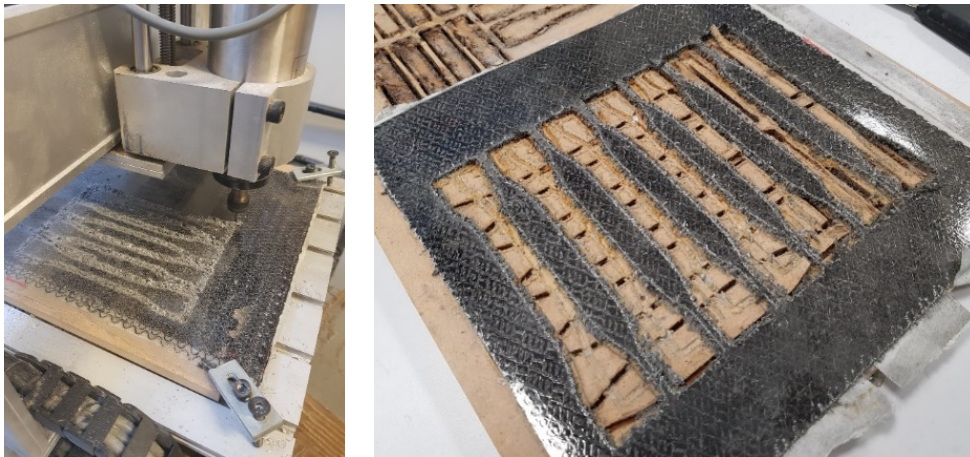


Figure 3. Samples cutting process with a mini CNC machine

3.3 Testing process

For the characterization of flexural effort, it was used the Universal Testing Machine (IBERTEST ELIB-50-W) to evaluate the samples. Due to the characteristics of the materials and the size of the samples, the 50 kN cell was selected and a distance between supports of 60 mm was set (figure 4).

3. RESULTS AND DISCUSSIONS

The obtained results were very promising as important improvements are observed in C-TFP even using less amount of reinforcement carbon fibre. In this case, C-TFP weights 122.64 g/m^2 less than S-TFP which is a reduction of a 19% of fibre consumption.

In table 1, it is observed that curvilinear designs like C-TFP improve flexural properties, increasing the maximum flexural strength till 105 MPa against the 89 MPa obtained by the S-TFP, which represents an improvement of 18%. In terms of elasticity, the Young Module also increases when using curvilinear fibres. In this case of study, curvilinear samples (C-TFP) obtained a Young Module of 3.234 MPa in contrast with the 2.352 MPa obtained by the S-TFP that does not use curvilinear fibres. This means that the C-TFP is more elastic and more resistant than the S-TFP as the Young Module and the

Flexural maximum Strength are higher. This improvement represents an increase of 37% in the Young Module for the C-TFP.



Figure 4. Universal Testing Machine used for flexural tests

Table 1. Flexural test results

Sample	S-TFP		C-TFP	
	Young Module (MPa)	Max. Strength (MPa)	Young Module (MPa)	Max. Strength (MPa)
1	2.488	93	3.405	108
2	2.333	85	3.420	105
3	2.234	89	2.876	102
Average	2.352 + 128	89 + 4	3.234 + 310	105 + 3

It is observed in the results showed in table 1 that samples with curvilinear alignment of fibres (C-TFP) improves the flexural strength properties.

One of the reasons which can explain this improvement of flexural properties with less amount of reinforcement fibre is the phenomenom of efforts decomposition in normal forces (figure 5).

When a generic effort called “F” is applied in warp direction a response is generated in the same direction but in the oposite sense. In the case of the S-TFP the response obtained in the weft direction is 0 as do not offers opposition or resistance.

$$F = F2 + F3 = F2 + 0 = F2 \quad (1)$$

However, in the case of C-TFP the effort applied in the curved fibres is decompose into normal forces improving the behaviour of the composite against an effort “F”.

$$F = F2 + F1y = F2 + F1 \cdot \text{sen}(\alpha) \quad (2)$$

This is the reason why composites reinforced with curved fibre alignment offers a better response againts flexural efforts even using less percentage of reinforcement fibre.

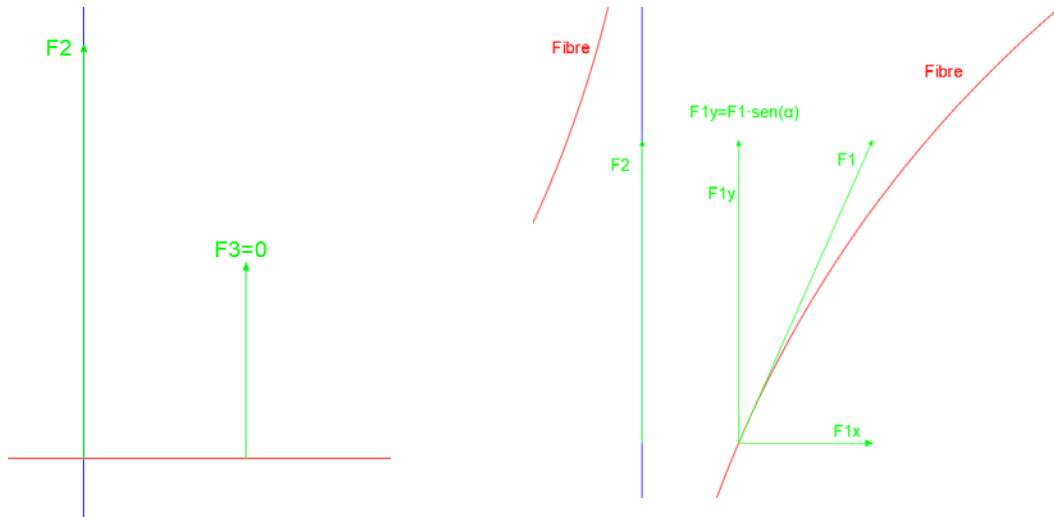


Figure 5. Schema of effort decomposition; on the left S-TFP and on the right image C-TFP

5. CONCLUSIONS

Composites with straight axial fibre placement like S-TFP have a good behaviour and good mechanical properties when the stress goes in the same direction than the fibre. In contrast, they obtain bad results when the stress is applied in a different direction (e.g., perpendicular) to the fibre. On the other hand, composites with aligned curvilinear fibres obtain better results due to the superposition of forces ($F_2 + F_{1y}$) and the phenomenon of loads decomposition into normal components (vertical and horizontal) as described in figure 5 and equation 2 along the fibres and interface of the resin matrix. This decomposition of efforts explains why the maximum flexural strength is higher in C-TFP than in S-TFP, since the added forces in C-TFP are greater than the force supported by S-TFP.

In this case of study, it is obtained an improvement of 18% of flexural maximum strength, using the same amount of fibre in both composites or even less fibre like in C-TFP and without increasing the costs. This increase of 18% can be considered very interesting in some industrial sectors and for high technique and added value applications like in automotive or aerospace industry. In this sense, C-TFP is less rigid than sample S-TFP and has a more elastic behaviour.

Also, for some specific applications not only strength but also elasticity is a very important factor to be considered due to its implications in aerodynamics. In this sense, curved oriented fibres has lot of potential as can improve both, elasticity and strength.

Nowadays this new and promising research line is researching new textile structures made with Tailored Fibre Placement technology with the objective to obtain composites with better mechanical properties.

ACKNOWLEDGEMENTS

This study has been developed within the framework of the LIGHTCOMP 2021 project. The LIGHTCOMP 2021 project has the support of the Conselleria d'Economia Sostenible, Sectors Productius, Comerç i Treball de la Generalitat Valenciana through IVACE, and is co-financed by the ERDF funds from the EU, within the ERDF Operational Program of the Valencian Community 2014-2020. (IMDEEA/2021/44).

REFERENCES

- [1] Yukseloglu, S.M., Canoglu, S., *Natural fibre composites: a review on flax fibres*, In: Annals of the University of Oradea. Fascicle of Textiles, Leatherwork, 2017, 1, XVIII, 137-142
- [2] Chand, S., *Review Carbon fibers for composites*, In: Journal of Materials Science, 200, 35, 1303-1313, <https://doi.org/10.1023/A:1004780301489>
- [3] da Rocha, R.J.B., Pina, L.M.P., Gomes, M., Sousa, J.P., *Evaluation of impact resistant composites for aircraft cockpit*, In: Materiales Compuestos, 2020, 4, 1, 1-9
- [4] Keskin, R., Gocek, I., Ozkoc, G., *Polyamide 6.6 composites reinforced with short glass fibers*, In: Annals of the University of Oradea. Fascicle of Textiles, Leatherwork, 2013, 1, XIV, 61-65
- [5] Irina, M.M.W., Azmi, A.I., Tan, C.L., Lee, C.C., Khalil, A.N.M., *Evaluation of mechanical properties of hybrid fiber reinforced polymer composites and their architecture*, In: Procedia Manufacturing, 2015, 2, 236-240
- [6] Liang, Y., Wang, H., Gu, X., *In-plane shear response of unidirectional fiber reinforced and fabric reinforced carbon/epoxy composites*, In: Polymer Testing, 2013, 32, 3, 594-601
- [7] El-Dessouky, H.M., Saleh, M.N., Gautam, M., Han, G., Scaife, R.J., Potluri, P., *Tailored fibre placement of commingled carbon-thermoplastic fibres for notch-insensitive composites*, In: Composite Structures, 2019, 214, 348-358
- [8] Villegas, D.F., Pedraza-Rosas, S.L., Toloza-Meza, S.A., *Tensile mechanical behavior of a polymeric composite reinforced with 4-axial carbon fiber woven*, In: Journal of Physics: Conference Series, IOP Publishing, 2019, 1386, 1, 012034
- [9] Bittrich, L., Spickenheuer, A., Almeida, J.H.S., Müller, S., Kroll, L., Heinrich, G., *Optimizing variable-axial fiber-reinforced composite laminates: the direct fiber path optimization concept*, In: Mathematical Problems in Engineering, 2019



SELECTIVE DEPOSITION OF NANOFIBERS NET ON TEXTILE STRUCTURES

DOI: 10.35530/TT.2021.34

D. Minguez, E.B. Belda, I. Montava, P.D. García, M.B. Aracil*, J.G. Payá

DITEXPA, GIITEX, Universitat Politècnica de València, Spain

(E-mail: damingar@epsa.upv.es, evbobel@upv.es, imontava@txp.upv.es, pdiazga@txp.upv.es, maboar@txp.upv.es, jaigispa@txp.upv.es)

Abstract: Nanotechnology has evolved in the last years and nowadays there are many technologies related with the development of nanoparticles (NPs) or nanofibers (NFs). Due to the wide variety of polymers and diverse applications, filtration, medicine, cosmetic, etc., the study of those NFs is still of interest nowadays. In this work the NFs net created from electrospinning is used as a coating for fabrics. The aim of this work is to demonstrate how fibres are placed on the fabrics and if there is a tendency or they are located randomly. Two different fabrics were used a 100 % cotton plain 115g/m² and a 100% polyamide knitting fabric 60 g/m². A PVA solution (9% w/v) was used to create NFs which were placed on the fabrics. This solution was prepared by heating water at 80° C till complete solution of the polymer. Electrospinning was designed for a vertical collector with 15 cm distance from the needle. The flow rate was 0,5 mL/h with 15 or 20 kV for 15 minutes. Results evidenced the tendency of NFs net to be located on the fibres and consequently we could conclude the fabric is designing the position where the fibres would be placed. Furthermore, we could demonstrate that the presence of a fabric with reduced density implies deposition of NFs on both the fabric and the collector.

Keywords: electrospinning, located, nanofiber, substrate

1. INTRODUCTION

Nanotechnology has evolved in the last years and nowadays there are many technologies related with the development of nanoparticles (NPs) or with nanofibers (NFs). There is a wide field of application for NFs nets, they can be used for filtration [1,2], biomedicine [3-5] or even for protection against COVID-19 [6-8].

NFs net can be made of different polymers such as polypropylene (PP) [9], polyamide (PA) [10], polyvinyl alcohol (PVA) [11], Polylactic acid (PLA) [12], etc.

Electrospinning is a technique based on the use of electrical forces to produce polymeric fibres of small diameter, comprised in a range that varies from micrometres (10-100 µm) to nanometres (10 x 10⁻³ - 100 x 10⁻³ µm), and with a high specific area, in a relatively simple and inexpensive way [13].

The technique consists of the application of a high electrostatic field between a polymeric solution and a collecting surface. The positive pole is attached to an injection system, in this case the needle (metallic capillar) and the negative pole to a metallic plate or collector (connected to ground) which is generally between 5 cm and 30 cm away from the metallic capillar [13-14]. On the collector the nanometric fibres are deposited, forming a fabric (nonwoven) with a characteristic texture, density and color [14].

The liquid drop remains attached to the tip of the capillar thanks to the surface tension until the repulsion is greater and causes a force in the opposite direction to the contraction of the drop. As a consequence of this application, an electrified meniscus known as the Taylor

Cone is formed, it is due to polarization and charge, causing a transverse and a normal force. As the cone accelerates the elongation process, it reaches a point where the tangential and normal components are equal, at this time the cone solidifies creating fibres and depositing them on the collector plate [13-14].

Some parameters affect electrospinning, they can be classified into three groups: dissolution parameters (polymer solution), process parameters and environment parameters. All of them influence the morphology and properties of the fibres [13-14].

1.1 Solution properties

- *Concentration*: it is one of the most determining parameters in the size and morphology of the fibres. Concentration affects both viscosity and surface tension. If the concentration is considerably high, apart from making it difficult for the solution to pass through the capillary, the diameter of the fibre may increase. On the other hand, if there is a low concentration of polymer, the solution will be so liquid that the drops will break before reaching the collecting plate due to the effect of surface tension [13-14].

- *Molecular weight*: The molecular weight of the polymer has a significant effect on rheology and electrical properties such as viscosity, surface tension, conductivity, and dielectric strength. It has been observed that low molecular weight solutions tend to form beads rather than fibres, and a high molecular weight one tends to form fibres with large diameters. The molecular weight also influences the number of polymer chain entanglements in a solution, therefore, the viscosity and entanglement of the chain play an important role in the electrospinning process [14-15].

- *Viscosity*: As it is also named in the concentration, the viscosity plays a very important role in electrospinning, when the viscosity is very low there will not be a continuous formation of fibre, the drops will break before reaching the collector. On the other hand, when the viscosity is relatively high, the polymer could present difficulties in its passage through the capillary [13-15].

- *Surface tension*: The surface tension will depend on the polymer and the solvent used. It has a relevant role in obtaining fibres without the presence of beads. The surface tension determines the upper and lower limits of the electric field, if all other variables are kept constant [14].

- *Conductivity*: The conductivity of the solution is determined by the type of polymer, the solvent used, and the availability of ionizable salts [14]. Solutions with high conductivity will have greater capacity to carry charges than those with low conductivity. The addition of salts to the solution increases the conductivity and therefore the electrical force for stretching the jet, which means obtaining fibres with a smaller diameter [13]. The lack or low electrical conductivity of the solution causes the elongation of the jet by the electrical force to be insufficient, and therefore, prevents the production of uniform fibres.

- *Dielectric effect of the solvent*: The solvent performs two jobs within the electrospinning process; first, it dissolves the polymer molecules to form the electrically charged jet, and second, it carries the dissolved polymer molecules to the collector [13].

Because of this, generally a solution with good dielectric properties reduces the bead formation and also the diameter of the resulting fibres.

1.2 Process parameters

They are the parameters that can be modified during the process. These are parameters that can be easily manipulated directly from the displays of the machine that we use.

- *Voltage (applied voltage)*: Voltage is one of the most fundamental parameters, since only after reaching the threshold voltage does the formation of fibres occur [14]. It has been shown that when applying higher stress values, a greater stretching of the solution is allowed since the electrostatic repulsive force (Coulomb force) increases, causing a reduction in the

diameter of the fibres. Also increasing the voltage favours the rapid evaporation of the solvent. On the other hand, increasing the voltage is directly related with increasing the probability of obtaining fibres with defects (beads) [13-14].

- *Flow*: The flow or outlet flow is also an important parameter of the process. A lower flow rate would be desirable as it gives the solvent more time to evaporate, thus preventing the formation of defects in the fibre. On the other hand, when the outflow increases there is an increase in the diameter of the fibres and in the size of the defects. The minimum flow rate to achieve a stable Taylor cone is the one that should be maintained to avoid fibre defects and allow the solvent to evaporate [13-14].

- *Needle-collector distance*: A minimum distance is required between the needle and the collector; this is the minimum distance that must be given to the fibre to allow the solvent to evaporate. On the other hand, over very long distances, the fibres can break under their own weight or bead formation.

1.3 Room parameters

- *Temperature*: Temperature can decrease the evaporation time of the solvent. In addition, there is a direct relationship between temperature and viscosity, the higher the temperature, the lower the viscosity. The decrease in viscosity, as it was explained previously, can cause a decrease in the diameter of the fibre [13-14].

- *Humidity*: High humidity in the environment can cause small pores on the surface of the fibres due to the condensed water deposited on them as they go from the needle to the collector, having an influence on the morphology of the fibres, especially when working with volatile solvents [13]. On the other hand, a low humidity rate can cause the solvent to evaporate very quickly, causing that in some cases the process must be carried out in the shortest possible time in order to prevent the solution is dried at the tip of the needle obstructing it [14].

Due to the wide variety of polymers and diverse applications the study of those NFs is still of interest nowadays. In this work the NFs is used as a coating of fabrics. The aim of this work is to demonstrate how PVA NFs are placed on the fabrics surface and if there is a tendency created by the geometry of the collector surface, or they are located randomly despite the surface roughness on the collector. Table 1 summarizes the most important parameters with influence on NFs.

Table 1. Summary of parameters influence on NFs.

PARAMETER	Tendency	Behaviour
Solution parameters		
Concentration	Increase	Difficult for the solution to pass through the capillary
	Decrease	Drops before reaching the collector
Molecular weight	Increase	Difficult for the solution to pass through the capillary
	Decrease	Drops before reaching the collector
Viscosity	Increase	Difficult for the solution to pass through the capillary
	Decrease	Drops before reaching the collector
Surface tension	Increase	No beads in NFs
	Decrease	Beads presence in NFs
Conductivity	Increase	Reduction in fibres diameter
	Decrease	Electrostatic forces derive into jet enlargement and it is not possible to obtain NFs
Process parameters		
Voltage	Increase	Thick fibres, jet distosion, beds presence
	Decrease	Solution does not reach the collector
Flow rate	Increase	Thicker fibres, higher size for beds.
	Decrease	Solvent evaporation takes longer, homogeneous fibres.
	Increase	Broken fibres due to its weight.

Needle-collector distance		Higher enlargement of the solution. Thinner fibres
	Decrease	Not enough time for solvent evaporation, wet fibres reach the collector.
Environment parameters		
Temperature	Increase	Solvent evaporates too quickly and dry polymer appears in the needle.
	Decrease	Solvent does not evaporate. Difficult for the solution to pass through the capillary
Humidity	Increase	Solvent does not evaporate properly. Porous NFs
	Decrease	Fast evaporation of solvent. Dry polymer appears in the needle.

2. MATERIALS AND METHODS

2.1 Materials

A Nanospider system supplied by Bioinicia was used to produce the nanofibers. Nanofibers were made of Polyvinyl alcohol (PVA) Mw 61000 g/mol, supplied by Sigma-Aldrich. Solutions were prepared with distilled water.

The collector of the Nanospider system was covered by different fabrics. One of the fabrics was a plain fabric 100% cotton, 115 g/m². The other one was a 100% polyamide knitting fabric 60 g/m².

2.2 Methods

Nanofibers were electro spun from polymer solution containing 9% w/v which was prepared with PVA and distilled water at 80° C until complete solution. The electrospinning process was conducted with the same Nozzle-collector distance (15 cm) The collector was placed vertically. Identical flow rate (0.5 ml/h) was used but different Voltage (12, 15 or 20 kV) for 15 minutes.

Scanning Electron Microscopy (SEM) was used to observe the fabrics surface and the NFs formation. FIB microscope from Zeiss was used as a Scanning Electron Microscopy (SEM) to analyse the fabrics' surface at 1.5 kV and a suitable magnification. Samples were previously sputtered with a gold/platinum coating.

3. RESULTS AND DISCUSSION

As it has been explained in the introduction section the nanofibers are placed on a collector. In this study we covered the collector system with two different fabrics, a weave with a plain rapport, and a Knitting one with low density. The electrospun fibres were placed on different fabrics a plain wave or a knitting one. Initially the voltage should be adapted in order to avoid the presence of beads on the NFs. Figure 1a shows the presence of polymer on the cotton fibres without NFs formation when the voltage is 12 kV. Polyamide fabric (60 g/m²) worked perfectly with 15 kV but cotton due to its higher density (115 g/m²) interfered on the voltage at the collector and 15 kV produced NFs but plenty of beads (figure 1b), and consequently it should be increased up to 20 kV (figure 1, c).

Figure 2 shows the microscopy images where it can be appreciated the coating of PVA nanofibers regularly placed on the surface of cotton fibres and with no beads. Results evidenced that the nanofibers were placed on the fabric acting as a nanospider net coating the fabric, which was also demonstrated by some authors [11]. This web of NFs is placed on the collector or on the fabric when the fabric is covering the collector.

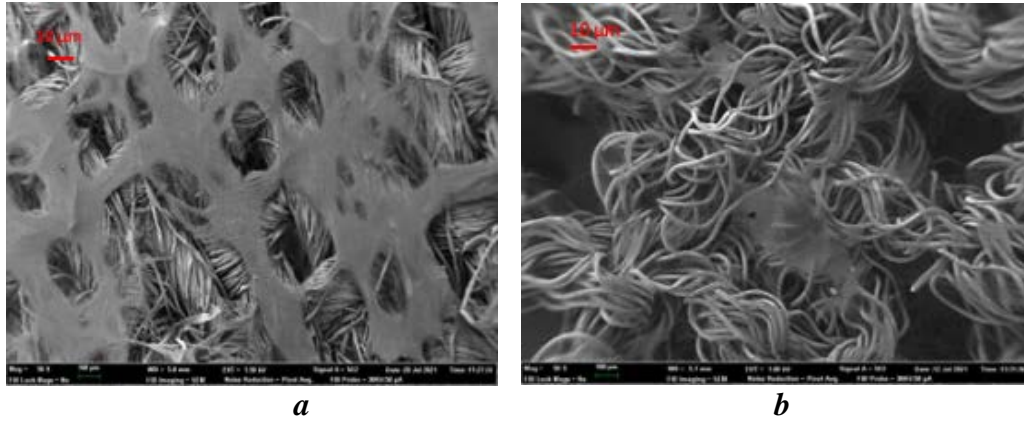


Figure 3. PVA nanofibers coating fabrics: a - plain fabric; b - knitted fabric

Nanofibers width is measured and results reveal there is a similar value obtained for nanofibers deposited on both fabrics, 128 nm for the weaving and 114 nm for the knitting. As the NFs are deposited on the fibres, it is clearly observed there is a higher presence of the nonwoven on the weave than on the knitted fabric due to the higher number of fibres. This is not due to the fabric technology used, weaving or knitting structure it is due to the presence of yarns. Weaving or knitting will only influence on the paths created by the nanofibers.

Figure 4 shows the appearance of the collector once the knitting fabric was removed. It is clearly appreciated a spotted surface. The spots observed can be attributed to the nanofibers which were not placed on the knitting fabric as there was a small holes or spaces between yarns.



Figure 4. Spotted collector once the knitted fabric is removed from collector

It has been demonstrated there is a clear tendency of NFs to be deposited on the fibres from the fabrics. Figure 3 evidences the grid formed by the NFs net on the plain fabric created. Furthermore, the results showed it is possible to create a micronets on the collector when the fabric shows reduced density of yarns, as the NFs pass through the fabric pores.

4. CONCLUSION

The observation of fabric surface at low enlargement, once nanofibers coating was placed on the fabric's surface evidenced the effect that the substrate has on the deposition of nanofibers onto the fabric. Despite being the collector the one which attracts the polymer we have demonstrated that there is a preference for nanofibers to be placed on the yarns of the fabrics, and not only on the collector. Thus, when the density of yarns is not too high the nanofibers are placed both on the collector and on the fabric fibres.

This behaviour allows to conclude that a suitable design with a specific raport can deal

into a selective coating of nanofibers which can be used for different applications such as selective filtration, electric conductivity circuits, etc., or even to create specific NFs nets with concrete shapes throughout the pores of a fabric.

ACKNOWLEDGMENT

The authors would like to express appreciation for the support of the sponsor. The research has been funded by the INSTITUTO VALENCIANO DE COMPETITIVIDAD (IVACE), with the nominative line in favour of the Universitat Politècnica de València, approved by the Budget Law of the Generalitat Valenciana on the year 2021.

REFERENCES

- [1] Wang, X., Xiang, H., Song, C., Zhu, D., Sui, J., Liu, Q., Long, Y., *Highly efficient transparent air filter prepared by collecting-electrode-free bipolar electrospinning apparatus*, In: Journal of hazardous materials, 2020, 385, 121535.
- [2] Liu, C., Hsu, P. C., Lee, H. W., Ye, M., Zheng, G., Liu, N., Cui, Y., *Transparent air filter for high-efficiency PM 2.5 capture*, In: Nature communications, 2015, 6, 1, 1-9
- [3] Whang, C., Wang, X., Zhang, E., Yang, L., Yuan, H., Tu, W., Zhang, Y., *An epigenetic bioactive composite scaffold with well-aligned nanofibers for functional tendon tissue engineering*. In: Acta biomaterialia, 2018, 66,141-156
- [4] Ren, G., Xu, X., Liu, Q., Cheng, J., Yuan, X., Wu, L., Wan, Y., *Electrospun poly (vinyl alcohol)/glucose oxidase biocomposite membranes for biosensor applications*, In: Reactive and Functional Polymers, 2006, 66, 12, 1559-1564
- [5] Si, Y., Zhang, Z., Wu, W., Fu, Q., Huang, K., Nitin, N., Sun, G., *Daylight-driven rechargeable antibacterial and antiviral nanofibrous membranes for bioprotective applications*, In: Science advances, 2018, 4, 3, eaar5931
- [6] Khanzada, H., Salam, A., Qadir, M. B., Phan, D. N., Hassan, T., Munir, M. U., Kim, I. S., *Fabrication of Promising Antimicrobial Aloe Vera/PVA Electrospun Nanofibers for Protective Clothing*, In: Materials, 2020, 13, 17, 3884
- [7] Zhang, L., Li, L., Wang, L., Nie, J., & Ma, G., *Multilayer electrospun nanofibrous membranes with antibacterial property for air filtration*, In: Applied Surface Science, 2020, 145962
- [8] Chowdhury, M. A., Shuvho, M. B. A., Shahid, M. A., Haque, A. M., Kashem, M. A., Lam, S. S., Mofijur, M., *Prospect of biobased antiviral face mask to limit the coronavirus outbreak*, In: Environmental Research, 2020, 192, 110294
- [9] Cho, D., Zhou, H., Cho, Y., Audus, D., Joo, Y.L., *Structural properties and superhydrophobicity of electrospun polypropylene fibers from solution and melt*, In: Polymer, 2010, 51, 25, 6005-6012
- [10] Heikkilä, P., Harlin, A., *Parameter study of electrospinning of polyamide-6*, In: European Polymer Journal, 2008, 44, 10, 3067-3079
- [11] Koski, A., Yim, K., Shivkumar, S., *Effect of molecular weight on fibrous PVA produced by electrospinning*, In: Materials Letters, 2004, 58, 3-4, 493-497
- [12] Chen, Y., Lin, J., Fei, Y., Wang, H., Gao, W., *Preparation and characterization of electrospinning PLA/curcumin composite membranes*, In: Fibers and Polymers, 2010, 11, 8, 1128-1131
- [13] Diaz, R.E., *Micro/Nanofibras coaxiales de PLA/PEG para el encapsulamiento de microorganismos de interés biomédico y alimentario*, In: Ingeniería Química, Escola Tècnica Superior d'Enginyeria Industrial de Barcelona, 2015
- [14] Gandía, A.S., *Estudio del proceso de electrohilatura del DL-PLG para optimizar su biodegradación en aplicaciones médicas*, In: Ingeniería química, Universitat Politècnica de València, 2016
- [15] Bhardwaj, N., Kundu, S.C., *Electrospinning: A fascinating fiber fabrication technique*, 2010, 28, 325-347.



EFFECTS OF ARAMID SEWING YARN TYPE AND FABRIC COMPOSITIONS ON SOME SEAM PROPERTIES OF HIGH PERFORMANCE FIRE RETARDANT FABRICS

DOI: 10.35530/TT.2021.16

S. Kara

Textile Engineering Department, Engineering Faculty, Dokuz Eylul University, Turkey
(E-mail: sukran.kara@deu.edu.tr)

Abstract: High performance fire retardant textiles are utilized in different end-use areas such as workwear, firefighter garments, military textiles etc. These textiles are produced to protect the wearer against harsh environmental/occupational hazards and to bear forces during occupation. In the literature, fire-retardancy and mechanical performance of high performance fire retardant textiles are searched in details. Nevertheless, in most of these studies, samples were in the form of fibres or fabrics. When the fabrics are cut and sewn together to form a textile article, their mechanical properties change along the seam lines. In spite of this fact, seam properties of high performance fire retardant fabrics were not studied in the literature, systematically. Therefore, in this study, some seam properties of high performance fire retardant fabrics were studied as a preliminary work in this subject. According to results, seam strength of all samples were considerably lower when compared to strength of non-sewn reference samples. Strength differences were detected between the samples sewn with meta-aramid sewing yarn and para-aramid sewing yarn. Seam elongation and seam slippage values were similar for both sewing yarn types.

Keywords: aramid fabric, aramid sewing yarn, seam strength, seam slippage, elongation

1. INTRODUCTION

Protective garments can be defined as technical textile products those are produced to protect the wearer against various threats and harsh environmental conditions [1,2]. Fire retardant garments are an important branch of protective garments. Fire retardant textiles are used in several end-use areas such as firefighter garments, industrial protective garments, military textiles and curtains/upholsteries for public places [3-6].

There are several studies about fire retardant fibres and fabrics, in the literature [7-26]. These studies have importance but they are not sufficient to evaluate the total protective performance of the garment. Because, fabrics are cut and sewn together to produce 3-D garments. Continuity of fabric structure deteriorates along the seam-lines. The amount of weak points and sewing induced risks increase as the amount of seams increase in the garment. If the seams break during usage, the unity of the garment disrupts and body or lower layers are exposed to flame or high heat. Therefore, evaluating the sewing yarns and seam lines are of great importance for the researches in fire retardant textiles. Despite the fact that there are a plenty of researches on fire retardancy of fibres

and fabrics, there is no systematical research on the seam performance of fire-retardant textiles.

The main goal of this study was to determine the seam strength changes of fire retardant textiles stitched with aramid sewing yarns, as a complementary work to the literature.

2. MATERIALS AND METHODS

Aramid sewing yarns with 2 types of raw materials were used for this study. In addition, 3 types of fire retardant fabrics were utilized. Properties of sewing yarns and fabrics are given in table 1. Tensile strength and breaking elongation of sewing yarns were determined according to TS EN ISO 2062 [27] standard, utilizing Instron 5969 Model Universal Test Machine.

Table 1. Materials of the study

Yarn/ Fabric code	Raw Material	Material type	Yarn density (tex)	Twist (tpm)	Tensile strength (cN)	Breaking elongation (%)	Weave	Unit mass (g/m ²)	Weft density (yarns/cm)	Warp density (yarns/cm)
P	100 % para-aramid	3-ply sewing yarn	40	530	2852	4.7	-	-	-	-
M	100 % meta-aramid	3-ply sewing yarn	55	510	1490	22.4	-	-	-	-
FR1	93% meta- aramid 5% para- aramid 2% antistatic yarn	Fabric	-	-	-	-	2/1 twill	200	26	30
FR2	75% meta- aramid 23% para- aramid 2% antistatic yarn	Fabric	-	-	-	-	2/1 twill	195	24	30
FR3	49% meta- aramid 50% viscose FR 1% antistatic yarn	Fabric	-	-	-	-	2/1 twill	220	18	38

Samples were prepared by sewing FR1, FR2 and FR3 fabrics with lock stitch. Stitch density was 3 stitches/cm and seam allowance was 8 mm, for all samples. Tests were repeated 5 times for warp and weft samples of each sample type.

Seam strengths and elongations of samples were determined according to TS EN ISO 13935-2 standard [28], by using an Instron 5969 Model Universal Test Machine. The gauge length was 100 mm and the test speed was 50 mm/min for the tests. Also, strength

and elongation of non-sewn reference samples were determined according to same procedure. 6 mm seam slippage of samples was determined according to TS EN ISO 13936-1 standard [29]. All of the specimens were conditioned under standard atmosphere conditions ($20\pm 2^{\circ}\text{C}$, $65\pm 4\%$ relative humidity) for 24 hours before the tests.

3. RESULTS AND DISCUSSIONS

Strength and elongation results of samples are given table 2, with standard deviation values. Also, strength results of non-sewn reference fabrics and sewn samples are visualized in figure 1, a. According to results, FR1 and FR2 fabrics had similar strength values in warp direction that reached to 1000 N. In weft direction, FR1 sample showed higher strength value. FR3 fabric, that contained 49% meta-aramid and 50% viscose FR, exhibited lower strength both in warp and weft directions when compared to FR1 and FR2 fabrics, those were highly composed of aramid fibre types.

Table 2. Strength, failure type and elongation results of samples

Sample code	Strength/Seam strength						Elongation			
	Warp			Weft			Warp		Weft	
	Mean (N)	St. Dev. (N)	Failure type	Mean (N)	St. Dev. (N)	Failure type	Mean (mm)	St. Dev. (mm)	Mean (mm)	St. Dev. (mm)
FR1- No Seam	1002.09	33.09	-	946.51	18.34	-	25.34	0.45	23.13	0.61
FR1-M	234.47	20.96	Seam breakage	239.00	23.39	Seam breakage	14.03	0.77	12.82	0.39
FR1-P	218.79	14.88	Seam breakage	226.77	13.59	Seam breakage	12.96	0.29	12.36	0.29
FR2-No Seam	959.24	48.75	-	674.54	43.93	-	15.90	0.40	12.31	0.29
FR2-M	234.08	22.00	Seam breakage	239.50	19.56	Seam breakage	12.56	0.46	12.31	0.40
FR2-P	237.58	24.99	Seam breakage	226.13	10.86	Seam breakage	12.25	0.59	11.87	0.26
FR3- No Seam	667.50	22.71	-	292.10	3.63	-	19.07	0.63	16.87	0.21
FR3-M	227.41	28.98	Seam breakage	185.80	14.15	Fabric tear at seam, seam breakage	11.92	0.87	17.15	1.49
FR3-P	185.98	14.98	Seam breakage	201.56	17.28	Fabric tear at the seam	10.33	0.51	17.33	1.93

Seam strengths of all samples were importantly lower when compared to non-sewn reference fabrics. Samples sewn with meta-aramid sewing yarn (M) had seam strengths between 185-240N. For these samples, sewing yarn broke as the failure type except than FR3-M in weft direction. FR1-M and FR2-M showed the same seam strength in both directions. In contrary, FR3-M possessed less seam strength. This can be a result of lower

strength of FR3 fabric, especially in weft direction. The failure of FR3-M was observed as fabric tear at the seam.

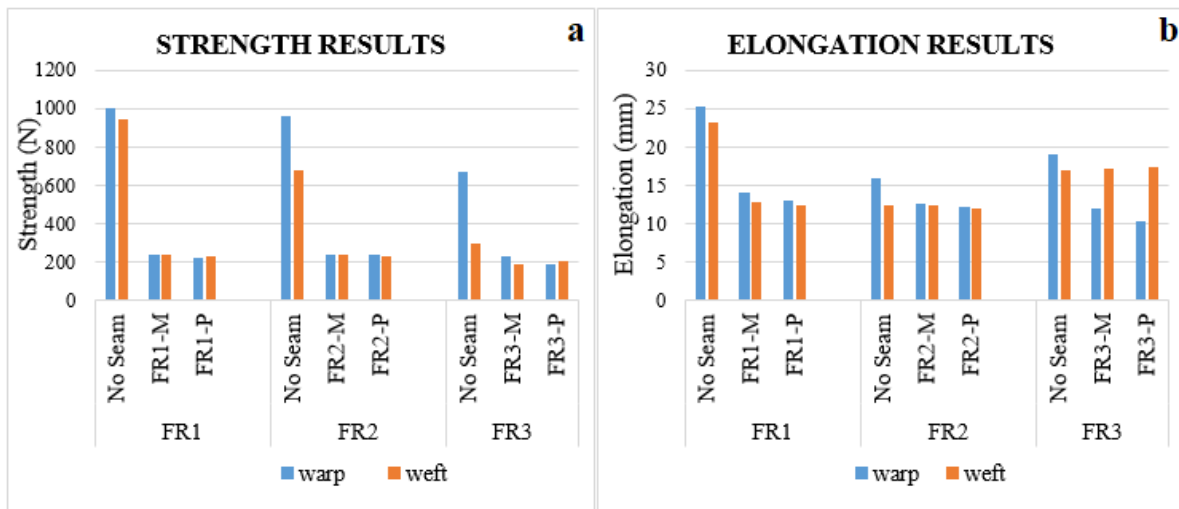


Figure 1. Strength, seam strength and elongation of samples

For samples sewn with 100% para-aramid sewing yarn (P), results were variable. In warp direction, FR2-P exhibited the highest seam strength, while in weft direction FR1-P and FR2-P showed exactly the same seam strength value. As for samples sewn with meta-aramid sewing yarn (M), sewing yarn breakage was observed for FR1-P and FR2-P samples, while fabric tear at the seam was observed for FR3-P samples in the weft direction. In warp direction, all the samples showed sewing yarn breakage as the failure type.

As the tensile strengths of para-aramid and meta-aramid sewing yarns were too high when compared to the strength of FR3 fabric in weft direction, it lead to the fabric tears at seam positions of FR3-M and FR3-P samples.

Elongation of samples are given in figure 1, b. Among all reference fabrics, FR1 had the highest elongation values while FR2 had the lowest in both warp and weft directions. After sewing, elongation of all warp samples decreased. For weft samples, elongation decreased only for FR1 samples after sewing. Elongation of samples sewn with M or P sewing yarns was close to each other, in both warp and weft directions.

Seam slippage results of samples (corresponding to 6 mm seam slippage) are given in table 3. According to results, FR1 and FR2 samples exhibited seam slippage forces higher than 200 N, for both warp and weft samples. These samples did not show enough seam openings during the tests, even the force reached 200 N. Similarly, required seam openings were not obtained for FR3 samples, but some of these samples broke before 200N, as noted in table 3.

4. CONCLUSION

In this study, effects of aramid sewing yarn type and fabric compositions are examined on the seam strength, elongation and seam slippage of high performance fabrics.

Table 3. 6 mm seam slippage results of samples

Sample code	Warp slippage (N)	Weft slippage (N)	Notes
FR1-No Seam	/	/	* Only one seam breakdown < 200 N
FR1-M	>200	>200	
FR3-P	>200	>200	
FR2- No Seam	/	/	** Only one value> 200 N and four breakdowns< 200 N (mean= 181.2 N)
FR2-M	>200	>200	
FR2-P	>200	>200	
FR3- No Seam	/	/	*** Only two values> 200N and three breakdowns< 200N (mean= 176.7 N)
FR3-M	**	>200 *	
FR3-P	>200 *	***	

For this purpose, 2 types of aramid sewing yarn (para-aramid and meta-aramid) and 3 types of high performance fire retardant fabrics were utilized.

According to test results, although the para-aramid sewing yarn was finer, its strength was higher than meta-aramid sewing yarn. When the fabric samples were considered, samples with higher aramid compositions exhibited similar and high strengths while sample with 50% aramid exhibited lower strength values.

When the samples were sewn, independent of the sewing yarn strength, all the strength values dropped to 185-240N range. In general, samples sewn with meta-aramid sewing yarn exhibited higher strength in this range. On the other hand, elongation of all sewn samples was close to each other. Although meta-aramid sewing yarn had higher strain value when compared to para-aramid sewing yarn, it did not reflect to sewn fabric elongation values. Similarly, 6 mm seam slippage forces were determined above 200 N for most of the samples that showed that sewing yarn type did not have an effect on seam slippage for these samples. Here, the effect of fabric type was more detectable.

This study was a preliminary work for a more detailed study on the seam properties of high performance garments. In the further studies, effects of aging on the seam properties of high performance fabrics sewn with aramid yarns is planned to be determined.

ACKNOWLEDGEMENT

The author would like to thank Kıvanç Kimya for providing the fabrics of the study, kindly. Also, author thanks Prof. Dr. Vildan Sular (Dokuz Eylul University, Textile Engineering Department) for her technical support during seam slippage evaluations.

REFERENCES

- [1] Scott, R A. (Ed.), *Textiles for protection*, Woodhead Publishing Ltd., 2005
- [2] Pan, N., Sun, G., *Functional Textiles for Improved Performance, Protection and Health*, Woodhead Publishing Ltd, 2011
- [3] Horrocks, A.R., Anand, S.C. (Eds.), *Handbook of technical textiles*, Woodhead Publishing Ltd., 2000

- [4] Den Hartog, E.A., *Challenges in future personal protective equipment-an overview of developments in user needs*, In: Research Journal of Textile and Apparel, 2010, 14, 4, 22
- [5] Dolez, P.I., Tomer, N.S., Malajati, Y., *A quantitative method to compare the effect of thermal aging on the mechanical performance of fire protective fabrics*, In: Journal of Applied Polymer Science, 2019, 136, 6, 47045
- [6] Orndoff, E., *Flame Retardant Fibers for Human Space Exploration - Past, Present, and Future*, In: NASA STI Collection, 2017, Available at: <https://ntrs.nasa.gov/search.jsp?R=20170008542> [Access on February 2020]
- [7] Eryürük, S.H., *Analysis of thermal properties of firefighter's protective clothings*, In: Tekstil ve Konfeksiyon, 2016, 26, 3, 270-279
- [8] Boguslawska-Bączek, M., Hes, L., *Thermal conductivity and resistance of Nomex fabrics exposed to salty water*, In: Tekstil ve Konfeksiyon, 2014, 24, 2, 180-185
- [9] Feng, Q., Zhu, F.L., Hu, J., *Estimation of the radiant performance of flame-retardant fabrics considering thermal degradation effect*, In: Journal of Engineered Fibers and Fabrics, 2019, 14, 1-10
- [10] Mandal, S., Annaheim, S., Greve, J., Camenzind, M., Rossi, R.M., *Modeling for predicting the thermal protective and thermo-physiological comfort performance of fabrics used in firefighters' clothing*, In: Textile Research Journal, 2019, 89, 14, 2836-2849
- [11] Wang, M., Li, J., *Thermal protection retention of fire protective clothing after repeated flash fire exposure*, In: Journal of Industrial Textiles, 2016, 46, 3, 737-755
- [12] Li, X., Lu, Y., Zhai, L., Wang, M., Li, J., Wang, Y., *Analyzing thermal shrinkage of fire-protective clothing exposed to flash fire*, In: Fire Technology, 2015, 51, 1, 195-211
- [13] Jin, L., Park, P.K., Hong, K.A., Yoon, K.J., *Effect of aluminized fabrics on radiant protective performance of fire proximity suit materials*, In: Annals of Occupational Hygiene, 2015, 59, 2, 243-252
- [14] Ertekin, M., Kırtay, E., *Burning behaviour and mechanical properties of fabrics woven with ring spun aramid and flame retardant polyester yarns*, In: Tekstil ve Konfeksiyon, 2014, 24, 3, 259-265
- [15] Mandal, S., Song, G., *An empirical analysis of thermal protective performance of fabrics used in protective clothing*, In: Annals of Occupational Hygiene, 2014, 58, 8, 1065-1077
- [16] Baltusnikaitė, J., Suminskiene, R., Milasius, R., *Influence of Woven Fabrics Structure upon Flammability Properties*, In: Materials Science (Medziagotyra), 2006, 12, 167-70
- [17] Kutlu, B., Cireli, A., *Thermal analysis and performance properties of thermal protective clothing*, In: Fibres and Textiles in Eastern Europe, 2005, 13, 3, 58-62
- [18] Stull, J. O., Dodgen, C. R., Connor, M. B., McCarthy, R. T., *Evaluating the effectiveness of different laundering approaches for decontaminating structural firefighting protective clothing*, In: Performance of Protective Clothing, ASTM International, 5th edn, 1996
- [19] Behnke, W.P., Geshury, A.J., Barker, R.L., *Thermo-Man® and Thermo-Leg: Large Scale Test Methods for Evaluating Thermal Protective Performance*, In: Performance of Protective Clothing, ASTM International, 4th edn, 1992
- [20] Türk, M., Şardağ, S., *Meta-aramid/yün karışımı dokuma kumaşların mukavemet ve eğilme özelliklerinin incelenmesi*, In: Tekstil ve Mühendis, 2019, 26, 113, 14-24
- [21] Mazari, A., Akçagün, E., Mazari, F.B., Kezlar, P., *Effect of sewing speed on the physical properties of firefighter sewing threads*, In: Industria Textila, 2016, 67, 5, 333-337
- [22] Ertekin, M., Kırtay, E., *Tensile properties of some technical core spun yarns developed for protective textiles*, In: Tekstil ve Konfeksiyon, 2015, 25, 2, 104-110
- [23] McQuerry, M., Klausung, S., Cotterill, D., Easter, E., *A post-use evaluation of turnout gear using NFPA 1971 standard on protective ensembles for structural firefighting and NFPA 1851 on selection, care and maintenance*, In: Fire Technology, 2015, 51, 5, 1149-1166
- [24] Özgen, B., *Physical properties of Kevlar and Nomex plied and covered yarns*, In: Textile Research Journal, 2013, 83, 7, 752-760

- [25] Thorpe, P.A., Torvi, D.A., *Development of non-destructive test methods for assessing effects of thermal exposures on fire fighters' turnout gear*, In: Journal of ASTM International, 2004, 1, 6, 1-14
- [26] Wu, Z., Li, F., Huang, L., Shi, Y., Jin, X., Fang, S., Chuang, K., Lyon, R.E., Harris, F.W., Cheng, S.Z.D., *The thermal degradation mechanism and thermal mechanical properties of two high performance heterocyclic polymer fibers*, In: Journal of Thermal Analysis and Calorimetry, 2000, 59(1-2), 361-373
- [27] TS EN ISO 2062. Textiles - Yarns from packages - Determination of single-end breaking force and elongation at break using constant rate of extension (CRE) tester, 2014
- [28] TS EN ISO 13935-2. Textiles - Seam tensile properties of fabrics and made-up textile articles - Part 2: Determination of maximum force to seam rupture using the grab method, 2014
- [29] TS EN ISO 13936-1. Textiles - Determination of slippage resistance of yarns at a seam in woven fabrics - Part 1: Fixed seam opening method, 2004



AQUEOUS SOLUTIONS OF CHITOSAN: VISCOMETRIC AND FLOCCULATION PROPERTIES

DOI: 10.35530/TT.2021.21

C.-E. Brunchi*, L. Ghimici

Natural Polymers, Biocompatible and Bioactive Materials, "Petru Poni" Institute of Macromolecular Chemistry, Romania
(E-mail: brunchic@icmpp.ro, lghimici@icmpp.ro)

Abstract: *The hydrodynamic and flocculation properties of aqueous solution of chitosan (CS) were investigated at room temperature. The viscometric data of dilute CS solutions were discussed in terms of Wolf method as a function of polymer concentration, salt nature (NaCl, NaNO₃, and CaCl₂) and concentration. The flocculation properties in emulsions of some commercial pyrethroid insecticides (Fastac 10 EC (F), Decis (Dc) and Karate Zeon (KZ)) were evaluated. The viscosity measurements reveal that the experimental data fit well with the Wolf model and the $[\eta]$ values decrease in salt aqueous solutions. For the same insecticide concentration (0.02%, v/v), UV-Vis spectroscopy measurements show maximum removal efficiency around 90% for Fastac 10EC and Decis and 80% for Karate Zeon. The residual KZ absorbance decreased with the increase of insecticide concentration in the initial emulsion, from 80% for the lowest concentration (0.02%, v/v) to around 90% for the highest one (0.06%, v/v). The supernatant zeta potential dependence on the chitosan dose pleads for the charge neutralization as the main mechanism for the flocculation of pyrethroid insecticide particles.*

Keywords: *chitosan, flocculation, insecticides, salt solution, viscosity*

1. INTRODUCTION

Chitosan is a well-known cationic polysaccharide made of glucosamine and a fraction of acetylglucosamine residues [1]. The main characteristics of chitosan, namely biodegradability, nontoxicity, hydrophilicity, easy chemical derivatisation, etc., are the consequence of the –OH and primary amino groups presence in its chemical structure. By virtue of these properties, chitosan has found applications in many fields such as medical, agriculture, food, textile, cosmetics, pharmaceutical, papermaking industries [2-4]. Its using in the above mentioned fields has challenged the researchers to investigate the dynamic (viscosity, rheology, etc.) and electrochemical (conductometry, activity, etc.) properties in solution with different characteristics (pH, ionic strength, etc.). The viscosity measurements provide valuable information about interactions between polymer chains or with solvent molecules, conformational transition of the chains and some hydrodynamic parameters of the polymer chains in solution [5,6]. In this context, a first aim of this paper was the investigation of some salts effect on the hydrodynamic properties of CS chains in aqueous solution and determination of the intrinsic viscosity by the Wolf method [7]. Also, the high ability of CS to interact with a wide range of compounds (salts, clays, oils, dyes, metal ions, etc.) has directed its application in the wastewater treatment field [2,8]. The presence of pesticides, a group of highly toxic materials for the living organisms in the environment (surface water and industrial/agriculture wastewater), has determined an increasing interest in their removal by

different physico-chemical methods [9,10]. However, the application of soluble polysaccharides including chitosan in removal of pesticides from wastewater was less investigated [9, 10]. The good removal efficiency (around 90%) obtained when dextran [9] and pullulan [10] derivatives were used as flocculants encouraged us to test the efficiency of chitosan solution in decreasing of some commercial pyrethroid insecticides content from wastewater. The insecticides chosen in this work (widespread applied in agricultural crops, forestry as well as in public and animal health) were Fastac 10 EC, Decis and Karate Zeon. The flocculation efficacy of CS in pyrethroid insecticides emulsions was followed by UV-Vis spectroscopy as a function of dosage (polymer dose represents the flocculant concentration in its mixture with pesticide emulsions). In addition zeta potential measurements were performed in order to establish the possible mechanisms that control the insecticides removal process.

2. MATERIALS AND METHODS

2.1. Materials

Chitosan (CS, chemical structure in figure 1, a, acetic acid (AcOH) and used salts (NaCl, NaNO₃ and CaCl₂) were purchased from Sigma-Aldrich, and were used as received.

The viscometric average molar mass of CS ($M_v = 189$ kDa) was estimated from the intrinsic viscosity, $[\eta]$, according to the equation proposed by Gamzazade et al. [11]:

$$[\eta] = 1.38 \times 10^{-4} M_v^{0.85} \text{ (dL}\cdot\text{g}^{-1}) \quad (1)$$

Degree of acetylation (DA) of chitosan was evaluated by infrared spectroscopy (Vertex 70 Bruker FTIR spectrometer). Transmission spectra were recorded in KBr pellets. For DA determination, Equation (2) was used taking the 1420 cm⁻¹ band as reference and the band located at 1320 cm⁻¹ as characteristic band for the N-acetylglucosamine [12]:

$$A_{1320}/A_{1420} = 0.3822 + 0.03133 \text{ DA} \quad (2)$$

An average value of DA =15%, obtained from three measurements, was taken into consideration.

The insecticide called in the paper *F* is commercially available as Fastac 10 EC (BASF), in small bottles: 2 ml solution (α -Cypermethrin: 100 g·l⁻¹; solvent naphtha (petroleum), light arom.) (chemical structure in figure 1, b). The insecticide called in the paper *Dc* is commercially available as Decis, in vials with 2 mL solution (Deltamethrin: 50 g·L⁻¹; solvent naphtha (petroleum), heavy arom.) (chemical structure in figure 1, c). The insecticide called in the paper *KZ* is commercially available as Karate Zeon (Syngenta Limited, England) in small bottles/vials: 2 ml solution (lambda-Cyhalothrin: 50 g·l⁻¹; solvent naphtha (petroleum), heavy aromatics, propylene glycol) (chemical structure in figure 1, d).

2.2. Methods

Viscometric measurements

An automatic viscometer (Instrument LAUDA LMV 830) equipped with a water bath (ECO ET 155) and an Ubbelohde suspended-level viscometer with capillary diameter of 0.64 mm (Type 531 10, Schott-Geräte) was used to perform the viscometric measurements for the aqueous solutions of CS (in the absence/presence of salts). The measurements were made at room temperature ($\pm 0.01^\circ\text{C}$) and repeated at least twice in order to check the reliability of the data, which was $\pm 3\%$. The chitosan solutions in aqueous AcOH (1%, v/v) and salt

solution with different concentration (0.1, 1 and 10 mM) were prepared one day before the viscometric measurements.

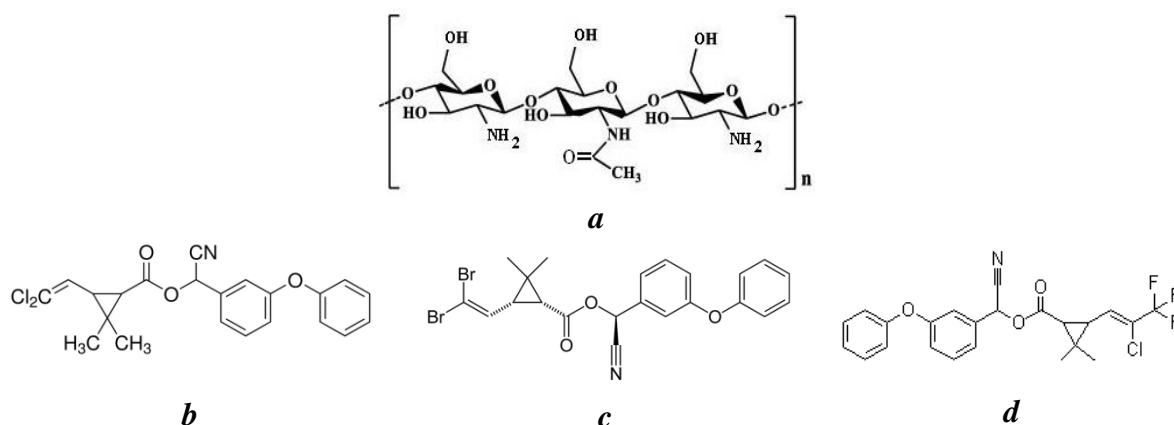


Figure 1. Chemical structure of: a – chitosan and used insecticides b - alpha-Cypermethrin; c – Delthametrin; d - lambda-Cyhalothrin

Flocculation procedure

The stock chitosan solution was prepared (CS powder was dissolved in aqueous solution of acetic acid (1%, v/v)) under magnetic stirring for 24 h at room temperature, 1 day before the flocculation experiments. Insecticide emulsions were also obtained in highly purified deionized water with the next concentrations (c_{ie} %, v/v): (i) F emulsion (the initial pH = 4.4, $\zeta = -24.6$ mV and $c_{ie} = 0.02$); (ii) Dc (the initial pH = 4.5, $\zeta = -28.2$ mV and $c_{ie} = 0.02$); (iii) KZ (the initial pH = 4.5, $\zeta = -26.5$ mV and $c_{ie} = 0.02, 0.04$ and 0.06). The concentration of polymer in its stock solution was $1\text{g}\cdot\text{L}^{-1}$. In order to obtain stable insecticides emulsions, the stock ones (sample volume of 500 mL) were sonicated for 15 min using an ultrasonicator with VCX 750 SONICS, USA. The flocculation measurements were carried out at room temperature, using a Cole Parmer stirrer/hotplate 9 places, according to the method already described [9]. After 1200 min settling time, 10 ml of supernatant was taken out for both the absorbance (spectrophotometer SPECOL 1300 Analytik Jena) and zeta potential measurements (Zetasizer Nano-ZS, ZEN-3500 model (Malvern Instruments, Malvern, England). The absorbance measurements were recorded at wavelength (λ , nm) = 276 nm for F, 267 nm for Dc and 270 nm for KZ. The pesticide removal was expressed as percent of the initial absorbance recorded for the insecticide particle emulsions, at time zero (without polymer). Triplicate experiments were made and the mean values were calculated. Standard deviation determined for the experiments was $\pm 4\%$.

3. RESULTS AND DISCUSSION

3.1. Viscosity data

The viscometric behaviour of aqueous solution of CS as a function of polymer concentration in terms of reduced viscosity (η_{sp}/c) and relative viscosity ($\ln\eta_r$) is presented in figure 2.

η_{sp} is the specific viscosity ($\eta_{sp} = \eta_r - 1$) which shows the change in viscosity of the polymer solution by the addition of the solvent. η_r represents the relative viscosity determined as the ratio between by the viscosities of the polymer solution and the solvent (experimentally determined as t/t_0 , where t and t_0 represents the flow time of polymer solution and solvent, respectively).

The plot of $\eta_{sp}/c-c$ (figure 2, a) points out the following aspects: *i*) in salt solutions, the values of reduced viscosity decrease linearly with CS concentration like the neutral polymers; *ii*) in the absence of salt, the reduced viscosity increases at high dilution (namely, for polymer concentrations lower than $0.002 \text{ g}\cdot\text{dL}^{-1}$) that is characteristic for the polyelectrolyte behaviour. This is due to the electrostatic repulsion interactions between the charged groups ($-\text{NH}_3^+$) which lead to the chain expansion; consequently, the determination of the intrinsic viscosity ($[\eta]$) by the Huggins method becomes difficult. For this reason we have chosen to determine the $[\eta]$ according to the method proposed by Wolf [7].

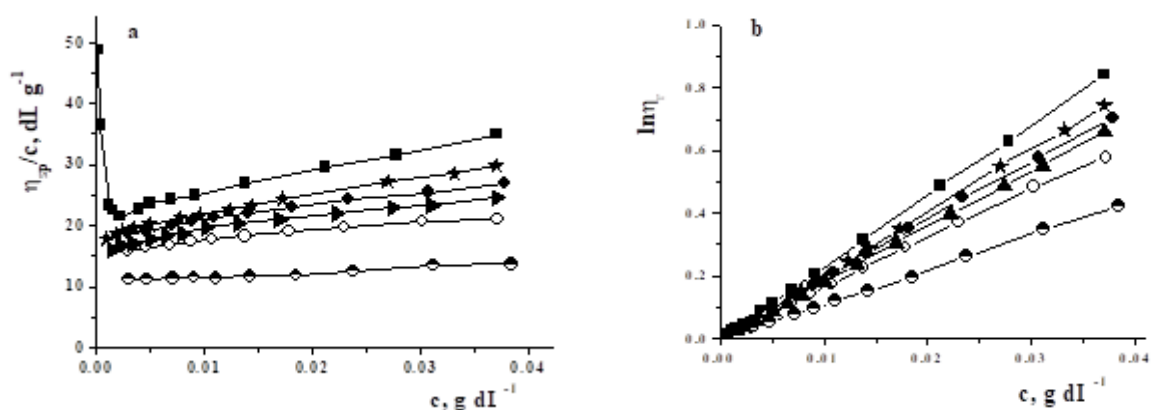


Figure 2. Dependence on: a - chitosan concentration, c , of reduced viscosity and b - relative viscosity in AcOH (full square) and in aqueous salt solutions: 0.1 mM NaCl (full circle), 1 mM NaCl (empty circle), 10 mM NaCl (half empty circle), 0.1 mM NaNO_3 (full star) and 0.1 mM CaCl_2 (full triangle).

This model allows the evaluation of the $[\eta]$ values from the initial slope of dependence of $\ln\eta_r$ as a function of polymer solution concentration (c) at sufficiently low shear rates and c , according to the following equation:

$$\ln\eta_r = \frac{c[\eta] + Bc^2[\eta][\eta]^*}{1 + Bc[\eta]} \quad (3)$$

where: η_r = the relative viscosity, $[\eta]$ = the intrinsic viscosity, B = the viscometric interaction parameter and $[\eta]^*$ = the characteristic specific hydrodynamic volume which incorporate the effects of electrostatic interaction.

Figure 2, b presents the evaluation of the experimental data from figure 2, a according to the Wolf model. The results demonstrate that all of calculated lines coincided well with the experimental points proving the ability of Equation (3) to determine the intrinsic viscosity and to describe the viscosity behaviour of CS in the absence/presence of salts.

Table 1 emphasizes (i) the higher values of $[\eta]$ for chitosan in AcAc solution than those in all salt solutions (the same concentration); (ii) for the same salt (NaCl), the decrease of $[\eta]$ with enhancing its concentration.

By adding salt, the electrostatic repulsion interactions between charged groups are screened, chains adopt a more compact conformation and thus intrinsic viscosity values decrease. The macromolecular chain conformation in solution is reflected in the value of c^* . In the present study, the increase of c^* from 0.04 to $0.093 \text{ g}\cdot\text{dL}^{-1}$ with salt concentration reveals the transition of chitosan chains from the extended conformation to a coiled one (table 1).

Table 1. Viscometric parameters determined by eq. 1 for CS aqueous solutions

Solvent/salt concentration	$[\eta]$ ($\text{dl}\cdot\text{g}^{-1}$)	$c^* = [\eta]^{-1}$ ($\text{g}\cdot\text{dl}^{-1}$)
AcOH 1%	22.7	0.044
AcOH(1%)/NaCl (0.1 mM)	19.534	0.050
AcOH(1%)/NaCl (1 mM)	16.718	0.059
AcOH(1%)/NaCl (10 mM)	10.740	0.093
AcOH(1%)/NaNO ₃ (0.1mM)	19.954	0.051
AcOH(1%)/CaCl ₂ (0.1 mM)	17.793	0.056

3.2 Flocculation data

Influence of chitosan dose

One of the most important parameters which gives an indication of the performance in coagulation/flocculation process of a compound (inorganic salts or polymer) is the optimum dose (dose_{op}), which is the polymer dose corresponding to the maximum removal efficiency. Hence, the percent of insecticides removal dependence on the chitosan dose was followed for all of the insecticides under study; insecticide emulsions with c_{ie} (% , v/v) = 0.02 were used (figure 3, a).

The maximum removal efficiency (RE%) more than 90% has been found in the polymer dose interval between $1.2 \text{ mg}\cdot\text{l}^{-1}$ and $1.4 \text{ mg}\cdot\text{l}^{-1}$ for *F* and between $1 \text{ mg}\cdot\text{l}^{-1}$ and $1.1 \text{ mg}\cdot\text{l}^{-1}$ for *Dc*. A slightly lower efficacy of chitosan was found in case of *KZ*, around 80% at a polymer dose of $0.8 \text{ mg}\cdot\text{l}^{-1}$. The explanation for this behavior could be found looking at the chemical structure of the partners implied in the systems investigated. Thus, the chitosan sample used in this investigation is a high charge density polycation (DA = 15%, see Materials and Methods part, 2.1. Materials subsection); the pKa of chitosan with a degree of deacetylation above 70% is around 6.3-6.4 [14].

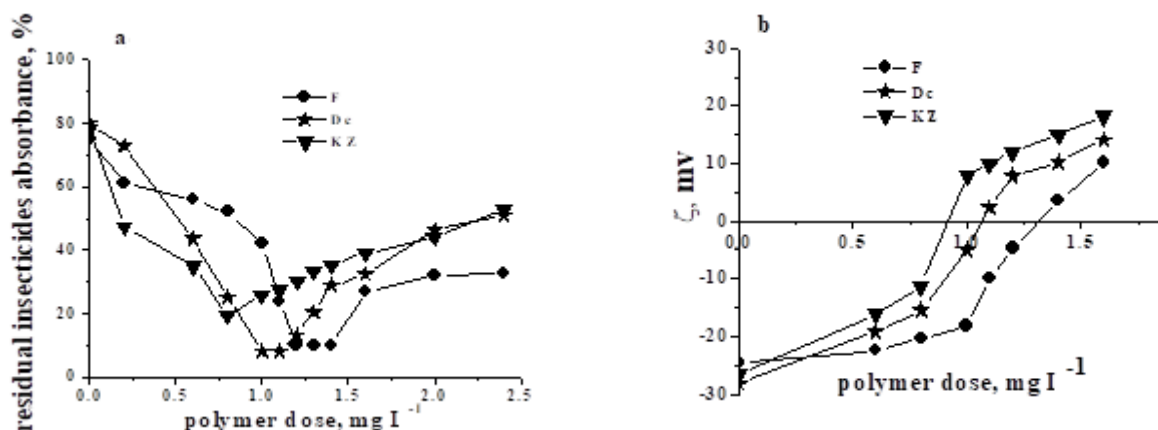


Figure 3. Graph of: a - residual insecticides absorbance (%); b - zeta potential (ζ) dependence on the chitosan dose; c_{ie} (% , v/v) = 0.02

On the other hand, the insecticides (i) α -Cypermethrin, the active ingredient of *F*, is a racemic mixture of (S)- α -cyano-3-phenoxybenzyl-(1R,3R)-3-(2,2-dichlorovinyl)-2,2-dimethylcyclopropanecarboxylate and (1R)- α -cyano-3-phenoxybenzyl-(1S,3S)-3-(2,2-dichlorovinyl)-2,2-dimethylcyclopropanecarboxylate, (ii) Deltamethrin- the active ingredient of *Dc* is [(S)-Cyano-(3-phenoxyphenyl)-methyl] (1R,3R)-3-(2,2-dibromoethenyl)-2,2-dimethyl-cyclopropane-1-carboxylate and (iii) lambda-Cyhalothrin- the active ingredient of *KZ*, is a mixture of (1R)-lambda-cyano-3-phenoxybenzyl (1S)-cis-3-[(Z)-2-chloro-3,3,3-trifluoropropenyl]-2,2-dimethylcyclopropanecarboxylate and (S)-lambda-cyano-3-phenoxybenzyl (1R)-cis-3-[(Z)-2-chloro-3,3,3-trifluoropropenyl]-2,2 dimethylcyclopropane-

carboxylate; zeta potential values of the insecticide particles emulsions without chitosan are $\zeta = -24.6$ mV for *F*, $\zeta = -28.2$ mV for *Dc* and $\zeta = -26.5$ mV for *KZ* (see Materials and Methods part, 2.2.2 Methods subsection). Based on this information one may surmise that the flocculation of suspended particles by CS results from mechanisms which, mainly, imply electrostatic attraction between oppositely charged groups on the particles and chitosan chains (neutralization and patch). In the neutralization mechanism, the surface charges are neutralized by the oppositely charged groups of the polyelectrolytes and the particles attract each other by van der Waals forces, while in the charge patch one, aggregation takes place as a result of the electrostatic attraction between oppositely charged regions on particles [15]. Zeta potential measurements can discriminate between these mechanisms. In case of the charge neutralization mechanism, the maximum removal efficiency takes place at a polymer dose around that required to obtain a zeta potential close to zero [16], while for the patch mechanism, zeta potential needs not to be zero [17]. Zeta potential measurements were undertaken on the same supernatant samples as that used for the absorbance measurements (figure 5, b). Irrespective of the insecticide used, ζ values increased over the entire domain of chitosan doses investigated, from the initial emulsion negative value (see above) to positive ones, namely 10.2 mV (*F*), 14.1 mV (*Dc*) and 18.2 mV (*KZ*). Worthy of note are the values of ζ , close to zero, recorded in cases of *F* and *Dc* (between -4.7 mV and 3.6 mV for *F* and between -4.93 mV and 2.33 mV for *Dc*) that points to charge neutralization mechanism for both insecticide particles removal by chitosan. The negative value of ζ at optimum dose (-11.3 mV) noticed for *KZ* reveals the weaker interactions with chitosan than *F* and *Dc*. This finding could be caused by the more bulky trifluoropropenyl groups in lambda-Cyhalothrin than dichlorovinyl and dibromoethenyl in α -Cypermethrin and Deltamethrin, respectively, which might impede in a certain extent the polymer-insecticide particles interactions. Also, the slightly higher optimum chitosan dose recorded in case of *F* than *Dc* and *KZ* could be assigned to the higher content of active ingredient in *F* (α -Cypermethrin: 20 mg·l⁻¹) than that in *Dc* and *KZ* (Deltamethrin and lambda-Cyhalothrin: 10 mg·l⁻¹).

Influence of insecticide concentration

The insecticides concentration in wastewaters can vary. Therefore, it is necessary to examine the impact of this parameter on the chitosan efficiency in flocculation process. Thus, in addition to the model wastewaters with c_{ie} (% v/v) = 0.02, we carried out experiments with insecticide emulsions having c_{ie} (% v/v) = 0.04 and 0.06 at the natural emulsions pH.

Figure 4 displays the results obtained in case of *KZ* which has been chosen as example.

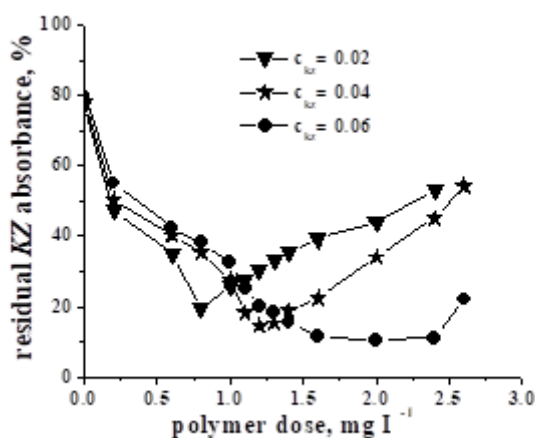


Figure 4. The residual *KZ* absorbance (%) dependence on the chitosan dose for different concentrations of *KZ* (c_{KZ})

One observes a clear increase of the removal percent of KZ with the increase of (c_{KZ}), namely from around 80% for the lowest c_{KZ} to around 90% for the highest one.

Worthy to note is the increase of $dose_{op}$ with c_{KZ} (% v/v), as follows: 0.8 mg·l⁻¹ for $c_{KZ} = 0.02$, 1.2 mg·l⁻¹ for $c_{KZ} = 0.04$, 2 mg·l⁻¹ for $c_{KZ} = 0.06$. At higher KZ concentration, more polycation chains were necessary for the neutralization of particle charge surface, hence the increasing $dose_{op}$.

4. CONCLUSIONS

1. Wolf equation is proper to describe the viscosity behaviour of chitosan aqueous solution in the presence/absence of salt;

2. The salt addition diminishes the electrostatic repulsive interactions between the charged groups along the chains, and so, the macromolecules adopt a more coiled conformation and hence, the intrinsic viscosity decrease;

3. The increase of flocculants dosage led to the drastic decrease of residual insecticides absorbance until the optimum dose is reached;

4. The optimum chitosan doses ($dose_{op}$, mg·l⁻¹) were found to increase as the KZ concentrations increase;

5. Zeta potential data indicate charge neutralization as the common mechanism contributing to the separation of investigated insecticide particles.

ACKNOWLEDGMENT

This work was supported by a grant of the Romanian National Authority for Scientific Research, CNCS-UEFISCDI, project number PN-III-P4-ID-PCE-2020-0296.

REFERENCES

- [1] Krishnapriya, K.R., Kandaswamy, M., *A new chitosan biopolymer derivative as metal-complexing agent: Synthesis, characterization, and metal (II) ion adsorption studies*, In: Carbohydr. Res., 2010, 345, 14, 2013-2022, <https://doi.org/10.1016/j.carres.2010.06.005>
- [2] Prado, H.J., Matulewicz, M.C., *Cationization of polysaccharides: A path to greener derivatives with many industrial applications*, In: Eur. Polym. J., 2014, 52, 53-75, <https://doi.org/10.1016/j.eurpolymj.2013.12.011>
- [3] Thomas, S., Ninan, N., Mohan, S., Francis, E., *Natural Polymers, Biopolymers, Biomaterials, and Their Composites, Blends, and IPNs*, Apple Academic Press Toronto New Jersey, 2013
- [4] Dutta, K., Duta, J., Tripathi, V.S., *Chitin and Chitosan: chemistry, properties and applications*, In: J. Sci. Ind. Res., 2004, 63, 1, 20-31, <https://dx.doi.org/10.1016/j.foodhyd.2010.08.008>
- [5] Costa, C.N., Teixeira, V.G., Delpech, M.C., Souza, J.V.S., Costa, M.A.S., *Viscometric study of chitosan solutions in acetic acid/sodium acetate and acetic acid/sodium chloride*, In: Carbohydr. Polym., 2015, 133, 245-250, <https://doi.org/10.1016/j.carbpol.2015.06.094>
- [6] Morariu, S., Brunchi, C.-E., Bercea, M., *The behavior of chitosan in solvents with different ionic strengths*, In: Ind. Eng. Chem. Res. 2012, 51, 12959-12966, <https://doi.org/10.1021/ie301309g>
- [7] Wolf, B.A., *Polyelectrolytes revised: Reliable determination of intrinsic viscosities*, In: Macromol. Rapid Commun., 2007, 28, 164-170, <https://doi.org/10.1002/marc.200600650>
- [8] Guibal, E., van Vooren, M., Dempsey, B.A., Roussy, J., *A review of the use of chitosan for the removal of particulate and dissolved contaminants*, In: Sep. Sci. Technol., 2006, 41, 11, 2487-2514, <https://doi.org/10.1080/01496390600742807>
- [9] Ghimici, L., Nichifor, M., *Ionic dextran derivatives for removal of Fastac 10 EC from its aqueous emulsions*, In: Carbohydr. Polym., 2015, 134, 46-51, <https://doi.org/10.1016/j.carbpol.2015.07.100>
- [10] Ghimici, L., Constantin, M., *The separation of the pyrethroid insecticide Fastac 10 EC by cationic pullulan derivatives*, In: React. Funct. Polym., 2015, 95, 12-18, <https://doi.org/10.1016/j.reactfunctpolym.2015.08.001>

- [11] Gamzazade, A.I., Šlimak, V.M., Skljar, A.M., Štykova, E.V., Pavlova, S.-S.A., Rogožin S.V., *Investigation of the hydrodynamic properties of chitosan solutions*, In: Acta Polymerica, 1985, 36, 8, 420-424, <https://doi.org/10.1002/actp.1985.010360805>
- [12] Brugnerotto, J., Lizardi, J., Goycoolea, F.M., Argüelles-Monal, W., Desbrières, J., Rinaudo, M., *An infrared investigation in relation with chitin and chitosan characterization*, In: Polymer, 2001, 42, 3569-3580, [https://doi.org/10.1016/S0032-3861\(00\)00713-8](https://doi.org/10.1016/S0032-3861(00)00713-8)
- [13] Brunchi, C.-E., Morariu, S., Bercea, M., *Impact of ethanol addition on the behaviour of xanthan gum in aqueous media*, In: Food. Hydrocolloid, 2021, 120, 106928, <https://doi.org/10.1016/j.foodhyd.2021.106928>
- [14] Sorlier, P., Denuziere, A., Viton, C., Domard, A., *Relation between the degree of acetylation and the electrostatic properties of chitin and chitosan*, In: Biomacromolecules, 2001, 2, 765-772, <https://doi.org/10.1021/bm015531+>
- [15] Bolto, B., Gregory, J., *Organic polyelectrolytes in water treatment*, In: Water Res., 2007, 41, 2301-2324, <https://doi.org/10.1016/j.watres.2007.03.012>
- [16] Kleimann, J., Gehin-Delval, C., Auweter, H., Borkovec, M., *Super-stoichiometric charge-neutralization in particle-polyelectrolyte systems*, In: Langmuir, 2005, 21, 3688-3698, <https://doi.org/10.1021/la046911u>
- [17] Bobacka, V., Eklund, D., *The influence of charge density of cationic starch on dissolved and colloidal material from peroxide bleached thermomechanical pulp*, In: Colloids Surf. A, 1999, 152, 285-291, [https://doi.org/10.1016/S0927-7757\(98\)00731-6](https://doi.org/10.1016/S0927-7757(98)00731-6)



A RESEARCH ON THE BREATHABILITY PROPERTY OF BABY DIAPER BACKSHEET

DOI: 10.35530/TT.2021.18

H.K. Kaynak, M. Alsayed*

Textile Engineering Department, Gaziantep University, Gaziantep, Turkey
(E-mail: tuluca@gantep.edu.tr, maheralsayyed99@gmail.com)

Abstract: Disposable breathable diapers are considered as one of the most important developments in diaper sector. Breathable diapers keep the child's skin dry and provide a comfortable feeling to the child. Breathability of diapers is obtained by using the breathable back sheet layer which is the most outer layer that the diaper comprises. In this study, the effects of laminating and printing processes on back sheet material breathability are studied. For this aim, four types of back sheet samples namely; film, printed film, laminated film and printed-laminated film are tested for breathability. For breathability testing, water vapour permeability test was applied with two different test devices which principally operate in different ambient conditions. As a result of the study, it is seen that, the breathability of back sheet component decreases as a result of printing and laminating processes. Also, it can be concluded that the ambient conditions for standard textile fabrics is not convenient for testing back sheet samples. Since, the test does not simulate the real ambient conditions of microclimate between the diaper and the child's skin during diaper use.

Keywords: back sheet, breathable diapers, breathability, water vapour permeability

1. INTRODUCTION

Baby diapers are used all over the world for many years. The crucial innovation in diapers is undoubtable the production of disposable diapers which are appeared in the middle of the twentieth century [1-3]. The disposable diapers are composed of different basic layers namely; top sheet, absorbent layer and back sheet. Each layer plays a different role, where the top sheet transports the liquid to the inner absorbent layer, while the absorbent layer is in charge of absorbing the liquid and the back sheet provides a liquid barrier effect [1-4].

In the literature there are some studies which deal with different performance properties of diapers. Yaman et al. investigated the surface, the mechanical and liquid absorption properties of commercial disposable diapers to determine their performance in use [4]. Özen et al. presented a study on the thermal comfort properties of multi-layered diaper structures regarding the breathability, thermal conductivity, and warmth-cool feeling in dry and wet conditions. They used different breathable films that were deliberately produced for the study in comparison to a commercial breathable film. They also used different top sheet layers [5]. Gündüz investigated the performance properties of commercially available baby diapers [6].

Baby's skin may be affected negatively by diapers. Since the skin is in contact with the diaper in wet and warm microclimate for a long time period [4]. To prevent the negative

effects of diapers, breathable diapers are developed by providing a breathable back sheet layer which has a good level of water vapour permeability. Breathable diapers keep the child's skin dry and provide a comfortable feeling to the child. Earlier studies show that the breathable disposable diapers retain the skin in dry condition and inhibit the increase of heat, owing to having a good level of water vapour permeability. So, they are superior to non-breathable diapers regarding the comfort property. It can be said that the infants who wear breathable diapers are less likely to get rash than the ones who use the non-breathable diapers. One of the most effective solution for DD (Diaper dermatitis) or diaper rash is concluded as using breathable disposable diaper for infants [5, 7-12].

In order to produce a breathable disposable diaper, a breathable back sheet layer must be provided. Baby diapers can be called as breathable if only the back sheet layer provides breathability. Back sheet is composed of spun bonded nonwoven layer which is laminated with PE (polyethylene) film layer. It should be regarded that spun bonded nonwoven layer has water vapour permeability or breathability since it has a porous structure. On the other hand, it is fundamentally critical to present water vapour permeability for PE film layer which is originally used for liquid barrier functionality. Even if the PE film layer is originally breathable, there are some production processes such as printing that decrease the breathability of the component. The PE film layer is generally printed with different designs to provide an attractive look. The other deteriorative process for water vapour permeability is lamination of PE film with spun bonded nonwoven fabric by the adhesive material. Even though the spun bonded nonwoven fabric has breathability due to its porous structure, lamination of this textile layer by an adhesive with PE film deteriorates the breathability of end product.

In this study, the effects of printing and lamination processes on the breathability of baby diaper back sheet component were investigated by two different test devices which principally apply different ambient conditions.

2. MATERIALS AND METHODS

In this study, breathability of different configurations of diaper back sheet layers was investigated to discuss the effects of printing and lamination processes on water vapour permeability. For this aim, PE film, printed PE film, laminated PE film and laminated-printed PE film samples were tested. The mass and thickness values of the samples were determined according to the standards of TS 12127 [13] and TS 7128 EN ISO 5084 [14] and given in table 1.

Table 1. Fabric mass and thickness of the samples

Samples	Fabric mass (g/m ²)	Thickness (mm)
PE film	15	0.014
Laminated PE film	25	0.024
Printed PE film	15	0.128
Laminated & Printed PE film	26	0.116

For breathability determination water vapour permeability tests were performed. In this study, two different types of water vapour permeability tests were applied to samples. The first test method is evaporative dish method by BS 7209:1990 [15] which is generally used for textile fabrics. In this method, three test specimens are mounted over the test dishes containing 46 ml of distilled water at 20±2°C. These dishes are placed on a rotating turntable. The samples are rotated with turntable for one hour to establish equilibrium of water vapour

pressure gradient across the sample (figure 1).

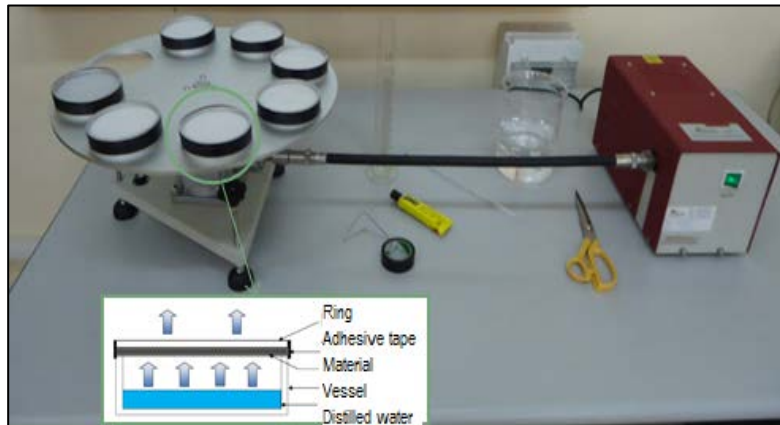


Figure 1. Water vapour permeability test device for evaporative dish method

After one hour rotating period for equilibrium the mass of the dishes are determined. The turntable with dishes is then rotated for a further period of 5 hours. The mass values of the dishes are determined after 5 hours duration. Then the water vapour permeability (WVP) of the samples is calculated in $\text{g/m}^2/\text{day}$ by the given equation 1. The ambient conditions of the test are $20\pm 2^\circ\text{C}$ temperature and $65\pm 4\%$ relative humidity, as generally used for textile fabrics:

$$\text{WVP} = \frac{24M}{At} \quad (1)$$

where t is test period in hours, A - area of the sample in $5.41 \times 10^{-3} \text{ m}^2$, M - mass difference in grams.

The second type of breathability test was done by Mocon test device (figure 2) according to standard test method of ASTM D6701 – 21 [16], at 38°C .



Figure 2. Mocon water vapour permeability test device

3. RESULTS AND DISCUSSIONS

Table 2 and figure 3 represents the experimental results of water vapour permeability test results determined by two different test principals.

Table 2. The results of water vapour permeability tests

Samples	Evaporative Dish Method		Breathability by Mocon	
	WVP (g/m ² /day)	Average	WVP (g/m ² /day)	Average
Film	557	457	4763	4400
	448		4339	
	474		4288	
	420		4248	
	383		4363	
Laminated film	511	466	3912	3711
	471		3872	
	510		3789	
	426		3416	
	411		3564	
Printed film	362	407	3418	3558
	428		3716	
	440		3571	
	369		3335	
	437		3750	
Printed laminated film	413	466	2754	2522
	573		2582	
	392		2166	
	424		2335	
	527		2774	

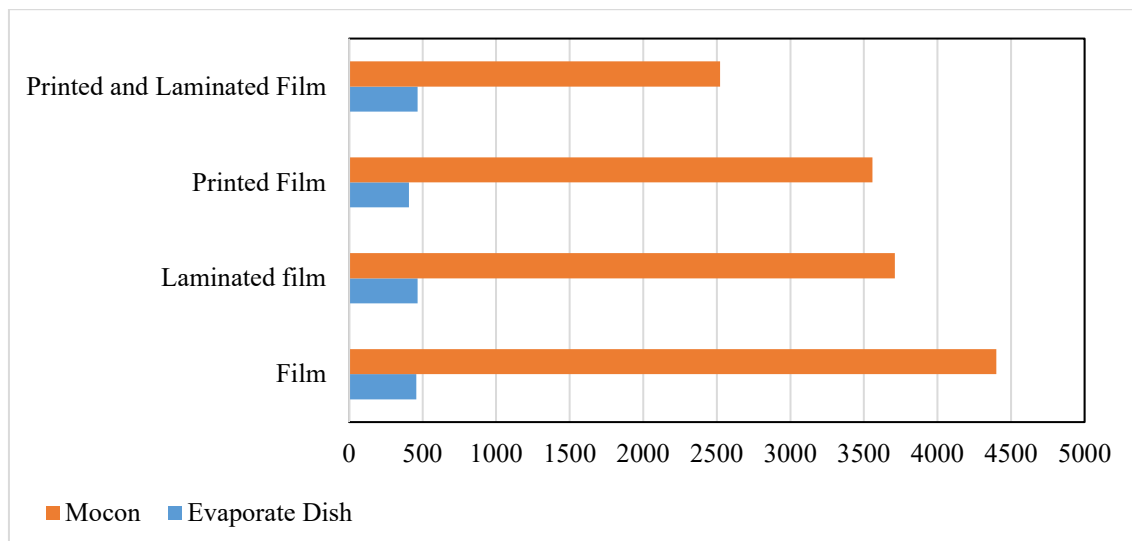


Figure 3. Water vapour permeability test results

As it can be seen from both table 2 and figure 3, the WVP results for two different test principles are considerably different. The situation is a result of ambient conditions that are generated by different test principles. The water vapour transfer through the samples is achieved by water vapour gradient between textile surfaces. If the water vapour pressure that is generated in the microclimate between the textile surface and water vapour source, the water vapour is enforced harder to be transferred through the textile surface. On the other hand, it can be seen from the results that the WVP of samples do not have an important difference for evaporative dish method, whereas there is a significant difference among the

samples for WVP measured by Mocon test device. Since, Mocon test device ensures higher temperature and humidity during water vapour permeability test. The ambient conditions that the test device performs during the WVP measurement provide a better simulation of real usage conditions. According to WVP results measured by Mocon test device, the highest value is obtained for breathable film material. In comparison to film material, laminated film and printed film samples have lower WVP values. Both lamination and printing processes cause a decrease on WVP. In lamination process film material is laminated with a spun bonded nonwoven fabric layer by using adhesive. So, it is an expected result to have lower WVP value due to providing higher thickness and more amount of material in unit area for the obtained textile surface. On the other hand, printing process decreased the WVP more than lamination process. This is a critical result that even if the printing process does not provide coloration and covering the entire surface by a colorant material, there is an important level of WVP decrease after the process. The situation may be attributed to the pressure that is applied to the entire surface of the film material by rotary screens during printing process. The printing process may negatively affect the pore structure of the film surface. The lowest WVP value is obtained with the printed-laminated sample. Regarding the WVP values of the printed sample and laminated sample, it is an expected result for the printed-laminated sample to have the lowest WVP value. Since, both lamination and printing processes have a decreasing effect on WVP.

ANOVA results for evaporative dish method and Mocon test device are given in table 3 and table 4, respectively.

Table 3. ANOVA results for Evaporative Dish method

Groups	Sum of Squares	df	Mean Square	F	Sig.
Between groups	11831.600	3	3943.867	1.108	0.375
Within groups	56941.600	16	3558.850		
Total	68773.200	19			

Table 4. ANOVA results for Mocon test device

Groups	Sum of Squares	df	Mean Square	F	Sig.
Between groups	9025244.950	3	3008414.983	62.716	0.000
Within groups	767505.800	16	47969.050		
Total	9792749.750	19			

According to ANOVA results of evaporative dish method, there is no statistically significant difference among WVP values of the samples, whereas there is statistically significant difference among the samples tested by Mocon test device.

4. CONCLUSION

Disposable diapers can be divided into two groups as breathable and non-breathable. Today generally breathable disposable diapers are used due to keeping child's skin dry, providing a comfortable feeling to the child and prevent diaper rash. The production of breathable diapers is possible by using the breathable back sheet layer which is the most outer layer of the disposable diaper. The back sheet is composed of spun bonded nonwoven layer and PE film. The laminated layer is then printed for an attractive look.

This study aims to investigate the effects of laminating and printing processes on baby diaper back sheet material breathability. For this aim, WVP of breathable film material is determined and compared with the products after printing, lamination and printing-lamination. Consequently, it is observed that, the printing and lamination processes have nearly same deterioration effect on the breathability back sheet material. In addition, WVP value is decreased with approximately 45% as a result of both lamination and printing processes in comparison to film layer. It can be concluded that even if the film material is produced with a high level of breathability, the process parameters of the post processes must be controlled precisely for a good level of end product breathability.

REFERENCES

- [1] Uyanık, S., Kaynak H.K., *Non-Breathable Baby Diaper Back Sheet*, In: Technical Journal, 2018, 12, 2, 74-78
- [2] Dyer, D., *Seven decades of disposable diapers. A Record of Continuous Innovation and Expanding Benefit*, 2005, Available at: https://www.edana.org/docs/default-source/absorbent-hygiene-products/edana---seven-decades-of-diapers.pdf?sfvrsn=3e24da15_2 [Accessed on June 2021]
- [3] Krafchik, B., *History of diapers and diapering*, In: International Journal of Dermatology, 2016, 55, 11, 4-6
- [4] Yaman, N., Senol M.F., Tayyar, A.E., *Alternative test methods for assessing mechanical properties of disposable diapers*, In: Fibres and Textiles in Eastern Europe, 2007, 15, 2, 80-84
- [5] Özen, İ., Çinçik, E., Şimşek, S., *Thermal comfort properties of simulated multilayered diaper structures in dry and wet conditions*, In: Journal of Industrial Textiles, 2016, 46, 1, 256-278
- [6] Gündüz Oktay, E., *Research About Influential Factors On Performance Characteristics Of Different Brand Disposable Baby Diapers And Their Comparison*, PhD Thesis, Pamukkale University Institute Of Science Textile Engineering, 2018
- [7] Akin, F., Spraker, M., Aly, R., Leyden, J., Raynor, W., Landin, W., *Effects of Breathable Disposable Diapers: Reduced Prevalence of Candida and Common Diaper Dermatitis*, In: Pediatric Dermatology, 2001, 18, 4, 282-290
- [8] Yuan, C., Takagi, R., Yao, X.Q., Xu, Y.F., Ishida, K., Toyoshima, H., *Comparison of the Effectiveness of New Material Diapers versus Standard Diapers for the Prevention of Diaper Rash in Chinese Babies: A Double-Blinded, Randomized, Controlled, Cross-Over Study*, In: BioMed Research International, 2018, 6
- [9] Owa, A.B., Oladokun, R.E., Osinusi, K., *Diaper dermatitis among children in Ibadan, Nigeria: frequency and predisposing factors*, In: Eur. J. Pediatr. Dermatol., 2016, 26, 135-141
- [10] Srinivas, S.M., Dhar, S., *Advances in diaper technology*, In: Indian J Paediatr Dermatol, 2016, 17, 83-86
- [11] Wright, A., Akin, F., *Comfort Perception of Breathable and Nonbreathable Diapers*, In: International Nonwovens Journal, 2005, 14, 3, 19-22
- [12] Grove, G.L., Lemmen, J.T., Garafalo, M., Akin, F.J., *Assessment of Skin Hydration Caused by Diapers and Incontinence Articles*, In: Skin Bioengineering Techniques and Applications in Dermatology and Cosmetology, Basel, Karger, 1998, 26, 183-195
- [13] TS 12127 Tekstil-Kumaşlar-Küçük numuneler kullanarak birim alan başına kütlenin tayini
- [14] TS 7128 EN ISO 5084 Tekstil-Tekstil ve tekstil mamullerinin kalınlık tayini
- [15] BS 7209:1990 Specification for water vapour permeable apparel fabrics
- [16] ASTM D6701 – 21 Standard Test Method for Determining Water Vapor Transmission Rates Through Nonwoven and Plastic Barriers



DEGRADATION OF NONWOVEN FABRICS SUITABLE FOR WET WIPES BURIED IN SOIL

DOI: 10.35530/TT.2021.53

V. Sular^{1*}, B. Keçeci²

¹Dokuz Eylul University, Textile Engineering Department, Turkey
(E-mail: vildan.sular@deu.edu.tr)

²Dokuz Eylul University, The Graduate School of Natural and Applied Sciences, Turkey
(E-mail: busra.salman271@gmail.com)

Abstract: *In this research, biodegradation behaviour of nonwoven fabrics suitable for wet wipes having different fibre types such as regenerated cellulose (viscose and Tencel), polyethylene terephthalate (PET) and their blends were investigated. Each nonwoven fabric was buried in soil and test samples were controlled in regular periods. Visual appearance was reported and examined by photographs and microscopic views. According to the changes in visual appearance and weight loss, biodegradation was examined in a systematic way. It has been observed that regenerated cellulose nonwoven fabrics and the PET nonwoven fabrics show big difference under the same degradation conditions. PET fibre content delays biodegradation in the soil and degradation behaviour is similar the content of PET fibre in fabric structure. The higher PET, lower degradation, and the higher cellulosic fibre, the higher degradation was determined for nonwoven fabrics suitable for wet wipes.*

Keywords: *degradation, nonwoven, soil burial, wet wipes*

1. INTRODUCTION

Nonwoven products, which are increasingly attracted by both manufacturers and consumers as faster and cheaper production, continue to be used in new areas every day. In particular, the ease of use of disposable products has created dynamism in the nonwoven sector and caused the sector to grow. Important developments are taking place in the disposable care and hygiene products market, which has an important place in daily life [1]. Most of these developments are aimed at increasing the qualities of disposable textile products. Wet wipes belonging to the care and hygiene products group meet the expectations of consumers in terms of both hygiene and ease of use.

In recent years, non-biodegradable materials have been a subject of discussion due to the damage they cause in the environment and their waste loads, and many studies have been initiated accordingly. Environmentally friendly products have started to be produced with appropriate technology. The need for environmentally friendly applications in frequently encountered products clearly reveals the importance of biodegradation in the textile industry. Biodegradation is the breakdown of organic materials by microorganisms such as bacteria and fungi. In last decade, there are many studies on biodegradation and new biodegradable fibres. Many researches were conducted on biodegradability of different materials and also textiles for different degradability conditions [2-8,10-11]. While the efforts to create new biodegradable nonwovens are continuing, the post-use journeys and waste load of wet wipes,

which are consumed every day in the market were studied [9]. In the context of this study, nonwoven fabrics suitable for wet wipes in landfill environment conditions is examined.

By the increasing consumption of wet wipes in daily life and getting higher with day by day with continuing Covid 19 pandemic, the researches on degradation of single use nonwoven fabrics is getting importance.

2. MATERIAL AND METHOD

In this research, nonwoven fabric suitable for commercial wet wipes were supplied from a producer company and analysed before degradation tests. Six nonwoven fabrics by different raw materials having different fibre contents were selected to examine the differences in biodegradation behaviour. The properties of the fabrics are shown in table 1. As can be seen in table 1, selected fabrics consist of different contents of viscose, Tencel and PET fibres.

Table 1. Structural parameters of nonwoven test fabrics

Fabric No	Raw material	Mass per unit area(g/m ²)	Thickness (mm)	Density (g/cm ³)
1K	100% Tencel	73.2	0.68	0.093
2K	70/30% Tencel/CV	66.0	0.60	0.088
3K	50/50% PET/CV	48.9	0.55	0.084
4K	60/40% PET/CV	70.4	0.38	0.089
5K	80/20% PET/CV	54.4	0.71	0.100
6K	100% PET	42.4	0.57	0.094

All samples were conditioned in the Physical Textile Testing Laboratory of Dokuz Eylül University Textile Engineering Department under standard atmospheric conditions before mass per unit area and thickness measurements. Samples were prepared in a square shape to be buried for 1 month and 2 months period and were weighed to make comparisons before and after burial period. The test samples for soil burial test were shown in figure 1. After that stage all samples were covered with soil. During the degradation process, relative humidity measurements were made in soil and water was sprayed to protect the moisture of the soil in constant such as 95% RH.



Figure 1. The test samples in plexiglass boxes for soil burial test

3. RESULTS

After the burial period completed, test samples were taken from soil and rinsed with ethanol/water solution and dried at room temperature. Weight loss (%) values were calculated after measuring the mass of samples under standard atmospheric conditions. Besides visual appearance of buried test samples was examined and recorded for two different burial periods. These visual examinations were given in table 2 and figure 2.

Table 2. Visual observation results of test samples for two different burial periods

Sample code	Visual appearance after 1 month soil burial	Visual appearance after 2 months soil burial
1K	Hard, brittle, dark spotting, hole and tear occurred	Completely disintegrated
2K	Completely disintegrated	-
3K	Yellow spotting, thinner areas were seen	Increased yellow staining, very thin areas were seen
4K	Yellow spotting, thinner areas were seen	Yellow staining and thinner areas were observed.
5K	Light spotting was observed	Yellow spotting increased
6K	No obvious change	Yellow spotting was seen



Figure 2. The test samples after two months soil burial period

As seen in table 2 and figure 2, Tencel/viscose nonwoven fabric was degraded in the first month. Pure Tencel nonwoven fabric was in degraded after the second month burial period. For fabrics 3K-5K, some thinner places were observed and colour change was seen. Fabric coded 6K (100 PET %) was the test sample having least changing after two months.

According to weight loss values, it has been observed that regenerated cellulose nonwoven fabrics and the PET nonwoven fabrics show big difference under the same degradation conditions. PET fibre content delays biodegradation in the soil and degradation behaviour is similar the content of PET fibre in fabric structure (figure 3).

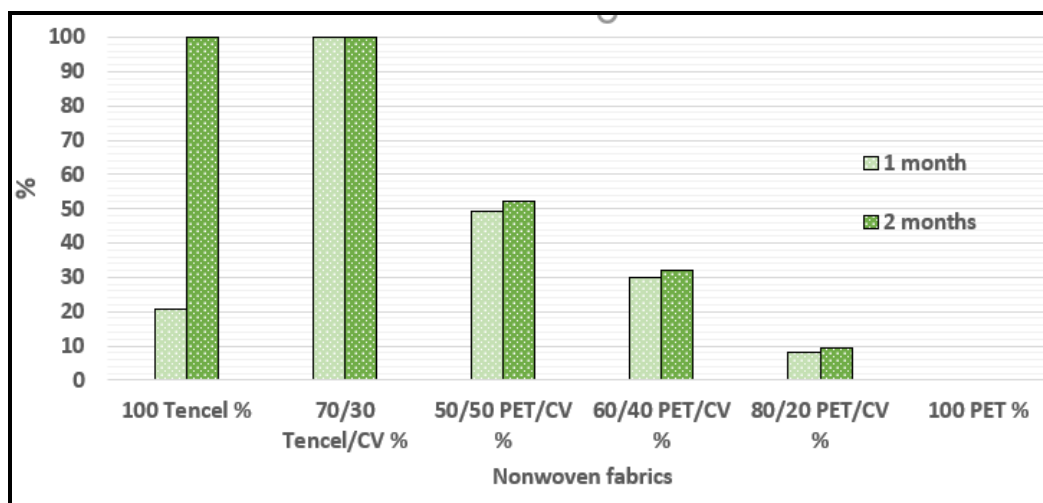


Figure 3. Weight loss values (%) after one month and two months soil burial periods

4. CONCLUSION

In this research, the biodegradability behaviours of nonwoven fabrics suitable for wet wipes and having different fibre types, such as viscose, Tencel, polyethylene terephthalate (PET) and its blends were studied in soil burial tests. Degradation of nonwoven fabrics suitable for wet wipes were evaluated by examining the changes in the fabrics.

Having higher cellulosic fibre in its content supplies relatively faster degradation of nonwoven fabrics in comparison to the other fabrics used in the study. As a general view, nonwoven fabrics having cellulosic fibres in its structure have shown good degradation behaviour. It is possible to conclude that to bury wet wipes is a good idea to decrease the waste load of wet wipes and to make disposing these materials easier if the fabrics have no virus, no microbial contamination and etc.

For further studies, it will be better to simulate soil degradation of wet wipes having different fibre content and carrying different wetting solutions.

ACKNOWLEDGEMENTS

The authors would like to express appreciation to Prof. Dr. Sibel Kaplan for her kind help to supply the fabric samples and besides authors would thank to Dokuz Eylul University, The Graduate School of Natural and Applied Sciences for their support.

REFERENCES

- [1] European Disposables and Nonwovens Association, EDANA publications, *Worldwide Outlook for the Nonwovens Industry 2018-2023*, Brussels, Belgium: EDANA, Available at: <https://www.edana.org/publications/statistics-nonwovens-report> [Accessed on June 2021]
- [2] Alimuzzaman, S., Gong, R.H., Akonda, M., *Biodegradability of Nonwoven Flax Fiber Reinforced Polylactic Acid Biocomposites*, In: *Polymer Composites*, 2014, 2094-2102
- [3] Alshehrei, F., *Biodegradation of Synthetic and Natural Plastic by Microorganisms* In: *Journal of Applied & Environmental Microbiology*, 2017, 5 1, 8-19
- [4] Chee, S.S., Jawaida, M., Sultan, M.T.H., Alothman, O. Y., Abdullah, L.C., *Accelerated weathering and soil burial effects on colour, biodegradability and thermal properties of bamboo/kenaf/epoxy hybrid composites*, In: *Polymer Testing*, 2019, 79, 106054
- [5] Sülar, V., Devrim, G., *Biodegradation Behaviour of Different Textile Fibres: Visual, Morphological, Structural Properties and Soil Analyses*, In: *Fibres and Textiles in Eastern Europe*, 2019, 1, 133
- [6] Choi, S., Jeon, H., Jang, M., Kim, H., Shin, G., Koo, J.M., Lee, M., Sung, H.G., Eom, Y., Yang, H.S., Jegal, J., Park, J., Oh, D. X., Hwang, S. Y., *Biodegradable, efficient, and breathable Multi-Use Face Mask Filter*, In: *Advance Science*, 2021, 8, 2003155
- [7] Gregorich, E.G., Carter, M.R., Angers, D.A., Monreal, C.M., Ellert, B.H., *Towards a minimum data set to assess soil organic matter quality in agricultural soils*, In: *Can. J. Soil Sci.*, 1994, 74, 367-385
- [8] ISO 11721-1:2001. Textiles – Determination of resistance of cellulose-containing textiles to microorganisms – Soil burial test – Part 1: Assessment of rot-retardant finishing
- [9] Klug, P., *Clariant product for wet wipes*, Clariant R & D Personal Care Report, 2008
- [10] Miros-Kudra, P., Gzyra-Jagiela, K., Kudra, M., *Physicochemical Assessment of the Biodegradability of Agricultural Nonwovens Made of PLA*, In: *Fibres and Textiles in Eastern Europe*, 2021, 29, 1, 145, 26-34
- [11] Park, C.H., Kyung, Y., Seung, K., Im, S., *Biodegradability of cellulose fabrics*, In: *Journal of Applied Polymer Science*, 2004, 94, 1, 248-253



A CASE STUDY FOR WATER FOOTPRINT ASSESSMENT OF A DENIM PRODUCT

DOI: 10.35530/TT.2021.55

V. Sular^{1*}, B. Soy¹, K. Yağci²

¹Dokuz Eylul University Textile Engineering Department, Turkey
(E-mail: vildan.sular@deu.edu.tr, berkaysoy96@gmail.com)

²Roteks Tekstil San. ve Tic.A.Ş.
(E-mail: korhanyagci@roteks.com.tr)

Abstract: *The awareness of the fact that the leading cause of the bad environmental conditions in our world is the human factor, has been increasing in recent years. This awareness enables people, companies, and organizations to decrease water consumption, to decrease carbon emission, to decrease using harmful chemicals, consequently people who are aware of global warming and depletion of resources are taking actions to save our planet for a sustainable life. Textile is one of the big sectors affecting the environmental pollution in a very bad way. For that reason, the present water footprint research was conducted on textiles and a denim company was especially chosen to examine the water footprint because of denim sector's being one of the biggest polluters and wasting water in a huge amount in the textile industry.*

Firstly, the limits of the research were obtained as finishing operations under the scope of water footprint. The production steps and wastewater occurring points were obtained carefully for different denim finishing processes. After that stage, personal water consumption during denim apparel production was examined in detail. To create a good inventory analysis, many meetings were performed, and a survey was prepared to collect the data about wastewater of the company. By the help of this water footprint evaluation, the processes that create the most wastewater and the distribution of water footprint according to processes and other sources that cause water consumption were determined for one pair of denim trouser accepted as a functional unit in the context of the research.

Keywords: *denim, inventory analysis, textile, water footprint*

1. INTRODUCTION

Textile is an industry branch where water is used intensively. In the textile industry, denim fabric production is the foremost sector in terms of consuming/polluting water. Approximately 10000 litres of water are consumed for one denim trousers. In addition, dyeing, finishing and washing processes pollute the water as much as they consume [1]. Today, consumers care not only for the quality and appearance of a product, but also for its environmental affect, and this factor drives companies towards an environmentally friendly production. Firms or organizations, with "water footprint" calculation; can create a roadmap for improvement works related to its own water consumption and water footprint. The water footprint also allows the calculation of the effect of water consumption in a particular region or geography on thirst or water scarcity in that region [2].

The total water consumption isn't sufficient to evaluate a footprint, it is necessary to transform these environmental impacts in order that it can be reported as water footprint (ISO

14046, 2011) and is defined as “the total amount of water produced by impact processes, products, or services at all stages of their life cycle” [3].

The fact that its fresh water is a central source may mean that the water will come. If the water becomes untreatable, it will be able to be made safe in terms of water resources, which are becoming sustainable to be completed in a short time. The water becoming non-recoverable can become sustainable to become complete over time. The amount of water used to produce a product or service is called “Water Footprint”. In 2002, UNESCO - I Arjen Hoekstra, which is probably not found in the total volume during the time spent, can be repeated for the first time with the "water footprint", which determines the plan of the used water volume [1]. Changes in climate conditions, water consumption and water pollution force humans to think about water resources and water quality. This situation causes water scarcity that should be calculated, assessed, estimated, and taken precautions.

Water footprint is grouped under three headings as blue, green and grey water footprints [1]. These are green, blue and grey water footprint. Green and blue water footprint consider total consumption and whereas grey measures the amount of freshwater polluted. The blue water footprint refers to the volume of surface and groundwater consumption along the supply chain of a product or service. ‘Consumption’ refers to the losses that occur when water evaporates, returns to another catchment area or the sea or is incorporated into a product. It also includes water that does not return in the same period (i.e., withdrawn in a scarce period and returned in a wet period).

2. MATERIAL AND METHOD

The research was carried out in a denim clothing company that supplies denim fabric and carries out garment, washing (finishing), packaging and shipping processes. The company was established in 1986 in Izmir. In the company where 1000 workers are employed, approximately 300 thousand pieces of denim products are produced monthly.

For the data collection stages to be healthy, meetings were held in the company within the scope of the research and the production processes were examined on site. Detailed information was obtained on dry and wet processes, spray and laser processes and end products. The water footprint of a pair of jeans considers the sum of the water footprint of each step, or process, required to manufacture it. From fibre production to fabric and apparel production, many production steps are taken place such as ginning, yarn production, indigo dyeing, weaving, sewing and finishing treatment operations. For that reason, the limits of water footprint calculations were determined in the present research and as a border, the finishing operations department of the company was determined. One pair of denim trouser (0.577 grams) was determined as the functional unit. The system limit of the research is shown in figure 1 and blue water footprint given in figure 2 was decided to evaluate for the company.

The two most produced products in the company were decided to calculate water footprint. These products, which are named as Product 1 and Product 2 in the research, constitute 80% of the production of the washing department of the company such as 40% and 40% (table 1).

In order to determine water consumption of the selected denim product, an inventory analysis was conducted for operational stages and personal use and cleaning. Input water was taken into consideration for every process stage, no recycled or reused water were not processed in the company. A detailed form was prepared, and the form was fulfilled by all staff working in the finishing department of the denim company. By interviewing a total of 28 people in this department and other staff supporting the production was considered during personal consumption calculation.

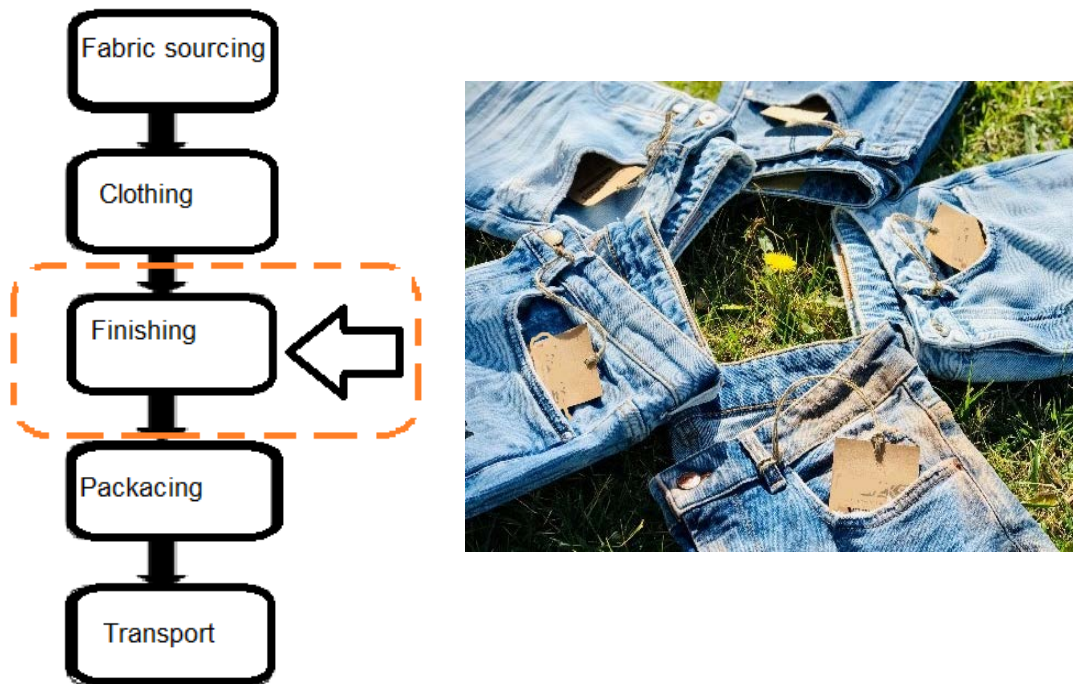


Figure 1. General process flow of the denim company and system limits of the research

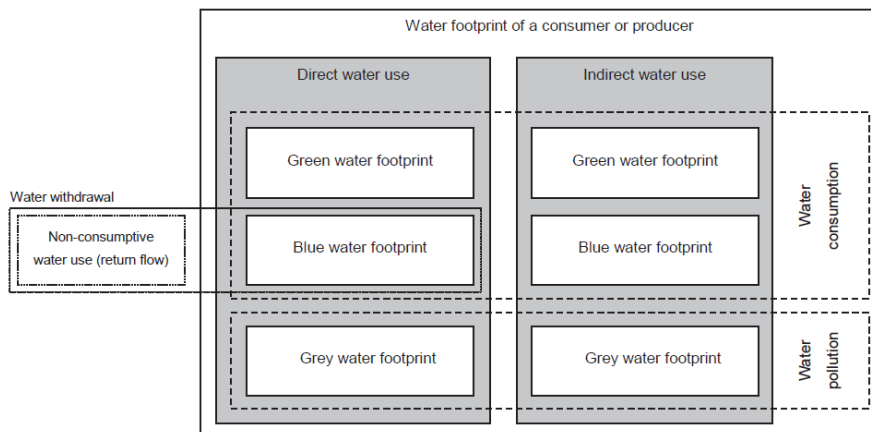


Figure 2. Schematic representation of the components of a water footprint [4]

Table 1. Process flow for product 1 and product 2

Product 1		Product 2
Rinse		Rinse
Stone washing		Stone washing
Bleaching		Softening
Neutralization		Wringing
Softening		Drying
Spray		
Wringing		
Drying		

Water consumption according to different finishing processes was shown in figure 3 and figure 4. The highest consumption values were determined for bleaching and neutralization after bleaching. Operational and personal consumption were considered

together, it can be said that a process improvement is needed to decrease water footprint for product 1 (figure 5).

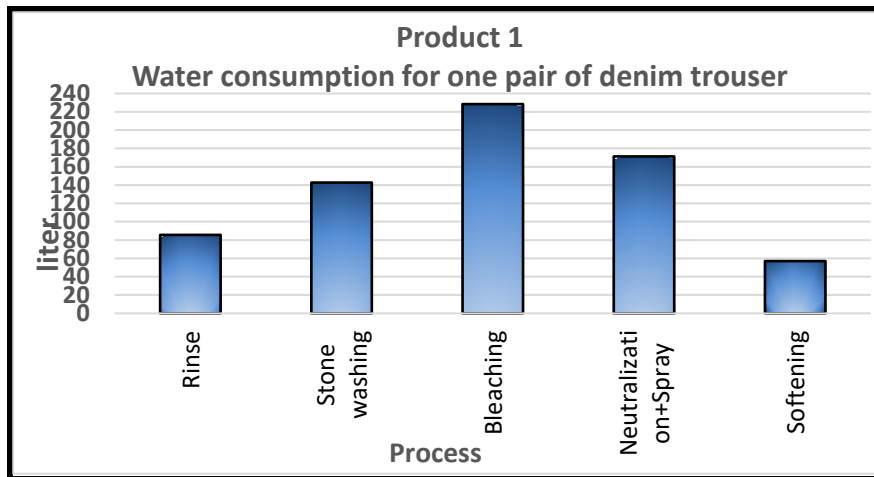


Figure 3. Water consumption of product 1 according to different finishing processes

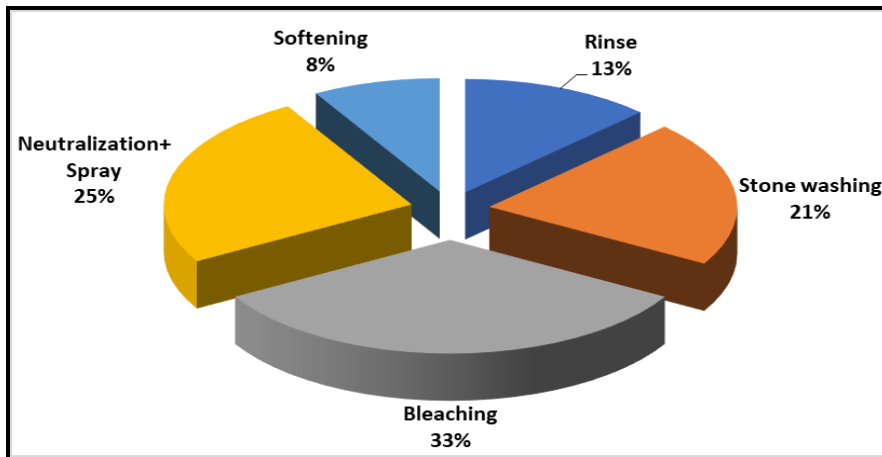


Figure 4. Water consumption distribution for processes of product 1

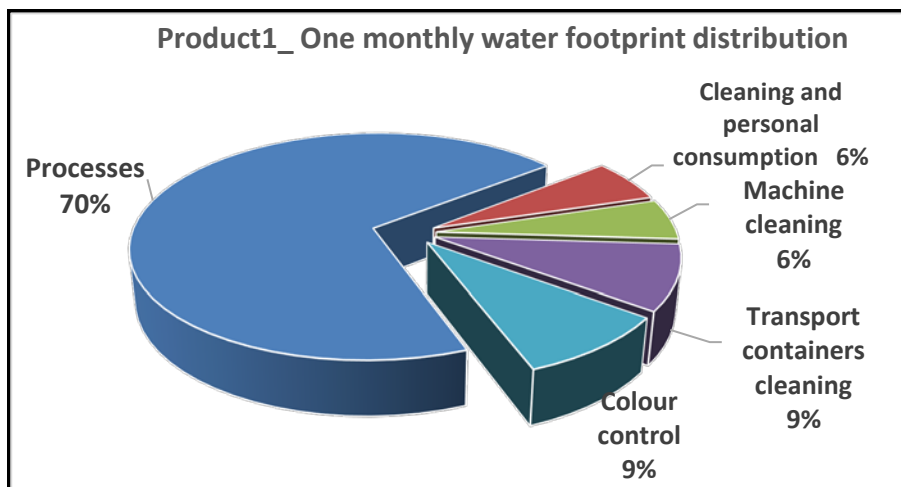


Figure 5. Water footprint of operational consumption and human consumption for product 1

As seen in figure 6-7, when bleaching process was not used in production, the total

consumption of water decreases dramatically. By not using bleaching also neutralization, a darker colour is obtained obviously but if it can be explained to the customers well and customers are persuaded to use it, a high amount of water saving is possible.

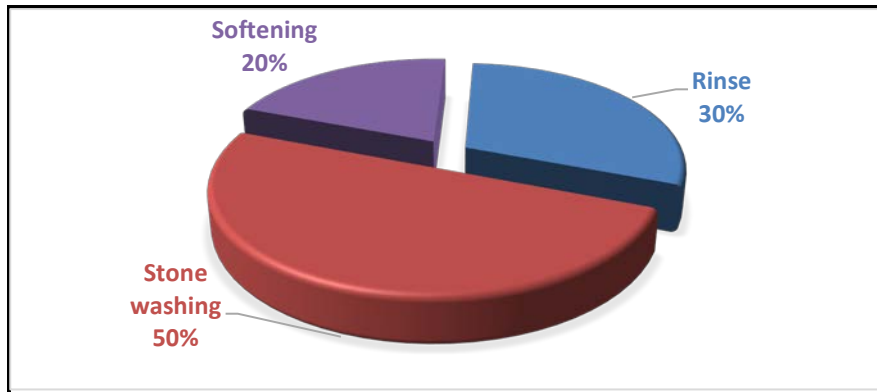


Figure 6. Water consumption of product 2 according to different finishing processes

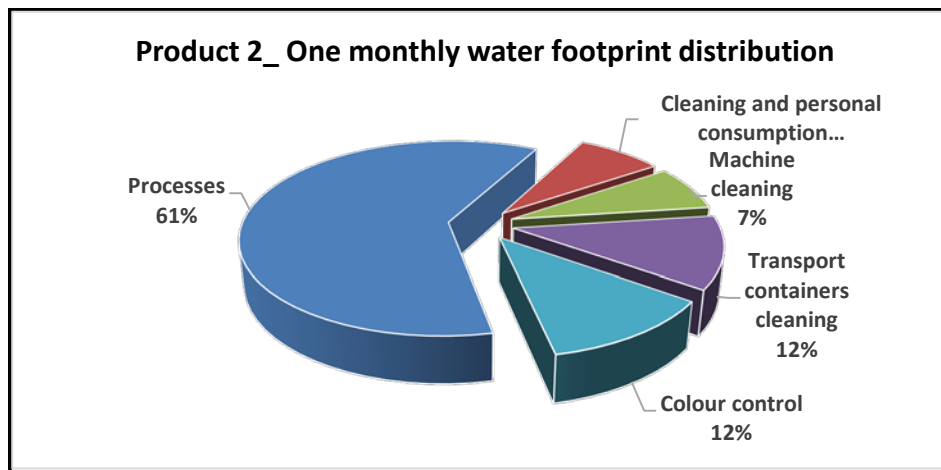


Figure 7. Water footprint of operational consumption and human consumption for product 2

3. CONCLUSION

Today, determination the impact of any production or any action on the environment and reducing these impacts by taking precautions and saving our planet has become one of our biggest tasks. Carbon and water footprint evaluations may help to determine these harmful impacts on environment before acting for any precaution. In this research, within the washing limits of denim fabric production, which processes, or stages cause harm to the environment on the basis of water footprints were examined and evaluated for one pair of trouser as a functional unit.

Certainly, assessment of water footprint does not solve all environmental problems of a company, but it simply shows the road map if the company want to start to do something for our world. As a result of the research, there are some advice for the denim company.

- Attempts may be done to reduce the amount of water used in Product 1, which includes the bleaching process.
- Ways to optimize the water level used in the current production processes in the company and ways to reuse or recycle the water that is currently used in the same process or in a different area should be planned.
- Low-flow water nozzles and faucets or faucet aerators can be used.

- It can be focused on alternative finishing methods that can be made without water or with less water.
- Particular attention can be given to colouring and patterning with laser applications which is more environment-friendly and sustainable process amongst other processes for denim apparel production.

ACKNOWLEDGEMENTS

The authors would like to express appreciation for their valuable support of Bahadır Güneşoğlu as a coordinator of the denim company and the staff of Finishing Department and R&D Department in Roteks Tekstil San.ve Tic.A.Ş. for their contribution to the study during data collection.

REFERENCES

- [1] Muthu, S.S., *Environmental Water Footprints Agricultural and Consumer Products*, 1st ed, Edition, Kindle Edition, 2019
- [2] *Sustainable Environmental Management*, 2021, Available at: <https://www.semtrio.com/en> [Accessed on September 2021]
- [3] Klemes, J.J., *Assesing and Measuring Environmental Impact and Sustainability*, Chapter 7, Oxford, UK, 2015
- [4] Hoekstra, A.Y., Ashok K.C., Maite M.A., Mesfin M.M., *The Water Footprint Assessment Manual*, Earthscan Ltd, UK, 2011
- [5] Tickner, D., Kumar Chapagain, A., *Water Footprint Assesment, A guide for Businesses*, 2017



ENCAPSULATION LAVENDER OIL BY SPRAY DRYING FOR SPORTSWEAR

DOI: 10.35530/TT.2021.23

G. Erkan^{1*}, G.C. Türkoğlu¹, S.Y. Karavana², A.M. Sarişik¹, B. Ütebay³,
A.Ç. Bakadur³, A. Popescu⁴

¹Dokuz Eylül University, Textile Engineering, İzmir, Turkey

(E-Mail: gokhan.erkan@deu.edu.tr, gizem.turkoglu@deu.edu.tr, merih.sariisik@deu.edu.tr)

²Ege University, Faculty of Pharmacy, Department of Pharmaceutical Technology, İzmir, Turkey

(E-Mail: sinemyaprak@hotmail.com)

³Uniteks, R&D Center, İzmir, Turkey

(E-Mail: burcin@uniteks.com.tr, aysegul.cetmeli@uniteks.com.tr)

⁴National Research Development Institute for Textiles and Leather, Bucharest, Romania

(E-Mail: alina.popescu@incdtp.ro)

Abstract: *Microencapsulation technology has been increasingly used in textile industry due to give some peculiarities such as controlled released etc. In this study we aim to make aromatherapy sportswear using lavender oil. Lavender oil is encapsulated by different wall materials. Microcapsules were obtained by spray drying method. Differential scanning calorimetry, thermal gravimetric analysis, Fourier Transform infrared spectroscopy, morphological analyses were applied to microcapsules. Optimum microcapsules were applied to different fabrics. Fastness to washing and rubbing, SEM and antibacterial tests were carried out.*

Keywords: *aromatherapy, lavender oil, microencapsulation, spray drying, textile finishing*

1. INTRODUCTION

Microencapsulation is a technique used to protect active substances from external influences by coating them in small droplets. This technology has preferably been used in the pharmaceutical, chemical and food industries to preserve and prolong fragrance, flavour or therapeutic effect [1,2]. Microencapsulation applications have succeeded in becoming one of the products that add value in the textile industry, create a competitive environment and difference, and increase its market share. In this study, it is aimed to obtain essential oil from *Lavandula angustifolia* plant, which has a pleasant smell and known antibacterial effect [3], and to use it in textile products. In this way, while the effect of this product, which has a limited lifespan, will be increased, and alternative sports and leisure clothes will be developed.

2. MATERIALS AND METHODS

In this study, knitted fabric from different natural and synthetic fibres was used. Gelatin (Gel), gum arabic (GA) and ethyl cellulose (EC) was used as shell material. Gel

was kindly donated from Sel Gel. Sigma-Aldrich branded GA and EC was employed. Lavender oil used as core material was obtained from by Doğal Destek A.Ş. (Tabia). Tween 80 was used as a surface-active agent and obtained from Merck. Tanatex Nano PU was employed as a binder. All other auxiliary chemicals used in the study are technical grade.

Plants grown in the Southern and Central Aegean were harvested and lavender essential oil was obtained by using the water vapour distillation method. The composition of the essential oil was determined by gas chromatography-mass spectrometry (GC-MS). Microcapsules were obtained in different shells and core ratios using selected polymers by spray-drying method. The solutions prepared at the different concentrations were sprayed from the 0.5 mm nozzle into the spray dryer cabinet. The formulation of lavender oil capsules are given in table 1.

Table 1. Formulation of Lavender oil microcapsules

Formulation	Polymer	Lavender oil (%)	Pump speed (ml/min)	Inlet temperature (°C)	Outlet temperature (°C)	Yield (%)
L1	5% Gel	4	10	140	90	34.2
L2		6	5	140	90	31.9
L3		8	5	140	90	32.8
L4	3% Gel	5	2.5	125	85	37.7
L5		10	2.5	125	85	26.6
L6	2.1% Gel	0.5	2.5	125	85	39.1
L7*	1.25% Gel 0.85% GA	0.5	2	125	85	61.1
L8	3% EC	3	2.5	115	85	63.0
L9		6	2.5	115	85	72.4
L10		9	2.5	115	85	78.1

The compressor and air circulation speed were operated at maximum. The experiments were carried out in a Lab Plant brand SD-Basic spray drying device with a main cabinet size of 380 mm x 110 mm. The production yield of the lavender microcapsules was calculated according to the following equation:

$$(\%)Yield = \frac{Actual\ capsule\ amount\ (g)}{Theoretical\ capsule\ amount\ (g)} \times 100 \quad (1)$$

Morphology of the microcapsules is a good indicator for ideal capsule formation. Therefore, scanning electron microscopy (SEM) micrographs were taken. The chemical properties of microcapsules were examined by Fourier transformed infrared (FT-IR) spectrometry. The thermal resistance of microcapsules and behaviour of the essential oil were investigated through thermogravimetric analysis and differential thermal analysis system (DT/TGA). The optimum microcapsule formulation was applied to the different knitted fabrics used in sports and leisure garments according to the exhaustion method. The fabrics were examined using SEM micrographs for the presence of capsules on the fabrics and the determination of the effect of domestic washing and rubbing. The effect of microcapsule finishing on colour was determined. The antibacterial effect of the microcapsule treated fabrics was studied according to AATCC 147 standard. Permeability properties were evaluated before and after microcapsule application regarding air permeability and water vapour permeability tests using ISO 9237 and BS 7209 standards respectively.

3. RESULTS AND DISCUSSIONS

The composition of the lavender oil was revealed as 39.2% linalool and 34.7% linalyl acetate. The other active agents found in the essential oil were camphor, 1,8-Cineole, β -ocimene, β -caryophyllene and borneol. Photomicrographs of gelatine, gelatine-gum arabic and ethyl cellulose micro particles formed using lavender oil are given in Figure 1. When the images of micro particles with 5% gelatine concentration were examined (L1-L3), collapses were observed in the capsule structure. It was thought that this could be due to the relatively high temperature required to dry solutions with high polymer concentrations. The drying effect at lower temperature, provided by using a low polymer concentration, resulted in an improvement in the capsule morphology (L4-L6). A lower aggregation tendency was observed in L7 coded micro particles prepared using a combination of gelatine and gum arabic polymer. When the images of the L8, L9 and L10 samples, which were created using ethyl cellulose, were examined, it was determined that the micro particles obtained were small, spherical and had a smooth surface compared to other formulations. Microcapsules with ethyl cellulose walls were less likely to agglomerate, and the capsules were found to be more rounded. The production yield of the optimum formulation was calculated as 72.4%, which has one of the highest yield.

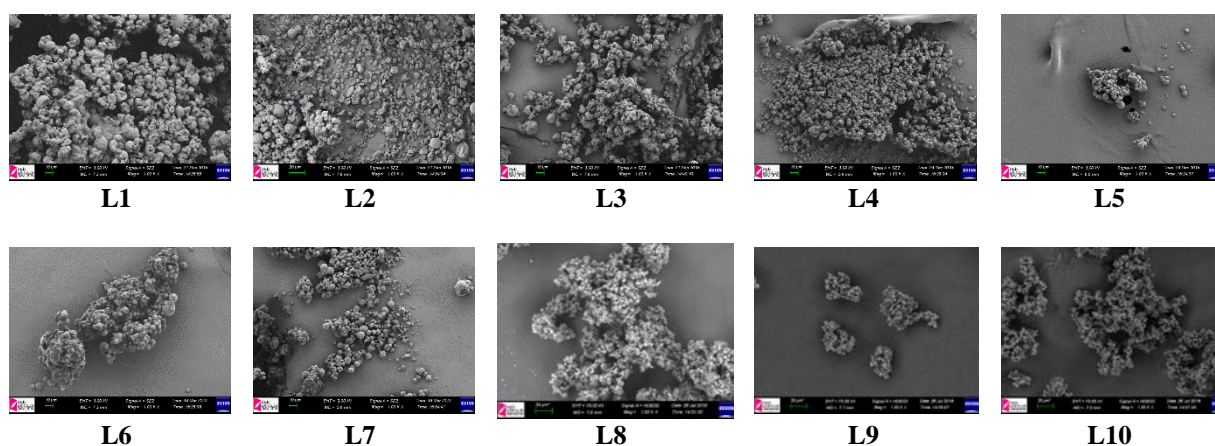


Figure 1. SEM Micrograph of the optimum microcapsule formulation with lavender oil

When the spectrum of lavender oil was examined, the broad band of the OH groups was seen in the range of $3600\text{-}3200\text{ cm}^{-1}$, and the peak of the CH_3 groups was around 2900 cm^{-1} . The characteristic molecular groups of COOR and C=O and the peak of C=O stretching at 1735 cm^{-1} were determined. Both lavender and ethyl cellulose peaks were found in lavender microcapsules (figure 2).

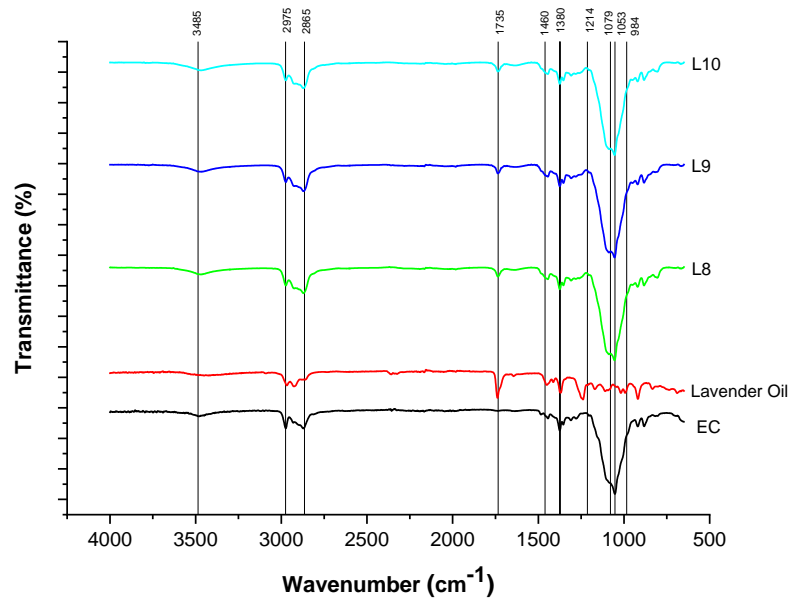


Figure 2. FT-IR Spectra of EC-Lavender capsules

TGA thermograms and DSC diagrams of ethyl cellulose, lavender oil and microcapsules formed with the oil are given in figure 3.

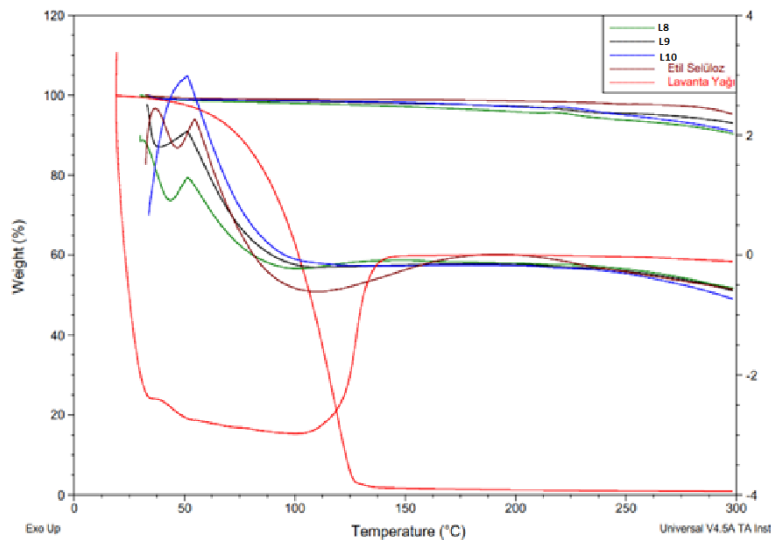


Figure 3. TGA thermograms and DSC diagrams of lavender oil and EC micro particles

When the TGA graph of ethyl cellulose is examined, a weight loss was observed at 100°C due to the moisture in the material. Pyrolysis starts around 225°C and accelerates at 300°C. It is known that the degradation temperature of ethyl cellulose is around 440°C [4]. When the graphs of lavender oil are examined, it is seen that the weight loss starts around 35°C and degrades around 125°C. A wide endothermic peak was observed in the range of 30-120°C in the DSC curve of lavender oil. TGA curves similar to ethyl cellulose were obtained when this oil, which evaporated at low temperatures, was confined to the ethyl cellulose shell. The mass loss at 150°C, where lavender oil is completely decomposed, is around 5% in L8, L9 and L10 formulations.

SEM images of knitted fabrics with L9 formulation before washing, after 1 and 10 washings are shown in figure 4. It was determined that the micro particles were successfully transferred to all the fabrics. It has been observed that the micro particles on the fabric and in the fibre spaces are especially concentrated in the areas covered with binder. A low rate of removal of micro particles from the fabric surface after washing indicates that permanent bonding based on 10 washings is achieved.

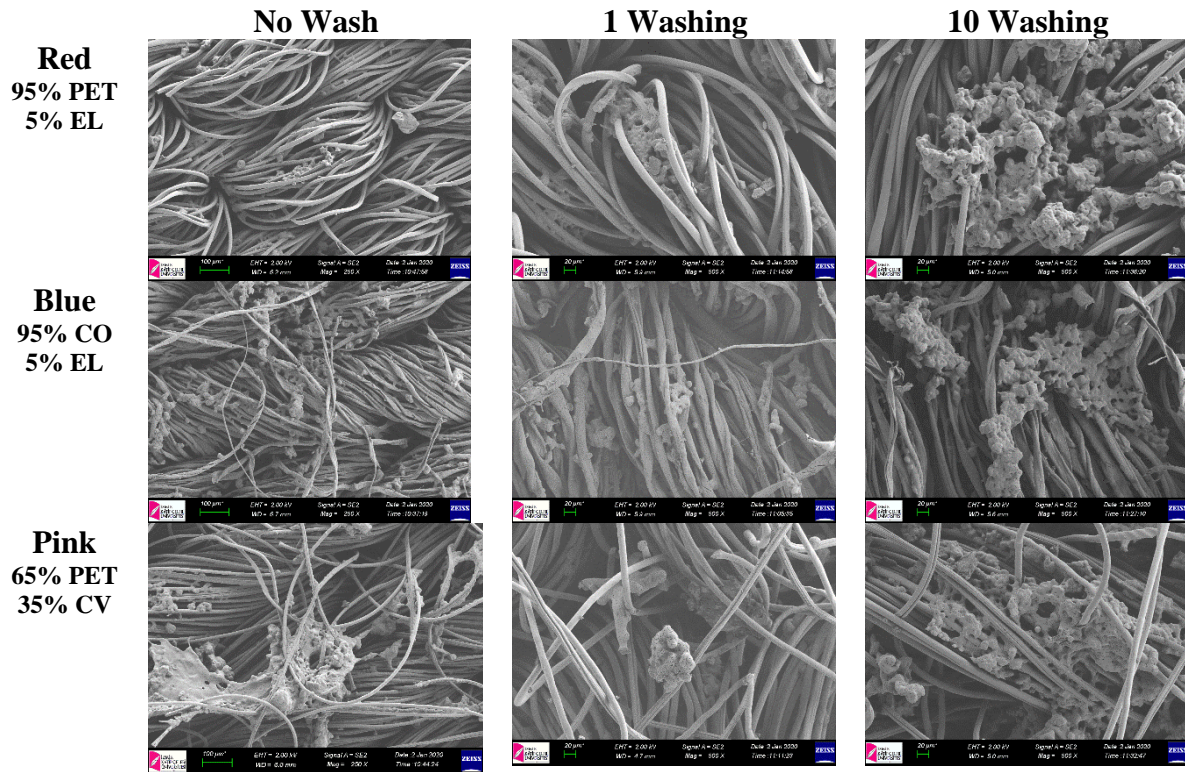


Figure 4. Washing resistance of fabrics containing lavender oil microcapsules

Another of the highest mechanical effects that leisure clothing faces is rubbing. It is important that the micro particles are permanently attached to the fabric exposed to friction. The images of the samples taken after the rub test from the lavender microcapsules applied fabrics are presented in figure 5. It was determined that the micro particles remained on the fabric after rubbing.

Antibacterial assay results on fabrics containing lavender oil capsules are given in table 2. Gram-negative and gram-positive bacterial types were heavily grown for the control samples. Zone of inhibition was not observed against both *E. coli* and *S. aureus* bacteria in lavender-containing fabrics and lower bacterial growth was observed on the contact surface.

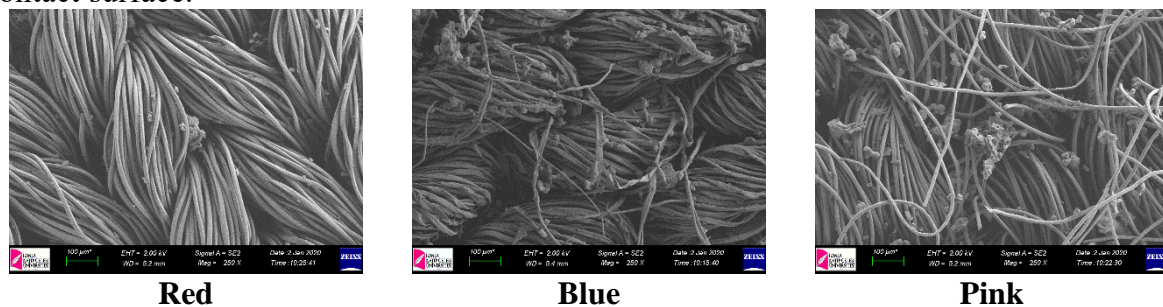
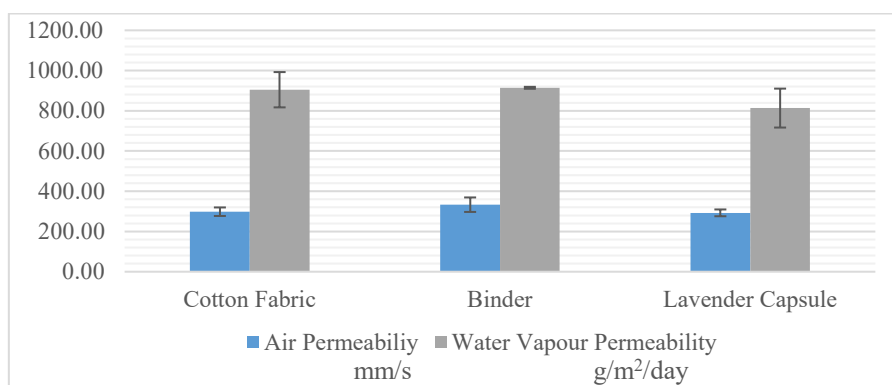


Figure 5. Rubbing resistance of fabrics containing lavender oil microcapsules

Table 2. Antibacterial analysis results of fabrics containing lavender microcapsules

Sample	Gram Negative Bacteria		Gram Positive Bacteria	
	<i>E.coli</i>		<i>S.aureus</i>	
	Inhibition Zone	Growth on the Surface	Inhibition Zone	Growth on the Surface
Control	Not observed	High bacterial growth	Not observed	High bacterial growth
Microcapsule Treated Fabric	Not observed	Medium bacterial growth	Not observed	Medium bacterial growth

Permeability properties of the cotton fabrics were determined before and after microcapsule application. Accordingly, capsule application was decreased the permeability of the fabrics due to blocking the spaces. Theoretically, binder and microcapsule applications are expected to reduce the permeability of fabrics as they block the pores in the fabric. While pristine cotton fabrics have 298.3 mm/s air permeability and 904.7 g/m²/day water vapour permeability, lavender capsule applied fabrics reveal 292.7 mm/s and 813.5 g/m²/day, respectively. However, there was no statistically significant decrease in both air and water permeability results (figure 6).

**Figure 6.** Permeability properties of fabrics containing lavender oil microcapsules

4. CONCLUSION

The aim of this study is to develop sports and leisure clothes containing nano and micro sized capsules with lavender oil. In the manufacture of the capsules, polymers that skin-safe are used as shell polymers. An industrially applicable method, the spray drying, was chosen as the capsule production technique. Lavender oil was selected to provide both aromatherapy effect and odour control that may occur during workout. The developed products have potential for commercialization and suitable for industrial production.

ACKNOWLEDGMENT

This work is produced by the project named “AromaTex” which is supported by MANUNET as international project collaboration between Romania and Republic of Turkey. It is funded by TUBITAK Scientific and Technological Research Council in the frame of the TEYDEB Project 917 0 25 and by UEFISCDI as MNET17 / NMAT-1240. Also we acknowledge to Doğal Destek A.Ş. (Tabia).

REFERENCES

- [1] Ghosh, S.K., *Functional coatings and microencapsulation: a general perspective*, In: Ghosh S.K. (Ed.), *Functional Coatings*, WILEY-VCH Verlag GmbH & Co. KGaA Weinheim, 2006, 1-28
- [2] Salaün, F., *Microencapsulation technology for smart textile coatings*, In: Hu, J. (Ed), *Active Coatings for Smart Textiles* (Woodhead Publishing, 2016, 179-220
- [3] Sienkiewicz, M., Lysakowska, M., Ciecwierz, J., et al., *Antibacterial activity of thyme and lavender essential oils*, In: *Medicinal Chemistry*, 2011, 7, 6, 674-689, <https://doi.org/10.2174/157340611797928488>
- [4] Turkoğlu, G.C., Sarıışık, A.M., Erkan, G., Kayalar, H., Kontart, O., Öztuna, S., *Determination of antioxidant capacity of capsule loaded textiles*, In: *Indian Journal of Fibre & Textile Research (IJFTR)*, 2017, 42, 2, 189-195



GROWING MATERIALS: EXPLORING NEW DESIGN PRACTICES TOWARDS A SUSTAINABLE FASHION SECTOR

DOI: 10.35530/TT.2021.24

E. D'Itria*, P. Bolzan, F. Papile

Department of Design, Politecnico di Milano, Italy
(E-mail: erminia.ditria@polimi.it, patrizia.bolzan@polimi.it, flavia.papile@polimi.it)

Abstract: *Today, sustainability is an imperative for industry, in all its sectors. The common focus is on achieving development that meets the needs of the present without compromising the future of the Planet and its People.*

In the field of fashion and textiles, this momentum toward sustainability translates also into an embryonic process of transformation of the material dimension. This positive transformation is characterized by the choice of new textile solutions supported by growing investments, radical experimentation, and a strong commitment to sustainability. Within this framework, there is a growing interest in bio-based materials, not only from material engineering experts, but also from designers who are starting to explore the possibilities offered by these materials through experiments more focused on design and aesthetics. According to the presented scenario, the proposed article investigates how to strategically implement the systematization of experiments in order to promote the development of an efficient and effective production chain for the growth of bacterial cellulose (BC). To do so, the authors will draw on the knowledge reservoir produced by the De-FORMA project - of which they are all members. This project has just initiated experimentation around the systematization of growth processes and characterization of bacterial cellulose. Specifically, the materials and methods used during the project's initial research phases will be here introduced and illustrated.

Keywords: *bio-based materials; digital fabrication; fashion design; industrial transformation; sustainability*

1. INTRODUCTION

Today, Fashion finds itself in an era of transformation of the material dimension, and the driver behind the choice of new textile solutions is growing investment, radical experimentation, and a firm commitment to sustainability. Precisely, the theme of sustainability can be addressed according to different interpretations, which can touch the aspects of design, process, material and distribution, but also cultural and perceived. The modern spirit of textile innovation is characterised by the expansion of synthetic and re-engineered fibres. Within this framework, there is a growing interest in bio-based materials, not only by materials experts with an engineering background, but also in a relevant way by designers [1-4], who are exploring the possibilities offered by these materials through experiments more focused on the design and aesthetic aspects. This industry is one of the largest industrial sectors in the world. The fashion supply chain is dynamic and complex, extending over several tiers including design, raw material production, manufacturing, distribution, and collection. The commitment to textile research and development should come as no surprise. On one hand, fashion industry needs to address its impacts as it is considered a key contributor to several environmental and social issues. Its negative action

is reported all along its supply chain from the production process to consumer disposal [5-7]. Here, particular attention is paid to the stages in the procurement process and manufacturing flows. According to Chaves and Villalobos (2021) the industry is responsible for exploitation of natural resources, energy consumption, waste production, CO₂ emission, indiscriminate use of synthetic materials, among others [8]. Quantis reported that apparel and footwear industries account for 8% of the world's greenhouse gas emissions, almost as much as the total carbon impact of the EU. The apparel industry alone accounts for 6.7% of the world's greenhouse gas emissions, with more than 50% coming from 3 phases: fibre production (15%), yarn preparation (28%), and the highest impact phase – dyeing & finishing (36%) [9]. About water usage, almost 93 billion cubic metres of water are consumed every year in the garment industry, which could be enough to satisfy the needs of 5 million people. In addition, around 20% of the world's wastewater is the direct result of dyeing and fabric treatment practices. Often at the end of the cycle, this untreated wastewater is pumped back into our water systems, contaminating its contents with toxins and heavy metals [10]. Furthermore, textiles are the largest source of primary micro plastics (specifically manufactured to be smaller than 5mm), accounting for 34.8% of global micro plastic pollution [11]. In parallel with these environmental aspects, social aspects cannot be neglected. As discussed by Mukherjee (2015), the industry has an important role in nurturing an unfair system based on globalisation, vulnerability of global capital and subsequent volatile employment opportunities in the developing countries, growing feminization of the workforce, workers' rights, their health and safety, among the others [12]. On the other hand, Fashion is a cultural and creative industry which has as its main objective the production or reproduction, the promotion, distribution or commercialization of goods, services and activities of content derived from cultural, artistic or heritage origins [13]. Thus, Fashion industry combines two separate dimensions: an intangible – its cultural, artistic or heritage origins - with a tangible one. This material medium through which to express all these meanings is precisely the textiles. Because materials serve as this medium, their role is critical. It is therefore not surprising that fashion is intransigent when it comes to fabrics. Aesthetic-symbolic parameters become fundamental when choosing a particular material: even a small change can have a big impact on the selection of that material [14]. Considering the importance of materials in the fashion industry, it is easy to see why textiles are a fertile ground for experimentation. Specifically, the last few years have seen an increasing interest around biomaterials. This because brands search for more sustainable alternatives against their environmental and social impacts. Wider trends are further contributing to this interest such as climate change, the potential for lower carbon footprints, the will to abandon fossil based synthetic materials, and the war on plastics [14]. Thus, the next big thing in fashion could be bio-based materials as they are focusing the industry attention, as well as shaping its sustainable future [1]. In this context, the paper explores the innovative character of the project De_FORMA. De_FORMA (Design Explorations on bio-Fabricated ORganic MATerials) research project aims to support the shift of focus from the simple growth of the crop to its planning and design in relation to possible applications. By building a material from scratch, it is possible to modify the traditional processing chain, anticipating needs and constraints currently left to post-production. This could enable new production and business paradigms.

2. DEFINING BIOS

Today, bio-based textiles are catalysing sustainable innovation efforts in material development. Increasingly more companies and designers are starting to work on radical and green innovations for the production of naturally-based materials characterized by

sustainable performances. Several research and development opportunities are therefore being pursued in the bio-based materials area. Of these many opportunities available for fashion designers, this paper will focus on a specific dimension: the bio-fabricated materials, which, thanks to their intrinsic characteristics of sustainability and flexibility, offer new ways of thinking about conventional textile manufacturing. But what a bio-fabricated material is? To define it, the terminology about biomaterials and their derivatives has been adapted from the biomedical field, but the authors select the interpretation that fits more for the fashion industry. According to this, the definition adopted is the one proposed by Biofabricate and Fashion for Good in their last report "Understanding 'bio' material innovation". This report considers everything falling under the umbrella term "biomaterial". All biomaterials are bio based but the biological component can largely vary from less than 10% to 100% [15] (figure 1).

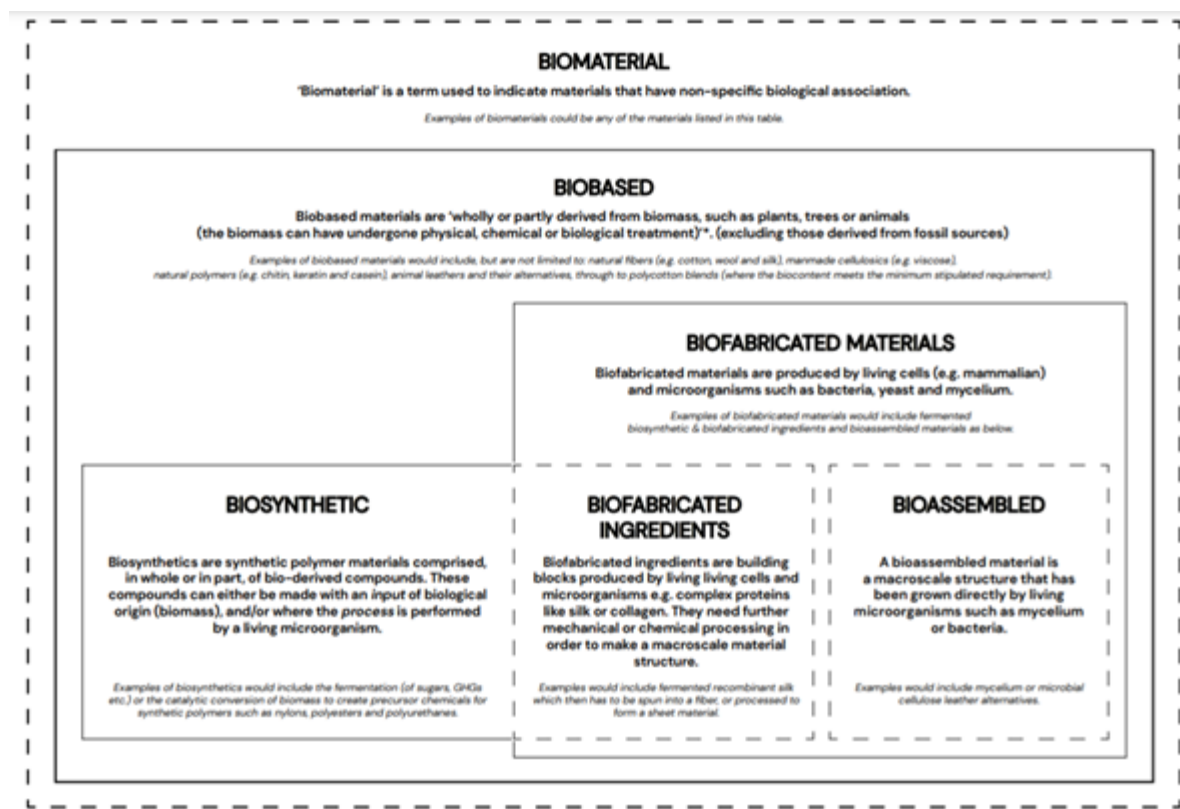


Figure 1. 'Defining Bio' Biofabricate and Fashion for Good, UNDERSTANDING "BIO" MATERIAL INNOVATION: a primer for the fashion industry, December 2020

Bio-fabricated material is "the production of complex living and non-living biological products from raw materials such as living cells, molecules, extracellular matrices, and biomaterials." [15]. This kind of materials cover two sub-categories: Bio-fabricated ingredients and bio-assembled materials. Bio-fabricated ingredients "are building blocks produced by living cells and microorganisms e.g. complex proteins like silk or collagen. They need further mechanical or chemical processing in order to make a macroscale material structure"[15]. Bio-assembled material "is a macroscale structure that has been grown directly by living microorganisms such as mycelium or bacteria" [15]. The present work focuses on one specific bio-assembled material: the bacterial cellulose (BC). As discussed by Amorin, BC is composed of cellulose nanofibers secreted extracellularly by

some bacteria [16]. This is an innovative raw material characterized by ecological, renewable and organic properties [17,18]. BC has a high degree of crystallinity, tensile strength, thermal stability, biodegradability, elasticity and porosity [19]. Furthermore, it is to be safe for contact with the human body [17].

BC appearance, which is similar to leather, allows it to be considered as a new type of sustainable fabric that can be manufactured from several sources [17]. Despite the interesting characteristics of bacterial cellulose, there is still no systematization of the several experimentations and the possibility of scaling up the one-off experiments into a systematized process for the fashion industry seems yet a long-term perspective. BC is inherently sustainable as it is renewable and biodegradable, but current experiments do not consider the production system from the perspective of circularity, integration, and optimization with potential applications.

3. MATERIALS AND METHODS

According to the aforementioned issues, the authors are part of a research group in Politecnico di Milano that launched experimentation around the systematization of growth processes and characterization of BC. The experimentation explores and verifies the mutual collaboration between bio-manufacturing processes and Digital Fabrication (DF) through the filter of design as a holistic discipline. These are the premises from which the De_FORMA project was born. Through the use of DF as an enabler for the construction of ecosystems for the cultivation of BC, De_FORMA aims to explore the possibility of constructing an experimental and flexible production system. The developed system could allow innovative practices such as a prior integration of formal choices, surface/aesthetic treatments, and additional elements, in a logic of zero waste. Methodologically the project follows four consecutive phases to produce iterative knowledge: (1) theoretical analysis, (2) research methodologies, (3) experimental verification of evidences, (4) dissemination of results. The whole process is being conducted in a systematic way, including the analysis and evaluation of results and errors. Now, the project is in progress and heading towards the conclusion of the third step with mature crops being hacked to understand the possibilities offered to the designers. The first step (1) was a theoretical analysis of the state of the art to frame BC research and design opportunities. This analysis phase allowed an exploration of BC evolution through an in depth literature review and mapping of case studies. The case studies were all best practices that have distinguished themselves for their work on two specific dimensions. Some case studies focus their work on enhancing growth processes in terms of production (e.g. culture techniques, morphogenesis, and processes), integration (e.g. other materials, colours, sensors, and actuators), and application (e.g. fashion, health, and lighting). Other case studies work on production chains in the DF context. Furthermore, this step has led to identifying inferences between GM and process and product design. The second step (2) aimed at defining a set-up for bacterial cellulose culture. The methodology applied to carry out this second step was akin with the experimental research [20] which creates a filter for the systemic analysis of the causal relationships between the variables involved, such as: growth of the material, manufacturing process(es) and insertion of components within the material itself. This dichotic process of controlling and monitoring was repeated in an iterative manner and supported by the application of techniques and processes typical of the design activity (design and realisation of tools, supports and prototypes). As a result, a suitable configuration for the culture of bacterial cellulose was identified. The third step is currently happening and is based on experimental verification of the evidence for the formulation of replicable standards. In this phase (3), empirical tests are

carried out to verify the processes of culture and growth of BC and its hybridisation with other materials and/or sensors, in order to define and evaluate possible fields of application. Various set-ups are being defined and applied for the culture of BCs, to be monitored according to qualitative and quantitative parameters (e.g. time and homogeneity of growth, olfactory quality). The monitoring of the growth process, is allowing understanding how to intervene through ad-hoc systems and instruments, realised using DF technologies present in the laboratories involved in the project (figure 2). This further step will now allow to define material and formal characterisation variables, with particular attention to surface qualities (e.g. texture and flexibility), optical qualities (e.g. transparency and colour), volumetric qualities (e.g. thickness), and the relative technical profile.



Figure 2. BC monitoring. Credit: De_FORMA project (2021)

In this context, the heterogeneous competences of the teammates are functionally used as a resource to identify possible fields of application and to support the next and last step of the project which aims at the dissemination of the findings.

4. RESULTS AND DISCUSSIONS

In regard to the broader investigative picture conducted in De_FORMA, the contribution focuses on the strategy implemented for the systemization of experiments, in order to promote the development of an efficient and effective production chain for the growth of bacterial cellulose. In detail, through the use of digital fabrication, it is possible to prototype pilot experiences on a small scale, to test the real feasibility of some insights, such as the approach to a zero-waste production system, the integration of additional elements during the growth of the material, the a priori design of the aesthetic and perceptual parameters of the material. Thanks to the use of additive manufacturing, it was possible to create growth chambers specifically designed to optimize some fundamental steps that bacterial cultures require. Just the redesign of these elements within the prototyping of the production chain has made it possible to make the growth of the material more efficient and controllable the final result. As designers, the

components of sustainability and quality and attention to aesthetics are crucial when conducting materials investigations. From the sustainability point of view, Although GMs are inherently sustainable as they are renewable and biodegradable, current experiments do not consider the production system in terms of circularity, integration and optimization with potential applications. We frequently witness a design exercise, which does not consider the applicative and functional evidence of the material's technical, sensory and intangible characteristics. De_FORMA wants to be the missing link between this experimental trend and the concrete possibility of transforming bacterial cellulose into a material that can be integrated into sustainable production chains and re-produced according to stable effective systems. In this sense we can recognize a level of attention to environmental sustainability:

- of the material, which is bio-based and pre-designed to avoid the generation of subsequent waste;
- of the production process, which adopts Digital Fabrication as an enabler, thus using organic polymers;
- of the impact on the application fields, for example, counteracting the impact that is being recorded in the textile sector (due to fast-fashion), or in the lighting and consumer electronics sector (with regard to the disassembly and recycling of components).

Transforming the traditional manufacturing processes through design thinking and digital fabrication has implications in terms of cultural sustainability in the definition of new knowledge useful to be encoded in new open-ended knowledge systems. Besides, De_FORMA project focuses on the programmability and assessment of the aesthetic features of the bio-manufactured living materials, functionalized to the application in the initial design stages. The aesthetics dimension is closely dependent both on functional aspects and sensory perception. Working on the intrinsic characterization of a "living" and "growing" material is a significant and attractive challenge for designers, who can operate on colonies of bacteria/yeasts to encode the aesthetic aspects of the final bio-fabricated material (figure 3).

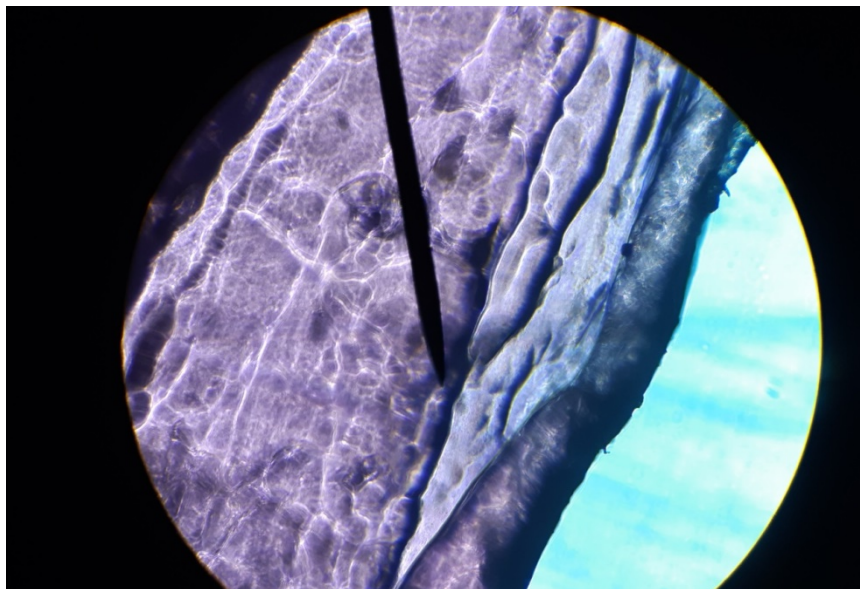


Figure 3. BC "growing" material enlarged under the microscope. Credit: De_FORMA project (2021).

The aesthetic aspects, on which it is intended to intervene, because relevantly perceived by users in contact with the finished product, are:

- surface qualities, e.g. consistency, flexibility, texture;
- optical qualities, e.g. transparency, colours, photoluminescence;
- volumetric qualities, e.g. thickness and weight.

When sensors and actuators are integrated into the material, it will be able to transform itself according to predefined inputs or to variation of parameters subject to direct monitoring, creating in fact a "smart" material, whose aesthetic features are dynamic and programmable. The characteristics of the sobby to be water resistant but not waterproof once dried, ensures easy disassembly of electronic components from the smart material, promoting its environmental sustainability at the end of its life cycle. The whole growing process will offer practitioners a direct feedback on materials properties, showing the direct correlation and interdependence between conceptual ideas and real-life ones. In this way, the aesthetic of a single material will become an expression of the process itself and of the cooperation between designers and other beings, increasing awareness of prime matter use and design. Aesthetics evaluation will be performed taking into account users' tactile, visual, and olfactory experiences along with assessing their emotional and intangible impact. To further all these aspects, the best geometries for the construction of the growth chambers are currently still being tested, as well as different mediums in which to grow BC in the shortest time and with the best aesthetic quality.

5. NEW POSSIBLE SCENARIOS

Within the vision of scaling up the production process of these promising materials, the systematisation of experiments, procedures and process monitoring are basic steps to ensure an appropriate starting point for producing grown bacterial cellulose on a larger scale [6]. Certain studies [21,22] affirm that the gestation time between the discovery of a new material and its widespread commercialisation may present a gestation time of about 20 years in average. To speed up this process, it becomes fundamental to build a concept with the innovation, demonstrate its potential and formally being approved into, e.g., new products to access the market [23]. Imagining growing materials as industrial level products or semi-products requires, then, a well-known data and an accurate repeatability for the production process itself. Defining some standards to be maintained all along the production line is fundamental to envision the application of BC as a material for the fashion industry. Therefore, the properties and intrinsic qualities of the grown material need to be accurately measured, but also material behaviour under operational processes and compatibility with other materials as well will be analysed. Also, an accurate reflection on the possibility to reuse the material at the end of product's life could be an interesting insight on which future works could be addressed. However, whatever the purpose of the investigation it will be, it becomes mandatory to start with the characterisation of the obtained materials towards technical, sensorial, aesthetical and sustainability properties analysis, to effectively envision the grown BC as a candidate alternative in the competitive market of materials for design, and specifically, for the fashion industry. In this perspective, future works on the project will focus on the material characterisation with a particular attempt to correlate production process and material properties, creating a portfolio of possible combinations, or enlightening the procedures to grow materials with already intended properties.

6. CONCLUSIONS

Given the initial results collected and the reflections made on possible future application scenarios, a program for the development of the experiment has been outlined.

The innovative character of the project De_FORMA lies in the shift of attention from the simple growth of the crop to its programming and design, depending on possible applications. By building material from scratch, it will be possible to modify the traditional production chain, anticipating needs and constraints that are currently delegated to post-production. This could enable new productive and entrepreneurial paradigms. The participants in the project, although they all have a background that can be associated with the discipline of Design, come from very divergent fields of research and practice, giving a strong added value of multidisciplinary. The transversal know-how of the participants offers a synergistic intersection able to enhance, integrate and develop knowledge, converging on methods, tools and models. In summary, the innovative character of De_FORMA is to have addressed a topic related to the growth of microorganisms with a design approach. The ultimate aim of the project is to expand the material production potential in view of design and circular economy, embracing a sustainable development perspective and following the material biological cycle.

Although the experiments have not yet reached a level of maturity, we can already confirm some of the insights gained at the beginning of the project, while other optimizations have not yet been achieved. In particular, the idea of making products completely zero waste starting from the use of this material has not yet found a viable solution in a standardized and effective way: this is because during the drying phases, the edges of the BC assume greater rigidity and a different colour than the rest of the piece. For this reason the project cannot yet be said to be concluded and scalable, although interesting observations have already been developed that are producing two derived lines: one starting from the intrinsic chromatic changes of the material, one from the reuse of filaments considered as waste. Current evidence is suggesting that the development of strategies around BC can lead to a deep systemic renewal of the production cycle of new materials all to be designed, thanks also to the typical design culture of designers.

ACKNOWLEDGEMENTS

Participants in the De_FORMA research project, funded within the Farb and Mini-Farb calls by the Department of Design of Politecnico di Milano, are: Patrizia Bolzan (coordinator), Daria Casciani, Erminia D'Itria, Flavia Papile, Stefano Parisi, Barbara Pollini and Carlo Emilio Standoli.

REFERENCES

- [1] Bof-Mckinsey, *State of Fashion 2020*, Available at: <https://www.mckinsey.com/~/media/McKinsey/Industries/Retail/Our%20Insights/The%20state%20of%20fashion%202020%20Navigating%20uncertainty/The-State-of-Fashion-2020-final.ashx> [Accessed on June 2021]
- [2] *A New Textiles Economy: Redesigning Fashion's Future*. Available at: https://www.ellenmacarthurfoundation.org/assets/downloads/publications/A-New-Textiles-Economy_Full-Report_Updated_1-12-17.pdf [Accessed on July 2, 2021]
- [3] Camere, S., Karana, E., *Fabricating materials from living organisms: An emerging design practice*, In: *Journal of Cleaner Production*, 2018, 186, 570-584
- [4] Mihaleva, G., *Bio matter in creative practises for fashion and design*, In: *AI & Soc*, 2020, <https://doi.org/10.1007/s00146-020-00957-5>

- [5] da Silva, C.J.G., de Medeiros, A.D.M., de Amorim, J.D.P., et al., *Bacterial cellulose biotextiles for the future of sustainable fashion: a review*, In: *Environ Chem Lett*, 2021, 19, 2967-2980, <https://doi.org/10.1007/s10311-021-01214-x>
- [6] Laavanya, D., Shirkole, S., Balasubramanian, P., *Current challenges, applications and future perspectives of SCOBY cellulose of Kombucha fermentation*, In: *Journal of Cleaner Production*, 2021, 295, 126454, <https://doi.org/10.1016/j.jclepro.2021.126454>
- [7] Shafie, S., Kamis, A., Ramli, M.F., Abu Bedor, S., Ahmad Puad, F.N., *Fashion Sustainability: Benefits of Using Sustainable Practices in Producing Sustainable Fashion Designs*, In: *International Business Education Journal*, 2021, 14, 1, 103-111, <https://doi.org/10.37134/ibej.vol14.1.9.2021>
- [8] Chaves, B.L., Villalobos, A.S., *Sustainable Fashion*. In: *Gardetti M.Á., Larios-Francia R.P. (eds) Sustainable Fashion and Textiles in Latin America*, In: *Textile Science and Clothing Technology*, Springer, Singapore, 2021, https://doi.org/10.1007/978-981-16-1850-5_15
- [9] *Measuring Fashion: Insights from the Environmental Impact of the Global Apparel and Footwear Industries*, Available at: <https://quantis-intl.com/report/measuring-fashion-report/> [Accessed on August 14, 2021]
- [10] *Fast Fashion's Environmental Impact: The True Price Of Trendiness*, Available at: <https://goodonyou.eco/fast-fashions-environmental-impact/> [Accessed on August 14, 2021]
- [11] Boucher, J., Friot, D., *Primary Microplastics in the Oceans: A Global Evaluation of Sources*, IUCN, 2017, Available at: <https://portals.iucn.org/library/sites/library/files/documents/2017-002-En.pdf> [Accessed on August 14, 2021]
- [12] Mukherjee, S., *Environmental and Social Impact of Fashion: Towards an Eco-friendly, Ethical Fashion*, In: *Journal of Interdisciplinary and Multidisciplinary Studies (IJIMS)*, 2015, 2, 3, 22-35
- [13] *What do we Mean by the Cultural and Creative Industries?*, Available online: <https://unstats.un.org/unsd/iiss/The-UNESCO-Framework-for-Cultural-Statistics-FCS.ashx> [Accessed on August 14, 2021]
- [14] Richetti, M., *Neomateriali nell'economia circolare*, Moda. Ediz. a colori, Milano: Edizioni Ambiente, 2017
- [15] Lee, S., Congdon, A., Parker, G., Borst, C., *Understanding 'Bio' Material Innovations. A primer for the Fashion industry*, In: *Biofabricate & Fashion for Good*, 2020
- [16] Amorim, J.D.P., Souza, K.C., Duarte, C.R., Duarte, I.S., Ribeiro, F.A.Z., Silva, G.S., Farias, P.M.A., Stingl, A., Costa, A.F.S., Vinhas, G.M., *Plant and bacterial nanocellulose: production, properties and applications in medicine, food, cosmetics, electronics and engineering. A review*, In: *Environ Chem Lett*, 2020, 18, 851-869
- [17] Sederavičiūtė, F., Bekampienė, P., Domskienė, J., *Effect of pretreatment procedure on properties of Kombucha fermented bacterial cellulose membrane*, In: *Polymer Testing*, 2019, 78, 105941
- [18] Shi, Z., Zhang, Y., Phillips, G.O., Yang, G., *Utilization of bacterial cellulose in food*, In: *Food hydrocolloids*, 2014, 35, 539-545
- [19] Machado, R.T., Meneguim, A.B., Sábio, R.M., Franco, D.F., Antonio, S.G., Gutierrez, J., Barud, H.S., *Komagataeibacter rhaeticus grown in sugarcane molasses-supplemented culture medium as a strategy for enhancing bacterial cellulose production*, In: *Industrial Crops and Products*, 2018, 122, 637-646
- [20] Bang, A.L., Eriksen, M.A., *Experiments all the way in programmatic design research*, In: *Artifact*, 2014, 3, 2, 1-4
- [21] Eagar, T.W., *Bringing new materials to market*, In: *Technology Review*, 1995, 98, 2, 42-49
- [22] Karana, E., Barati, B., Rognoli, V., Zeeuw Van Der Laan, A., *Material driven design (MDD): A method to design for material experiences*, 2015
- [23] Markham, S.K., *Moving technologies from lab to market*, In: *Research-technology management*, 2002, 45, 6, 31-42



TWO-STEP CROSSLINKING OF PVP/GEL NANOFIBERS

DOI: 10.35530/TT.2021.25

H.K. Güler*, F.C. Çallıoğlu

Textile Engineering Department, Engineering Faculty, Süleyman Demirel University, Turkey
(E-mail: hulyakesici@sdu.edu.tr, fundacengiz@sdu.edu.tr)

Abstract: *In this study, it was achieved that crosslinking of PVP/GEL nanofibers with two-steps. Crosslinking is a process highly important for water-soluble polymers in terms of application areas and mechanical properties. Firstly, crosslinking of PVP polymers experimental studies were carried out via heat treatment at different temperatures and times. Then, GEL polymers were crosslinked with GTA vapour at different times. Morphological analysis was carried out via SEM images and chemical characteristics were determined via FT-IR analysis. Moreover, after the crosslinking process, SD and WL values were calculated. All results showed that before crosslinking of SEM images, nanofibers were smooth, fine and without beads. The average fiber diameter is 196 nm and the fiber diameter distribution is quite uniform. After crosslinking of SEM images, it is expected that all nanowebs will turn from fibrous surfaces to membranous. Generally, SD and WL values decrease with crosslinking time increase. According to all of the SEM images, SD and WL values, optimum conditions were determined for PVP as 4 hours at 180°C and for GEL as 24 hours. Lastly, the presence of PVP and GEL polymers in the nanofiber structure was verified chemically with FT-IR analysis.*

Keywords: *crosslinking, electrospinning, gelatin, nanofiber, poly(vinyl pyrrolidone)*

1. INTRODUCTION

Poly (vinyl pyrrolidone) (PVP) is a water soluble, biocompatible, nontoxic, synthetic and hydrophilic polymer. Similarly, gelatin (GEL) is a natural, protein-based, non-immunogenic, biodegradable, and biocompatible polymer. All of these features are critical in biomedical and cosmetic applications such as wound dressing, tissue engineering, drug delivery and controlled release systems [1-3].

Electrospun nanofibers have unique properties than conventional fibers, such as small fiber diameter (nm), high porosity, small and open pore structure, large specific surface area (m²/g), and high loading capacity. However, if a water-soluble polymer is used during the production of nanofibers, it may be necessary to make them water resistant depending on the application areas. Crosslinking is a method used to make nanofibers water resistant. After the crosslinking process, the polymers become stable in water and aqueous environments. When the literature is analyzed, generally, the PVP polymer is crosslinked using heat treatment or UV light. It is seen in the literature that PVP based nanofibers are crosslinked using heat with different temperature ranges from 140°C to 210°C and different times, such as 14 min., 30 min., 1 hour, 2 hours, 3 hours etc. [4-5]. GEL nanofibers are mostly crosslinked chemically using glutaraldehyde (GTA). Here, GTA was either added directly into the polymer solution or the nanofibrous surface was exposed to GTA vapors for different times (1 hour, 3 hours, 6 hours, 12 hours, 24 hours, and 48 hours etc.) at room temperature. Moreover, some

researchers immersed the gelatin based nanoweb into the GTA solutions for crosslinking [6-7].

In this study, it was aimed at crosslinking and characterizing PVP/GEL nanofibers. Crosslinking of two different water-soluble polymers in a single nanoweb is very limited in the literature. Moreover, crosslinking of nanofibers consisting of both PVP and GEL polymers has not been reported in the literature yet.

2. MATERIALS AND METHODS

2.1 Materials

In this study, PVP (360.000 g mol⁻¹) was used as a polymer and GEL from porcine skin (gel strength 300, Type A) was used as a copolymer. Ultra-pure water (UPW) and acetic acid (AA) were used as the solvents. Glutaraldehyde (GTA) was used as a crosslinker. PVP, GEL, GTA, and AA were purchased from Sigma-Aldrich Corporation (St. Louis, MO, USA) and UPW was obtained from a Millipore Milli-Q System with a conductivity of 18.0MΩ.cm. The polymer concentrations were kept constant for PVP and GEL at 12 wt % and 0.72 % wt, respectively.

2.2 Methods

Nanofibers were produced using an electrospinning method. During the electrospinning process, 26.4 kV voltage, 0.3 mL/h feed rate, 17.0 cm distance between electrodes, 33±2% humidity, and 23.5±1°C temperature were applied. The optimum process parameters were determined from our preliminary studies.

The crosslinking process was carried out in two steps. Firstly, optimum conditions in terms of temperature and time were determined by performing crosslinking of PVP polymer in a vacuum oven at different temperatures (150°C, 180°C, and 200°C) and at different times (1, 2, 3, 4, and 5 hours). In the second step, the GEL polymer was crosslinked with GTA vapors. For this purpose, optimization studies were carried out by placing the nanofibers on the perforated porcelain tray of a 25 cm diameter desiccator containing 10 mL of GTA and keeping them at room temperature (24°C) for 3, 6, 12, 24, and 48 hours.

After crosslinking optimization studies, nanoweb were investigated morphologically by SEM images with 5.000x magnification. Then, the crosslinked nanofibers were soaked in distilled water at room temperature (24°C) for 24 hours and the weight loss (WL) and swelling degrees (SD) were calculated. The samples' water resistance was tested, and the weight loss ratio of the samples was determined using Eq. 1, where W_0 represents the initial weight of the samples and W_1 represents the dry weight of the samples after water treatment. The swelling ratio was evaluated in the same method as the weight loss tests, using Eq 2, where W_2 is the weight of the swelled samples and W_1 is the weight of the dry samples after water treatment was applied.

$$WL(\%) = \frac{W_0 - W_1}{W_0} \quad (1)$$

$$SD(\%) = \frac{W_2 - W_1}{W_1} \quad (2)$$

In addition, a Fourier Transform Infrared Spectrophotometer (FT-IR) was used to chemically determine the presence of polymers (PVP and GEL) in the structure of nanofibers. The device used was a Perkin Elmer Spectrum BX model device with a 2 cm⁻¹

resolution between 400 and 4000 cm^{-1} wavelength and was used in accordance with the KBr disc technique to obtain the results.

3. RESULTS AND DISCUSSIONS

For this study, SEM images of PVP/GEL nanofibers were taken (with various magnifications) before and after the crosslinking process. Before the crosslinking process, SEM results and histogram curve of electrospun PVP/GEL nanofibers are given in figure 1.

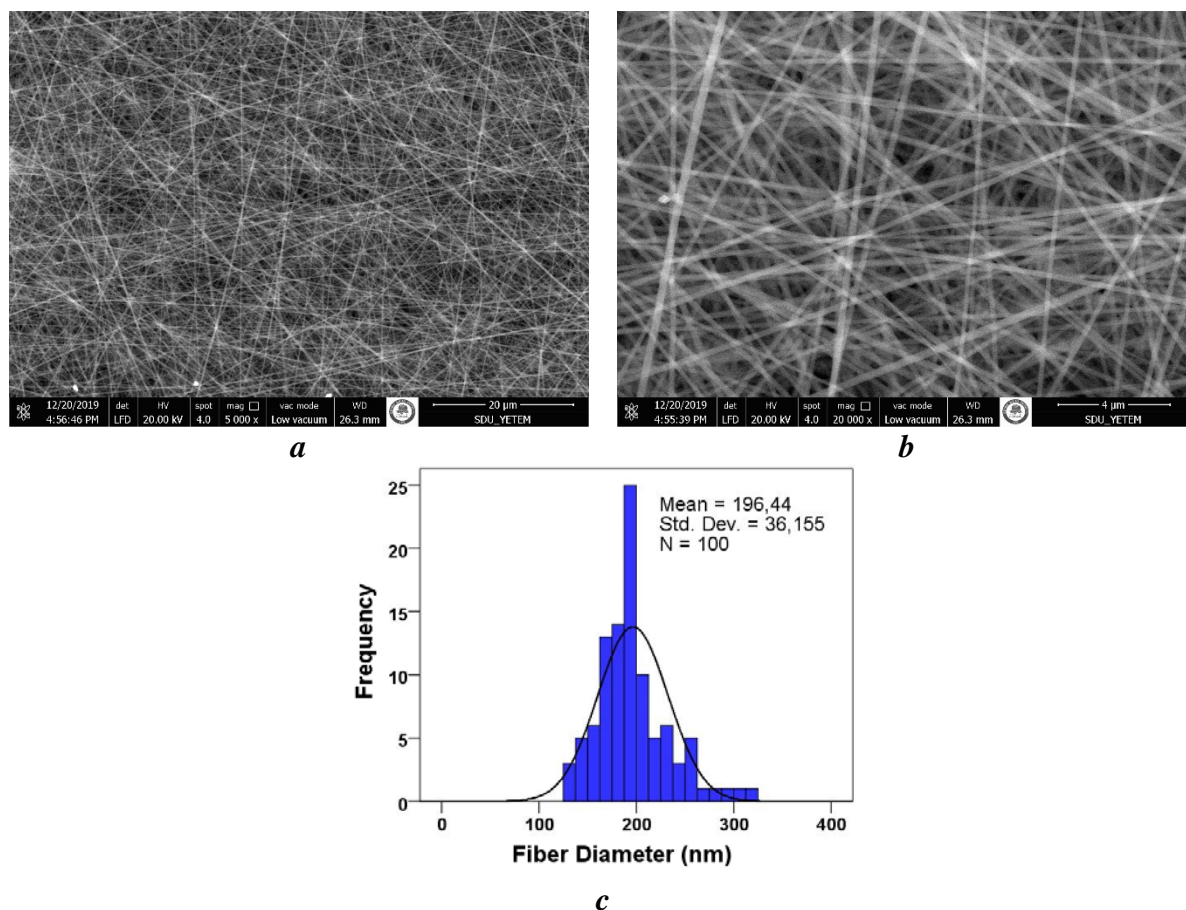


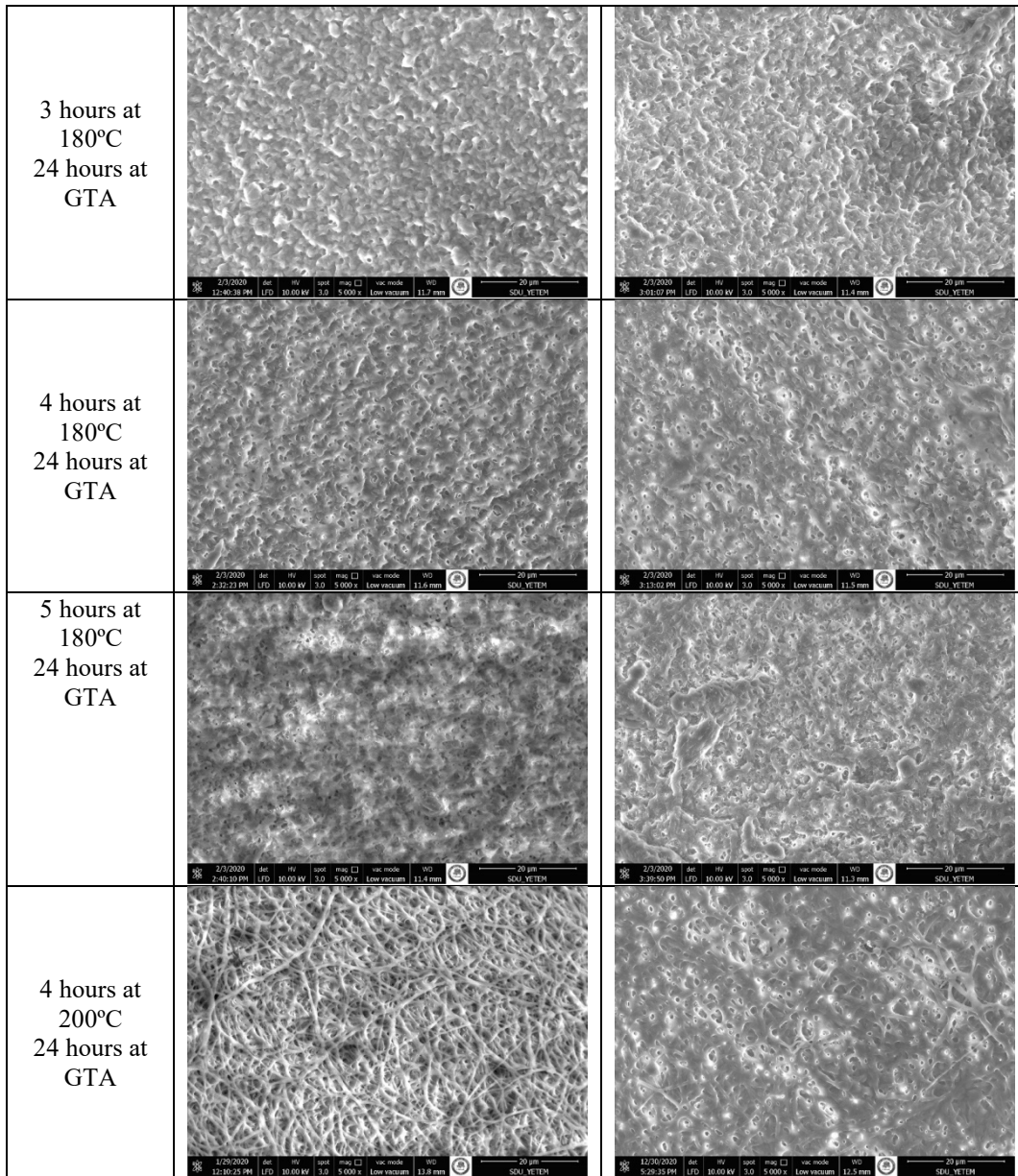
Figure 1. SEM images and fiber diameter histogram of PVP/GEL nanofibers before crosslinking

According to figure 1, it has been seen clearly that nanoweb quality is good and quite smooth and fine nanofibers can be obtained. Furthermore, the average fiber diameter is 196 nm, there is a unimodal histogram curve, and the fiber diameter distribution is uniform.

SEM images of crosslinked PVP/GEL nanofibers at optimum process parameters are given in table 1. SEM images showed that all crosslinked nanofibrous surfaces turned into membranous structures as expected result. It is seen that the fibrous structure is more preserved as the processing time and temperature increase.

Table 1. SEM images of PVP/GEL nanofibers after crosslinking and swelling tests at various conditions.

Crosslinking conditions	SEM image after two-step crosslinking	SEM image after 24 hours in distilled water at room temperature (24°C)
4 hours at 180°C 3 hours at GTA		
4 hours at 180°C 6 hours at GTA		
4 hours at 180°C 12 hours at GTA		
4 hours at 180°C 48 hours at GTA		
2 hours at 180°C 24 hours at GTA		



After swelling tests, SD and WL values of PVP/GEL nanofibers were calculated under various crosslinking conditions using equations 1 and 2 which were explained in the methods part. The results are given in table 2.

Table 2. SD and WL values of PVP/GEL nanofibers after swelling test

Crosslinking conditions	SD (%)	WL (%)
4 hours at 180°C 3 hours at GTA	1130	27.71
4 hours at 180°C 6 hours at GTA	862.29	23.75
4 hours at 180°C 12 hours at GTA	356.60	15.87
4 hours at 180°C 24 hours at GTA	271.62	11.90
4 hours at 180°C 48 hours at GTA	281.96	12.85

2 hours at 180°C 24 hours at GTA	268.86	23.39
3 hours at 180°C 24 hours at GTA	214.49	20.28
4 hours at 180°C 24 hours at GTA	224	9.63
200 °C'de 4 saat GTA'da 24 saat	282.83	18.78

Crosslinking results show that crosslinking could not be achieved at 150°C. Although experiments were carried out at different times, it was seen that the temperature was insufficient. As the holding time at 180°C decreases, it is clearly seen that the surface passes through from the fiber form to the membrane form. It was observed that the nanofiber surface almost completely preserved the fiber form from the SEM images taken after crosslinking at 200°C, but this fiber form disappeared in SEM pictures captured after the swelling test. It was decided that the temperature of 200°C was not suitable for the crosslinking process for PVP polymer, considering both the high temperature and the values of SD and WL. For this reason, in the first stage of the study, it was decided that the process time of 4 hours at 180°C was optimum.

Similarly, in the second stage of the study, it was observed that the nanofibrous surfaces tried to protect the fiber form as the processing time increased in the GTA application. However, because the SD and WL values were higher, there was no significant difference between SEM images, and the procedure duration was longer, it was determined that the optimum time would be 24 hours rather than 48 hours.

FT-IR spectroscopy confirmed the presence of PVP and GEL polymers in the chemical structures of the nanofibers (figure 2).

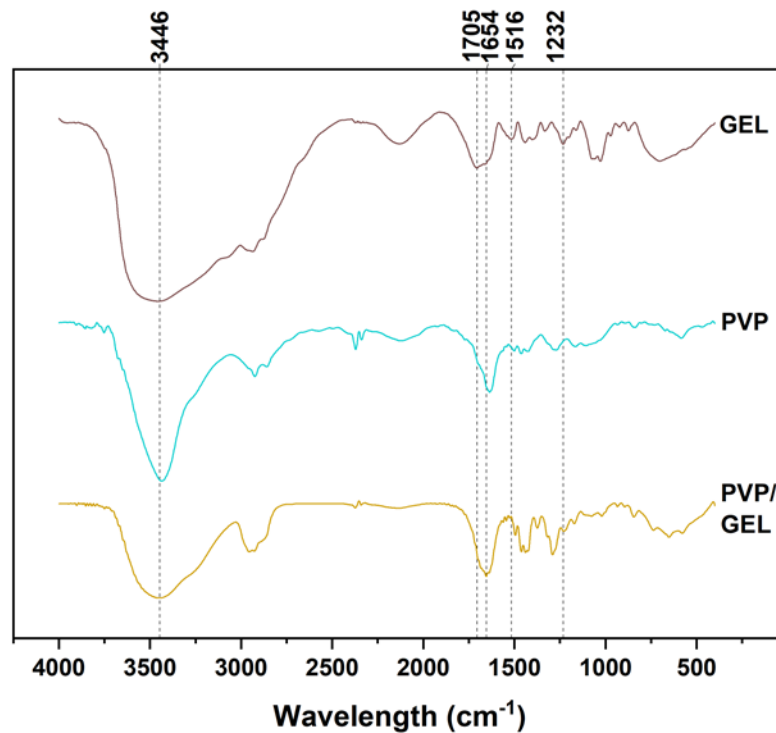


Figure 2. FT-IR spectra of PVP and GEL polymers and PVP/GEL nanofibers

There is an OH stretching intensive peak that was attributed to the presence of water at 3434 cm^{-1} . This intensive peak appeared crosslinked PVP/GEL nanofibers at 3446 cm^{-1} . There is another peak that occurred related to C=O at 1654 cm^{-1} in the spectra of PVP. This peak arises from the spectra of PVP/GEL nanofibers at 1659 cm^{-1} . Similarly, there were three major absorption bands in the spectra of gelatin and nanofiber samples: amide I (C=O stretch), amide II (N–H bend and C–H stretch), and amide III (C–N stretch plus N–H in-phase bending). In the spectra of gelatin, amide I, amide II, and amide III peaks were shown at around 1705 cm^{-1} , 1516 cm^{-1} , and 1232 cm^{-1} , respectively. These characteristic peaks were determined in the spectra of the nanofibers [8].

4. CONCLUSIONS

This study achieved optimization and characterization of crosslinked PVP/GEL nanofibers. According to the results, 4 hours at 180°C for PVP and 24 hours at GTA vapors for GEL were selected as the optimum. Crosslinking of PVP/GEL nanofibers in two steps could be carried out successfully. At the end of this study, these two polymers can be used in many application areas involving aqueous media. Thus, it is thought that the crosslinking of these two polymers commonly used in biomedical applications in a nanoweb will contribute significantly to the literature.

ACKNOWLEDGEMENTS

The authors would like to express appreciation for the financial support of the Süleyman Demirel University Scientific Researches Project Unit [Project Number = FDK-2019-6761] and The Scientific and Technological Research Council of Turkey [Project Number = 119M880].

REFERENCES

- [1] Dhandayuthapani, B., Krishnan, U.M., Sethuraman S., *Fabrication and characterization of chitosan-gelatin blend nanofibers for skin tissue engineering*, In: J. Biomed. Mater. Res. - B Appl. Biomater., 2010, 94, 1, 264-272, <https://doi.org/10.1002/jbm.b.31651>
- [2] Wang, L., Chang, M. W., Ahmad, Z., et al., *Mass and controlled fabrication of aligned PVP fibers for matrix type antibiotic drug delivery systems*, In: Chem. Eng. J., 2017, 307, 661-669, <http://dx.doi.org/10.1016/j.cej.2016.08.135>
- [3] Ki, C.S., Baek, D.H., Gang, K.D., et al., *Characterization of gelatin nanofiber prepared from gelatin-formic acid solution*, In: Polymer, 2005, 46, 14, 5094-5102, <https://doi.org/10.1016/j.polymer.2005.04.040>
- [4] Rosa, R.M., Silva, J.C., Sanches, I.S., et al., *Simultaneous photo-induced cross-linking and silver nanoparticle formation in a PVP electrospun wound dressing*, In: Mater. Lett., 2017, 207, 145-148, <https://doi.org/10.1016/j.matlet.2017.07.046>
- [5] Lubasova, D., Niu, H., Zhao, X., et al., *Hydrogel properties of electrospun polyvinylpyrrolidone and polyvinylpyrrolidone/poly (acrylic acid) blend nanofibers*, In: RSC Adv., 2015, 5, 67, 54481-54487, <https://doi.org/10.1039/C5RA07514A>
- [6] Laha, A., Sharma, C.S., Majumdar, S., *Sustained drug release from multi-layered sequentially crosslinked electrospun gelatin nanofiber mesh*, In: Mater. Sci. Eng. C, 2017, 76, 782-786
- [7] Zhang, Y.Z., Venugopal, J., Huang, Z.M., et al., *Crosslinking of the electrospun gelatin nanofibers*, In: Polymer, 2006, 47, 8, 2911-2917
- [8] Cengiz Çallıoğlu, F., Kesici Güler, H., Sesli Çetin, E., *Emulsion electrospinning of bicomponent poly (vinyl pyrrolidone)/gelatin nanofibers with thyme essential oil*, In: Materials Research Express, 2019, 6, 12, 125013, <https://doi.org/10.1088/2053-1591/ab5387>



ELECTROSPINNING OF ST. JOHN'S WORT OIL LOADED MICROCAPSULES BASED PVA NANOFIBERS

DOI: 10.35530/TT.2021.26

H.K. Güler^{1*}, F.C. Çalhoğlu¹, İ.Y. Mol¹, M. Geysoglu²

¹Textile Engineering Department, Engineering Faculty, Süleyman Demirel University, Turkey
(E-mail: hulyakesici@sdu.edu.tr, fundacengiz@sdu.edu.tr, iremyagmurmol@gmail.com)

²Bioengineering Department, Engineering Faculty, Süleyman Demirel University, Turkey
(E-mail: mustafageysoglu@sdu.edu.tr)

Abstract: In this study, it was achieved that the production of St. John's Wort oil loaded Eudragit RS 100/PVA microcapsules by emulsion/solvent evaporation method and the microcapsules were embedded in PVA nanofibers. Morphological analysis was carried out with SEM images of both microcapsules and nanofibers. The presence of St. John's Wort oil, PVA and Eudragit RS 100 polymers were confirmed in the chemical structure of microcapsules and nanofibers by FT-IR. According to experimental studies, microcapsules were produced to have a smooth surface, a spherical shape and a uniform particle size. The PVA concentration was kept constant at 10% wt and microcapsule concentrations were applied as 1, 3, 5, 7, and 9 wt %. Then, polymer solution properties were measured, such as conductivity, viscosity, and surface tension. It was determined that viscosity and surface tension values increased with microcapsule concentration increase, while conductivity did not change significantly. Nanofiber production was realized via the electrospinning method under the optimum process parameters. According to the SEM images and histogram, nanowebs have a fine fiber diameter, smooth surface, high quality and no bead structure. In addition, the average microcapsule size is 30 µm, average fiber diameter is 430 nm and the fiber diameter uniformity coefficient is 1,014. It is thought that this nanofiber surface containing microcapsules embedded in St. John's Wort has the potential to be used as a wound dressing.

Keywords: electrospinning, emulsion/solvent evaporation, microcapsule, nanofiber; St. John's Wort oil

1. INTRODUCTION

Eudragit RS 100 is a biocompatible, low-cost, high-strength, water-insoluble polymer that is commonly utilized as a wall material in extended-release microcapsules. Due to its low permeability, it is advantageous for drug release. In addition, Eudragit RS 100 is an easy-to-use and easy-to-process polymer in all forms, such as aqueous dispersions, granules, organic solutions, powders or ready-to-use powders [1]. As a core material to load into microcapsules within the scope of the study, St. John's Wort oil is a medicinal plant that has been used for centuries for burns, wounds, inflammation of the skin, nerve pain and stopping bleeding. *Hypericum perforatum* L. has antibacterial, antimicrobial, antiviral, and anti-inflammatory effects as a pharmacological effect [2-4]. The emulsion/solvent evaporation method is the most common method used for microencapsulation of water-insoluble agents. Furthermore, the fact that oil-loaded microcapsules do not leak or crack after production contributes to the advantages of this technology. As that solvent can be evaporated rapidly by itself, by heat, or by mixing

during production, there is no need for an addition to the system, making production easier and faster [5-6].

In literature, nanofiber incorporation of St. John's Wort oil studies are very limited. Girgin and Cengiz Çallıoğlu produced Poly(vinyl pyrrolidone) based nanofibers with different concentrations of St. John's Wort oil by emulsion electrospinning. They incorporated St. John's Wort oil into the nanofibers successfully and indicated that the biocompatible nanofibrous surfaces can be used as a wound dressing [7]. In this study, it was aimed at producing St. John's Wort oil loaded microcapsules via the emulsion/solvent evaporation method and then, production of PVA nanofibers containing microcapsules by the electrospinning method. In addition, considering the limited number of studies about nanofibers containing microcapsules in the literature, it can be said that this study will make a great contribution to the literature.

2. MATERIALS AND METHODS

2.1 Materials

For microcapsule production, Eudragit RS 100 (Evonik Röhm GmbH) and Polyvinyl alcohol (Mn=88,000, 88% hydrolyzed) were used as shell materials. St. John's Wort oil (Botalife, Isparta, Turkey) was used as a core material. Polyvinyl alcohol (Mn=88,000, 88% hydrolyzed) was used as the main polymer, distilled water and chloroform (Sigma-Aldrich Corporation (St. Louis, MO, USA)) were used as the solvent for nanofiber production.

2.2 Methods

Initially, microcapsules were produced by a solvent/evaporation technique. While producing microcapsules first, the oil phase and water phase were prepared to generate emulsion. The Eudragit RS 100 polymer was dissolved in chloroform to form an oil phase. The core ingredient, St. John's Wort oil, was then added. Meanwhile, the water phase was prepared by stirring PVA and the surfactant with pure water in a high-speed mixer. Then, the oil phase was added dropwise to the water phase and mixed in a high-speed mixer for 1.5 hours at 350 rpm. Finally, washing with 100 mL distilled water, filtering, and drying processes at room temperature were carried out. Then, a polymer solution containing 10 wt % PVA and 1, 3, 5, 7 and 9 wt % microcapsules were prepared to produce nanofibers (Table 1). The polymer solutions were characterized by conductivity (Selecta CD 2005), viscosity (Lamy Rheology, B-One Touch Screen) under shear rate of 5 s^{-1} and surface tension (Biolin Scientific Sigma 702) by the Du Noüy ring measurements. Nanofibers were produced with the electrospinning method under process parameters such as 21.7 kV voltage, 1.5 mL/h feed rate, 18.1 cm distance between electrodes, $30 \pm 2\%$ humidity, and $25.5 \pm 1^\circ\text{C}$ temperature. The composition of PVA polymer solutions with various microcapsule concentrations is given in table 1.

Table 1. Composition of PVA polymer solutions with microcapsules

Sample Codes	PVA Concentration (%)	Microcapsule Concentration (%)
PVA-0	10	0
PVA-1	10	1
PVA-3	10	3
PVA-5	10	5
PVA-7	10	7
PVA-9	10	9

After experimental studies, both microcapsules and nanowebs were investigated morphologically by SEM images with different magnifications. ImageJ software was used

to measure the diameters of 100 fibers obtained from various parts of the electrospun web. The number average and weight average values were estimated using the following equations.

$$A_n = \frac{\sum n_i d_i}{\sum n_i} \text{ (number average)} \quad (1)$$

$$A_w = \frac{\sum n_i d_i^2}{\sum n_i d_i} \text{ (weight average)} \quad (2)$$

where d_i is fiber diameter, n_i - fiber number.

The ratio of A_w/A_n was used to obtain the fiber uniformity coefficient, the same as it did for molar mass distributions. An optimum value is close to 1, which indicates fibers that are uniform in size [8]. The histogram curve for fiber diameter was provided in the form of SPSS.

In addition, FT-IR analysis was performed to determine the presence of microcapsules in the nanofiber structures.

3. RESULTS AND DISCUSSION

For this study, firstly microcapsule production was carried out via the emulsion/solvent evaporation method. SEM images of St. John's Wort oil loaded Eudragit RS 100/PVA microcapsules are shown in figure 1.

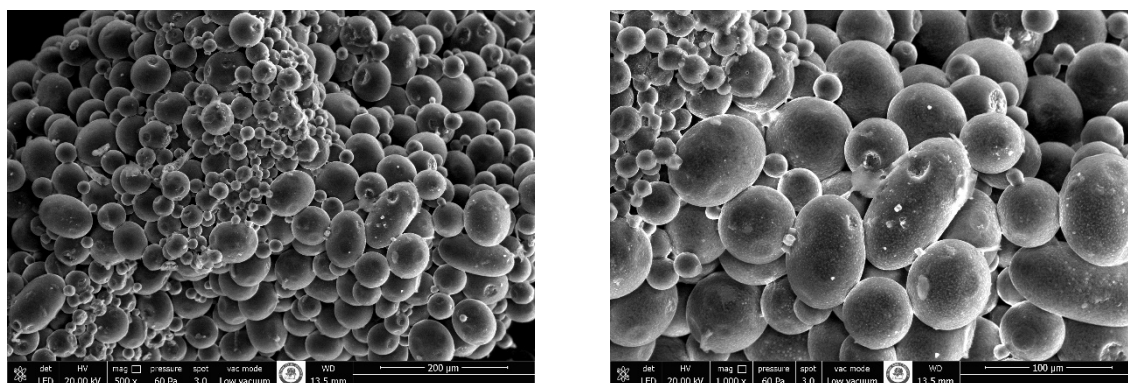


Figure 1. SEM images of microcapsules (500x and 1.000x)

As seen from the SEM images, St. John's Wort oil loaded Eudragit RS 100/PVA microcapsules have a spherical shape, a smooth surface and uniform particle size distribution. Average microcapsule size is 30 μm . Solution properties (conductivity, viscosity and surface tension) of PVA solutions include different concentrations of microcapsules' were measured. The results of solution properties are given in figure 2.

According to figure 2, it has been seen clearly that viscosity and surface tension increased with microcapsule concentration increase. However, conductivity did not change significantly. The morphology of PVA-0 nanofibers was investigated via SEM images and histogram (figure 3).

From the SEM images of figure 3, it has been observed that good nano web quality, fine, uniform and bead-free nanofibers were obtained. As it has been seen from the histogram, the average fiber diameter is 430 nm and the fiber diameter uniformity coefficient is 1.01. Moreover, there is a unimodal histogram curve and the nanofibers are quite uniform.

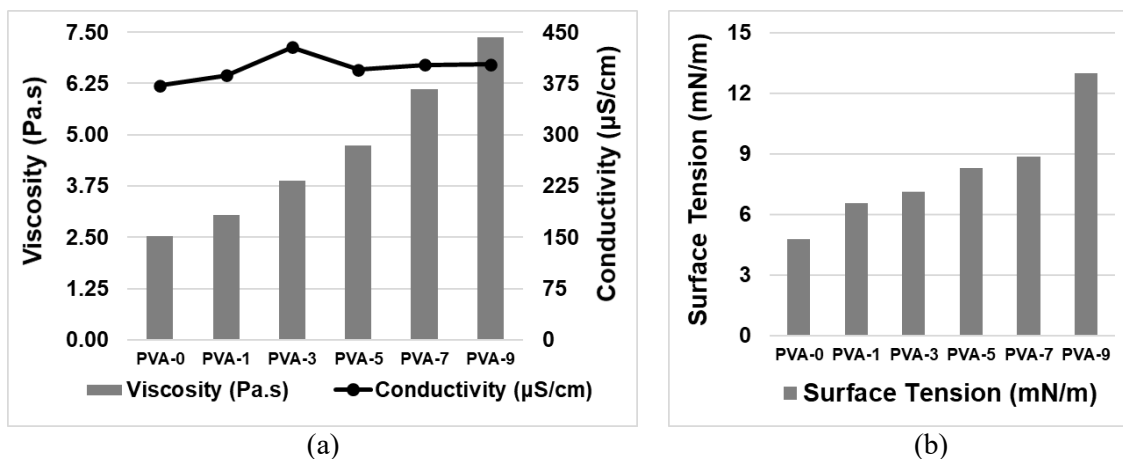


Figure 2. Solutions properties of PVA polymer solutions with different concentration of microcapsules a) Viscosity and conductivity b) Surface tension

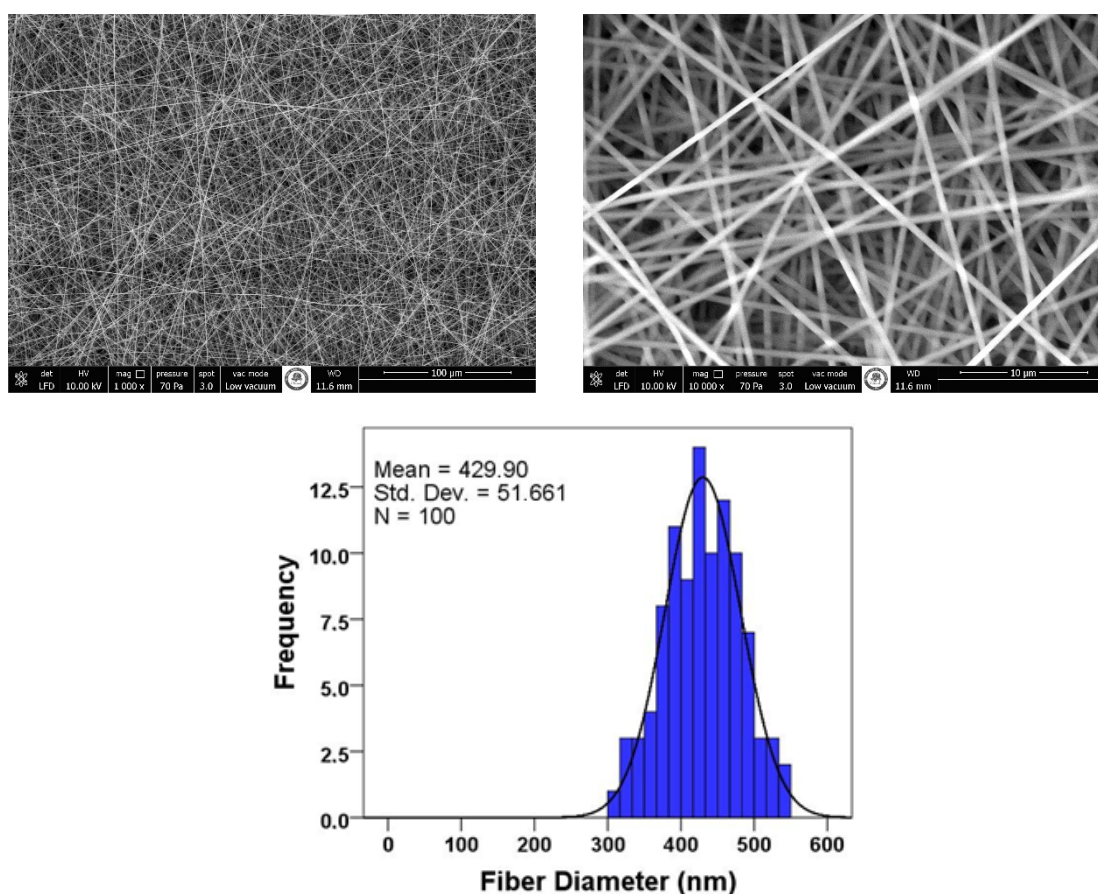


Figure 3. SEM images (1.000x and 10.000x) and histogram of PVA-0 nanofibers

The morphology of PVA nanofibers with various concentrations of microcapsules such as 1, 3, 5, 7, and 9 wt % was investigated via SEM images (figure 4).

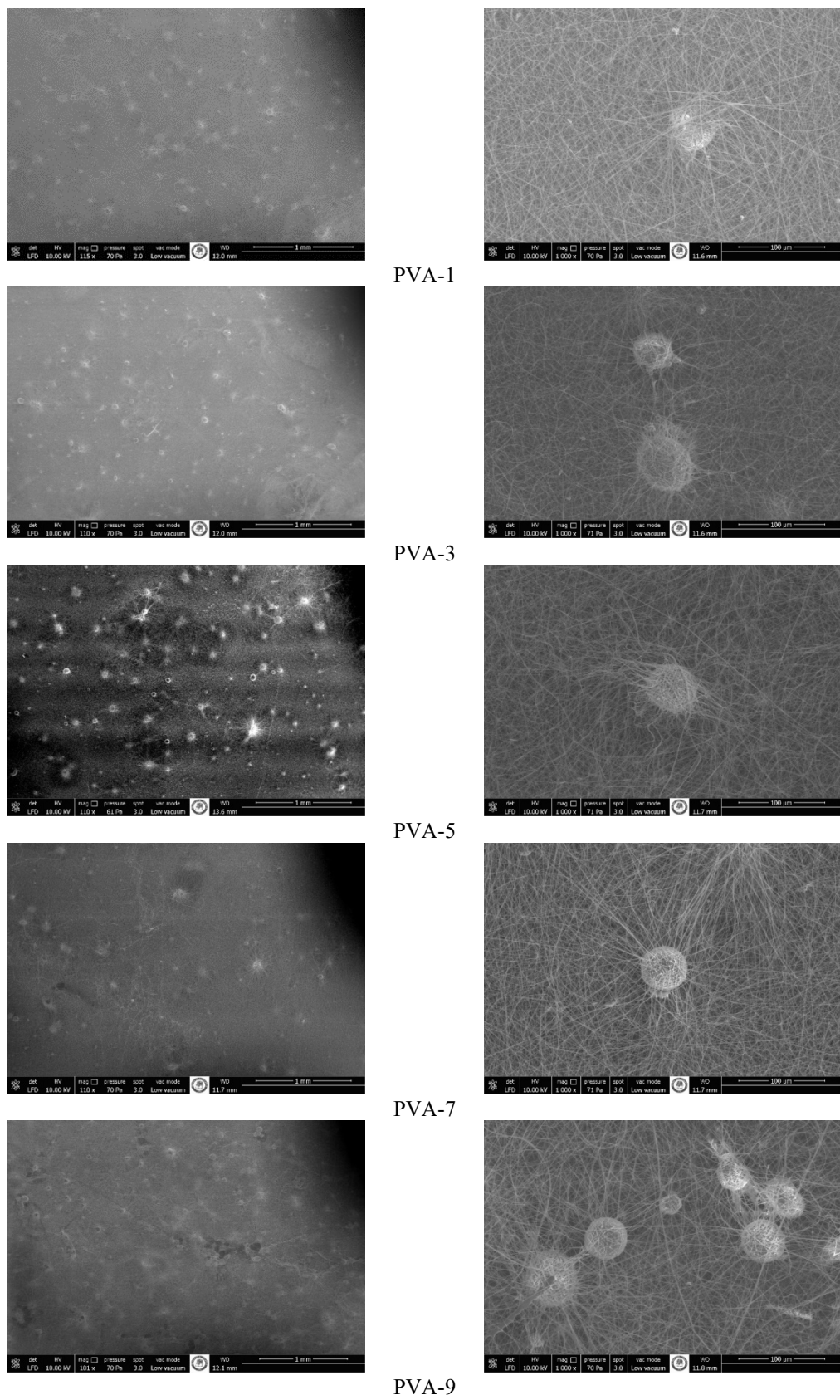


Figure 4. SEM images of PVA nanofibers with various concentrations of microcapsules

As shown in the SEM photos, microcapsules were successfully incorporated into a nanofibrous structure. All of the nanowebs are quite fine, smooth, uniform and without

beads. Additionally, it is observed that the density of microcapsules in the nanoweb increases as the microcapsule concentration increases.

In addition to these results, FT-IR spectroscopy confirmed the presence of PVA polymer and St. John's Wort oil loaded microcapsules in the chemical structures of the nanofibers (figure 5).

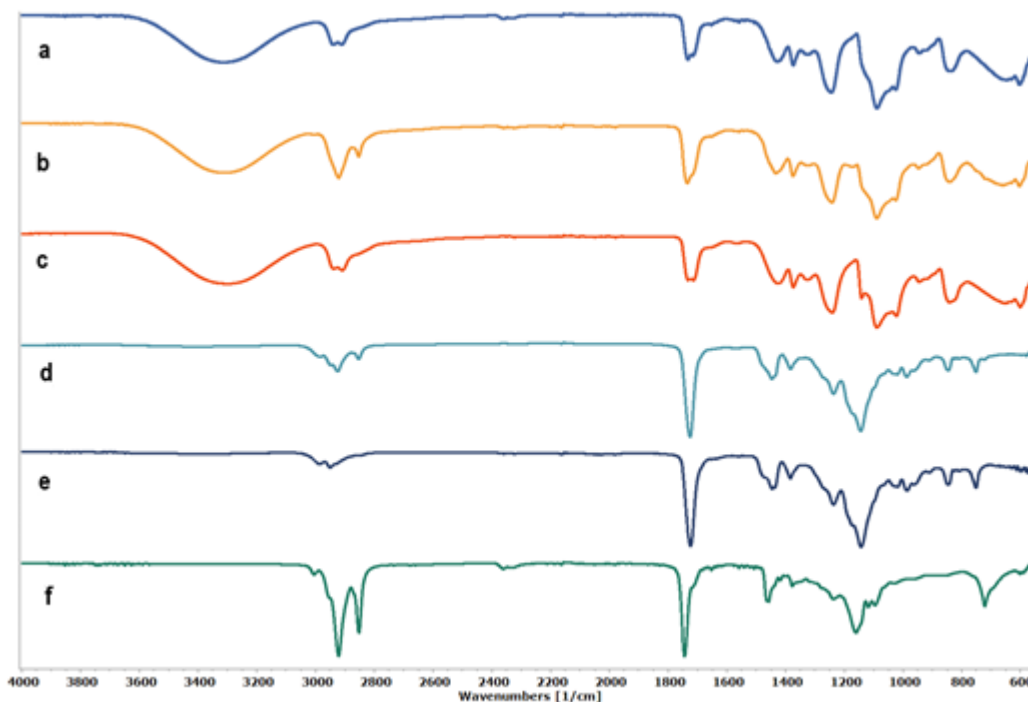


Figure 5. FT-IR spectra of: a - PVA-0 nanofibers; b - PVA-9 nanofibers; c - PVA polymers; d - St. John's Wort oil loaded PVA/ Eudragit RS 100 microcapsules; e - Eudragit RS 100 polymers; f - St. John's Wort oil

The FT-IR spectrum of PVA demonstrates the primary peaks linked with PVA and PVA nanofibers quite clearly. For instance, the typical strong hydrogen bonded band occurred at approximately $3400\text{-}3200\text{ cm}^{-1}$ wavelength in the spectra of PVA polymer, PVA-0 and PVA-9 nanofibers. Because of the high hydrophilic forces, intramolecular and intermolecular hydrogen bonding is expected to occur among PVA chains. Another important absorption peak was confirmed at 1141 cm^{-1} . This peak arises at 1243 cm^{-1} and 1245 cm^{-1} in the spectra of PVA-0 and PVA-9 nanofibers, respectively. The crystallinity of PVA is primarily responsible for this vibrational band, which is related to the carboxyl stretching band (C–O) [9]. The most intense peak in the spectrum of St. John's Wort oil related to C-H stretching peak appearances at 2922 cm^{-1} and 2853 cm^{-1} . These peaks are seen clearly at 2922 cm^{-1} and 2853 cm^{-1} for PVA-9 nanofiber and 2925 cm^{-1} and 2854 cm^{-1} for microcapsule spectra [10]. The carbonyl stretching vibration of the ester group is responsible for the stretching bands of Eudragit RS 100 at 1143 cm^{-1} and 1237 cm^{-1} . These stretching bands are attributed to 1173 cm^{-1} and 1243 cm^{-1} for PVA-9 nanofibers and to 1237 cm^{-1} and 1145 cm^{-1} for spectra of microcapsules [11].

5. CONCLUSIONS

This study achieved the production of St. John's Wort oil loaded microcapsules by the solvent/emulsion evaporation method and electrospinning of PVA nanofibers

incorporated into the microcapsules successfully. Small, uniform and spherical microcapsules were produced, solution properties of PVA includes different concentrations of microcapsules were determined and also fine, uniform nanofibers incorporated St. John's Wort oil loaded microcapsules were electrospun during the experimental studies. As a result of this study, it is considered that the nanofiber surface containing microcapsules has a high potential for end use as a wound dressing in biomedical applications due to the superior properties of St. John's Wort oil and nanofibers.

REFERENCES

- [1] Bolourchian, N., Bahjat, M., *Design and In Vitro Evaluation of Eudragit-Based Extended Release Diltiazem Microspheres for Once-and Twice-Daily Administration: The Effect of Coating on Drug Release Behavior*, In: Turk J Pharm Sci, 2019, 16, 3, 340-347, <https://doi.org/10.4274/tjps.galenos.2018.24861>
- [2] Çoban, D.Z., Yener, M., et al., *Molecular View to The The Effect of Centaury Oil on Wound Healing*, In: Cumhuriyet Medical Journal, 2016, 38, 4, 231-239, <http://dx.doi.org/10.7197/cmj.v38i2.5000144674>
- [3] Mukherjee, P.K., Verporte, Rob., et al., *Evaluation of In-Vivo Wound Healing Activity of Hypericum Perforatum Leaf Extract on Different Wound Model in Rast*, In: Journal of Ethnopharmacology, 2000, 70, 315-321, [https://doi.org/10.1016/S0378-8741\(99\)00172-5](https://doi.org/10.1016/S0378-8741(99)00172-5)
- [4] Greeson, M.J., Sanford, B., et al., *St. John's Wort (Hypericum Perforatum): a Review of The Current Pharmacology, Toxicological and Clinical Literature*, In: Journal of Psychopharmacology, 2001, 153, 402-414, [https://doi.org/10.1016/S0378-8741\(99\)00172-5](https://doi.org/10.1016/S0378-8741(99)00172-5)
- [5] Heiskanen, H., Denifl, P., Pitkänen, P., et al., *Effect of Concentration and Temperature on The Properties of The Microspheres Prepared Using an Emulsion–Solvent Extraction Process*, In: Adv Powder Technol, 2012, 23, 6, 779-786, <https://doi.org/10.1016/j.appt.2011.10.007>
- [6] Hong, Y., Gao, C., Shi, Y., et al., *Preparation of Porous Polylactide Microspheres by Emulsion-Solvent Evaporation Based on Solution Induced Phase Separation*, In: Polym. Adv. Technol., 2005, 16, 8, 622-627, <https://doi.org/10.1002/pat.629>
- [7] Girgin, S., Cengiz Çalhoğlu, F., *Production of Polyvinylpyrrolidone (Pvp)/ St. John's Wort Oil Based Nanofibrous Material*, In: National Çukurova Textile Congress (UÇTEK'19), 2019, 337-344
- [8] Cengiz, F., Jirsak, O., *The effect of salt on the roller electrospinning of polyurethane nanofibers*, In: Fibers and Polymers, 2009, 10, 2, 177-184, <https://doi.org/10.1007/s12221-009-0177-7>
- [9] Mansur, H.S., Oréfice, R.L., Mansur, A.A., *Characterization of poly (vinyl alcohol)/poly (ethylene glycol) hydrogels and PVA-derived hybrids by small-angle X-ray scattering and FTIR spectroscopy*, In: Polymer, 2004, 45, 21, 7193-7202, <https://doi.org/10.1016/j.polymer.2004.08.036>
- [10] Eğri, Ö., Erdemir, N., *Production of Hypericum Perforatum Oil-Loaded Membranes For Wound Dressing Material And in Vitro Tests, Artificial Cells*, In: Nanomedicine and Biotechnology An International Journal, 2019, 1404-1415, <https://doi.org/10.1080/21691401.2019.1596933>
- [11] Park, J.M., Park, S.J., *Preparation and characterization of water-soluble microcapsule for sustained drug release using Eudragit RS 100*, In: Macromolecular Research, 2010, 18, 12, 1191-1194, <https://doi.org/10.1007/s13233-010-1203-8>



SOLVENT OPTIMIZATION OF ELECTROSPUN POLY(ACRYLIC ACID) NANOFIBERS

DOI: 10.35530/TT.2021.27

M. Geysoglu^{1*}, F.C. Çallioğlu²

¹Bioengineering Department, Institute of Natural and Applied Sciences, Süleyman Demirel University, Turkey

(E-mail: mustafageysoglu@sdu.edu.tr)

²Textile Engineering Department, Engineering Faculty, Süleyman Demirel University, Turkey

(E-mail: fundacengiz@sdu.edu.tr)

Abstract: *In this study, it was investigated experimentally the influence of various solvents (distilled water and ethanol) on the solution properties, spinning performance, and fibre morphology of the electro spun Poly (acrylic acid) nanofibers. Firstly, polymer solutions were prepared at 5 wt % PAA with various solvent ratios of ethanol and distilled water. Then, solution properties such as viscosity, density, pH, conductivity, and surface tension were determined. The production of nanofiber samples was carried out by electrospinning under the optimum process parameters (voltage, distance between electrodes, feed rate, and atmospheric conditions). Finally, the morphological characterization of the nanofiber surface was carried out with SEM. According to the results, it was observed that conductivity, surface tension and the density of the solution increase as the ethanol ratio decreases. On the other hand, pH value increases as the ethanol ratio increases and, so, the acidic value of the solutions decreases. The viscosity increased until the ethanol/distilled water ratio was 50/50 and then decreased as the ethanol percentage decreased to under 50%. In addition, average fibre diameter decreases with ethanol ratio decreases. It is possible to say that solvent type affects solution properties, fibre morphology and spinning performance significantly. Generally, fine, uniform and bead free nanofibers could be electro spun and the PAA solution containing 70 wt % distilled water and 30 wt % ethanol was selected as the optimum in terms of fibre morphology, web quality and spinning performance.*

Keywords: *electrospinning, ethanol, nanofiber, poly(acrylic acid), solvent optimization*

1. INTRODUCTION

In this study, it was aimed at achieving electrospinning of Poly (acrylic acid) (PAA) nanofibers with various solvents such as distilled water and ethanol. It is known from the literature that these solvents can be used to solve PAA separately or together [1-3].

PAA is a superabsorbent, water soluble, innocuous [4], synthetic, and high molecular weight polymer of acrylic acid [3]. PAA is also non-toxic and very sensitive to temperature and pH changes. Therefore, PAA has attracted great interest in different fields, especially biomedical applications [5].

Nanofibers have unequalled properties, such as very small fibre diameter, high porosity, small controllable pore size, very high specific surface area (m²/g) etc. [6]. Thanks to their unique features, nanofibers can be a promising material for a variety of applications, from medical to consumer products, and industrial to high-tech applications. In literature, there are several studies on the medical application areas of PAA based

nanofibers, such as drug delivery [7,8], tissue engineering, implant coatings, wound dressing [9], etc.

Solvent selection is an important step in obtaining uniform and fine nanofibers by electrospinning. There are some studies about solvent optimization and solvent effects on solution properties and fibre morphology in literature. Yang et al. investigated the influence of solvents on the morphology of the poly (vinylpyrrolidone) (PVP) nanofibers prepared by electrospinning with different solvents, including ethanol, dichloromethane, and dimethylformamide, and they specified that solution properties and fiber morphology were affected by solvent type [10]. Gee et al. compared the effects of three solvents (dimethylformamide, N-methylpyrrolidone, and dimethyl sulfoxide) on fiber formation. These researchers also observed that fiber morphology, such as fiber diameters, web thickness, and pore area, were affected by solvent ratio [11].

This study aims to analyse the effect of ethanol and distilled water on PAA-based nanofiber morphology and contribute to the literature.

2. MATERIALS AND METHODS

For this study, PAA was used as a polymer. Distilled water and ethanol were used as the solvents to obtain nanofibrous surfaces. PAA with a viscosity-average molecular weight of 450,000 was purchased from Sigma–Aldrich (St. Louis, MO, USA) and ethanol was purchased from ISOLAB (Izmir, Turkey). The PAA polymer concentration was kept constant at 5 wt% and details of solvent ratios are given below in Table 1.

Table 1. Different solvents ratios of PAA solutions with sample codes

Sample Codes	Distilled Water Ratio (wt%)	Ethanol Ratio (wt%)
S1	0	100
S2	10	90
S3	30	70
S4	50	50
S5	70	30
S6	90	10
S7	100	0

It is known from the literature that process parameters of electrospinning, such as applied voltage, solvent selection, distance between needle and collector, solution flow rate, etc., have to be optimized to obtain uniform, fine, and bead-free nanofibers [3]. All process parameters were kept constant except solvent ratios during the spinning process.

The study consists of three stages. In the first stage, PAA solution properties such as viscosity, conductivity, pH, surface tension, and solution density were measured. At the second stage, a needle electrospinning process using optimum process parameters carried out nanofiber production. During the nanofiber production process, 14 kV voltage, 0.6 ml/h solution feed rate, and 22.5 cm distance between the electrodes were applied for all solutions. Also, spinning experiments were achieved under ambient conditions of 32% (± 1) humidity and 25°C (± 1) degree temperature for all samples. All nanofibers were produced for 20 minutes and collected on an alumina foil.

The last step of the study is the characterization of PAA nanofibers in terms of fibre diameter, fibre diameter uniformity, and web surface structure (bead, stickiness etc.). The morphology was analysed with a Scanning Electron Microscope (SEM). By using image J analysing software, the average fibre diameters were calculated. The findings

were analysed statistically with the SPSS analysis program. The fibre uniformity coefficient was calculated using equations 1 and 2 which are given below [12]:

$$A_n = \frac{\sum n_i d_i}{\sum n_i} \text{ (number average)} \quad (1)$$

$$A_w = \frac{\sum n_i d_i^2}{\sum n_i d_i} \text{ (weight average)} \quad (2)$$

where d_i is fibre diameter and n_i - fibre number.

The fibre diameter uniformity coefficient was determined by the ratio of A_w / A_n and optimum value should be very close to 1 for uniform fibres.

3. RESULTS AND DISCUSSIONS

3.1. Solution Properties

From the solution results are given in figure 1, it was observed that conductivity, surface tension, and the density of the solution increase as the ethanol ratio decreases.

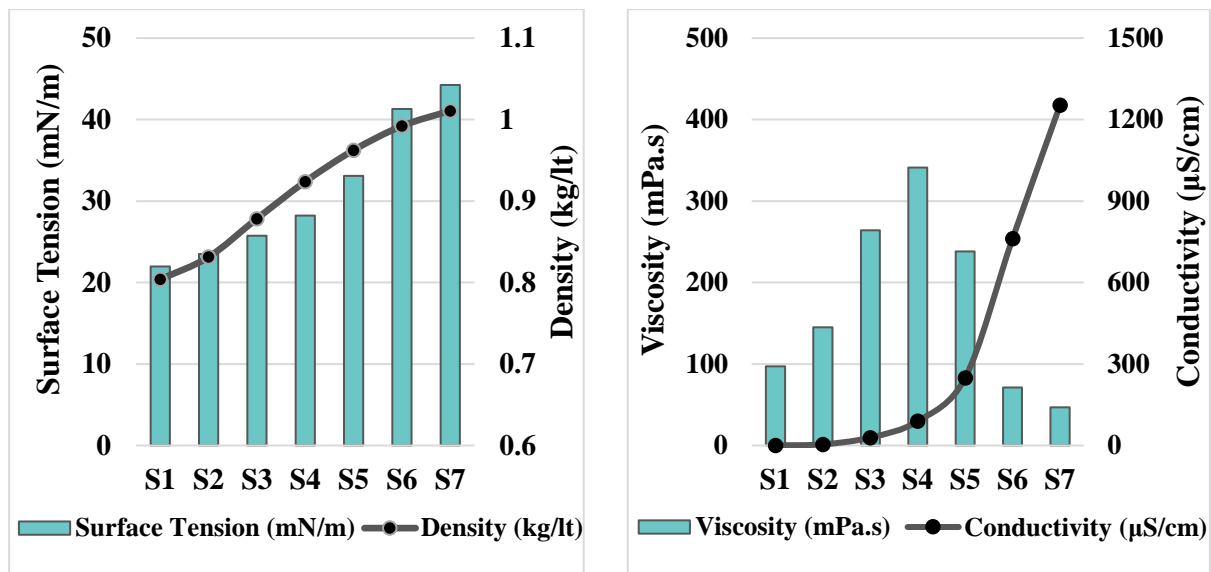
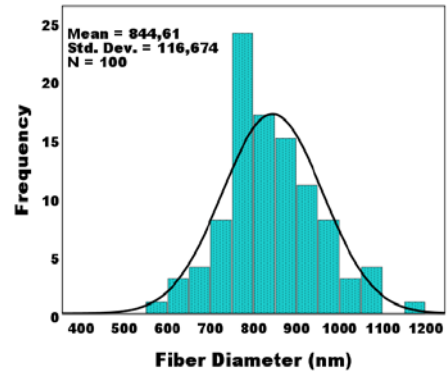
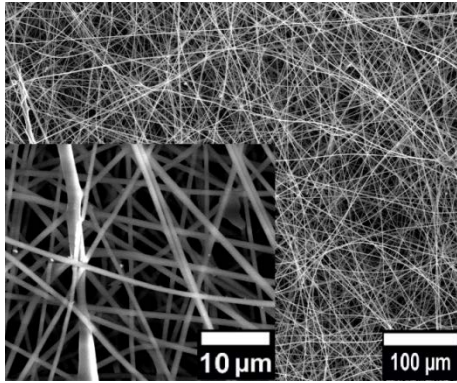


Figure 1. Results of solution properties such as surface tension, density, viscosity and conductivity of PAA with various solvent ratios

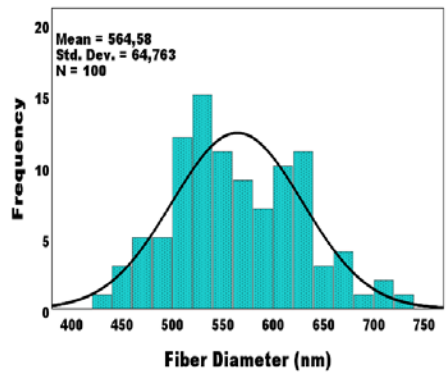
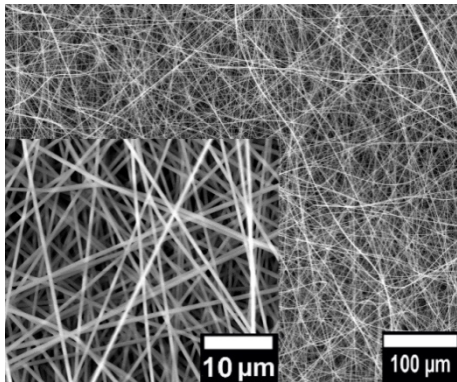
On the other hand, pH value increases as the ethanol ratio increases and, so, the acidic value of the solutions decreases. The viscosity increased until the ethanol/distilled water ratio was 50/50 and then decreased as the ethanol percentage decreased to under 50%. The viscosity has the highest value where the solvent ratios are equalized (S4).

3.2. Fiber Morphology

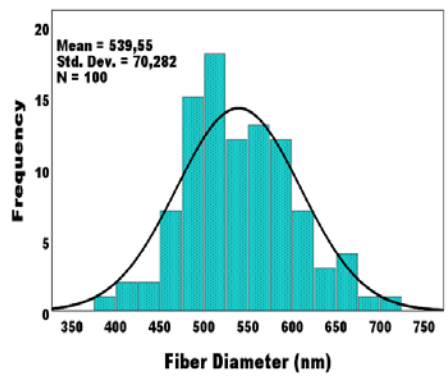
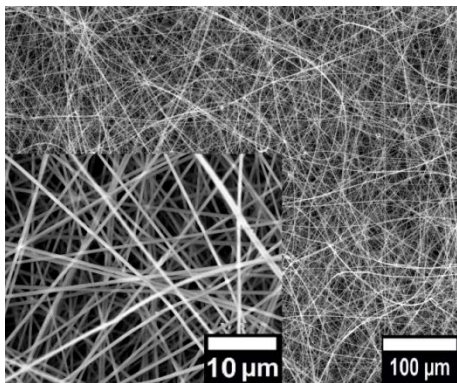
SEM pictures of PAA nanofibers with different solvents ratios of distilled water and ethanol are given in figure 2. Spinning could not be achieved with PAA solutions include only distilled water (S1) and only ethanol (S7) as a solvent.



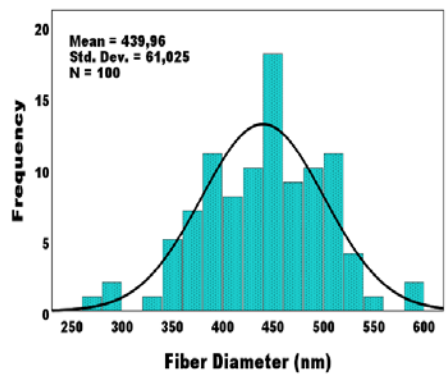
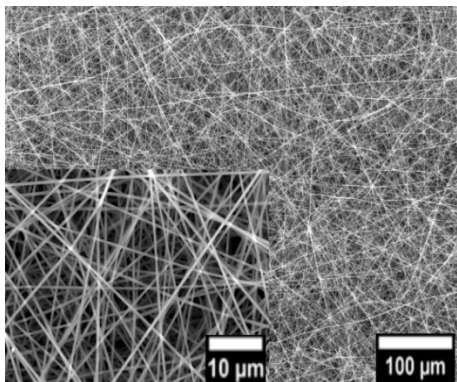
(S2)



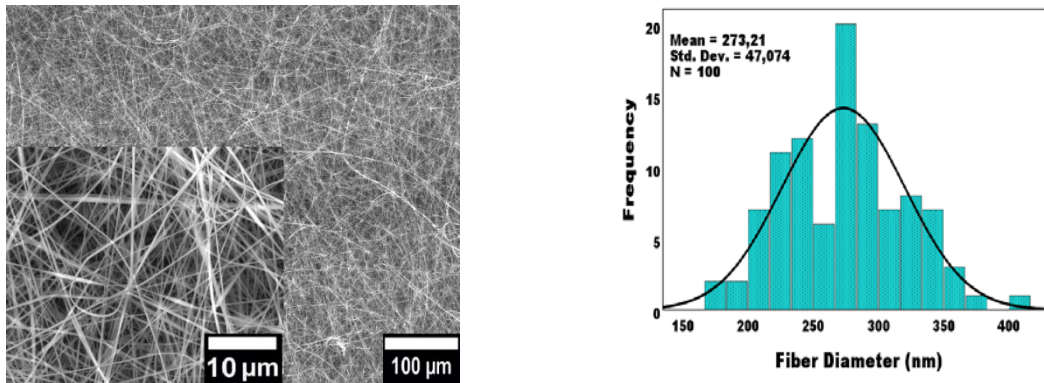
(S3)



(S4)



(S5)



(S6)

Figure 2. SEM images and fibre diameter histograms of PAA nanofibers (1.000x, 10.000x) produced with different solvents ratios of distilled water and ethanol.

It was clearly observed from the SEM images that generally, uniform and smooth nanofibers were produced and unimodal histogram curves were obtained. In addition, all fibre structures are bead-free and bead formation was not observed with the change of solvent ratio.

The effect of different solvent ratios on the average fibre diameter and fibre diameter uniformity coefficient was shown in Figure 3.

According to Figure 3, it was determined that average fibre diameter decreased as the ethanol concentration decreased. This result is compatible with solution properties and literature [2]. The finest fibres were obtained from an S6 sample (273 nm) including 10 wt % ethanol. Fibre diameter uniformity coefficient values are very close to 1 for all samples and the most uniform sample is S3 with a 1.013 value. It is possible to say that uniform, smooth nanofibers, good web quality without beads and unimodal fibre diameter histograms were obtained.

The PAA solution containing 70 wt % distilled water and 30 wt % ethanol (S5) was selected as the optimum in terms of fibre morphology, web quality, and spinning performance. From the calculations, it was specified that the average fibre diameter is 440 nm and the fibre diameter uniformity coefficient is 1.019.

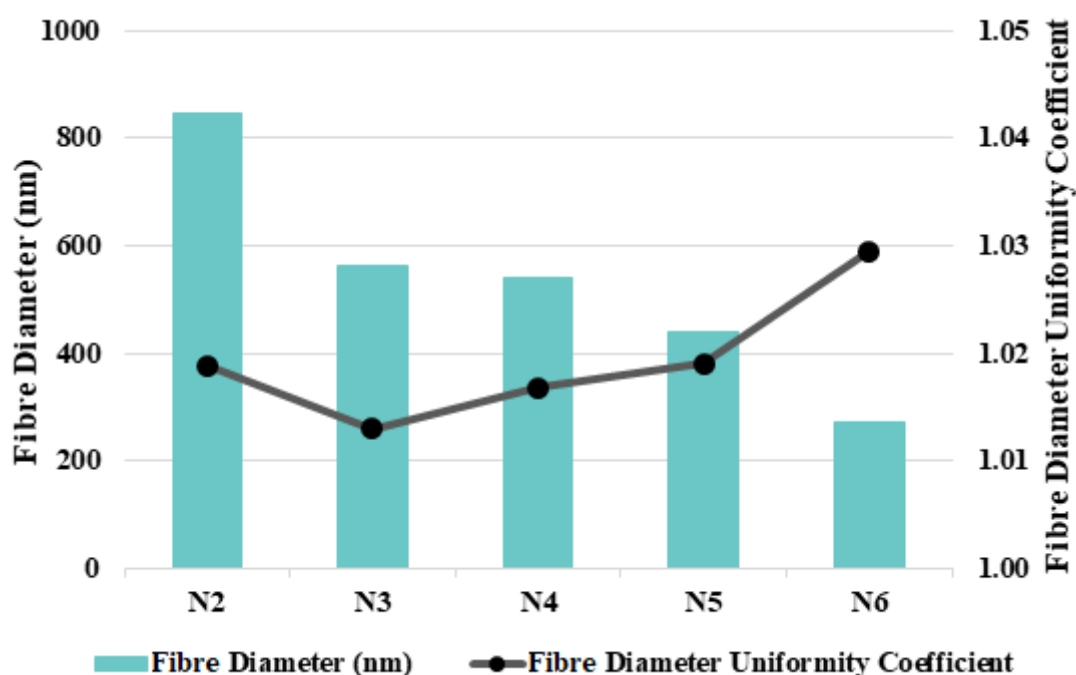


Figure 3. The effect of different solvent ratios on the average fibre diameter and fibre diameter uniformity coefficient

4. CONCLUSION

The production and characterization of PAA nanofibers prepared with different solvent ratios were achieved in this study. From the results, it is clearly seen that solvent type affects solution properties, fibre morphology and spinning performance distinctively. After the analysis of all the results, the PAA solution containing 70 wt % distilled water and 30 wt % ethanol was selected as the optimum in terms of fibre morphology, web quality, and spinning performance.

ACKNOWLEDGMENT

The authors would like to express appreciation for the financial support of the Süleyman Demirel University Scientific Researches Project Unit [Project Number = FDK-2019-7164].

REFERENCES

- [1] Kim, B., Park, H., Lee, S., et al., *Poly(acrylic acid) nanofibers by electrospinning*, In: Mater. Lett., 2005, 59, 829-832, <https://doi.org/10.1016/j.matlet.2004.11.032>
- [2] Theron, S.A., Zussman, E., Yarin, A.L., *Experimental investigation of the governing parameters in the electrospinning of polymer solutions*, In: Polymer, 2004, 45, 6, 2017-2030, <https://doi.org/10.1016/j.polymer.2004.01.024>
- [3] Khampieng, T., Wnek, G.E., Supaphol, P., *Electrospun DOXY-h loaded-poly(acrylic acid) nanofiber mats: in vitro drug release and antibacterial properties investigation*, In: J. Biomater. Sci. Polym. Ed., 2014, 25, 12, 1292-1305, <http://dx.doi.org/10.1080/09205063.2014.929431>
- [4] Shukla, N.B., Darabonia, N., Madras, G., *Ultrasonic degradation of poly(acrylic acid)*, In: J. Appl. Polym. Sci., 2009, 112, 2, 991-997, <https://doi.org/10.1002/app.29460>

- [5] Chen, K., Wang, S., Guo, X., *Confinement effect on the aqueous behaviors of free poly(acrylic acid) and poly(acrylic acid) grafted on a nanoparticle surface*, In: Colloid Polym. Sci., 2019, 297, 1223-1231, <https://doi.org/10.1007/s00396-019-04541-2>
- [6] Bhardwaj, N., Kundu S.C., *Electrospinning: a fascinating fiber fabrication technique*, In: Biotechnol. Adv., 2010, 28, 3, 325-347, <https://doi.org/10.1016/j.biotechadv.2010.01.004>
- [7] Velasco-Barraza, R.D., Vera-Graziano, R., López-Maldonado, E.A., et al., *Study of nanofiber scaffolds of PAA, PAA/CS, and PAA/ALG for its potential use in biotechnological applications*, In: Int J Polym Mater., 2018, 67, 13, 800-807, <https://doi.org/10.1080/00914037.2017.1378887>
- [8] Chunder, A., Sarkar, S., Yu, Y., et al., *Fabrication of ultrathin polyelectrolyte fibers and their controlled release properties*. In: Colloids Surf. B Biointerfaces, 2007, 58, 172-179, <https://doi.org/10.1016/j.colsurfb.2007.03.004>
- [9] Bandeira, M., Chee, B.S., Frassini, R., et al., *Antimicrobial PAA/PAH Electrospun Fiber Containing Green Synthesized Zinc Oxide Nanoparticles for Wound Healing*. In: Materials, 2021, 14, 2889, <https://doi.org/10.3390/ma14112889>
- [10] Yang, Q., Li, Z., Hong, Y., et al., *Influence of solvents on the formation of ultrathin uniform poly(vinyl pyrrolidone) nanofibers with electrospinning*, In: J. Polym. Sci. B Polym. Phys., 2004, 42, 3721-3726, <https://doi.org/10.1002/polb.20222>
- [11] Gee, S., Johnson, B., Smith, A.L., *Optimizing electrospinning parameters for piezoelectric PVDF nanofiber membranes*, In: J. Membr. Sci., 2018, 563, 804-812, <https://doi.org/10.1016/j.memsci.2018.06.050>
- [12] Cengiz, F., Jirsak, O., *The Effect of Salt on the Roller Electrospinning of Polyurethane Nanofibers*, In: Fibers Polym., 2009, 10, 2, 177-184, <https://doi.org/10.1007/s12221-009-0177-7>



ELECTROSPINNING OF ANTIBACTERIAL POLYURETHANE/ZnO NANOFIBERS

DOI: 10.35530/TT.2021.29

İ.Y. Mol*, F.C. Çallioğlu

Textile Engineering Department, Engineering Faculty, Süleyman Demirel University, Turkey
(E-mail: iremyagmurmol@gmail.com, fundacengiz@sdu.edu.tr)

Abstract: *In this study, it is aimed to produce and characterize antibacterial polyurethane (PU)/Zinc oxide (ZnO) nanofibers by electrospinning method. Firstly, polymer solutions were prepared at various ZnO concentrations such as 0, 0.2, 0.4, 0.6, 0.8, 1. Then solution properties (conductivity, viscosity, surface tension) were determined and analysed the effects of ZnO concentration on the solution properties. PU/ZnO nanofibers produced via electrospinning under the optimum process parameters (voltage, distance between electrodes, feed rate and atmospheric conditions). Finally, the nanofibers were characterized in terms of fibre morphology, thermal stability, permeability and antibacterial activity using SEM-EDS, DSC-TGA, water vapour permeability and disk diffusion methods. According to the solution results; it was observed that conductivity and surface tension decrease significantly with ZnO addition. On the other hand, solution viscosity increases as the ZnO concentration increases. From the SEM images, it has been seen clearly that average fibre diameter increases with ZnO concentration and incorporation of ZnO particles to the fibre structure was verified by SEM-EDS. According to the thermal analyse result, nanofibers begin to degrade between 271.94 °C and 298.73 °C. In addition, water vapour permeability increases as the ZnO concentration increase. Lastly antibacterial activity against gram negative (E.coli) and gram positive (S. aureus) was determined with specific zone diameter.*

Keywords: antibacterial, electrospinning, nanofiber, polyurethane, Zinc oxide

1. INTRODUCTION

Protective textiles are the materials to prevent the risk of exposure to harmful substances (virus, bacteria etc.) and bad environmental conditions, to protect them from this risk and/or to reduce this risk. Especially fibre structure, thermal, chemical, microbiological, pore size, air permeability, barrier etc. properties are important for this aim [1].

In recent years, various polymers can be easily electro spun to obtain advanced fibrous materials [2,3]. Among them, polyurethane based nanofibers are the most common and functional materials due to their high elasticity, good mechanical, protective and barrier properties. Polyurethane based nanofibers are especially used in medical, filtration, protective textiles, etc. [4-6]. Antibacterial nanofibers are also important for these application areas. In the literature, there are many studies about PU nanofibers containing various antibacterial agents [7,8].

For this study, ZnO was chosen as an antibacterial agent because of its non-toxicity, compatibility with the skin, and its chemical stability when exposed to both high temperatures and UV [9]. There are some studies on ZnO based nanofibers in the literature. Lee studied PU/ZnO based nanofibers to obtain UV protective textile materials. He noted that very thin electro spun ZnO nanocomposite fibre layer significantly

increased UV blocking for both the UV-A and UV-B ranges and exhibited excellent UV protection. In addition, it was observed that the UV protective properties increased with increasing ZnO concentrations [10]. Wu and Pan also prepared ZnO nanofibers by electrospinning. They found that the fibre diameter increased with ZnO content and the morphology of inorganic ZnO fibres was affected by the calcination time.

2. MATERIALS AND METHODS

In this study, polyurethane (PU) was used as a polymer, dimethylformamide (DMF) was used as a solvent and zinc oxide (ZnO) was used as an additive to provide antibacterial activity. During the experimental studies, PU polymer concentration was kept constant at 15 wt % and this value was determined from our preliminary studies. Zinc oxide concentrations such as 0, 0.2, 0.4, 0.6, 0.8 and 1 wt % were applied to the PU/DMF solutions. All solutions were prepared under the same conditions (mixing time, temperature, etc.).

First of all, solution properties such as conductivity, viscosity (shear rate 5 s^{-1}) and surface tension were measured. Then, nanofiber production was carried out by electrospinning method under the optimum process parameters. During the spinning process, 24 kV voltage, 0.2 ml/h solution feed rate and 22 cm distance between the electrodes were applied for all solutions. In addition, all nanofibers were produced under ambient conditions of $36 \pm 2\%$ humidity and $23 \pm 2^\circ\text{C}$ temperature. All nanofibers were produced for 30 minutes and collected on an aluminium foil.

Nanofiber morphology such as fibre diameter, diameter uniformity and nanoweb surface structure were analysed by Scanning Electron Microscopy (SEM). Fibre diameter histograms were obtained from the SPSS program. The presence of ZnO was determined by EDS and the thermal behaviour of nanofibers was analysed by DSC and TGA. In addition, the water vapour permeability test was performed according to BS 7209, BS 3424 standards. Finally, antibacterial activity against gram negative (*E. coli*) and gram positive (*S. aureus*) was determined by disc diffusion method.

3. RESULTS AND DISCUSSIONS

Viscosity, conductivity and surface tension results of PU/DMF solutions with various ZnO wt % concentrations are given in table 1.

Table 1. Solution results of PU/DMF with various concentrations of ZnO wt %

Samples	Viscosity (mPa.s) (Shear rate: 5 s^{-1})	Conductivity ($\mu\text{S/cm}$)	Surface Tension (mN/m)
PU0	2240	5.16	36.4
PU0.2	3970	1.01	6.74
PU0.4	4570	0.93	7.63
PU0.6	5680	0.82	7.29
PU0.8	5080	1.17	6.77
PU1	7680	0.72	7.53

Also figure 1 shows the changing of viscosity, conductivity and surface tension of PU/DMF solutions with ZnO concentrations.

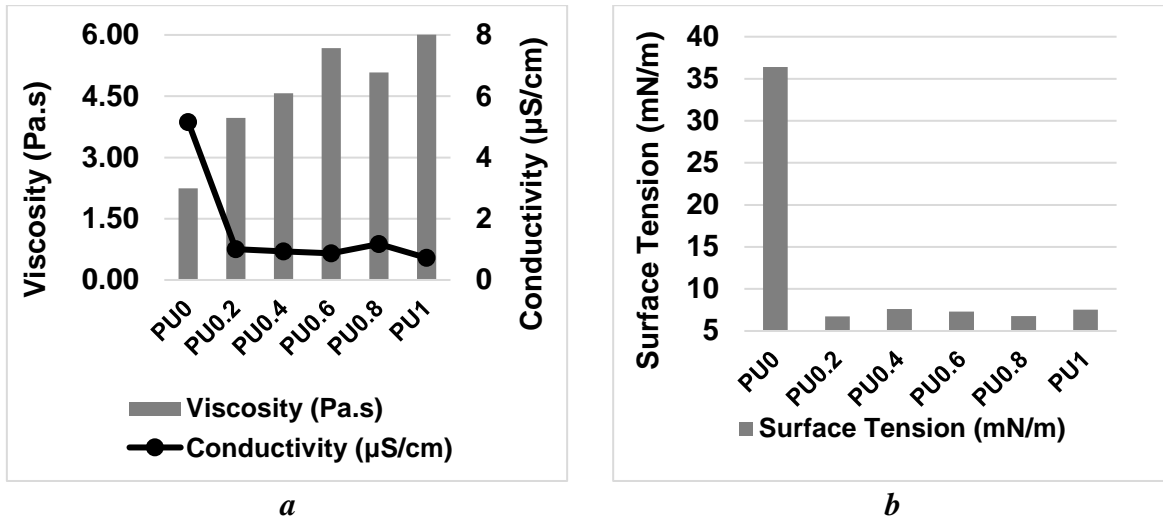
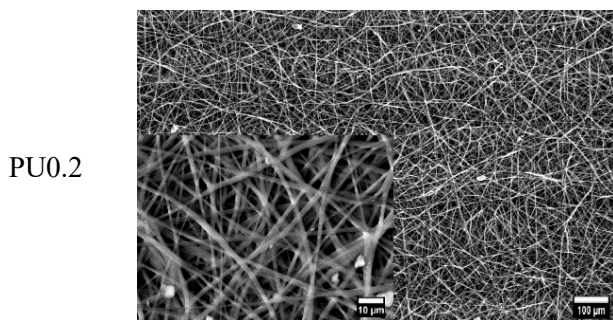
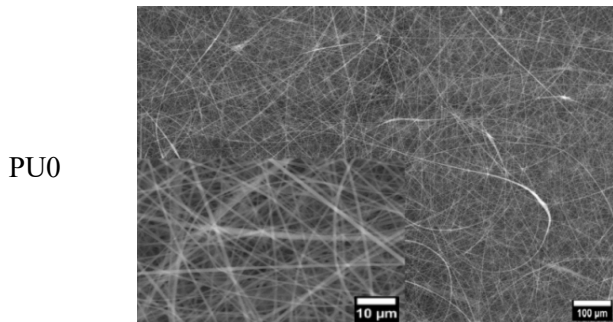
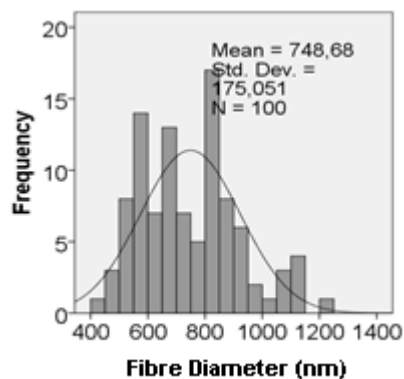
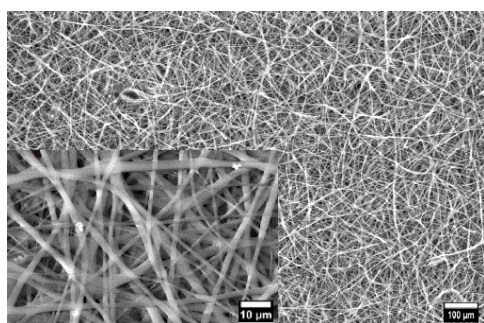


Figure 1. Graphical representation of: a - viscosity and conductivity of PU/ZnO solutions; b - surface tension of PU/ZnO solutions

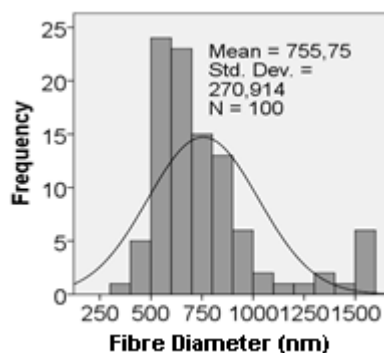
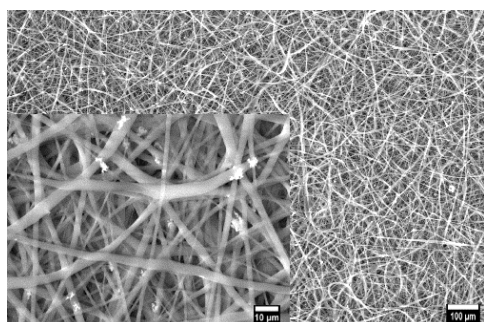
It is clearly seen that from table 1 and figure 1, solution viscosity increases with ZnO concentration while conductivity decreases. On the other hand, with the initial addition of ZnO, conductivity and surface tension decreases significantly, but is not affected by the ZnO concentration increase. This result is compatible with literature [11]. Figure 2 shows the SEM images and histograms of PU/ZnO nano webs.



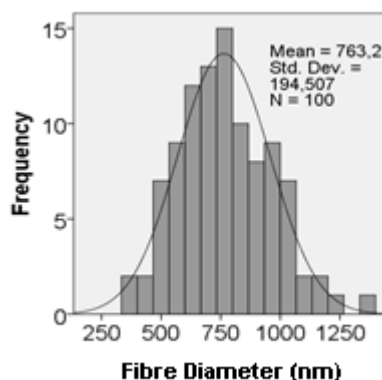
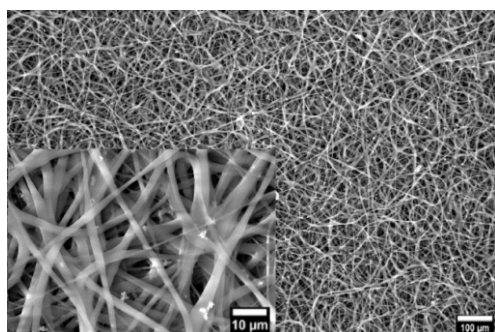
PU0.4



PU0.6



PU0.8



PU1

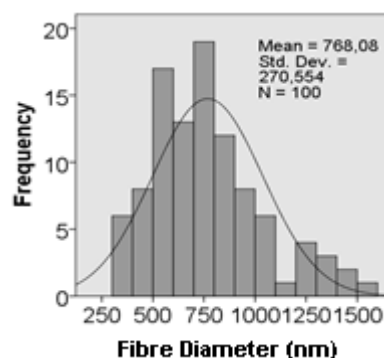
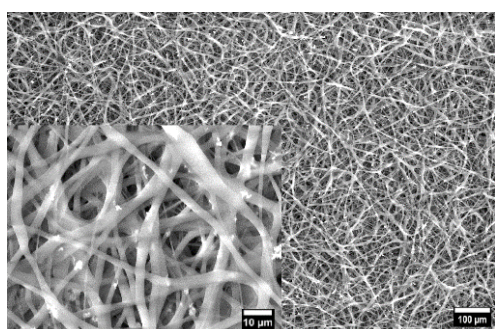


Figure 2. SEM images and fibre diameter histograms of PU/DMF nanofibers

From the SEM images, it was observed that the fibre diameter and stickiness increased with the addition of ZnO. Average fibre diameter was calculated as 550 nm for PU/DMF without ZnO (PU0). On the other hand, average fibre diameter increased to approximately 750 nm with addition of various concentrations of ZnO. It is clearly seen

from the SEM images that incorporation of ZnO particles to the nanofibers were achieved successfully. Unimodal histogram curves were obtained from PU0, PU0.2, PU0.8 samples.

The changing of average fibre diameter and fibre diameter uniformity with ZnO concentration increase is shown in figure 3.

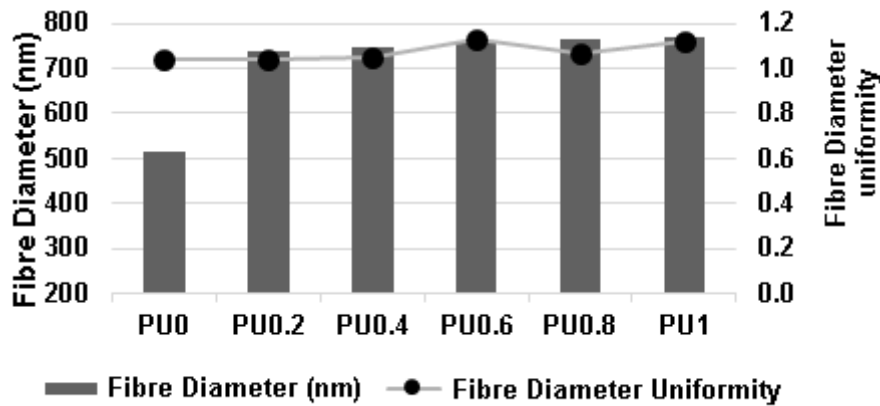


Figure 3. Average fibre diameter and diameter uniformity coefficient of PU/ZnO nanofibers

Figure 3 presents that average fibre diameter increased significantly with the first addition of ZnO to the PU nanofibers. Fibre diameter uniformity coefficient is not effected from ZnO concentration. It is possible to say that uniform PU/ZnO nanofibers were obtained. From the water vapour permeability test results, it was determined that water vapour permeability increased with addition of ZnO (PU0: 2484.62 g/m²/day and PU0.8: 2910.28 g/m²/day).

ZnO particles can be seen clearly into the fibre structure and also ZnO existence was verified by SEM-EDS (figure 4).

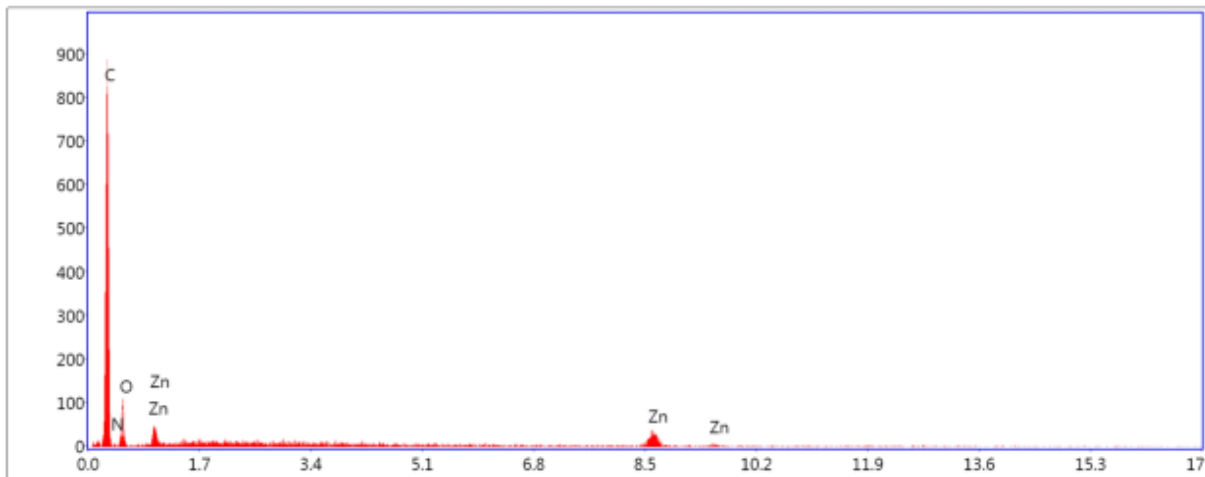
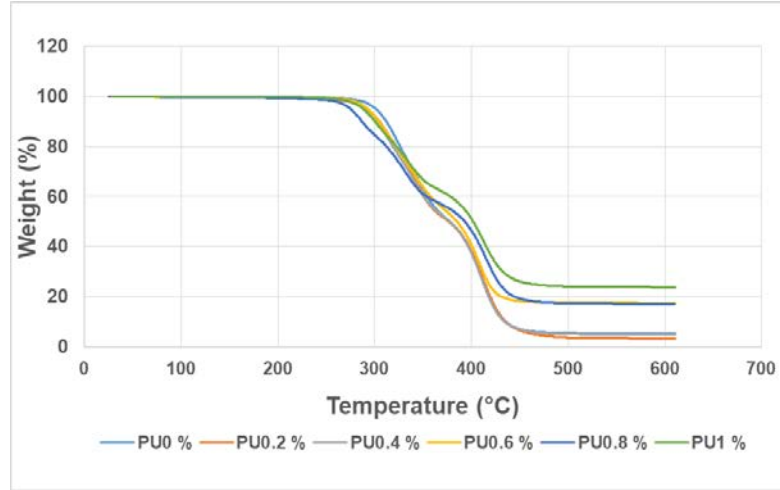


Figure 4. SEM-EDS Spectroscopy of PU nanofibers with 0.8 wt % ZnO

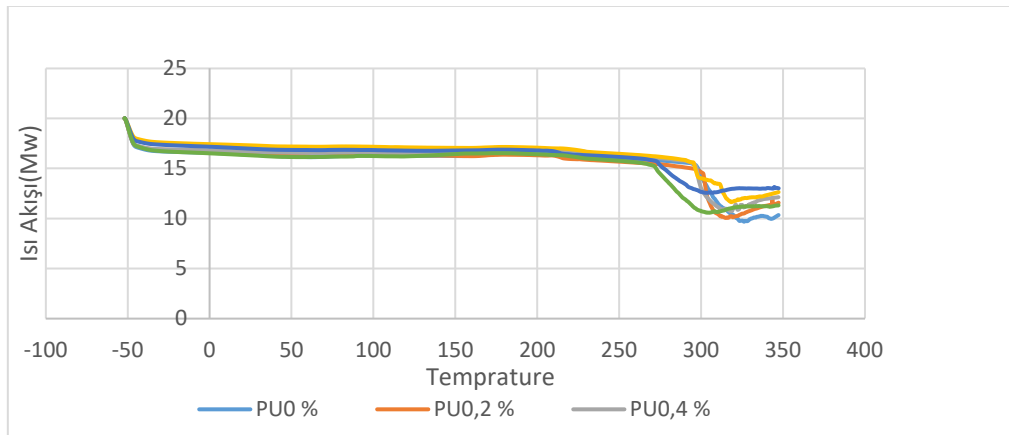
Elemental analysis results of Pu/ZnO nanofibers are given in table 2. Thermal behaviour of Pu/ZnO nanofibers were analysed by DSC-TGA (figure 5, figure 6).

Table 2. SEM-EDS results of PU/ZnO nanofiber samples

Sample code	C (%)	N (%)	O (%)	Zn (%)	Mg (%)	Al (%)	Na (%)
PU0.2	68.13	7.20	19.95	-	0.27	3.89	0.55
PU0.4	75.76	-	23.25	0.99	-	-	-
PU0.6	76.41	-	21.02	1.38	-	1.19	-
PU0.8	70.87	6.57	20.22	2.34	-	-	-
PU1	70.63	7.28	20.01	2.07	-	-	-

**Figure 5.** TGA analysis of PU nanofibers with various concentrations of ZnO

As shown, the amount of ZnO is visibly changing the temperature of any thermal resistance value. The major mass loss for PU/ZnO is around 275-280°. In the PU/ZnO curve, after 430 degrees, PU1 % containing the most zinc oxide remained the most residues and this ratio was 25%. PU0, PU0.2 and PU0.4 left the least residues close to each other. This rate is 1%.

**Figure 6.** DSC analysis of PU nanofibers with various concentrations of ZnO

Thermal characterization of polymers was investigated in nitrogen atmosphere using differential scanning calorimetry (DSC) and glass transition temperature (T_g) and melting temperature (T_m) were determined. Analysis -50°C to 350°C at a scan rate of $10^\circ\text{C}/\text{min}$ has been carried out. In general, the temperatures at which nanofibers begin to degrade are between 271.94°C and 298.73°C . Similarly, the temperature at which the mass loss ends is close to each other and varies between 308.11°C and 330.90°C .

Lastly, antibacterial activity against gram negative (*E.coli*) and gram positive (*S. aureus*) was determined with specific zone diameter for PU nanofibers with 0.8 wt % ZnO.

4. CONCLUSION

This study was carried out for the fabrication and characterization of antibacterial PU/ZnO nanofiber surface with various ZnO concentrations by electrospinning. According to the solution results; viscosity increased with ZnO concentration while conductivity and surface tension decreased. In addition, average fibre diameter increased and fibre stickiness was observed with ZnO concentration increase. On the other hand, fibre diameter uniformity was not affected from ZnO addition. ZnO incorporation to the PU nanofibers was shown by SEM images and ZnO presence was verified via SEM-EDS. Also it was determined that water vapour permeability increased with ZnO addition. Thermal behaviour of PU nanofibers with various concentrations of ZnO was investigated by DSC-TGA analysis. Lastly, good antibacterial activity against gram negative (*E. coli*) and gram positive (*S. aureus*) was determined.

ACKNOWLEDGMENT

The authors would like to express appreciation for the financial support of the Süleyman Demirel University Scientific Researches Project Unit [Project Number = FYL-2020-8206]. I would like to thank the Scientific and Technological Research Council of Turkey for their support to the 2247-C Trainee Researcher Scholarship Program (STAR) 2020/1.

REFERENCES

- [1] Duran, K., Bahtiyari, M.İ., Atav, R., *Protective nonwoven technical textiles*, In: Textile and Apparel, 2007, 17, 3, 174-177, <https://hdl.handle.net/11454/64515>
- [2] Huang, Z.M., Zhang, Y.Z., Kotaki, M., et al., *A review on polymer nanofibers by electrospinning and their applications in nanocomposites*, In: Compos. Sci. Technol., 2003, 63, 15, 2223-2253, [https://doi.org/10.1016/S0266-3538\(03\)00178-7](https://doi.org/10.1016/S0266-3538(03)00178-7)
- [3] Mirjalili, M., Zohoori, S., *Review for application of electrospinning and electrospun nanofibers technology in textile industry*, In: J. Nanostructure. chem., 2016, 6, 3, 207-213, <https://doi.org/10.1007/s40097-016-0189-y>
- [4] Gorji, M., Jeddi, A.A., Gharehaghaji, A.A., *Fabrication and characterization of polyurethane electrospun nanofiber membranes for protective clothing applications*, In: J. Appl. Polym. Sci., 2012, 125, 5, 4135-4141, <https://doi.org/10.1002/app.36611>
- [5] Mohraz, M.H., Golbabaei, F., Yu, I.J., Mansournia, M.A., et. al., *Preparation and optimization of multifunctional electrospun polyurethane/chitosan nanofibers for air pollution control applications*, In: IJEST., 2019, 16, 2, 681-694, <https://doi.org/10.1007/s13762-018-1649-3>
- [6] Akduman, C., Özgüney, I., Kumbasar, E.P.A., *Preparation and characterization of naproxen-loaded electrospun thermoplastic polyurethane nanofibers as a drug delivery system*, In: Mater. Sci. Eng. C., 2016, 64, 383-390, <https://doi.org/10.1016/j.msec.2016.04.005>
- [7] Jatoi, A.W., *Polyurethane nanofibers incorporated with ZnAg composite nanoparticles for antibacterial wound dressing applications*, In: Compos. Commun., 2020, 19, 103-107, <https://doi.org/10.1016/j.coco.2020.03.004>
- [8] Lee, J.H., Park, S.H., Kim, S.H., *Fabrication of bio-based polyurethane nanofibers incorporated with a triclosan/cyclodextrin complex for antibacterial applications*, In: RSC. Adv., 2020, 10, 6, 3450-3458, <https://doi.org/10.3390/polym13040576>
- [9] Yang, H., Zhu, S., Pan, N., *Studying the mechanisms of titanium dioxide as ultraviolet-blocking additive for films and fabrics by an improved scheme*, In: J. Appl. Polym. Sci., 2004, 92, 5, 3201-3210,

<https://doi.org/10.1002/app.20327>

[10] Lee, S., *Developing UV-protective textiles based on electrospun zinc oxide nanocomposite fibers*, In: *Fibers Polym.*, 2009, 10, 3, 295-301, <https://doi.org/10.1007/s12221-009-0295-2>

[11] Aydemir, E.H., *Topical treatment (part two): Vehicles, nature and functions*, In: *Turkderm*, 2012, 46, 4, 175, <https://doi.org/10.4274/Turkderm.42275>



EMULSION ELECTROSPINNING OF POLYVINYLPIRROLIDONE (PVP)/PARACETAMOL NANOFIBERS

DOI: 10.35530/TT.2021.28

M. Geysoğlu^{1*}, H.K. Güler², F.C. Çalhoğlu², İ.Y. Mol²

¹Bioengineering Department, Institute of Natural and Applied Sciences, Süleyman Demirel University, Turkey

(E-mail: mustafageysoglu@sdu.edu.tr)

²Textile Engineering Department, Engineering Faculty, Süleyman Demirel University, Turkey

(E-mail: hulyakesici@sdu.edu.tr, fundacengiz@sdu.edu.tr, iremyagmurmol@gmail.com)

Abstract: This study aimed to achieve Polyvinylpyrrolidone (PVP) nanofiber production including paracetamol (PCT) by oil-in-water emulsion electrospinning. At first, emulsions were prepared at 14 wt % PVP with various PCT concentrations (0, 0.1, 0.3, 0.5, 0.7, 0.9 wt %). Then, solution properties such as viscosity, conductivity, and surface tension were determined. The production of nanofiber samples was carried out by emulsion electrospinning under the optimum process parameters (voltage, distance between electrodes, feed rate, and atmospheric conditions). Finally, the morphological and structural characterization of the nanofiber surface was carried out with SEM and FT-IR. According to the results of emulsion properties, although the change is not remarkable, it tends to increase the viscosity with an increase in PCT concentration. On the other hand, it was observed that surface tension did not change significantly with PCT concentration increase and while the conductivity of emulsions decreased slightly. When the fibre structure was investigated, average fibre diameter and fibre diameter uniformity were not affected prominently by PCT concentration. From the SEM images, it is possible to say that generally fine, uniform and bead-free drug-loaded nanofibers were obtained. The finest (326 nm) and most uniform (1.03) nanofibers were achieved from the sample N4 which included 0.5 wt % PCT. Also, the FT-IR results verified that PVP and PCT exist in the nanofiber structure.

Keywords: emulsion electrospinning, nanofiber, paracetamol, Polyvinylpyrrolidone

1. INTRODUCTION

In this study, it was aimed at achieving Polyvinylpyrrolidone (PVP) nanofiber production including paracetamol (PCT) by oil-in-water emulsion electrospinning and characterization in terms of fibre morphology by Scanning Electron Microscope (SEM) and chemically exhibition of PCT presence in the structure of nanofibers by FT-IR analysis.

It is known from the literature that nanofibers can be used in several fields, such as medical applications, drug delivery systems, energy storage, battery separators, aerospace, information technology, etc. [1]. Recently, there have been lots of possible biomedical uses for nanofibers, owing to their unequalled mechanical strength, elasticity, very small fibre diameter, small controllable pore size, high porosity, very high specific surface area (m²/g), high load capacity, and ease of fabrication [2,3].

Emulsion electrospinning is an efficient and new method for the production of nanofibers. From immiscible liquids such as essential oils and hydrophobic drugs and

proteins can be produced as nanofibers by this new approach. The preparation of homogenous and stable emulsion solutions to produce nanofibers is much easier with emulsion electrospinning. Another advantage of this method is that there is no need for an extra apparatus compared to the classical electrospinning system [4].

PVP is a highly hydrophilic polymer and is used because of its remarkable properties, such as high surface activity, good biocompatibility, low toxicity, and strong adsorption capacity. PVP based nanofibers have a wide variety of applications in biomedical, pharmacy, food and cosmetics [5].

PCT is a non-inflammatory [6], antipyretic and analgesic agent which is used to relieve pain in the body and to reduce body temperature [7]. Recently, there has been research about electro spun nanofibers, including PCT. Yang et al. prepared PCT loaded poly (vinyl alcohol) (PVA) nanofibers by electrospinning [8]. Yıldız and Uyar successfully obtained free-standing, easy to handle nanofibrous films of paracetamol/HPCD-IC and paracetamol/SBE--CD-IC by electrospinning [9]. Illangakoon et al., successfully produced fast-dissolving drug delivery systems for the simultaneous release of paracetamol and caffeine. This work was achieved by processing them into electro spun fibres using PVP as the filament forming agent [7].

It is thought that the results obtained from this study will contribute to the literature on medical textile materials.

2. MATERIALS AND METHODS

In this study, PVP (360.000 g/mol) (Sigma–Aldrich (St. Louis, MO, USA) was used as a polymer, PCT was used as a drug (Atabay Pharmaceuticals and Fine Chemicals Inc.), dimethylformamide (DMF) (Sigma–Aldrich (St. Louis, MO, USA) and distilled water were used as solvents. In addition, Cremophor RH 40 was used as a surfactant and was supplied by Ersa Chemistry (Izmir, Turkey).

PVP concentration and surfactant concentration were kept constant at 14 wt % and 1 wt %, respectively. PCT was added at different concentrations, such as 0.1, 0.3, 0.5, 0.7, and 0.9 wt%.

According to the experimental studies, initially, polymer solutions were prepared as an emulsion with PVP and PCT. The emulsion was stirred at room temperature for about 20 hours. After emulsion preparation, the emulsion properties were determined. The conductivity, viscosity, and surface tension (by the Du Noüy ring) of emulsions were measured.

Then, the nanofibers were produced by an emulsion electrospinning approach. The process parameters of the electrospinning given in table 1, such as applied voltage, distance between needle and collector, solution flow rate etc., were optimized. All process parameters were kept constant as in table 1 during the spinning process. Also, the spinning process was achieved under the same ambient conditions for all samples. The nanofibers were produced for 20 minutes and collected on an aluminium sheet.

Table 1. Process parameters of the electrospinning

Voltage (kV)	Distance between electrodes (cm)	Feed rate (ml/h)	Humidity (%)	Temperature (°C)
21	19.5	0.3	28	25

Finally, the nanofiber morphology, such as fibre diameter, diameter uniformity, and web surface structure, was determined and analysed with SEM. The fibre diameters

were calculated by image J analysing software. The SPSS analysis program was used to statistically analyse the findings about morphological parameters such as fibre diameter histogram. FT-IR was performed to determine the presence of PVP and PCT in the nanofiber structure chemically.

3. RESULTS AND DISCUSSIONS

In this study, emulsion properties such as viscosity, conductivity, and surface tension were measured and the effects of PCT concentration on the solution properties were analysed. From figure 1, it was determined that there was no significant change in surface tension, viscosity, and conductivity with different PCT concentrations.

According to the results of emulsion properties, although the change is not significant, it tends to increase the viscosity with an increase in PCT concentration except N6.

On the other hand, it was observed that surface tension tends to decrease as the PCT concentration increases, except for the N4 sample, but the changes are not significant. The conductivity of emulsions decreases with PCT increase except N2. It is possible to say that emulsion conductivity increases with the first addition of PCT to the PVP emulsion and then decreases as the PCT concentration increases.

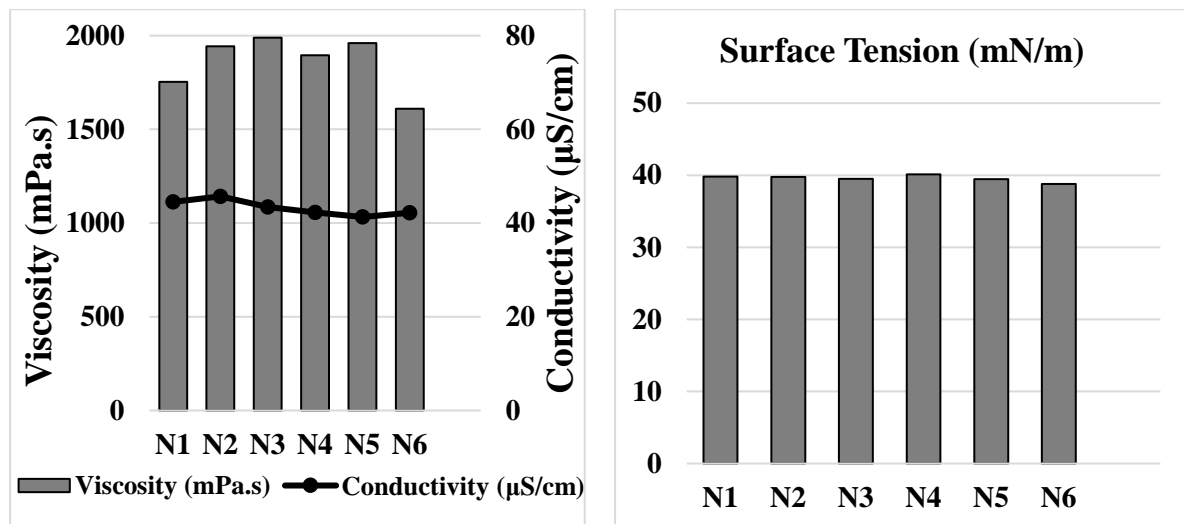
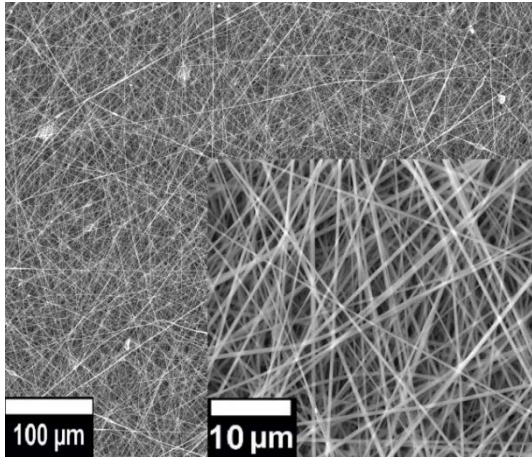
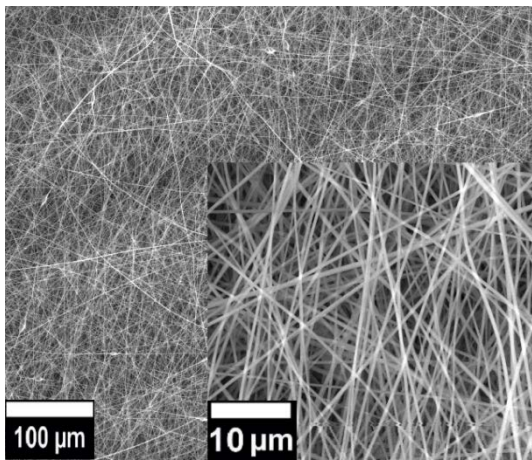
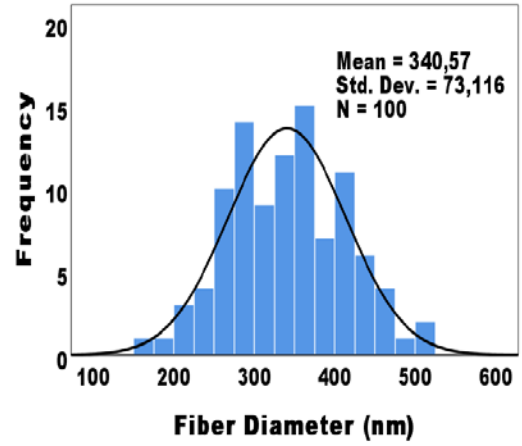


Figure 1. Results of solution properties (surface tension, viscosity and conductivity) of PVP with various PCT concentrations.

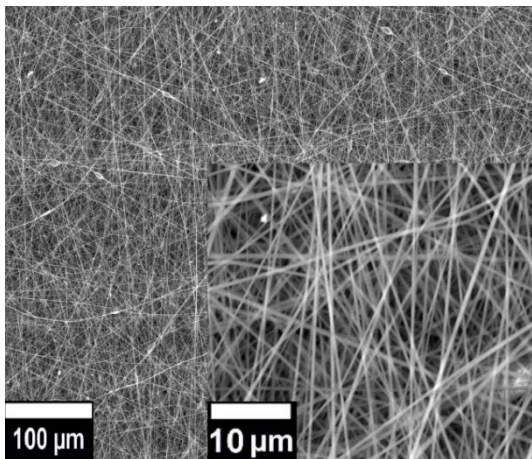
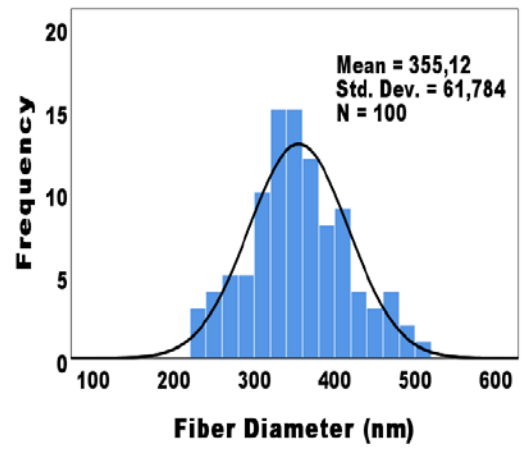
SEM images and fibre diameter histograms of PVP nanofiber samples (1.000x, 10.000x) produced with various PCT concentrations are given in figure 2.



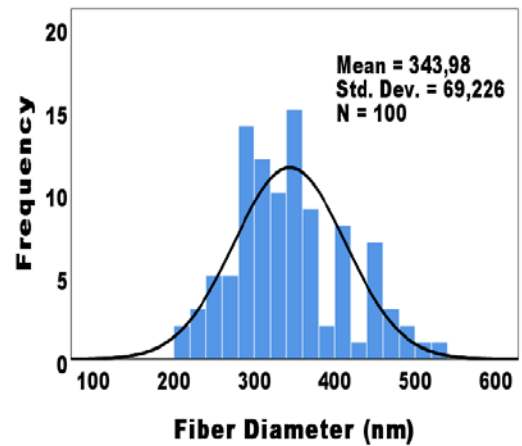
(N1)

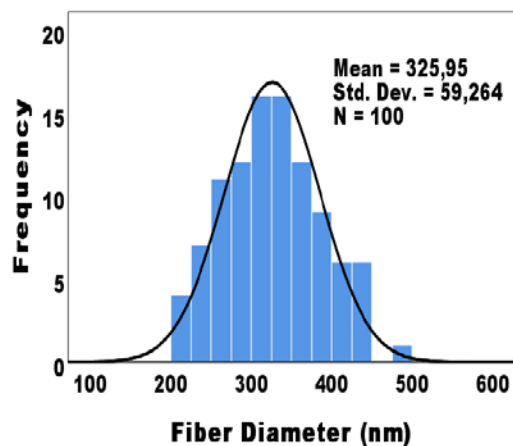
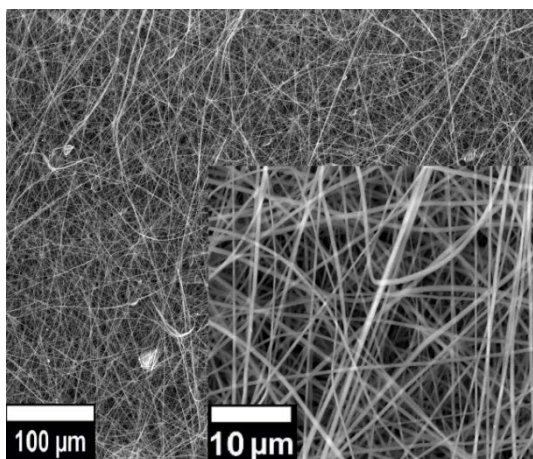


(N2)

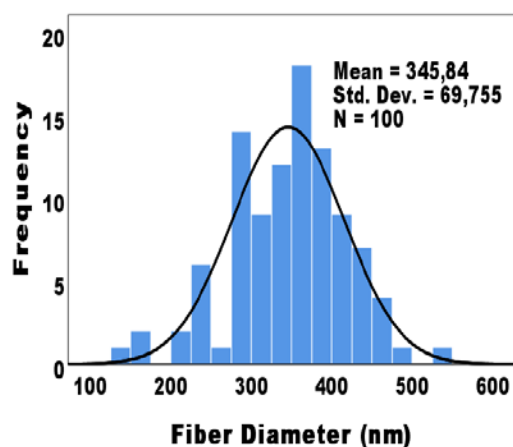
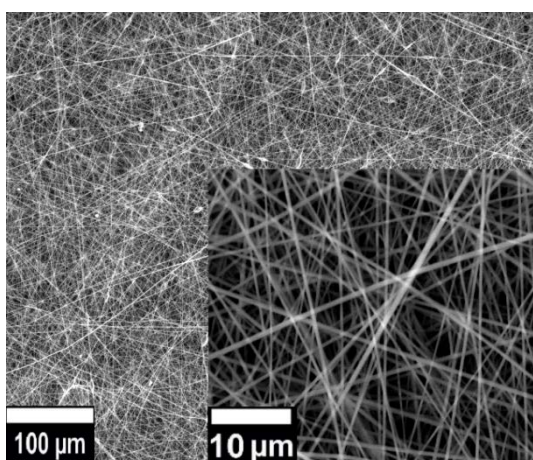


(N3)

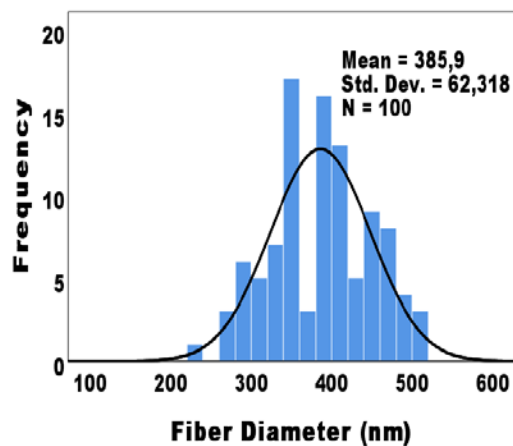
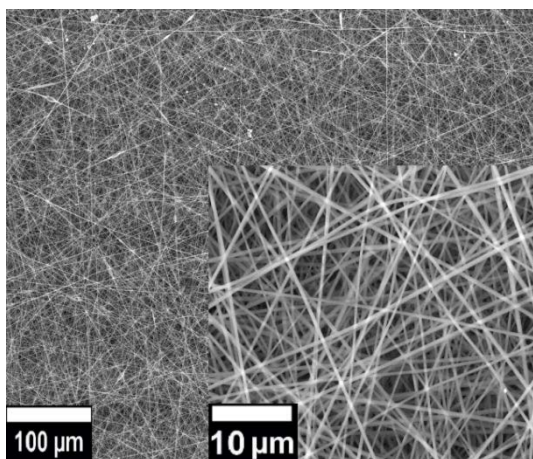




(N4)



(N5)



(N6)

Figure 2. SEM images and fibre diameter histograms of PVP nanofiber samples produced with various PCT concentrations (1.000x, 10.000x)

When figure 2 was analysed, it was seen that uniform and smooth nanofibers, good web quality without beads, and unimodal fibre diameter histograms were obtained. There was no bead formation in any fibre structure and the PCT concentration did not affect the bead formation.

The effect of PCT concentration on the average fibre diameter and fibre diameter

uniformity coefficient was shown in figure 3.

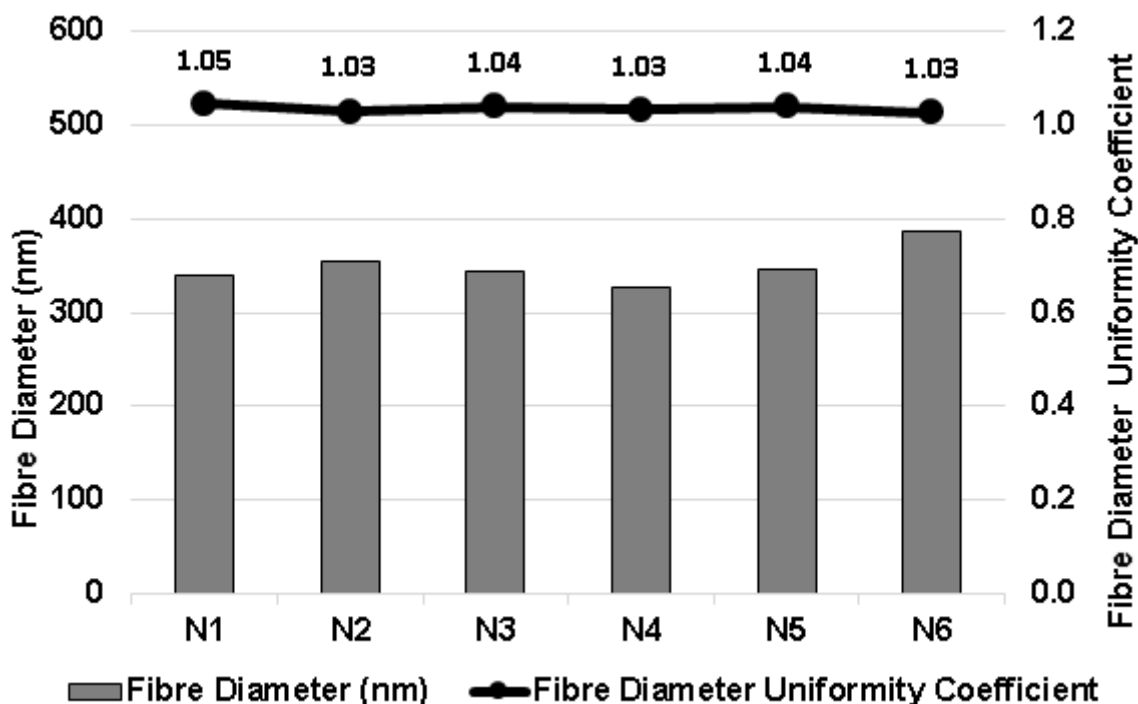


Figure 3. The effect of PCT concentration on the average fibre diameter and fibre diameter uniformity coefficient of PVP nanofibers

According to Figure 3, there isn't any specific variation in the fibre diameter and diameter uniformity coefficient with change in PCT concentration. The smallest average fibre diameter is 326 nm (N4) and the highest one is 385 nm (N6) for all fibre structures among all PCT concentrations. Fibre diameter uniformity coefficient values are very close to 1 for all samples. The smoothest histogram was again seen in the N4 sample.

Lastly, the presence of PVP and PCT were confirmed in the nanofiber structure via FT-IR analysis (Figure 4). According to FT-IR spectra of the PVP, there is a peak at 2949 cm^{-1} . This peak appeared at 2949 cm^{-1} in N1, and 2953 cm^{-1} in N4. There is another sharp peak at 1652 cm^{-1} due to the C=O in the spectra of the PVP polymer. This peak appeared at 1657 cm^{-1} and 1655 cm^{-1} in the spectra of N1 and N4 respectively. Due to the C–N stretch from PVP, there is a peak at 1284 cm^{-1} . This peak appeared at 1288 cm^{-1} in both N1 and N4. On the other hand, pure PCT has a peak at 1561 cm^{-1} . This peak appeared at 1559 cm^{-1} in an N4 sample that included 0.5 wt %.

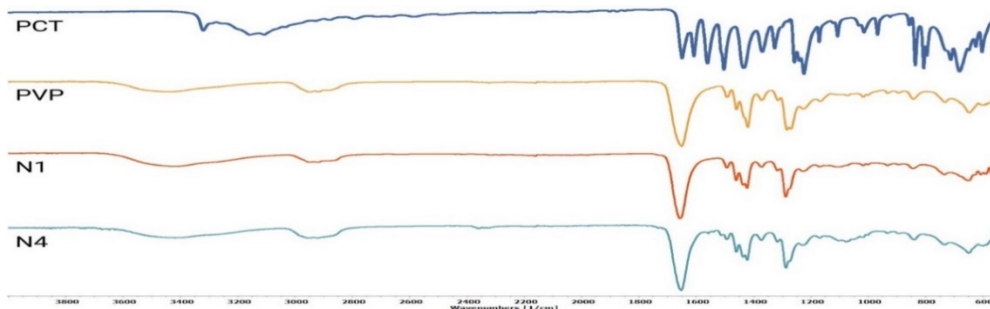


Figure 4. FT-IR spectra of PVP, PCT and PCT loaded PVP nanofiber samples

4. CONCLUSION

The production and characterization of PVP nanofibers with various concentrations of PCT were achieved via an emulsion electrospinning approach. According to the results, it was observed that quite uniform, smooth and fine, drug-loaded emulsion electro spun nanofibers were produced. In addition, good web quality without beads and a unimodal histogram curve of fibre diameter were determined. It is thought that this nanofibrous medical textile surface obtained has the application potential for controlled drug delivery applications.

REFERENCES

- [1] Fang, J., Niu, H., Lin, T., et al., *Applications of electrospun nanofibers*, In: Chi. Sci. Bull., 2008, 53, 15, 2265-2265-2286, <https://doi.org/10.1007/s11434-008-0319-0>
- [2] Bhardwaj, N., Kundu S.C., *Electrospinning: a fascinating fiber fabrication technique*, In: Biotechnol. Adv., 2010, 28, 3, 325-347, <https://doi.org/10.1016/j.biotechadv.2010.01.004>
- [3] Shanmugam, V., Selvakumar, S., Yeh, C.S., *Near-infrared light-responsive nanomaterials in cancer therapeutics*, In: Chem. Soc. Rev., 2014, 43, 17, 6254-6287, <https://doi.org/10.1039/C4CS00011K>
- [4] Cengiz Çalhoğlu, F., Kesici Güler, H., *Production of essential oil-based composite nanofibers by emulsion electrospinning*, In: PAJES, 2020, 26, 7, 1178-1185, <https://doi.org/10.5505/pajes.2019.67424>
- [5] Xie, J., Mao, H., Yu, D.G., et al., *Highly stable coated polyvinylpyrrolidone nanofibers prepared using modified coaxial electrospinning*, In: Fibers Polym., 2014, 15, 1, 78-83, <https://doi.org/10.1007/s12221-014-0078-2>
- [6] Li, L., Zhou, T., Sun, G., et al., *Ultrasensitive electrospun nickel-doped carbon nanofibers electrode for sensing paracetamol and glucose*, In: Electrochim. Acta, 2015, 152, 31-37, <https://doi.org/10.1016/j.electacta.2014.11.048>
- [7] Illangakoon, U.E., Gill, H., Shearman, G.C., et al., *Fast dissolving paracetamol/caffeine nanofibers prepared by electrospinning*, In: Int. J. Pharm., 2014, 477, 369-379, <https://doi.org/10.1016/j.ijpharm.2014.10.036>
- [8] Yang, G., Wang, L., Yang, Y., et al., *4-phosphatephenyl covalently modified glassy carbon electrode for real-time electrochemical monitoring of paracetamol release from electrospun nanofibers*, In: Electroanalysis, 2012, 24, 1937-1944, <https://doi.org/10.1002/elan.201200230>
- [9] Yıldız, Z.I., Uyar, T., *Fast-dissolving electrospun nanofibrous films of paracetamol/cyclodextrin inclusion complexes*, In: Appl. Surf. Sci., 2019, 492, 626-633, <https://doi.org/10.1016/j.apsusc.2019.06.220>



PARACETAMOL DRUG LOADED MICROCAPSULE BASED NANOFIBER PRODUCTION

DOI: 10.35530/TT.2021.30

İ.Y. Mol^{1*}, F.C. Çallıoğlu¹, H.K. Güler¹, M. Geyssoğlu²

¹Textile Engineering Department, Engineering Faculty, Süleyman Demirel University, Turkey
(E-mail: iremyagmurmol@gmail.com, fundacengiz@sdu.edu.tr, hulyakesici@sdu.edu.tr)

²Bioengineering Department, Institute of Natural and Applied Sciences, Süleyman Demirel University, Turkey
(E-mail: mustafageysoglu@sdu.edu.tr)

Abstract: *In this study, it was aimed to production and characterization of paracetamol (PCT) loaded microcapsules and microcapsule added electro spun PVA nanofibers. Eudragit RS 100 and PVA were used as the shell in the microcapsule structure, and PCT was used as the core material. First of all, the PCT loaded Eudragit RS 100/PVA microcapsules were produced by solvent evaporation method under the optimum process parameters. Then, properties such as conductivity, viscosity and surface tension of the microcapsule loaded PVA solution were measured and the effects of microcapsule concentration on the solution properties were determined. According to the solution results, while the viscosity increased with the microcapsule concentration, conductivity and surface tension did not change significantly except for the PVA-10 sample. After the electrospinning process, fibre morphology was determined by SEM and incorporation of microcapsules into the nanofibers was clearly demonstrated. It was calculated from the SEM images that average microcapsule size is 9.81µm, average fibre diameter is 550 nm and fibre diameter uniformity coefficient is 1.025. Finally, the incorporation of PCT loaded microcapsules into the nanofibers was chemically confirmed by FT-IR analysis. It is thought that the results of this study will be useful for controlled drug release, especially in medical textiles.*

Keywords: *electrospinning, medical textile, microcapsule, nanofiber, paracetamol*

1. INTRODUCTION

Microcapsules have become very popular in recent years, especially for the development of functional fabrics in the textile industry. With the microencapsulation technique, controlled/delayed release, masking of taste, odour and color, protection against UV, heat, oxidation, acids and bases, stabilization of volatile compounds, antibacterial, antimicrobial, long-term flaming, retardant, insect repellent and thermal insulation properties can be achieved on textile surfaces [1]. As the core material, volatile, drug-active substances, taste, odour, etc. substances can be microencapsulated [2]. Microcapsules can be produced by physical or chemical methods [3].

Eudragit RS 100 is a copolymer of ethyl acrylate, methyl methacrylate, and a small amount of methacrylic acid ester containing quaternary ammonium groups [4]. Eudragit RS 100 used in the shell material is an easy to use and process polymer in any form as aqueous dispersions, granules, organic solutions, powders or ready-to-use powders [5]. Eudragit RS 100 is a biocompatible, inexpensive, easily produced polymer with good stability. It is a common polymer that is insoluble in water and is often used as a wall material in extended-release microcapsules [6]. Eudragit RS 100 has a wide use in coating,

that is, microencapsulation, of drug-active substances that do not dissolve in water [7]. The main ingredient, paracetamol (PCT), is an active drug substance with analgesic and antipyretic effects. Paracetamol is a white, odourless, crystalline powder. It has a bitter taste [8]. Although it is slightly soluble in water, its analgesic effect is milder than other new generation pain relievers, PCT was preferred in the study due to its safety and lack of side effects in the digestive system. Solvent evaporation method was chosen as the microcapsule production method. The emulsion/solvent removal method is the most common method used for microencapsulation of water-insoluble drugs [9]. In the solvent evaporation method, the production conditions such as mixing speed, mixing time, solvent ratio, solution concentration have a great influence on the microcapsule morphology [10]. In addition, the fact that drug-loaded microcapsules do not leak or crack after production makes this method even more advantageous. During the experiments, the production is simpler as the solvent can be evaporated quickly by itself, by temperature or by mixing, that is, there is no need for an extra addition to the system.

Nanofiber textiles are materials with high porosity and specific surface area, pore size smaller than 1 micrometre, have water vapor permeability and air permeability. Electrospinning is a simple, inexpensive, easy and fast process used to obtain micro-nano size fibres suitable for commercial production, suitable for spinning many different polymers [11]. The Poly (vinyl alcohol) (PVA) used is a biocompatible and biodegradable semi-crystalline polymer and has a very good ability to form fibrous materials. It is water soluble, has very good chemical resistance, physical and mechanical properties and flexibility. It shows excellent electro-absorbability in aqueous environments [12]. It is thought that PCT loaded microcapsule added nanofiber material produced for this study will have an important place for medical textiles.

2. MATERIALS AND METHODS

2.1 Materials

For microencapsulation process, Eudragit ® RS 100 (Evonik Röhm GmbH) and Polyvinyl alcohol (Mn=88,000, 88% hydrolysed) were used as shell materials, paracetamol (PCT) (Atabay Kimya, Turkey) was used as a core material, chloroform (Iso Lab) and distilled water were used as solvents and Span20 (Sigma-Aldrich Corporation (St. Louis, MO, USA)) was used as a surfactant. During nanofiber production experiments, Polyvinyl alcohol (Mn=88,000, 88% hydrolysed) was used as a main polymer and distilled water was used as a solvent. PVA polymer concentration was kept constant as 10 wt % and PCT loaded microcapsule concentration was applied as 0, 2, 4, 6, 8, 10.

2.2 Methods

Microencapsulation was achieved by solvent/evaporation method which is the simple and physical method. In this method, the polymer is first dissolved with the solvent. Then the active ingredient is added. The dissolved polymer formed the oil phase, that is, the droplet phase. The surfactant forms the second and continuous phase by mechanical mixing in an aqueous solution. The polymer solution containing the insoluble substance from these two solutions was added to the droplets in the aqueous solution high speed mixer. Finally, the solvent is evaporated by mechanical action. The resulting microcapsules are washed with water, filtered with filter paper and dried. Composition of microcapsule loaded PVA solutions is given in table 1.

Table 1. Composition of microcapsule loaded PVA polymer solutions

Sample codes	PVA concentration (wt %)	Microcapsule concentration (wt %)
PVA-0	10	0
PVA-2	10	2
PVA-4	10	4
PVA-6	10	6
PVA-8	10	8
PVA-10	10	10

First of all, microcapsule loaded PVA solution properties such as conductivity, viscosity (shear rate 5 s^{-1}) and surface tension were measured. Then, nanofiber production was carried out by conventional electrospinning method under the same process parameters. During the spinning process, 21.7 kV voltage, 1.5 ml/h solution feed rate and 18.1 cm distance between the electrodes, $29 \pm 2\%$ humidity and, $25.9 \pm 2^\circ\text{C}$ ambient conditions were applied for all solutions. All nanofibers were produced for 15 minutes and collected on aluminium foil. Microcapsules and nanofiber morphology such as capsule size, fibre diameter, diameter uniformity and nanoweb quality were analysed by Scanning Electron Microscopy (SEM).

It was used to measure the diameters of 100 fibres obtained from various parts of the nanoweb with the Image J program. The number mean and weight mean values were estimated using the following formulas: (1) and (2).

$$A_n = \frac{\sum n_i d_i}{\sum n_i} \text{ (number average)} \quad (1)$$

$$A_w = \frac{\sum n_i d_i^2}{\sum n_i d_i} \text{ (weight average)} \quad (2)$$

The A_w/A_n ratio was used to obtain the fibre uniformity coefficient as well as for the molar mass distributions. A_n optimum value close to 1 indicates fibres of the same type in size [13]. Fibre diameter histogram was obtained by SPSS statistical program.

Lastly, FT-IR analysis was performed to determine the presence of PCT loaded microcapsules into the nanofiber structures.

3. RESULTS AND DISCUSSION

Microcapsule production was carried out by emulsion/solvent evaporation method under the optimum process parameters. SEM images of paracetamol loaded Eudragit RS 100/PVA microcapsules are shown in figure 1.

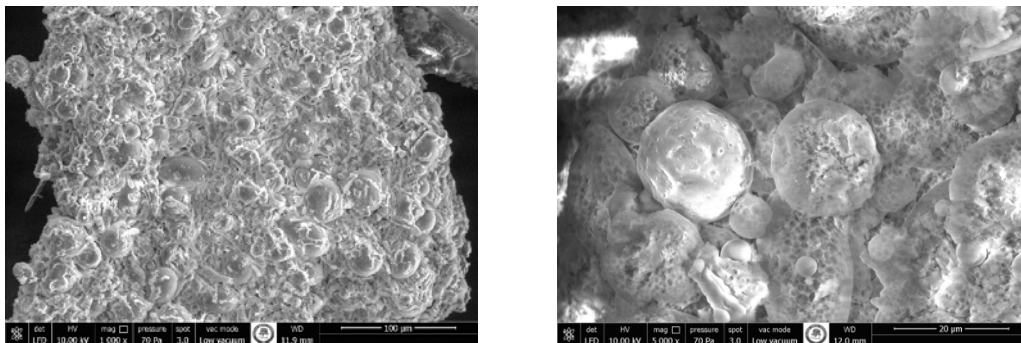


Figure 1. SEM images of PCT loaded Eudragit RS 100/PVA microcapsules (1.000x, 5.000x)

As seen from the SEM images, PCT loaded Eudragit RS 100/PVA microcapsules have a partial spherical shape and also there are some cracks. Average microcapsule size is 9.81 μm . Then, solution properties (conductivity, viscosity and surface tension) of PVA solutions include different concentrations of microcapsules, were measured. The results of solution properties are given in figure 2.

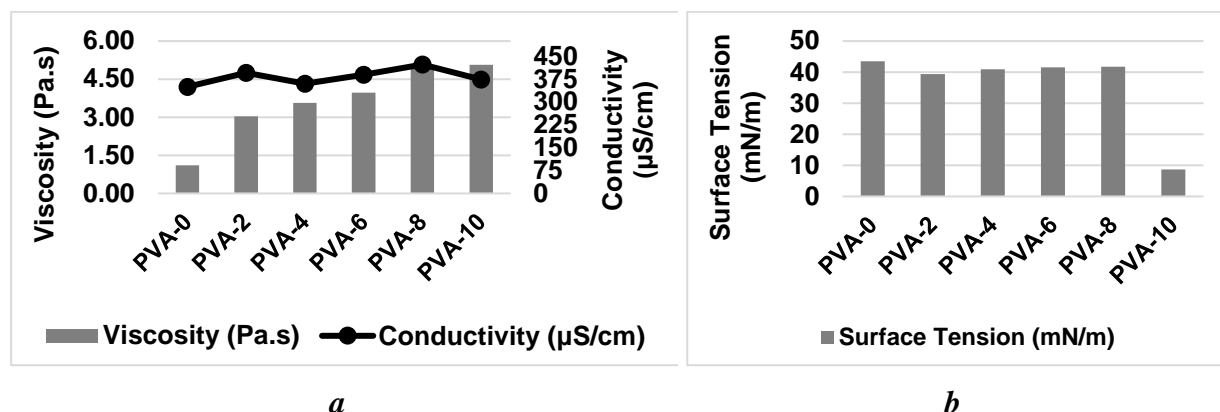
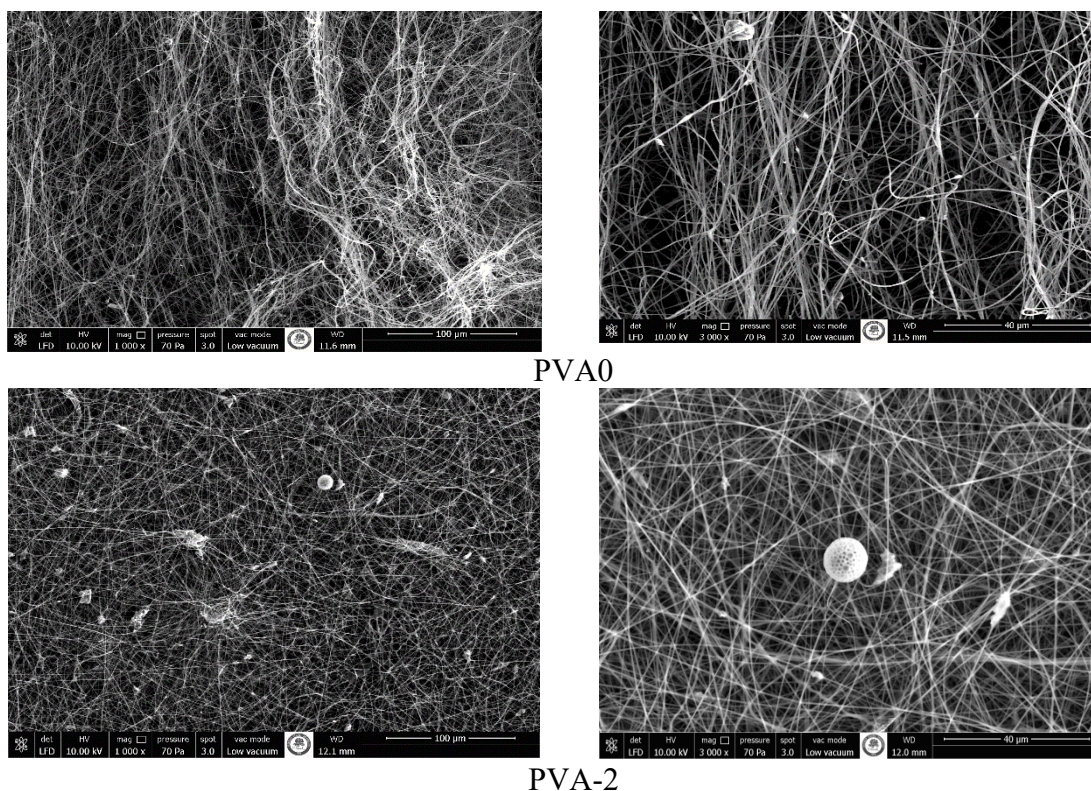
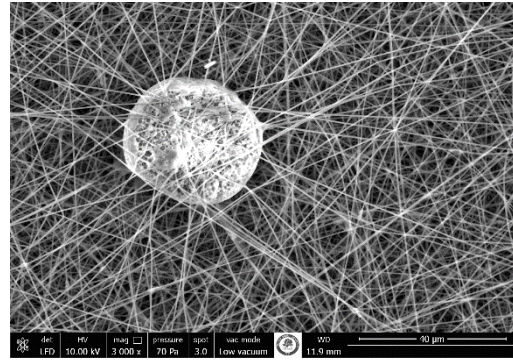
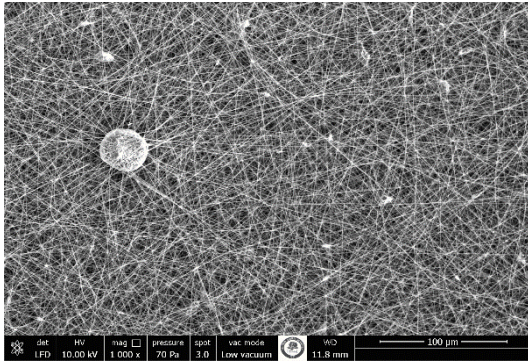


Figure 2. Solutions properties of PVA polymer solutions with different concentrations of microcapsules: a - viscosity and conductivity; b- surface tension

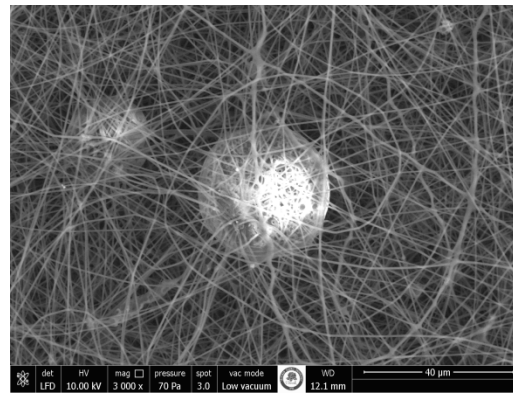
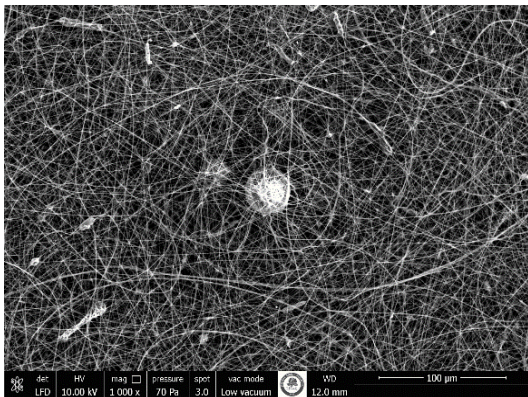
According to figure 2, viscosity increases with microcapsule concentration increasement while conductivity and surface tension were not significantly change except sample PVA-10. Surface tension decreased drastically at 10 wt% concentration of PCT loaded microcapsules (PVA-10).

Morphology of PVA nanofibers at various concentrations of PCT loaded microcapsules such as 0, 2, 4, 6, 8 and 10 wt% were examined by SEM images (figure 3).

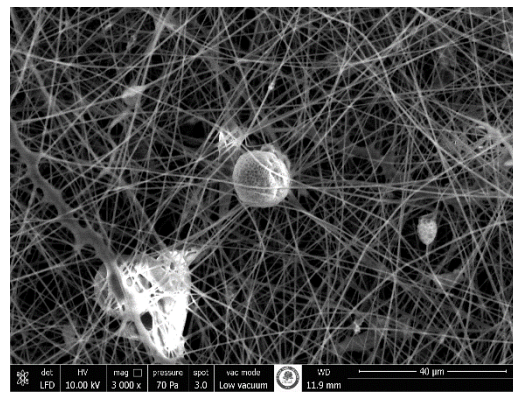
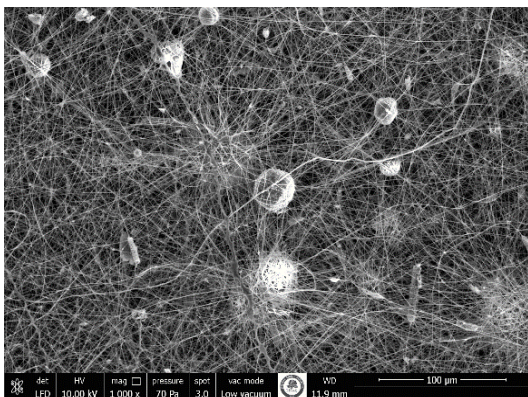




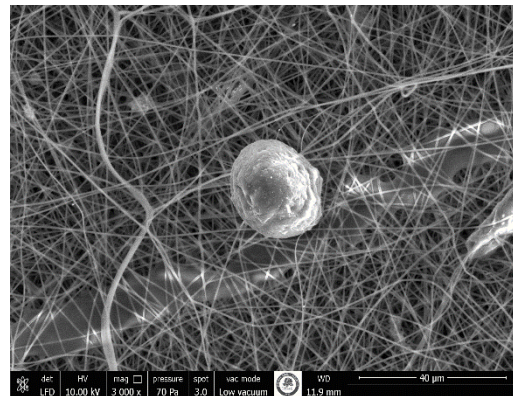
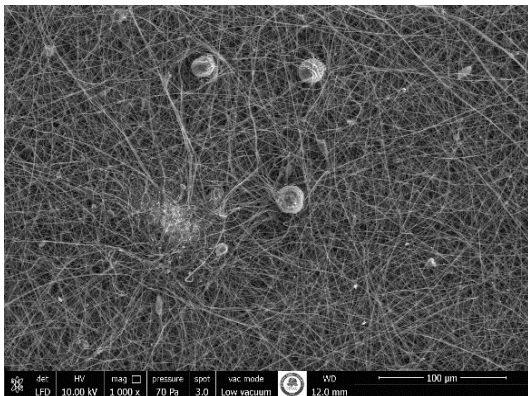
PVA-4



PVA-6



PVA-8



PVA-10

Figure 3. SEM images of PVA nanofibers with various concentrations of microcapsules (1,000x, 3,000x)

As shown in the SEM images, PCT loaded microcapsules were successfully incorporated into the nanofibrous structure. Generally, quite fine, smooth and uniform nanofibers were obtained. PVA nanofibers diameter histogram is given in figure 4.

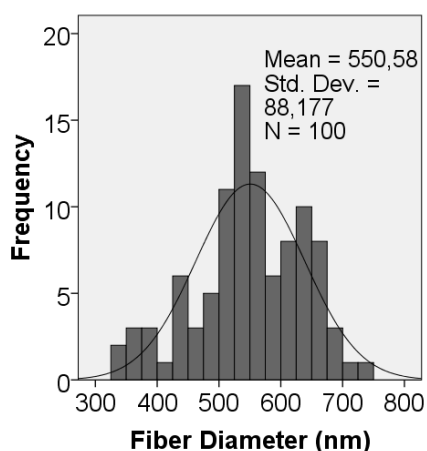


Figure 4. Electro spun PVA nanofiber diameter histogram

From the calculations; average fibre diameter is 550 nm and fibre diameter uniformity coefficient are 1.025. Unimodal histogram curve was obtained from the SPSS diagram. In addition, it is possible to say that fibre morphology (diameter, diameter uniformity) was not affected from the microcapsule concentration.

FT-IR spectroscopy confirmed the presence of PVA polymer and PCT loaded microcapsules in the chemical structures of the nanofibers (figure 5).

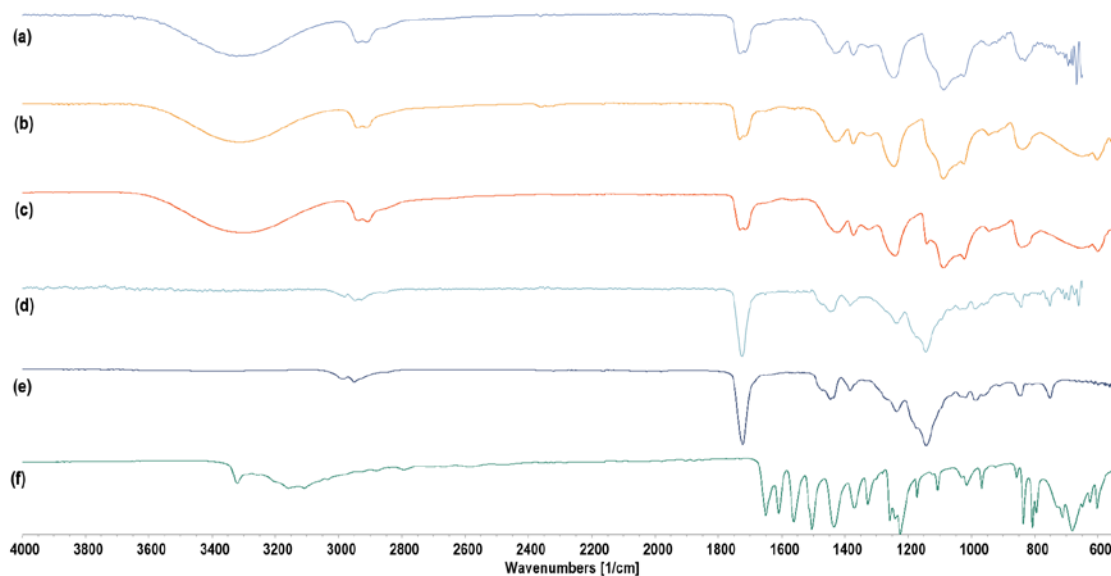


Figure 5. FT-IR spectra of: a - PVA-0 nanofibers; b- PVA-10 nanofibers; c- PVA polymers; d- PCT/PVA/Eudragit RS 100 microcapsules; e- Eudragit RS 100 polymers; f- PCT

The FT-IR spectrum of PVA demonstrates the primary peaks linked with PVA and PVA nanofibers quite clearly. For instance, the typical strong hydrogen bonded band occurred at approximately $2940\text{-}2912\text{ cm}^{-1}$ wavelength in the spectra of PVA polymer, PVA-0 and PVA-10 nanofibers. Because of the high hydrophilic forces, intramolecular and

intermolecular hydrogen bonding is expected to occur among PVA chains. Another important absorption peak was confirmed at 1141 cm^{-1} . This peak arises at 1243 cm^{-1} and 1245 cm^{-1} in the spectra of PVA-0 and PVA-10 nanofibers, respectively. The crystallinity of PVA is primarily responsible for this vibrational band, which is related to the carboxyl stretching band (C–O) [14]. The most intense peak in the spectrum, pure PCT has a peak at 1561 cm^{-1} . These peaks are seen at 2922 cm^{-1} and 2853 cm^{-1} for PVA-10 nanofiber and 2925 cm^{-1} and 2854 cm^{-1} for microcapsule spectra [15]. The carbonyl stretching vibration of the ester group is responsible for the stretching bands of Eudragit RS 100 at 1143 cm^{-1} and 1237 cm^{-1} . These stretching bands are attributed to 1173 cm^{-1} and 1243 cm^{-1} for PVA-10 nanofibers and to 1237 cm^{-1} and 1145 cm^{-1} for spectra of microcapsules [16,17].

5. CONCLUSIONS

This study was carried out for the production and characterization of PCT loaded microcapsules by solvent/emulsion method and PCT loaded microcapsule incorporation to the PVA nanofibers with various concentrations by electrospinning. Generally, partial spherical and some cracks shapes of capsules were synthesized and incorporate to the PVA nanofibers at various concentrations. The incorporation of PCT loaded microcapsules to the PVA nanofibers was verified with SEM images and FT-IR results. It is thought that this research results will be useful for the medical textile-based materials in future.

REFERENCES

- [1] Eyüpoğlu, Ş., Kut, D., *Microencapsulation technology and the use of microencapsulation technology in textile industry*, In: Istanbul Commerce University Journal of Technologies and Applied Sciences, 2016, 15, 29, 9-28
- [2] Kesici Güler, H., *Bazı bitki ekstratlarının eldesi, mikrokapsülasyonu ve pamuklu kumaşa uygulaması*, Master's Thesis, At: Institute of Natural and Applied Sciences Süleyman Demirel University, 2015
- [3] Çimen, E., *Possibilities of bring in new properties to woven fabrics by microencapsulation method*, PhD thesis, At: Institute of Natural and Applied Sciences, Istanbul Technical University, 2007
- [4] Reddy, Y., Dastagiri D., et al., *Formulation and in vitro evaluation of antineoplastic drug loaded nanoparticles as drug delivery system*, In: AJPP, 2013, 7, 23, 1592-1604, <https://doi.org/10.5897/AJPP2013.3436>
- [5] Thakral, S., Thakral, N. K., Majumdar, D. K., *Eudragit®: a technology evaluation. expert opinion on drug delivery*, 2013, 10, 1, 131-149. <https://doi.org/10.1517/17425247.2013.736962>
- [6] Pignatello, R., Amico, D., Chiechio, S., Spadaro, C., Puglisi, G., Giunchedi, P., *Preparation and analgesic activity of eudragit rs100® microparticles containing diflunisal*, In: Drug Deliv., 2001, 8, 1, 35-45, <https://doi.org/10.1080/107175401300002748>
- [7] Bolourchian, N., Bahjat M., *Design and in vitro evaluation of eudragit-based extended release diltiazem microspheres for once- and twice-daily administration: the effect of coating on drug release behaviour*, In: Turkish J. Pharm. Sci., 2019, 16, 3, 340-347, <https://doi.org/10.4274/tjps.galenos.2018.24861>
- [8] Selimoğlu, F., *Quantitative analysis of combined pharmaceutical preparations containin paracetamol by UPLC method*, PhD Thesis, At: Institute of Health Sciences, Ataturk University, 2013
- [9] Heiskanen, H., Denifl, P., Pitkänen, et al., *Effect of concentration and temperature on the properties of the microspheres prepared using an emulsion–solvent extraction proces*, In: Adv. Powder. Technol., 2012, 23, 6, 779-786, <https://doi.org/10.1016/j.ap.2011.10.007>
- [10] Hong, Y., Gao, C., Shi, et. al., *Preparation of porous polylactide microspheres by emulsion-solvent evaporation based on solution induced phase separation*, In: Polym. Adv. Technol., 2005, 16, 8, 622-627, <https://doi.org/10.1002/pat.629>

- [11] Yüksel, İ., *Effect of Process Parameters on Morphology of Electrospun PVA Nanofibers*, In: PAJES, 2009, 15, 3, 363-369
- [12] Üstündağ, G. C., Karaca, E., *Production of electrospun nanofibrous mat containing alginate and providing of water resistance with crosslinking*, In: Textile and Engineering, 2009, 16, 75
- [13] Cengiz, F., Jirsak, O., *The effect of salt on the roller electrospinning of polyurethane nanofibers*, In: Fibers and Polymers, 2009, 10, 2, 177-184
- [14] Mansur, H.S., Oréface, R.L., Mansur, A.A., *Characterization of poly (vinyl alcohol)/poly (ethylene glycol) hydrogels and PVA-derived hybrids by small-angle X-ray scattering and FTIR spectroscopy*, In: Polymer, 2004, 45, 21, 7193-7202
- [15] Eğri, Ö., Erdemir, N., *Production of Hyperivum Perforatum Oil-Loaded Membranes For Wound Dressing Material And in Vitro Tests, Artificial Cells*, In: Nanomedicine and Biotechnology An International Journal, 2019, 1404-1415
- [16] Park, J.M., Park, S.J., *Preparation and characterization of water-soluble microcapsule for sustained drug release using Eudragit RS 100*, In: Macromolecular Research, 2010, 18, 12, 1191-1194
- [17] Behera, B.C., Sahoo, S. K., Dhal, S., Barik, B.B., Gupta, B.K., *Characterization of glipizide-loaded polymethacrylate microspheres prepared by an emulsion solvent Evaporation Method*, In: Trop. J. Pharm. Res., 2008, 7, 1, 879-885, <https://doi.org/10.4314/tjpr.v7i1.14672>



PERFORMANCE PROPERTIES OF KNITTED FABRICS PRODUCED FROM rPET AND COTTON/rPET BLENDED VORTEX AND RING YARNS

DOI: 10.35530/TT.2021.32

A. Oruç*, Y. Arıkan, E. İlanbey, K. Özşahin

MEM Tekstil San. Ve Tic. A.Ş., Kahramanmaraş/Turkey
(E-mail: aoruc@memtextile.com, kaliteguvence@memtextile.com, argel1@memtextile.com, arge2@memtextile.com)

Abstract: An awareness of environmental issues is crucial for textile engineering due to increasing consumption of textile fibres. In addition, levels of pollution are ever increasing due to single use polymeric packaging materials in our daily life. Single use polymeric packaging materials, such as PET beverage bottles, have impacts on the consumption of raw materials and energy, on the contamination of our water and atmosphere, on human health, on global climate change. In this point of view, the ability of the textile producers to recycle the disposed PET beverage bottles into textile products has a critical importance. In this study, performance properties of knitted fabrics produced from rPET and cotton/rPET blended vortex and ring yarns are investigated to figure out the reproducibility of environmentally friendly textile products. For this aim, 100% rPET, 50-50% rPET-Co and 50-50% VPET-Co yarns were produced by Vortex and Ring Spinning technologies with same yarn number as Ne 30/1. Then the knitted fabric samples were produced from these sample yarns and the fabrics were dyed. Dimensional stability, bursting strength and pilling resistance properties of the fabrics were examined. Dimensional stability properties of rPET used fabrics were found to be similar with the ones which VPET used. Pilling resistance and bursting strength of the sample fabrics were close to each other that rPET usage does not demonstrate any disadvantage. Consequently, rPET fibre usage instead of VPET fibre is found to be appropriate.

Keywords: knitted fabric; r-PET yarn; recycle; ring spinning; vortex spinning

1. INTRODUCTION

Economic and population growth, industrialization in the world together causes an increase in the amount of waste. As a consequence of all these, while the more intensive use of natural resources is inevitable, the wastes created by the ever-increasing consumption tendency have reached the huge amounts that threaten the environment and human health due to their quantity and harmful contents [1,2]. The most favourable packaging material is polyethylene terephthalate (PET) is versatile owing to its transparent color, lightweight, strength, food safe, inexpensive price, fully recyclability etc. In addition to all these advantages, PET as a waste material takes up considerable space in nature and needs to be recycled for the disposal of these wastes. In this regard, recycling enables conservation of raw materials, reduce energy use in order to produce virgin PET and reduce greenhouse gas emissions. Today, PET is the most widely recycled plastic in the world. Eco-friendly products obtained by recycling of PET are mainly used as textile fibres [3]. In

the literature there are some studies which deal with rPET fibre usage in yarn and fabric production [3-12].

2. MATERIALS AND METHODS

In this study, it is aimed to compare the performance properties of knitted fabrics which are produced from Regenerated Polyester (rPET) and blends of Virgin Polyester (VPET) and rPET with Cotton (Co). The PET fibre and cotton fibre properties used in the study are given in table 1 and table 2, respectively.

Table 1. Properties of PET fibres used in the study

Characteristics	rPET	VPET
Fibre linear density (dtex)	1.3	1.3
Fibre length (mm)	38	40
Fibre strength (g/den)	6	6.95

Table 2. Properties of cotton fibres used in the study

Characteristics	Vortex	Ring
Fibre fineness (mic.)	4.57	4.20
Fibre length (mm)	29.9	30.4
Fibre strength (g/tex)	32.5	25.6

In this study, 100% rPET, 50-50% rPET-Co and 50-50% VPET-Co yarns were produced by Vortex and Ring Spinning technologies with same yarn number as Ne 30/1. The unevenness, imperfections and hairiness parameters were tested by USTER Tester by taking samples from 5 bobbins. Strength and breaking elongation parameters were tested by USTER Tensojet. Yarn quality parameters are given in table 3.

Table 3. Quality parameters of the sample yarns

Parameter	Ring			Vortex		
	100% rPET	50-50% rPET-Co	50-50% VPET-Co	100% rPET	50-50% rPET-Co	50-50% VPET-Co
U (%)	11.07	10.63	10.15	11.54	11.64	10.98
CVm	14.00	13.43	12.85	14.55	14.67	13.83
Thin-50%/km	9.5	2.5	0.5	42.5	32.5	20.5
Thick +50%/km	53.5	58	43	46	61.5	40
Neps +200%/km	78	65	58.5	-	-	-
Neps +280%/km	-	-	-	3	4	3
Hairiness	6.14	6.27	5.93	3.55	4.16	4.27
Strength (cN/tex)	17.61	14.07	18.62	16.64	13.70	17.25
Breaking elongation (%)	10.52	5.66	7.19	9.09	5.84	6.94

The knitted fabric samples were produced from the sample yarns by a 32 inches diameter and 28 fein single jersey circular knitting machine. Then, the fabric samples were dyed. 100% Polyester fabric samples and 50-50% Polyester-Cotton fabric samples were dyed according to the processes given in figure 1 and 2, respectively.

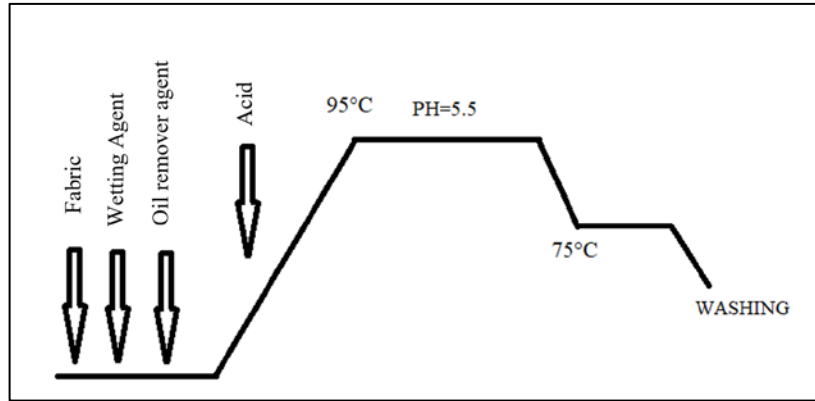


Figure 1. Dyeing curve for 100% Polyester fabric samples

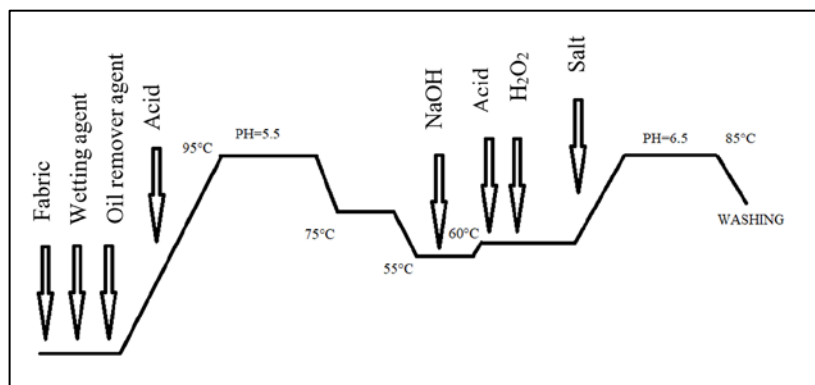


Figure 2. Dyeing curve for Polyester-Cotton blended fabric samples

All fabric samples were conditioned according to TS EN ISO 139 [13] before the tests and measurements. The tests were performed in the standard atmosphere of $20\pm 2^\circ\text{C}$ and $65\pm 4\%$ relative humidity. Fabric structural parameters namely; fabric mass, loop density and loop length properties of the dyed samples were determined according to standards of TS EN 12127 [14], TS EN 14971 [15] and TS EN 14970 [16], respectively. The fabric structural parameters are given in table 4.

Table 4. Structural parameters of sample fabrics

Parameter	Ring			Vortex		
	100% rPET	50-50% rPET-Co	50-50% VPET-Co	100% rPET	50-50% rPET-Co	50-50% VPET-Co
Fabric mass (g/m^2)	151	161	173	153	185	174
Number of courses (loops/cm)	18	21	21	20	23	21
Number of wales (loops/cm)	14	14	15	15	14	14
Loop length (mm)	3	2.8	2.8	3	2.8	2.8

Dimensional stability and skewness performance after home laundering were determined according to the standards of TS EN ISO 6330 [17] and AATCC 179 [18], respectively. In addition, bursting strength and pilling resistance of the samples were tested according to the standards of TS EN ISO 13938-2 [19] and TS EN ISO 12945-2[20], respectively.

3. RESULTS AND DISCUSSIONS

3.1. Dimensional Stability and Skewness After Home Laundering

Dimensional stability of the fabric samples produced from ring yarns and vortex yarns are given in figure 3 and figure 4, respectively.

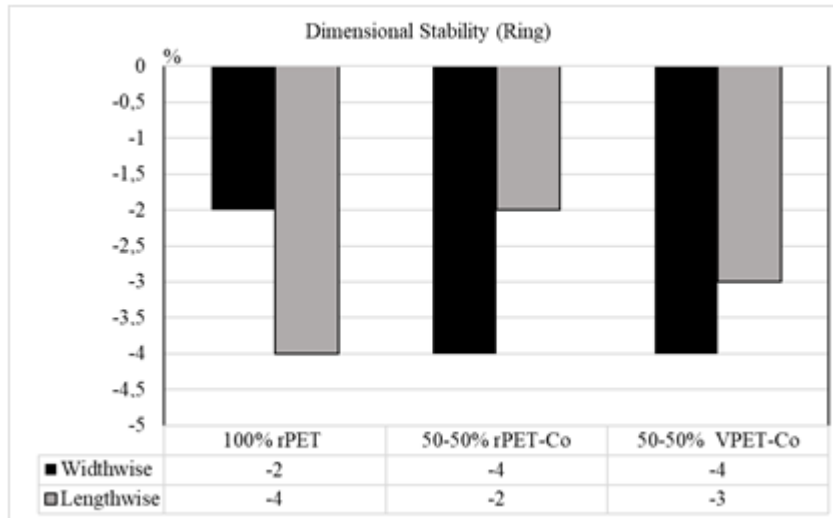


Figure 3. Dimensional stability of the ring yarn samples

It can be seen from figure 3 that the dimensional stability results of all fabric samples are below the commercial acceptability limits (5%). For ring yarn samples 50-50% rPET-Co and 50-50% VPET-Co samples show very similar dimensional stability results. So, it can be concluded that usage of rPET instead of VPET for widely used 50-50 PET-Co blend single jersey fabrics provide a similar fabric performance regarding the dimensional stability after home laundering. With respect to 100% rPET sample, it is seen that dimensional change values in width wise and lengthwise direction are contrary to other samples. This situation may be attributed to the usage of 50% cotton fibre.

Dimensional change results below commercial acceptability limits (5%) are observed for vortex yarn samples similar with ring samples. Figure 4 exhibits that the usage of rPET fibre instead of VPET causes an increase for width wise shrinkage. On the other hand, lengthwise direction shrinkage decreases by the use of rPET fibre instead of VPET. This is a very important result to keep in mind during the production of rPET blended fabrics that some precautions may be taken during commercial production. Also, it can be concluded that the 100% rPET vortex samples has a more dimensionally stable fabric structure than other samples.

According to the skewness after home laundering results, all fabric samples provided no skewness. So, it can be concluded that usage of rPET fibre instead of rPET has no disadvantage regarding the skewness performance.

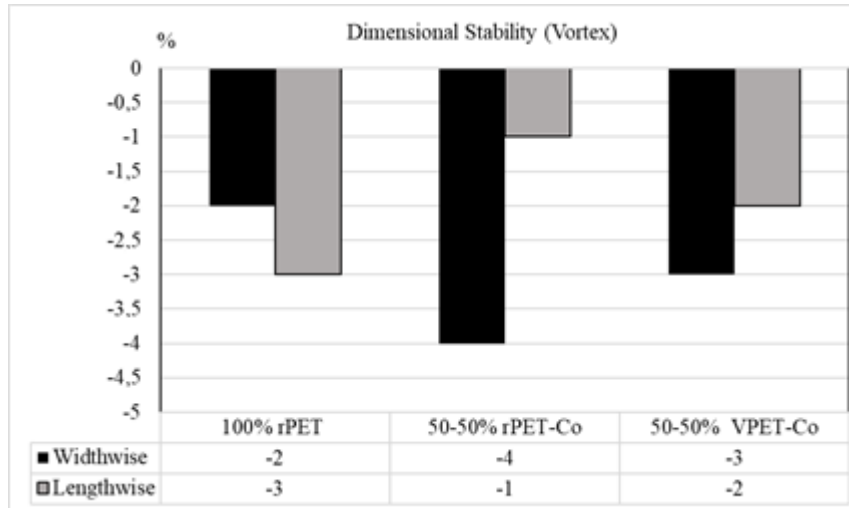


Figure 4. Dimensional stability of the vortex yarn samples

3.2. Bursting Strength

Bursting strength test results of the samples are given in figure 5.

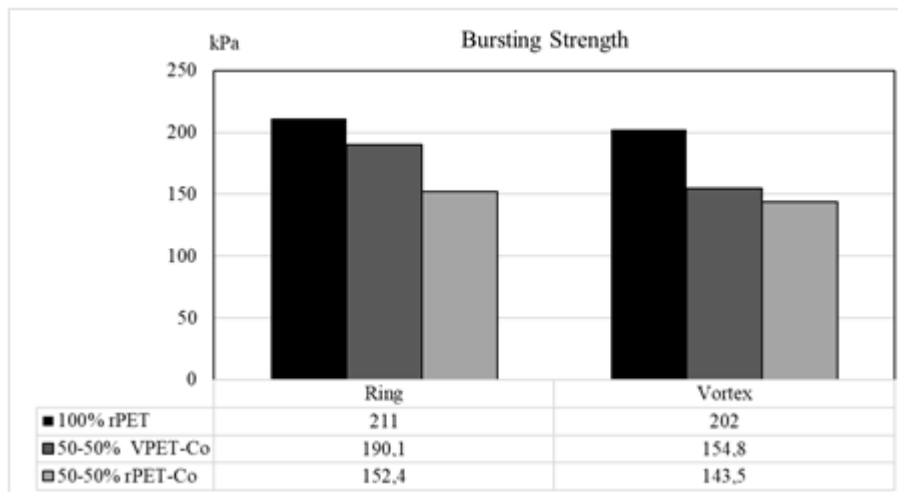


Figure 5. Bursting strength test results of the samples

Figure 5 exhibits the bursting strength values of the samples that the highest bursting strength value is obtained by the 100% rPET samples for both spinning technologies due to the higher fibre strength of rPET than cotton. 50-50% VPET-Co samples have higher bursting strength in comparison to 50-50% rPET-Co samples for both spinning technologies. This situation can be attributed the higher fibre strength of VPET fibre than rPET fibre. On the other hand, it can be seen that the difference between 50-50% VPET-Co and 50-50% rPET-Co samples is lower for vortex samples. So, it can be concluded that yarn structure that is obtained by vortex spinning technology may compensate the decrease in bursting strength of the fabrics.

3.3. Pilling Resistance

Pilling resistance of the samples are given in table 5. It can be seen that ring yarn samples provide higher pilling tendency than vortex samples. This situation arises from the higher number of protruding fibres ends from yarn structure in ring spinning technology

than vortex yarn. In vortex spinning technology, there is a group of fibres that provides wrapping around the yarn body. By this way, the number of protruding yarns ends from yarn body is decreased. The fabrics that are produced from ring spun yarns have hairier surface that causes pilling. In addition, it can be seen that usage of rPET fibre instead of VPET cause a slight decrease in pilling resistance for both ring yarn sample. With respect to vortex spinning, rPET usage instead of VPET results in enhancing the pilling resistance surprisingly.

Table 5. Pilling resistance of sample fabrics

Fibre composition	Ring	Vortex
100% rPET	1/2	2/3
50-50% rPET-Co	1/2	³ / ₄
50-50% VPET-Co	2	2/3

4. CONCLUSION

Increasing the rPET usage in textile production is an important issue and also a critical responsibility of commercial textile mills. Owing to this environmental responsibility, in this study it is aimed to investigate the reproducibility of rPET yarns and fabrics produced thereof by the most widely used spinning technologies as ring and vortex spinning. As a result of yarn production, it is seen that rPET and rPET-Co blended yarns have a good level of quality parameters for both spinning technologies except the yarn strength of rPET-Co blended yarns. Also, single jersey knitted fabrics were produced and dimensional stability, bursting strength and pilling resistance properties were demonstrated. As a result of fabric performance tests, it can be concluded that with respect to pilling resistance and skewness rPET usage do not provide any negative effect for both ring and vortex spinning technologies. Dimensional change values of all fabric types used in the study are below the commercially acceptable limits. Regarding the bursting strength performance, the decrease caused by usage rPET usage may be compensated by using vortex spinning technology instead of ring spinning. Consequently, by the important know-how gained by this study, it can be concluded that it is possible for textile mills to produce environmentally friendly rPET knitted fabrics commercially.

REFERENCES

- [1] Tayyar, A.E., Üstün, S., *Usage of Recycled PET*. In: Pamukkale University, Journal of Engineering Sciences. 2010, 16, 53-62
- [2] European Commission DG ENV, *Plastic waste in the environment* , 2011, Available at: <http://ec.europa.eu/environment/waste/studies/pdf/plastics.pdf> [Accessed on June 2021]
- [3] Sarioğlu, E., Kaynak, H.K., *PET bottle recycling for sustainable textiles*. In: Polyester - Production, Characterization and Innovative Applications, InTech Publishing, 2018, ISBN: 978-953-51-3882-2, Print ISBN: 978-953-51-3881-5, doi: 10.5772/intechopen.69941
- [4] Yuksekkaya, E.M., Celep, G., Dogan, G., Tercan M., Urhan B., *Comparative study of physical properties of yarns and fabrics produced from virgin and recycled fibers*, In: Journal of Engineered Fibers and Fabrics, 2016, 11, 2, 68-76
- [5] Inoue, M., Yamatomo, S., *Performance and durability of woven fabrics including recycled PET fibers*, In: Journal of Textile Engineering, 2004, 50, 2, 25-30

- [6] Rajamanickam, S., Vasudevan, K., *Study of Antibacterial Activity of Chitosan on Lyocell and Recycled Polyester Yarns*, In: International Journal of Innovative Research in Science Engineering and Technology, 2014, 3, 2, 9480-9486
- [7] Sariođlu, E., *Ecological Approaches in Textile Sector: The Effect of r-PET Blend Ratio on Ring Spun Yarn Tenacity*, In: Periodicals of Engineering and Natural Sciences, 2017, 5, 2, 176-180
- [8] Nohut, S., Sariođlu, E., Yayla, O., Kaynak, İ., Vuruskan, D., *Ring Eđirme Yöntemi ile Üretilen Geri Dönüşüm Poliester (r-PET) Karışımli İpliklerin Karakterizasyonu*, At: 3rd International Mediterranean Science and Engineering Congress, 2018, 971-975
- [9] Sariođlu E., *An investigation on performance optimization of r-PET/cotton and v-PET/cotton knitted fabric*, In: International Journal of Clothing Science and Technology, 2019, 31, 1, 439-452
- [10] Uyanık, S., *A study on the suitability of which yarn number to use for recycle poliester fiber*, In: The Journal of the Textile Institute, 2019, 110, 7, 1012-1031
- [11] Sariođlu, E., Vuruskan, D., Yayla, O., Satil, E.A., Çelikten, E., *Investigation of yarn properties produced from 100% recycled poliester (r-PET) by different spinning systems*, At: The International Conference of Materials and Engineering Technologies, 2019, 450-456
- [12] Sariođlu, E., Nohut, S., Vuruşkan, D., Yayla, O., *Production and characterization of recycled poliester (r-PET) blend vortex and ring spun yarns*, In: The Journal of The Textile Institute, 2020, 111, 12, 1705-1712
- [13] TS EN ISO 139 Tekstil - Şartlandırma ve deney için standart ortamlar
- [14] TS EN 12127 Tekstil-Kumaşlar-Küçük numuneler kullanarak birim alan başına kütleinin tayini
- [15] TS EN 14971 Tekstil- Örülmüş kumaşlar- Birim uzunluk ve birim alan başına örgü ilmeđi sayısının tayini
- [16] TS EN 14970 Tekstil- Örülmüş kumaş- Tek iplikli örme kumaşlarda örgü ilmeđi ve iplik doğrusal yoğunluđunun tayini
- [17] TS EN ISO 6330 Tekstil- Tekstil deneyleri için- Ev tipi çamaşır makinesi ile yıkama ve kurutma işlemleri
- [18] AATCC Test Method 179 Skewness Change in Fabric and Garment Twist Resulting from Automatic Home Laundering
- [19] TS EN ISO 13938-2 Tekstil-Kumaşların patlama özellikleri - Bölüm 2: Patlama mukavemetinin ve patlama gerilmesinin tayini için pnömatik metot
- [20] TS EN ISO 12945-2 Tekstil - Kumaşlarda yüzey boncuklanması, tüylenmesi ve matlaşması yatkinliđının tayini - Bölüm 2: Geliştirilmiş Martindale metodu



OPTIMIZATION OF SOME WEAVING MACHINE PARTS DESIGN. THEORETICAL APPROACH

DOI: 10.35530/TT.2021.33

A. Mostafa*¹, W. Hashima¹, S. El-Gholmy¹, A. Al-Oufy^{1,3}, M. Hassan²

¹Textile Engineering department, Faculty of Engineering, Alexandria University, Alexandria, Egypt.

²Mechanical Engineering department, Faculty of Engineering, Alexandria University, Alexandria, Egypt

³Material & Manufacturing Engineering, Faculty of Engineering, Galala University, Galala City, Egypt

Abstract: *The factors of increasing productivity, reducing the cost and the quality improvement are the most important research concerns in weaving machinery. Increasing the effectiveness and productivity of production were achieved by increasing the operating time and efficiency of weaving looms. Thus, the manufacturers of weaving equipment attempt to minimize factors that limit production speed and production conditions. Heald frame is one of the known parts of the weaving machine that causes vibrations and noise which are important factors that influence high-speed development of looms. In this research work, study of mechanical factors (stresses and vibration) has been investigated for heald shaft. Finite element model of the heald frame was constructed to simulate different type of material. Then some important natural frequencies and vibration modes are calculated and the results. Results show a major improvement with the usage of these different material. As well as the failure of heald shaft is mainly due to friction and vibration and not due to the stresses or weight.*

Keywords: *heald frame, composite, carbon-fibre, glass-fibre, vibration, finite element, weaving machine*

1. INTRODUCTION

It is fundamentally a known fact that the heald frames move constantly in a vertical reciprocated movement in order to raise the warp yarns to provide the interlacing with weft yarns. The minimum number of heald frames is two. In case of complex weaving patterns, more heald frames are required [1]. Consequently, the shedding motion and warp tension are strongly influenced by the heald shaft's motion. Looms should be equipped with more heald frames and moving at high speed [2]. Vibration of the heald frame may causes breakage of yarns and reduces weaving efficiency that leads to limiting and reducing the speed of the loom. So, a lot of researches have been done to develop and improve the performance of the heald shaft. The design and development of heald frame mechanism was carried out in Air-jet weaving machine in order to save energy newly developed high-volume-low-pressure relay nozzles had been used also for very high operating speeds [3,7]. The dynamic force of the heald is less than the resultant forces influencing the heald. Under the influence of pulling the warp ends down ward, the heald changes its movement direction and moves in the direction of the carrying healds movement[4].

Composite material was proposed to be used in manufacturing the heald frame. Composite materials are formed by combining two or more materials so that they have better engineering properties than conventional materials, e.g., metals. Some of the properties that can be improved by forming a composite material are hardness, strength, weight reduction,

wear resistance, fatigue life and wear resistance. Composite materials are commonly formed in fibrous structure, which is made up of fibres and a resin as a matrix material [5,6].

Thus, the aim of this work is to compare between the traditional heald frame that is used in industry and a modified heald frame made of composite material to reduce the stresses and vibration on heald shaft using different materials on the performance of the loom using simulation software - ABAQUS platform [8].

2. MATERIALS

The material properties which were used in this study are illustrated in table 1 and table 2. As well all the measurements and experiments in this research were performed on air jet weaving machine heald shaft frame.

Table 1. Material properties used in traditional model

Material	Modulus of elasticity (MPa)	Poisson ratio	Density (tonne/mm ³)
Steel	210000	0.3	7.874 E-9
Aluminium	70000	0.34	2.7 E-9

Table 2. Material properties used in modified model

Material	Density	Modulus of elasticity			Poisson ratio			Shear modulus		
	(tonne/mm ³)	E1 (GPa)	E2 (GPa)	E3 (GPa)	γ_{12}	γ_{13}	γ_{32}	G12 (GPa)	G13 (GPa)	G23 (GPa)
Glass fibre composite	1.57778E-09	23.62	9.87	9.87	0.23	0.23	0.23	4.0	4.0	4.0
Carbon fibre composite	1.56E-09	136	11.9	11.9	0.29	0.29	0.4	4.86	4.86	4.4

3. FINITE ELEMENT MODEL (FEA) & METHODOLOGY

The modelling of the orthotropic materials was made using Abaqus CAE software to construct finite element model of the heald frame, the properties of materials used in structure of the old heald shaft frame as shown in table 1, the properties of materials used in structure of the new modelling of the heald shaft frame via Abaqus software is shown in table 2. Figure 1 illustrate the model of conventional heald shaft frame that is used in industry, with length of 2000 mm, height 550 mm and thickness 20mm. Assuming the motion of heald shaft frame is a simple harmonic motion with maximum displacement 80 mm and dwell period of 120 degree. Figure 2 illustrates the part meshing shape of heald shaft frame.

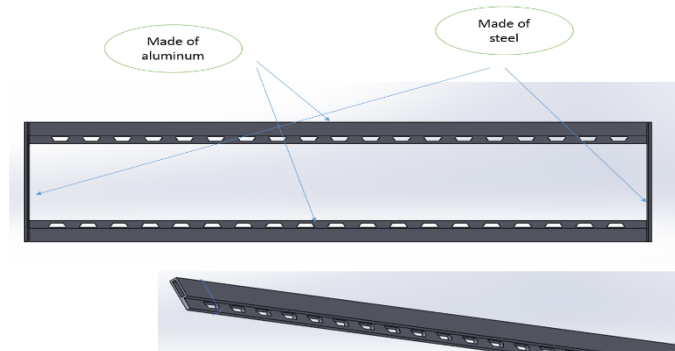


Figure 1. The model of conventional heald shaft frame

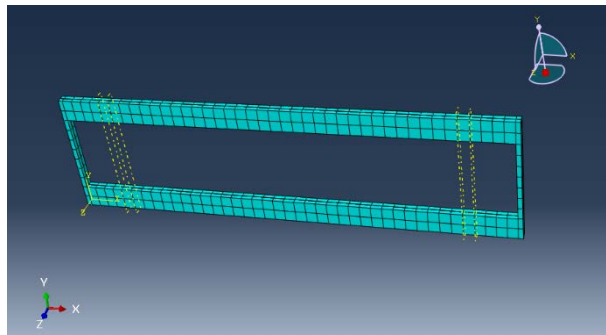


Figure 2. The part meshing shape of heald shaft frame

Figure 3. shows the arrangements of the various composite layup and the orientation of the fibres, the composite layup is shown for zero-degree, forty-five-degree, ninety-degree, forty-five-degree, zero-degree, forty-five-degree, ninety-degree, forty-five degree, and zero-degree. The model consists of nine laminae.

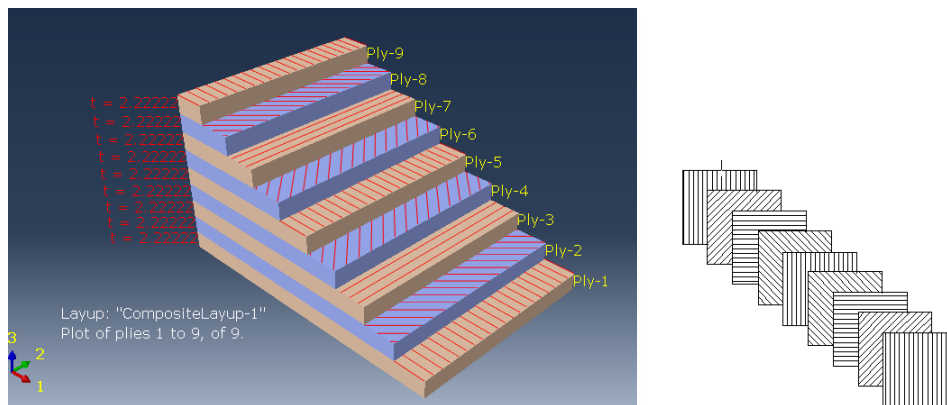


Figure 3. The arrangements of the various composite laminates

4. RESULTS

The following part enlightens the results obtained from the analysis of finite element design of heald frame.

4.1 Stresses

Figure 4 illustrates the stress analysis of the heald shaft made of aluminium alloy, the maximum stress obtained was 24.68 MPa concerted at the side edges of heald frame. Figure 5 shows the stresses analysis of the heald shaft made of glass fibre; the maximum stress obtained was 9.064 MPa concerted at the side edges of heald frame. Figure 6 displays the stresses analysis of the heald shaft made of carbon fibre, the maximum stress obtained was 7.78 MPa concerted at the upper middle part of heald frame. All the obtained results of the stresses were within the design factor of safety.

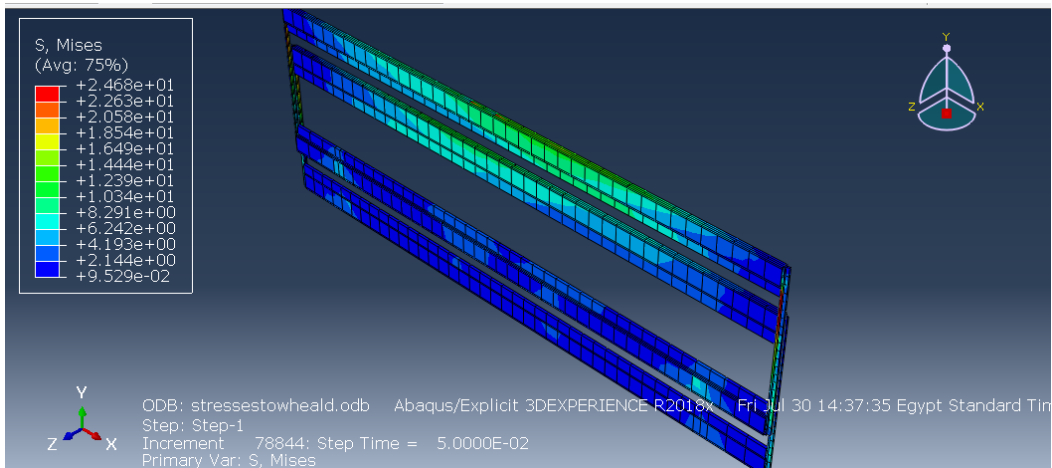


Figure 4. The maximum stress of heald shaft made of aluminium alloy

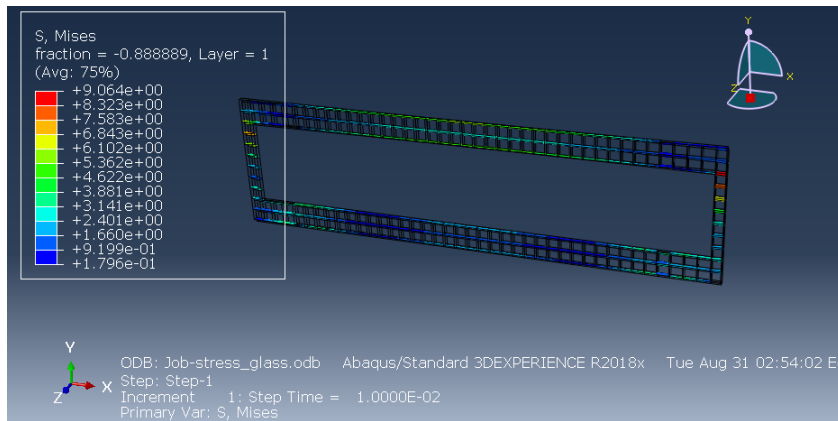


Figure 5. The maximum stress of heald shaft made of composite of glass-fibre

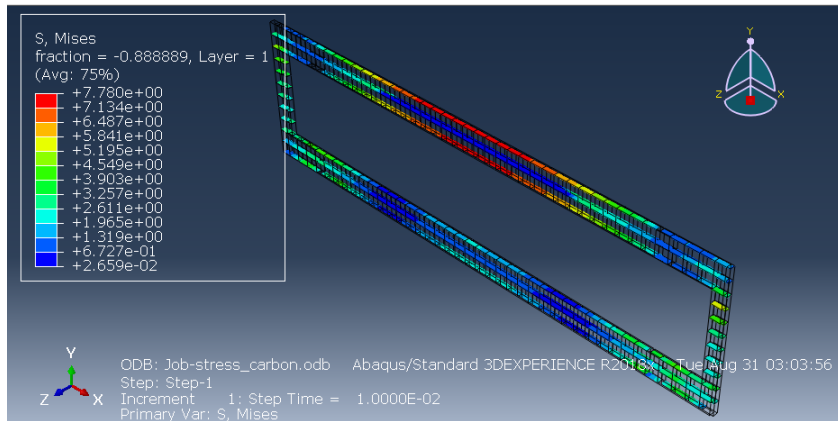


Figure 6. The maximum stress of heald shaft made of composite of carbon-fibre

4.2 Vibration

Figure 7 shows the natural frequency analysis of the heald shaft made of aluminium alloy; the natural frequency obtained was 14.76 Hz. Figure 8 illustrates the natural frequency analysis of the heald shaft made of glass fibre the natural frequency obtained was 9.064 Hz. Figure 9 demonstrates the natural frequency analysis of the heald shaft made of carbon fibre the natural frequency obtained was 7.78 Hz. Results show low frequency range for composite material which requires more research work.

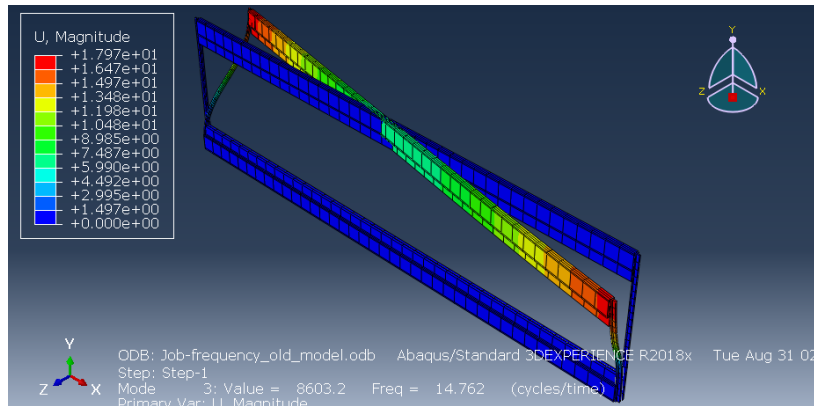


Figure 7. The Natural frequency of heald shaft made of aluminium alloy

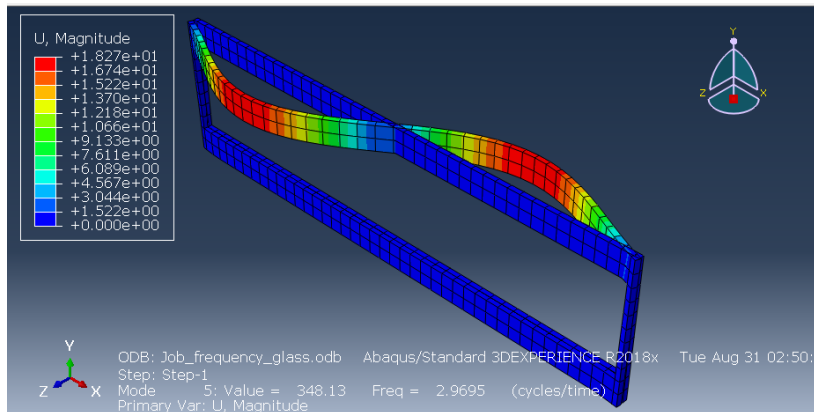


Figure 8. The Natural frequency of heald shaft made of Glass fibre composite

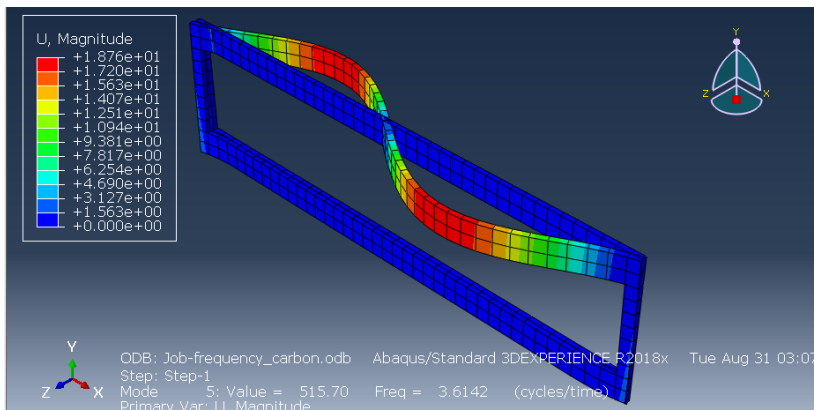


Figure 9. The Natural frequency of heald shaft which made of carbon fibre composite

Table 3 demonstrates the comparison between the results of traditional heald frame made of aluminium and the modified model made from glass and carbon composite material. Figure 10 presents the comparison of natural frequency between traditional heald shaft and modified model made from glass and carbon composite material. Figure 11 illustrates the comparison of stresses between traditional heald shaft and the modified model made from glass and carbon composite material.

Table 3. Natural frequency and the stresses of two type of models

Materials	Aluminium alloy	Glass fibre composite	Carbon fibre composite
Frequency (Hz)	14.76	2.96	3.61
Stresses (MPa)	24.68	9.064	7.78

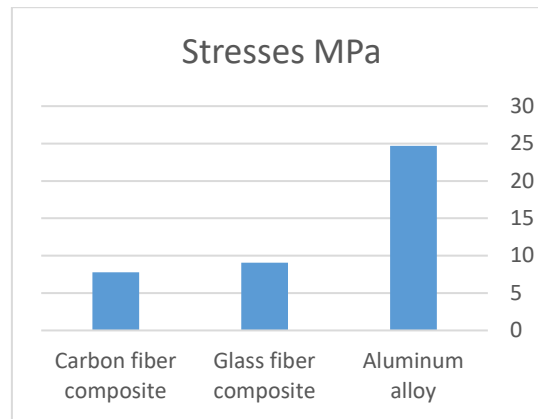


Fig. 10. The comparison of natural frequency

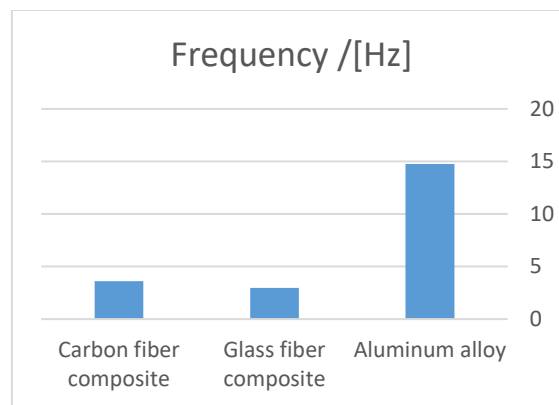


Fig. 11. The comparison of the stresses

As seen from figures 10 and 11, when the composite of carbon-fibre and the composite of glass-fibre were used as the material of heald frame, the natural frequency obviously decreased compared to aluminium alloy material. The smallest value makes fundamental frequency of heald frame decreased to 2.96 Hz. that is less than 11.8 Hz. of the aluminium alloy material, leading to the reduction of the loom's speed. Also, the stresses decreased obviously relative to aluminium alloy material.

5. CONCLUSIONS

The study estimates the dynamic nature of the movement of the heald shaft with relative to each other. For predicting low stresses, a computer program based on this model was developed. The finite element model of heald frame with composite of carbon-fibre and glass-fibre were constructed. The stresses obtained from the Abaqus is very low compare to the maximum load from yarn tension during operation case, therefore, the heald shaft is recommended to be made from another material. The composite model provided low cost and low strength, but the fundamental frequency of this method is decreased by 11.8 Hz to that of the heald frame with aluminium alloy. So, the vibration in working condition of looms is effectively decreased.

REFERENCES

- [1] Hall, A.J., *The Standard Hand book of Textiles*, 8th, 1975
- [2] Gokarneshana, N., Jegadeesan, N., Dhanapal, P., *Recent innovations in loom shedding mechanisms*, In: Indian Journal of Fibre & Textile Research, 2010, 35, 85-94

- [3] Koç, E., Çinçik, E., *Analysis of Energy Consumption in Woven Fabric*, In: Production. FIBRES & TEXTILES in Eastern Europe, 2010, 18, 2, 79, 14-20
- [4] Bilek, M., Kovář, S., Skřivánek, J., *Mathematical modelling of the heald shaft*, In: Autex Research Journal, DOI: 10.1515/aut-2015-0041
- [5] Rao, K.S., Mahendra, M., Aithal, K., *Study of Composite Glass Laminate Reinforced with Carbon Fiber at Cutout Locations*, In: American Journal of Materials Science, 2017, 7, 5, 170-173
- [6] Haifei, O., Songlin, W.Y.W., *The Study on Dynamic Characteristics for Heald Frame Designed by new Type Composite of Carbon-Fibre*, In: Advanced Materials Research, 2013, 804, 353-357
- [7] Schwarzfischer, F., Kurtenbach, S., Onischke, J., Corves, B., *Design and Development of a Heddle Shaft Mechanism for Air-Jet Weaving Machines*
- [8] Abaqus Cae, Available at: <https://edu.3ds.com/en/software/abaqus-student-edition> [Accessed on June 2021]



INTERACTION OF CLOTHING IN THERMOREGULATION IN THE CASE OF PRETERM INFANTS

DOI: 10.35530/TT.2021.12

V. Danila^{1*}, A. Curteza¹, S. Balan²

¹Technical University „Gheorghe Asachi” Iasi, Romania, Faculty of Industrial Design and Business Management, Iasi, Romania

(E-mail: victoriavasiledanila@gmail.com, acurteza@gmail.com)

²Technical University of Moldova, Faculty of Textile and Polygraphy, Department of Design and Technologies in Textile and Polygraphy, Chisinau, Republic of Moldova

(E-mail: stela.balan@adm.utm.md)

Abstract: *The paper presents a study about the thermoregulation in the case of premature babies and the importance and influence of their clothing in this complex process. The temperature of premature babies has to be between 36.5 - 37.5°C but, hypothermia (axillary temperature <36.5°C) is a common situation. This is primarily due to a large surface area and metabolic mass ratio that results in heat loss. Hypothermia among new-borns is considered an important contributor to neonatal morbidity and mortality. In this context, it has been identified that clothing products are recommended to maintain the optimal body temperature for those born prematurely. The elaborate clothing products aim at maintaining a thermal comfort and certain physiological indicators. Skin temperature and tactile sensations also play an important role in the growth and development of premature babies. In this regard, 15 premature infants were used as study subjects and their temperature profile was recorded. The proposed clothes aimed to maintain the baby's temperature in the normal range and provide a pleasant aesthetic appearance, while helping to improve the medical manipulations to which these children are subjected.*

Keywords: *body temperature, thermoregulation, clothing, comfort, premature babies*

1. INTRODUCTION

The World Health Organization (WHO) has recognized neonatal hypothermia as a contributing factor to the risk of morbidity and mortality in newborns. Hypothermia was defined by the WHO as body temperature below normal (36.5°C - 37.5°C) and was sub-classified into three grades: mild (36.0°C - 36.5°C), moderate (32.0°C - 35.9°C) and severe hypothermia (<32.0°C) [1]. For each of these classifications, there are guidelines in place to respond to or manage hypothermia [2]. Furthermore, the WHO has published guidelines on thermal care and has included thermal care for newborns as one of the essential elements of essential care for newborns (ENC) that should be provided to all newborns, regardless of how the temperature is taken [3].

The American Academy of Pediatrics (PAA) [4] and the American College of Obstetricians and Gynecologists (ACOG) (1997) [5] and the World Health Organization (WHO) [1] define normal axillary temperatures to be between 36.5°C and 37.5°C.

2. NEONATAL THERMOREGULATION

Hypothermia occurs when the axillary temperature of the newborn drops below 36.3°C [5] or below 36.5°C [1,4]. We highlight the following characteristics of preterm infants with a higher risk of heat loss:

- A high ratio between surface and body
- Decreased subcutaneous fat
- Higher water content for the body
- Immature skin that leads to increased water by evaporation and heat loss
- Poorly developed metabolic mechanism to respond to thermal stress (eg no tremors)
- Altered blood flow (eg peripheral cyanosis) [1,6-8].

Premature neonates are at an increased risk of developing hypothermia and are more vulnerable to cold stress than the term ones. The axillary temperature (figure 1) should be monitored within the first 30 minutes of life, and then every 1 hour, and should be maintained between 97.7°F and 99.5°F (36.5°C and 37.5°C) [9].

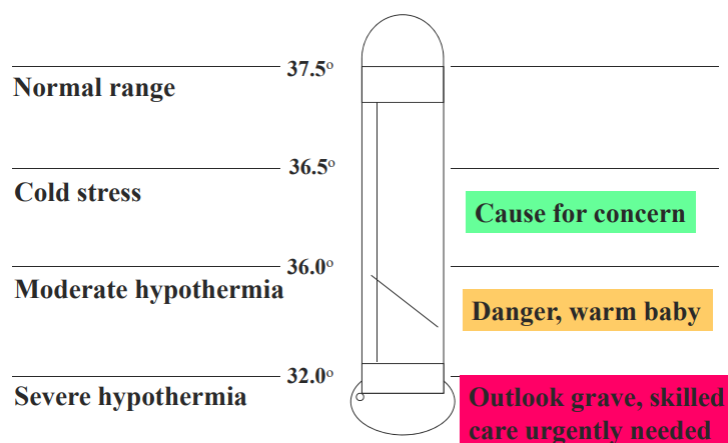


Figure 1. Newborn temperature (°C)

Early clinical signs which should arouse suspicion of cold stress due to hypothermia are: the feet are cold to the touch; weak sucking ability - inability to nurse; reduction in activity - lethargy; and a weak cry [10]. Thermoregulation is a biological priority for all homeothermic species [11]. New-borns, particularly preterm and low-birth weight (LBW) infants, have limited capacity for thermoregulation during the first weeks of life. The optimal environmental temperature is named thermal neutral temperature, at which metabolic requirements of the organism are minimal [12,13]. Both a decreased and an increased core temperature increase the metabolic rate of newborns, [13] who have only very limited ability to maintain a normal temperature and easily become hypothermic or hyperthermic (tables 1 and 2).

Table 1. Normal human body temperature and hypothermia [1]

Description	Range
Normal	36.5 - 37.5°C
Cold Stress Moderate	36.5 – 36°C
Hypothermia	36 – 32°C
Severe Hypothermia	< 32°C

Table 2. Risk factors of prematurity for hypothermia [14-16]

No.	Risk factors
1	Increased surface area to body mass ratio
2	Decreased subcutaneous and brown fat
3	Greater body water content
4	Increased evaporative water and heat losses due to immature skin barrier
5	Decreased body tone
6	Immature thermoregulatory system

Below we present ways to lose body heat: evaporation, conduction, convection and radiation (figure 2).

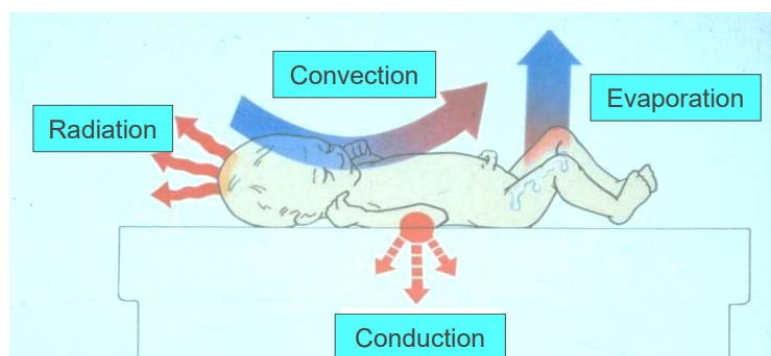


Figure 2. Ways of heat loss [13]

3. THERMAL SUPPORT OF MODERATELY PREMATURE NEONATES

From the above discussion one can realize the importance of providing thermal regulation that supports the immature structural and functional integrity of premature neonates. Thermal regulation is important because heat production requires oxygen consumption and energy use:

Persistent hypothermia (table 3) may deplete energy stores impairing weight gain. The following section will present the study of interventions that mainly reduce premature neonates heat lost by the four modes (table 2) and support the conservation of energy balance [17].

3.1. Measures to prevent hypothermia

The main measures that may prevent hypothermia include:

1. Increase the room/delivery room temperature $> 25^{\circ}\text{C}$ (77°F).
2. Use of radiant warmer for resuscitation if available.
3. Use of chemical warming mattress.
4. Use of occlusive/polyethylene wrap or large plastic bag (i.e. gallon size food grade storage bag) for neonates $< 28-30$ weeks' gestation.
5. Use of knit hat.
6. Neonates born at more than 32 weeks gestation may be placed skin-to-skin with mother, if stable.
7. To avoid burns, hot water bottles or gloves filled with hot water, to warm the neonate, are forbidden [18].

3.2. Materials and methods

The aim of this study was to maintain the warmth of premature and low birth weight babies, to improve infant state and to determine the safety and efficacy of designed clothing products. The study took place inside the Gh. Paladi or Chisinau hospital, where the medical histories of premature babies were studied. During the study were present medical sisters and doctors responsible for the given department. Premature babies were dressed in ordinary products and products of appropriate size (body and pants, socks, gloves, hat) were subsequently monitored to monitor body temperature. The time interval was 15 minutes at the first measurement of body temperature after every 30 minutes for 24 hours. The data were collected in subsequently processed documents.

Local reactions, if any, due to the texture and quality of the textile material that come in contact with the baby's skin, have also been closely monitored.

We observed 15 premature and low birth weight infants who were hospitalized in the NICU and were kept in an incubator or under radiant heating conditions. Each child's temperature started at 36.5°C - 37.5°C. These infants were constantly monitored for their temperature profile. The average weight of these infants was 1.65 kg, and the average gestational age was 34.75 weeks.

3.3. Results

The data of the study were collected in the form presented in table 4, which shows the values of body temperature of children dressed in different products. From the analysis of these data we conclude that children who have been dressed in morphometrically adapted products show an insignificant decrease in body temperature.

Table 3. Study sample

Time, min/no.	0	15	30	45	60	90	120	150	180	210
1	37	37.3	36.8	37.2	37	36.5	36.9	37	37.2	36.8
2	36.6	37.4	37.3	37.2	37	36.6	36.4	37.3	37.1	37
3	36.6	37.5	37.6	37.2	37	37.4	37	36.5	-	-
4	36.6	37.6	37.8	37.3	37.4	37.2	37.3	36.4	36.7	37
5	36.8	37.3	37.5	37.3	36.7	36.8	37	37.2	36.3	36.6
6	37.2	36.8	37.3	37.6	37.2	36.6	37	36.5	37.2	36.5
7	36.8	37	37.4	36.9	37	37	37.5	37	37.4	36.5
8	36.8	37.5	37.6	37.4	37	37.4	37	36.5	-	-
9	36.9	37.6	37.8	37.6	37.4	37.2	37.3	36.4	36.7	36.5
10	37	37.3	36.8	37.2	37	36.5	36.9	37	37.2	37
11	36.8	37.4	37.3	37.2	37	36.6	36.4	37.3	37.1	37
12	36.7	37.5	37.6	37.2	37	37.4	37	36.5	-	-
13	36.9	37.6	37.8	37.3	37.4	37.2	37.3	36.4	36.7	36.5
14	37	37.3	37.5	37.3	36.7	36.8	37	37.2	36.3	36.5
15	36.8	37.6	37.1	36.8	37.2	37	36.6	36.9	36.8	37

4. CLOTHING INFLUENCE ON THERMOREGULATION

Temperature regulation is an important function for homeothermic organisms, because body temperature ensures the balance of metabolic chemical reactions and its optimal overall state. The study [19] focused on aspects of thermoregulation at the birth of

VLBW (small children with birth weight), including epidermal water loss and temperature control, during stabilization and on admission to the neonatal intensive care unit.

Clothing plays an important role in this context. It is known that clothing products form a microenvironment, an insulating layer with properties to reduce the degree of heat loss by evaporation. The developed clothing products aim at increasing the thermal insulation, offering psychosensory and thermal comfort to the child. Therefore, one of the benefits of manufactured products is increased functionality and reduced heat loss.

We took also into consideration that advances in textile research have identified that thermoregulation can be improved through the use of materials with hygienic, aesthetic and physical-mechanical properties. The materials used to make these products were those with the fibrous composition of natural fibers (organic cotton, flax, lyocel). The materials have high hygienic properties, are soft and allow the exchange of heat and humidity with the environment.

In the development of the functional clothes (figure 3) some important aspects were taken into account, such as:

- infants have a large body surface area in relation to their weight;
- the ratio between surface and body weight is two to three times higher than in adults;
- the head of an infant is large regarding the proportion of the body;
- in the case of newborns, up to 75% of the body heat loss may be from an uncovered head;
- premature and low birth weight babies have less subcutaneous fat for insulation and thus lose heat more easily;
- because babies do not have body fat, they cannot regulate their body temperature; prolonged exposure to environmental factors outside the incubator cools babies' bodies.

The given products are qualitative; they correspond to all the clothing requirements for premature babies, which take into account their degree of development and needs, in order to allow them an easy and comfortable growth. Thus we satisfy the mothers and the medical staff with hygienic, aesthetic products and adequate given situation.



Figure 3. Functional clothes for premature babies

The shape of the product is obtained by winding, the closing system is on the upper and inner edges, with buttons, and has no contact with the child's body, and the product has holes for: head, upper and lower limbs.

Thermal comfort is ensured by the constructive and technological solution proposed for premature babies. The anthropomorphological adaptation of the products to the requirements and needs of premature babies for static and dynamic positions, offers the possibility to provide medical help in a short time.

5. CONCLUSION

The proposed solution is one of the strategies applied in order to increase the efforts of medical institutions as well as of parents whose final goal is to improve the chances of survival and rehabilitation of preterm babies.

Particularities of the premature child's physical development, including the thermoregulation system, determine the hygienic and thermal insulation requirements imposed on clothing products.

This specific problem is behind ongoing efforts to find solutions to eliminate hypothermia in the case of premature infants. One of the issues addressed is the use of appropriate clothing products for premature babies. The products offer thermal insulation and convenience when performing various medical movements and manipulations.

REFERENCES

- [1] World Health Organization, *Thermal protection of the newborn: A practical guide*, Geneva, 1997, Report No.: WHO/RHT/MSM/97.2
- [2] World Health Organization, *Pregnancy, childbirth, postpartum, and neonatal care: A guide for essential practice*, Geneva, 2007
- [3] World Health Organization, *Essential newborn care*, 1996, Report No.: WHO/FRH/MSM/96.13
- [4] American Academy of Pediatrics (AAP), Available at: www.aap.org [Accessed on June 2021]
- [5] American Academy of Pediatrics & American College of Obstetricians and Gynecologists, , *Acute care of at-risk newborns: A resource and learning tool for health care professionals*, ACoRN Editorial Board, Vancouver, 2012
- [6] Blackburn, S.T., *Maternal, fetal, & neonatal physiology: A clinical perspective*, 3rd ed., St. Louis: Saunders Elsevier, 2007
- [7] Hackman, P., *Recognizing and understanding the cold-stressed term infant*, In: Neonatal Network, 2001, 20, 8, 35-41
- [8] Galligan, M., *Proposed guidelines for skin-to-skin treatment of neonatal hypothermia*, In: American Journal of Maternal/Child Nursing, 2006, 31, 5, 298-304
- [9] Pejaver, Dr. Ranjan K., *Interview on Infant Hypothermia*, Personal interview, June-July, 2012
- [10] World Health Organization, *Thermal control of the newborn: a practical guide*, 1993, Available at: <https://apps.who.int/iris/handle/10665/60042> [accessed on June 2021]
- [11] Hey, E., *Thermal neutrality*, In: Br Med Bull, 1975, 31, 69-74
- [12] Baumgart, S., *Iatrogenic hyperthermia and hypothermia in the neonate*, In: Clin Perinatol, 2008, 35, 183-197, ix-x
- [13] Sherman, T.I., Greenspan, J.S., St. Clair, N., Touch, S.M., Shaffer, T.H., *Optimizing the neonatal thermal environment*, In: Neonatal Newt, 2006, 25, 251-260
- [14] Aylott, M., *The neonatal energy triangle. Part2: Thermoregulatory and respiratory adaption*, In: Paediatric Nursing, 2006, 18, 7, 38-42
- [15] Knobel, R., Holditch-Davis, D., *Thermoregulation and heat loss prevention after birth and during neonatal intensive-care unit stabilization of extremely low-birthweight infants*, In: Journal of Obstetric, Gynecologic, and Neonatal Nursing: JOGNN / NAACOG, 2007, 36, 3, 280-287
- [16] Sedin, G., Agren, J., *Water and heat--the priority for the newborn infant*, In: Upsala Journal of Medical Sciences, 2006, 111, 1, 45-59
- [17] Lewis, L.A., *Nursing care procedures, thermal regulation and growth of the moderately premature neonate in the neonatal intensive care unit*, Kent State University College of Nursing, Dissertation thesis, 2014, 128
- [18] *Illinois ESF-8 Plan: Paediatric and Neonatal Surge Annex Paediatric and Neonatal Care Guidelines*, 2017, June

[19] Danila, V., Curteza, A., *Thermoregulatory clothes for premature babies: effectiveness and risks*, In: Proceedings 17th Romanian Textiles and Leather Conference – CORTEP 2018, Iasi, 7-9 November 2018, ISSN-L 2285-5378, 95-100



ACTIVE PRINCIPLES APPLIED ON BIOMATERIALS FOR THE CURATIVE THERAPY OF INFLAMMATORY SKIN DISEASES - A REVIEW

DOI: 10.35530/TT.2021.04

A. Țigău*, G. Vasile, L. Chirilă, A. Popescu, S. Olaru

National Research & Development Institute for Textiles and Leather, Bucharest, Romania
(E-mail: andreea.tigau@incdtp.ro, georgiana.vasile@incdtp.ro,
laura.chirila@incdtp.ro, alina.popescu@incdtp.ro, sabina.olaru@incdtp.ro)

Abstract: Every year, millions of peoples are affected by skin injuries of either an acute or chronic nature. Worldwide 300,000 people die every year in lower-middle-income countries due to chronic wounds and burn injuries. Wounds are described as the disruption in the skin integrity and function, which arises from different causes such as trauma, surgery, diabetes, and burns. Skin provides a mechanical barrier against the external environment and has further roles in thermoregulation, metabolism and regulation of fluid balance. Skin diseases can affect each of these regions and they can be influenced by body size, sex, age, medications, diet, and microenvironment. Also, they can manifest whether the skin is healthy or diseased. Wound dressings are critical to wound care, providing a physical barrier between the wound and the external environment to prevent further damage or infection. The most promising wound dressings are biocompatible, enable physical protection of the wound milieu against penetration of bacteria and are highly porous. The use of natural biocompatible drugs is highly desirable in wound dressing compared to synthetic chemicals. To achieve an adequate therapeutic effect, different polymeric systems are used for drug delivery. To improve drug efficacy, safety, patient compliance and convenience a drug delivery system is modified to enhance drug release profile, absorption, distribution and elimination of the drug. The present review is an attempt to brief readers about the engineering of wound dressing materials from natural and synthetic sources upfront using active principles, such as bee products, drugs, essential oils, metallic nanoparticles and vitamins.

Keywords: drug delivery; essential oils; hydrogels; metallic nanoparticles; wound dressings

1. INTRODUCTION

The skin is the largest organ in the human body. It accounts for about 15% of the total body weight of an adult and has a surface area of 1.5-2 m² and it plays an important role in continuously maintaining life [1,2].

Wound healing is a dynamic process that comprises a synchronized effort by a multitude of biological pathways and is generally divided into multiple phases such as swelling, angiogenesis, proliferation and final development [3].

Bacterial wound infection delays wound healing and may lead to life-threatening complications. Human skin is colonized by trillions of microorganisms, referred to as the skin microbiome. Breakdown of the symbiotic relationship between the human host and microbiome can contribute to the pathogenesis of many skin diseases, including atopic dermatitis, psoriasis and acne [2,4].

Bacterial infection during the wound healing process is also a common challenge, resulting in hard-to-heal or chronic wounds. Up to now, different materials with antibacterial properties have been reported for wound dressing application, such as biopolymers (chitosan, ϵ -polylysine, alginate, xanthan, gelatine, etc.), metallic particles (ZnO, Ag, etc.), essential oils, and so forth [5].

The development of wound dressings has partly improved the effect of wound management. There is an urgent need to develop a new type of wound dressing with comprehensive performance to achieve multiple effects such as protecting the wound site from the external environment, absorbing wound exudate, anti-inflammatory, antibacterial, and accelerating the wound healing process [6].

2. GENERAL INFORMATION

2.1. Structure and function of the skin

Structurally, the skin is divided into three distinct layers (figure 1.):

- **Epidermis:** The epidermal layer is the outermost layer and is populated mostly by keratinocytes and it is responsible for skin colour, texture, and moisture.
- **Dermis:** The dermis is composed of a thin, looser papillary dermis and a thicker, denser reticular dermis and it is responsible for the regional variation in skin thickness. It is composed primarily of collagen, but also contains elastin, blood vessels, nerves, and sweat glands [7].
- **Subcutaneous layer:** The subcutaneous tissue is made of fat and connective tissue [8].

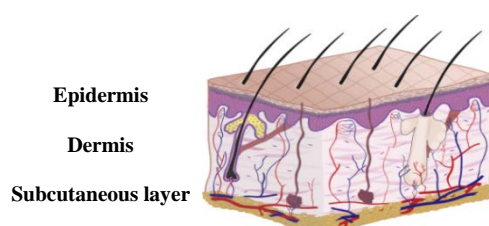


Figure 1. An illustration of the skin anatomy [9]

Some of the crucial functions of the skin are listed below:

- Skin provides a physical barrier against the external environment and helps to reduce water loss through the water-impermeable stratum corneum.
- The skin is important for thermoregulation
- Skin contributes to innate and adaptive immunity. Keratinocyte-derived endogenous antimicrobial peptides are active against a variety of bacteria, viruses and fungi.
- The skin is important for sensory perception because of its rich supply of free nerve endings and end-corpules.
- Subcutaneous fat is important in cushioning trauma and providing insulation.
- Skin is important for the synthesis of vitamin D (bone formation, calcium metabolism and aspects of immune regulation) [2].

2.2. Wound dressings

Skin wound dressings are a crucial segment of the wound care industry and trade worldwide.

The wound dressings currently available in the market are typically in the form of hydrogels, films, sponges, and foams. As a relatively new class of wound dressing materials, nanofibers have emerged that offer distinct advantages [10].

A favourable wound dressing must prevent the wound from infection, provide adequate moisture, eliminate wound exudates, and encourage further tissue restoration. Accelerating the recovery rate of a tissue injury with minor scarring and the highest regeneration is the primary goal of wound healing [11].

The ideal wound dressing material is biocompatible, moisture-retaining, gas permeable, adequate as a barrier against dust and microorganisms, and non-adhesive so that it can be removed easily with no trauma [4].

3. HEALING PROCESS

The wound healing process is regulated by complex molecular mechanisms and is susceptible to interruption by many factors, such as size, depth, origin, and level of contamination [6].

Traditionally, wound healing processes have been divided into four overlapping phases of hemostasis, inflammation, proliferation, and remodelling. Wound healing represents a very complex process that requires a long time to be complete, as the remodelling phase to form the proper environment can last from 21 days to 1 year [1,12].

4. ACTIVE PRINCIPLES

There are many antibacterial agents available to cure infections, but the systemic use of antibacterial agents is not only less effective to manage skin infection but also causes of increasing microbial resistance. Encapsulation of bioactive compounds, for antibacterial activity, has been remained a hot topic since the last decade. These compounds are both synthetic and natural. Encapsulation of bioactive compounds is a possible strategy to increase the physical stability of the active substances [13,14].

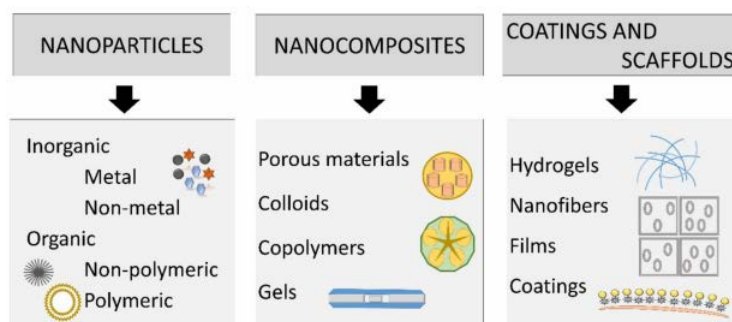


Figure 3. Main types of nanomaterials can be used for wound treatment [12]

4.1. Vitamins

Recently, the target delivery of vitamins has gained increased interest for wound-dressing applications [15].

Vitamin C is a well-known natural antioxidant involved in all phases of wound healing, mainly in the collagen formation phase. This vitamin is extensively used for the prevention of colds and bacterial and viral illnesses [16].

Vitamin A and E can increase collagen deposition in the repair zone of a wound.

However, they suffer from stability issues. Thus, derivatives have been developed: Vitamin A palmitate is a lipid-soluble substance used for the treatment of skin diseases and offers greater stability than vitamin A [17].

Recent studies reported that Vitamin E can significantly contribute to the healing of wounds, through diverse mechanisms such as protection of biological membranes against lipid peroxidation, antioxidant and anti-inflammatory activities [15].

Vitamin D3 (1, 25-dihydroxy vitamin D3), is one of the most effective therapeutic agents which has fascinating impacts on the skin wound healing process [18].

4.2. Drugs

Infections provoke tissue necrosis, subsequently delay the healing process and extend the healing period with dramatic consequences for the patient. Even though polymers have outstanding cytocompatibility, their antibacterial characteristics are unsatisfactory in preventing infections. Infected wounds request the use of antibacterial dressings to eradicate bacterial colonization in order to allow the beginning of the healing process. As necrotic tissues are poorly irrigated, local treatments give better results than systemic administration [19,20].

Table 1. Different types of drugs used in the synthesis of wound dressings

Active principle	Matrix	Wounds	Highlights
Heparin	PLGA/ Curcumin nanofiber membrane	Diabetic wound healing	Accelerates wound closure by promoting re-epithelization, angiogenesis and collagen deposition [21]
Chlorhexidine	PET/ Chitosan	All types (antiseptic)	Antibacterial activity against <i>S. aureus</i> up to 30 days [19]
Bacitracin	Poly-3-hydroxybutyric acid/ Alginate	Dermal reconstruction	Good in vitro biocompatibility, cell proliferation and antimicrobial activity [22]
Gentamicin	Chitosan/ Alginate nanofiber	Skin regeneration	High antibacterial performance [20]

4.3. Bee products

Honey is an ancient therapeutic nutrition that also shows remarkable antimicrobial, anti-inflammatory and antioxidant performance, thanks to its acidic nature. Conventionally, honey has been applied to treating burns, non-healing and infected ulcers and wounds, pilonidal sinus, venous and diabetic foot boils [10].

Propolis extract, another bee product can be combined with different polymers and used for bone tissue engineering and wound dressing applications. In the study made by Ceylan (2021) was proved that propolis incorporation into membranes based on PVA/chitosan significantly promoted cell proliferation and adhesion. Water uptake and contact angle measurements showed that water uptake capacity and hydrophilicity are increasing with propolis concentration [23].

All types of propolis have antibacterial properties. Veiga et al. (2017) reported that poplar propolis has antibacterial effects against both Gram-positive and Gram-negative microorganisms including multidrug-resistant bacteria such as MRSA.

Honey samples and aqueous propolis extracts have antimicrobial activity against the *S. aureus*, *P. aeruginosa*, *E. coli*, *B. cereus*, and *C. albicans* strains [24].

4.4. Metallic nanoparticles

Researches have shown that metal and metal oxide nanoparticles provide broad

antimicrobial activities.

Silver nanoparticles (Ag-NPs) are among the most effective and investigated nanoparticles that have been shown to be effective against multidrug-resistant bacteria. However, researches have demonstrated that a high concentration of Ag-NPs could be cytotoxic to human cells due to the uptake of Ag-NPs by cells and/or reactive oxygen species (ROS) related to oxidative stress [25].

ZnO on a nano-scale presented higher antibacterial behaviour because of the higher amount of zinc ions on the surface for improving re-epithelialization, reducing inflammation and bacterial growth [26].

Table 2. Different types of wound dressings based on metallic nanoparticles

Metallic nanoparticle	Matrix	Name of materials	Highlights
Ag NPs	Nanofibrous matrices and Scaffolds	Silk fibroin /Ag NPs	Antibacterial [4]
	Gum	Persian gum/ Ag NPs	High bacterial efficiency against both gram-positive <i>S. aureus</i> and gram-negative <i>P. aeruginosa</i> [25]
TiO ₂ NPs	Nanofibrous matrices and Scaffolds	Silk fibroin /TiO ₂	Antibacterial activity demonstrated against <i>E. coli</i> bacteria under UV light [27]
	Hydrogels	PVA/SA/TiO ₂ -CUR	Exceptional wound healing ability by restricting bacterial growth and enhancing tissue regeneration [28]
ZnO	Bi-layered hydrogel films	Sodium alginate/ZnO	Good antibacterial properties and no significant cytotoxicity [29]
	Hydrogels	PVA/Chitosan/ZnO	Biocompatible and nontoxic, and were significantly able to protect the wounds against microorganisms [30]
	Hydrogel	Silk fibroin /ZnO	Significant antibacterial property; adherence, growth, and proliferation of the fibroblast cells [31]

4.5. Essential oils

Essential oils, also called volatile natural mixtures, are plant secondary metabolites that exhibit antioxidant, antiviral, anticancer, insecticidal, anti-inflammatory, anti-allergic and antimicrobial properties. The plant essential oils destroy the cytoplasmic membrane of bacteria through demolishing the cell membrane and inducing coagulation in bacteria cell matters, but they can be rapidly decomposed under inappropriate conditions of heat, humidity, light, oxygen, and so forth [14, 32].

Table 3. Different types of wound dressings based on essential oils

Essential oil	Matrix	Highlights
Tea tree	Hydrogel	Significant antiedematogenic and wound healing effect [33]
Oregano	PLCL/Silk fibroin	Excellent antibacterial activity [13]
Clove	Wax	A good inhibition of the butyryl and acetylcholinesterase enzymes [34]
Cinnamon	Emulsion	Effective against <i>E. coli</i> growth and <i>C. albicans</i> [35]
Peppermint	Emulsion	Effective against <i>E. coli</i> growth and <i>C. albicans</i> [35]
Lemongrass	Emulsion	Effective against <i>E. coli</i> growth and <i>C. albicans</i> [35]

5. CONTROLLED DRUG RELEASE

Drug delivery devices are promising tools in the pharmaceutical field, as they are able to maximize the therapeutic effects of the delivered drug while minimizing the undesired side effects [36].

A formulation that will provide a continuous discharge of its active agent at a fixed rate for a predetermined time sums up as a controlled release dosage. It had begun with the oral administration but recently found its place in parenteral administration, ocular insertion and transdermal application too [37].

Advanced wound dressings are divided into seven categories: semi-permeable films, semipermeable foam dressings, hydrogel dressings, hydrocolloid dressings, alginate dressings, non-adherent contact layer dressings, and multilayer dressings [12].

As the matrix, hydrogels provide a convenient delivery platform for the controlled release of loaded drugs, growth factors, cytokines, and even cells [38].

The types of wounds that may heal faster-using hydrogel wound dressing include:

- Hydrogel wound dressing provides a soothing effect in order to alleviate excruciating pain and tenderness of the skin in minor burns.
- Hydrogel provides sufficient hydration to help with skin moisture retention and provide effective healing in dry wounds.
- Applying hydrogel wound dressing for depressed wounds will likely improve tissue growth and minimize the risk of having a healed but dented wound site.
- Hydrogel wound dressing promotes faster healing since it does not stick or allow necrotic tissue to slough off during healing [6].

6. CONCLUSIONS

This review briefly presents the wound healing process, wound dressing function and introduces different dressings fabricated using biopolymers (chitosan, poly(lactic-co-glycolic acid), polyethylene glycol, alginate, xanthan, gelatine, etc.) functionalized with active principles (bee products, drugs, essential oils, metallic nanoparticles, and vitamins).

With the advent of new technologies, a wide range of antimicrobial/antibacterial textile products is now available for the benefit of medicinal applications. The development of new biocompatible and biodegradable nanomaterials, which are capable of regulating all phases of wound healing, incorporate antibacterial properties and have self-healing and excellent mechanical properties, is an essential and increasing issue worldwide.

ACKNOWLEDGEMENTS

This work was carried out through the Nucleu Programme, with the support of MEC, project no. 4N/08.02.2019, PN 19 17 03 01, project title: “Multifunctional integrated systems based on nanocomposites and pharmacodynamic therapeutic agents for different skin conditions – BIOPANTEX”.

REFERENCES

- [1] Zhang, M., Zhao, X., *Alginate hydrogel dressings for advanced wound management*, In: Int. J. Biol. Macromol., 2020, 1, 162, 1414-1428, <https://doi.org/10.1016/j.ijbiomac.2020.07.311>
- [2] Lai-Cheong, J.E., Mcgrath, J.A., *Structure and function of skin, hair and nails*. In: Medicine, 2021, <https://doi.org/10.1016/j.mpmed.2021.03.001>

- [3] Ullah, S., et al., *An update on stem cells applications in burn wound healing*, In: *Tissue Cell*, 2021, 101527, <https://doi.org/10.1016/j.tice.2021.101527>
- [4] Patil, P.P., Reagan, M.R., Bohara, R.A., *Silk fibroin and silk-based biomaterial derivatives for ideal wound dressings*, In: *Int. J. Biol. Macromol.*, 2020, 1, 164, 4613-4627, <https://doi.org/10.1016/j.ijbiomac.2020.08.041>
- [5] Ling, Z., et al., *A novel self-healing polydopamine-functionalized chitosan-arginine hydrogel with enhanced angiogenic and antibacterial activities for accelerating skin wound healing*, In: *Chem. Eng. Sci.*, 2021, 130302, <https://doi.org/10.1016/j.ces.2021.130302>
- [6] Zeng, D., Shen, S., Fan, D., *Molecular design, synthesis strategies and recent advances of hydrogels for wound dressing applications*, In: *Chin. J. Chem. Eng.*, 2021, 30, 308-320, <https://doi.org/10.1016/j.cjche.2020.12.005>
- [7] William, D.L., *Anatomy of the Skin and the Pathogenesis of Nonmelanoma Skin Cancer*, In: *Facial. Plast. Surg. Clin. North. Am.*, 2017, 25, 3, 283-289, <http://doi.org/10.1016/j.fsc.2017.03.001>
- [8] Onishi, H., Machida, Y., Santhini, E., Vadodaria, K., *8 – Novel textiles in managing burns and other chronic wounds*, Editor(s): Rajendran, S., In: *The Textile Institute Book Series, Advanced Textiles for Wound Care (Second Edition)*, Woodhead Publishing, 2019, 211-260
- [9] Chin, J. S., et al., *Drug therapies and delivery mechanisms to treat perturbed skin wound healing*, In: *Adv. Drug Deliv. Rev.*, 2019, 149, 2-18, <http://doi.org/10.1016/j.addr.2019.03.006>
- [10] Homaeigohar, S., Boccaccini, A.R., *Antibacterial biohybrid nanofibers for wound dressings*, In: *Acta Biomater.*, 2020, 107, 25-49, <http://doi.org/10.1016/j.actbio.2020.02.022>
- [11] Hemmatgir, F., Koupaei, N., Poorazizi, E., *Characterization of a Novel Semi-interpenetrating Hydrogel Network Fabricated by Polyethylene Glycol Diacrylate/Polyvinyl Alcohol/Tragacanth Gum as a Wound Dressing*, In: *Burns*, 2021, <https://doi.org/10.1016/j.burns.2021.04.025>
- [12] Stoica, A.E., Chircov, C., Grumezescu, A.M., *Nanomaterials for Wound Dressings: An Up-to-Date Overview*, In: *Molecules*, 2020, 25, 11, 2699, <http://doi.org/10.3390/molecules25112699>
- [13] Huang, K., et al., *PLCL/Silk fibroin based antibacterial nano wound dressing encapsulating oregano essential oil: Fabrication, characterization and biological evaluation*, In: *Colloids Surf. B Biointerfaces*, 2020, 196, 111352, <http://doi.org/10.1016/j.colsurfb.2020.111352>
- [14] Farahpour, M.R., et al., *Effectiveness of topical caraway essential oil loaded into nanostructured lipid carrier as a promising platform for the treatment of infected wounds*, In: *Colloids Surf. A Physicochem. Eng. Asp.*, 2021, 610, 125748, <http://doi.org/10.1016/j.colsurfa.2020.125748>
- [15] Cerchiara, T., et al., *New spanish broom dressings based on vitamin E and Lactobacillus plantarum for superficial skin wounds*, In: *J. Drug Deliv. Sci. Technol.*, 2020, 56, 101499, <http://doi.org/10.1016/j.jddst.2020.101499>
- [16] Voss, G.T., et al., *Polysaccharide-based film loaded with vitamin C and propolis: A promising device to accelerate diabetic wound healing*, In: *Int. J. Pharm.*, 2018, 552, 1-2, 340-351, <http://doi.org/10.1016/j.ijpharm.2018.10.009>
- [17] Wang, L.H., Williams, M., Wu, G.R., et al., *Electrospun gelatin nanofibers loaded with vitamins A and E as antibacterial wound dressing materials*, In: *RSC Adv.*, 2016, 6, 55, 50267–50277, <https://doi.org/10.1039/C6RA05092A>
- [18] Ehterami, A., et al., *A promising wound dressing based on alginate hydrogels containing vitamin D3 cross-linked by calcium carbonate/d-glucono- δ -lactone*, In: *Biomed. Eng. Lett.*, 2020, 1-11, <https://doi.org/10.1007/s13534-020-00155-8>
- [19] Aubert-Viard, F., et al., *Evaluation of antibacterial textile covered by layer-by-layer coating and loaded with chlorhexidine for wound dressing application*, In: *Mater. Sci. Eng. C.*, 2019, 100, 554-563, <http://doi.org/10.1016/j.msec.2019.03.044>
- [20] Bakhsheshi-Rad, H.R., et al., *In vitro and in vivo evaluation of chitosan-alginate/gentamicin wound dressing nanofibrous with high antibacterial performance*, In: *Polym. Test.*, 2020, 82, 106298, <http://doi.org/10.1016/j.polymertesting.2019.106298>

- [21] Liao, H.T., et al., *A bioactive multi-functional heparin-grafted aligned poly (lactide-co-glycolide)/curcumin nanofiber membrane to accelerate diabetic wound healing*, In: Mater. Sci. Eng. C., 2021, 120, 111689, <http://doi.org/10.1016/j.msec.2020.111689>
- [22] Shiny, P.J., et al., *In vitro and in vivo evaluation of poly-3-hydroxybutyric acid-sodium alginate as a core-shell nanofibrous matrix with arginine and bacitracin-nanoclay complex for dermal reconstruction of excision wound*, In: Int. J. Biol. Macromol., 2021, 168, 46-58, <http://doi.org/10.1016/j.ijbiomac.2020.12.025>
- [23] Ceylan, S., *Propolis loaded and genipin-crosslinked PVA/chitosan membranes; characterization properties and cytocompatibility/genotoxicity response for wound dressing applications*, In: Int. J. Biol. Macromol., 2021, 30, 181, 1196-1206, <https://doi.org/10.1016/j.ijbiomac.2021.05.069>
- [24] Vică, M.L., et al., *The antimicrobial activity of honey and propolis extracts from the central region of Romania*, In: Food Biosci., 2021, 41, 101014, <http://doi.org/10.1016/j.fbio.2021.101014>
- [25] Amirsadeghi, A., et al., *Sprayable antibacterial Persian gum-silver nanoparticle dressing for wound healing acceleration*, In: Mater. Today Commun., 2021, 27, 102225, <https://doi.org/10.1016/j.mtcomm.2021.102225>
- [26] Ghiyasi, Y., Salahi, E., Esfahani, H., *Synergy effect of Urtica dioica and ZnO NPs on microstructure, antibacterial activity and cytotoxicity of electrospun PCL scaffold for wound dressing application*, In: Mater. Today Commun., 2021, 26, 102163, <http://doi.org/10.1016/j.mtcomm.2021.102163>
- [27] Jao, W., et al., *Fabrication and characterization of electrospun silk fibroin/TiO₂ nanofibrous mats for wound dressings*, In: Polym. Adv. Technol., 2012, 23, 7, 1066-1076, <https://doi.org/10.1002/pat.2014>
- [28] Niranjana, R., et al., *PVA/SA/TiO₂-CUR patch for enhanced wound healing application: In vitro and in vivo analysis*, In: Int. J. Biol. Macromol., 2019, 138, 704-717, <http://doi.org/10.1016/j.ijbiomac.2019.07.125>
- [29] Wang, T., Wang, J., Wang, R., Yuan, P., Fan, Z., Yang, S., *Preparation and property of ZnO/sodium alginate bi-layered hydrogel films as novel wound dressings*, In: New J. Chem., 2019, <https://doi.org/10.1039/c9nj00402e>
- [30] Khorasani, M.T., et al., *Design and optimization of process parameters of polyvinyl (alcohol)/chitosan/nano zinc oxide hydrogels as wound healing materials*, In: Carbohydr. Polym., 2019, 207, 542-554, <http://doi.org/10.1016/j.carbpol.2018.12.021>
- [31] Majumder, S., Ranjan Dahiya, U., Yadav, S., Sharma, P., Ghosh, D., Rao, G.K., et al., *Zinc Oxide Nanoparticles Functionalized on Hydrogel Grafted Silk Fibroin Fabrics as Efficient Composite Dressing*, In: Biomolecules, 2020, 10, 5, 710, <http://doi.org/10.3390/biom10050710>
- [32] Simões, D., Miguel, S.P., Ribeiro, M.P., Coutinho, P., Mendonça, A.G., Correia, I.J., *Recent advances on antimicrobial wound dressing: A review*, In: Eur. J. Pharm. Biopharm., 2018, 127, 130-141, <http://doi.org/10.1016/j.ejpb.2018.02.022>
- [33] Flores, F.C., et al., *Hydrogels containing nanocapsules and nanoemulsions of tea tree oil provide antiedematogenic effect and improved skin wound healing*, In: J. Nanosci. Nanotechnol., 2015, 15, 1, 800-809, <http://doi.org/10.1166/jnn.2015.9176>
- [34] De Meneses, A.C., et al., *Encapsulation of clove oil in nanostructured lipid carriers from natural waxes: Preparation, characterization and in vitro evaluation of the cholinesterase enzymes*, In: Colloids Surf. A Physicochem. Eng., 2019, 583, 123879, <https://doi.org/10.1016/j.colsurfa.2019.123879>
- [35] Liakos, I., et al., *All-natural composite wound dressing films of essential oils encapsulated in sodium alginate with antimicrobial properties*, In: Int. J. Pharm., 2014, 463, 2, 137-145, <http://doi.org/10.1016/j.ijpharm.2013.10.046>
- [36] Luraghi, A., Peri, F., Moroni, L., *Electrospinning for drug delivery applications: A review*, In: J. Control Release, 2021, 334, 463-484, <https://doi.org/10.1016/j.jconrel.2021.03.033>
- [37] George, B., Suchithra, T.V., *Plant-derived bioadhesives for wound dressing and drug delivery system*, In: Fitoterapia, 2019, 137, 104241, <http://doi.org/10.1016/j.fitote.2019.104241>

[38] Cheng, H., et al., *Sprayable hydrogel dressing accelerates wound healing with combined reactive oxygen species-scavenging and antibacterial abilities*, In: Acta Biomater., 2021, 124, 219-232, <http://doi.org/10.1016/j.actbio.2021.02.002>



THEORETICAL CONSIDERATIONS REGARDING VIRTUAL METHODS TO OBTAIN THE GARMENT PROTOTYPE (2D/3D AND 3D/2D)

DOI: 10.35530/TT.2021.47

M. Avadanei^{1*}, A. Talpa², A. Curteza¹, D. Viziteu¹, I. Dulgheriu¹

¹Faculty of Industrial Design and Business Management, “Gheorghe Asachi” Technical University of Iasi-Romania
(E-mail: mavad@tex.tuiasi.ro, acurteza@gmail.com, viziteudianaroxana@gmail.com, ionut.dulgheriu@yahoo.com)

²SC Katty Fashion Company SRL, Romania
(E-mail: talpa.andreea@yahoo.com)

Abstract: *With the progress and development of science and technology, virtual reality technology is becoming more and more present, its application in digital creations is becoming more and more widespread. Everything the user does is calculated by the computer and has real-time feedback, making this virtual environment more realistic and giving the user an immersive experience. This technology integrates the latest developments in computer science, computer simulation, artificial intelligence, recognition, display and online parallel processing. Virtual prototyping offers a new way to explore the design and subsequent changes that need to be made to the product before it is manufactured in larger quantities or put into production. The development of new product models using virtual tools requires a certain level of training of the designer; he/she must have skills in understanding and using the specific tools for CAD systems (2D and 3D) and technical knowledge regarding the ways of conceptual product development. This paper presents the methodology of the virtual development process for an apparel product model, using the tools of the 2D and 3D digital environments. The first solution is to design the 2D patterns of the components of an apparel product, followed by a 3D simulation that verifies the aforementioned solution. The second solution is to design the 3D components using the tools of the 3D digital environment (the software used is Clo3D) and then extract the 2D parts required for the classical manufacturing process.*

Keywords: *digitalisation, virtual prototype, 2D patterns, 3D simulation*

1. DIGITALISATION-THE NEW REALITY

Digitalisation is regarded as a major phenomenon that has drastically changed society. Technological advancement ensures a better quality of life, as well as social evolution. Digital technology lies at the forefront of technological development, and its effects are felt in all economic and social sectors [1].

A report from early 2021 shows that the number of people that use internet for socialising, communication, professional activities, product/service acquisition is currently increasing [2].

Even though 3D technology has been used in engineering fields for many years (furniture industry, automotive, aerospace, etc.), it has been used in the apparel industry for a relatively short period of time. This kind of technology comes with a whole range of advantages. It can be used at every stage of the product development process, from design

and sampling, as well as for 3D images and videos for product website pages or fashion shows (figure 1).

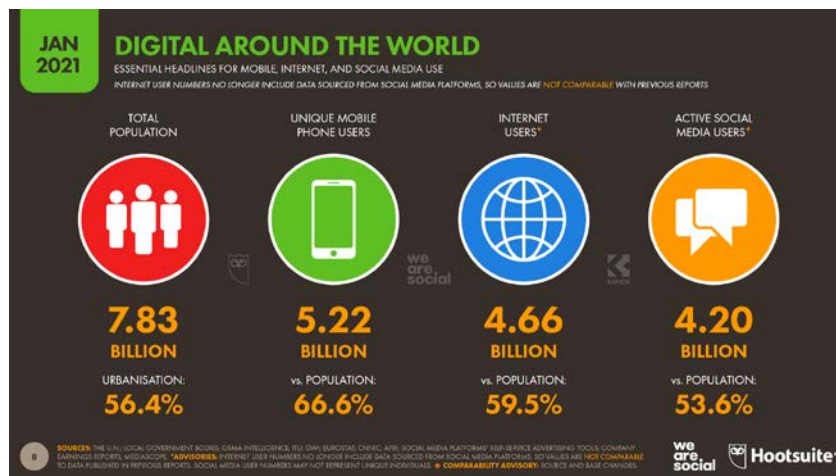


Figure 1. Digital Around The World – Jan 2021[2]

Virtual prototypes provide the designer with new methods of creating products and of simulating what they will be like in reality, before being physically manufactured.

The development of 3D technologies has a positive impact on the field of consumer goods. This kind of technology provides the environment and tools that are necessary in order to simulate the desired product in a virtual space. At the same time, it allows the user to validate the design solution, and to cut down on production costs, energy consumption, pollutants, labour, thus making the design process sustainable [3,4].

The paper presents the main steps of the virtual development process for an apparel product model, which uses the tools provided by 2D and 3D digital environments:

- Designing the 2D patterns of the components of a garment product, followed by a 3D simulation which verifies the aforementioned solution;
- Constructing the 3D components by using the tools of the 3D digital environment (the software that has been used is Clo3D) and then obtaining the 2D pieces which necessary for the classic manufacturing process.

2. VIRTUAL METHODS OF DESIGNING GARMENTS

Digitalisation boils down to "the transformation of interactions, communications, relationships, business functions, and business models into multiple digital processes, often reduced to a combination of digital and physical processes. Digitalisation involves the use of digitised information (or information directly received in a digital format) [3].

Increasingly many apparel companies are using digital tools, and this comes with several advantages:

- the reduction of the time that is necessary to produce the first prototype,
- a significant reduction of the manufacturing costs,
- the reduction of waste,
- the possibility of making changes in real time, and of viewing them,
- the possibility of diversifying the model – by combining or altering the textures of materials,
- the possibility of co-creation service,
- improved communication between the development and production departments,

- online promotion of the created model.

The digital approach to the virtual development of apparel product models can be implemented in two ways:

-a 2D design process of the product components, followed by a 3D simulation on the corresponding virtual mannequin;

-a 3D design process that is directly carried out on the mannequin, followed by the extraction of the 2D patterns that are necessary for the manufacturing process of the selected model.

In CAD applications based on the first type of approach (from 2D → 3D), one edits the shape of the components are performed in the 2D module, and then proceeds to the 3D simulation stage. 3D simulations enable one to visualise the behaviour of the materials in the final product (in this way, one can verify that they have been chosen in accordance with the model and the intended purpose).

In applications based on 3D design, one makes the changes in the design area (3D), and then extracts the 2D shapes of the parts (if the product is made with classical technology, the sewing). The 3D shape of the model (if one can be created) can be exported to a 3D printer in order to obtain the desired product.

The two methods of virtual development of the clothing product models are illustrated for a product with shoulder support (woman dress). The model has both symmetrical and asymmetrical markings, as well as division lines at the top for adjusting and volume at the bottom. The sleeve of the product is fitted with a cuff at the end (figure 2).

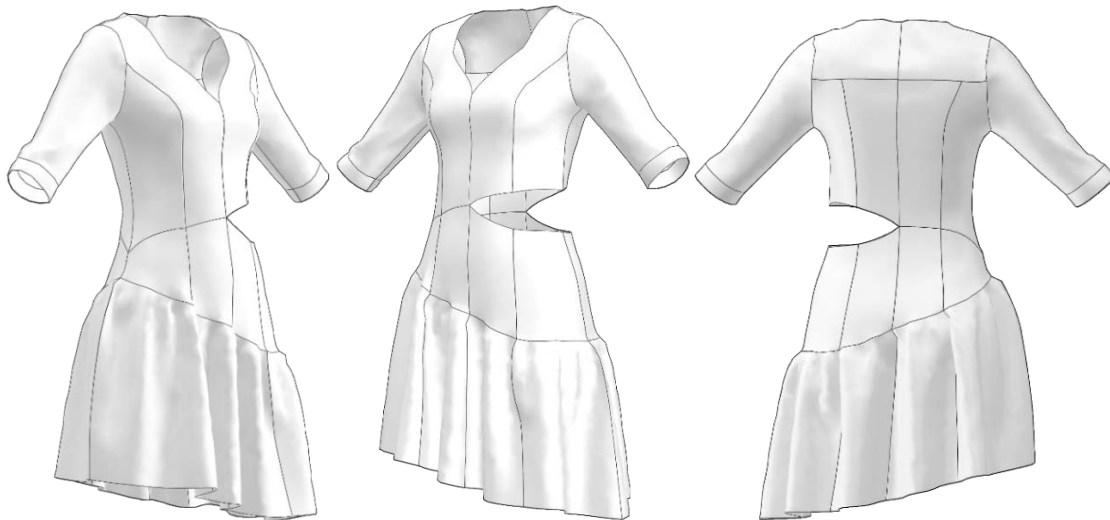


Figure 2. Model sketch

2.1. Designing the model in 2D and validating the resulting prototype via 3D simulation

Manufacturers of software for the clothing sector have developed software packages that allow an individualised / customised design of the patterns (Lectra, Gemini, Graphis, etc.) that takes into account the constructive aesthetic characteristics of the model and the physical characteristics of the wearer (conformation, proportions). For the selected model, the 2D design process of its components was carried out using the MTM module of the Gemini CAD system. In this design environment, depending on the chosen solution, the user picks certain initial data and processes certain mathematical relations in order to decide upon the dimensions of the components of the product. The structure of the initial data or of

the mathematical relations can be changed very easily depending on the requirements for the model/component. The design process of the shapes of the product components is carried out in a layer called the geometric layer. If the product components are still linked with the geometrical layer in which the design was made, then any change in the size, volume and values of the initial data, or in the structure of mathematical relations determine the alteration of the product elements (figures 3, 4 and 5) [5,6].

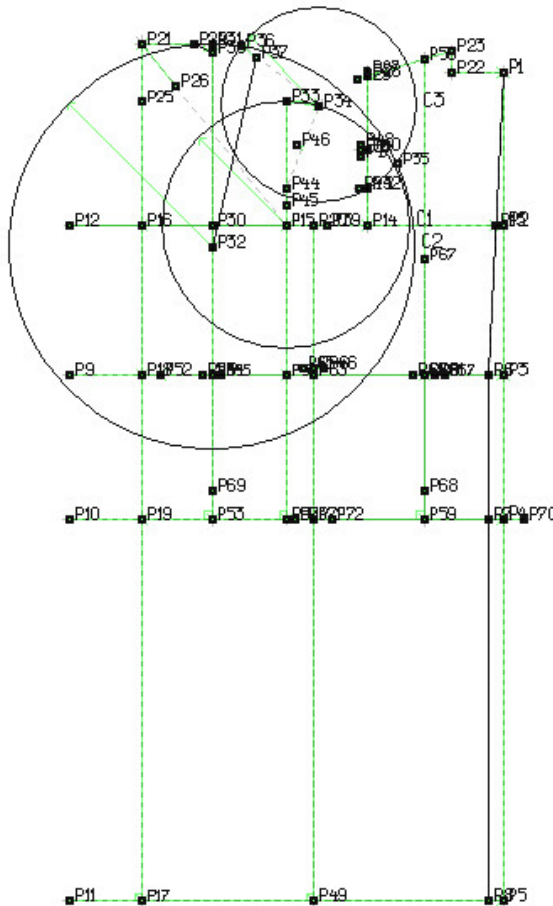


Figure 3. The network for the main elements (front and back)

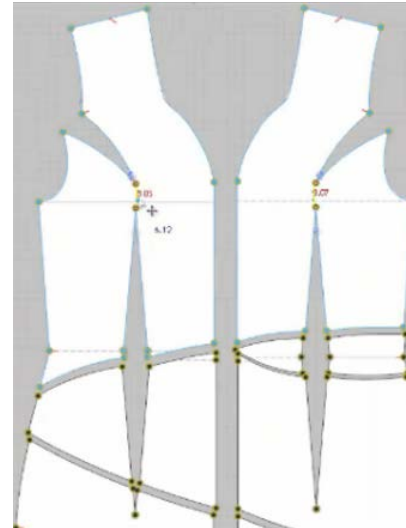


Figure 4. The front model pieces

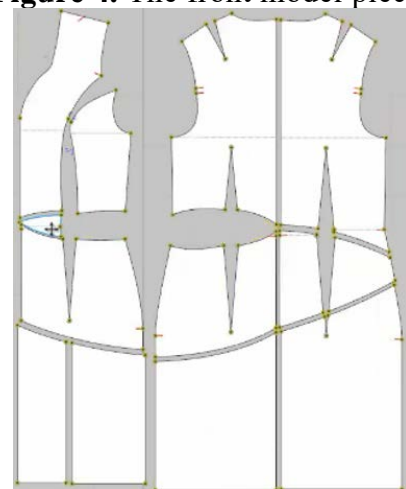


Figure 5. The back model pieces

After obtaining the shape of the components of the model, we proceed to the 3D simulation, which is performed in Clo3D [7,8]. In the simulation process, one takes into account the physical and mechanical properties of the materials, the manufacturing technology and a mannequin corresponding to the one used in the 2D design stage.

The simulation process consists of:

- selecting the avatar (the mannequin), choosing an appropriate shape and dimensions (size and posture), and scaling the mannequin until they are achieved. The values of body dimensions are similar with the one which were used in the design scenario (personalised);
- placing the pieces near the avatar;
- declaring the assembly lines;

- selecting the material (basic, since it is a single product);
- simulating the sewing process, and checking the length of the assembly lines (figures 6, 7, 8 and 9).

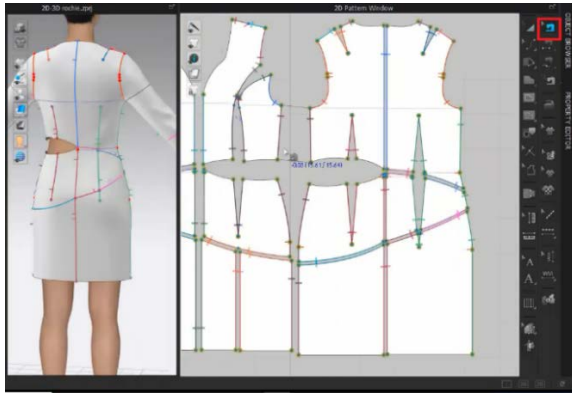


Figure 6. Checking the length of the sewing lines

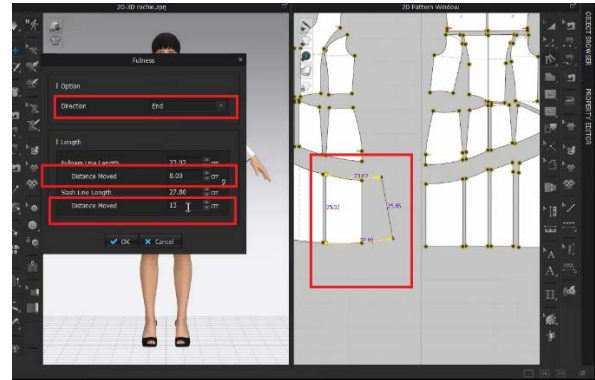


Figure 7. Establish the orientation of the fullness



Figure 8. Product simulation- checking the distribution of the fullness

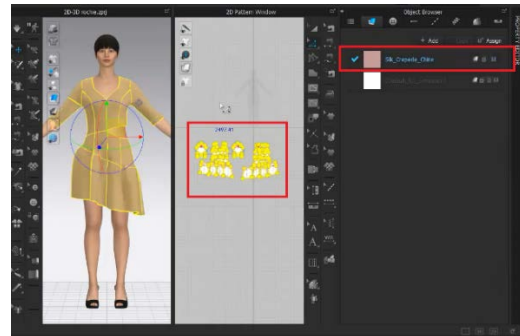


Figure 9. 3D final model (virtual representation)

During the simulation process, if the designer finds problems with the fit and position of the product on the avatar, he will return to the previous phase (2D design phase) and make the necessary changes to eliminate the problems. He will run the 3D simulation process again to be sure that the problems have been solved (figure 10).

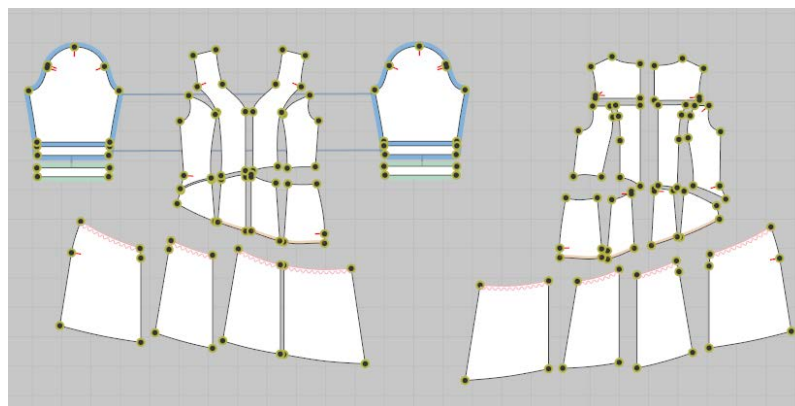


Figure 10. 2D model pieces

2.2. Directly designing the product on the avatar in a 3D virtual environment. Obtaining the corresponding 2D patterns.

The direct 3D design of the product on the virtual mannequin requires knowledge and skills pertaining to the steps that are used in order to obtain the product components, physiochemical properties of textiles, expertise in anthropometry (static and dynamic regime), and in the usage of the tools provided by CAD systems. In order to obtain the shape of the component, the designer needs to know what they want to achieve, the logical and necessary steps for drawing the contour lines (model lines), the relationship between the product components and their support surfaces, and the contour, control and magnetisation points between the product and the body [9-11].

The designer selects the tools that are needed in order to draw the shape of the product component. The direct 3D dimensioning of the latter takes the silhouette and the details of the model into account.

Before the 3D design phase, the designer analyses the silhouette of the model, evaluates the additions that are necessary in order to maintain the silhouette, and takes these details into account when drawing the product components on the avatar (figures 11-19) [5,7,8].

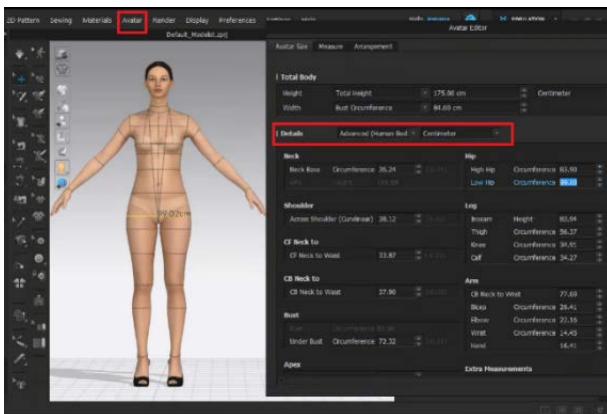


Figure 11. Change the avatar dimensions and position

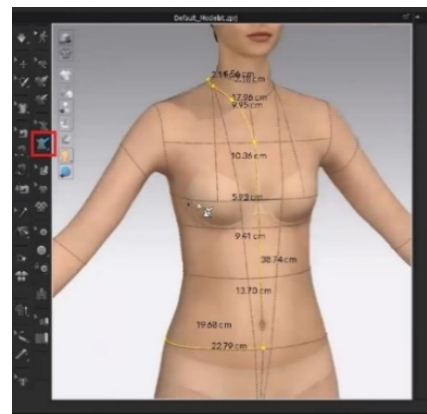


Figure 12. Draw the model lines linked with specific points on the avatar

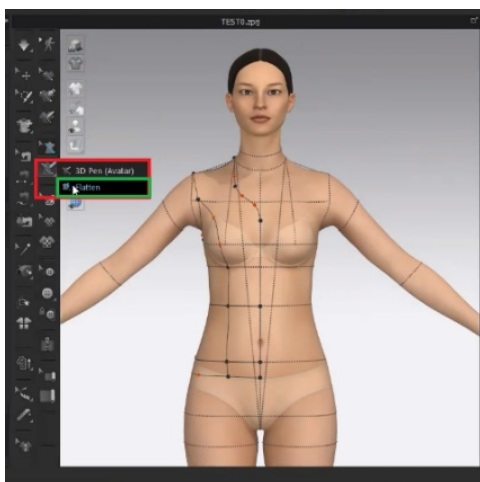


Figure 13. Preparation of piece extraction

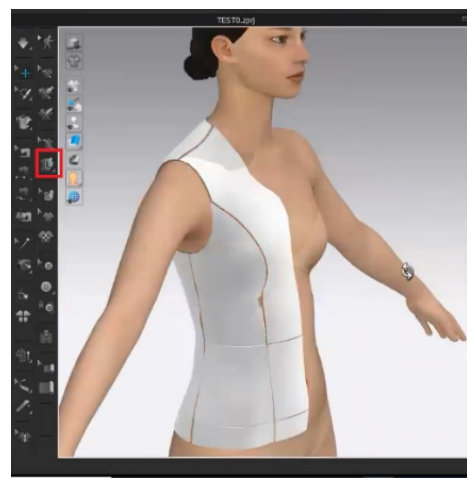


Figure 14. Model pieces (bodice pieces)

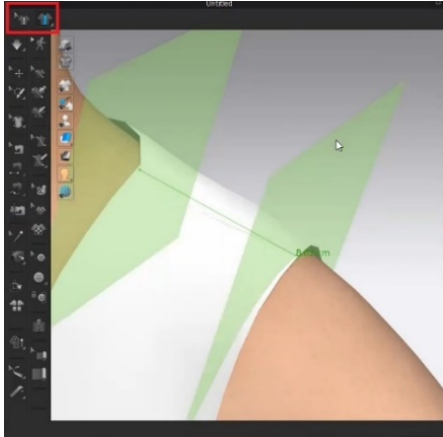


Figure 15. Checking the model dimensions (the length of the shoulder line)



Figure 16. Product simulation



Figure 17. Material selection

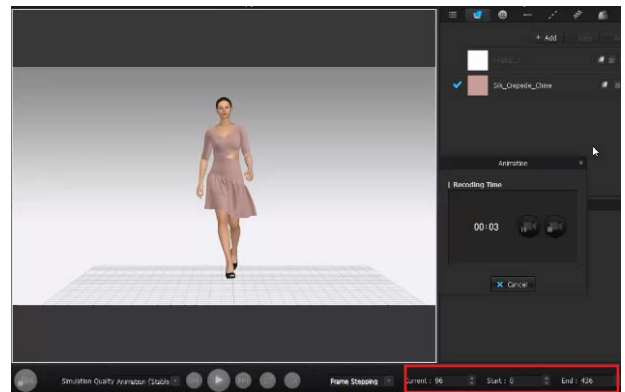


Figure 18. Avatar movement

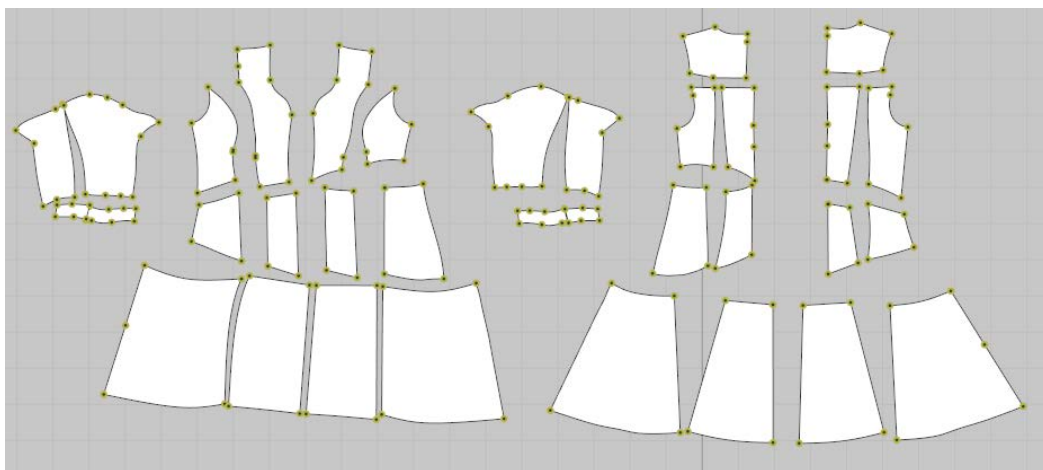


Figure 19. The model pieces (design 3D and exported in 2D)

5. RESULTS AND DISCUSSIONS

By analysing the shapes of the model components obtained by using the two aforementioned methods, one can notice certain differences in the geometry of the contour lines and of their surface. The shape and geometry of the contour lines drawn directly on the 3D avatar depend on the following factors: the complexity of the model, the anatomical

characteristics of the mannequin, the experience of the user in identifying and defining the position of the magnetisation/pinning points of the components of the avatar, and in choosing the right methods of technical modelling for the surface of some parts (volumes), in order to obtain the desired model.

The modelling in the 2D work mode is done by using decorative-constructive lines, while in the 3D work version the same process is carried out automatically by extracting the pieces drawn on the avatar. The shape of the latter is then altered according to the one of the body. In order to obtain their correct shape, the designer must take the following into account: the details of the model, the necessary technical means, the position of the body of the avatar and the physical and mechanical properties of the materials.

In the 2D work mode, after having decided upon a type of material (depending on the elasticity level of the material), the shape of the contour line of every component will have to be adapted to the shape of the body during the 3D simulation process, depending on the elasticity of the material (in the landmark, it remains a straight line). If you draw the pattern directly on the avatar (direct 3D construction), its shape is going to imitate the one of the corresponding area of the avatar. After having extracted the corresponding 2D pattern, the shape of the contour lines will have to be adjusted depending on the type and model of the product.

In the direct 3D design scenario for dimensionally stable products (multilayers), the one must take consider the thickness of the layers of the components, the number of intermediate layers, the extra material between the layers, and the physical and mechanical interactions between them and with the intermediates the avatar.

6. CONCLUSIONS

The whole process of pattern design is increasingly carried out by software programs that enable one to visualise the resulting components in a virtual environment.

The designer that wishes to employ the direct 3D design method must take into account the constructive-aesthetic characteristics of the model, the aesthetic and technological impact of the material, the manufacturing technology, and the characteristics of the wearer's body in terms of posture or conformation. Knowing this information enables one to obtain a product that meets the requirements specified in the technical documentation (by the customer).

In summary, digital transformation comes with costs, efforts and risks. It is crucial to keep up with the global technological evolution and to remain competitive.

Investing in digitalisation and training employees in using specialised software for their tasks should be a top priority for both business owners and managers. At the same time, everyone should be provided with resources that enable them to adapt to the digital age.

REFERENCES

- [1] Knell, M., *The digital revolution and digitalised network society*, Springer Link, 2021, Available at: <https://link.springer.com/article/10.1007/s43253-021-00037-4> [Accessed on June 2021]
- [2] Kemp, S., *DataReportal*, 2021, Available at: <https://datareportal.com/reports/digital-2021-global-overview-report> [Accessed on June 2021]
- [3] Yuwei, M., Mok, P.Y., et al., *Computer aided clothing pattern design with 3D editing and pattern alteration*, Available at: <https://www.sciencedirect.com/science/article/abs/pii/S001044851200067X> [Accessed on June 2021]

- [4] Avadanei, M., Olaru, S., Ionescu, I., Ursache, M., Ciobanu, L., Alexa, L., Luca, A., Olmos, M., Aslanidis, T., Belakova, D., Silva, C., *ICT new tools for a sustainable textile and clothing industry*, In: *Industria Textila*, 2020, 71, 5, 504-512, <http://doi.org/10.35530/IT.071.05.1811>
- [5] M. Avădanei, *Principii de construcție și modelare ale produselor vestimentare*, Iași: Casa de Editura Venus, 2005
- [6] Gemini Cad, Available at: <http://www.geminiCAD.com> [Accessed on June 2021]
- [7] C. 3D, 2021, Available at: <https://www.clo3d.com/> [Accessed on June 2021]
- [8] Clo3D, Available at: <http://www.clo3d.com> [Accessed on June 2021]
- [9] Olaru, S., Filipescu, E., Filipescu, E., Niculescu, C., Salistean, A., *Software solution to assess morphological body through 3D scanning results*, In: *Proceeding of the 9th International Scientific Conference eLearning and software for Education Bucharest*, April 25-26, 2013, 3, 391-398
- [10] Özbek, A., *Online customized T-shirt design and evaluation of online websites for customization*, In: *Industria Textila*, 2020, 71, 4, 371-379, <http://doi.org/10.35530/IT.071.04.1674>
- [11] Dimitrijević, D., Spaić, O., Đurić, Ž., Urošević, S., Nikolić, M., *CAD/CAM system implementation criteria in the process generating of optimal and efficient models for clothing industry*, In: *Industria Textila*, 2020, 71, 5, 467–472, <http://doi.org/10.35530/IT.071.05.1741>



ANALYSIS OF THE PHYSICO-MECHANICAL PROPERTIES OF DIFFERENT WOVEN STRUCTURES WITH POTENTIAL APPLICATIONS IN THE HEALTHCARE AND HYGIENE SECTOR

DOI: 10.35530/TT.2021.37

C.E. Stroe*, T. Sârbu

R&D Department – Textile Materials and Processes Engineering, National Research Development Institute for Textiles and Leather, Romania
(E-mail: cristina.stroe@incdtp.ro, teodor.sarbu@incdtp.ro)

Abstract: *This study aimed at creating different woven textile fabrics with potential applications related to healthcare and hygiene by using textile yarns obtained from diverse fibre blends and by varying the structural parameters of the fabrics. Four different weave patterns were used to create the fabrics: warp rib, 2/2 twill, 2/2-pointed twill and hopsack. Cotton fibres were mostly used, but fibres made from regenerated cellulose with extra antibacterial properties (silver ions) and from ultra-high tenacity polyethylene (UHMWPE) were also used in different proportions. The choice and combination of these types of yarns, along with the rational design for making the fabrics contribute to supporting the sustainability of the textile field, improving the quality of life of people, especially those with special needs (the elderly, people with disabilities, or people with various diseases that limit their free movement) and also ensuring a longer usage time and manifestation of functionalities. A comparative analysis regarding the influence of structural parameters, but also the influence of fibre types on the physico-mechanical performance of the created fabrics was made.*

Keywords: *functionality, mechanical performance, sustainability, weave pattern*

1. INTRODUCTION

In a constantly changing and developing world, functional textiles have gained increasing attention lately due to their potential to bring added value and increased performance in many of the essential areas of life (Personal Protection, Medical, Hygiene, Sports and Leisure, Military/war, Constructions, Geotextiles, etc.) [1].

We need innovative ideas for creating new materials that meet the needs, requirements and expectations of consumers, but also bring appropriate costs and take into account an important part of our future existence, sustainability. Thus, with the upgrading of technology, compared to the basic purposes of textiles (aesthetics, comfort and protection), currently other functions can be given to textile materials and products to meet special needs: to last longer, to be lighter, stronger, more flexible, be breathable or fireproof or other features that give them an advantage.

From the point of view of product development, the selection of materials is the most critical aspect in determining its performance. If we talk about the hygiene and healthcare products sector, important performance characteristics must be met by the product made (table 1) to ensure consumers physical well-being, mental health and increased safety.

In addition, compared to the characteristics of the type of material used, the structural attributions of the realized product are equally important. Thus, at the level of textile fabric

design, a series of parameters must be considered, which through different combinations of their values can be obtained superior performances.

Table 1. Needed performance characteristics and contributing parameters of healthcare/hygiene textile products [2]

Performance characteristics	Contributing parameters
Comfort	Fibre type
Cleanliness	Fibre fineness, compactness
Antibacterial ability	Arrangement and mobility
Minimum cross infection	Fibre contamination
Durability	Fabric weight
High filter capacity	Fabric absorption
Light support	Fabric air permeability
Mechanical protection	Fabric porosity
Permeable to oxygen	Fabric thickness
Non-toxic or non-allergenic	Fabric bulkiness and loftiness

Many key factors determine the increasing growth in the use of textiles in applications related to the healthcare and hygiene sector. These include: raising number of accidents, increasing number of surgeries, increasing number of patients with chronic diseases, increasing demand to limit nosocomial infections, increasing health spending around the globe, raising public awareness of health and hygiene, and innovations in technologies and products [3,4]. Also, awareness and promotion of a healthy and physically active lifestyle contribute greatly to increasing the consumption of textiles to ensure health and hygiene among sportsmen, especially textiles with antimicrobial properties. Thus, according to the report published by MaketsandMarkets, the healthcare textile market is projected to reach USD 23.3 billion by 2025 from USD 16.8 billion in 2020, at a CAGR of 6.7% [4], and the textile market with antimicrobial properties will show a CAGR of 9.8% by 2026, according to Global Market Insights [5].

The market is based on nonwoven, woven and knitted fabrics, but nonwovens will have the largest market share due to their extensive use in many different applications and due to their cost-effectiveness. Hygiene products are also expected to dominate the market over the next 4 years due to increased consumption of baby diapers and sanitary napkins in developing economies [6].

Unfortunately, all these developments and the excessive consumption of resources will lead to destruction if we do not find solutions that maintain a balance between man-nature-economy. We are therefore forced to rethink our economy, to use resources efficiently and to move to alternative, renewable materials, but also to transform the way we use and consume resources and create waste. It is impossible to imagine a world without textiles, but we can turn this industry into an extremely functional, interesting and responsible industry [7], if we contribute to raising awareness, if we address strict environmental regulations and if we will change the way we live.

This paper presents an investigation of the influence of structural parameters on the physico-mechanical performance of many woven fabrics with potential applications related to healthcare and hygiene that were obtained from the same warp yarns and different weft yarns and with four different weave patterns: warp rib, 2/2 twill, 2/2-pointed twill and hopsack.

To obtain textile materials that support the sustainability of the field, but that also offer functionality by increasing comfort and by conferring a superior resistance to mechanical action, it was chosen to use mainly natural cotton fibres blended with man-made fibres from regenerated cellulose, but also with high-tech fibres from ultra-high tenacity polyethylene (UHMWPE), with a reinforcing role. Moreover, to add additional functionality, silver ions with an antibacterial role were used on regenerated cellulose fibres by functionalizing them in

the polymeric mass, in this way the functionality at the level of the fibres manifesting itself for a longer time.

2. MATERIALS AND METHODS

2.1 Materials

In this research, 11 types of woven fabrics were made with four different weaving patterns, namely: warp rib, 2/2 twill, 2/2-pointed twill and hopsack (figure 1). All fabrics were produced on the same type of equipment from the experimental station of INCDTP.

Five types of yarns were used in this research, keeping the same warp for all the fabrics and different weft yarns:

- 100% cotton, 25x2 tex;
- 98% cellulosic blend of cotton and regenerated cellulose fibres with 2% Ag⁺ ions incorporated in the polymeric mass before spinning, 20x2 tex (figure 2);
- cotton fibres blended with 2%, 5% and 10% of UHMWPE fibres, 30x1 tex.

For each type of weave pattern 3 fabrics were made, except for the rib structure for which only 2 were made, being considered the reference for comparing the properties between fabrics. For a better understanding, in table 2 are found the characteristics of the fabrics made.



Figure 1. The appearance of the 4 types of used weave patterns



Figure 2. Optical microscope view of the cotton fibres and also the regenerated cellulose with Ag⁺ ions fibre at 400x magnification

These types of yarns could contribute to create functional fabrics that can ensure skin comfort and good absorption properties by using cellulosic fibres, protection against the proliferation of microorganisms on the skin and odour control through the action of Ag⁺ ions, safety and protection against skin lesions or to the intense frictional stresses by the insertion of UHMWPE fibres especially in the most exposed areas of the body. At the same time, cellulosic fibres correspond to the actual eco-friendly criteria.

Table 2. Structural characteristics of the woven fabrics

Fabric code	Weave pattern	Weft composition	Weft yarn linear density (tex)	Warp composition	Warp yarn linear density (tex)	Yarn tenacity at break (N/tex)
V01	Warp rib	100 % cotton	25x2	90% cotton + 9% regenerated cellulose + 1% Ag ⁺ ions	Alternating yarns 25x2 Tex (100% cotton) and 20x2 Tex (80% cotton + 18% regenerated cellulose + 2% Ag ⁺ ions)	0.181
V02		80% cotton+ 18% regenerated cellulose + 2% Ag ⁺ ions	20x2			0.147
V03	Hopsack	98% cotton + 2% UHMWPE	30x1			0.167
V04		95% cotton + 5%UHMWPE	30x1			0.181
V05		90% cotton + 10% UHMWPE	30x1			0.192
V06	2/2 Twill	98% cotton + 2% UHMWPE	30x1			-
V07		95% cotton + 5% UHMWPE	30x1			-
V08		90% cotton + 10% UHMWPE	30x1			-
V09	2/2- Pointed twill	98% cotton + 2% UHMWPE	30x1			-
V10		95% cotton + 5% UHMWPE	30x1			-
V11		90% cotton + 10% UHMWPE	30x1			-

2.2 Methods for investigating the physico-mechanical properties of the fabrics

After making the fabrics with functional properties, they were tested in the raw state, unfinished, by various investigation methods, to highlight their physico-mechanical properties with the variation of the chosen structural parameters.

Fabric testing plays a crucial role in evaluating product quality, ensuring compliance with applicable regulations and evaluating the performance of textiles. Among the critical factors that control the properties of the fabric can be mentioned the properties of the yarns (composition, fineness, strength), the thickness of the fabrics and their weave pattern. The manipulation of these elements and the way they interact produces fabrics with different physical and mechanical properties.

- *Testing the tensile strength and elongation*

The strength and elongation at break of all fabrics were tested in both weft and warp directions, on James Heal-Titan equipment according to the standard EN ISO 13934-1/2013- *Tensile properties of fabrics-Part 1: Determination of maximum force and elongation at maximum force using the strip method*. The tested specimens had the size 350 mm x 50 mm and their number was 5 in the warp direction & 5 in the weft direction. The applied test speed was 100 mm/min and a load cell of 5 kN, and the distance between the clamps was 200 mm.

- *Testing the tearing strength*

The tensile strength by tearing was tested on the same James Heal-Titan device on 5 specimens for both yarn systems according to the standard EN ISO 13937-2/2001 *Tear properties of fabrics - Part 2: Determination of tear force of trouser-shaped test specimens (Single tear method)*. The tear test speed was 100 mm/min and the distance between the clamps was 100 mm.

- *Determining the propensity of fabrics to form pilling on the surface and the resistance to perforation*

This test was performed on James Heal-Orbitor equipment. Two square specimens with a size of 125 mm were made for warp and weft for each of the 11 fabrics. The specimens were subjected to a number of 10800 rotation cycles.

- *Determining the air permeability of the fabrics*

Air permeability test was done to each type of weave structure. Air permeability tests were conducted using Textest FX 3300 model Air Permeability Tester at a test pressure drop of 200 Pa for 20 cm² test area (EN ISO 9237:1999).

3. RESULTS AND DISCUSSIONS

3.1 Breaking strength and elongation at break

Breaking strength and elongation are the most important properties of fabrics that govern their performance during use. The average results obtained after testing the specimens with the dynamometer can be seen in table 3 and figures 3 and 4. Thus, overall, the breaking strength in the warp direction was better than in the weft direction, as expected, due to the higher density of the yarns. Except for the results of the resistance in the weft of the variants V09, V10 and V11 with pointed twill 2/2 pattern which had higher values, exceeding 1000 N. The breaking strength in the warp direction was maintained at almost the same level for all variants, because the same type of yarn was used, as well as composition and fineness, the highest values also being registered in the case of variants with pointed twill 2/2 pattern. The fabrics with the warp rib pattern registered slightly higher resistance in the warp direction than in the case of the hopsack or twill 2/2 patterns.

The yarns resulting from the blend of cotton-regenerated cellulose-Ag⁺ ions fibres gave the fabrics a much better resistance than those with various percentages of UHMWPE in the weft, although this material is known for its superior strength. However, an influence on this fact most likely had the lower fineness of the used yarns and the warp rib pattern. In the weft direction, the variants with the highest breaking strength and the only ones that exceeded the breaking strength from the warp were obtained for pointed twill 2/2 pattern, for which the way of binding the yarns in the structure had a significant influence.

If we consider the tenacity of the yarns as can be seen from table 2, the higher tenacity was obtained for the yarns with 10% UHMWPE, the rest with 2% and 5 % being comparable with the tenacity of 100% cotton yarns. The lowest tenacity was obtained for the yarns with cotton-regenerated cellulose-Ag⁺ ions and yet it appears that the hopsack and D2/2 patterns had a much lower influence on the strength, regardless of the type of yarn used both in the weft and in the warp. In the case of fabrics with 2%, 5% and 10% UHMWPE, the breaking strength increased in correlation with the increase in the percentage of UHMWPE.

The elongation in the warp direction was higher than in the weft, and the highest elongation in the warp was obtained for the variants with pointed twill 2/2 pattern in agreement with the high resistance. The smallest elongation in the warp direction was obtained for the warp rib pattern. Fabrics with yarns with different percentages of UHMWPE indicated less elongation in the weft direction compared to cotton yarns fabrics and to cotton-regenerated cellulose yarns fabrics.

3.2. Tearing strength

The results of tear strength can be seen in table 3 and figure 5. For warp yarns with a blend of cotton and regenerated cellulose fibres, the average tear strengths resulted were generally lower than for weft yarns with percentages of UHMWPE, which demonstrates the ability to resist to mechanical stress of UHMWPE fibres. In general, the average tear strength for warp yarns was between 40N and 50N. Only variants V01, V02, V05, V06, and V07 with rib, hopsack and twill 2/2 patterns had a warp tearing strength higher or almost equal to the

weft strength, but some of them also showed higher standard deviations. The lowest average tear strength, below 40 N, was recorded for the V02 variant in both warp and weft, but for the warp resistance, it can be also noticed the fairly high standard deviation.

For the weft with cotton yarns and various percentages of UHMWPE, the tear resistance had an ascending trend in relation to the increase in the percentage of UHMWPE, only the V11 variant does not follow this trend, with a high standard deviation of ± 19.6 N.

Table 3. Average results of the performed analysis and confidence intervals for dispersion

Fabric code	Breaking strength (N)		Elongation at break (%)		Tearing strength (N)	
	Warp	Weft	Warp	Weft	Warp	Weft
V01	923.53 \pm 33.06	675.78 \pm 27.35	10.05 \pm 0.6	15.75 \pm 0.37	51.12 \pm 8.24	50.70 \pm 3.47
V02	959.60 \pm 49.83	659.87 \pm 30.66	11.48 \pm 0.59	14.72 \pm 0.36	36.34 \pm 11.39	30.65 \pm 0.88
V03	856.31 \pm 9.67	489.20 \pm 10.81	12.69 \pm 0.36	7.90 \pm 0.13	45.72 \pm 18.42	52.97 \pm 6.21
V04	841.50 \pm 32.07	518.01 \pm 13.37	13.22 \pm 0.20	8.23 \pm 0.11	48.59 \pm 16.79	60.17 \pm 4.54
V05	868.70 \pm 20.10	535.07 \pm 7.76	12.95 \pm 0.26	8.56 \pm 0.18	65.78 \pm 2.75	61.46 \pm 3.31
V06	871.32 \pm 43.37	401.08 \pm 31.14	16.65 \pm 0.93	10.54 \pm 0.56	46.40 \pm 1.85	35.83 \pm 0.71
V07	881.21 \pm 7.84	531.48 \pm 16.63	14.69 \pm 0.25	9.95 \pm 0.28	42.79 \pm 1.78	42.94 \pm 1.50
V08	894.53 \pm 43.36	591.85 \pm 13.26	13.78 \pm 0.55	10.54 \pm 0.17	44.46 \pm 2.21	54.93 \pm 0.68
V09	976.52 \pm 26.47	1062.49 \pm 20.86	16.81 \pm 0.30	11.48 \pm 0.24	43.85 \pm 1.06	53.19 \pm 1.05
V10	972.38 \pm 26.37	1170.07 \pm 37.30	17.11 \pm 0.29	11.28 \pm 1.11	43.78 \pm 2.07	67.35 \pm 2.59
V11	966.64 \pm 19.73	1296.99 \pm 17.93	16.41 \pm 0.42	12.56 \pm 0.20	41.81 \pm 2.05	55.22 \pm 17.18

3.3 The propensity of pilling formation on the fabric surface and perforation resistance

The pilling effect on the surface of fabrics consists in the appearance of small pills of tangled fibres that can form during wearing or washing, giving an unsightly appearance to the material. Following the analysis, all the fabrics were evaluated with maximum score regarding the propensity of pilling formation and the perforation resistance, 4-5, thus noting a very good quality of the fabrics, with a very poorly produced or even non-existent pilling effect or snagged yarns. This is due to the reduced migratory tendency of the fibres in the constituent yarn used to make the fabrics.

3.4 Air permeability of the fabrics

Air permeability of the fabrics is a special property that must be fulfilled by them when it is intended to be used in the health sector, especially for clothing or different items that comes into contact with the skin. Air permeability is influenced by several factors such as the type of fabric structure, the design fabric density, the amount of twist in yarns, the size of the yarns, the type of yarn structure, the size of the interstices in the fabric, etc. [8]. The average results for air permeability of the fabrics are presented in table 4. The best air permeability was recorded for the hopsack weave pattern and also for the 2/2 twill pattern, therefore ensuring very good thermal ventilation.

Table 4. Air permeability of the four types of weave patterns

Weave pattern	Warp rib	Hopsack	2/2 Twill	2/2-Pointed Twill
Air permeability (l/m ² /s)	165.2	412.8	343.8	119

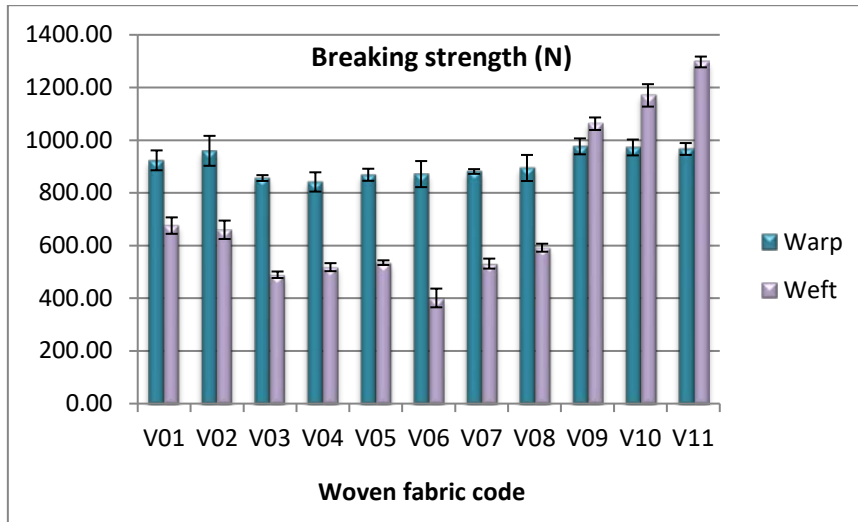


Figure 3. The results of the breaking strength for weft and warp of the 11 fabrics

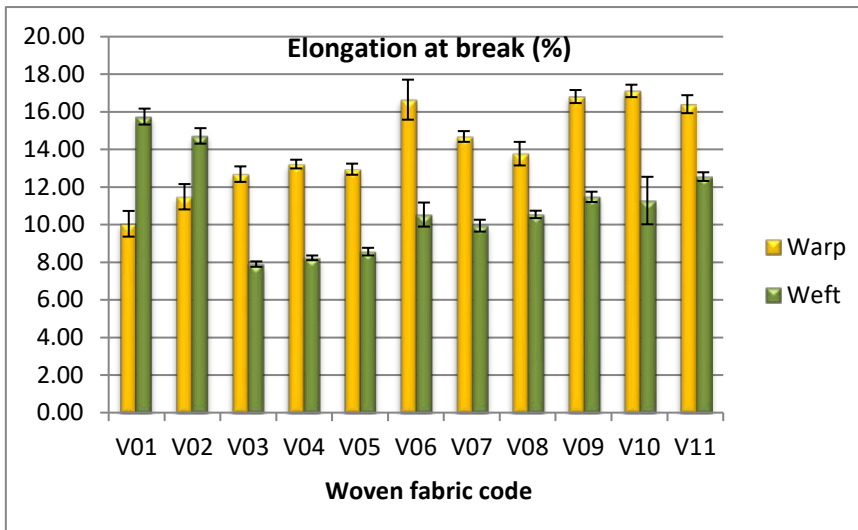


Figure 4. Elongation at break of the woven fabrics in warp and weft direction

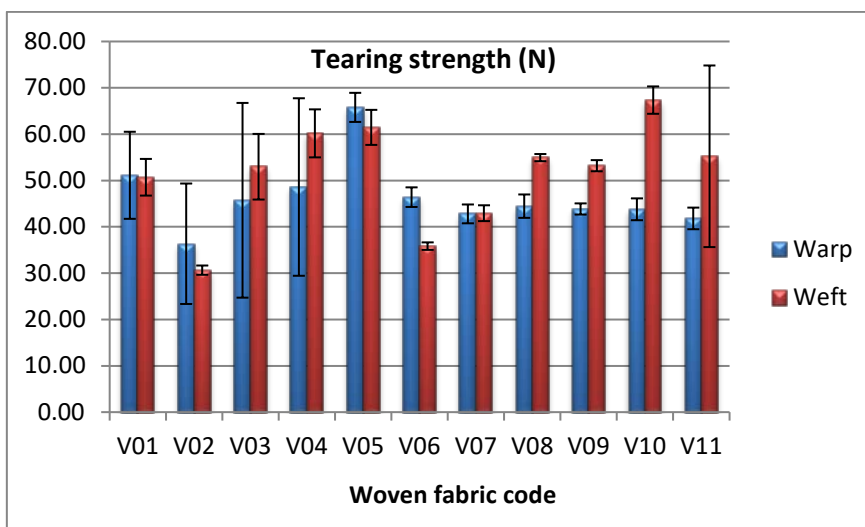


Figure 5. Tearing strength of the woven fabrics in warp and weft direction

4. CONCLUSIONS

The investigations made it possible to demonstrate the following aspects:

- The weave pattern influences the mechanical properties of fabrics. The fabrics with pointed twill 2/2 and warp rib weave patterns showed the best breaking resistance both in the warp direction and in the weft direction, thus demonstrating the effectiveness of these two ways of binding the yarns in relation to the breaking strength.
- The weaving of fabrics with warp rib pattern and yarns resulting from the blend of cotton – regenerated cellulose and Ag⁺ ions fibres showed a higher breaking strength than weft of fabrics with hopsack and twill 2/2 fabrics with yarns from the blend of cotton and UHMWPE fibres, this result demonstrating that although the yarns have lower tenacities, the way they are bonded in the structure influence the mechanical properties positively.
- The breaking strengths in the weft of the fabrics with yarns made of cotton and different amounts of UHMWPE fibres increased with the increase in the percentage of UHMWPE, and depending on the weave pattern, the resistances were situated in ascending order as follows: hopsack < 2/2 twill < 2/2-pointed twill.
- It was noticed by the tearing analysis the superior resistance of the fabrics from yarns with different percentages of UHMWPE from the 3 variants of weave. Thus, fabrics with reinforcing elements such as UHMWPE fibres are ideal for making clothing or different textile items that provide support and protection to mechanical actions. Significantly stronger products can be made without compromising comfort.
- A very good pilling and perforation resistance was obtained for all the fabrics; as for air permeability, the best ability to create optimal conditions for the skin was shown by the fabrics with hopsack and 2/2 twill patterns.
- The use of natural and renewable resources such as cellulose extracted from wood for obtaining fibres and the development of textile materials ensures high performance, compared to those of synthetic fibres. Also, increasing their use will considerably alleviate the harmful effects of the textile industry on pollution and will support the sustainability of the field.
- The use of advanced techniques such as design thinking allows the realization of a rational design at the level of use of fibres and functionalities, but also at the level of product, which allows modulation.

ACKNOWLEDGEMENTS

Funds support this work from Ministry of Research, Innovation and Digitization, Romania, National Project “Macro-mezo-micro advanced materials meant for health and improvement of life quality (AkSuTex)” [Project Number PN 19 17 03 03].

REFERENCES

- [1] Persistence Market Research, *Functional Textiles Market: Global Industry Analysis and Forecast 2016 – 2024*, Available at: <https://www.persistencemarketresearch.com/market-research/functional-textiles-market.asp> [Accessed on June 2021]
- [2] Mogahzy, Y.E.El, *Engineering textiles, Integrating the design and manufacture of textile products*, Woodhead Publishing Ltd, 2009, ISBN 978-1-84569-048-9
- [3] Brandessence Market Research and Consulting Pvt Ltd, *Medical Textiles Industry 2021 Insights & Forecast*, 2021, Available at: <https://www.mynewsdesk.com/us/brandessence/pressreleases/medical-textiles-industry-2021-insights-and-forecast-3083982> [Accessed on June 2021]
- [4] MarketsandMarkets Research Private Ltd, *Healthcare Fabrics Market by Raw Material, Fabric Type, Application, Region - Global Forecast to 2025*, 2021, Available at:

<https://www.marketsandmarkets.com/Market-Reports/healthcare-fabric-market-220548133.html>
[Accessed on June 2021]

[5] Global Market Insights Inc., *Antimicrobial Textiles Market Size By Fabric, By Application, By Active Agents, Industry Analysis Report, Regional Outlook, Growth Potential, Price Trends, Competitive Market Share & Forecast, 2020 – 2026*, 2020, Available at: <https://www.gminsights.com/toc/detail/antimicrobial-textiles-market> [Accessed on June 2021]

[6] Zion Market Research, *Global Healthcare Fabrics Market Raw Material, by Fabric Type, and by Application: Global Industry Perspective, Comprehensive Analysis, and Forecast, 2018–2025*, 2019, Available at: <https://www.globenewswire.com/fr/news-release/2019/03/14/1752927/0/en/Global-Healthcare-Fabrics-Market-Will-Reach-USD-15-7-Billion-By-2025-Zion-Market-Research.html>
[Accessed on June 2021]

[7] Kerkhof, R., Lenzing A.G., *Time to act!*, 2018, Available at: https://unece.org/fileadmin/DAM/timber/meetings/2018/20181105/COFFI2018_-Circular_Economy_-_van_de_Kerkhof.pdf [Accessed on June 2021]

[8] Ogulata,, R.T., *Air permeability of woven fabrics*, In: *Journal of Textile and Apparel, Technology and Management*, 2006, 5, 2, 1-10



CLOTHES DEVELOPMENT BASED ON METHODS OF HANDLING OF PREMATURE BABIES IN THE INTENSIVE CARE UNIT

DOI: 10.35530/TT.2021.13

V. Danila^{1*}, A. Curteza¹, S. Balan²

¹Technical University „Gheorghe Asachi” Iasi, Romania, Faculty of Industrial Design and Business Management, Iasi, Romania

(E-mail: victoriavasiledanila@gmail.com, acurteza@gmail.com)

²Technical University of Moldova, Faculty of Textile and Polygraphy, Department of Design and Technologies in Textile and Polygraphy, Chisinau, Republic of Moldova

(E-mail: stela.balan@adm.utm.md)

Abstract: *The health of children born prematurely remains a significant challenge, but clothing products designed considering medical requirements and handling methods used in the intensive care unit, may contribute to the reduction of neonatal mortality. Assistants in the therapy unit implement practices based on the needs of vulnerable infants, from the very first second of life.*

This pilot clinical study was conducted in a specialised neonatal intensive care unit, at the IMSP Municipal Clinical Hospital Gheorghe Paladi from Chisinau. Informed consent of parents and/or caregivers was required. All users (nurses and doctors) were informed about the product and instructed regarding dressing and undressing process. This controlled study was conducted under the supervision of doctors and nurses. As the study was exploratory in nature, aspects of grounded theory have been used for qualitative data collection.

The sample studied consists of preterm infants less than 30 weeks GA, admitted by UTIN in 2018. The population eligible for qualitative data collection was made up of neonatology nurses from the clinic. To obtain a heterogeneous sample, aspects such as age, work experience, environment, and education were considered. The method of observation and subsequent testing used of the newly designed products and every manipulation under medical conditions was intensely studied. Local reactions, if any, due to the texture and quality of the textile material that come into contact with the baby's skin, were also carefully monitored. The process of dressing and stripping off the products, carrying out medical manipulations (in case of neonatal emergencies), were also carefully observed for developing ease of use clothes.

Keywords: *manipulation, observation, nurses, premature babies, clothes*

1. INTRODUCTION

There are few studies that identify the scope of healthcare procedures at a NICU (Neonatal Intensive Care Unit) [1-5]. The healthcare procedures were described as follows: heart rate, temperature, blood pressure, and weight assessment; laboratory tests; care equipment and response to vital signs; change of position; feeding; changing diapers or bathing, changing linen; reaching; holding or behaving without care [4-6]. Unfortunately, these reports did not quantify the number of healthcare procedures, a premature newborn received, at a NICU.

2. THE STUDY OF DEVELOPMENT CLOTHES

The development of comfortable and aesthetic products with functional and constructive elements that facilitate the performance of medical procedures (in the case of premature babies) can increase the efficiency of rehabilitation and improve the quality of life of these children.

The elaborated clothing models ensure an easier dressing and undressing process of the products, without any discomfort during the medical manipulations. Medical staff and parents confirm that these clothing products by being this ergonomic, could facilitate the medical procedures and save time without losing their effectiveness of healthcare. It contributes to the proper work process of the nurse in the stages of rehabilitation during intensive care units [7,8].

The most important role in the development and provision of high-quality medical care is assigned to the neonatologist and nurses at all stages in the department of neonatology of premature babies.

The decisive and critical period in the life of a premature baby is at his first stage in the neonatal intensive care unit, where the speed of decision making and the professional training of the medical staff is directly proportional with the chances of life. The purpose of the first stage of healthcare is to exclude the chance of situations that can endanger the child's life. In achieving these goals, the importance of medical care also lies in creating a supportive environment, not only for the premature babies, but also for taking the right approach by the family.

The provision of effective medical care staff is somehow restricted by the insufficiency of types of clothing products adapted to medical equipment and facilities, significantly affecting the possibility of using such high medical technologies.

Existing products regrettably does not meet current requirements and does not have the flexibility of using modern technologies. The properties of new materials and their special finishes not only solves these problems and improve the quality of medical procedures, but also help to improve the ergonomic properties of clothing for premature babies.

The creation of adapted, comfortable, and aesthetic clothing products, with functional and constructive elements, facilitate medical procedures (considering the specifics of handling), will not only contribute to the rehabilitation of premature babies, but will also increase the level of social protection and patients'life quality.

3. METHODOLOGY

The study was performed based on the Chisinau's №1 Municipal Maternity Hospital, the Intensive Care Unit. The eligible population from the quantitative data collection were premature infants and nurses. The premature babies were under 30 weeks of gestation age, selected and admitted to the NICU in 2018. The nurses were selected by heterogeneous sampling, and aspects such as age, work experience, education and work environment were considered. Students and temporary staff were excluded due to the need for a solid work experience in therapy. Attendees were asked to participate and received an email with additional information about the study.

On the base of the observations and recommendations made during the study, clothing products were designed according to the need to provide medical help in a short and effective time for premature babies. For the development of functional clothing for premature babies, we considered the following aspects: functional elements, medical

manipulations, the destination of the product, the location of medical devices, etc., these are described in figure 1.

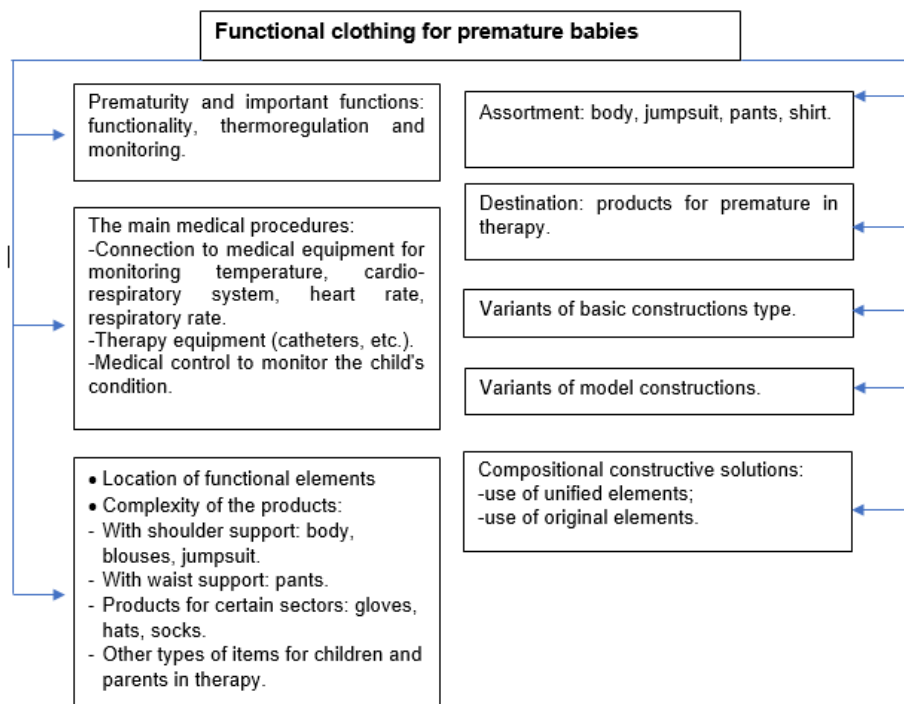


Figure 1. Information scheme for the development of clothing for premature children in the intensive care unit

Due to medical equipment, premature babies are now much more likely to survive than before. In the worst case, with a minimum of equipment, the premature baby can be heated and monitored with equipment that may include:

- ✓ closed or open incubator;
- ✓ thermometer for permanent monitoring of body temperature;
- ✓ cardio-respiratory monitoring system device for monitoring heart and respiratory rate;
- ✓ pulse oximeter, to monitor the level of oxygen in blood.

4. THE IMPACT OF MEDICAL MANIPULATIONS ON THE DESIGN OF STRUCTURALLY FUNCTIONAL ELEMENTS OF CLOTHING

To increase the degree of functionality of products intended for premature infants, and to perform various medical manipulations, were developed adapted clothing designed in accordance with the needs and anthropo-morphological requirements of this group of carriers.

Therefore, it was decided to design the products taking into account the wrapping method, which gives us the possibility to cover the child's body, minimizing the number of stitches and optimizing the dressing and undressing process through holes specially adapted for medical equipment.

Experimental research conducted to the design of several types of products that can be used for children, in the incubator. The models are original and designed in accordance with the requirements imposed on clothing for premature babies. A „prema body” product has been defined and designed, which forms holes by folding, for the head, upper limbs and

lower limbs; it is a bag type product, which allows the attaching of the needed elements. The dimensions of the products have been designed accordingly.

The clothing products are made of natural materials, which will allow the child's skin to breathe and will ensure the protection of the child from various chemicals and pathogens. The elements of the products were processed by edging, and the endings of the products were processed with coating seams. The products meet all the requirements and standards regarding the manufacture of products for premature babies, with reduced body weight [9].

The design of clothing for premature babies should ensure an easy dressing and undressing, the handling without causing pain or discomfort and, most important, to ensure free access to the equipment and appliances, as shown in figure 2.

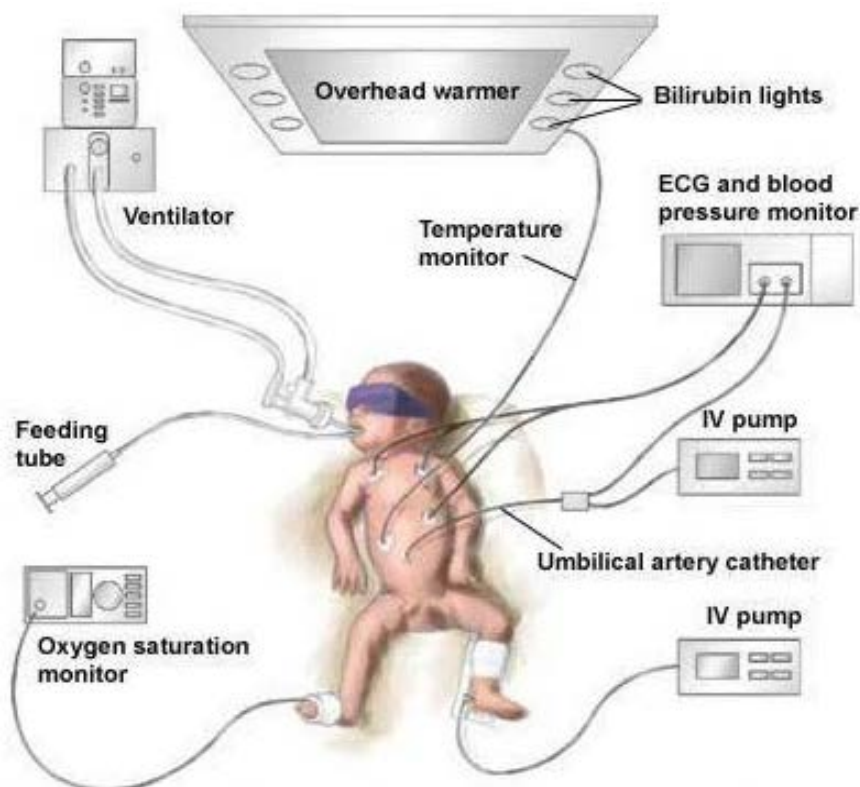


Figure 2. Equipment and devices to which premature babies are subjected [8]

Following the establishment of the equipment and devices that are applied to premature babies in intensive care section, the following areas of the premature body free access is required during medical manipulations (figure 3):

1. the area of the hands (for intravenous therapy) - the placement of catheters in the veins of babies to provide fluids, nutrients and drugs or blood;
2. subaxillary and chest area to have access for monitoring vital parameters: temperature, cardiac, apnea, etc., as well as for neonatal control;
3. the leg area to have access to intravenous therapy as well as to the monitoring of oxygen saturation by applying the pulse oximeter;
4. the back area to have access to the neonatologist's control;
5. buttock access area (intramuscular injections).

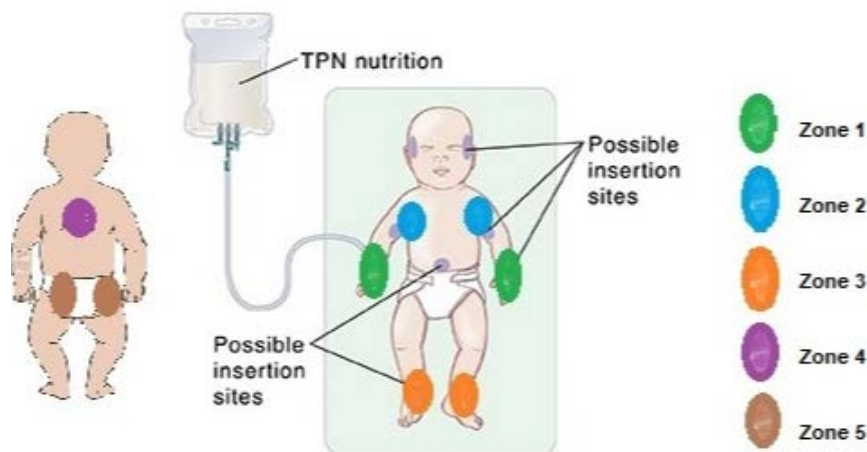


Figure 3. Topography of procedures and medical manipulations in the case of premature babies

It can be concluded that the knowledge of the types of manipulations and procedures, to which premature babies are subjected, determines the complexity and functionality of the elaborated clothing products. Therefore, the functionality of the products (Figure 4) can be obtained using:

- structural elements for folding the front and rear elements;
- closing systems placed on the ends of the products, by simply attaching press buttons ;
- minimal types of seams that does not scratch the baby's skin.

Thus, the proposed products allow free access to the:

- shoulder, chest and back for equipment and neonatologist control but also for monitoring vital parameters;
- sleeve line by closing with the help of press buttons;
- foot, for the needed equipment.

Detachable side seams, front and back folds can be used for free intramuscular injections. The use of the winding at the top of the side seams of the pants will release the needed area for the intramuscular injection without completely undressing the child, thus, the heat losses will be smaller. The use of functional structural elements in the side, shoulder and lower seams of clothing products will provide premature children with comfort and safety, giving them the necessary care and handling without creating discomfort.

The developed functional-structural elements of the clothing offer free access to the procedure area based on the following morphological elements:

- ✓ adjustment method - changing the geometric parameters of the product, the type of „adjustment-fixing”;
- ✓ wrapping the flat back and front elements offering the possibility of easy dressing-undressing without traumatizing the child, and providing help in a short time in case of neonatal emergencies;
- ✓ products adapted to the anthropomorphological parameters of the carriers.

The opening of certain parts of the product is convenient in operation because, at the time of the procedure, part of the body is released, and the rest of the time is covered and protected from external influences. The proposed functional and constructive elements are

easy to use, during the intensive neonatal therapy, being a support for both children and medical staff.

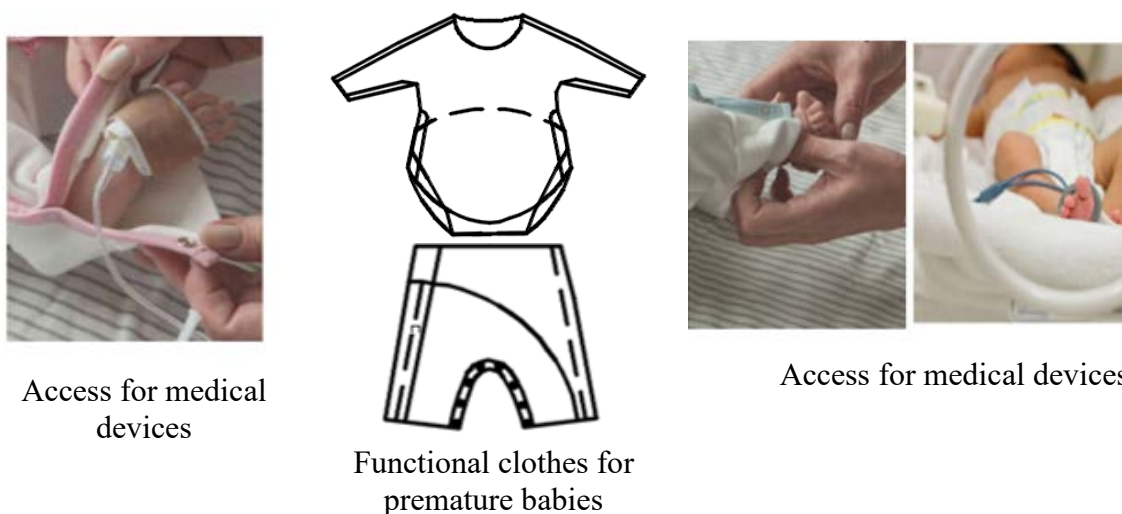


Figura 4. Functional model - overalls with long sleeves

The „adjustment-fixing” method of the product is used for premature babies; it depends on the degree of prematurity and assures the right adjustment of the sleeve, product and pants length. This type of transformation is used to control the width of the pants on the waistline, with the help of folding, in the case of clothing with waist support. Buttons or staples are recommended as fasteners for this type of clothing, allowing an easy and fast opening.

An important requirement in the design of structural-functional elements of clothing for premature babies is their reliable fixation, as some medical procedures are performed over a long period of time. The reliable fixation of the clothing products will ensure the maintenance of the sterility of the area of application of medical procedures, as well as comfortable condition for the child. It should be noted that most respondents, both hospital staff and parents, considers the functional textile products convenient during medical procedures by reducing the needed time.

5. DISCUSSIONS

A case study was conducted in intensive care units, where were examined the nurse’s types of medical manipulations, in order to meet the pre-established requirements of basis of products development. During the study were used the method of observation and subsequent testing of newly designed products. Each manipulation in medical conditions has been intensively studied.

The developed products were made of a cotton fabric. In terms of testing and use, the nurses indicated that the products provide an easy access. They have a locking system that favours the opening to certain parts of the body; it will take more than 3 seconds to put on and take off the product. There are also holes on purpose, which allow connecting devices and recording the vital signs of the baby. The ease of cleaning the products has been tested, and corresponding instructions have been provided.

Some limitations of this pilot clinical study refer to the fact that the products were not tested in the case of infants whose temperature was adjusted without an incubator. The

products developed favour the proper provision of medical care and handling for this group of carriers.

6. CONCLUSIONS

The pilot study was focused on the dressing and undressing process, performing medical manipulations even in case of neonatal emergencies. The textile products were tested, the results were analyzed according to the data obtained during the study, it confirms the easiness in use.

The health of premature babies remains a significant challenge in NICU, and functional clothing, designed according to the requirements and methods of handling these little ones could be one of the potential methods to reduce neonatal mortality.

The products correspond to the morphometry of the premature baby and are made of natural materials. The main advantage of the developed products consists in the wrapping system to obtain the shape of the product. This system allows obtaining the products based on flat elements and the exclusion of the seams, which can be traumatic for the premature baby. The products cover, by folding, the parts of the flat elements, forming soft holes for the head and limbs, and offering the possibility of moving the limbs without twisting or pressing the attached medical devices. The selected closing system consists of buttons which are placed on the edges of the flat elements, without any contact with the child's body, and is ergonomic at the same time.

For the upbringing and development of premature babies in the intensive care unit, the presence of functionally adapted clothing plays an important role; they meet several important requirements during medical manipulations and procedures to which they are subjected. These products offer functionality, ergonomics, easy access to medical devices, comfort and safety for healthy growth and speedy recovery of the premature babies.

REFERENCES

- [1] Montes Bueno, T., et al., *Effect of hygiene interventions on the thermal stability of extremely low-birth-weight newborns in the first two weeks of life*, Spain: Elsevier España, 2005
- [2] Fraser, D., *Association of Women's Health, Obstetric, and Neonatal Nurses. & AWHONN Late Preterm Infant Initiative, (Eds.), Late preterm infant assessment guide*, Washington D.C., Association of Women's Health Obstetric and Neonatal Nurses, 2007
- [3] Liaw, J., et al., *Caregiving and positioning effects on preterm infant states over 24 hours in a neonatal unit in Taiwan*, In: *Research in Nursing & Health*, 2012, 35, 2, 132-145, <https://doi.org/10.1002/nur.21458>
- [4] Mok, Q., et al., *Temperature instability during nursing procedures in preterm neonates*, IN: *Archives of Disease in Childhood*, 1991, 66, 7, 783-786
- [5] Newnham, C.A., et al., *Measuring preterm cumulative stressors within the NICU: The neonatal infant stressor scale*, In: *Early Human Development*, 2009, 85, 9, 549-555, <https://doi.org/10.1016/j.earlhumdev.2009.05.002>
- [6] Carbajal, R., et al., *Epidemiology and treatment of painful procedures in neonates in intensive care units*, In: *JAMA: The Journal of the American Medical Association*, 2008, 300, 1, 60-70, <https://doi.org/10.1001/jama.300.1.60>
- [7] Волова, М.В., *Статья в сборнике трудов конференции. Этапы реабилитационной помощи недоношенным детям*, 2016, 21-28
- [8] Equipment in the NICU: What does what?, available at: <https://www.earlybaby.info/en/in-the-nicu/equipment-in-the-nicu-what-does-what.html> [Accessed on February 2020]
- [9] SM GOST R 50713:2005. Articles for newborns and children nursery. General technical conditions



CHARACTERIZATION OF AIRBORNE PARTICLES IN MECHANICAL TEXTILE YARNS PROCESSING

DOI: 10.35530/TT.2021.58

E. Visileanu*, C. Mihai, A. Ene, M.C. Grosu, R. Scarlat, A. Vladu

National Research Development Institute for Textile and Leather, Romania
(E-mail: e.visileanu@incdtp.ro)

Abstract: Nano and micro plastics (NP/MPs) represent one of the most challenging classes of micro-pollutants, with occurrence across all ecosystems and size distributions ranging from the nanometre to the millimetre scale. Natural environments are receiving MPs in the form of anthropogenic direct release as well as disintegrated and loose products of larger plastics via biological activities, mechanical abrasion, and UV radiation. During the processing steps, the textile yarns are subjected to friction either by different driving organs or between themselves at the binding points. The magnitude of the friction forces is influenced by the nature of the yarns, the structure of the yarn, the type, and the raw material from which the driving organs of the machines are made. The paper presents the shape and dimensions of the particle that is released in the air during the abrasion resistance test of three types of polyester yarns: spun yarn, multifilament yarn, and monofilament yarn. The structure composition of the particles consists of more microfibrils (34%) in the case of spun yarn and the finest microparticles were obtained from monofilament yarn (0,004 μ m).

Keywords: health, particles, fibres, stiffness, abrasion

1. INTRODUCTION

Plastics are highly versatile materials that have brought huge societal benefits. They can be manufactured at low cost and their lightweight and adaptable nature has a myriad of applications in all aspects of everyday life, including food packaging, consumer products, medical devices, and construction. By 2050, however, it is anticipated that an extra 33 billion tonnes of plastic will be added to the planet. Given that most currently used plastic polymers are highly resistant to degradation, this influx of persistent, complex materials is a risk to human and environmental health. Continuous daily interaction with plastic items allows oral, dermal, and inhalation exposure to chemical components, leading to the widespread presence in the human body of chemicals associated with plastics [1-3].

Nano and micro plastics (NP/MPs) represent one of the most challenging classes of micro-pollutants, with occurrence across all ecosystems and size distributions ranging from the nanometre to the millimetre scale. These broad composition and size distribution ranges limit the efficiency of detection methods, often inherently focused on a single and narrow class of NP/MPs sizes. In addition to their demonstrated native toxicity, NP/MPs may act as efficient carriers of pollutants and pathogens onto their surface, facilitating the transfer and penetration of other classes of hazardous materials [4-6].

The mismanagement and dumping of domestic and commercial plastic wastes are the major cause of pollution in a natural setting. Natural environments are receiving MPs in the form of anthropogenic direct release as well as disintegrated and loose products of larger

plastics via biological activities, mechanical abrasion, and UV radiation. NPs, imposed more potential risk in comparison to MPs as they can easily able to enter cells/ tissues. Complexity in separation and identification of NPs, their abundance in the environmental setting has been generally overlooked to date. Hence, the physical presence and health menace of NPs may be underrated [7-8].

2. MATERIALS AND METHODS

Textile fabric may be defined as the flexible assembly of fibres or yarns, either natural or manmade. It may be produced by several techniques, the most common of which are weaving, knitting, bonding, felting, or tufting. Conventional fabrics (woven, knitted) are produced in such a way that the fibres are first converted into yarn and subsequently this yarn is converted into fabric [9]. During the processing steps, the yarns are subjected to friction either by different driving organs or between themselves at the binding points. The magnitude of the friction forces is influenced by the nature of the yarns, the structure of the yarn, the type, and the raw material from which the driving organs of the machines are made.

Due to the friction forces, bending, stretching of the yarns, that take place during these processes, degradations of fibres/yarns occur and micro plastics/microfibres are released into the air/water. A series of laboratory devices simulate these actions to determine the strength of yarns or semi-finished products to the action of frictional forces.

Fibre fragments are one of the dominant types of micro plastics in environmental samples, suggesting that synthetic textiles are a potential source of microplastics for the environment. Textile abrasion can induce fibre fibrillation and therefore lead to the formation of much finer fibre fragments. To determine the abrasion resistance of the yarns, a testing device was built (figure 1), whose constructive principle consists in simulating the friction phenomena, which the textile yarns are subjected to, during the steps of textile mechanical processing (spinning, warping, weaving knitting) and electronic monitoring of their behaviour.

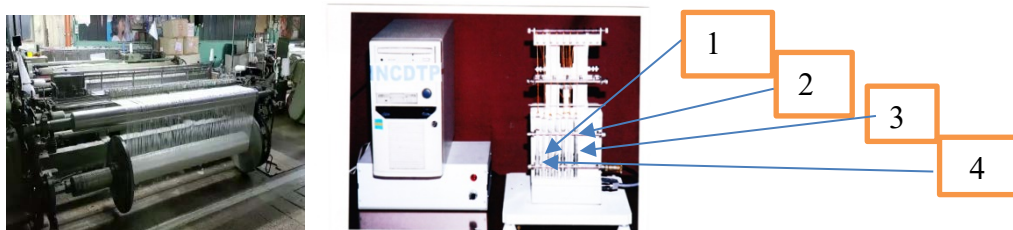


Figure 1. Weaving machine and yarn rubbing device: 1 - tensioning mechanism; 2 - friction mechanism; 3 - the drive mechanism; 4 - the weaving simulation mechanism

The device consists of the following components: 1 - tensioning mechanism, 2 - friction mechanism, 3 - the drive mechanism, 4 - the weaving simulation mechanism. The device simultaneously performs the friction of 10 yarns in the cockles, their movement, with a stroke length of 0-40 mm is generated by a motor whose speed can be varied. The preliminary pretension load of the yarns can be modified in increments of 10 g, within the limits: 50-140 mg.

The method for determining the abrasion resistance of textile yarns is in accordance with the international standards ISO 9290 and ASTM-D 1422. To collect the particles released during the rubbing of the cochlear yarns, the device was covered with a box with

antistatic walls. The collection of particles was done by the static method (deposition) in Petri dishes, sterile in the flow, with ventilation, with a diameter of 90 mm.

2. RESULTS AND DISCUSSION

For the laboratory experiments, 3 variants of 100% PES yarns with the different structures were used: Nm 20/2 spun yarn (FPES), 195/32f dtex multifilament yarn (MPES), and 0.19 mm monofilament yarn (MOPES) of whose characteristics are presented in table 1 and in figures 3, 4, 5 and 6 are their diagrams by comparison.

Table 1. Type sizes for camera-ready papers

No.	Yarn feature / variant	UM	Spun yarn	Multifilament yarn	Monofilament yarn
			100% PES-FPES	100%PES - MPES	100%PES-MOPES
1	Length density	Tex/Nm	50.6 x2/19.8/2	-	-
		Den/dtex	-	175.5/32f/195.0/32f	342/380
	Coefficient of variation	%	4.9	1.34	-
	Standard deviation	-	4.96	0.26	-
2	Diameter	mm	0.22	0.14	0.190
	Breaking strength	N	35.51	6.25	16.7
	Coefficient of variation	%	4.2	8.61	2.9
3	Standard deviation	-	1.5	0.53	0.45
	Elongation at break	%	16.23	32.08	28.35
	Coefficient of variation	%	2.84	8.83	7.9
4	Standard deviation	-	0.46	2.83	2.2
	Torsion/twist	t/m	469.0/321.2	39.6	-
	Coefficient of variation	%	3.57/3.67	11.61	-
5	Standard deviation	-	8.38/2.93	2.3	-
	Deformation resistance	KPa	147.7	119.0	114.1
	Coefficient of variation	%	6.89	1.62	3.67
6	Standard deviation	-	10.13	1.93	4.19
	Deformation	mm	14.4	14.2	9.5
	Coefficient of variation	%	22.8	4.93	11.75
7	Standard deviation	-	3.29	0.70	1.12
	Young's modulus	MPa	7142.8	1660.6	5357.0

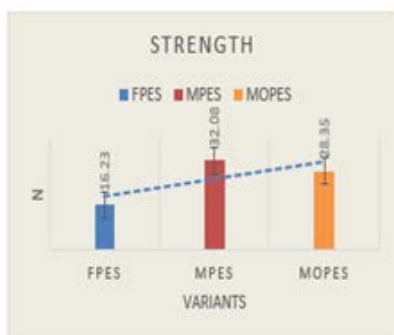


Figure 3. Breaking resistance

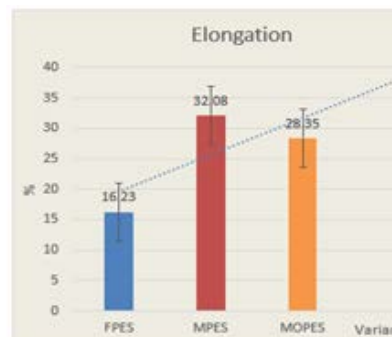


Figure 4. Elongation

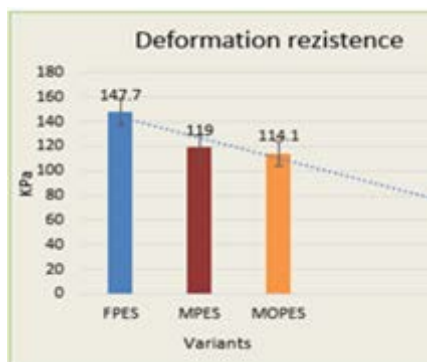


Figure 5. Deformation resistance

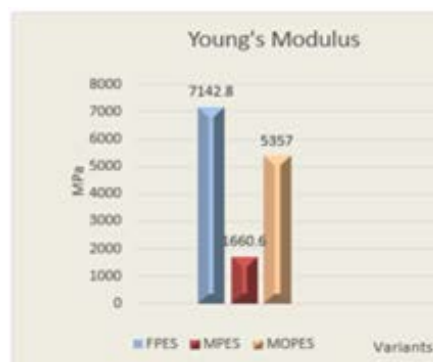


Figure 6. Young's modulus

The deformation resistance of the yarns was determined on the Tru Burst3 Bursting Strength Tester having upper-pressure limit – 100 kPa and distension range between: 0.1-70 mm and the method applied according to SR EN ISO13937-4 / 2003 (adapted). The highest breaking strength (N) is obtained for the FPES variant (35.51N) which records the highest values of deformation resistance of 147.7 KPa, deformation (14.4 mm), and modulus of elasticity (7142.8 MPa), but with the lowest value of elongation at break (16.23%).

The same correlation between the breaking strength and young's modulus is also maintained in the case of the MOPES variant (16.7 N and respectively 5357.0 KPa) and MPES (6.25N and respectively 1660.6 KPa). The highest resistance to deformation is obtained for the FPES variant (147.7 KPa), followed by MPES (119.0 KPa) and MOPES (114.1 KPa). The deformation variation (mm) follows the same order: FPES (14.4 mm), MPES (14.2 mm) and MOPES (9.5 mm). The laboratory experiments of collecting the particles released in the air during the frictional stress of the three yarn variants were performed using the working parameters presented in table 2.

Table 2. Experiments' parameters

No.	Working parameters	FPES yarn	MPES yarn	MOPES yarn
1	Time (hours)	16.10	15.00	15.00
2	No. of cycles/min	600		
3	No. of cycles/total	582000	540000	528000
4	Pretention (mg)	40		

Morphological characterization of the collected particles was achieved by scanning electron microscopy (SEM), using an FEI Quanta 200 instrument, equipped with an Everhart-Thornley (ET) detector and using an acceleration voltage of 15 kV, in low vacuum mode. Microparticles were taken on the device tablet directly from the collecting Petri dishes (figures 7, 8 and 9).

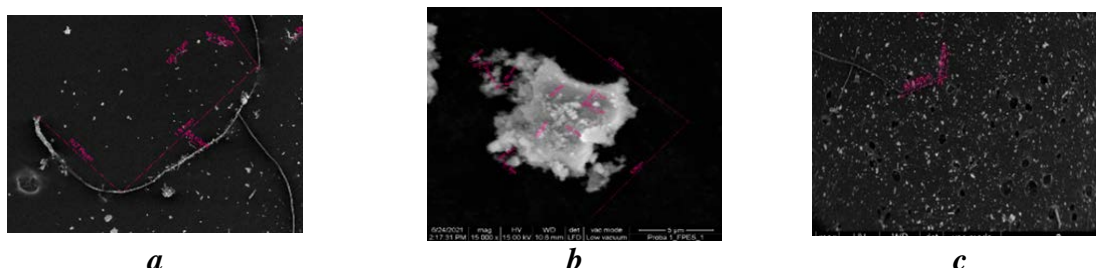


Figure 7. SEM images FPES sample: a – microfibrils; b – agglomerations; c - particles

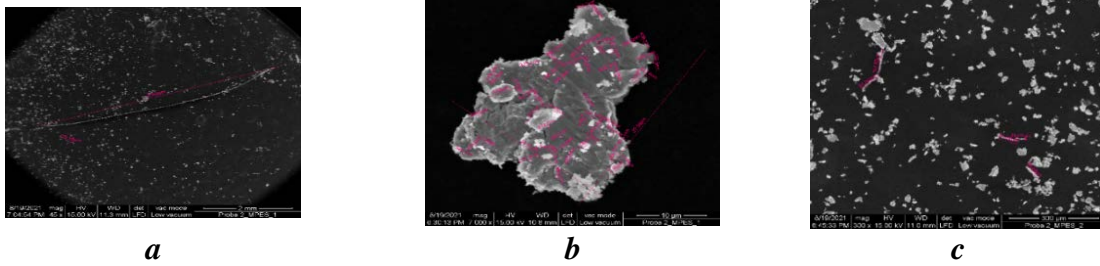


Figure 8. SEM images MPES sample: a) microfibrils b) agglomerations c) particles

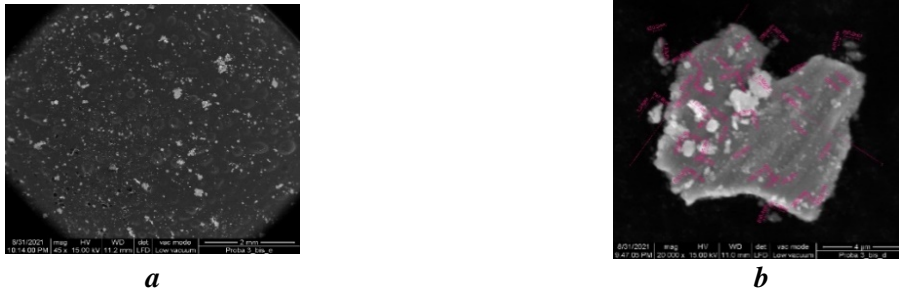


Figure 9. SEM images MOPES sample: a) agglomerations b) particles

In figures 7, 8 and 9 SEM images of airborne particles resulting from the application of the FPES, MPES si MOPES yarns friction test are presented.

The shape and size of particles, agglomerations, and fibrils in μm were determined. The characterization of the 3 statistical populations considered to define the type and size of the collected particles were performed, using specialized software, which allowed the analysis of the obtained data (using the ANALYZE menu) and their visualization (GRAPHS menu).

Variables that entered the analysis: particle area (round, rectangular) in μm^2 , the surface of particle agglomerations in μm^2 and fibril sizes (length) in μm .

The scores obtained from the experiments (for each statistical population studied) allowed the calculation of the main parameters of the distributions for each variable. The obtained values and the afferent histograms are presented in table 3 and figure 10.

FPES variant (Figure 10)

The variables “rectangle FPES1” and “circle FPES1” do not show great variability of the results, the “boxes” having small dimensions. However, for “FPES1 circle”, the value no. 12 ($0.116 \mu\text{m}^2$) is an extreme case, being located at a distance of more than 3 box lengths.

The variable “FPES1 agglomerations” highlights the distribution of 50% of the values, the lower edge representing the 25% percentile value, and the upper one the 75% percentile value. Thus, it is found that 25% of the values are below $5.55 \mu\text{m}^2$, 25% are between $5.55 - 12.37 \mu\text{m}^2$, 25% between $12.37 - 127.1 \mu\text{m}^2$ and 25% over $127.1 \mu\text{m}^2$. The value identified by 1 in the database (real value $324.48 \mu\text{m}^2$) is considered extreme in the range of 1.5 - 3 lengths. Also, the median is directed towards the lower edge of the "box", so it can be stated that the distribution is directed to the left and the small values are predominant (figure 11).

Table 3. Statistical indicators

Shapes	Mean	Median	Std. Deviation	Variance	Skewness	Kurtosis	Min.	Max.	Percentiles		
									25	50	75
Rectangular shape FPES1	0.79	0.37	1.42	2.04	4.64	25.38	0.04	9.23	0.18	0.37	0.74
Circle FPES1	0.02	0.01	0.02	0	3.14	11	0	0.11	0.01	0.01	0.02
Agglomeration FPES1	69.51	12.37	96.6	9332.61	1.87	3.21	3.27	338.64	5.55	12.37	127.1
Microfibrils FPES1	361.2	279.1	223.21	49826.31	0.98	0.03	109	973.17	196	279.1	520.9
Rectangular shape MFILPES2	1.25	0.55	1.8	3.25	2.6	6.73	0.03	8.38	0.21	0.55	1.44
Circle MFILPES2	0.08	0.06	0.06	0	1.88	4.27	0.01	0.33	0.03	0.06	0.11
Agglomeration MFILPES2	71.92	10.24	120.79	14592.41	1.73	1.53	2.11	325.96	5.67	10.24	119.3
Microfibrils MFILPES2	160.9	150.28	96.92	9394.06	0.68	-0.21	35.2	352	65.8	150.3	229.5
Rectangular shape MOPES3	0.68	0.43	0.72	0.52	1.59	2.5	0.01	3.23	0.13	0.43	0.92
Circle MOPES3	0.04	0.03	0.048	0	2.71	10.27	0	0.26	0.01	0.03	0.06
Agglomeration MOPES3	387.8	230.58	567.38	321924	1.63	1.33	2.8	1614	6.86	230.6	317.2
Microfibrils MOPES3	68.64	87.13	59.01	3482.22	-1.27	-	2.6	116.2	2.6	87.13	-

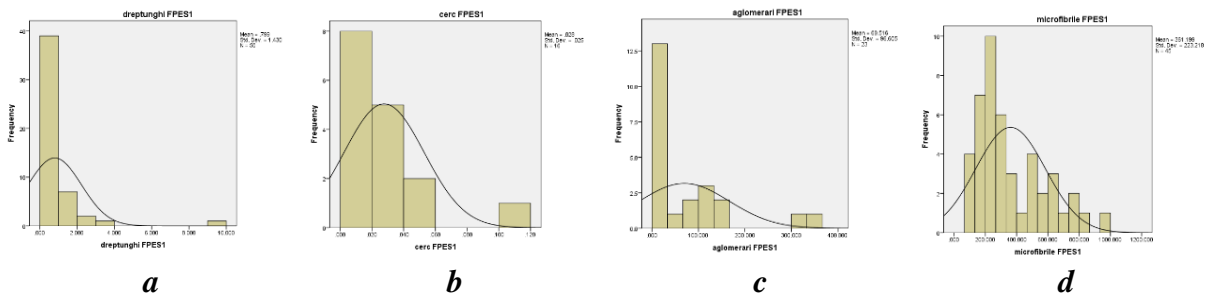


Figure 10. Histograms for particle surface variables: a – round; b – rectangular; c - surface of particle agglomerations; d - fibril dimensions (length) - FILPES1

The variable microfibrils FPES1 does not present extreme cases, the median being directed as in the previous case, towards the lower edge of the “box”, so the small values being predominant. Additionally, 50% of the values are in the range [196; 520.9] μm^2 .

MPES variant

As in the previous case, the first 2 variables (related to the shape of the identified particles) do not show large variations of the values, but in the case of the variable “rectangle MFILPES2”, value no. 6 from the database (real value 8,385 μm^2) is considered extreme value is located in the range of 1.5 - 3 box lengths.

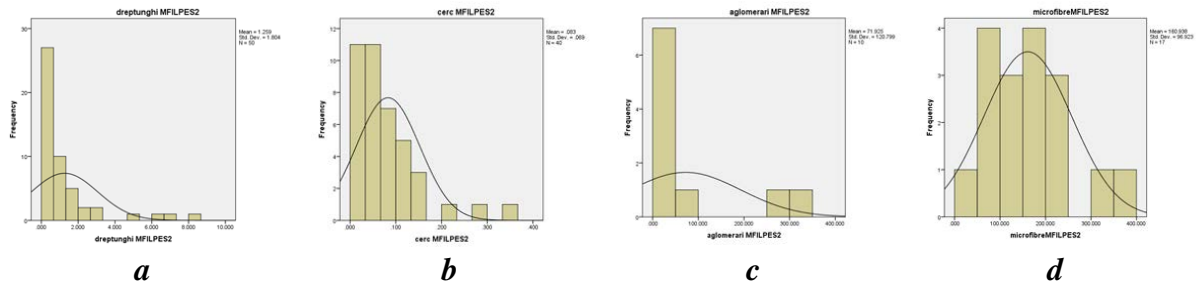


Figure 11. Histograms for particle surface variables: a – round; b – rectangular; c - surface of particle agglomerations; d - fibril dimensions (length) - MFILPES2

The variable “agglomerations MFILPES2” presents the median placed towards the lower edge of the box, so the distribution is directed to the left and the small values are predominant. The outer limits of the graph highlight the small values within 1.5 lengths. The values 5 and 6 in the base, respectively $267.05 \mu\text{m}^2$ and $325.96 \mu\text{m}^2$ are considered extreme. In this case, there is a large spread of values, 25% of the values being located below $5.67 \mu\text{m}^2$, 50% are located in the range $[5.67; 119.32] \mu\text{m}^2$ and 25% over $119.32 \mu\text{m}^2$.

The variable “microfibrils MFILPES2” does not present extreme cases, however, there is a very high variability of the data, 50% of the values being located in the range $[65.78; 229.50] \mu\text{m}^2$.

MOPES variant

There is no large data scattering for the variables “rectangle MOPES3”, “circle MOPES3”, and “microfiber MOPES3”. In the case of this last variable, the median is placed towards the upper edge of the box, so the distribution is inclined to the right, and therefore the large values predominate.

The variable “MOPES3 agglomerations” shows the median placed towards the lower edge of the box (figure 13) so the distribution is directed to the left and the small values are predominant. However, there is a very high variability of the data, with 50% of the values being in the range $[6.86; 317.23] \mu\text{m}^2$.

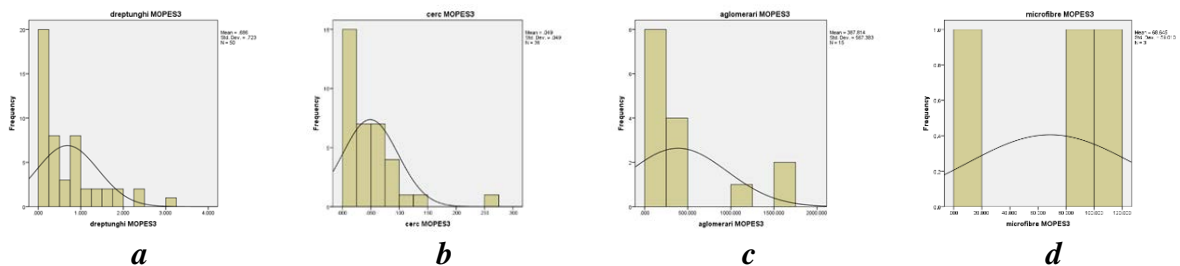


Figure 12. Histograms for particle surface variables: a – round; b – rectangular; c - surface of particle agglomerations; d - fibril dimensions (length) - MOPES3

For all variables, the coefficient of variability is higher than 30%, so the arithmetic mean is not representative for any sample, the groups being inhomogeneous.

The skewness index for 8 of the 12 variables does not exceed ± 1.96 , highlighting, in this case, the extent to which the average moves away from the median and implicitly the curve of normal data distribution moves away from the middle, moving to the left (at FPES1 agglomerations, FPES1 microfibers, MFILPES2 circle, MFILPES2 agglomerations, MFILPES2 microfibers, MOPES3 rectangle, MOPES3 agglomerations) and to the right for MOPES3 microfibers, respectively. For the other 4 variables, it is found to be out of normal.

The vaulting index (kurtosis) has positive values, so the distribution is leptocortical - within the limits of a normal distribution for FPES1 microfibers, MFILPES2 agglomerations, and MOPES3 agglomerations, and MFILPES2 microfiber plasticurtica. For the other 8 variables, it is found that the distributions are out of normal.

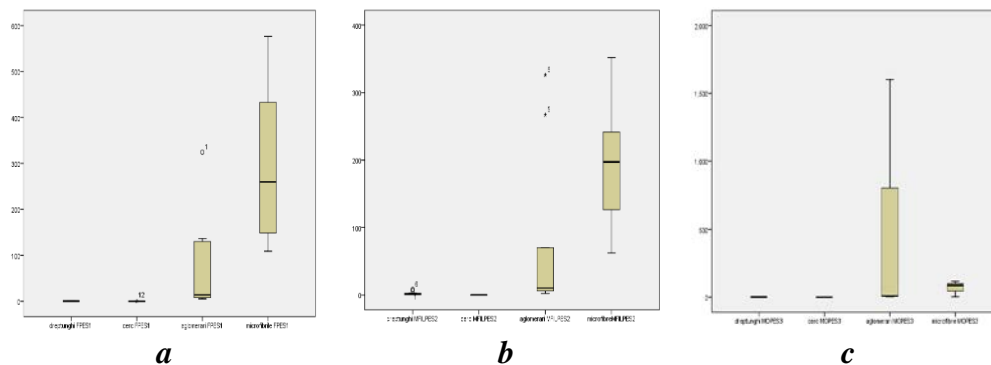


Figure 13. Boxplot graphs for particle surface variables:
a - round; b - rectangular; c - the surface of the particle agglomerations;
d - the dimensions of the fibrils (length)

5. CONCLUSIONS

Polyester particles were collected in laboratory experiments that simulated the rubbing of threads in the cochleae of weaving machines. The morphological analysis of the particles showed that:

- for variant FPES - 37% of the identified particles have a parallelepiped shape, 12% have a spherical shape, 17% are agglomerations of particles and 34% are microfibrils;
- for MPES variant - 43% of the identified particles have a parallelepiped shape, 34% have a spherical shape, 9% are agglomerations of particles and 14% are microfibrils;
- for MOPES variant - 48% of the identified particles have a parallelepiped shape, 35% have a spherical shape, 14% are agglomerations of particles and 3% are microfibrils.

ACKNOWLEDGEMENTS

This research is carried out within the project:” Understanding exposure and toxicity of Micro- and Nano-Plastic contaminants in humans, POLYRISK” - Horizon 2020, Call: H2020-SC1-BHC-2018-2020” (Better Health and care, economic growth and sustainable health systems).

REFERENCES

- [1] Galloway, T.S., *Micro- and Nano-plastics and Human Health*, Bergmann M., Gutow L., Klages M. (eds) Marine Anthropogenic Litter. Springer, Cham., 2015
- [2] Marie, E., Cyril, H., Peter, D.H., Veeriah, J., Johannes, V., Damien, L.C., Judy, L., Ludovic, F.D., *Nano/micro plastics – Challenges on quantification and remediation: A review*, In: Journal of Water Process Engineering, 2021, 42, 102128, ISSN 2214-7144
- [3] Manish, K., Hongyu, C., Surendra, S., Shiyi, Q., Huimin, L., Mukesh, K.A., Sunil, K., Lal, S., Zengqiang, Z., Nanthi, S.B., Ashok, P., Sunita, V., Mohammad, J.T., *Current research trends on micro- and nano-plastics as an emerging threat to global environment: A review*, In: Journal of Hazardous Materials, 2021, 409, 124967, ISSN 0304-3894
- [4] *Plastics Europe*, 2018, Available at: https://www.plasticseurope.org/application/files/6315/4510/9658/Plastics_the_facts_2018_AF_web.pdf [Accessed on June 2021]

- [5] Gigault, J., Halle, A., Baudrimont, M., Pascal, P.Y., Gauffre, F., Phi, T.L., El Hadri, H., Grassl, B., Reynaud, S., *Current opinion: what is a nanoplastic*, In: Environ. Pollut., 2018, 235, 1030-1034
- [6] Yee, Maxine S.-L., Hii, L.-W., Looi, C.K., Lim, W.-M., Wong, S.-F., Kok, Y.-Y., Tan, B.-K., Wong, C.-Y., Leong, C.-O., *Impact of Microplastics and Nanoplastics on Human Health*, Nanomaterials, 2021, 11, 2, 496
- [7] Ma, Y.N., Wang, L., Wang, T., Chen, Q.Q., Ji, R., *Microplastics as vectors of chemicals and microorganisms in the environment*, In: Bolan, N.S., Kirkham, M.B., Halsband, C., Nuggeoda, D., Ok, Y.S. (Eds.), Particulate Plastics in Terrestrial and Aquatic Environments, CRC Press, 2020, 209-230
- [8] Chibuisi, G.A., Caterina, F., Saravanadevi, S., Adebayo, L.O., Kannan, K., *Micro(nano)-plastics in the environment and risk of carcinogenesis: Insight into possible mechanisms*, In: Journal of Hazardous Materials, 2021, 416, 126143, ISSN 0304-3894
- [9] Gopinath, P.M., Saranya, V., Vijayakumar, S., Mythili Meera, M., Ruprekha, S., Kunal, R., Pranay, A., Thomas, J., Mukherjee, A., Chandrasekaran, N., *Assessment on interactive prospectives of nanoplastics with plasma proteins and the toxicological impacts of virgin, coronated and environmentally released-nanoplastics*, In: Sci. Rep., 2019, 9, 1-15
- [10] Marks, R., Robinson, ATC., *Woven cloth construction*. Manchester: The Textile Institute, 1973



DEVELOPMENT OF TEXTILE-RUBBER COMPOSITE MATERIALS USING RECYCLED RUBBER AND TEXTILES WITH APPLICATIONS IN INDUSTRY

DOI: 10.35530/TT.2021.15

F.St. C. Mustata*, A. Curteza

“Gheorghe Asachi” Technical University of Iasi, Romania
(E-mail: florinmustata@gmail.com)

Abstract: This paper study methods to obtain composite materials based on recycled rubber from End-of-Life tires and scrap textile. Rubber particles was obtained by industrial shredding procedures and separated by dimension, using sieves. Recycled cotton weave was obtained from scrap cotton textiles. The composite material was produced mixing the recycled rubber powder with a solution of acrylate rubber (AR), (NipolR AR 51) in acetone/ethyl acetate, then coating that composition on a 100% recycled cotton weave. After application, the composite was dried in a dryer with ventilation. The final composite material will be chemical characterized. Attempts will be made to determine whether the composite can be used as isolation material with temperature dissipation characteristics.

Keywords: recycled rubber and textiles, composite materials, circular economy

1. INTRODUCTION

The necessity of transportation generates a steady growth the demand in car tires. The quantity of the End-of-Life tires increase despite all the recycle policies implemented over the earth. Global recycling policies adopted in Europe and United States, limit a portion of the waste generation. A big portion of the recycled End-of-life tires is used for energy generation in kilns, as raw material in the chemical industry (carbon black) and in construction applications as the asphalt mixtures [1]. Despite all these uses, there is no annual reduction in waste rubber generation. Some unconventional approach was done in few countries to try to use rubber ash or waste rubber powder as fertilizers to enhance soil deficiencies in Zn and Fe [2].

Another big portion of the global waste it is the textile waste generated by textile industry. The textile waste quantity in 1980 year in United States was around 5 billion pounds which increased up to 32,44 billion pounds in 2014. The textile waste in United States excide yearly 9.5% of municipal solid waste, the deficiency of landfills generates greenhouse gases. As an example in the processing cotton, there are by-products who generate pollution (pesticides, nitrous oxide, greenhouse gas), as around 0.15 kg of pesticide is used for one shirt produced [3,4]. The large majority (about 95%) of the textile waste has a good potential to be recycled, however in the reality being that only 15% of the waste is recycled [5-7].

The objective of the present paper is to do experimental analysis that will provide information about methods to obtain End-of-Life tire-textile composites and their characterization as temperature isolators. The evaluation of the textile-rubber composite

was done using applying a heated electrode on the rubbery surface of the composite and measuring the thermal transfer thorough the material to another electrode, mounted on the textile surface of the composite.

2. MATERIALS AND METHODS

2.1 Materials

The materials used to obtain the rubber/textile composite are:

- a) Rubber powder
- b) Textile scraps material
- c) Acrylate rubber, NipolR AR, rubber solution

The rubber powder was obtained by grinding rubber from a motorcycle tire, known having more natural rubber in composition vs a car tire. Black, solid rubber powder with particles size up to 100 μm , moisture content < 0,25 %, density(ρ) = 1058 Kg/m^3 , measured with digital microscope VT-101 (figure 1, a)

Acrylate rubber (AR), NipolR AR 51 (density ρ = 1100 kgm^{-3} at 25°C, Mooney viscosity ML (1+4) at 100°C = 55; T_g = -4°C containing epoxy cure site monomer was obtained from Nippon Zeon Co. Ltd., Tokyo, Japan.

Acetone/ethyl acetate 75/25 g/g was a reactive grade purity (b.p. = 56.5°C, ρ =784 Kg/m^3 , b.p. = 77.1°C, ρ =902 Kg/m^3)

The AR solution in acetone/ethyl acetate had a concentration of 16 wt.%.

The recycled textile used for the composite is a 100% cotton base (natural cellulosic fibre) (Tesatura Iasi, Romania) with the thickness of 0.28 mm and weave mass of 143g/m² (figure 1, b)

2.2. Methods

Fourier transform infrared (FTIR) spectra were used to analyse the chemical structure of AR rubber and their blends with powder rubber. The FTIR spectra were registered at room temperature using a Vertex 70 (Bruker-Germany) apparatus equipped with a MIRacle™ ATR accessory with diamond crystal plate with 1.8 mm diameter for wave number between 500 to 4000 cm^{-1} . The spectra were processed with OPUS 6.5 software.

Density of the powder sample was measured using a pycnometer (ASTM D854 - 14 Standard Test Methods for Specific Gravity of Soil Solids by Water Pycnometer) (rectangular sample 10 mm x 5 mm x 2 mm).

For the evaluation of humidity, the samples are dried, at 105°C until they reached a constant weight. The samples humidity was calculated with the next formula:

$$H (\%) = 100 \times (W_i - W_d) / W_i \quad (1)$$

where H is the percent of the humidity; W_i is the weight of initial sample and W_d is the weight of dried sample.

The dimension of rubber powder was measured with digital microscope VT-101 (figure 1, a).

The structure of the cotton weave from the recycled textile is revealed under digital microscope (figure 2, b).

AR rubber solution was done using rubber pellets with dimensions as 15 mm length, 10 mm width and 1.5 mm thickness at weight ratio 84 g acetone/ethyl acetate/16 g rubber. The pellets were grinded at dimensions of 3 mm/1 mm/1.5 mm. To the mixture acetone/ethyl acetate, AR rubber was added under agitation at 40°C and 200 rotations

per minute (rpm) till complete solving process. After the process is completed, filtration method is used to extract unsolved rubber particles.

The recycled rubber powder was obtained by mechanical grinding of a motorcycle tire. Then, the steel residue was magnetically separated. The sorting by sieving with a metal laboratory sieve with hole sizes up to 0.149 mm (MRC Laboratory-Instruments, Sieve mesh for laboratories, ASTM mesh 100, holes 0.149 mm) allowed to obtain an assortment with the dimensions between 0.01 mm - 0.12 mm.

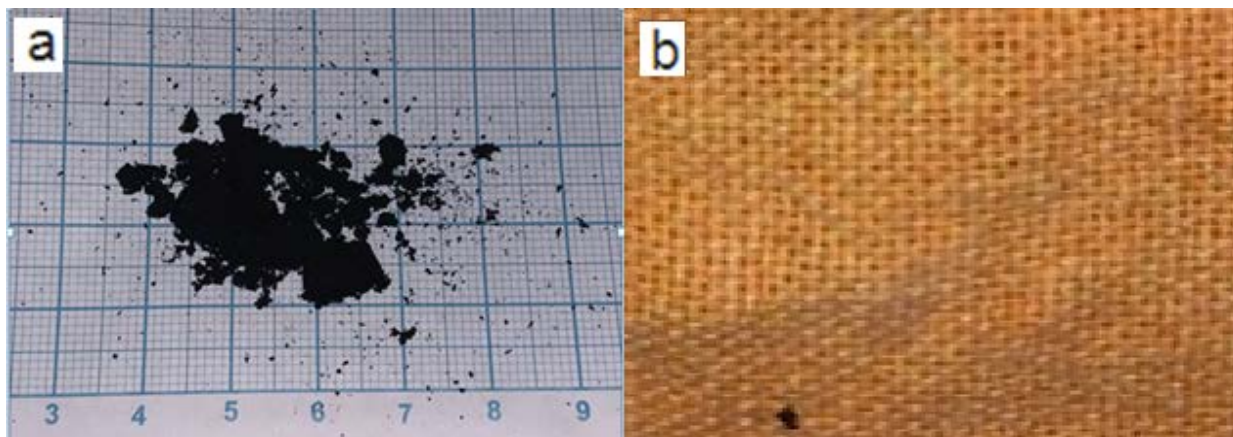


Figure 1. Materials: a - rubber powder; b - recycled cotton

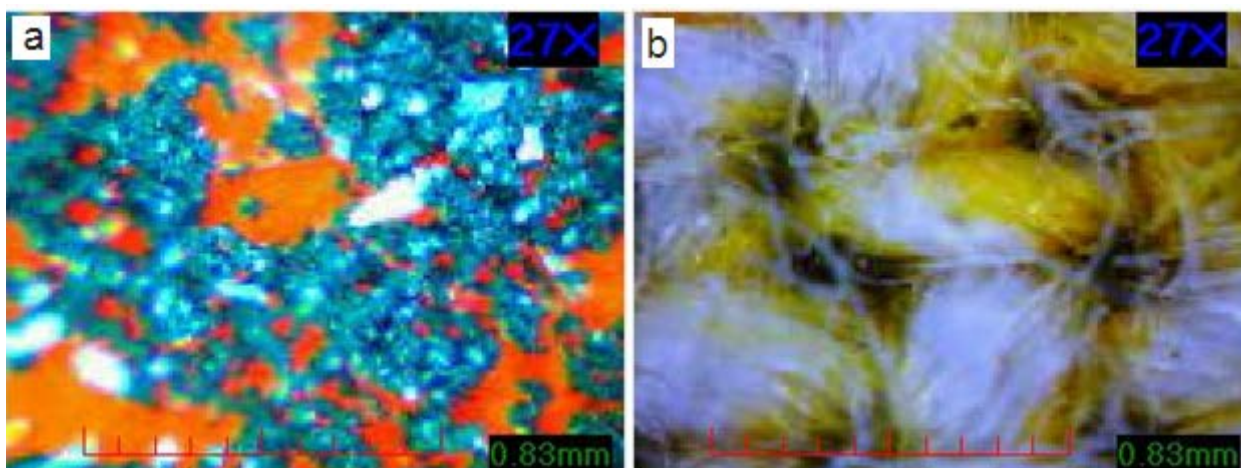


Figure 2. Digital microscope images: a - rubber powder; b - cotton weaves

The structure of rubber powder and the cotton weave are registered under digital microscope (figure 2, b). The rubber composite at weight ratio 1/1 rubber powder/AR rubber were obtained by mixing of 16 g of the rubber powder and a 100 g solution of 16% AR rubber in acetone/ethyl acetate. The powder was added slowly under agitation during 10 minutes. The rubbery solution with 50% recycled rubber powder content resulted was applied on the cotton weave as a thin film with the scope of forming a rubber-textile composite material. The solution was applied with a coating knife on the textile support at a desired thickness. The opposite face of the textile support stayed on a silicone paper with role in easing the application effort. After depositing the rubbery solution on the textile surface, will dry the surface at cold during 60 min, and then hot drying 60 min at 30°C, 120 min at 40°C, 180 min at 50°C, this process being done in a dryer with forced ventilation.

The visual aspect of the samples was evaluated with a digital microscope VT-101. The thickness of the material obtained was measured with a high accuracy

micrometer Mitutoyo MDH-25MB with 0.0001 mm resolution. The structure of the rubbery surface of the composite material under digital microscope (figure 3, a), the back textile surface is presented in figure 3, b.

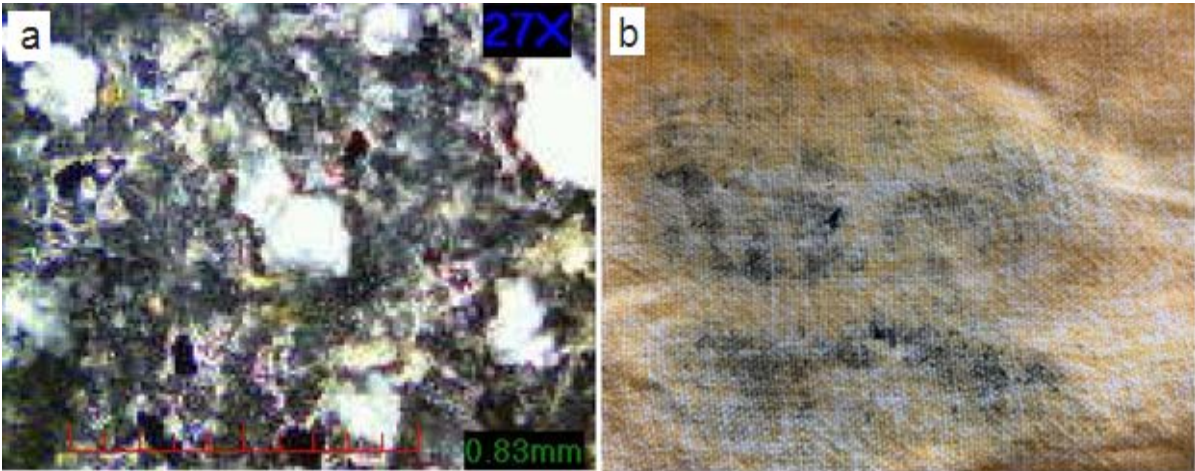


Figure 3. Digital microscope images: a - rubber-textile composite material front; b - material back

After applying the rubber mix solution on the cotton weave and drying at 24°C, were obtain 4 samples with thickness of: with 0.38 mm, 0.54 mm, 0.65 mm - 0.68 mm, 1.38 mm. The aspect of the obtained composite material at weight ratio 1/1 rubber powder/AR rubber with 0.54 mm is presented in figure 4.

Table 1 show the quantities of rubber powder and acetone/ethyl acetate AR rubber solution used in the manufacturing process of the four composite samples.

Table 1. Quantities used in the manufacturing process

Recycled rubber powder (g)	AR solution (g)	Composite thickness (mm)
2.60	11.96	0.38
3.69	17.00	0.54
4.65	21.40	0.68
9.44	43.40	1.38

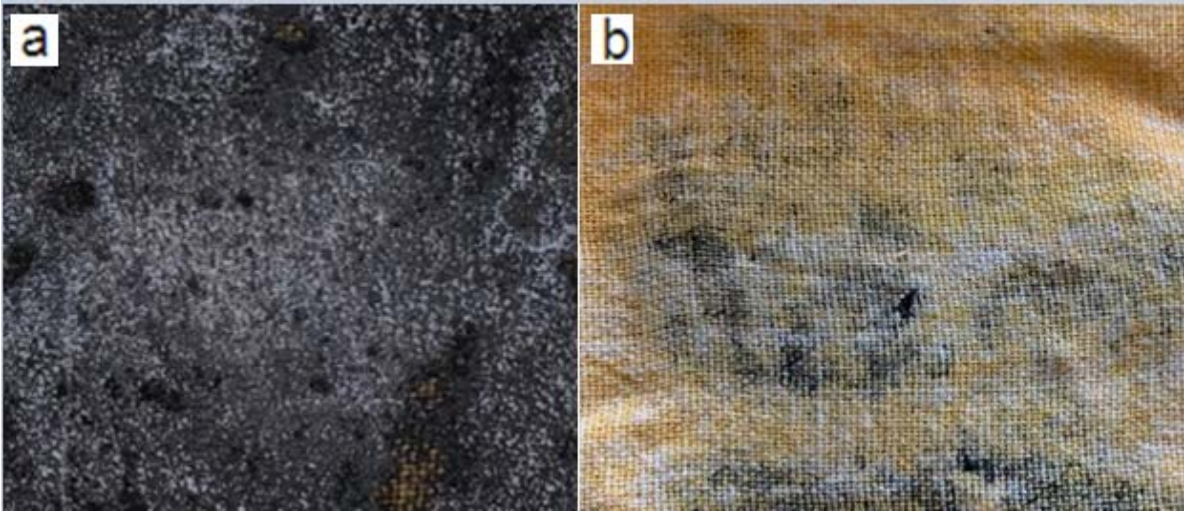


Figure 4. Rubber-textile composite material: a - front; b - back

Resistance at thermal transfer and heat damage was measured. The material thickness was measured with a precision micrometre. Measurements are done at 24°C, air relative humidity 35%. The temperature transfer was measured in between of two aluminium electrodes with useful surface of 7 mm, one electrically heated with a resistance. The temperature loss function of exposure time was measured. The measurement was done on four composite probes with 0.38 mm, 0.54 mm, 0.65 mm - 0.68 mm, 1.38 mm.



Figure 5. Rubber-textile composite material heat transfer measurement

The temperature variation was measured using two thermocouple coupled at an industrial thermometer-controller.

3. RESULTS AND DISCUSSION

3.1 Appearance

The composite material resulted can be seen in figure 6. The rubber solution didn't get through the textile component as seen on the back of the composite.



Figure 6. Rubber-textile composite material

3.2. Infrared spectroscopy

Infrared spectroscopy is a method for the determination of the structure of AR and AR/recycled rubber blend, the FTIR spectra were collected. In figure 7, the spectra of pure AR and AR/recycled rubber blend are shown. The assignment of the most important infrared bands was made according to literature data [8-12]. In the spectrum of both samples the signals located in the range between 3100 and 2800 cm^{-1} can be assigned to the CH, CH₂ and CH₃ stretching frequency, signals that can also be detected in the region 1500-1400 cm^{-1} with the medium values at 1488 cm^{-1} , and at 1220 cm^{-1} for CH groups. The signals present at 1726 cm^{-1} can be assigned to the CO groups from ester groups from the macromolecular chain. Resistance at thermal transfer of the

rubber-textile composite is a function of the chemical structure and the material thickness.

3.3. Thermal characterization of rubber/textile composite

Resistance at thermal transfer of the rubber-textile composite is a function of the chemical structure and the material thickness. The temperature loss function depending of exposure time was presented in figure 8. As can be seen in figure 8, the temperature variation between the two faces of the composite at a given time is a function of the layer thickness, having relatively constant values until the temperature reaches about 70°C indicating that up to this temperature the composite has good thermal insulator properties. Above this temperature the composite begins to deteriorate, starting in the first wrinkle with its melting (figure 9).

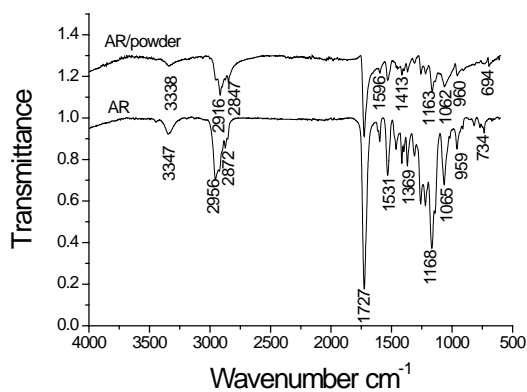


Figure 7. IR spectra of AR and AR/rubber powder

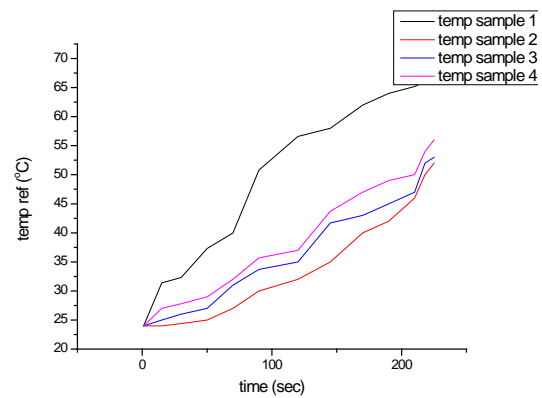


Figure 8. Variation of the surface temperature on composite samples with 0.35 mm, 0.54 mm, 0.68 mm, 1.38 mm thickness depending on the exposure time

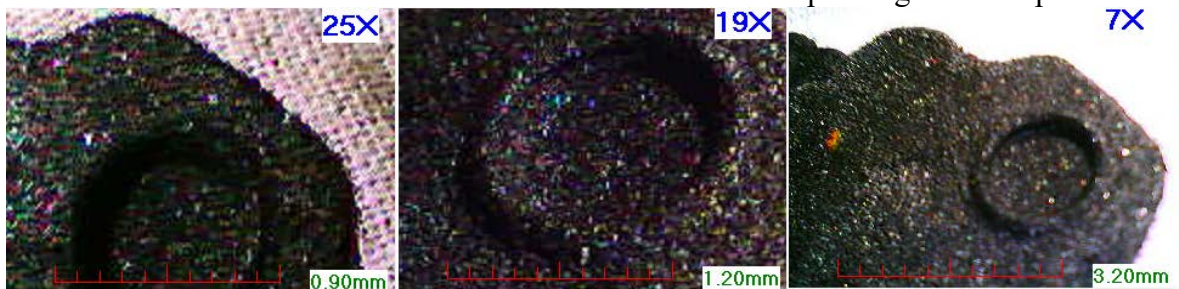


Figure 9. Rubber-textile composite material damage after heat exposure

4. CONCLUSION

The composite material obtained keep textile qualities on one of the faces, this being an important quality for future applications.

The thickness of the composite can be increased, generating a wide range of industrial application.

This research can provide a path to obtain textile composite materials with possible sound and vibration absorption applications and with low thermal isolation abilities (under 70°C), out of recycled materials as End-Of-Life tires and recycled textiles.

Future research on sound and vibration absorption will be done.

All of those prime materials can be provided from the same recycle facility.

Obtaining composites with good properties can be done using up to 50 wt% from recycle materials as powdered rubber obtained from used tires and scrap textiles. Starting from these researches, we can propose recycle plans, using the concepts of Circular Economy, with the possibility to utilize used tires and scrap textiles as prime materials for industry.

REFERENCES

- [1] Peterson, M.K., Lemay, J.C., Shubin, S.P., Prueitt, R.L., *Comprehensive multipathway risk assessment of chemicals associated with recycled ("crumb") rubber in synthetic turf fields*, In: Environmental Research, 2018, 160, 256-268, <http://dx.doi.org/10.1016/j.envres.2017.09.019>
- [2] Taheri, S., Khoshgoftarmanesh, A.H., Shariatmadari, H., Chaney, R.L., *Kinetics of zinc release from ground tire rubber and rubber ash in a calcareous soil as alternatives to Zn fertilizers*, In: Environmental Research, 2018, 160, 256-268
- [3] Navone, L., Moffitt, K., Hansen, K.-A.J., Blinco, J., Payne, A., Speight, R., *Closing the textile loop: Enzymatic fibre separation and recycling of wool/polyester fabric blends*, In: Waste Management, 2020, 102, 149-160, <https://doi.org/10.1016/j.wasman.2019.10.026>
- [4] Muthu, S.S., Li, Y., Hu, J.-Y., Mok, P.Y., *Recyclability Potential Index (RPI): The concept and quantification of RPI for textile fibres*, In: Ecological Indicators, 2012, 18, 58-62, <https://doi.org/10.1016/j.ecolind.2011.10.003>
- [5] Islam, S., Bhat, G., *Environmentally-friendly thermal and acoustic insulation materials from recycled textile.*, In: Journal of Environmental Management, 2019, 251, 109536, <https://doi.org/10.1016/j.jenvman.2019.109536>
- [6] Shirvanimoghaddama, K., Motamed, B., Ramakrishna, S., Naebe, M., *Death by waste: Fashion and textile circular economy case*, In: Science of the Total Environment, 2020, 718, 137317, <https://doi.org/10.1016/j.scitotenv.2020.137317>
- [7] Manohar, N., Jayaramudu, J., Suchismita, S., Rajkumar, K., Reddy, A.B., Sadiku, E.R., Priti, R., Maurya, D.J., *A unique application of the second order derivative of FTIR-ATR spectra for compositional analyses of natural rubber and polychloroprene rubber and their blends*, In: Polymer Testing, 2017, 62, 447-453
- [8] Bandyopadhyay, A., Bhowmick, A.K., De Sarkar, M., *Synthesis and characterization of acrylic rubber/silica hybrid composites prepared by sol-gel technique*, In: J. Appl. Polym. Sci., 2004, 93, 2579-2589
- [9] Kader, A., anil k. Bhowmick, A.K., *Novel thermoplastic elastomers from fluorocarbon elastomer, acrylate rubber and acrylate plastic*, In: Rubber Chem. Technol., 2001, 73, 662-676



AN INTEGRATED SOLUTION FOR THE ONLINE MARKETING OF CUSTOM-MADE GARMENTS THAT INCORPORATES A VIRTUAL FITTING ROOM

DOI: 10.35530/TT.2021.48

M. Avadanei^{1*}, A. Matasel², I. Ionescu¹, E. Loghin¹, D. Ionesi¹

¹Faculty of Industrial Design and Business Management, “Gheorghe Asachi” Technical University of Iasi, Romania

(E-mail: mavad@tex.tuiasi.ro, loghin.emil@gmail.com, iirina@tex.tuiasi.ro, dionesi@tex.tuiasi.ro)

²SC LIZZET SRL Company, Romania

(E-mail: matasel.alice@yahoo.com)

Abstract: We use IT applications to solve various problems, such as buying various things, communication or professional matters. Everything seems to be solved faster when we shop on online platforms (virtual stores) because we can analyse several offers, see the best deals and then decide which one suits our purpose. Sometimes the items bought online are returned for the following reasons: they do not look as they were presented on the website; these items have functional problems or do not fit (this is the situation with clothing and footwear products). Usually, the fit problems occur because the customer did not choose the right size, the model does not have a size range that fits the customer, or the customer has a particular body shape. The return rate (fit problem) can decrease if the customer can virtually try on the selected model during the purchase process to check how it looks on their body. Assuming that customers also have the option to personalise the product according to their body shape or desires, their satisfaction increases. In this case, the number of returned or unsold products is reduced, and a dynamic and positive advertising campaign for the brand can be carried out (based on customer reviews). This paper proposes an integrated solution for online marketing of customised clothing products (website for medium or small companies), using a virtual test room that simulates the product on the virtual mannequin in different positions (360°).

Keywords: avatar, body shape, custom made garments, virtual fitting room

1. INTRODUCTION

Through the Internet, new business models (e-business) have emerged that have redefined human interaction, the way organisations conduct their operations and monetise social interaction or trade different types of stocks. The activity of companies has been focusing on the virtual space because in this area, customers are active, present and they inform themselves in order to purchase certain goods or services. Textile companies are constantly looking for viable solutions in order to promote their products in the virtual space, which is very rich in products, to attract new customers and to reduce the number of products that are returned to the best possible extent (non-compliant) [1,2].

If the customers have the possibility of personalising/individualising the product according to the shape of their body, and to perform a virtual test of the selected item, then the level of their satisfaction increases, the amount of returned or unsold products (that do

not fit in terms of size) is reduced, and a dynamic and positive advertising campaign can be carried out for of the brand (based on customer reviews) [3,4].

The paper proposes a method of developing an integrated solution for the online marketing (website) of custom-made clothing products that uses a virtual test room which allows the simulation of the product on the virtual mannequin in different positions (360°).

2. GENERAL PRESENTATION OF THE WEBSITE

Technological advancements have enabled manufacturers, users, and retailers to enhance their sales service through various virtual platforms that have eliminated the line between traditional/conventional stores and online stores [2].

An online store (clothing) must provide:

1. A collection of models, in 3D digital format, accessible to the customer. The models must be accompanied by complete descriptions of the corresponding products (measurements, the types of materials from which it is made, photos, shipping costs, etc.), which are taken into account by the customer in order to decide whether or not to buy the product. It is advisable to provide tables that allow the customer to estimate the size that they need, based on the details that they have specified, colour charts, matching accessories, etc.;
2. Similar products suggestions (along with the corresponding links);
3. The “Add to Cart” button, optimally placed on the page and easily distinguishable;
4. Payment methods ;
5. Blog (about new products and special offers that can influence the purchase decision);
6. Customer reviews;
7. Social networking links;
8. Return Policy;
9. Page with information about the company (“About us”).

A collection of 3D digital models consists of the following elements:

1. virtual avatar library → scalable for customisation
2. 3D virtual library of patterns corresponding to some clothing products → the models are designed in a way that allows them to be modified according to the customer's requirements.

3. THE ELEMENTS OF THE 3D CUSTOM MADE DIGITAL MODEL COLLECTION

3.1. Creating the database of virtual mannequins

There are several 3D CAD software solutions for the clothing industry (such as Lectra, Optitex, Gerber, Clo3D, Assyst, Graphis, etc.) with the following special features: a database of virtual bodies (scalable, to a certain extent), suitable tools that allow the designer to directly design the clothing product on the virtual mannequin, a library of raw materials which can be used during the virtual design process of the clothing product model, and tools that enable one to animate the mannequin in order to evaluate the fitting degree of the product [1,3].

The virtual mannequins (avatars) database is created by using the information in accordance to the anthropometric standard and is also based on the company's experience (customer network); avatars are created for EU sizes (e.g., 36, 38, 40, 42, 44, 46, 48, 50, 52, 54), with different silhouettes, postures and heights (figures 1-4).

This paper uses the virtual avatar database (certain shapes and sizes) that is provided by Clo3D in order to create a new one for a specific category of customers. By using a

virtual database (mannequins), the changes made during the design process are realistic (the program has certain limitations in applying certain transformations) [5,6].



Figure 1. Scaling the virtual avatar

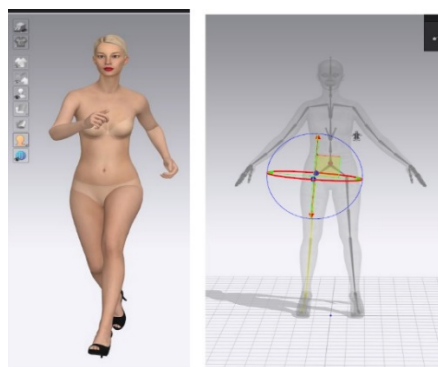


Figure 2 Changing the avatar position

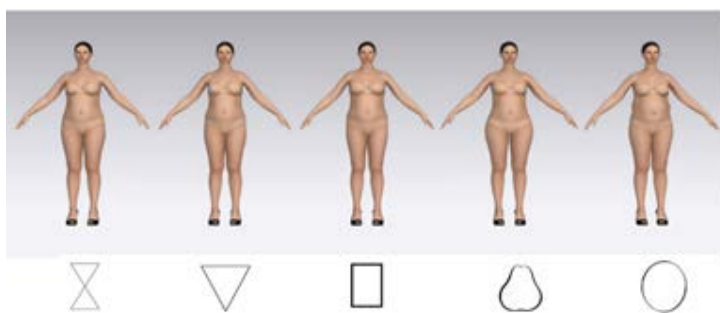


Figure 3. The virtual avatar database (different silhouette)

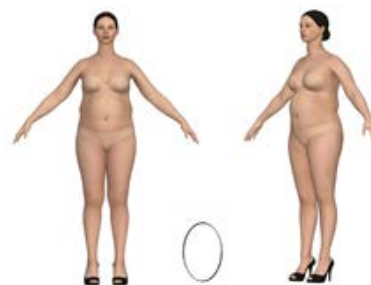


Figure 4 Virtual avatar, size 46 EU

The virtual avatar database is stored for later use (in the virtual test room).

3.2. The 3D virtual library of custom-designed models.

Design the patterns

The virtual library consists of custom-designed models. The applications created by the CAD systems producers for textile clothing allow the custom design (for custom made products) to be carried out in two ways:

a) by designing the 2D patterns for the model components by using special 2D design tools that allow the data provided by the customer (dimensions of the body, as well as information regarding its conformation and posture) and the ones corresponding to the model to be integrated in the process. The designer carries out the design process for a collection of models that is in accordance with the customers' requirements and the fashion trends. The components that are stored in the virtual library can be automatically modified (resized) by altering the data used in their corresponding design process.

b) by directly constructing the 3D model (with all of its characteristics) on the virtual avatar. The specific lines of the model (geometry, shape and size) are suitable only for a customer whose body dimensions are very similar to the ones of the avatar used in the 3D design process of the model.

A new version of the designed model can be generated for a different customer in any of the following ways:

-by scaling the avatar and the model (which is attached to it at its support points from the contact area);

-by remodelling the details of the model on another avatar.

In this paper, we use the first method of creating the 3D virtual library, which consists of designing the 2D patterns for the components of the model (while also checking their fitting degree on the assembly lines), saving the model and preparing it for the 3D simulation (in the Clo3D virtual environment). The components designed in the 2D working environment can be combined in order to develop new models by taking into account the fitting rules and their roles.

Custom design in a Gemini CAD can be done by following the geometric design method principles (classical method) and of technical design for the shape of components to obtain the pattern for the model. In this software environment, the design process is carried out in a special layer (geometric layer), in which the user can edit various mathematical relations (depending on the geometric design solution) by using the data provided at the beginning of the design session (figure 6). They can add or remove data or change the structure of the mathematical relations at any time; the components of the model alter their shape in accordance with the changes made by the user (figures 7 and 8) [7,8].

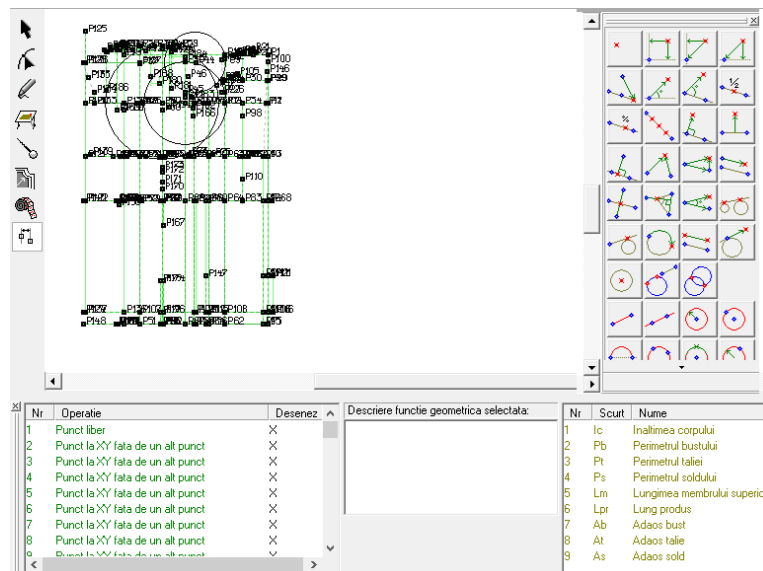


Figure 6. The design scenario of the geometric network (Gemini CAD)

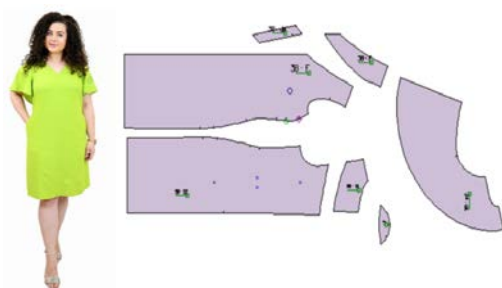


Figure 7. Model1- patterns of the model pieces

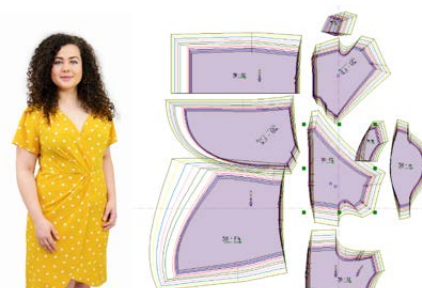
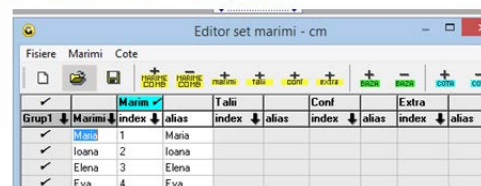


Figure 8. Model 2- patterns of the model, for different clients



The model designed for only one customer by using the Made-to-Measure module of the Gemini CAD (figure 8) software solution can be adapted for multiple customers by simply entering some values in the fields related to the data that has been used in the design scenario. The shapes of the components of the model are automatically generated and overlaid (figure 8).

The models constructed in the 2D environment are saved. In the next phase, they are imported into a 3D working environment in order to carry out the simulation process necessary for developing the virtual collection (the presentation of a model that is tested on several virtual avatars).

The construction of the material database that is necessary for the garment collection

The concept of rendering is limited to a process of manipulating digital information, including reflected and absorbed light, textures, and volumes. Their corresponding parameters are introduced into and processed in the graphical 3D modelling environment (figure 9). This process enables one to obtain editable images that are used for the purpose of transforming the presented objects into reality (a database containing textile materials with physical-mechanical properties). The virtual database of the materials needed for the collection is developed in the Clo3D software environment [5].

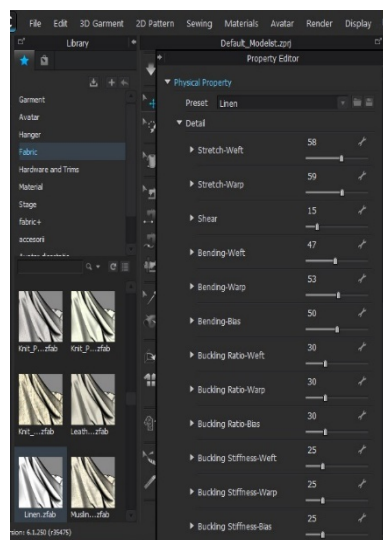


Figure 9. The material database

3D Simulation of the virtual models on the mannequins

The 2D patterns (that have been created using the Gemini CAD software) are imported into Clo3D. Afterwards, the user simulates the sewing process and evaluates the fitting degree of the product on the virtual avatar (whose technical details were used in the design process) (figure 10).

The designer obtains the 3D shape of the model by:

- Selecting of the avatar with the correct shape and dimensions (size and posture);
- Importing the 2D model into the Clo3D program;
- Placing the components of the model next to the virtual avatar;
- Declaring the assembly lines;
- Choosing the material;
- Simulating the sewing parts and checking the length of the assembly lines.



Figure 10. Simulation process

In order to get a more accurate picture, the product has to be rendered. This process produces a clear image, similar to that of a physical prototype, which can be later used in another context. Afterwards, the designer saves the product, along with all of its technical specifications: size, format (video or image), resolution and background. In this way, one constructs a virtual 3D database of the model that covers various sizes (figure 11).

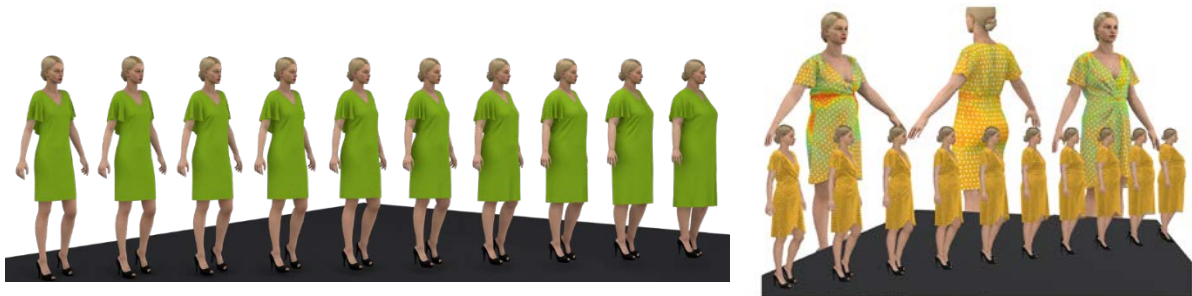


Figure 11. 3D custom made models (different sizes and body positions)

Clo3D, like any other 3D CAD software, offers the possibility of displaying the tension forces that occur in the product (in certain areas) when it is worn on the body. One checks whether the model is perfectly balanced on the virtual avatar, and if it fits it. This is done by displaying the stress map. The meaning of the colours is the following:

- Green - the ideal colour, which means the product fits properly, and is balanced on the avatar;
- Yellow - the product is too loose (oversized) on the avatar;
- Red - the product is undersized (too small for the selected avatar).

4. INTEGRATING THE 3D VIRTUAL MODEL INTO THE WEBSITE

After having been saved, the model is integrated into the website. The customer accesses the website, analyses the information that is provided (collection of models), selects the desired model, the customer reaches the point where they have to choose the right size [9,10]. The customer looks at the model on a virtual avatar of a certain size. It is

possible to alter the dimensions so that they match the desired ones by using the “Test the size of the product” option (figure 12).

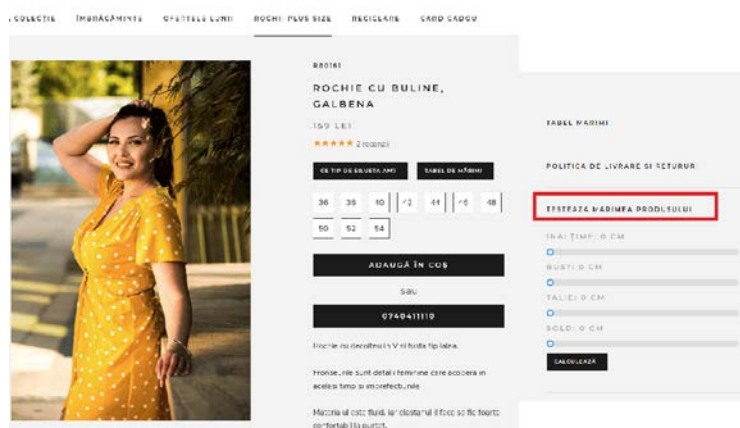


Figure 12. Website screenshot

According to the instructions, the customer enters their own values for the dimensions, expressed in centimetres. In the next stage, the software displays the shape of the avatar (in accordance with the changes that have been made). If the entered values result in a standard silhouette, the customer receives information about the correct size. The dressed modified avatar can be viewed from several positions, as it is exported into the 3D working environment. In this way, by changing the viewing scale and the positioning distance (display scale), all of the details of the model can be analysed (figure 13).

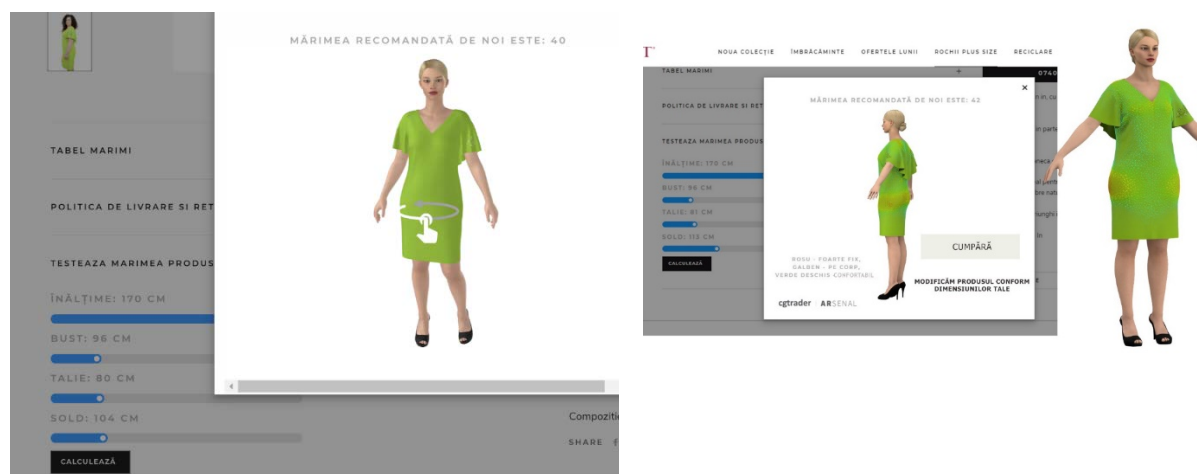


Figure 13. Website screenshot

If the resulting virtual avatar has an atypical shape, the product might not properly fit it. In this case, the designer will have to analyse the 3D image of the model and to alter the shape of the patterns in order to address the issue. In this way, the virtual model is adapted to the shape of the customer’s body without any additional costs.

If the customer accepts the adjustments (they receive a notification in order to get the chance to see what the model looks like after the changes have been applied), the order can be finalised and the product can be manufactured and delivered in accordance with the customer’s requirements.

5. CONCLUSIONS

Companies must adapt to these digital changes by developing and properly pursuing strategies to leverage digital technologies, in order to maintain or increase competitiveness in global markets.

The number of returned products can be reduced by showing what the products would look like when dressed on “virtual bodies”, and by tailoring products to the customer’s needs.

The technology must be adapted to the target audience; the market must be analysed in terms of financial resources that are allocated to these categories of fashion products, and of familiarity with the use of websites.

Virtuality in fashion involves a virtual fitting room that can be used at any place and at any time, without space and time constraints, and without the need to be physically present.

Virtual/digital goods that exist only virtually represent an innovative and futuristic approach, but they are mostly inaccessible for the vast majority of the population.

Providing the customer with the chance of customising the desired products by creating their own designs comes with its own set of challenges, due to their limited ability to identify and develop their own preferences. The customer can also easily feel overwhelmed by the large number of design options.

REFERENCES

- [1] Franke, P.K.M.S.N., *Complementing mass customisation toolkits with user communities: how peer input improves customer self-design*, 2004, Available at: <https://onlinelibrary.wiley.com/doi/full/10.1111/j.1540-5885.2008.00321.x> [Accessed on June 2021]
- [2] Pousttchi, K., *Digital Transformation*, *Encyclopedia of Business Informatics*, Available at: <http://www.enzyklopaedie-derwirtschaftsinformatik.de/lexikon/technologien-methoden/Informatik--Grundlagen/digitalisierung/digitale-transformation/digitaletransformation> [Accessed on June 2021]
- [3] Fuller, H.M.K.M.G.J.J., *Consumer empowerment through internet-based co-creation*, 2009, 71-102
- [4] Avadanei, M., Olaru, S., Ionescu, I., Ursache, M., Ciobanu, L., Alexa, L., Luca, A., Olmos, M., Aslanidis, T., Belakova, D., Silva, C., *ICT new tools for a sustainable textile and clothing industry*, In: *Industria Textila*, 2020, 71, 5, 504-512, <http://doi.org/10.35530/IT.071.05.1811>
- [5] Clo3D, Available at: <http://www.clo3d.com> [Accessed on June 2021]
- [6] Olaru S., Popescu, G., Anastasiu, A., Mihăilă, G., Săliștean, A., *Innovative concept for personalized pattern design of safety equipment*, In: *Industria Textila*, 2020, 71, 1, 50-54, <http://doi.org/10.35530/IT.071.01.1620>
- [7] Gemini Cad, Available at: <http://www.geminiCAD.com> [Accessed on June 2021]
- [8] Avădanei, M., *Principii de construcție și modelare ale produselor vestimentare*, Iași: Casa de Editura Venus, 2005
- [9] Hernández-Gracia, T.J., Duana, D.-A., *Creators of competitiveness in the textile and clothing industry from the Hidalgo state*, In: *Industria Textila*, 2020, 71, 3, 241-244, <http://doi.org/10.35530/IT.071.03.1705>
- [10] Abrudan, D.B., Maticiuc, M.D., Năstase, M., Florescu, M.S., Dăianu, D.C., *The challenge of young Romanian designers: creativity in business*, In: *Industria Textila*, 2020, 71, 3, 245-251, <http://doi.org/10.35530/IT.071.03.1818>



ANALYSIS OF THE MECHANICAL PROPERTIES OF SOME HIGH-TECH YARNS WITH DIFFERENT FUNCTIONS

DOI: 10.35530/TT.2021.38

T. Sârbu, C.E. Stroe

R&D Department – Textile Materials and Processes Engineering, National Research and Development Institute for Textiles and Leather, Romania
(e-mail: teodor.sarbu@incdtp.ro, cristina.stroe@incdtp.ro)

Abstract: *We live in a knowledge-based society, which is facing an increasing impact of science and technology on all aspects of life through products, services and consumer needs. In the future, society will be oriented towards the individual and his needs, which will be more and more complex and varied. The present paper comparatively presents a series of variants of cotton fibre yarns: made of blended cotton fibres with ultra-high molecular weight polyethylene fibres; yarns of cotton fibres blended with regenerated cellulose fibres, that were functionalized with Ag ions and yarns obtained from fibre blends of recycled organic cotton, virgin cotton with recovered cotton fibres in order to observe their mechanical potential. The built-in functionalities allow their use in areas such as healthcare and hygiene, sports and leisure activities. The recovery of textile waste in a circular approach and the transition to a circular economy is an important direction for research. The repercussions that the consumption of raw materials in the textile industry has, on the environment, as well as on sustainability, determine us to reason in a judicious way when we select the different materials that we use in making the products.*

Keywords: *eco nanotechnologies, functional textiles, high-tech yarns*

1. INTRODUCTION

Functional textiles are an interdisciplinary field that incorporates science, technology and design, and its future lies in the potential to combine different technologies [1].

Functional cotton textiles blended with cellulose that incorporate silver ions, through their antimicrobial properties lead to improved quality of life and contribute to significant savings for the health budget [2].

For the production of advanced textile materials, the research methodology includes innovative techniques for functionalizing the materials by:

- high-tech yarn processing, with nano and micro functionalization through classic, flexible, ecological technologies;
- incorporation of passive and / or active interactive elements in textile structures;
- eco-nanotechnologies such as electroplating and 3D printing;
- closing the value chain through eco-innovative waste processing technologies.

The most frequently used yarns for making clothing items are:

- 100% cotton yarns;
- cotton yarns blended with cellulose;
- recycled cotton yarns.

The main purpose of yarn functionalization is to create the basic relationships

between properties and effects in fibrous materials, reagents, additives, reactive media and reaction parameters.

With modern finishing, coating and treatment technologies, innovative and highly functional technical textiles are developed for a wide range of applications, including power generation, textile architecture, medical materials, conductive / sensor materials or high temperature textile protection [3].

These yarns can be a set of variants that underlie the generation of an experimental matrix of woven and / or knits with comfort and performance functionalities and recovered fibre elements in the current context of research.

2. MATERIALS AND METHODS

2.1. Materials

High-tech high molecular weight polyethylene fibre (UHMWPE) offers maximum strength with minimum specific mass.

Regenerated cellulose fibre was obtained through an eco-friendly technology, and by adding silver (Ag) ions to the polymeric mass before spinning, remarkable antibacterial properties are obtained. This type of functionalisation also offers a longer time to use the yarns.

The yarns used in this research, had the following characteristics:

- 2 variants of cotton spun yarns:
 - Variant 1 (V1), tex: 23,05x2 - 100% cotton fibres;
 - Variant 2 (V2), tex: 19x2 - blend of 80% cotton fibres and 18% regenerated cellulose fibres functionalized mass with 2% Ag ions particles.
- 3 variants of spun yarns from a blend of cotton fibres with different percentages of UHMWPE fibres:
 - Variant 3 (V3), tex: 30x1 - 98% cotton and 2% UHMWPE;
 - Variant 4 (V4), tex: 30x1 - 95% cotton and 5% UHMWPE;
 - Variant 5 (V5), tex: 30x1 - 90% cotton and 10% UHMWPE.
- 4 variants of yarns made of recycled organic cotton, virgin cotton and recovered cotton fibres:
 - Variant 6 (V6), tex: 21,42x2 - thread R-EARTH / E 50, 50% recycled cotton + 50% organic cotton (Hilaturas Ferre);
 - Variant 7 (V7), tex: 33,06x2 - thread R-EARTH / E 50, 50% recycled cotton + 50% organic cotton (Hilaturas Ferre);
 - Variant 8 (V8), tex: 63,52x2 - R-Jeans / J 30 yarn: 27% recycled cotton + 70 % organic cotton + 3% other recycled yarn (Hilaturas Ferre);
 - Variant 9 (V9), tex: 63,06x1 - thread R-Jeans / J 30: 27% recycled cotton + 70 % organic cotton + 3% other recycled yarn (Hilaturas Ferre).

The two types of fibres from regenerated cellulose and UHMWPE, are distinguished by different properties, exemplified in table 1.

Table 1. Lyocell and Dyneema fibres properties [4-6]

Lyocell fibre properties	Dyneema fibre properties
High tensile strength (2X rayon dry / 3X rayon wet)	Extremely strong (up to 15 times stronger than steel and up to 40% stronger than aramid fibres)
Highly absorbent	Cut and tear resistance
Higher water vapour permeability than cotton which means that garments are comfortably cool to wear	Low elongation
High wet and dry modulus	Low density

Easily dyeable to strong color-fast shades	Low coefficient of friction
Stable at high temperatures (above 170°C the fibre will start to lose strength gradually)	High abrasion resistance
It biodegrades completely during biological treatment, such as burial or anaerobic digestion	High pliability
-	Soft as silk
-	Hydrophobicity

2.2. Methods

The tests on the yarns were performed on the equipment from the testing laboratories, INCDTP accredited by Romanian Accreditation Association (RENAR).

During the research, the following physical and mechanical properties were determined:

- length density (tex); C.V. (%);
- torsion/ twist (no. tors./m); C.V. (%);
- breaking tenacity (N); C.V. (%);
- elongation at break (%); C.V. (%).

3. RESULTS AND DISCUSSIONS

The yarns made of 100% cotton and those made of the blend cotton and regenerated cellulose with Ag ions were analysed to compare their properties with the high-performance yarns, and those with content of recovered fibres from waste, in order to highlight the mechanical potential and to identify areas of use. Tables 2, 3 and 4 show the results of the tests performed for the three categories of yarns.

Table 2. Yarns length density

Variants	V1	V2	V3	V4	V5	V6	V7	V8	V9
Length density (tex)	23.05x2	19x2	30x1	30x1	30x1	21.42x2	33.06x2	63.52x2	63.06x1
CV (%)	10.21	5.79	9.23	5.31	5.86	3.38	5.41	4.4	3.38

Table 3. Breaking tenacity of cotton yarns

Determination	Breaking tenacity (N/tex)		Elongation at break (%)	
Variants, tex	V1 23.05x2	V2 19x2	V1 23.05x2	V2 19x2
Average	0.1810	0.1476	8.4800	8.6500
Standard deviation	0.0079	0.1315	0.4237	0.5580
CV (%)	0.0694	0.8909	4.995	6.4500

The breaking tenacity of cotton and regenerated cellulose yarn is close to that of 100% cotton yarn, but in relation to the lower fineness, this aspect demonstrating the ability of this yarn to withstand mechanical stress (figure 1).

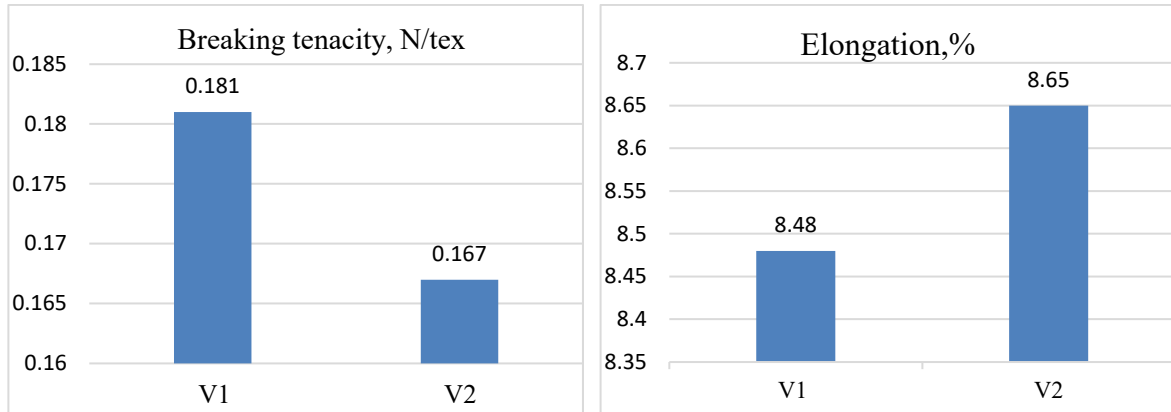


Figure 1. Breaking tenacity (N/tex) and elongation at break (%) for cotton yarns

Table 4. Breaking tenacity of yarns made of cotton and UHMWPE fibres

Determination	Breaking tenacity (N/tex)			Elongation at break (%)		
	V3 30x1; 2%	V4 30x1; 5%	V5 30x1; 10%	V3 30x1; 2%	V4 30x1; 5%	V5 30x1; 10%
Average	0.1670	0.1810	0.1916	8.6500	8.48	8.2900
Standard deviation	0.0297	0.0079	0.1111	0.558	0.4237	0.4270
CV (%)	0.1778	0.0694	0.1019	6.4500	4.9950	5.1500

Following the determinations, it was observed that the V5 yarn has the highest breaking tenacity; elongation at break for yarns containing decreases in correlation with increasing the percentage of UHMWPE fibres, demonstrating the ability of this type of yarn to resist at mechanical stresses. Only a content of 5 and 10% UHMWPE brings improvements in the breaking tenacity of the yarns (table 4).

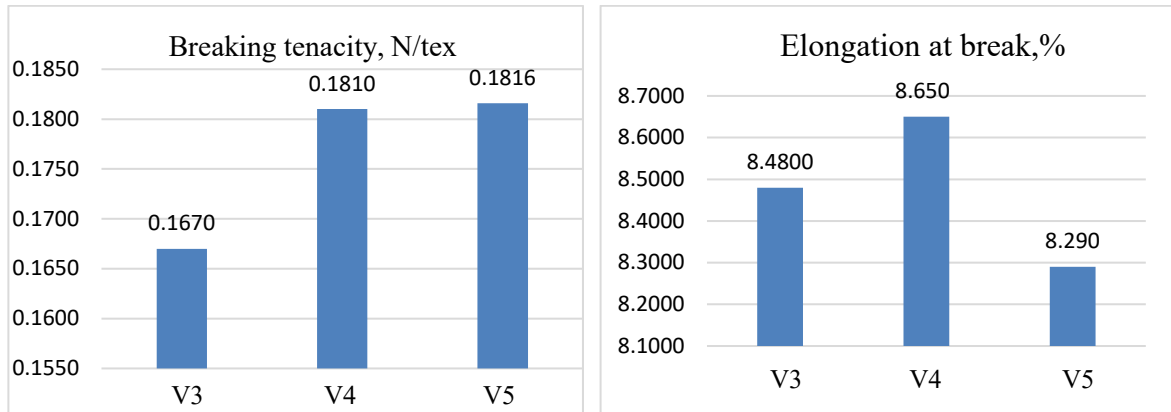
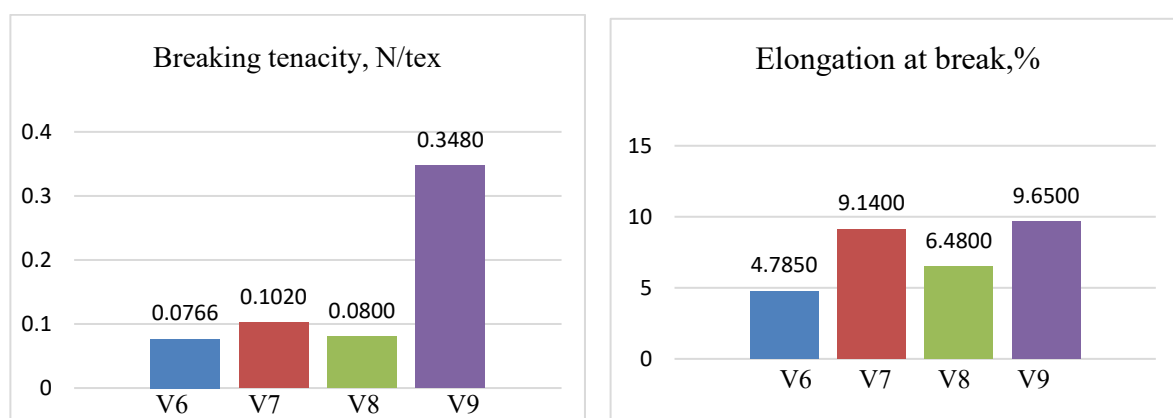


Figure 2. Breaking tenacity (N/tex) and elongation at break (%) for cotton with UHMWPE yarns

The lowest tenacity values were registered in the case of yarns with a percentage of recovered fibres, with the exception of V9, with a higher breaking tenacity even than those with 2%, 5%, 10% of UHMWPE fibres and the V7 variant has the breaking tenacity close to the results of cotton-UHMWPE yarns.

Table 5. Breaking tenacity of yarns made of recycled and organic cotton fibres

Determination	Breaking tenacity (N/tex)				Elongation at break (%)			
	V6	V7	V8	V9	V6	V7	V8	V9
Variants, tex	21.42x 2	33.06x 2	63.52x 2	63.06x 1	21.42x 2	33.06x 2	63.52x 2	63.06x 1
Average	0.0766	0.1020	0.0800	0.3480	4.7850	9.1400	6.4800	9.6500
Standard deviation	0.0063	0.0070	0.0061	0.0202	0.5280	0.7960	0.3926	0.5150
CV (%)	8.1600	6.8500	7.6400	5.8100	11.0400	8.7100	6.0600	5.3400

**Figure 3.** Breaking tenacity (N/tex) and Elongation at break (%) for recycled organic cotton yarns

Therefore, due to the superior resistance, these types of yarns from regenerated fibre content can be used in favour of the synthetic ones, supporting the concept of circular economy and sustainability.

4. CONCLUSIONS

It is recommended that the performance yarns be used in a judicious manner.

Yarns with 2% UHMWPE can be used for making clothing or non-clothing products entirely in relation to the textile surface.

The increase of the percentage imposes the realization of clothing or non-clothing products of modulated type, and the yarns with content of 5% or 10% UHMWPE to correspond exactly to the areas where it is necessary to manifest its performance.

The yarns may be used with a suitable design, including in combination with yarns containing a certain percentage of recovered fibres.

The values of the mechanical potential of yarns obtained from the blending of fibrous organic cotton with recovered cotton fibres can be compared even with conventional yarns of virgin fibres of the same fineness.

Also, the results of breaking resistance, obtained in laboratory, recommend the use of these types of yarns both in warp and weft, given that the yarns obtained from waste are mainly used in weft or in the production of low-strength products.

ACKNOWLEDGEMENTS

The results presented in this paper were obtained in the projects:

- PN 19 17 03 03 “Macro-meso-micro advanced materials for health and quality of life improvement (AkSuTex).
- LIFE17 ENV/ES/000290 “A 100% rel circular economy process for vegane-organic-recycled footwear”.

REFERENCES

- [1] European Environment Agency, *Circular by design - Products in the circular economy*, ISSN 1977-8449, 2017
- [2] Piscis, V., *Circular Design Project*, 2021, Available at: <https://vesicapiscisfootwear.com/en/content/19-RECYCLABLE> [Accessed on June 2021]
- [3] Tatusa, H., Glin, O.P., Makiko, T., *New millenium fibres – applied examples of high tech fiber*, The Textile Institute Woodhead Publishing Limited, 2005
- [4] *Engineered fibres technology, Tencel® lyocell short cut fiber*, Available at: http://www.eftfibers.com/prod_lyocell.php [Accessed on June 2021]
- [5] Parul, G., Pankaj, G., Singh, S.S.J., *Lyocell Properties and applications*, In: *Man-Made Textiles in India*, 2002
- [6] *FibrXL smart performance fibres Dyneema®*, Available at: <https://fibrxl.com/fibrxl-performance/fibers/dyneema/> [Accessed on June 2021]



VIRTUAL 3D KINEMATIC HUMAN MODEL PROTOTYPE

DOI: 10.35530/TT.2021.35

D.R. Viziteu, A. Curteza, M.L. Avadanei

“Gheorghe Asachi” Technical University of Iasi, Doctoral School - Faculty of Industrial Design and Business Management, Iasi, Romania
(E-mail: viziteudianaroxana@gmail.com, acurteza@gmail.com, mavad@tex.tuiasi.ro)

Abstract: *In the past several years, the application of 3D technologies in the textile and clothing design industry has considerably increased and become more accessible to designers and patternmakers. With digitisation in garment engineering and virtual prototype and modelling techniques becoming more mainstream, a new generation of virtual human models starts to develop to fulfil the demand for protective and functional products designed for specific athletes, such as climbers and mountaineers. We must base our work on an improved understanding of the behaviour of the musculoskeletal system to develop garment patterns that minimise discomfort and improve performance under dynamic body deformations and muscle contractions associated with specific movements. For this study, we explored the possibilities of using existing software packages for virtual prototyping based on human kinematic models for functional clothing.*

Keywords: *clothing design, digitalization, kinematic human model, virtual prototyping*

1. INTRODUCTION

Patternmakers are still developing clothes based on the standard anthropometric static protocol defined by ergonomic standards or size charts: standing and looking straight ahead, with shoulders relaxed, arms at sides, and legs hip widespread [1]. When the size charts do not cover the requirements of personal protective equipment, there are measurements during movements as standing, sitting, kneeling, etc. [2]. Since the human body is engaged in permanent movement, and the demand for functional garments for work or sportswear is a modern concern, understanding how the human body alters in dynamic is an essential and contemporary research topic.

In current practice, dynamic anthropometry in the clothing industry was first applied for functional and aesthetic sportswear products [3]. Because functional clothing, especially for sports athletes, has complex requirements regarding increased physical comfort, performance, ease, and range of motion, the 2D flat pattern methods fail to capture the complex form of the human body shape in movement. In this case, an efficient method that can enhance body mobility and fitting test in movement is using 3D human body data and 3D technology in order to develop clothing.

Several changes have been implemented to bring virtual humans closer to our everyday lives in the past years. These human body models can be found in many interactive applications for virtual reality (VR) and augmented reality (AR), including games, movies or commercials. Virtual prototyping is usually based on avatars, garment patterns and textile materials. In the garment industry, most virtual models use realistic virtual representations of humans based on 3D anatomy scan data or used to the body measurement standard charts. Commercially available software package for garment

industry that offers avatars includes CLO 3D by CLO Virtual Fashion, Vidya by Assyst, V Stitcher by Browzwear Solutions, Modaris by Lectra and various others.

Morlock et al. were the first to investigate the differences between body measurements for work or sports associated positions for both men and women [4]. 3D garment simulation software can be used for fit assessment in dynamic positions for garments developed for work or sportswear.

We can mention various skin deformation software avatars such as:

- Linear Blend Skinning - (LBS) - standard and popular method where the deformation of the character skin is driven via an underlying skeleton. The linear models of male and female body shape are obtained from the CAESAR dataset [5] (approximately 2000 scans per gender) [6][7];
- Skinned Multi-Person Linear - (SMPL) - skinned vertex-based model (male, female, gender-neutral) that precisely characterises a wide variety of body shapes in real human poses, from thousands of 3D body scans [8];
- Dynamic Multi-Person Linear - (DMPL) - an extended version of SMPL model that captures soft-tissue in dynamic [9];
- Bone-Level Skinned Model (BLSM) - the bone scales are set prior to template synthesis; the human body mesh first sets bone lengths and joint angles to specify the skeleton [10].

Researchers proposed a method based on the BLSM model, capable of precisely reconstructing 3D human body pose in the outdoor environment [11]. Klepser et. al [12], compared avatars from three 3D garment simulation software systems (CLO 3D, VStitcher, Vidya) with 4D scans of real test persons, revealing their limitations, especially in movement. Some authors have synthesised that 3D product development based on the kinematic human body and 3D technology is an efficient way to create close-fitting clothes straight on the body. Kanika et al. [13] proposed an efficient method to design functional clothing, developing virtual 3D patterns for specific body postures of a motorcycle rider. We considered the human kinematic models presented in the literature, which can be combined with different software applications into the digital process to develop functional garments [14].

2. MATERIALS AND METHODS

The garment simulation method is usually performed in the following stages: an avatar is selected according to defined body measurements, the pattern parts are assembled at the seams and digitally sewn together, the garment is placed and draped on the avatar, the properties of the fabric are defined, fit assessment and evaluation of the model.

Body movement is recorded by motion-capture technology in other fields such as video game design, animation, virtual reality, recuperative pain medicine and sport. There are different methods for studying body motion having the same fundamental principle of triangulation - e.g., 3D scanners, photogrammetry software, inertial sensors, etc.

Kinematics, in this paper, is an interdisciplinary field that analyses human movement. It describes the motion of points, objects and systems of groups of objects without reference to the causes of motion (e.g., forces). The study of kinematics is often referred to as the “geometry of motion”. Through the lens of kinematics, we must consider information about the movement of the body, limbs and joints, that occurs during rock climbing [15]. There are big variances in geometry between the genders in body forms, proportions and muscle manifestations. In most cases, the kinematic 3D model is built of skeleton, muscles and skin.

The sport of rock climbing or bouldering involves both lower and upper limbs, with movement between rests (figure 1). There are different phases in climbing on a rock surface, through continuous upward body movements, such as posture equilibrium, arm release, climbing-specific foot raise, resting and another route-finding [16,17]. The climber's success is based on the skill of moving fluidly between the rest points while maintaining the centre of gravity over one or, depending on the given route, on both feet. Rock climbing is interesting and complex because of the unequal spreading of the holds that come in so many angles and sizes. Based on that, the athlete has to perform a complex form of locomotion with extreme and contorted postures, combining key physiological components like power, strength and muscular endurance at variable angles.

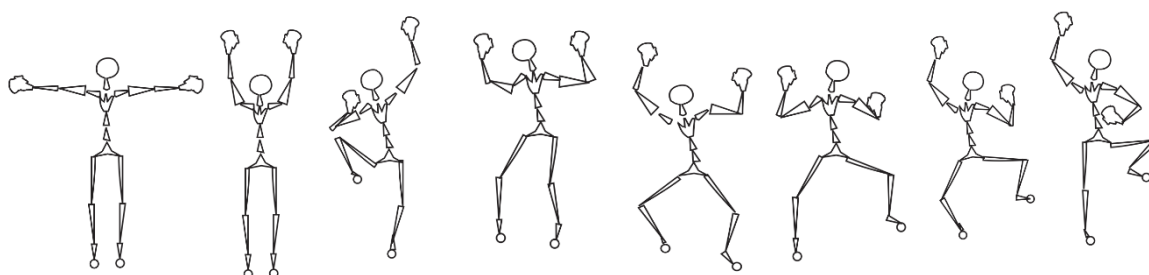


Figure 1. Climbing movements synthesised on body skeleton

The simulation was performed using a generated male muscular avatar revised to define body measurements [18]. In our case, we considered that muscle deformation is an important design component in clothes deformation. We integrated the avatar into auto-rigging online service Mixamo to insert animation structures from joints and bones, similar to those from rock climbing [19]. We placed the markers on the avatar joint positions for chin, wrists, elbows, knees and groin (figure 2).

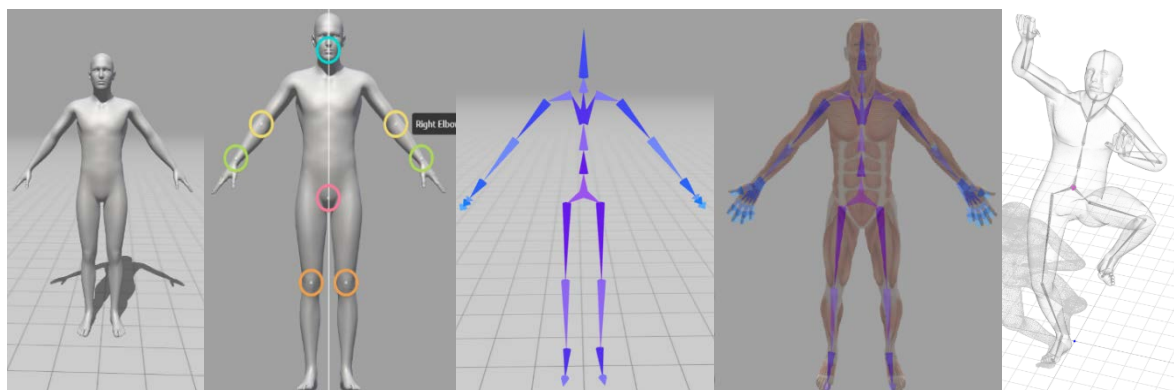


Figure 2. Auto-rigging: 3d body surface, place markers on joints, inserts skeleton generation of animated 3d avatar

The skeleton can be used as a framework for scan data. To test the interaction between the animated avatar and the virtual garment prototype for fitting, we used Clo3d [20]. The auto-rigged avatar is imported in FBX format. The rigged avatars can be utilised across the current platforms for garment simulation.

3. RESULTS AND DISCUSSIONS

3D virtual prototyping of garment products enables the designers to easily see how their new or existing 2D pattern will look with a wide range of materials and diverse strain situations. Additionally, 3D animation with apparel design can be used in e-

commerce. Digitalisation in garment development involves applying a great diversity of CAD systems with integrated 3D modules to develop the pattern designs and assess their fit to the 3D body model. The great advantage is that we can check the fit simulation and the virtual wearing comfort of functional clothing by using pressure tools and analysing stress, pressure points, strain and fit maps.

We tested the animated dummy as an import into Clo3d and designed clothing on it. Examining avatars exposes alterations between software in appearance and shape. Various methods to study 3D garment simulation were reviewed. The obtained results are:

- (1) identifying climbing phases through kinematic analysis;
- (2) generating a rigged avatar;
- (3) obtaining postures with muscle deformation;
- (4) case I - garment pattern construction using the traditional 2D method, then analyse fit in motion;
- (5) case II - garment pattern created with 3D flattening technique direct on dynamic posture;
- (6) findings.

The postures obtained from the generated rigged avatar are reliable in considering which areas of the body are exposed to extreme tension. The kinematic analysis showed that the knee, hip and crotch region are the stress points during bouldering specific movements.

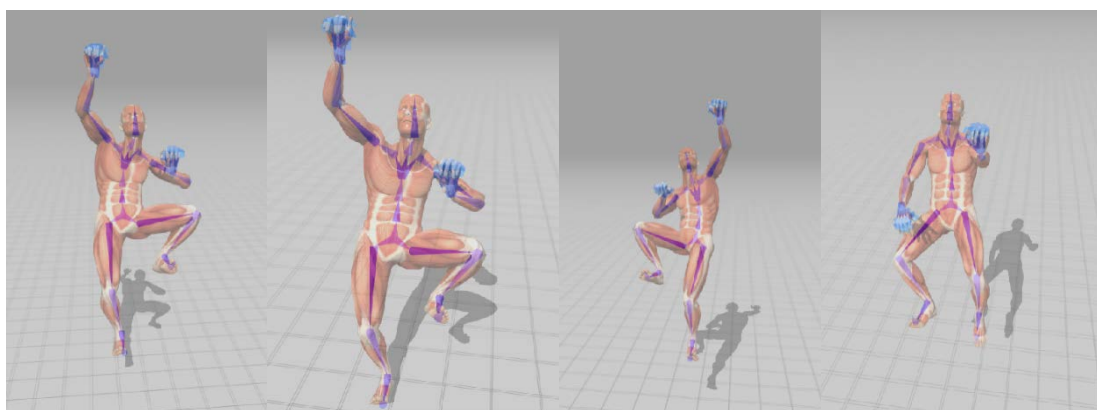


Figure 3. Postures with muscle deformation

In case I, starting from the avatar static posture, we adopted the traditional 2D method of garment pattern construction for outdoor climbing pants, animated in Mixamo and then analysed fit in motion. We observed that the dressed avatar in motion shows a disturbing effect at the hip and knee joints (figure 4).

The garment pattern for the second case of outdoor pants design will consider the mapped red zones on the avatar (figure 4). We can observe muscle deformation during the knee and hip flexion, where, normally, the fabric should extend the same as the muscle will contract during bouldering movement, being like a second skin. Following the avatar shape from the dynamic posture, we can trace the body skin deformation to create lines and shapes (figure 5). The lines are drawn with the 3D Pen (Avatar) directly on the virtual climber. It is essential to draw and close shapes on the avatar because the flattening function only recognises and extracts closed surfaces as patterns.

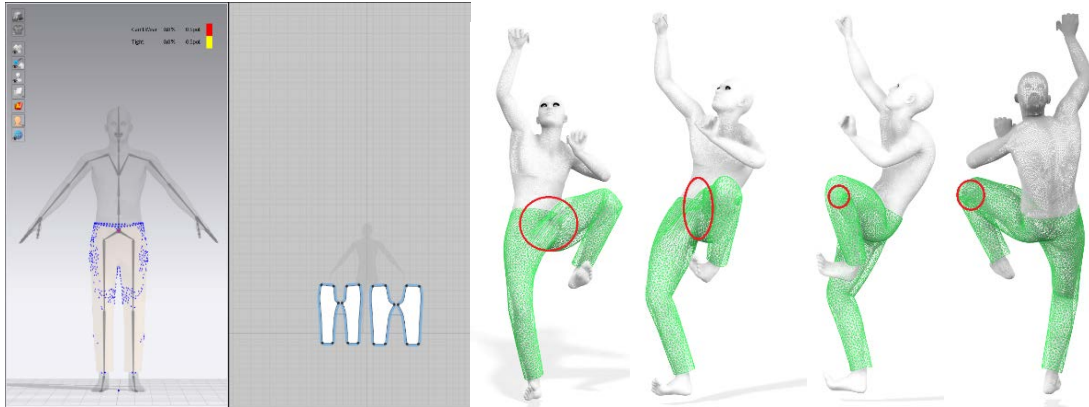


Figure 4. Case I - 3D simulation and fit analysis

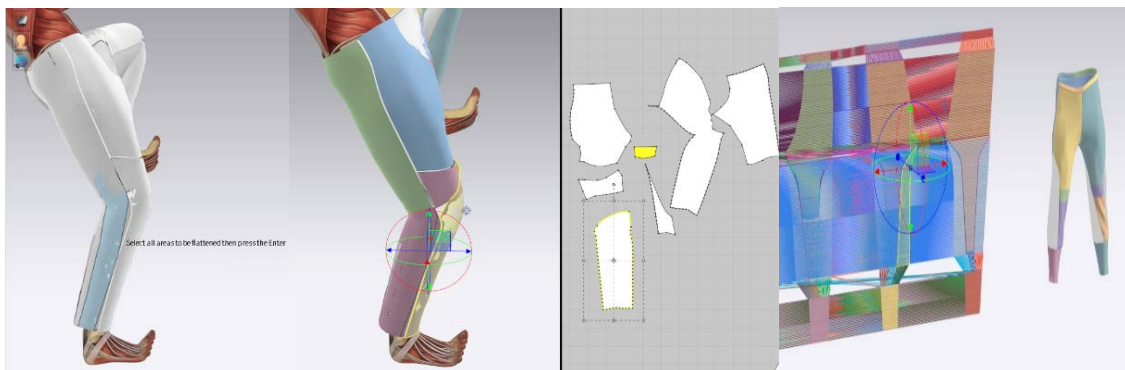


Figure 5. Case II – Pattern flattening and 3D prototype

When designing garments alongside 3D avatars, we can test the fit against flexed limbs and muscle bunches in real-time and dynamic motion, which vary the diameter and overall shape of limbs. In these situations, it is much clearer where garments need to be elastic or have fabric folds that compensate for dynamic shape differences between static and dynamic states of the body. While avatars are a very useful emergent tool in garment design, one must consider the shortcomings of incipient states of technology – e.g., the first avatars somewhat struggle to recreate soft tissue folds along large joints. We must further include and update 3D models with anthropometric parameter data sets to achieve a 100% accurate, complete form-fitting dynamic mannequin. There has been interesting in the perfection of 3D fabric dynamic and draping on scans and models. The area lacking is making the actual dynamic models accurate, taking into account scan data and adapting to it. Hence, this paper aims to assess virtual prototyping using personalised kinematic human models.

4. CONCLUSION

Animating digital humans with clothes has numerous applications, especially with 3D content for fashion runway collections, e-commerce, entertainment or virtual try on.

The proposed method for virtual prototyping using an avatar has proven to be efficient in the kinematic analysis of rock climbing. Simulating bouldering is quite difficult because it requires high degrees of freedom considering the climber's body and, consequently, a wide range of climbing movements.

We presented different methods for creating a personalised virtual kinematic human model prototype regarding compatibility, the right mix of existing software packages and digital transformation.

In the first case, we find body areas that are compressed or restructured by the simulated movement or virtual garment. The fact that the avatars zones overlap at a certain point cannot be reproduced accurately. The second case, with 3D to 2D pattern flattening method for sports garments, gives the impression of a viable solution in understanding the anthropometric dimensions through dynamic body movement and extreme postures.

Virtual prototyping based on human kinematic models can be the new go-to method in functional clothing design. Our future work will compare traditionally patterns and patterns obtained with the flattening (model unwrapping) procedure.

Product development designers can communicate faster with textile engineers and deliver more inspiring collections at a lower cost with digital visualisation and prototyping. With 3D technologies in the textile and clothing design industry, the line between “realities” and “virtual” fade even more. A 3D modelling environment provides the logistical advantages of a virtual medium, giving designers free rein when it comes to pursuing perfection. Having the luxury of testing countless iterations of a product without committing (and wasting) endless amounts of resources is also an advantage when it comes to reducing the carbon footprint of the fashion industry.

REFERENCES

- [1] Filipescu, E., Avadanei M., *Structura si proiectarea confectiilor textile*, Ed. Performantica, Iasi, 2007
- [2] Loercher, C., Morlock, S., Schenk A., *Motion-oriented 3D analysis of body measurements*, In: IOP Conf. Ser.: Mater. Sci. Eng., 2017, 254 172016, <https://doi.org/10.1088/1757-899X/254/17/172016>
- [3] Teyeme, Y., Malengier, B., Tesfaye, T., Ciesielska, I., Musa, A., Van Langenhove, L., *A Review of Contemporary Techniques for Measuring Ergonomic Wear Comfort of Protective and Sport Clothing*, In: Autex Research Journal, 2020, 21, <https://doi.org/10.2478/aut-2019-0076>
- [4] Loercher, C., Morlock, S., Schenk, A., *Design of a Motion-Oriented Size System for Optimizing Professional Clothing and Personal Protective Equipment*, In: Journal of Fashion Technology & Textile Engineering, 2018, <https://doi.org/10.4172/2329-9568.S4-014>
- [5] Robinette, K., Blackwell, S., Daanen, H., Boehmer, M., Fleming, S., Brill, T., Hoeflerlin, D., Burnside, D., Anthropometry resource (caesar) final report, volume I: Summary, 2002
- [6] Pan, J., Chen, L., Yang, J., Qin, H., *Automatic skinning and weight retargeting of articulated characters using extended position-based dynamics*, In: The Visual Computer, 2018, 34. 1-13. <https://doi.org/10.1007/s00371-017-1413-6>
- [7] Aburumman, N., Fratarcangeli, M., *Skin Deformation Methods for Interactive Character Animation*, In: Communications in Computer and Information Science, 2017, 8, 153-174, https://doi.org/10.1007/978-3-319-64870-5_8
- [8] *SMPL. A Skinned Multi-Person Linear Model*, Available at: <https://smpl.is.tue.mpg.de/> [Accessed on July 28, 2021]
- [9] *Dyna. A Model of Dynamic Human Shape in Motion*, Available at: <http://dyna.is.tue.mpg.de/> [Accessed on July 28, 2021]
- [10] Wang, H., Guler, R.A., Kokkinos, I., Papandreou, G., Zafeiriou, S., *BLSM: A Bone-Level Skinned Model of the Human Mesh*, In: Proceedings of the European Conference on Computer Vision (ECCV), 2020, August
- [11] Marcard, T., Henschel, R., Black, M., Rosenhahn, B., Pons-Moll, G., *Recovering Accurate 3D Human Pose in the Wild Using IMUs and a Moving Camera*, At: 15th European Conference, Munich, Germany, 2018, Proceedings, Part X. https://doi.org/10.1007/978-3-030-01249-6_37
- [12] Klepser, A., Pirch, C., Zangue, F., Loercher, C., & Chen, A., Morlock, S., *Is this real? Avatar Generation for 3D Garment Simulation*, In: Journal of Textile and Apparel, Technology and Management, 2021
- [13] Jolly, K., Krzywinski, S., Rao, P.V.M., Gupta, D., *Kinematic modeling of a motorcycle rider for design of functional clothing*, In: International Journal of Clothing Science and Technology, 2019, <https://doi.org/10.1108/IJCST-02-2019-0020>

- [14] Zhang, D., Krzywinski, S., *Development of a Kinematic Human Model for Clothing and High Performance Garments*, 2019, <https://doi.org/68-73>. 10.15221/19.068
- [15] Legreneur, P., Rogowski, I., Durif, T., *Kinematic analysis of the speed climbing event at the 2018 Youth Olympic Games*, In: *Computer Methods in Biomechanics and Biomedical Engineering*, 2019, 22. S264-S266. <https://doi.org/10.1080/10255842.2020.1714907>
- [16] Quaine, F., Martin, L., *A biomechanical study of equilibrium in sport rock climbing*. *Gait and Posture*, 1999, 10, 233-239
- [17] Hörst, E.J., *Training for Climbing: The Definitive Guide to Improving your Climbing Performance*, In: Guildford, CT: Falcon Guides, Globe Pequot Press, 2003
- [18] *3D Models*, Available at: <https://www.turbosquid.com/3d-models/> [Accessed on July 28, 2021]
- [19] *Mixamo*, Available at: <https://www.mixamo.com/#/> [Accessed on July 30, 2021]
- [20] *CLO-3D Fashion Design Software*, CLO Official Site, Available at: <https://www.clo3d.com> [Accessed on July 30, 2021]



CORRELATIVE AND COVARIANCE ANALYSIS OF THE ELECTROCONDUCTIVE FABRICS

DOI: 10.35530/TT.2021.42

R.M. Aileni*, L. Chiriac

National Research Development Institute for Textiles and Leather, Romania
(E-mail: aileni.raluca@incdtp.ro, laura.chiriac@incdtp.ro)

Abstract: This paper presents the correlation and covariance analysis of the electrical resistance dependence of mass, thickness and air permeability of textile structures coated with magneto-conductive materials and used for protection against electromagnetic waves. For this scientific approach, 9 experimental models of composites-based fabrics with electroconductive properties were made by applying different pastes based on organic polymeric matrices polyvinyl alcohol (PVA), copper (Cu), aluminium (Al), zinc (Zn), iron oxide (Fe_3O_4) and polypyrrole (PPY) solution using a classical deposition method such as scraping. The surface resistance was evaluated using a resistance meter device based on two parallel electrodes. From all samples analysed 5 samples based PPY, PVA-Ni, PVA-Ni-Al and PVA-Zn present a surface resistance between 10^3 and $10^5 \Omega$. Because the surface resistance has a lower value this means that the samples have a good conductivity to be used as layers for electromagnetic shielding systems.

Keywords: coating, conductive, electrical resistance, electromagnetic shielding, textile

1. INTRODUCTION

The investigation of the electrical properties of textiles was a challenge in numerous scientific papers because of the variation with temperature and moisture [1]. However, the ambient temperature and humidity, in real condition, is impossible to be controlled and this leads to variation in the surface resistance of the textile materials which tends to increase the conductivity with moisture contents even if are not previously treated with conductive pastes. In addition, the temperature and moisture at the skin level cannot be controlled and this can lead also to a variation of the surface resistance in the case of the textile conductive electrodes in contact with the skin. An increasing interest is in using the conductive inks composed of a polyurethane-based elastomer containing Ag flakes or polypyrrole [2,3] for smart textile applications [4-6]. In addition, the practical methods to obtain the conductive fabrics include metal or graphene coating and conducting polymer (polyaniline, polythiophene, PEDOT: PSS, and polypyrrole) coating [7-11].

The scientific literature presents several aspects concerning the influence of textile moisture or temperature on the surface electrical resistance of textiles [12-14]. The use of copper-coated lyocell cellulose fabric for flexible strain sensor [15] or nano copper loaded nonwoven polypropylene-based textile ECG electrodes was presented in numerous scientific papers [16-18]. In addition, the use of coatings-based nickel and titanium presents a good application for actuators [19,20]. Special attention is on using the Fe_3O_4 nanoparticles on cotton fabrics by the Pad-Dry-Cure process for the elaboration of magnetic and conductive

textiles [21]. Aluminium and nickel were applied in numerous applications for electromagnetic shielding [22,23].

In the context of electroconductive textile development and characterization, this paper is divided into the following parts: experimental part section introduce the specific aspects of the coatings and materials physico-mechanical and electrical characterization; correlative/covariance analysis section introduces the main aspects concerning the covariance and correlation matrix, principal components analysis and correlation coefficients; the discussions section introduce explanations about correlation coefficient values signification and finally, the conclusion section concludes the paper.

2. EXPERIMENTAL PART

In the framework of the 3D Electrotex project, 9 experimental samples were obtained using different pastes based organic polymeric matrices PVA and metallic nonferrous or ferrous microparticles such as zinc (Zn), copper (Cu), nickel (Ni), aluminium (Al), iron oxide (Fe₃O₄) and polypyrrole (PPY). The physico-mechanical and electrical properties were evaluated in the laboratory. In table 1 are presented the investigation results for the 9 samples treated with conductive pastes and the standard sample (M).

Table 1. Physico-mechanical and electrical characterization

No.	PPY	Ni	Cu	Al	Zn	Fe ₃ O ₄	H ₂ O	Rs*(Ω)	M**(g/m ²)	δ*** (mm)	Pa**** (l/m ² /sec)
M	-	-	-	-	-	-	x	10 ¹²	518	1.36	107
1	-	x	-	-	-	-	x	10 ³	590.8	1.5	113.4
2	-	x	x	-	-	-	x	10 ⁷	623.2	1.424	109.4
3	-	-	x	-	-	-	x	10 ¹¹	623.6	1.42	121.8
4	x	-	-	-	-	-	x	10 ⁸	513.6	1.472	187.4
5	x	-	-	-	-	X	-	10 ⁵	513.6	1.472	55.68
6	-	-	-	-	-	x	x	10 ⁸	602.8	2.408	55.73
7	-	x	-	x	-	-	x	10 ³	769.6	3.878	143
8	-	-	-	x	-	-	x	10 ⁵	577.2	1.25	88.14
9	-	-	-	-	x	-	x	10 ⁵	559.2	1.684	16.2

Note: *Rs – electrical resistance; **M - mass; ***δ – thickness; ****Pa – air permeability. Pressure difference used: 200 Pa; Standard conditions: T=20,2°C, RH=64,5%.

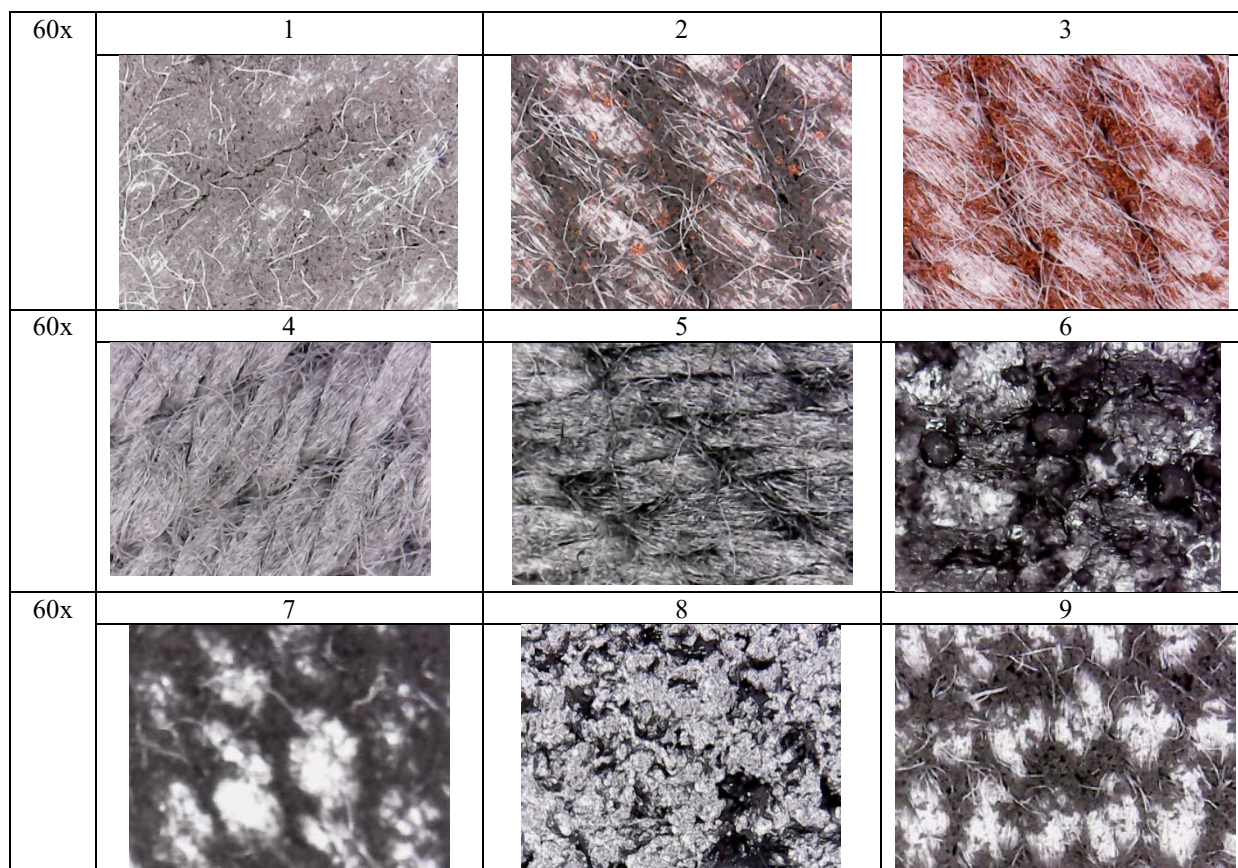
In table 2 are presented the optical view of the samples captured using the optical microscope with a magnification of 60x.

2. CORRELATIVE/COVARIANCE ANALYSIS

Using the results from physico-mechanical and electrical investigations were evaluated the correlations and covariance between dependent (Rs) and independent variables (M, δ, Pa) using the analysis of principal components (ACP) to resolve the following issues:

- Data complexity reduction and correlation/covariance matrix (table 3-9);
- Establishing of the correlations and covariances (table 3 and table 6);
- The determination of the latent variables and the behaviour. However, the variant of the variables measured can be found in the variant of hidden variables (influencing factors), which are determined by the association. In addition, considering the variables x_1, x_2, \dots, x_p , it is necessary to determine certain components C_1, C_2, \dots, C_m , where $C_i = w_{i1}X_1 + w_{i2}X_2 + \dots + w_{ip}X_p$, to obtain $m \ll p$.

Table 2. Analysis of the surface topography of the fabric by optical digital microscopy



- Correlative analysis

Table 3. Eigen analysis of the Correlation Matrix

Eigenvalue	1.9947	1.0649	0.7666	0.1738
Proportion	0.499	0.266	0.192	0.043
Cumulative	0.499	0.765	0.957	1.000

Table 4. Eigenvectors

Variable	PC1	PC2	PC3	PC4
Rs	-0.327	0.608	0.714	0.117
M	0.667	0.029	0.162	0.727
Δ	0.638	0.029	0.378	-0.670
Pa	0.204	0.793	-0.567	-0.092

- Covariance analysis

Table 5. Eigen analysis of the Covariance Matrix

Eigenvalue	9.87726×10^{22}	5516	2121	-3
Proportion	1.000	0.000	0.000	-0.000
Cumulative	1.000	1.000	1.000	1.000

Table 6. Eigenvectors

Variable	PC1	PC2	PC3	PC4
Rs	1.000	0.000	0.000	-0.000
M	-0.000	0.964	0.267	-0.009
Δ	-0.000	0.008	0.003	1.000
Pa	0.000	0.267	-0.964	0.001

Table 7. Unrotated Factor Loadings and Communalities

Variable	Factor1	Factor2	Factor3	Factor4	Communality
Rs	-0.462	0.627	0.625	0.049	1.000
M	0.942	0.030	0.142	0.303	1.000
δ	0.901	0.030	0.331	-0.280	1.000
Pa	0.288	0.818	-0.496	-0.038	1.000
Variance	1.9947	1.0649	0.7666	0.1738	4.0000
% Var	0.499	0.266	0.192	0.043	1.000

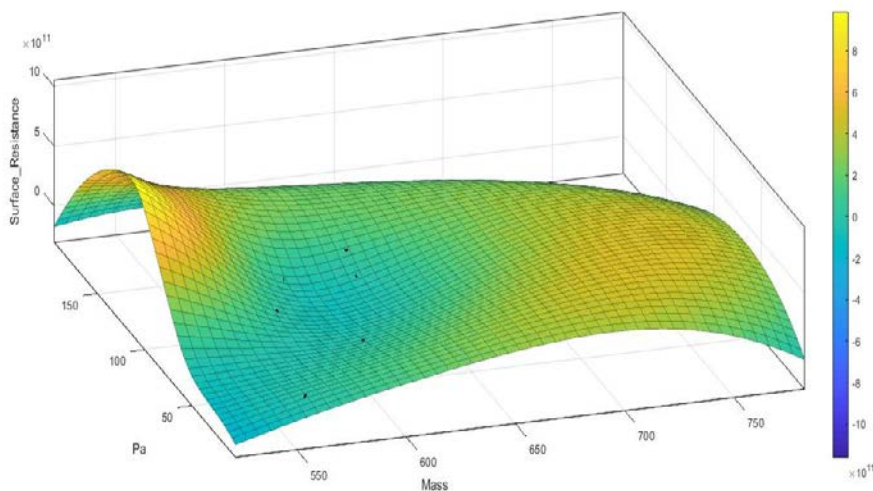
Table 8. Rotated Factor Loadings using Quartimax Rotation and Communalities

Variable	Factor1	Factor2	Factor3	Factor4	Communality
Rs	-0.173	0.045	0.984	-0.003	1.000
M	0.927	0.114	-0.160	0.318	1.000
δ	0.960	0.023	-0.041	-0.276	1.000
Pa	0.114	0.992	0.044	0.003	1.000
Variance	1.8246	1.0007	0.9971	0.1776	4.0000
% Var	0.456	0.250	0.249	0.044	1.000

Table 9. Factor Score Coefficients

Variable	Factor1	Factor2	Factor3	Factor4
Rs	0.110	-0.059	1.039	0.222
M	0.506	-0.067	0.098	1.740
δ	0.582	-0.067	0.100	-1.620
Pa	-0.077	1.020	-0.061	-0.173

In figures 1 – 3, are presented the 3D representations for the Rs depending on the mass (M), thickness (δ), and air permeability (Pa).

**Figure 1.** 3D surface representation $R_s = f(Pa, M)$

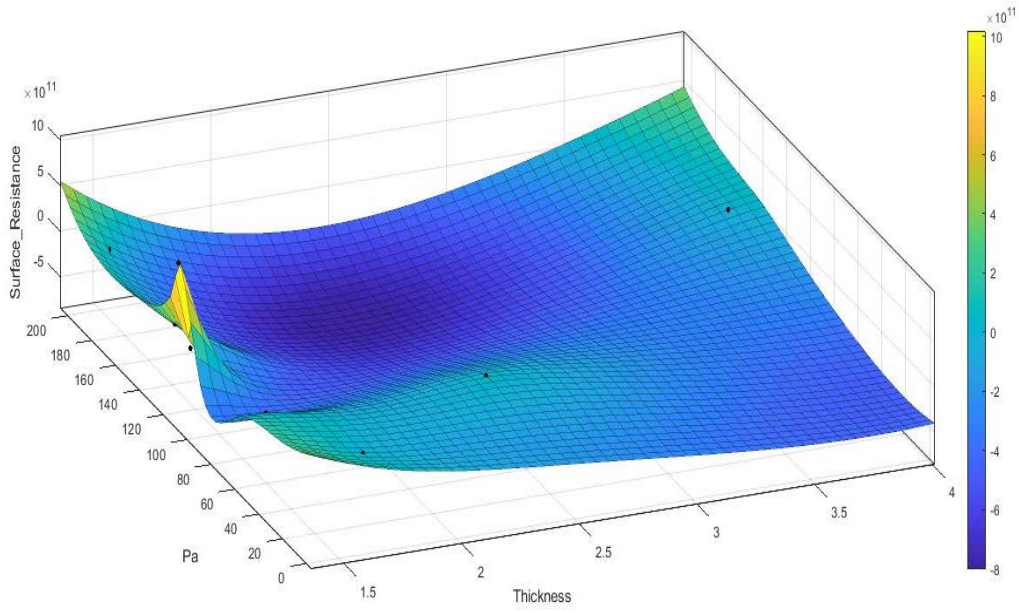


Figure 2. 3D surface representation $R_s = f(Pa, \delta)$

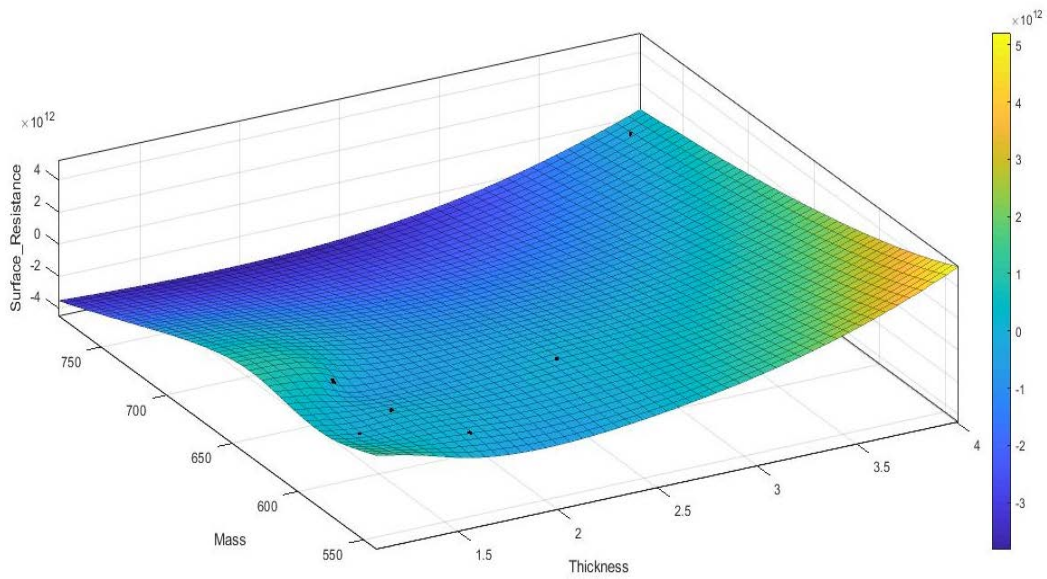


Figure 3. 3D surface representation $R_s = f(M, \delta)$

In the math expressions 1-6 are presented the correlation coefficients $r_{R_s,Pa}$, $r_{R_s,M}$, $r_{R_s,\delta}$, $r_{M,\delta}$, $r_{M,Pa}$, $r_{\delta,Pa}$.

$$r_{R_s,Pa} = \begin{vmatrix} 1.0000 & 0.0684 \\ 0.0684 & 1.0000 \end{vmatrix} \Leftrightarrow r_{12_{R_s,Pa}} = r_{21_{R_s,Pa}} = 0.0684 \quad (1)$$

$$r_{R_s,M} = \begin{vmatrix} 1.0000 & -0.3131 \\ -0.3131 & 1.0000 \end{vmatrix} \Leftrightarrow r_{12_{R_s,M}} = r_{21_{R_s,M}} = -0.3131 \quad (2)$$

$$r_{R_s,\delta} = \begin{vmatrix} 1.0000 & -0.2043 \\ -0.2043 & 1.0000 \end{vmatrix} \Leftrightarrow r_{12_{R_s,\delta}} = r_{21_{R_s,\delta}} = -0.2043 \quad (3)$$

$$r_{M,\delta} = \begin{vmatrix} 1.0000 & 0.8116 \\ 0.8116 & 1.0000 \end{vmatrix} \Leftrightarrow r_{12_{M,\delta}} = r_{21_{M,\delta}} = 0.8116 \quad (4)$$

$$r_{M,Pa} = \begin{vmatrix} 1.0000 & 0.2132 \\ 0.2132 & 1.0000 \end{vmatrix} \Leftrightarrow r_{12_{M,Pa}} = r_{21_{M,Pa}} = 0.2132 \quad (5)$$

$$r_{\delta,Pa} = \begin{vmatrix} 1.0000 & 0.1297 \\ 0.1297 & 1.0000 \end{vmatrix} \Leftrightarrow r_{12_{\delta,Pa}} = r_{21_{\delta,Pa}} = 0.1297 \quad (6)$$

4. RESULTS AND DISCUSSIONS

The results obtained following the experimental plan (Table 1), in comparison with an insulative material (M), consists in:

- 5 samples (1, 5, 7, 8, 9) based on Ni, PPY+Fe₃O₄, Ni+Al, Al and Zn having the electrical resistance specific to the conductive materials (10³-10⁵Ω) with potential to be used such as electrodes in sensors, actuators or electromagnetic shield for electromagnetic waves attenuation;

- 4 samples (2, 3, 4 and 6) based on Ni+Cu, Cu, PPY and Fe₃O₄ having the electrical resistance specific to the static dissipative materials (10⁷-10¹¹ Ω) with potentially safe in ESD (electrostatic discharge) environment and prevent the damage of the sensitive equipment.

Evaluating the math expressions 1-6 concerning the correlation coefficients $r_{R_s, Pa}$, $r_{R_s, M}$, $r_{R_s, \delta}$, $r_{M, \delta}$, $r_{M, Pa}$ and $r_{\delta, Pa}$, we found that:

→ The greatest correlation coefficient is between the mass and thickness and the lowest one is between the surface resistance and the mass: $r_{M, \delta} > r_{M, Pa} > r_{\delta, Pa} > r_{R_s, Pa} > r_{R_s, \delta} > r_{R_s, M}$. This means that between the mass and thickness it is a strong dependence. Withal, between surface resistance and mass is a moderate negative correlation which means if the independent variable (mass) increases, the dependent variable (surface resistance) tends to decrease.

→ Between surface resistance and air permeability it is a strong and positive correlation and which means that by increasing the air permeability (independent variable) of the fabric, the discontinuities and pores in the fabric increase and the distance between metallic conductive particles increase and this led to the reduction of the surface conductivity and increasing the surface resistance (dependent variable). As a result, the surface resistance has increased due to the air insulation and the reduction of the distance between the conductive microparticles in a certain level of the fabric.

→ Between the surface resistance and thickness, it is a negative dependence which means if the independent variable (thickness) increases due to the conductive layer thickness, the dependent variable (surface resistance) tends to decrease.

5. CONCLUSIONS

In conclusion, the samples obtained have an electrical resistance specific to the conductive materials (10³-10⁵ Ω) used for sensors, actuators or EM shields, respective for dissipation of the static energy (10⁷-10¹¹ Ω).

In addition, the analysis of the principal components is important because it generates:

- the reduction of the redundant data;
- establish the correlations and covariance between variables necessary in the prediction of the variable's dependencies;
- discover the latent variables;
- establish the correlation and covariance matrix.

The analysis of the correlation coefficient conducts to conclusions that the surface resistance is not in a dependent relationship with the mass and thickness, and is in a dependent

relationship with air permeability. However, a higher value of the air permeability means that the conductive layer is not perfectly continuous, the conductivity is reduced and the surface resistance increase with the density of the air gaps in the fabric, because the air is a good insulator having a resistivity between 1.3×10^{16} to $3.3 \times 10^{16} \Omega$.

ACKNOWLEDGEMENTS

The research presented in this paper was prepared in the INCDTP laboratories. Funds support this work from MCI, National Project "Materiale textile composite electroconductive pe bază de matrici polimerice 3D pentru sisteme senzoriale de monitorizare și de atenuare a undelor electromagnetice (3D ELECTROTEX)", Contract PN 19 17 01 01.

REFERENCES

- [1] Wang, X., et al., *Study on the electrical resistance of textiles under wet conditions*, In: Textile Research Journal, 2009, 79,8, 753-760
- [2] Kuhn, H.H., et al., *Properties and applications of conductive textiles*, In: Synthetic Metals, 1993, 57, 1, 3707-3712
- [3] Attia, N.F., El Ebissy, A.A., Hassan, M.A., *Novel synthesis and characterization of conductive and flame retardant textile fabrics*, In: Polymers for Advanced Technologies, 2015, 26, 12, 1551-1557
- [4] Inoue, M., et al., *Development of highly conductive inks for smart textiles*, In: 14th International Conference on Electronic Materials and Packaging (EMAP), IEEE, 2012, 1-4
- [5] Kim, B., et al., *Electrical and morphological properties of PP and PET conductive polymer fibers*, In: Synthetic Metals, 2004, 146, 2, 167-174
- [6] Grancaric, A.M., et al., *Conductive polymers for smart textile applications*, In: Journal of Industrial Textiles, 2018, 48, 3, 612-642
- [7] Kuhn, H.H., et al., *Properties and applications of conductive textiles*, In: Synthetic Metals, 1993, 57, 1, 3707-3712
- [8] Neves, A.I., et al., *Towards conductive textiles: coating polymeric fibres with graphene*, In: Scientific reports, 2017, 7, 1, 1-10
- [9] Skeifvars, M., Rehnby, W., Gustafsson, M., *Coating of textile fabrics with conductive polymers for smart textile applications*, In: Ambience 08, Borås, Sweden, 2008
- [10] Tseghai, G.B., et al., *PEDOT: PSS-based conductive textiles and their applications*, In: Sensors, 2020, 20, 7, 1881
- [11] Kuhn, H.H., *Characterization and application of polypyrrole-coated textiles*, In: Intrinsically conducting polymers: an emerging technology. Springer, Dordrecht, 1993, 25-34
- [12] Wang, X., Xu, W., Li, W., Cui, W., *Study on the electrical resistance of textiles under wet conditions*, In: Textile Research Journal, 2009, 79, 8, 753-760
- [13] Hearle, J.W.S., *The Electrical Resistance of Textile Materials: III. Miscellaneous Effects*, In: Journal of the Textile Institute Transactions, 1953, 44, 4, T155-T176
- [14] Hearle, J.W.S., *The electrical resistance of textile materials: II. the effect of temperature*, In: Journal of the Textile Institute Transactions, 1953, 44, 4, T144-T154
- [15] Root, W., Wright, T., Caven, B., Bechtold, T., Pham, T., *Flexible textile strain sensor based on copper-coated lyocell type cellulose fabric*, In: Polymers, 2019, 11, 5, 784
- [16] Shaikh, T.N., Chaudhari, S., Patel, B.H., Patel, M., *Study of conductivity behavior of nano copper loaded nonwoven polypropylene based textile electrode for ECG*, In: International Journal of Emerging Science and Engineering, 2015, 3, 4, 11-14
- [17] Jang, S., Cho, J., Jeong, K., Cho, G., *Exploring possibilities of ECG electrodes for bio-monitoring smartwear with Cu sputtered fabrics*, In International Conference on Human-Computer Interaction, Springer, Berlin, Heidelberg, 2007, 1130-1137
- [18] Pani, D., Achilli, A., Bonfiglio, A., *Survey on textile electrode technologies for electrocardiographic (ECG) monitoring, from metal wires to polymers*, In: Advanced Materials Technologies, 2018, 3, 10, 1800008

- [19] Pequegnat, A., Daly, M., Wang, J., Zhou, Y., Khan, M.I., *Dynamic actuation of a novel laser-processed NiTi linear actuator*, In: Smart materials and structures, 2012, 21, 9, 094004
- [20] Lima, P.C., Rodrigues, P.F., Ramos, A.S., da Costa, J.D., Braz Fernandes, F.M., Vieira, M.T., *Experimental Analysis of NiTi Alloy during Strain-Controlled Low-Cycle Fatigue*, In: Materials, 2021, 14, 16, 4455
- [21] Nadi, A., Sbai, S.J., Bentiss, A., Belaiche, M., Briche, S., Gmouh, S., *Application of Fe₃O₄ nanoparticles on cotton fabrics by the Pad-Dry-Cure process for the elaboration of magnetic and conductive textiles*, In: IOP Conference Series: Materials Science and Engineering, 2020, 827, 1, 012021
- [22] Jiang, S.X., Guo, R.H., *Electromagnetic shielding and corrosion resistance of electroless Ni-P/Cu-Ni multilayer plated polyester fabric*, In: Surface and Coatings Technology, 2011, 205, 17-18, 4274-4279
- [23] Palanisamy, S., Tunakova, V., Militky, J., *Fiber-based structures for electromagnetic shielding—comparison of different materials and textile structures*, In: Textile Research Journal, 2018, 88, 17, 1992-2012



INTEGRATION OF MAGNETIC MATERIALS WITH ACTUATOR ROLE ON TEXTILE SUPPORTS

DOI: 10.35530/TT.2021.45

C. Grosu*, R.M. Aileni, S. Olaru

National Research Development Institute for Textiles and Leather, Romania
(E-mail: cristina.grosu@incdtp.ro; raluca.aileni@incdtp.ro; sabina.olaru@incdtp.ro)

Abstract: *Magnetic textile materials represent a new category of smart materials, whose properties are obtained either by adding magnetic materials during the technological processes of obtaining fibres and yarns, either by applying some magnetic materials on textile surfaces during the chemical finishing processes (electroless plating, electroplating, magnetron sputtering). Therefore, by adding magnetic nano powders in the spinning solution, fibres with magnetic properties are obtained, by adding metallic fibres, with magnetic properties, during the spinning process, magnetic yarns are obtained, and by the insertion of a certain percent of metallic/magnetic yarns during the weaving or knitting process, textile materials with magnetic properties are obtained. Thus, magnetic textile materials will possess the uniqueness of a textile structure due to specific features as flexibility, breathability or lightweight, but at the same time, also the magnetic properties necessary in multiple applications such as magnetic sensors, actuators and electromagnetic shielding used in technical applications for defence, automotive and aerospace.*

Keywords: *actuators, composites, filler, functionalization, magnetic materials, textiles*

1. INTRODUCTION

Magnetic textiles belong to the group of smart textiles, as independently of their natural textile features, they are characterized by new magnetic properties which depend on the type of magnetic material (the filler) included in the textile matrix, as well as on the filling degree [1]. For the magnetic functionalization of the textile materials, are usually used composites based on magnetic materials such as iron oxide nanoparticles (Fe_2O_3 or Fe_3O_4) combined with conductive polymers (polypyrrole (PPY), polyaniline (PANI), polythiophene (PTH)). Inherently, conductive polymers such as PPY or PANI, known as “synthetic metals”, are unique due to their electrical properties similar to those of metals, while maintaining the mechanical characteristics of polymers [2-4]. The resulted composite materials, consisting of two or more components with magnetic and electrical properties, gain significantly different electromagnetic, physical and chemical properties, as compared with the properties of initial materials. Thus, the added magnetic component allows the responses of the composite material under the influence of an external magnetic field [5,6] and is very useful in medical applications for drug delivery.

The parameters such as dielectric permittivity, magnetic permeability and electrical conductivity define the electromagnetic properties of a textile material [7].

This research paper presents a study of the magnetic textile materials – focused on the obtaining processes, their magnetic properties and applications.

2. OBTAINING PROCESSES OF MAGNETIC TEXTILE MATERIALS

Conventional textiles are generally obtained from non-magnetic and non-conductive polymeric materials, which means that they are magnetically negative. Table 1 shows the values of magnetic susceptibility (χ), for some reference raw textile materials.

Table 1. Magnetic susceptibility of some textile fibres [7]

Material	Magnetic susceptibility (χ)
Ethylene	-10.3×10^{-6}
Polypropylene	-10.1×10^{-6}
Fluorine	-47.8×10^{-6}
Polyester	-6.53×10^{-6}
Nylon 66	-9.55×10^{-6}

Magnetic functionalization of the textile materials can be achieved by:

- the introduction of some materials with special properties during the obtaining process of fibre/yarn/material;
- the deposition of some materials with specific characteristics on the fibre/yarn/material surface during the finishing process [7,8].

Therefore, magnetic functionalization of fibres, yarns and 2D and 3D textile surfaces can be obtained:

- a) during the fabrication process of the fibres;
- b) during the spinning process of the yarns;
- c) during the obtaining process of braided, woven, non-woven and knitted materials;
- d) during the finishing process of fibres, yarns and textile structures [7,9,10].

2.1 Fibres functionalization

During the spinning process of the textile fibres, metallic fibres, carbon/ graphite fibres, or intrinsic conductive polymeric materials, with intrinsic electromagnetic functionalities, can be used to replace partially or totally the conventional fibrous textile material. The most exploited raw material for obtaining magnetic textile fibres is cellulose, in the solution of which is possible to add powders with magnetic properties, such as iron, cobalt, nickel and different ferrites, by mixing during the spinning process [7,11].

Chemical finishing, in the case of conventional fibres that lack electromagnetic properties, allows the deposition on their surface of some metallic coatings or powders by different procedures, such as electroless plating, electroplating, magnetron sputtering, *in situ* polymerization, etc. [7]. The most exploited textile fibres suitable for magnetic functionalization by chemical finishing are natural vegetal fibres, like cotton, with high cellulose content, known for its important role in fixing and stabilizing the binder, with a high degree of hygroscopicity and retention of aqueous substances, but also new as mango fibres, etc. [12-15].

2.2 Yarns functionalization

The introduction of fibres with electromagnetic properties during the spinning process of yarns leads to magnetic yarns. Obtaining these yarns by processes like blending or enveloping, necessitates particular attention, especially regarding the ratio between the magnetic/metallic fibres and the conventional ones, knowing that metallic fibres are not suitable to be used alone for weaving because of their low elongation and poor toughness [7].

By inserting a microfilament with electromagnetic properties in the yarn structure, there could be obtained the following yarns with magnetic properties: i) yarns obtained by enveloping the exterior of a metallic microfilament with a fibrous layer; ii) twisted yarn obtained by twisting together a metallic microfilament with a conventional textile yarn; iii) plied yarn obtained by parallel feeding of the conventional textile yarn and the metallic filament [16].

Chemical finishing is a deposition process onto the yarn surface of a metallic coating or powder by processes like electroless plating, electroplating, magnetron sputtering, etc., to obtain the targeted magnetic properties [7,17].

2.3 Textile surfaces functionalization

During the weaving or knitting process of textile structures, the metallic yarn cannot be used as unicomponent element, due to its poor elongation and flexibility, necessitating additional processing steps like blending or enveloping with conventional fibres. Thus, there can be obtained functionalized yarns with magnetic properties, adequate for direct feeding of weaving or knitting machines, in different ratios with conventional yarns [7]. Several experimental reports have shown that both in the case of rectilinear or circular knitting machines, as well as in the case of classical weaving machines, feeding of yarns with metallic microfilament content was possible, in the same time establishing the relationship between the feeding ratio of metallic yarns and the electromagnetic shielding effectiveness [16].

Chemical finishing techniques, like solution impregnation, coating or scraping, represent the last step in the fabrication process of textile material and implies the addition of chemical products to the textile materials, their aspect remaining generally unchanged after these procedures [8].

Impregnation with a solution containing ferromagnetic microfilaments proved to be unsuitable in the case of functionalizing textile materials intended for shielding electromagnetic waves. By impregnation of a 100% cotton fabric with a 20% polyurethane solution, containing ferromagnetic filaments, an uneven distribution onto the fabric surface of the ferromagnetic microfilaments was obtained. Fibre agglomerations appeared even since the blending step with the polyurethane solution. Solving the problem of uneven distribution through solution impregnation in two steps proved to be inefficient in terms of the filling degree of the composite material, which increased proportionally with the polyurethane solution concentration [16].

In the case of metallic nanoparticles easily oxidized by air or aqueous solutions (e.g., nano copper), it is recommended the addition of a small quantity of ascorbic acid (Vitamin C) in the polymeric matrix of the doped solution with ferromagnetic filaments/powders [18].

The coating with neo dim magnetic microparticles onto textile substrates obtained by different technologies (knitting or weaving), revealed higher performances for the composite based on knitted structure compared to the woven structure, due to the higher energy present on the surface, due to the higher wetting capacity and rubbing coefficient, leading so to higher retention of magnetic powder [10].

Significant magnetic performances have been obtained by coating cotton with barium ferrite ($\text{BaFe}_{12}\text{O}_{19}$) doped aniline solution, resulting in a new composite material, with electromagnetic properties with particular values of remanent magnetization of 0.54 emu/g, as well as coercive value of 4700 G, under ambient conditions [19].

Scraper coating of some woven textile materials with solutions doped with hard magnetic powders of barium hexaferrite ($\text{BaFe}_{12}\text{O}_{19}$), demonstrated that the magnetic performances increase directly proportional to the percent of magnetic powder from the coating solution. For a more even deposition onto the textile surface, it is recommended that

the size of selected ferromagnetic powders to be at nano level [20]. Similar conclusions were elaborated, that the increase of the mass, thickness and air permeability of fabric will generate the decreasing of the conductivity, a fact explained by the decreased concentration of the magnetic nanoparticles onto the fabric surface, when multivariate regression analysis was applied [21].

Magnetron sputtering allows the deposition metallic layers, with nanometre thicknesses onto the textile structure surfaces. The tests have shown that by copper deposition onto the textile structure surfaces, the electromagnetic shielding effectiveness of textile materials grew significantly [22].

Plasma treatment at atmospheric pressure proved to be superior to conventional cleaning, by improving the hydrophily. The process is more friendly with the environment compared to conventional procedures, which implies the use of higher quantities of water and various chemical substances [23,24].

3. APPLICATIONS OF MAGNETIC TEXTILE MATERIALS

Due to the fundamental properties exhibited by the magnetic textiles, such as electrical conductivity, dielectric permittivity and magnetic permeability these are exploited in a large number of applications in the field of aerospace, automotive, medicine and smart clothing (sport, protection) [18].

Composites obtained by introducing ferromagnetic nano powders into the fibres spinning solution are also known as electromagnetic composites, due to their multiple applications in structures of microelectronic and nano-electronic micro-mechanical systems (MEMS) and bio-micro-mechanical systems (MioMEMS) [1].

Magnetic textiles exhibit a great potential for applications in the fields of medical devices (actuators and magnetic sensors). Magneto-active fabrics (MAFs), as magnetic dielectric tissues, obtained through soaking with silicone oil and iron oxide microfibers, represent a promising candidate for the fabrication of health monitoring systems and electromagnetic radiation absorbers [25].

Luminescent magnetic fibres obtained from the modification of the lyocell fibres through the NMNO (*N*-methyl morpholine-*N*-oxide) method are successfully used for the production of threads and yarns. Under UV light irradiation, this novel fibre glows and exhibits magnetization, being an innovative method of intellectual rights protection in the fashion industry, because the original garments become almost impossible to counterfeit [26].

4. CONCLUSIONS

Factors that influence the magnetic functionalization process of conventional textile materials, by integration of magnetic materials on the textile structure surfaces, are as follows:

- **Nature of the textile raw material:** *cotton* fibre is the most frequently used for the substrates of the composite materials designed with magnetic properties based on classical finishing processes with dispersions or pastes-based water. This is due to the multiple polar cellulose groups present on the cotton fibre, which gives its high hydrophilicity and an excellent wetting capacity, but also because improves the comfort properties of the resulted composite material. Even if synthetic fibres, such as polyamide and polyester, although possess polar groups, cannot absorb large quantities of water, due to their advanced crystallinity [2,10,16,18,19,22], but can be used successfully in case of using the coating technologies such as electroless plating, electroplating or magnetron sputtering.

- **Obtaining process of the textile substrate:** there are only a few studies regarding the obtaining of composite materials with magnetic properties, using knitted structures as substrates, compared with the using of woven structures. Knitwears, especially the 3D ones, possess a high potential for exploitation in this direction, due to high breathability given by the controllable porous structure, due to the controllable cross-section geometry by binding the external layers with yarns or other knitted structures having electromagnetic properties.

The high potential of the knitwears was also confirmed by several studies that compared the magnetic properties obtained by depositing under similar conditions of the solutions containing ferromagnetic materials on knitted and woven substrates, respectively [2,7,10].

Mainly, for magnetic composites development are used conductive polymers such as PPY, PANI, PTH mixed with magnetic nanoparticles. These composites obtained have numerous applications for actuators [2-4,27].

The higher the concentration of magnetic powder dopped in the coating solution of the textile substrate, the higher the magnetic induction intensity of the composite material [10,19,20].

To improve the electromagnetic properties of a textile structure it is possible to simultaneously use: the insertion of conductive yarns during the weaving/knitting process, followed by the deposition onto the surface material of a thin layer containing ferromagnetic nanoparticles [22,28].

ACKNOWLEDGEMENTS

This work was supported through the National Nucleu Programme, with the support of MEC, Contract PN 19 17 01 01, project title: “Composite materials with electroconductive properties, based on 3D polymeric array for sensorial monitoring systems and electromagnetic waves attenuation (3D ELECTROTEX)”.

REFERENCES

- [1] Rubacha, M., Zieba, J., *Magnetic Textile Elements*, In: *Fibres & Textiles in Eastern Europe*, 2006, 14, 59, 49-53
- [2] Loghin, C., Cianga, L., Ciobanu, L., Cianga, I., Yagci, Y., Nicolaiov, P., *Textile composites based on conductive polymers*, In: *Buletinul Institutului Politehnic din Iasi*, 2010, 57-66
- [3] Teslaru, T.L., *Caracterizarea filmelor de poliotiofen obținute în reactori cu plasmă la presiune atmosferică*, Iasi, 2015
- [4] Kongahage, D., Foroughi, J., *Actuator materials: review on recent advances and future outlook for smart textiles*, In: *Fibers*, 2019, 1-24
- [5] Loghin, C., *Composite textile structures for protective systems against electromagnetic radiations*, Iasi, 2007
- [6] INCD pentru Tehnologii Izotropice si Moleculare, *Cresterea capacitatii de transfer tehnologic si de cunoastere a INCDTIM in domeniul Bioeconomiei*, Cluj Napoca, 2018
- [7] Xiao, H., Shi, M., Chen, J., *Electromagnetic Function Textiles*, In: *Electromagnetic Materials*, IntechOpen, 2019, 1-32
- [8] Kumar, R.S., Sundaresan, S., *Advances in the dyeing and finishing of technical textiles*, In: M.L. Gulrajani, *Advances in the dyeing and finishing of technical textiles*, Woodhead Publishing, 2013, 270
- [9] Ehrmann, A., Blachowicz, T., *Magnetic Yarns, Fabrics, and Coatings*, In: *Examination of Textiles with Mathematical and Physical Methods*, Springer, 2016, 31-46, https://doi.org/10.1007/978-3-319-47408-3_3
- [10] Zhou, Y., Zhu, W., Zhang, L., Gong, J., Zhao, D., Liu, M., Sun, Y., *Magnetic properties of smart textile fabrics through a coating method with NdFeB flake-like microparticles*, In: *Journal of*

Engineered fibers and fabrics, 2019, 14, <https://journals.sagepub.com/doi/10.1177/1558925019865708>

- [11] Rubacha, M., Zieba, J., *Magnetic Cellulose Fibres and Their Application in Textronics*, In: *Fibres & Textiles in Eastern Europe*, 2007, 15, 5-6, 101-104
- [12] Small, A.C., Johnston, J., *Novel hybrid materials of magnetic nanoparticles and cellulose fibers*, In: *Journal of Colloid and Interface Science*, 2008, <https://doi.org/10.1016/j.jcis.2008.11.038>
- [13] Souza Junior, F.G., da Silva, A.M., de Oliveira, G.E., Costa, R.M., Fernandes, E.R., Pereira, E.D., *Conducting and magnetic mango fibers*, In: *Industrial Crops and Products*, 68 Special Issue, 2014, 97-104, <https://doi.org/10.1016/j.indcrop.2014.09.032>
- [14] Frydrysiak, M., Grosu, M. C., Zieba, J., Lupu, I.G., *Textile magnetic yarns – research and simulation*, In: *Industria Textila*, 2015, 66, 6, 322-328
- [15] Blachowicz, T., Ehrmann, A., *Simulation on magnetic coatings on textile fibers*, In: *Journal of Physics*, 2016, <http://doi.org/10.1088/1742-6596/738/1/012057>
- [16] Universitatea Tehnică "Gheorghe Asachi", *Sisteme mecatronice inteligente pentru echipamente textile*, Iasi, 2010
- [17] Grosu, M.C., Lupu, I.G., Cramariuc, O., Hogas, H.I., *Fabrication and characterization of magnetic cotton yarns for textile applications*, In: *The Journal of the Textile Institute*, 2018, 109, 10, 1348-1359, <https://doi.org/10.1080/00405000.2018.1423935>
- [18] Hassabo, A.G., El-Naggar, M.E., Mohamed, A.L., Hebeish, A.A., *Development of multifunctional modified cotton fabric with tri-component nanoparticles of silver, copper and zinc oxide*, In: *Carbohydrate Polymers*, 2019, 144-156
- [19] Onar, N., Akşit, A.C., Ebeoglugil, M.F., *Conductivity and magnetic properties of coated fabrics with barrium ferrite doped aniline solution*, In: *International Technical Textiles Congress, Istanbul*, ResearchGate, 2007, 200-208
- [20] Grosu, M.C., Lupu, I.G., Avram, D., Tudorache, F., *Magnetic woven fabrics - physical and magnetic properties*, In: *Annals of the University of Oradea. Fascicle of Textiles, Leatherwork*, 2015, 43-48
- [21] Aileni, R.M., Albici, S., Chiriac, L., Sandulache, I.M., *Multivariate regression analysis of the 3D composites with electroconductive*, In: *Industria Textila*, 2020, 71, 4, 334-339, <https://doi.org/10.35530/IT.071.04.1767>
- [22] Rădulescu, I.R., Surdu, L., Mitu, B., Morari, C., Costea, M., Golovanov, N., *Conductive textile structures and their contribution to electromagnetic shielding effectiveness*, In: *Industria Textila*, 2020, 71, 5, 432-437, <https://doi.org/10.35530/IT.071.05.1783>
- [23] Kan, C.-w., Lam, C.-f., *Atmospheric pressure plasma treatment for grey cotton knitted fabric*, In: *Polymers*, 2018, 1-16
- [24] Aileni, R.M., Albici, S., Dinca, L., Surdu, L., *Bivariate analysis of the hydrophobic textiles obtained by plasma treatment*, In: *Industria Textila*, 2019, 70, 6, 527-532, <https://doi.org/10.35530/IT.070.06.1476>
- [25] Bunoiu, M., Anitas, E. M., Pascu, G., Chirigiu, L. M., Bica, I., *Electrical and Magnetodielectric Properties of Magneto-Active Fabrics for Electromagnetic Shielding and Health Monitoring*, In: *International Journal of Molecular Sciences*, 2021, 21, 13, <https://doi.org/10.3390/ijms21134785>
- [26] Skwierczynska, M., Runowski, M., Goderski, S., Szczytko, J., Rybusinski, J., Kulpinski, P., Lis, S., *Luminescent-Magnetic Cellulose Fibers, Modified with lanthanide- Doped Core/ Shell Nanostructures*, In: *ACS OMEGA*, 2018, 3, 10393-10390, <https://doi.org/10.1021/acsomega.8b00965>
- [27] Pandey, D.N., Basu, A., Kumar, P., *Electro Conductive Knitted Structure: An Over View*, In: *Emerging Trends in Engineering & Technology*, 2016, 261-265
- [28] Maziz, A., Concas, A., Khaldi, A., Stalhald, J., Persson, N.-K., Jager, E., *Knitting and weaving artificial muscles*, In: *Applied Science and Engineering*, 2017, 1-11



ROLE OF THE E-LEARNING COURSES FOR CAPACITY BUILDING IN THE FIELD OF ADVANCED MATERIALS DEVELOPMENT

DOI: 10.35530/TT.2021.43

R.M. Aileni*, L. Chiriac

National Research Development Institute for Textiles and Leather, Romania
(E-mail: aileni.raluca@incdtp.ro, laura.chiriac@incdtp.ro)

Abstract: *This work presents several aspects concerning the e-learning courses about composite materials developed for capacity building in the field of advanced materials for new or upgraded research centers in Morocco and Jordan. The proposed course for capacity building in the field of advanced materials development is represented by 3D advanced composites obtained through textile technologies and additive manufacturing processes. This course presented using e-learning technologies received increased interest from students attending the learning sessions in the framework of the Fostex Erasmus+ project because can be applied to obtain composites for a large area of industries such as automotive, construction, medicine, electronics/electrotechnical and aerospace. The textile composites are materials made from 2/more constituent materials with different chemical, physical and electrical properties. When combined, these materials generate a material (composite) with different characteristics than the initial individual components. The design and development of the composite can lead to new materials with superior characteristics: more robust, lighter, flexible, and less expensive in comparison with traditional materials such as metal, ceramics.*

Keywords: *e-Learning, electroconductive, 3D composites, textiles*

1. INTRODUCTION

In the framework of the project, Fostex Erasmus+ has been developed several courses about technical textiles including composites development and testing. These e-learning courses were developed to enhance the knowledge of the students (Ph.D., Master) and to improve employability in the new or upgraded research centers developed in Morocco and Jordan with financial support obtained through the Fostex Erasmus+ project for purchasing new equipment. The course about composites investigation and development was very appreciated by the audience because the composite opens a new perspective for the textile industry in strong connection to other industrial areas such as automotive, aerospace, construction, medicine or electro technique.

In general, composite textiles used in aerospace, construction, automotive, medicine, sports, electronics (wearable – lighter / flexible electrodes) are complex structures that can be developed using multidisciplinary approaches such as material science, chemistry physics, mathematics, textile and mechanics knowledge. The textile components such as fibers, yarns, filaments, knits, woven and nonwoven can be used in advanced composites development for reinforcements. The principal textile components for composites and the interdependences between them are presented in figure 1.

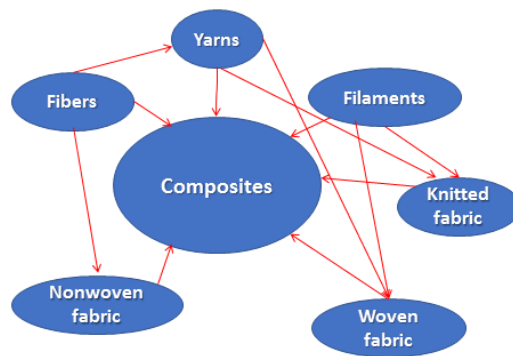


Figure 1. Textile components used in composites

2. COMPOSITES CLASSIFICATION

The classification of the composite materials is done according to the polymer type, reinforcements, and matrix types. According to the polymers used, the composites can be are thermoset and thermoplastic [1]:

- Thermoset composites are based on polymers such as epoxy, unsaturated polyester and vinyl-ester;
- Thermoplastic composites are based on the polymers such as polyester, high-density polyethylene (HDPE)

According to the reinforcements used, the composites can be classified on [2]:

- Laminated composites (lamination is done on the nonwoven, braided, fiber reinforced, 2D woven or knitted);
- 3D woven composites;
- 3D knitted composites.

According to matrix types used such as polymeric, metallic, ceramic or carbon/graphite), the composites [1,2] are:

1. Polymeric matrix thermoset (epoxides, polyester, polyamides) or thermoplastic reinforced with glass fibers, carbon fibre, aramid fibre or metallic fibre;
2. Metallic matrix;
3. Ceramic matrix (resistance at higher temperature 1000^0 C);
4. Carbon/graphite matrix (good resistance at high temperatures).

In line with the textile dimensions, the textile components used in composites can be 1D, 2D or 3D structures.

- **1D (fibers or yarns)**
- **2D nonwoven fabrics (nonwoven, knitted, woven)**
- **3D fabrics** (nonwoven, woven (figures 2 and 3), knitted (figures 4 and 5) offer through-the-thickness reinforcement, improve the interlaminar properties, and damage tolerance of the resulting composites.

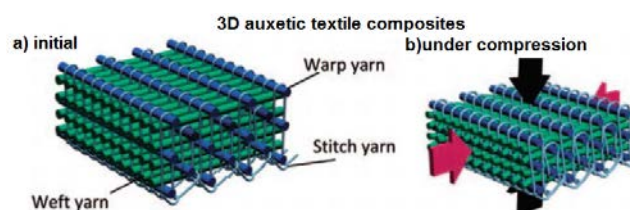


Figure 2. 3D composite fabrics [3]

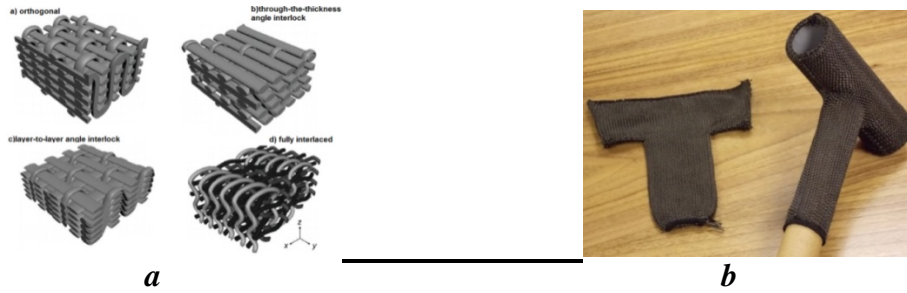


Figure 3. 3D woven composites: a - 3D woven structures [4]; b - UK, 3D carbon fibre preforms for composites [5]

The integrally knitted fabric preforms are produced by computer-controlled weft knitting machines (figure 4).

- **Multiaxial warp knit (MWK) fabrics** (figure 4)

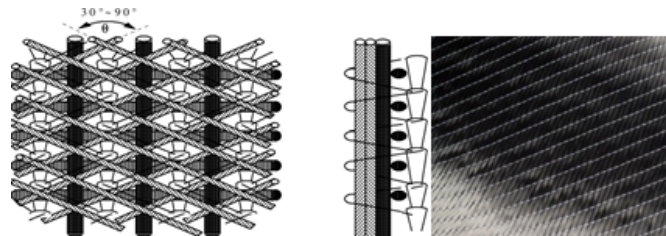


Figure 4. 3D composites based on warp knits (Karl Mayer –MWK) [6]

- **Spacer fabrics** (figure 5) are sandwich structures that consist of two knitted fabric layers connected by yarns.

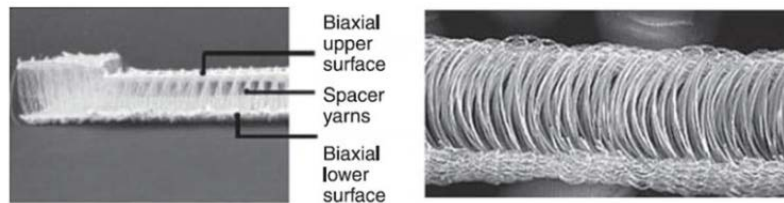


Figure 5. Spacer fabrics [7]

The 3D printing techniques are very versatile and offer an easy way to produce composites based on textile support (knits, nonwoven or woven fabrics) with applications in several industries:

- ➔ The fashion industry uses this hybrid technique to obtain innovative 3D knit shapes (figure 6).



Figure 6. 3D knits obtained through a 3D printing technique [8]

→ This technique is used in electronics to create circuits or sensors based on conductive filament (using filament melting) fused and deposited on the textile's surface. In this hybrid technique, the most important is the correlation between filament type, the plate's temperature and extruder head, and textile temperature resistance. In such a way can, be manufactured the tactile sensors using photopolymerization-based 3D printing (figure 7):

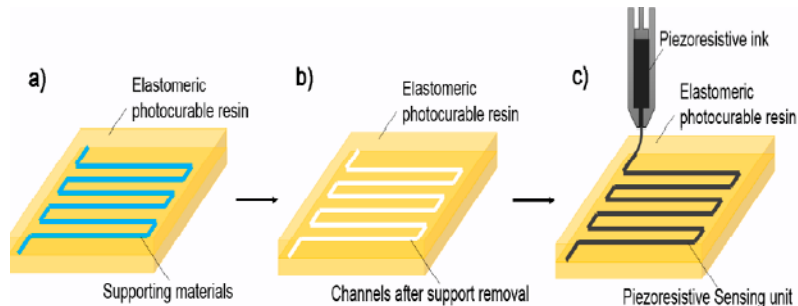


Figure 7. Tactile sensors fabrication using 3D printing [9]

- 3D printing techniques used in composite development are presented in figure 8.

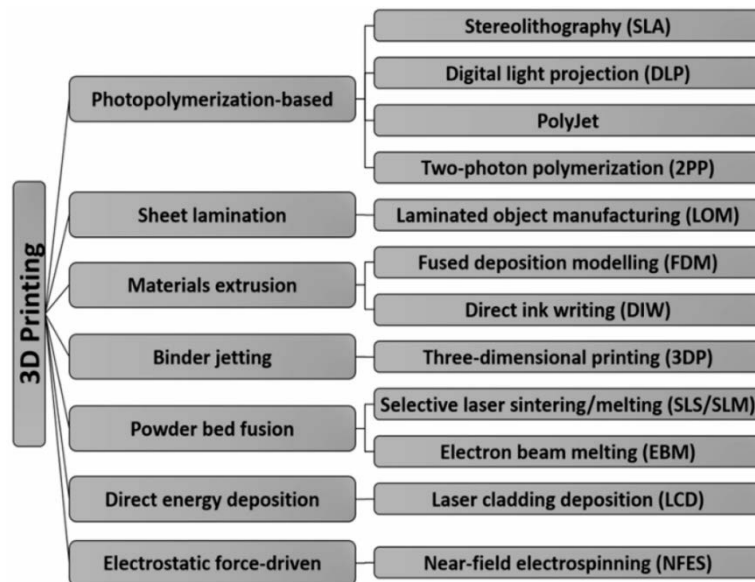


Figure 8. 3D printing technologies [9]

Composites-based polymeric matrix and micro/nanoparticles combined with textile support can be used to obtain textiles electrodes or tactile buttons integrated into textile. Very high importance in composites performance (mechanical properties) has the fiber-matrix interface.

To improve the fiber-matrix interface are used surface coating, plasma treatment, and chemical modification. The surface coating includes electrodeposition, chemical vapor deposition (CVD), metalorganic deposition, and vacuum deposition.

Table 1. Classification – Processes used for composite development [10]

Method	Matrix		State		Polymer melting
	Thermosetting	Thermoplastic	Liquid	Solid	
Hand lay-up	x		x		NO
Resin transform moulding (RTM)	x		x		NO
Autoclave moulding	x		x		NO
Compression molding	x		x		NO
Filament winding	x		x		NO
Resin infusion	x		x		NO
Resin pultrusion	x		x		NO
Injection moulding		x		x	YES
Thermoforming		x		x	YES

Hand lay-up is a simple manually molding process [10] for fabricating composites [10], consisting of applying the resin with a hand roller on the textile surfaces (woven, knitted, stitched, or bond fabrics) placed in the mold. The goal of the resin matrix is to reinforce the composite material.

Resin transfer moulding (RTM) processes [11] reinforce the fabric into the mould as a dry stack of materials, pre-compacted to the mould contour in some cases, and held together by a binder. Mainly this process is used in the automotive and aerospace industry.

The **autoclave moulding** process [12,13] is used to obtain moulded composite. The method consists of curing the composite parts at different high temperatures, pressure and time. Mainly this method is used for manufacturing composites for the automotive and aerospace industry.

The **compression moulding** process [14-16] consists of thermosetting composites for rubber gaskets, handles, car tires, electrical components, automotive parts, and polymer matrix composite parts.

In the compression moulding process [14-16], the polymer deposited in the mould cavity (liquid, pellets or powder) is heated and then placed into the lower half of the mould, and using a hydraulic system, the mould is closed, forming the piece shape in the mould cavity. After the polymerization, the raw material (polymers with contents of textiles components) is transformed into the closed mould's solid object. Finally, the mould is opened and the piece part resulted is removed. A good example is car tire manufacturing using textile materials as reinforcements.

The **filament winding** process [17] is an automated composite fabrication technique used to produce tubular structures such as storage tanks, vessels, missiles and rocket motor cases.

Resin pultrusion [18] develops advanced composite materials in which fibres and resin are pulled through a heated die.

The **resin infusion** process [19] is used to fill holes or gaps in porous material with liquid resin. Usually, this type of composite is used for aviation, yachts, train and truck body panels

The **injection moulding** process is used to fabricate composite materials by injecting molten material into a mould, using metals, glasses, elastomers, confections, thermoplastic/thermosetting polymers, fibres as reinforcements.

The **thermoforming** process [1] uses heat and pressure to transform flat sheet thermoplastics (unreinforced or reinforced) with fibre content into a desired three-dimensional shape.

5. CONCLUSIONS

In the framework of the Fostex Erasmus+ project was provided e-Learning courses about composite technical textiles development and investigation. The courses were very appreciated by the audience (Ph.D. and Master students) because can conduct to new challenging development of the textile for advanced multidisciplinary research and can generate new jobs and attractiveness to work in the new or upgraded research centers developed in Morocco and Jordan with financial support obtained through Fostex Erasmus+ project for purchasing new equipment.

ACKNOWLEDGEMENTS

The research presented in this paper was prepared within INCDTP. Funds support this work are from the Erasmus+ programme of the European Union, Project FOSTEX “Fostering innovation in the Jordan and Moroccan textile industry”, project no. 598347-EPP-1-2018-1-ES-EPPKA2-CBHE-JP.

This project has been funded with support from the European Commission. This publication [communication] reflects the views only of the author, and the Commission cannot be held responsible for any use which may be made of the information contained therein.

The logo for the FOSTEX project, featuring the word "FOSTEX" in a stylized, outlined font with a light blue and green color scheme.

Co-funded by the
Erasmus+ Programme
of the European Union 

REFERENCES

- [1] *Thermal conductivity applications*, Available at: thermtest.com/applications/fabric-thermal-conductivity [Accessed on June 2021]
- [2] Chilton, J., Velasco, R., *Applications of textile composites in the construction industry*, In: Design and manufacture of textile composites, Woodhead Publishing, 2005, 424-435
- [3] Ge, Z., Hu, H., *Innovative three-dimensional fabric structure with negative Poisson's ratio for composite reinforcement*, In: Textile Research Journal, 2013, 83, 5, 543-550
- [4] Liu, Y., de Araujo, M., Hu, H., *Advanced fibrous architectures for composites in aerospace engineering*, In: Advanced Composite Materials for Aerospace Engineering, Woodhead Publishing, 2016, 17-58
- [5] *Improved 3d knitted carbon fiber preforms developed*, Available at: advancedtextilesource.com/2017/08/01/improved-3d-knitted-carbon-fiber-preforms-developed [Accessed on June 2021]
- [6] *3D composites based on warp knits* (Karl Mayer –MWK), Available at: textiletuts.com/3d-textile [Accessed on June 2021]
- [7] Fangueiro, R., Soutinho, F., *Textile structures*. In: Fibrous and composite materials for civil engineering applications, Woodhead Publishing, 2011, 62-91
- [8] Sitotaw, D.B., Ahrendt, D., Kyosev, Y., Kabish, A.K., *Additive Manufacturing and Textiles—State-of-the-Art*, In: Applied Sciences, 2020, 10, 15, 5033
- [9] Liu, C., Huang, N., Xu, F., Tong, J., Chen, Z., Gui, X., Fu, Y., Lao, C., *3D printing technologies for flexible tactile sensors toward wearable electronics and electronic skin*, In: Polymers, 2018, 10, 6, 629
- [10] Raji, M., Abdellaoui, H., Essabir, H., Kakou, C.A., Bouhfid, R., *Prediction of the cyclic durability of woven-hybrid composites*, In: Durability and Life Prediction in Biocomposites, Fibre-Reinforced Composites and Hybrid Composites, Woodhead Publishing, 2019, 27-62
- [11] *Resin transfer moulding processes*, Available at: www.nal.res.in/en/techniques/resin-transfer-moulding-processes [Accessed on June 2021]
- [12] Manoj, K., *Autoclave molding*, Available at: www.slideshare.net/ManojK55/autoclave-molding [Accessed on June 2021]

- [13] Nele, L., Caggiano, A., Teti, R., *Autoclave cycle optimization for high-performance composite parts manufacturing*, In: Procedia CIRP, 572016, 241-246
- [14] Vallejo-Montesinos, J., Muñoz, U.M., Gonzalez-Calderon, J.A., *Mechanical Properties, Crystallization and Degradation of Polypropylene due to Nucleating Agents, Fillers and Additives*, In: Polypropylene: Uses and Benefits, chapter 4, 2016, 83
- [15] Tohidi, S.D., Rocha, A.M., Dencheva, N.V., Denchev, Z., *Single polymer laminate composites by compression molding of knitted textiles and microparticles of polyamide 6: Preparation and structure-properties relationship*, In: Composites Part A: Applied Science and Manufacturing, 2018, 109, 171-183
- [16] *Compression Molding – the manufacturing process*, Available at: www.engineeringclicks.com/compression-molding [Accessed on June 2021]
- [17] Lapkovskis, V., Mironovs, V., Kasperovich, A., Myadelets, V., Goljandin, D., *Crumb Rubber as a Secondary Raw Material from Waste Rubber: A Short Review of End-Of-Life Mechanical Processing Methods*, In: Recycling, 5, 4, 32
- [18] *Resin pultrusion*, Available at: olemiss.edu/depts/compmat1/pultrusion.html [Accessed on June 2021]
- [19] *Resin infusion*, Available at: netcomposites.com/guide/manufacturing/infusion-processes [Accessed on June 2021]



REVIEW ON DIFFERENT TYPES OF CLAY AND THEIR USE AS ANTIMICROBIAL AGENTS FOR TEXTILES TREATMENT

DOI: 10.35530/TT.2021.51

M.C. Lite¹, E.C. Tănăsescu¹, L.O. Secăreanu^{1,2}, I.M. Săndulache¹, O. Iordache¹,
E. Perdum¹

¹Material Research and Investigation Department, National Research Development Institute for Textiles and Leather, Romania

(E-mail: cristina.lite@incdtp.ro, cornelia.tanasescu@incdtp.ro, lucia.secareanu@incdtp.ro, irina.sandulache@incdtp.ro, ovidiu.iordache@incdtp.ro, elena.perdum@incdtp.ro)

²Faculty of Applied Chemistry and Materials Science, Romania

(E-mail: lucia.secareanu@incdtp.ro)

Abstract: *Traditional uses of clay as medicine started in prehistoric times (Aboriginal times). Natural clays have been used in ancient and modern medicine, but the mechanism that makes certain clays lethal to bacterial pathogens has not been yet identified. The aim of this paper is to identify the proper clays that could be used in textile industry for improving textiles` functionality, based on the information extracted from literature. It is important, to differentiate between the properties that make a clay `healing`, versus what makes it `antibacterial`. So far, literature is abundant in reports regarding `healing` clays, but, when tested against pathogens in vitro and compared to controls, they do not appear to have bactericidal properties. The studies carried out up to this point established that the physical adsorption of water and organic matter is the main feature which leads to healing properties of clays; however, the chemical interaction between clay and bacteria has received less attention. Clay properties, with potential application in medicine, have recently been started to be investigated and the results indicate that certain natural clays can have noticeable and extremely specific effects on microbial colonies. Further studies will be directed towards the characterization of the selected `clay-textile` pairs.*

Keywords: *antibacterial agents, clay, review, textile industry*

1. INTRODUCTION

Modern textile industry has an increasing contribution in ensuring a safe environment, by developing and supplying multifunctional textile materials and products that are safe to use.

Functional textiles have been developed since the late 1980s. The purpose of these textiles is to include a wide range of properties and to improve their performance [1]. In recent years, textile innovation has reached unsuspected levels. Thus, in a relatively short period of time, the textile industry had the most remarkable innovations.

One of the most important historical events which marked the progress of textiles manufacturing was the invention of steam engine, in 1782. Until that moment, textile production was mainly in domestic system [2].

Natural fibres (cotton, wool, silk, etc.) are aesthetic and intensively used to fabricate textile products (clothing, upholstery, carpets, etc.). With the advent of chemical fibres (which are divided into artificial and synthetic fibres), at the end of the 19th century - beginning of

the 20th century, the availability of materials / textiles with new characteristics and performances also provided superior technical properties. This gave rise to a starting point of replacing the natural fibres with chemical fibres, based on their similarities.

Multifunctional clothing products, by definition, are designed to meet the performance requirements of the users in extreme conditions, such as protective equipment for people exposed to hazardous environments, medical products or sportswear that facilitates movement and balance of the body, increasing endurance or reducing fatigue during sports activity [3].

Traditionally, textiles can be functionalized by printing processes, filming, etc. Other methods involve the incorporation of chemicals into textile finishing. The innovative techniques use specialized chemicals or new alternative media, such as microencapsulation (for example, by using cyclodextrins). Also, the emergence of nanotechnologies came along with a wide range of new possibilities regarding textile functionalization [3].

Textiles finishing with antimicrobial agents has been recently under intense investigation, leading to a development of the technologies and methods used. Of course, all these treatments also highlight the need to assess and ensure their ecological character [4].

The compounds evaluated and reported for their antimicrobial properties belong to various classes of substances, such as: gentamicin [5], antibiotics, salts, and esters of alkyl compounds with tin, alcohols, aldehydes, thiophenols, alkylphenols, thiocarbamate compounds, certain inorganic salts of heavy metals, imines and imides, certain organic structures, zeolites [6] and different types of gases [7-9].

As natural compounds present less side effects compared to synthetic pharmaceuticals, they are an attractive alternative for textiles finishing, from human health and ecological considerations [10].

It is known that clays can be found in large amounts, and they are relatively inexpensive. Clay is generally known as an earthy material that is flexible when moist and firm when dried, and it consists mainly of fine particles of silicates and other minerals [11]. Studies regarding clays as fine-grained rocks or soil components are essential for understanding the global biological and environmental processes. Clays were also used as a scientifically unsupported chelation treatment for heart disease and autism [12].

A wide variety of clays are used today for medicinal purposes - mainly for external applications (mud therapy). Among clays, the most used are kaolin clays and smectites, such as bentonite, montmorillonite, and *Fuller's earth* [13].

2. CLAYS – CLASSIFICATION AND SHORT HISTORY

In clays formation, the solvents, usually acidic, erode the rock after leaching through upper weathered layers. Apart from the weathering process, some clay minerals are formed through hydrothermal activity. There are two types of clay deposits: primary and secondary. Primary clays are residual deposits in soil and remain at the site of formation. Secondary clays are the clays that have been transported from the original location by water erosion and deposited in a new sedimentary deposit. Clay deposits are typically similar with extremely low energy depositional environments such as large lakes or marine basins [14].

Medicinal clays have been used in folk medicine from prehistoric times. Nowadays, clay is used by aboriginal people all over the world. The first recorded use of medicinal clay goes back to ancient Mesopotamia.

The *Ebers Papyrus* (an important medical text from ancient Egypt) describes the use of ochre (an earthy pigment containing ferric oxide, typically with clay, varying from light

yellow to brown or red) for a large range of health issues, including intestinal problems, as well as various eye problems [15].

The *Lemnian Earth* is a type of clay used to treat many health conditions in Classical Antiquity, (for example, as treatment for poisoning). It was mined on the island of Lemnos (the deposits may have been extinguished by then). It was used until the 19th century, as it was still listed in the pharmacopoeia from 1848. *Lemnian* clay is a red earth shaped into tablets with distinctive seals stamped on them, thus the name 'sealed earth' (terra sigillata-latin) [16]. The French naturalist Pierre Belon (1517–1564) was interested in investigating the mystery of the *Lemnian* clay. In 1543, he visited Constantinople and he encountered 18 types of different products marketed as *Lemnian Earth*. In the late 1540s Pierre Belon visited the island to investigate the clay and described it in his notes as *Terra Lemnia*. Then, He made a special journey to Lemnos, where he continued his investigation, and tried to find the source of the clay. He discovered that it was extracted only once a year (on 6 August) under the supervision of Christian monks and Turkish officials [17].

Soranus of Ephesus (100-140 AD) a Roman obstetrician, gynecologist and pediatrician also used to write prescriptions of clays as healing treatments [18].

Ibn al-Baitar, a Muslim scholar, born in Malaga, Spain, at the end of the 12th century, was the author of a famous pharmacology work – “Encyclopedia of the History of Arabic Science” about eight types of medicinal earth [19].

Furthermore, the effects of imponderability on human body were studied by NASA in the 1960s. Experiments demonstrated that imponderability leads to rapid bone depletion, so various remedies were explored in order to counter that. Many pharmaceutical companies tried to develop calcium supplements, but none of them were as effective as the ones with clay. The special clay that was used in this case was *Terramin*, reddish clay found in California. Benjamin Ershoff from the California Polytechnic Institute demonstrated that the ingestion of clay counters the effects of imponderability, pointing out that no important changes were made when calcium alone was added to the diet [20].

Depending on the academic source, clays are divided into four main categories: kaolinite, montmorillonite-smectite, illite, and chlorite. Chlorites are also considered to be part of a separate group, within the phyllosilicates. There are approximately 30 different types of "pure" clays in these categories, but most natural clay deposits are mixtures of these different types, along with other weathered minerals. *Varve* (or varved clay) is clay with visible annual layers, which are formed by seasonal deposition of those layers and are marked by differences in erosion and organic content. This type of deposit is common at the glacial lakes' formations. *Quick* clay is a unique type of marine clay indigenous to the glaciated lands of Norway, Canada, Northern Ireland, and Sweden. It is a highly sensitive clay, prone to liquefaction, which has been involved in several landslides [21].

There are different ways of clay manufacturing. These includes heating or even baking the clay. However, too much processing, may reduce the clay's curative potential [22]. Medicinal clay can usually be found in health food shops as dry powders, or in jars as a liquid (hydrated state) which is normally used for internal use. For external use, the clay may be added to the bath, or prepared as poultices in order to be applied to specific parts of the body. Warm packs are prepared to help the interaction of clay with the body, as the heat opens the pores of the skin. In the European health spas, the clay is prepared so that it can be used in a multitude of ways, but usually it is mixed with peat and matured in special pools for a few months or even up to two years [23].

Many types of skin conditions have been treated by applying the clay directly on the skin. *Montmorillonite* has shown its effectiveness in this area. Clay is used in many dermatological health problems, such as acne [25]. There are also many commercial remedies

intended for internal use, for examples Kaopectate®, Rheaban®, and Diar-Aid®. The labels on all of these showed that the active ingredient was *Attapulgate*, each tablet containing 600 to 750 mg of this component along with other adjuvants [26]. However, since April 2003, attapulgate medication was discontinued due to lack of evidence, according to the U.S. Foods and Drugs Administration [27]. Numerous medicines also use *Kaolinite* clay, which has been for long time a traditional remedy to heal an upset stomach. Also, *Kaolin* has been used to treat diarrhea and cholera around the start of the 20th century [28].

Compounds such as kaolin and attapulgate were formerly considered diarrhetic medication, until studies in this direction were rejected by the U.S. Food and Drug Administration (USFDA) [27].

3. DIFFERENT TYPES OF CLAYS AND THEIR INFLUENCE ON TEXTILE FABRIC INDUSTRY

Over time, different studies have been carried out in order to highlight clays properties on textile fabrics. Mostly, the research was in the area of dyed water decontamination. Dye removal from polluted water was carried out by various methods such as biological treatment, coagulation/flocculation, ozone treatment, chemical oxidation and photocatalytic processes, membrane processes, and adsorption. The adsorption is the most used method because of its easy handling and because it allows the removal of pollutants even from solutions with low pollutant concentration. Adsorption is a very used method, as researchers are continuously intending to use or discover innovative adsorbent materials that are efficient and less expensive. For example, Nejib Abidi and his team studied the removal of anionic dye (RR 120 – red dye) from textile industries' effluents by using as adsorbents *Tunisian* clays from Tabarka (a mixture of kaolinite and illite) and from Fouchana (a mixture of smectite, kaolinite, and illite). The overall data indicate the porosity, the surface area, and the cationic exchange capacity of the clay are not the key points, but the clay nature is the dominant factor controlling the efficiency of the dye removal from water [29].

Clays have a high adsorption capacity due to their lamellar structure which offers them high specific surface areas, which may even exceed that of activated carbon under the same conditions of temperature and pH. Considering the aspects above, and the fact that activated carbon is known to be an effective but expensive adsorbent due to its high costs of manufacturing and regeneration, R. Elmoubarki and his team studied the adsorption of textile dyes on raw and decanted *Moroccan* clays. The raw clays used in their work were collected from Safi and Berrechid regions in Morocco. Their study shows that *Moroccan* natural clays can successfully remove dyes from aqueous solutions. Therefore, the use of *Moroccan* natural clays presents a great potential for the removal of textile dyes from contaminated waters, as no costly equipment is needed [30].

In the review published by Abida Kausar and her team about dyes adsorption using clay and modified clay, they concluded that modified clays offer more efficiency. Different techniques were used in order to characterize the clays before and after the adsorption of dyes, however, most of the studies lack information about the complete characterization of clays used as an adsorbent, which needs to be investigated in future studies [31, 32].

Nanostructured coating on textiles is a novel way to impart various functional properties such as gas barrier, antibacterial, abrasion resistance, UV resistance, flame retardant and super hydrophobic. Nanomaterials such as layered silicate clays, carbon nanofiber/nanotubes, nano silica, nano TiO₂ have been incorporated in the base polymeric coating to enhance the performance of coated textiles to achieve these properties on fabrics [33].

Considerable research is being focused on the physical and mechanical properties of various polymers through mixing them with inorganic nanoparticles and nano clays to produce the layered clay-incorporated polymer composites by sol-gel processing, in situ polymerization and melt compounding [34-37].

The functionalization of silica and cotton surface helps to create strong bond between the fibre and particles. Thus, produced nano roughening on fibre surface is very robust and durable [38]. Besides the water repellent lotus effect, nano silica can also be used to develop wrinkle free silk [39], to reduce the friction and wear of nylon-6 [40] and polyurethane coating [41] and to increase the flame resistance property of textiles [42].

In Patent 5968203/ 1999, Harold M. Brown registered an invention relates to a composition for treating synthetic textile material and a method of using it. The composition comprises a smectite clay to scour the textile material, a wetting agent to enhance addition of the clay to other components of the composition, a sequestrant to sequester metal ions that inhibit the performance of the clay, and, when the composition is an aqueous slurry, a viscosity control agent to adjust the viscosity of the composition to prevent separating or settling of the clay [43].

5. CONCLUSIONS

These nanocomposites are often claimed to exhibit improved properties such as modulus, strength, stiffness, flame retardancy, dimensional stability, electrical conductivity, barrier performance, solvent and heat resistance, wettability and dyeability depending on the type and contents of clay mineral used [44].

The studies conducted so far are insufficient, because clays have a wide range of healing properties and there are also many ways to use them. Kaolin is one of the most promising clays, in terms of its healing properties, and is mainly used for external use. However, many laboratory tests are required to determine the best "textile-clay" pairs. Future studies will be carried out to characterize clay-treated textiles, as this area has recently begun to be developed.

ACKNOWLEDGEMENTS

This work was supported by a grant of the Romanian Ministry of Research and Innovation CCCDI-UEFISCDI, project number PN-III-P3-3.5-EUK-2017-02-0084, within PNCDI III.

REFERENCES

- [1] Rondao, R., de Melo, J.S., Schaberle, F., Voss, G., *Excited state characterization of a polymeric indigo*, In: Physical Chemistry Chemical Physics, 2012, 14, 1778
- [2] Wilson J., *Chapter I. An overview of textile and textile design from fibre to product purchase, Handbook of textile design – Principles, processes and practice*, Woodhead Publishing Ltd., 2000, 1
- [3] Almeida, L., *Functionalisation of Textiles - Future Perspectives*, 2015, Available at: <https://www.technicaltextile.net/articles/functionalisation-of-textiles-3174> [Accessed on June 2021]
- [4] Uddin, F., *Environmental Concerns in Antimicrobial Finishing of Textiles*, In: International Journal of Textile Science, 2014, 3, 1A, 15-20
- [5] Cho, J.S., Cho, G., *New approach for improving antimicrobial functions of cotton fabric*, In: Textile Research Journal, 1997, 67, 12, 875
- [6] Stevanato, R., Tedesco, R., *New antibacterial acrylic fiber*, In: Chemical Fibers International, 1998, 48, 5, 480
- [7] Ananthanarayan, R., Paniker, C.K.J, *Textbook of microbiology*, 6th edn (Orient Longman Limited), 2000

- [8] Sidwell, W.R., Dixon, G., Westbrook, L., Forzile, H.F., In: *Journal of Applied Microbiology*, 1971, 227
- [9] Pelezar, M.J., Chan, E.C.S., Kreig, N.R., *Microbiology*, 5th edn (Tata McGraw Hill Publishing Co. Ltd., India), 1993, 473
- [10] Singh, R., Jain, A., Panwar, S., Gupta, D., Khare, S.K., *Antimicrobial activity of some natural dyes*, In: *Dyes and Pigments*, 2005, 66, 99-102
- [11] ASTM International, *Standard Test Methods for Liquid Limit, Plastic Limit, and Plasticity Index of Soils. Annual Book of ASTM Standards*, West Conshohocken, PA., 2010
- [12] Immunization Safety Review Committee, Board on Health Promotion and Disease Prevention, *Institute of Medicine. Immunization Safety Review: Vaccines and Autism*, Washington, DC: The National Academies Press, 2004
- [13] Ferrell, R.E., *Medicinal clay and spiritual healing*, In: *Clays and Clay Minerals*, 2008, 56, 6, 751
- [14] *Environmental Characteristics of Clays and Clay Mineral Deposits*, Available at: usgs.gov [Accessed on June 2021]
- [15] Translated by Ebbell, B., *The Papyrus Ebers: The Greatest Egyptian Medical Document*, Copenhagen: Levin & Munksgaard, 1937
- [16] Selinus, O., Alloway, B.J., In: Academic Press., 2005, 446
- [17] Gudger, E.W., *The Five Great Naturalists of the Sixteenth Century: Belon, Rondelet, Salviani, Gesner and Aldrovandi: A Chapter in the History of Ichthyology*, In: *Isis.*, 1934, 22, 1, 21
- [18] Scarborough, J., *Roman Medicine*, New York: Cornell University Press, 1969, 39
- [19] *Encyclopedia of the History of Arabic Science. Volume 1: Astronomy, Theoretical and Applied*, Ed. Roshdi Rasheed. London: Routledge, 1996, 271
- [20] Ubick, S., *Mud, Mud, Glorious Mud*, California Wild, California Academy of Sciences, 2009
- [21] Guggenheim, S., Martin, R.T., *Definition of Clay and Clay Mineral: Joint Report of the Aipea Nomenclature and CMS Nomenclature Committees*, In: *Clays and Clay Minerals*, 1995, 255
- [22] Carretaro, M.I., Gomes, C.S.F., Tateo, F., In: *Clays And Human Health*, 2006, 724
- [23] Ramaekers, C.J., *Compositions for treating animal diseases and syndromes*, US patent, Table 1: Montmorillonite Components; Average Nutrient Content, 2005
- [24] Saary, J., Qureshi, R., Palada, V., DeKoven, J., Pratt, M., Skotnicki-Grant, S., Holness, L., *A systematic review of contact dermatitis treatment and prevention*, In: *Journal of the American Academy of Dermatology*, 2005, 53, 5, 845
- [25] Chu, P., Garwood, W.E., *Zeolite-clay composition and uses thereof*, US Patent 5079201, 1992
- [26] *Food and Drug Administration, Antidiarrheal Drug Products for Over-the-Counter Human Use; Final Monograph*, In: *Federal Register*, 2003, 68, 74, 18869
- [27] Walker, R.R., *Kaolin in the Treatment of Asiatic Cholera: Its Action and Uses*, In: *Proceedings of the Royal Society of Medicine*, 1921, 14, 23
- [28] Albert, K.S., DeSante, K.A., Welch, R.D., DiSanto, A.R., *Pharmacokinetic Evaluation of a Drug Interaction between Kaolin-Pectin and Clindamycin*, In: *Journal of Pharmaceutical Sciences*, 1978, 67, 11, 1579
- [29] Elmoubarkiab, R., Mahjoubia, F.Z., Tounsadia, H., Moustadrafa, J., Abdenmouria, M., Zouhrib, A., El Albanic, A., Barka, N., In: *Water Resources and Industry*, 2015, 9, 16
- [30] Kausara, A., Iqbalab, M., Javeda, A., Aftaba, K., Nazli, Z.H., Bhattic, H.N., Nourend, S., In: *Journal of Molecular Liquids*, 2018, 256, 395
- [31] Dastjerdi, R., Montazer, M., *A review on the application of inorganic nano-structured materials in the modification of textiles: Focus on anti-microbial properties*, In: *Colloids and Surfaces B: Biointerfaces*, 2010, 79, 5
- [32] Akca, C., *A new method: the usage of natural zeolite as a killer chemical for hydrogen peroxide during the hydrogen peroxide bleaching*, In: *Industria Textila*, 2019, 70, 6, 519-522, <http://doi.org/10.35530/IT.070.06.1523>
- [33] Joshi, M., Bhattacharyya, A., *Nanotechnology – a new route to high-performance functional textiles*, In: *Textile Progress*, 2011, 43, 3, 155
- [34] Sinha Ray, S., Okamoto, M., *Polymer/Layered Silicate Nanocomposites: A Review from Preparation to Processing*, In: *Progress in Polymer Science*, 2003, 28, 11, 1539

- [35] Parvinzadeh, M., Moradian, S., Rashidi, A., Yazdanshenas, M.E., *Surface characterization of polyethylene terephthalate/silica nanocomposites*, In: Applied Surface Science, 2010, 256, 9, 2792
- [36] Parvinzadeh, M., Memari, N., Shaver, M., Katozian, B., Ahmadi, S., Ziadi, I., In: Journal of Surfactants and Detergents, 2010, 10, 2, 219
- [37] Hajiraissi, R., Parvinzadeh, M., *Preparation of polybutylene terephthalate/silica nanocomposites by melt compounding: Evaluation of surface properties*, In: Applied Surface Science, 2011, 257, 20, 8443
- [38] Xue, C.H., Jia, S.T., Zhang, J., Tian, L.Q., *Superhydrophobic surfaces on cotton textiles by complex coating of silica nanoparticles and hydrophobization*, In: Thin Solid Films, 2009, 517, 4593
- [39] Wong, Y.W.H., Yuen, C.W.M, Leung, M.Y.S, Ku, S.K.A., Lam, H.L.I., *Selected applications of nanotechnology in textiles*, In: Autex Research Journal, 2006, 61
- [40] Garci, M., de Rooij, M., Winnubst, L., van Zyl, W.E., Verweij, H., *Friction and wear studies on nylon-6/SiO₂ nanocomposites*, In: Journal of Applied Polymer Science, 2004, 92, 1855
- [41] Song, H.J., Zhang, Z.Z., Men, X.H., *The tribological behaviors of the polyurethane coating filled with nano-SiO₂ under different lubrication conditions*, In: Composites: Part A, 2008, 39, 188
- [42] Kashiwagi, T., Morgan, A.B., Antonucci, J.M., Van Landingham, M.R., Harris Jr., R.H., Awad, W.H., Shields, J.R., *Thermal and flammability properties of a silica-poly(methylmethacrylate) nanocomposite*, In: Journal of Applied Polymer Science, 2003, 89, 2072
- [43] Brown, H.M., *Clay-containing textile material treating composition and method*, Patent number 5968203/19.10.1999, Assignee: Sybron Chemicals Inc., Appl. No.:09/031152, Filed: 26 Feb 1998
- [44] Njuguna, J., Pielichowski, K., Desai, S., *Nanofiller-reinforced polymer nanocomposites*, In: Polymers for Advanced Technologies, 2008, 19, 8, 947



ACCESSIBILITY AND USABILITY OF THE LEARNING TOOLS TO ACCELERATE INNOVATION IN THE FIELD OF SMART MATERIALS DEVELOPMENT

DOI: 10.35530/TT.2021.44

R. M. Aileni*, L. Chiriac

National Research Development Institute for Textiles and Leather, Romania
(E-mail: aileni.raluca@incdtp.ro)

Abstract: *This work presents the general aspects concerning the accessibility and usability of the learning tools existent for smart materials development using eco-design in the context of the circular economy. These learning tools will be used in part and some of them developed in the framework of the Erasmus+ project DigiTEX and will cover also the aspects of digital learning technologies capable to accelerate innovation in the field of healthcare and protective systems based on electroconductive materials. In DigiTEX Erasmus+ project will be developed solution-based software technologies, database development and creative methods for coaching the innovative ideas from design, development and production management in the context of circular economy and sustainable development with reduced environmental impact. This paper is structured in 5 sections such as introduction, smart materials overview, eco-design for smart materials, circular economy approach and conclusions.*

Keywords: *smart materials, e-learning, textiles, electroconductive, eco-design, environment*

1. INTRODUCTION

The market of smart materials was dominated by North America in the field of the aerospace & defence industry having a research budget allocated of USD 589 billion in 2017. Europe has the second position in the market due to the researches obtained in the developed countries such as Germany, the Netherlands and France using funds for research in the field of smart materials from research agencies from Germany, France and the Netherlands (figure 1). However, the global smart materials market is expected to reach 121.90 Bn by 2027 [1].

Unfortunately, the list of countries with substantial research results in the field of smart materials is limited to only 3 countries (Germany, the Netherlands and France) due to the lack of funding and expertise in designing systems based on smart materials and this generated barriers in the market. However, research and innovation strategies supported by the government and universities could accelerate the development of smart materials and the technological transfer to the industry [1].

The preferences for automated products and non-conventional energy sources increased the interest in developing research and product based on piezoelectric devices. In addition, can be observed an increased interest of the aerospace engineering sector in using smart systems implementation in aeronautical engineering and astronautical engineering. Also, in the defence industry exist an interest in using advanced smart materials to equip

their defines sectors [1].

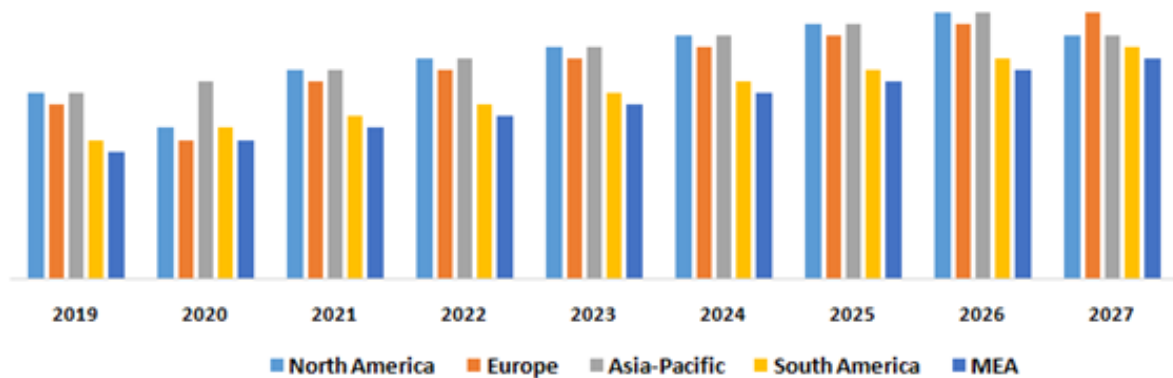


Figure 1. Global market segmentation in the field of smart materials [1]

This paper is structured in the introduction, smart materials overview section, eco-design, circular economy for smart materials with electroconductive properties and conclusion sections.

2. SMART MATERIALS OVERVIEW

Smart materials are advanced materials having one or more properties that can be modified by external stimuli, such as stress, moisture, electric or magnetic fields, light, temperature, pH, or chemical compounds. Especially smart materials are used for sensors and actuators consumer goods such as electronics, automotive, medical, aerospace and defence systems. Concerning the end-user consumer of smart materials, this segment is focused mainly on young or older adults.

The development of materials such as polymers, metal, and smart glass, generated new opportunities for various industries such as automotive, consumer electronics, and healthcare to integrate smart materials in classical or new devices.

The smart materials market is segmented by product such as [1]:

- piezoelectric (52%) for consumer goods, aerospace, defines, automotive, healthcare, information, communication, and manufacturing industries;
- shape memory alloys (19%) for medical applications including surgical devices, prosthetic devices, and stents;
- electro strictive smart materials.

The smart materials market is dominated in the field of application by actuators used as components of the machine that respond to change in the mechanical properties (viscosity or dimensional change) or as an amplifier that converts low energy into high energy signals, in sectors such as automotive, aerospace, defence and consumer goods.

The smart materials are advanced materials such as shape memory alloys, piezoelectric, electro strictive, magneto strictive and electrochromic materials. Generally, smart materials are used for sensors, actuators, structural materials and coatings.

The principal end-users of smart materials can be stakeholders from industrial, defence and aerospace, automotive, electronics, healthcare, civil engineering and retail.

The advanced materials used for actuators should exhibit an adaptive response to the different stimuli (mechanical, electrical, magnetic, pH, light, traction), the potential to change the physical properties (shape, stiffness, and viscosity) specifically and to have functionalities such as self-adaptability, self-sensing, self-healing, and memory enabling

their usage in numerous soft or hard robotics applications.

On the other hand, smart materials represent the foundation for smart textiles development. Moreover, according to standard ISO/TR 23383:2020 (Textiles and textile products — Smart (Intelligent) textiles— Definitions, categorization, applications and standardization needs), the smart (intelligent) textile products include chromic textile, phase change textile, Textile products with active ingredients inside the microcapsules, shape memory textile, super-absorbing polymers and gels, auxetic textile, dilating and shear-thickening textile, Piezoelectric textile, electroluminescent textile, thermo-electric textile, photovoltaic textile, electrolytic textile and capacitive textile products.

The existent software intended to be used for e-Learning courses are:

- Galileo for virtual testing, smart material design for the analysis, design and optimization of smart materials;
- Comsol Multiphysics;
- Matlab;
- software for smart materials simulation for 3D and 4D printing;
- software for rapid prototyping with 3D printing.

3. ECO DESIGN FOR SMART MATERIALS

The Eco-design involves a design with reduced environmental impact and avoiding the inputs considered with a high degree of toxicity.

The toxicity of inputs can be determined by consulting the guidelines such as the EU REACH Regulation [2], EU RoHS Directive [3], SIN List from the International Chemical Secretariat [4], and Banned Lists of Chemicals Cradle to Cradle Certified Product Standard [5]. However, lead, cadmium, polytetrafluoroethylene (PTFE), and polycyclic aromatic hydrocarbons (PAHs) are banned for use in materials where exposure to humans or the environment is highly likely to occur [5]. For example, the coatings, and finishes based on previously mentioned chemicals, that are used on the surface of products such as e-textiles, toys or other children's products and jewellery [5] are banned. However, there are concerns in the utilization of the oxides for the development of the actuators/sensors and generally for electronics components. In addition, the recommendation is to use mainly compounds such as barium titanate (BT), potassium bismuth titanate (KBT), sodium potassium niobate (KNN), and bismuth ferrite (BFO). In this way, according to the EU Directive on the Restriction of Hazardous Substances (RoHS), some oxides are restricted in the production process, because of environmental toxicity.

Eco-design in comparison with the classical design of the product integrates also the environmental performance assuming the responsibility of protecting the environment [6,7]. According to the Eco Design Directive, the eco-design goal is to optimize the environmental performance of products, while maintaining their functional qualities [8].

4. CIRCULAR ECONOMY CONTEXT

According to the European Circular Economy Plan [9], 80% of the product's environmental impact occurs at the design phase.

The circular economy is a model where products, components, energy and materials re-enter in manufacturing process involving waste minimization, product re-design through LCA approaches, and the use of bioresources [10].

Circular economy principles include:

- use of green technologies and use responsible the natural resources;

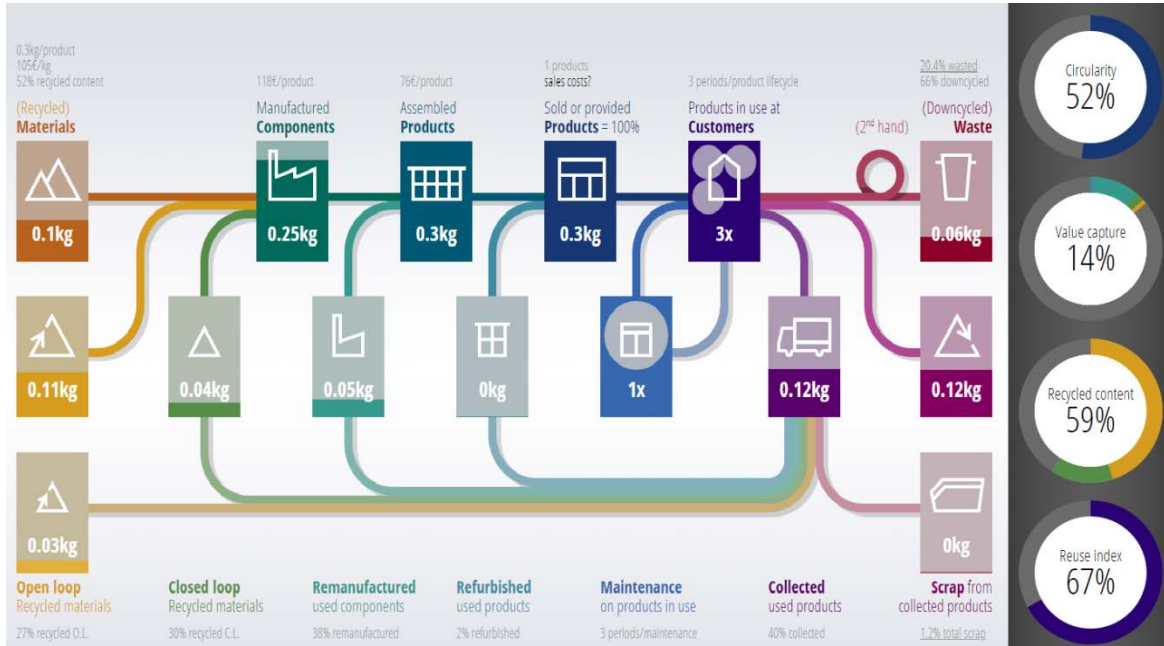


Figure 3. MCI calculation (©2016-2021 IDEAL&CO Explore BV)

Mainly, the electronics waste (e-waste) contains numerous toxic and hazardous chemicals (palladium, copper, iron, aluminium, fossil fuels, titanium, gold, and silver) that are released into the environment if are not dispose of adequately [17-19]. The e-waste collection rate is a report between the total e-waste recycled and total e-waste generated, equation 1. Approximately 80% of e-waste electronics end up in landfills and just 20% of e-waste is recycled [20-23].

$$E - waste\ collection\ rate = \frac{total\ e-waste\ recycled}{total\ e-waste\ generated} \times 100 \quad (1)$$

5. CONCLUSIONS

We can conclude that taking into account the eco-design and circular economy requirements is necessary to develop smart materials using the existing software for materials development and simulation. In addition, the smart material should provide good environmental performance, to reduce energy consumption, toxicity and increase the potential of recycling, reuse, or remanufacturing the new products using recycled components. However, this approach is very difficult to be achieved considering that some conductive parts are coated on textile surfaces and are not distinct elements attached to the textiles.

ACKNOWLEDGEMENTS

The research presented in this paper was prepared within INCDTP. Funds that support this work are from the Erasmus+ programme of the European Union, Project DigiTEX “Textile digitalization based on digital education and innovative e-Tools”, project no. 2020-1-RO01-KA226-HE-095335

REFERENCES

- [1] *Global Smart Materials Market*, Available at: www.maximizemarketresearch.com [Accessed on June 2021]
- [2] *Registration, Evaluation, Authorisation and Restriction of Chemicals (REACH)*, European Commission, 2006
- [3] *Restriction of Hazardous Substances Directive (RoHS)*, European Commission, 2002
- [4] *SIN List from the International Chemical Secretariat*, Available at: sinlist.chemsec.org [Accessed on June 2021]
- [5] *Banned Lists of Chemicals Cradle to Cradle Certified Product Standard*, MBDC, 2012
- [6] Mao, J., et al., *Circular economy and sustainable development enterprises*, Springer, 2018
- [7] Berndtsson, M., *Circular economy and sustainable development*, 2015
- [8] *Eco Design Directive*, European Commission, 2009
- [9] *European Circular Economy Plan*, European Commission, 2020
- [10] Tonelli, M., Cristoni, N., *Strategic management and the circular economy*, Routledge, 2018
- [11] Franco-García, M.L., Carpio-Aguilar, J.C., Bressers, H., *Towards zero waste, circular economy boost: waste to resources*, In: *Towards Zero Waste*, Springer, Cham, 2019, 1-8
- [12] Linder, M., Sarasini, S., van Loon, P., *A metric for quantifying product-level circularity*, In: *Journal of Industrial Ecology*, 2017, 21, 3, 545-558
- [13] Ashby, M., Vakhitova, T., *Analyzing and Measuring Circularity—Teaching and Industrial Tools by Granta Design*, In: *MRS Advances*, 2018, 3, 25, 1379-1386
- [14] Westerlund, N., *Circularity Indicator Calculation Tool, A comprehensive method and metric for measuring the circularity of a product* (Master's thesis), 2018
- [15] Mantalovas, K., Di Mino, G., *Integrating circularity in the sustainability assessment of asphalt mixtures*, In: *Sustainability*, 2020, 12, 2, 594
- [16] Glogic, E., *Towards sustainable energy materials: broadening life cycle assessment for emerging technology development and resource-effective choices*, PhD Thesis, 2020
- [17] Widmer, R., Oswald-Krapf, H., Sinha-Khetriwal, D., Schnellmann, M., Böni, H., *Global perspectives on e-waste*, In: *Environmental impact assessment review*, 2005, 25, 5, 436-458
- [18] Perkins, D.N., Drisse, M.N.B., Nxele, T., Sly, P.D., *E-waste: a global hazard*, In: *Annals of global health*, 2014, 80, 4, 286-295
- [19] Grant, K., Goldizen, F.C., Sly, P.D., Brune, M.N., Neira, M., van den Berg, M., Norman, R.E., *Health consequences of exposure to e-waste: a systematic review*, In: *The lancet global health*, 2013, 1, 6, e350-e361
- [20] *Introduction to Electronics (E-Waste) Recycling*, Available at: www.thebalancesmb.com [Accessed on June 2021]
- [21] Forti, V., Balde, C.P., Kuehr, R., Bel, G., *The Global E-waste Monitor 2020: Quantities, flows and the circular economy potential*, 2020
- [22] Kumar, A., Holuszko, M., Espinosa, D.C.R., *E-waste: An overview on generation, collection, legislation and recycling practices*, In: *Resources, Conservation and Recycling*, 2017, 122, 32-42
- [23] Dhir, A., Koshta, N., Goyal, R.K., Sakashita, M., Almotairi, M., *Behavioral reasoning theory (BRT) perspectives on E-waste recycling and management*, In: *Journal of Cleaner Production*, 2021, 280, 124269



DEVELOPMENT OF JACKET PATTERNS FOR TEENAGERS USING OPTITEX FLATTENING MODULE

DOI: 10.35530/TT.2021.52

G. Popescu*, S. Olaru, C. Grosu, I. Badea

National Research Development Institute for Textiles and Leather, Romania
(E-mail: georgeta.popescu@incdtp.ro, sabina.olaru@incdtp.ro, cristina.grosu@incdtp.ro, ionela.badea@incdtp.ro)

Abstract: Adolescence is a period of transition from childhood to adulthood, defined by major changes in physical, behavioural and social plan. The interest of teenagers for computer technology is in a perpetual growing and shopping online is one of their favourite activities. The garment industry is extremely competitive in terms of virtual simulation, consisting of 3D virtual bodies, virtual garments and virtual try-on systems. The paper presents the advanced method of designing 2D patterns, started from the 3D surfaces, obtained by real scanning of several teenager bodies. The development of a jacket model for girls, by using Optitex software with its high-performance modules 3D Flattening, 3D Simulations and PDS, based on the anthropometric standard for children, SR 13546: 2012, will be presented. These modules enable the designer to preview the shape of the product and its fitting to the body dimensions, which offer the possibility of developing to an infinite number of clothing collections just by changing the characteristics of the material, various seams, accessories or colours.

Keywords: anthropometric standard, basic pattern, 3D flattening, jacket for girls, 3D simulation

1. INTRODUCTION

Currently, most teenagers are users of computer technology. Online shop become more and more used by them, especially since they are also very interested in their physical appearance. From this point of view, the aim of the garment companies is to attract them as customers. In order to comply with customer preferences, the garment producers take into account two important aspects: the design and the fit. To achieve these two components, a complex process of product development is required, but even so, the results of the sales volume remain uncertain. A successful alternative in presenting the design of the clothing product, as well as evaluating the fit of the selected item, is the development of this process as a virtual one. The advanced systems for 3D design and body measurement, open a new door for researchers and specialists to provide a better comfort and fit and even to gain a new level of customization, especially in the field of garments [1,2].

The processing of patterns for garments can be obtained by various methods, generally classic geometric design, which is the basis for designing patterns in different specialized software. Currently, a garment can be developed using existing high-performance tools such as: garment design software, 3D scanning for anthropometric data collection and 2D/3D simulation, modelling and fitting software [3]. The final product ready for launch in production goes through a complex process of design, sampling, and validation, meticulous steps that are time, energy and material resources consuming. By using the pattern

processing method with 3D Flattening module from Optitex PDS design software and 3D simulation, the resources consumption is considerably reduced and the final quality is superior. Applying the specific functions of the module, the surface of the 3D object is converted in a 2D surface, respectively the human body on which the contour of the desired product is drawn. The result is a very accurate pattern – human body correspondence. The patterns are actually obtained from the unfolded surface of the body. Another advantage of this processing method is the direct visualization on the body model of the sewing lines between the product components, the shape of the product and the desired length. Surfaces are displayed in the PDS pattern processing window. These are the result of drawing the contour lines between anthropometric points necessary for the pattern, using the geometric method. The contour can be resized by modifying the main segments with a specific constructive addition, according to the product type, material type and product destination. Depending on the positioning on the body, garments are divided in two main categories: products with shoulder support (shirt, blouse, shirt and jacket) and products with waist support (tights, pants and skirt). The proposed method can be applied for obtaining basic patterns for both categories.

2. GENERAL DATA AND STEPS OF THE PROPOSED METHOD

The most important biological changes of the human body begin during adolescence. Thus, to girls who have reached the age of 14, the breast continues to develop and the hips get wider. To boys, the features of maturity appear 1 year later, around age 15. During this period, the waist is clearly pronounced for both, boys and girls. The proportions of adolescents' bodies are close to those of adults [4]. Product development for the 14- to 18-year-old age group, especially girls, is a difficult process due to these continuous body changes, very difficult to standardize. The anthropometric standard for children, SR 13546: 2012 – Clothing. Body dimensions for children between 6 and 19 years old [5], elaborated by INCDTP (table 1), provides a solid anthropometric database for garments development.

Table 1. The main standardized anthropometric dimensions for girls [5]

Girls age groups	Body height (cm)	Bust circumference (cm)	Hip circumference (cm)
14-15 years	152	85	91
	158	87	93
	164	89	95
	170	92	98
16-18 years	152	88	93
	158	89	95
	164	91	97
	170	92	99

Based on the information regarding lengths, dimensions, circumferences, conformations, the virtual mannequin is generated according to the type and dimensions from the corresponding age category. For girls, compared to the boys, due to the appearance of the breasts, additional anthropometric dimensions are needed to characterize this area.

The method consists in processing the flattened surfaces of a 3D product.

The first step to obtain the basic patterns for teenager's garments is to parameterize the virtual mannequin, by setting the values of different anthropometric dimensions (i.e., lengths and circumferences) in the "Model properties" window (figure 1).

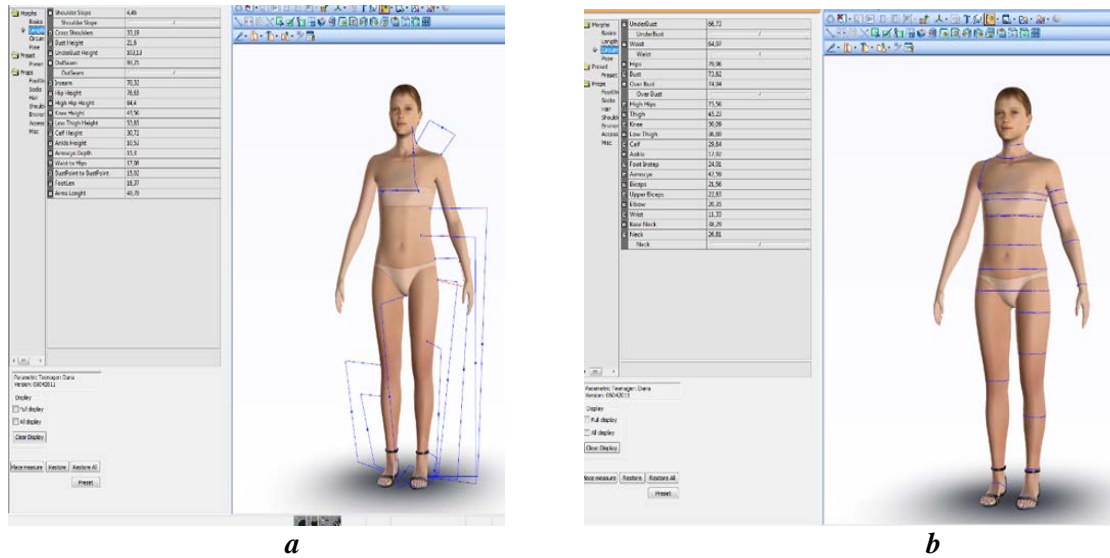


Figure 1. Application of standardized anthropometric dimensions for:
a - lengths; b - circumferences

By changing the anthropometric dimensions parameters in the „Model properties” window, the mannequin can be shaped in different sizes and conformations, which leads to the elimination of the pattern grading operation (figure 2) [6,7].

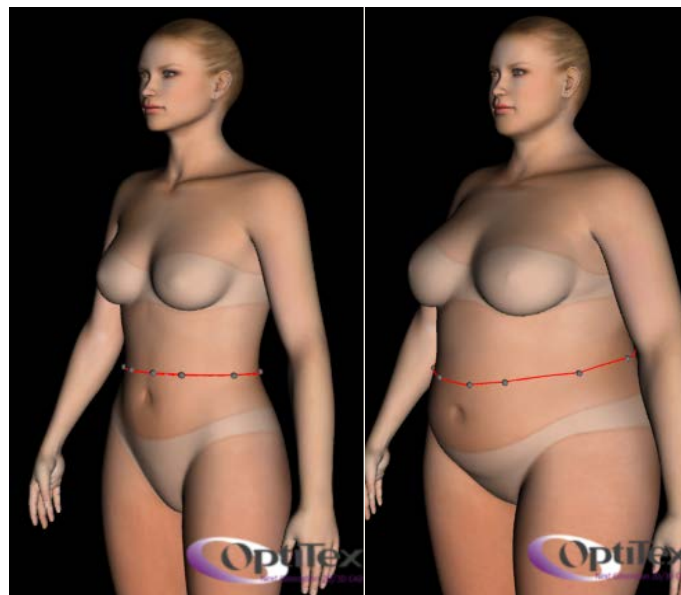


Figure 2. Marking in the waist area for two mannequins of different sizes

The process of obtaining 2D patterns from the 3D surface consists of the following steps (figure 3):

- creating standardized mannequins;
- placing the marking points on the virtual body using the “Draw Path” function;
- drawing the corresponding contour;
- extracting the resulted surface using the “Build Patch” function;
- checking and processing the contour of 2D surfaces;
- obtaining the desired pattern by adding constructive additions.

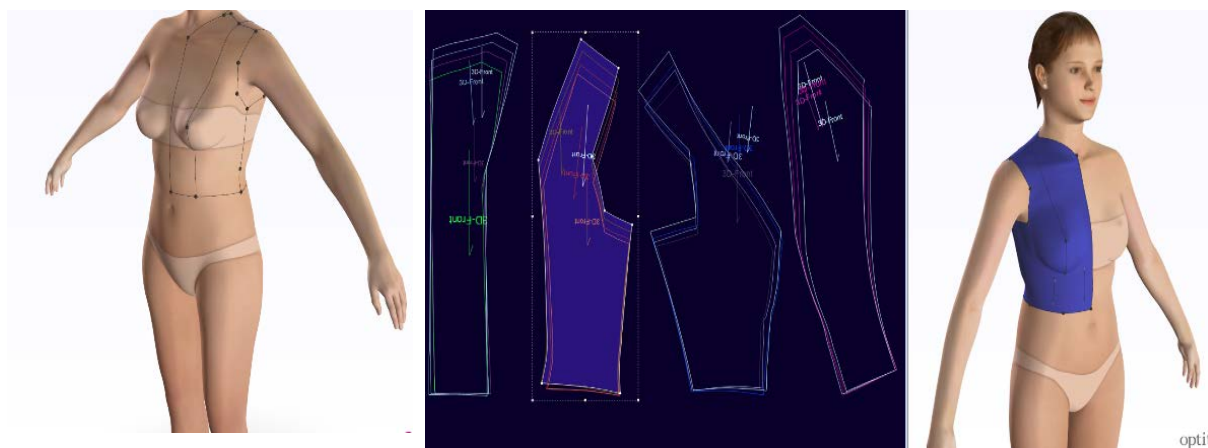


Figure 3. Steps for obtaining 2D patterns from the 3D surface

In parallel with the process of obtaining the patterns, the product is simulated on the virtual mannequin, thus having a real image of it. A virtual collection can be developed by changing materials and accessories directly in the software (figure 4).



Figure 4. Simulated garment on virtual mannequin

3. PROCESSING THE BASIC PATTERNS OF GIRLS JACKET

The jacket for teenagers can be the first or second layer on the body. The jacket for girls is designated for school activities or social events. The silhouette of the product is semi-adjusted, the basic pattern is composed of two front parts, two front side parts, two back parts, two back side parts and two sleeves formed by front and back parts. The bottom edge of the jacket corresponds to the hip line, and the bottom edge of the sleeves with the wrist line. In order to obtain the flattened surfaces, the marks corresponding to the main anthropometric points have to follow the below body parts, placed on the mannequin (figure 5):

- for the front: the circumference of the base of the neck, the cut of the sleeve, the waist, the hip and the nipple;
- for the back: the circumference of the base of the neck, the cut of the sleeve, the waist, the hip and the prominence of the shoulder blade.



Figure 5. Placing contour points

The placed points are joined together by contour lines and the body surface become flattened with “Build patch” function support (figure 6).

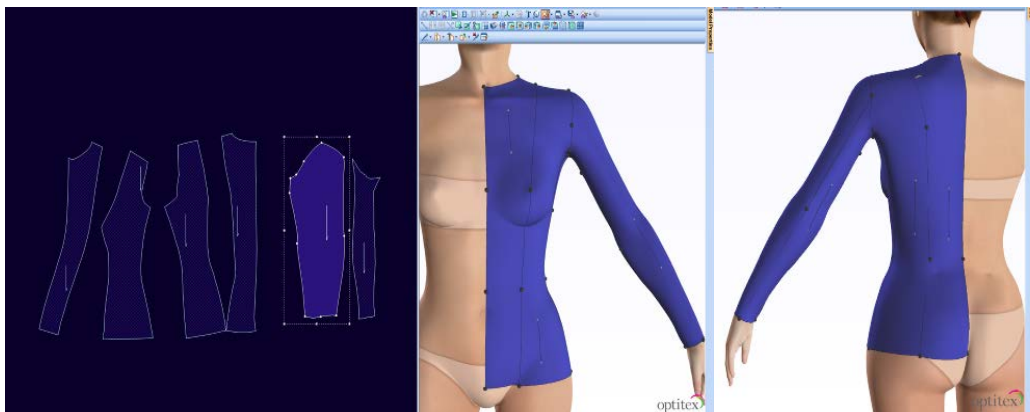


Figure .6 Flattening operation of 3D surfaces

Successively, contoured surfaces can be developed for all types of age groups for adolescents.

4. 3D SIMULATION AND VIRTUAL MODELLING OF THE JACKET

3D simulation and virtual modelling of a garment has the purpose to check the product - body correspondence and correct any technical issue. To obtain an image as close as possible to the reality of the garment, the 3D simulation and modelling is applied directly on the parameterized body, using the standard anthropometric values and the properties and appearance of the materials. Compared with the classic development of a product, this method saves the time and related costs of stages like model execution, prototyping and zero series execution.

The following steps are necessary to elaborate the basic patterns, using the 3D Optitex software parameterized mannequins:

- **Step 1.** Applying assembly directions between pattern parts: the sewing lines are defined with the help of the “Stitch” function.
- **Step 2.** Placing the patterns on the parameterized mannequin: the patterns must be replaced from the PDS work area to the 3D work area of the PDS program, by using

"Place cloth" button, which requires first to synchronize the patterns with the mannequin's position (figure 7).

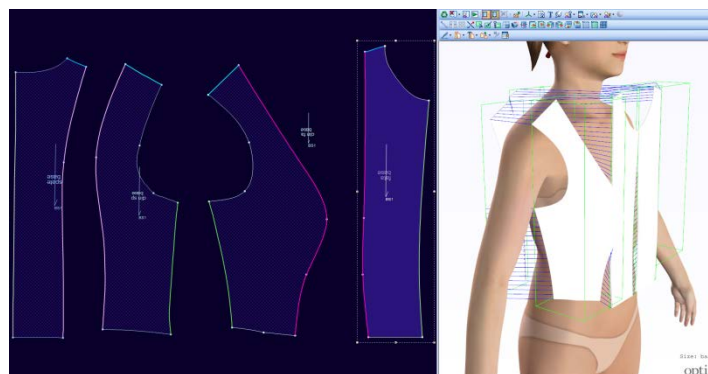


Figure 7. Applying assembly directions between pattern parts

- **Step 3.** Processing the simulation stage: Once the way of assembling the parts is correctly implemented, the simulation stage can start. The duration of the simulation process varies depending on the number of marks placed in the 3D simulation window, the complexity of the simulated model and the number of stitches (figure 8).

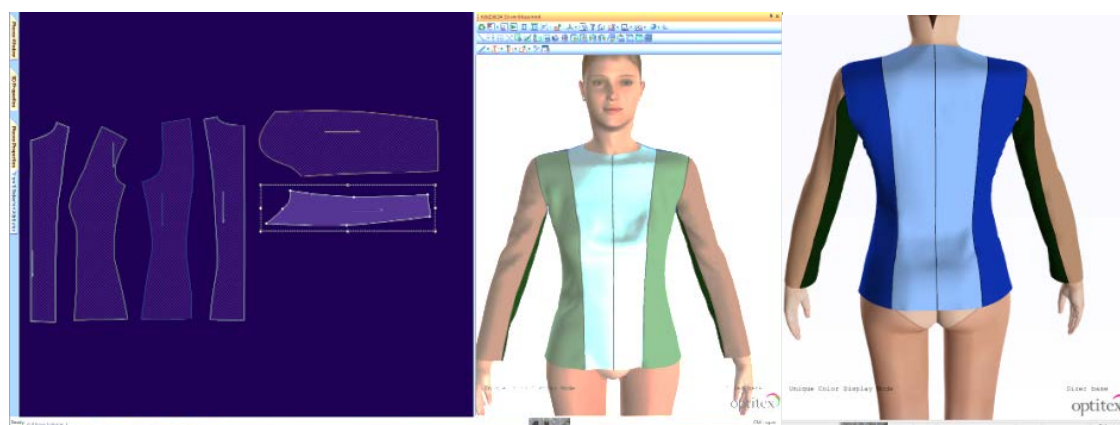


Figure 8. 3D simulation of the jacket

- **Step 4.** Checking the body-product correspondence: one of the multiple options offered by Optitex PDS, is to check the correctness correspondence between the body and the designed product, by using the “Tension map”, which indicates essential aspects regarding the necessary distance between the body and the product and the degree of comfort. 3 different colours are displayed on the virtual mannequin, as so (figure 9):
 - Red: indicates an increased pressure of the product on the body;
 - Green: a comfortable pressure (comfort zone);
 - Blue: lack of the tension of the product on the body.

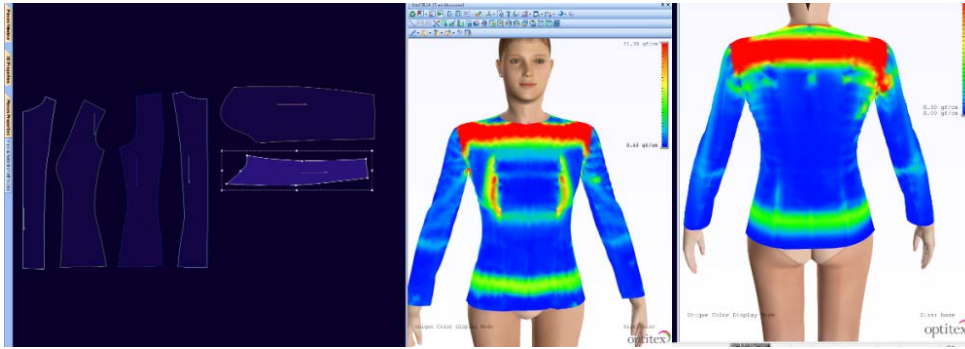


Figure 9. Visualization of the tension maps

- **Step 5.** Modifying patterns in non-conformities areas: in the Optitex PDS software, the patterns can be modified by moving the main points or correcting the contour. These changes are made simultaneously on the simulated product.

- **Step 6.** Repeating steps starting with step 3, after changing the patterns.

This method can be easily applied in the same sequence for any type of product. In our study, the basic patterns for the jacket product were obtained for the type dimensions 152, 158, 164, 170 for the two age groups, 14-15 years and 16-18 years (figure 10).

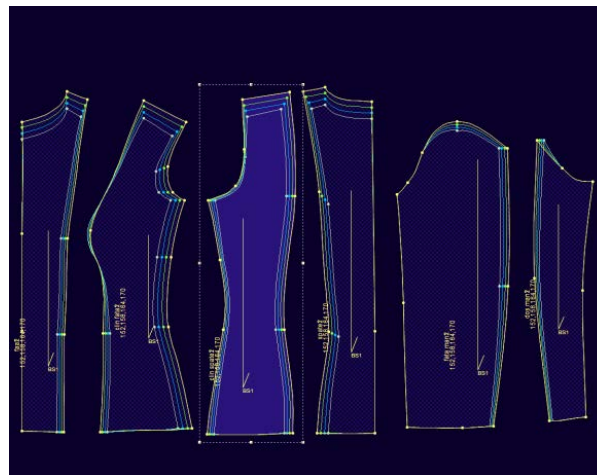


Figure 10. Basic patterns by type dimensions and age groups

5. CONCLUSIONS

The paper presents the method of pattern processing for girls jacket having as information the anthropometric data and the necessary knowledge for the garments design, from 3D body surfaces by using the Optitex Flattening module. This advanced method can be applied to all types of products and categories of people. The process of obtaining basic patterns by this method has the following features and advantages:

- the use of specific anthropometric dimensions, depending on the category destination and type of the product;
- developing algorithms for basic patterns;
- fitting the product on the parameterized virtual mannequin;
- visualizing the sewing lines for the product, its shape directly on the virtual body and correcting any non-conformities, through the “tension map” that express the distance between the body and the product in different areas;
- development of very precise patterns in a short time;

- creating virtual collections using various fabrics, accessories and colours.

REFERENCES

- [1] Zheng, R., Yu, W., Fan, J., *Development of a new Chinese bra sizing system based on breast anthropometric measurements*, In: Int. J. Indus. Ergon., 2007, 37, 697-705
- [2] Albu, A., Caciora, T., Berdenov, Z., Ilies, D.C., Sturzu, B., Sopota, D., Herman, G.V., Ilies, A., Kecse, G., Ghergheles, C.G., *Digitalization of garment in the context of circular economy*, In: Industria Textila, 2021, 72, 1, 102–107, <http://doi.org/10.35530/IT.072.01.1824>
- [3] Wang, Z., Xing, Y., Wang, J., Zeng, X., Yang, Y.L., Xu, S., *A knowledge-supported approach for garment pattern design using fuzzy logic and artificial neural networks*, In: Multimedia Tools and Applications, 2020, <https://doi.org/10.1007/s11042-020-10090-6>
- [4] Babcinetchi, V., *Cercetări în domeniul caracterizării corpului omenesc din punct de vedere antropomorfolologic cu aplicații în arta și proiectarea constructivă a vestimentației*, Ed. Politehniun, Iasi, 2011, ISBN 978-973-621-383-3
- [5] Standard SR 13546/2012, *Clothing. Body dimensions for children between 6 and 19 years old*
- [6] Liu, K., Zeng, X., Bruniaux, P., Tao, X., Yao, X., Li, V., Wang, J., *3D interactive garment pattern-making technology*, 2018, 104, 114
- [7] Pintilie, E., Ciubotaru, G., Avădanei, M., *Proiectarea confecțiilor textile asistate de calculator*, 2006, Ed. Performantica, Iași, ISBN 973-730-259-1



OVERVIEW OF THE KNITTED MATERIALS WITH VIBRATIONS DAMPING CAPACITY

DOI: 10.35530/TT.2021.54

C. Grosu^{*1,2}, M. Blaga¹

¹“Gheorghe Asachi” Technical University, Doctoral School, Romania

²National Research Development Institute for Textiles and Leather, Romania

(E-mail: cristina.grosu@academic.tuiasi.ro; mirela.blaga@academic.tuiasi.ro)

Abstract: Textile materials are often subjected to different stresses, acting on them in two phases: during the knitting phase, when the yarns and the obtained structure are subjected to cyclic stress, but also during the use phase, when the knitted structures are subjected to various stresses. The dynamic behaviour of knitted fabrics in a vibrating environment is usually evaluated by standardized methods, such as the method using vibration exciters (e.g., ISO 10819:2013). However, in recent years, the authors' collective has carried out research to characterize the behaviour of knitted structures in a vibrating environment, using a well-known method for generating vibrations by impact excitation, which is specific to the mechanical field but also has a high potential for application in the textile field. This method refers to the determination of the free vibrations of an elastic system. Its measurement in the design phase of the system is considered a crucial step, since by knowing the frequency range of the system, the resonance phenomenon in the operational phase can be avoided. Similar results obtained by applying standardized methods for measuring vibration transmissibility and the currently adapted method from the field of mechanics to the field of textiles, represent a validation for this type of investigation process and also show the high potential of knitwear to be used in the vibration environment.

Keywords: free vibrations, knitted structures, dynamic excitation, structural parameters

1. INTRODUCTION

Although exposure to vibration can have very different causes, a major source of exposure is the use of work equipment that emits transmitted vibrations to the hand-arm system (HAV) or the whole body (WBV).

Depending on the characteristic parameters of the transmitted vibrations, such as frequency and amplitude, but also on secondary factors, such as the duration of exposure or the ambient temperature, vibration exposure can cause clinical manifestations that endanger the health of the worker, such as kinetosis, dizziness, vomiting or even inflammation of the tendons and muscles, leading in rare cases to joint swelling, reduced mobility and gangrene of the fingers.

Any workplace where workers are exposed to vibration must implement a very strict policy to prevent and reduce the risks of exposure to HAV and WBV. Personal protective equipment (PPE) is the final barrier between the exposed person and the risk and is the ultimate solution to protect against risks at the workplace.

To provide the highest level of protection against vibration, PPE must be able to absorb energy efficiently and maintain an optimal level of rigidity to avoid crushing it, in

the event of an impact. It must also be of an acceptable thickness to allow handling of vibrating instruments without compromising dexterity and sense of touch [1].

2. MANUFACTURING METHODS OF SPACER KNITTED FABRICS

Spacer fabrics are one of the most widely used materials for engineering applications and the most widely used option for the manufacture of anti-vibration materials. Spacer fabrics (sandwiches) are complex three-dimensional constructions created by knitting two separate layers, joined by yarn segments or other knitted layers, in different bond ratios.

3D fabrics have great potential to replace commonly used materials as protective layers in PPE construction due to their high flexibility, good pressure recovery, and high tensile, flexural, and impact strength. Compared to most of the materials used, such as polyurethane, foam or rubber, they are more environmentally friendly, not easily flammable, have superior thermal comfort properties and also a low mass to volume ratio.

The structure of the outer layers, as well as the way in which the layers are bonded and the distance between them, offer a variety of possibilities for designing spacer fabrics with different physical-mechanical properties. Structures with outer layers made of the same raw material as well as structures with layers made of different raw materials can be produced [2].

Spacer knitted fabrics produced on warp knitting machines can be rigid or elastic structures, with open or closed stitches, this technology being by far the most inventive system for obtaining textiles. Double needle bar raschel knitting machines have the ability to produce the two outer layers on the front and back needle bars simultaneously with the process of feeding the binding yarns on these two needle bars to achieve the joining of the outer layers [3]. The 3D fabrics produced in this way are characterized by a very large volume with relatively low mass and offer high air permeability. The thickness of the fabrics ranges from 1.5 to 10 mm, depending on the spacing of the needle bars, and can be up to 60 mm for special applications.

Spacer knits made on weft machines can be made on both, flat knitting machines equipped with two needle bars and circular machines equipped with a cylinder and disc. While spacer fabrics joined by binding threads can be produced on both, warp and weft knitting machines, spacer fabrics joined by layers can only be produced on weft knitting machines, the basic principle being similar to that of sandwich structures joined by binding threads. The knitting of the two outer layers begins independently on the two needle bars and at a certain point in time this process stops and the knitting of the connecting layers starts. After the knitting of the connecting layer is completed, the knitting of the independent outer layers starts again.

3. EVALUATION OF THE SPACER KNITTED MATERIALS

3.1. Knitted materials

The dynamic behaviour of different variants of knitted structures produced by specific technologies for warp and weft spacer fabrics was analysed under the influence of vibrations. A wide range of raw materials was used, such as cotton, polyamide, polyester, polypropylene and polyacrylonitrile.

The raw materials from which the spacer fabrics with the best anti-vibration properties were obtained are polyamide and polyester with the below characteristics, according to the specific manufacturing process, as follows:

Spacer warp knits:

- for the outer layers: Polyester multifilament, in the fineness range 44-2500 dtex, with a number of filaments between 2 and 144 or polyamide multifilament, in the fineness range 44-167 dtex, with a number of filaments between 3 and 24;
- for the connecting yarns: Polyester monofilament, in the fineness range 33-680 dtex or polyamide monofilament, in the fineness range 22-33 dtex.
- the samples subjected to be evaluated, are represented in figure 1.



Fig. 1. Variants of spacer warp knitted structures [4]

Spacer weft knits:

- for the outer layers: Polyester/Elastan multifilament yarns, in different fineness range;
- for the connecting yarns: Polyester monofilament, in diameter range 0.13 mm - 0.3 mm;
- the needles sections of proposed knitted structures to be evaluated, are represented in figure 2.

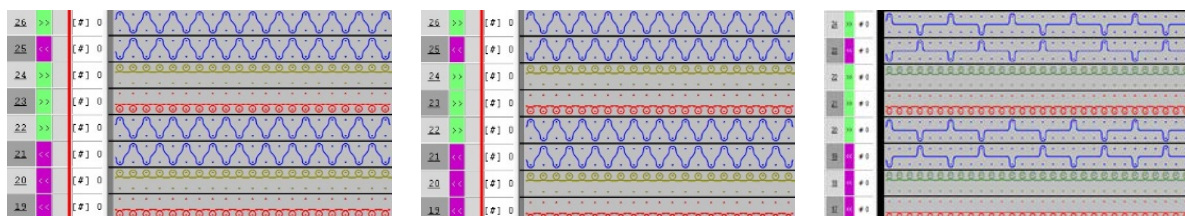


Fig. 2. Variants of spacer weft knitted structures

3.2. Testing method

PPE, such as anti-vibration gloves, must be marked with the symbol CE indicating that they have been tested and meet the requirements of the standard SR EN ISO 10819: 2013 - Mechanical vibration and shock - Hand-arm vibration - Measurement and evaluation of vibration transmissibility of gloves at the palm. The standard uses the method of vibration generation by excitation using a system equipped with a special handle to measure the clamping force and a device to measure the supply force of the system. A major disadvantage of this standard is that the measurement is only carried out in the area of the palm in the direction of the forearm.

The method proposed by the authors is based on the generation of vibrations by shock excitation to determine the natural frequencies of an elastic system, which plays a crucial role in avoiding, from the design stage, the possibility of resonance during use. This method is specific to the mechanical field and for its application it is necessary to use a specially designed test apparatus and carry out the following steps:

The application of the method refers to the excitation process of the elastic system, which consists of a metallic mass fixed to the knitted structure, to which an accelerometer is

attached. A piezoelectric impact hammer is used as the exciter. The vibrations are exerted and measured in three directions: transverse, longitudinal and vertical.

Data analysis is performed by characterizing the movements of the metal mass attached to the knitted fabric. The signal is processed by a data acquisition system, and the Fast Fourier Transform (FTT) decomposes the signal and allows the frequency spectrum of a data sequence to be calculated.

The evaluation of the results consists in the characterization of the dynamic vibration behaviour for the tested knitted variants and the interpretation of the obtained responses in correlation with different structural parameters of the knitted fabric.

4. PARAMETERS RELATED TO THE FABRICS BEHAVIOUR AT VIBRATIONS

4.1. Direction of producing and measuring vibration

The recorded frequencies showed comparable vibration responses in the coursewise and walewise directions, while significantly higher values of natural frequencies were recorded in the perpendicular direction of the test. Therefore, a first conclusion is that the perpendicular direction is recommended as a possible final application for vibration isolation [5].

4.2. Spacer fabrics properties with influence on the behaviour in vibration environment

The results obtained indicated that the properties of the spacer knitted fabrics with the strongest impact on vibration behaviour, proved to be:

Spacer yarn threading

The tests showed a higher stability of the knit, both, in the case of the comparative evaluation between two knits, fed with one yarn per needle, respectively two yarns per needle, in the same ratio of 1:5, for the knit with double number of fed yarns on a needle, but also in the case of two knits, fed with a single thread per needle, but in a ratio of 1:3 and 1:5, respectively.

In this second case, the knitted structure with a higher number of connecting yarns, the one in the ratio of 1:3, showed a higher rigidity, implicitly a better vibration behaviour, which led to the conclusion that a higher number of connecting yarns positively influences the resistance of the knit to vibration, by increasing its rigidity [1,6].

Spacer yarn diameter

The spacer yarns offer a better stability and structural balance as well as a positive effect on mechanical properties of the fabric.

Tests have shown that an insignificant increase of 0.02 mm in the spatial yarn diameter, significantly influences the behaviour of the knit, which increases its mass by about 15%. This consequently implies a higher stiffness of the knit, demonstrated by higher values of natural frequencies [1,6].

It can be hypothesized that the thicker the spacer yarn, the more rigid the knit will be, higher loading capacity will possess and implicitly higher values of natural frequencies will record.

Yarn consumption

From a range of 16 knitted structures, those made with the lowest yarn consumption, presented the lowest values of natural frequencies, implicitly the lowest level of rigidity. The variants made with the highest yarn consumption have registered the highest values of

natural frequencies and implicitly due to the increased mass they present a higher rigidity, which will lead to a much better response in vibration environment [7].

Fabric thickness

Tests have shown that the thickness of the knit directly influences the values of natural frequencies, so that the thicker the knit, the higher the values of natural frequencies, implicitly a higher rigidity. To validate these results, a second method was applied, specific to the textile field, to determine the flexibility of knitwear, which validated the ranking of knitwears stiffness, based on the method of determining free vibrations [4].

Raw materials of the outer layers

Tests with several knitting variants, in which the structure of the fabric and the diameter of the spacer yarns were maintained, but the type of yarns for the outer layers was varied, showed that polyester and polyamide were the most recommended raw materials for the outer layers, with extremely small differences registered between them at the maximum local stress, less than 0.1 MPa. The knitted fabrics made of synthetic fibres such as PES and PP showed higher natural frequencies than the knitted fabrics made of cotton and PNA, which reached similar values between them [5].

5. CONCLUSIONS

The study of the vibration behaviour of the knitted fabric using the method proposed by the authors to determine the natural frequencies is confirmed by the fact that similar results were obtained as in the literature, where the standardized method of generating vibrations by excitation was applied.

The application of existing methods led to the same conclusions regarding the influence of structural and physical-mechanical parameters of the knitted structures on the vibration behaviour, such as: type of raw material [3,8-11], thickness of the knitted fabric [3,12], yarn consumption and some particularities of the spacer yarn: threading type [3,13], yarn diameter [3,13].

Analysis of the recorded frequencies revealed comparable vibration responses in the longitudinal and transverse directions, while significantly higher values of natural frequencies were recorded in the perpendicular direction of the test. This suggests that this direction is the more suitable for vibration isolation [1-7].

ACKNOWLEDGEMENTS

This work is the result of the research activity for the doctoral thesis "Technical textiles for protection against vibrations", carried out by the doctoral student Grosu (Pavel) Cristina under the careful guidance of the doctoral supervisor, Prof. Dr. Habil. Eng. Blaga Mirela.

REFERENCES

- [1] Blaga, M., Seghedini, N.E., *Knitted Spacer Fabrics Behaviour at Vibrations*, In: Journal of Textile Engineering & Fashion Technology, 2017, 3, 2, 602-608, <https://doi.org/10.15406/jteft.2017.03.00092>
- [2] Buhai, C., *Cercetari privind utilizarea firelor din fibre speciale in realizarea produselor de imbracaminte din tricot*, Iasi, 2013
- [3] Sum, N.W., *Development of anti-vibration glove with weft knitted spacer fabric*, Hong Kong, 2013

- [4] Blaga, M., Harpa, R., Seghedin, N.E., Marmarali, A., Ertekin, G., *Evaluation of the knitted fabrics stiffness through dynamic testing*, In: Materials Science and Engineering. IOP Publishing, 2019, <https://doi.org/10.1088/1757-899X/459/1/012033>
- [5] Seghedin, N.E., Blaga, M., Ciobanu, R., *Weft knitted fabrics behaviour under dynamic testing.*, Autex 12th World textile Conference, Zadar, 2012
- [6] Blaga, M., Seghedin, N.E., Ciobanu, A.R., *Weft knitted spacer fabrics response to vibrations*, Autex World Textile Conference, Bursa, 2014
- [7] Blaga, M., Seghedin, N.E., Buhai, C., Chitariu, D., *Dinamic testing of the warp knitted spacer fabrics*, Autex World Textile Conference, Dresden, 2013
- [8] Liu, Y., Hu, H., *An Experimental Study of Compression Behavior of Warp-knitted Spacer Fabric*, In: Journal of Engineered Fibers and Fabrics, 2014, 9, 2, 61-69
- [9] Liu, Y., Hu, H., *Finite element analysis of compression behaviour of 3D spacer fabric structure*, In: International Journal of Mechanical Sciences, 2015, 94, 95, 244-259, <https://doi.org/10.1016/j.ijmecsci.2015.02.020>
- [10] Liu, Y., Hu, H., *Vibration isolation behaviour of 3D polymeric knitted spacer fabrics under harmonic vibration testing conditions*, In: Polymer Testing, 2015, 120-129
- [11] Liu, Y., Hu, H., Long, H., Zhao, L., *Impact compressive behavior of warp-knitted spacer fabrics for protective applications*, In: Textile Research Journal, 2012, 773-788, <https://doi.org/10.1177/0040517511433147>
- [12] Liu, Y., Hu, H., *Vibration Isolation Performance of Warp-knitted Spacer Fabrics*, Fiber Society Spring Conference, Hong Kong: Curran Associates, Inc., 2011, 63-64
- [13] Chaoyu, C., Junli, C., Fengxin, S., Huijuan, Y., Zhaoqun, D., *Analysis of the damping property of warp-knitted spacer fabrics under damped free vibration*, In: Textile Research Journal, 2017, 790-799



THE GAIN IN SHIELDING EFFECTIVENESS ACHIEVED BY SUPERPOSITION OF STAINLESS-STEEL PLASMA COATED WOVEN FABRICS

DOI: 10.35530/TT.2021.56

I.R. Radulescu^{1*}, L. Surdu¹, E. Visileanu¹, I. Sandulache¹, C. Morari², B. Mitu³

¹National Research Development Institute for Textiles and Leather, Romania
(E-mail: razvan.radulescu@incdtp.ro, lilioara.surdu@incdtp.ro, e.visileanu@incdtp.ro, irina.sandulache@incdtp.ro)

²ICPE-CA – Bucharest, Romania
(E-mail: cristian.morari@icpe-ca.ro)

³INFLPR – Magurele, Romania
(E-mail: bogdana.mitu@inflpr.ro)

Abstract: Electromagnetic shielding based on textile fabrics is important in applications for ensuring proper work of electronic equipment and for protection of human's health. Fibre-based materials include a good capability for a precise design of the physical and electric properties of the EM shields. There are two main methods to impart electroconductive properties to textile fabrics: insertion of conductive yarns into the fabric structure and coating with conductive layers. In our approach, both methods were applied: cotton woven fabrics with conductive yarns of stainless steel and silver, were coated by magnetron sputtering with stainless steel layers. Electromagnetic shielding effectiveness (EMSE) was determined by Transversal-Electric-Magnetic (TEM) cell measurement system, according to standard ASTM ES-07. Moreover, EMSE was determined for the superposition of the manufactured textile shields. The stainless-steel plasma coating improves EMSE with 20 dB in case of the fabrics with stainless steel yarns and with 15-17 dB in case of the fabrics with silver yarns, in the frequency range of 0.1-1000 MHz. By superposition of the plasma coated shields, the gain in EMSE achieved was of 6 dB for the fabrics with stainless steel yarns and of 5-8 dB for the fabrics with silver yarns, on the same frequency range. EMSE has significant higher values in case of the superposed shields with silver yarns and stainless-steel coating for the frequency domain of 100-1000 MHz, due to the higher thickness and the significant contribution of the multiple reflection term.

Keywords: fabrics, plasma coating, shielding, superposition

1. INTRODUCTION

Textile shields are used today in numerous applications for ensuring the proper work of electronic equipment and to protect human's health against non-ionizing radiation. The manufacturing of electromagnetic shields encompasses several solutions of fibre-based materials with electric conductive properties, and represents a niche domain with a lot of scientific contributions [1-4]. Main technological approaches to impart electric conductive properties to textile materials include insertion of conductive yarns into the fabric structure and coating with conductive layers [5]. In our approach, we propose textile woven fabrics with both inserted conductive yarns and plasma conductive coating. The inserted conductive yarns are made of silver and stainless steel, while the magnetron sputtering deposition conducted to stainless steel coatings. The current paper aims to tackle the gain in shielding

effectiveness achieved by superposition of two textile shields with same type of inserted conductive yarns, measured by means of the coaxial Transversal Electric-Magnetic (TEM) cell (standard ASTM ES-07).

2. EXPERIMENTAL

2.1 Materials

Insertion of conductive yarns in the woven fabric structure

Two types of woven fabrics with inserted conductive yarns were manufactured: stainless steel yarns (Bekinox BK50/2) were inserted both in warp and weft system of a cotton substrate at the experimental station of INCDTP–Bucharest and silver yarns (Statex 117/17 dtex) were inserted in weft system of a cotton substrate at SC Pamartex SRL, Giurgiu North Technological Park.

Figures 1, a and b present the warping beam and respectively the weaving loom of type SOMET width 1.90 m, at the experimental station of INCDTP. Table 1 presents the design parameters of the woven fabrics with conductive yarns as well as some of the main physical-mechanical parameters.

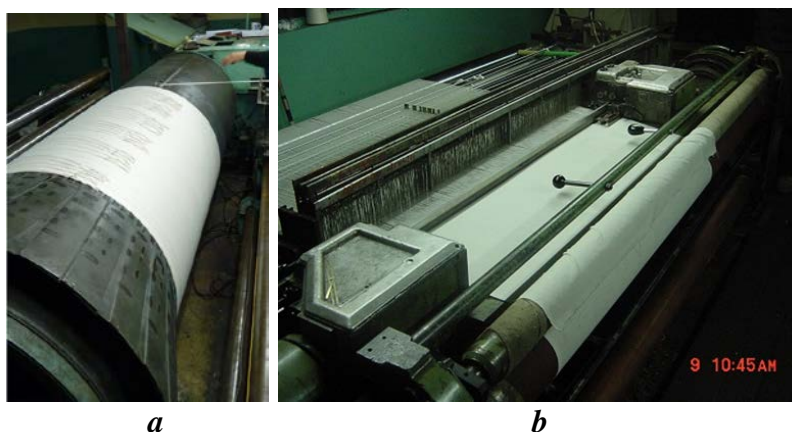


Figure 1. Equipment: a - warping beam; b - weaving loom

Table 1. Woven fabrics design parameters and main physical-mechanical properties

Parameters/Properties	F1	F4
Conductive yarns	Stainless steel (Bekinox BK50/2)	Silver (Statex 117/17 dtex)
Yarns fineness (dtex)	400	220
Density Warp (no. yarns/10 cm)	180	650
Density Weft (no. yarns/10 cm)	170	340
Float repeat Warp (cotton yarn: conductive yarn)	6:2	-
Float repeat Weft (cotton yarn: conductive yarn)	6:2	6:1
Specific mass (g/m ²)	143	329
Thickness (mm)	0.55	0.49
Distance between conductive yarns (mm)	4	4

Plasma coating technique

The stainless-steel coating of the textile fabrics was performed into a dedicated spherical stainless steel vacuum chamber (K.J. Lesker), pumped out by an assembly of a

fore pump and turbomolecular pump (Pfeiffer), which allowed the obtaining of a base pressure down to 3×10^{-5} mbar.

The chamber is provisioned with a magnetron sputtering gun from K.J. Lesker, accommodating a high purity Stainless steel target (99.999%). Enhanced deposition uniformity was achieved by rotating the samples during the deposition process (200 rotations/min). A constant Ar (6.0) flow of 50 sccm was continuously introduced into the chamber by means of a Bronkhorst mass flow controller, so that the pressure established during the process was 5.3×10^{-3} mbar. The discharge was ignited with an RF generator (13.56 MHz) – model CesarR provisioned with an automatic matching box.

The deposition time was set to insure a coating thickness of 400 nm and 1200 nm on both sides of the textile fabrics. Figure 2 presents the magnetron plasma equipment of INFLPR, evidencing the stainless-steel discharge above the textile surface.

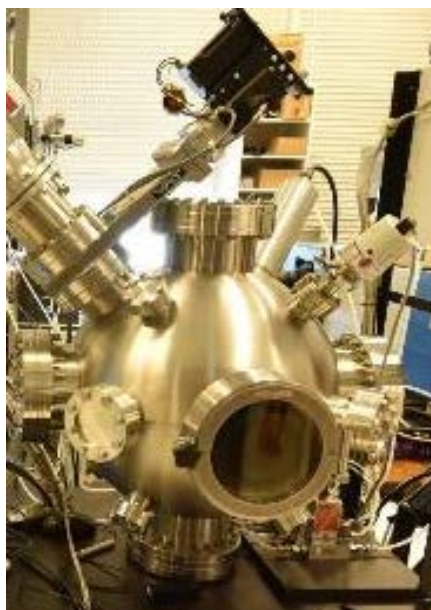


Figure 2. Magnetron plasma equipment

Figure 3 presents the experimental plan of achieved textile shields, considering the insertion of conductive yarns into the fabric structure and the magnetron plasma stainless steel coating.

Plasma coating 1200 nm x2	F3	F6
Plasma coating 400 nm x2	F2	F5
	F1	F4
	Stainless steel yarns	Silver yarns

Figure 3. Experimental plan of manufactured textile shields

2.2 Methods

Shielding effectiveness measurement

Electromagnetic shielding effectiveness (EMSE) is defined as:

$$EMSE = 10 \log \left(\frac{\text{power of incident signal}}{\text{power of transmitted signal}} \right) \quad (1)$$

Shielding effectiveness of fabric samples was measured via a coaxial TEM cell, according to standard ASTM ES-07. A picture of the measurement system, including the coaxial TEM cell is presented in figure 4.



Figure 4. TEM cell measurement system

Tested fabric samples were tailored in annular shape having an outer diameter of 100 mm and an inner diameter of 30 mm and they were fixed onto the cell by means of conductive colloidal Ag paste. The measurement system included a signal generator E8257D, a power amplifier model SMX5, the coaxial TEM cell model 2000 and an oscilloscope Tektronix model MDO3102.

3. RESULTS AND DISCUSSION

The electromagnetic shielding effectiveness (EMSE) was determined in the frequency range 0.1 – 1000 MHz. Results of EMSE are presented in figures 5 and 6.

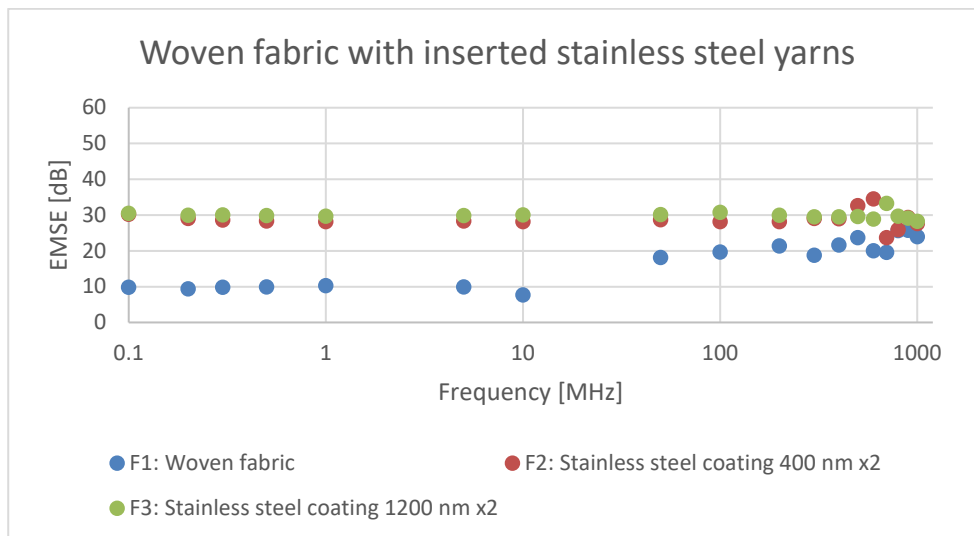


Figure 5. EMSE for fabrics with inserted stainless-steel yarns

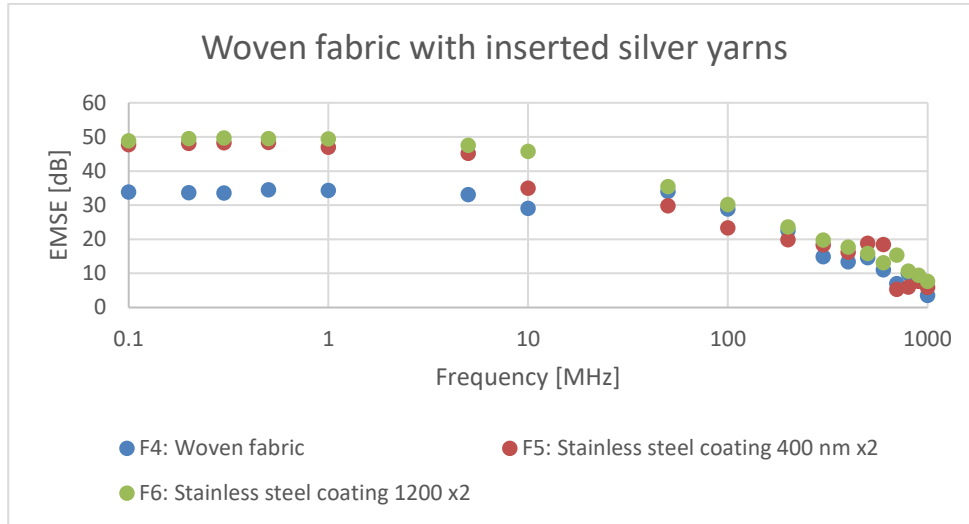


Figure 6. EMSE for fabrics with inserted silver yarns

According to experimental results evidenced in figure 5, stainless steel plasma coating improves EMSE of the fabrics with stainless steel yarns, in the frequency range of 0.1-1000 MHz with 20 dB. A slightly higher shielding (1-2 dB) was obtained in case of the coating with higher thickness (1200 nm on both faces). On the other hand, for the case of fabrics with silver yarns, the experimental results shown in figure 6 reveal that the same stainless steel plasma coatings improve EMSE with 15-17 dB on the same frequency range. This means a substantial improvement in EMSE of both types of textiles, due to magnetron plasma coating. The behaviour of EMSE in case of plasma coated woven structures with conductive yarns was analysed within paper [6]. The drop in EMSE for the woven fabrics with inserted silver yarns in the frequency range 100-1000 MHz, where the sample becomes electrically thick (sample thickness \gg skin depth), is due to the appearance of higher transmission modes in the coaxial TEM cell [9] that overdoses over the main transmission mode and can affect the measurement result.

As well, EMSE was determined for the shields built by superposition of two plasma coated samples, namely F2+F3 (fabrics based on stainless steel yarns) and F5+F6 (fabrics based on silver yarns). This approach was proposed in order to assess the gain in EMSE in case of superposition of the coated samples. Figure 7 and 8 present the EMSE in case of the superposition.

The superposition of the two plasma coated fabrics with stainless steel yarns increases EMSE with 6 dB on the entire frequency range, according to experimental results (figure 7). Figure 8 shows that superposition of the two plasma coated fabrics with silver yarns increases EMSE with 5-8 dB on the frequency range 0.1-100 MHz, with improved results in the range of 100-1000 MHz, of 10-12 dB. This behaviour in the high frequency range may be explained by the fact that by superposing the two fabrics, a thicker shield with an additional interface is obtained which leads to higher losses inside the shield due to the multiple reflection mechanism that occur both inside the two fabrics and at their interface [7-8]. Again, the deviation of the graphs, which according to theory [9] should have, for homogenous conductive materials, a straight trend at low frequencies (electrically thin samples) and an ascending trend at high frequencies (electrically thick samples), shows the occurrence of the higher order transmission modes that influences the measurement results.

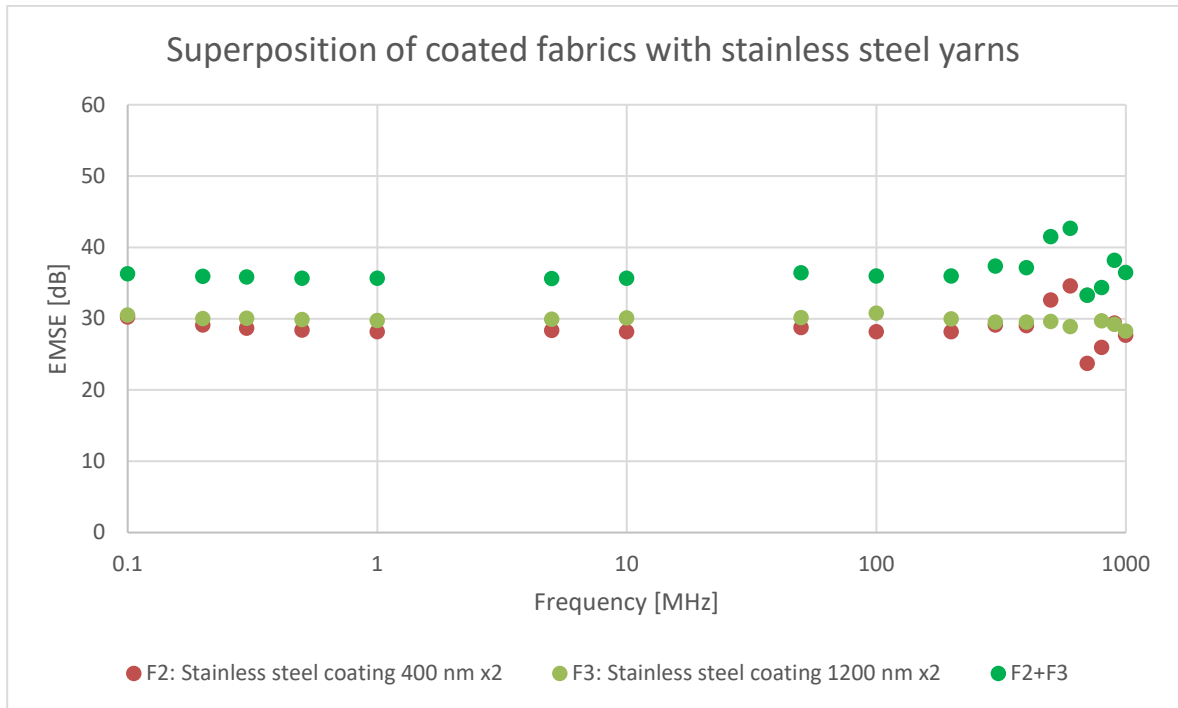


Figure 7. EMSE for superposition of coated fabrics with stainless steel yarns

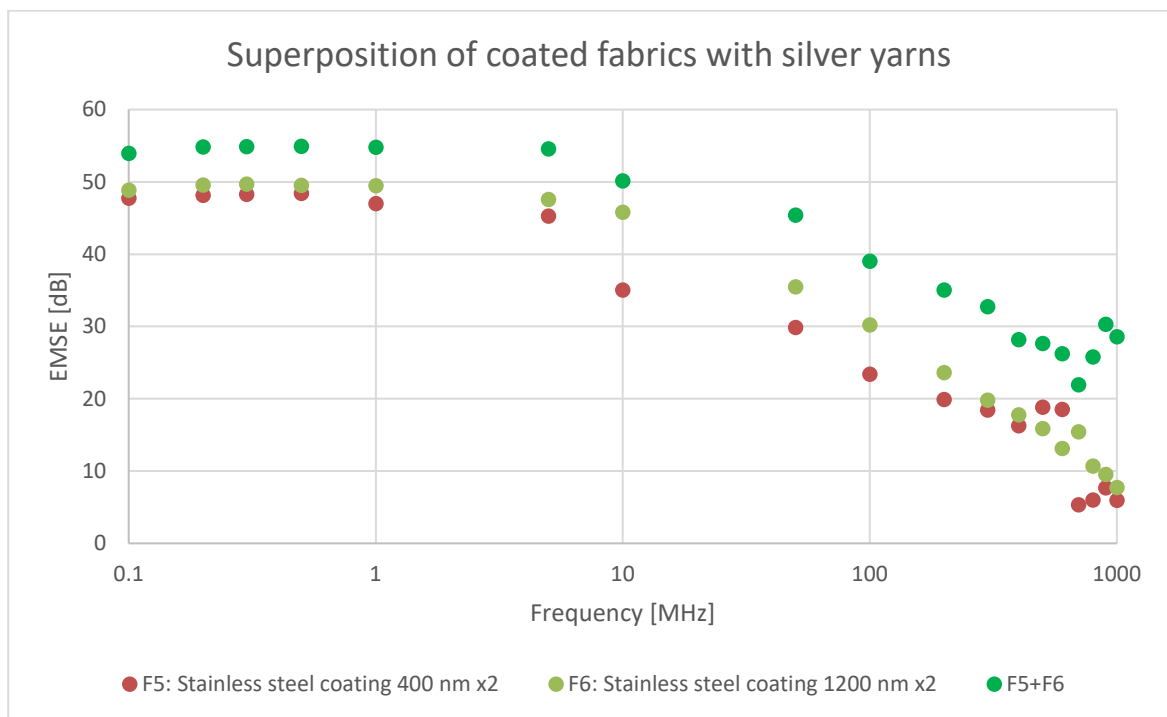


Figure 8. EMSE for superposition of coated fabrics with silver yarns

4. CONCLUSIONS

The paper was discussing on the shielding effectiveness for stainless steel plasma coated woven fabrics with inserted conductive yarns of stainless steel and silver. The manufactured EM shields were measured by superposition of two textile samples, based on the same type of inserted yarns and the coating thickness of 400 nm and 1200 nm, too. The results evidenced that the magnetron sputtering coatings of stainless steel improve EMSE

with 15-20 dB on the frequency domain of 0.1-1000 MHz for both types of woven fabrics. Superposition of samples conducted to an additional improvement of EMSE with 6-8 dB on the same frequency domain, when compared to the single samples.

ACKNOWLEDGEMENTS

Research work for this study has been performed within ERA-NET Manunet project C28/2018 TexEMFiRe – “Manufacturing textiles with electromagnetic shielding and fire-retardant properties by plasma-based methods”.

REFERENCES

- [1] Dai, M., Zhai, Y., Zhang, Y., *A green approach to preparing hydrophobic, electrically conductive textiles based on waterborne polyurethane for electromagnetic interference shielding with low reflectivity*, In: *Chemical Engineering Journal*, 2020, <https://doi.org/10.1016/j.cej.2020.127749>
- [2] Liu, Q., Yi, C., Chen, J., Xia, M., Lu, Y., Wang, Y., Liu, X., Li, M., Liu, K., Wang, D., *Flexible, breathable, and highly environmental-stable Ni/PPy/PET conductive fabrics for efficient electromagnetic interference shielding and wearable textile antennas*, In: *Composites*, 2021, Part B, 215, 108752, <https://doi.org/10.1016/j.compositesb.2021.108752>
- [3] Xu, C., Zhao, J., Chao, Z., Wang, J., Wang, W., Zhang, X., Li, Q., *Developing thermal regulating and electromagnetic shielding textiles using ultra-thin carbon nanotube films*, In: *Composites Communications*, 2020, 21, 100409, <https://doi.org/10.1016/j.coco.2020.100409>
- [4] Pakdel, E., Wang, J., Kashi, S., Sun, L., Wang, X., *Advances in photocatalytic self-cleaning, superhydrophobic and electromagnetic interference shielding textile treatments*, In: *Advances in Colloid and Interface Science*, 2020, 277, 102116, <https://doi.org/10.1016/j.cis.2020.102116>
- [5] Ziaja, J., Jaroszewski, M., *EMI Shielding using Composite Materials with Plasma Layers*, In: *Electromagnetic Waves*, Vitaliy Zhurbenko, IntechOpen, 2011, <https://doi.org/10.5772/16553>
- [6] Rădulescu, I.R., Surdu, L., Mitu, B., Morari, C., Costea, M., Golovanov, N., *Conductive textile structures and their contribution to electromagnetic shielding effectiveness*, In: *Industria Textila*, 2020, 71, 5, 432-437, <http://doi.org/10.35530/IT.071.05.1783>
- [7] Schwab, A., Kuerner, W., *Electromagnetische Verträglichkeit*, Springer, 2011, <https://doi.org/10.1007/978-3-642-16610-5>
- [8] Keiser, B., *Principles of electromagnetic compatibility*, CRC Press, 1981
- [9] Bădic, M., Marinescu, M-J., *The Failure of Coaxial TEM Cells ASTM Standards Methods in H.F. Range*, IEEE Xplore, <https://doi.org/10.1109/ISEMC.2002.1032442>



PREDICTIVE MATHEMATICAL MODEL FOR ABSORBANT SUBSTRATE ACHIEVEMENT, THROUGH ELECTROSPINNING PROCESS

DOI: 10.35530/TT.2021.59

C. Mihai¹, A.G. Ene¹, R.-G. Hertzog², D. Popescu², A.F. Vladu¹

¹IT Research Department in Industrial Engineering, National Research Development Institute for Textiles and Leather, Romania

(E-mail: carmen.mihai@incdtp.ro)

²Biological Research Department, “Cantacuzino” National Institute of Research, Bucharest, Romania

(E-mail: office.cantacuzino@mapn.ro)

Abstract: The new generations of wound dressings aim to create an optimal environment that allows epithelial cells to move easily in order to support regeneration. Such optimal conditions include a humid environment around the wound bed, efficient oxygen circulation to help regenerate cells and tissues, and low bacterial contamination. Composite matrices have several layers and can be used as primary or secondary dressings. Most composite dressings have three layers, respectively a semi-adherent or non-adherent layer, an absorbent layer, and a bacterial barrier layer. A method to obtaining these materials, which can be assimilated to layer-by-layer deposition, or which can be operated in this regime, is represented by electrospinning. However, the deposition technique by electrospinning on textile surfaces (fabrics or nonwovens) raises some problems related to the electrostatic behaviour of textile fibres with dielectric properties. In this case, the characteristics of the jet are affected directly proportional with the thickness of the textile material, resulting in defects of nano- or micro-fibrillar deposition, such as unevenness and/or sputter (formation of drops, which are deposited in mixture with electro spun fibres). The article presents a mathematical model that predicts the diameter of the fibres in the composition of the absorbent layer of the multilayer matrix structure for the treatment of burns or gunshot wounds, taking into account the nonlinear relationships between the parameters explained above and specific theories of electrodynamics for thin profiles (for instance, those used in aeronautics) for the prediction of the behaviour of the electrospinning jet.

Keywords: cellular matrix, electrospinning, mathematical modelling, textile substrate, skin regeneration

1. INTRODUCTION

Studies worldwide have shown that for biomedical applications, in case of the development of multilayer matrices for the treatment of wounds caused by burns or by shooting, the adhesion of fibroblast cells and their migration depends on the diameter of the fibres in the textile structure [1]. A method that can be assimilated to layer-by-layer deposition, or that can be operated in this regime, is represented by electrospinning. The resulting irregular layer of nanofibers can then be further processed by compaction/fusion in the form of extremely thin films, or by physico-chemical functionalization (for instance in cold plasma), followed by the continuation of deposition by the same technique, but using a different composition, or by any other technique [2,3].

However, the technique of deposition by electrospinning on textile surfaces (fabrics or nonwovens) raises some problems related to the electrostatic behaviour of textile fibres with dielectric properties. In their case, the characteristics of the jet are affected in directly proportional to the thickness of the textile material, resulting in defects of nano- or micro-fibrillar deposition, such as unevenness and/or sputter (formation of drops, which are deposited in mixture with electro spun fibres) [1,4].

It is possible to reach the complete collapse of the micro-nano-fibrillar layer and the formation of non-homogeneous, interrupted films. [4].

The article presents a mathematical model that predicts the diameter of the fibres in the composition of the absorbent layer of the multilayer matrix structure for the treatment of burns or gunshot wounds, taking into account the nonlinear relationship between the parameters explained above and specific theories of electrodynamics for thin profiles (for instance, in aeronautics) for the prediction of jet behaviour. Specifically, it has been proposed to explain, from a mathematical point of view, the interaction of the electric field with the properties of the fluid to predict the diameter of the final jet.

2. MATERIALS AND METHODS

The absorbent layer of the multilayer matrix, made by multilayer electrospinning must: have a moderate hydrophilic surface, dimensional stability (especially for deep burns), adequate microstructure, proper porosity, controllable biodegradability, allow adhesion and cell population growth [2].

i. Materials used to make the absorbent layer in case of burn wounds: natural polymers-collagen, gelatine, chitosan, fibrin, and their combinations (e.g., PLGA and collagen, to increase cell proliferation and the rapid development of extracellular matrix).

ii. Materials used to make the absorbent layer in case of gunshot wounds (blood vessels and bone tissue regeneration): chitosan, hyaluronic acid, collagen hydrolysed and colloidal silver.

Electrospinning is performed with a single nozzle; multiplication of the primary jet not been taken into account. After the formation of the Taylor cone, the molecular cohesion of the liquid is high and constant enough to prevent the flow from breaking (the electrospray phenomenon does not occur), generating the charged liquid jet [5].

The current flow changes from ohmic (linear) to convective (turbulent) as the load migrates to the fibre surface. The elongation of the jet takes place due to the whipping process caused by the electrostatic rejection initiated in the curved areas of the fibre. The visco-elastic behaviour of the polymer solution is described using the nonlinear model used in aerodynamics, considering the motion of the jet fluid element, and the mass transport of the solvent between the liquid jet and the gaseous medium is described by Frick's first law (stationary diffusion).

Fluid motion is defined by diffeomorphism $x=\mathfrak{N}(t,X)$, with X being the position vector of a particle in the initial configuration, x is the position vector of the same particle at time t . Consequently, the velocity and acceleration of the particle are given by the equation 1 [3-5]:

$$v(t,X) = \frac{d}{dt} \mathfrak{N}(t,X) \quad a(t,X) = \frac{d}{dt} v(t,X) \quad (1)$$

The fluid is a continuous medium, so the image through diffeomorphism is also a domain [6-8] and the intervening functions are of class $C_2(\mathfrak{F}_0)$ with the Jacobian 2:

$$J = \frac{\partial(\mathbf{x}_1, \mathbf{x}_2, \mathbf{x}_3)}{\partial(X_1, X_2, X_3)} \neq 0 \quad (2)$$

The equations of motion: the mass conservation principle 3, the continuity equation 4, the impulse variation principle 5, the energy balance equation 6 are the well-known ones, not insisting on the specific conditions of the studied case:

$$\frac{d}{dt} \int \rho dv = 0, \forall DC \mathfrak{B} \quad (3)$$

$$\dot{\rho} + \rho \operatorname{div} v = 0 \quad (4)$$

$$\frac{d}{dt} \int \rho v dv = - \int p n da + \int \rho f dv, \forall DC \mathfrak{B} \quad (5)$$

In this case, from (5) si $a = \frac{\partial v}{\partial t} + (v \cdot \nabla)v$ is result in the Euler equation:

$$\rho \left[\frac{\partial v}{\partial t} + (v \cdot \nabla)v \right] = \rho f - \operatorname{grad} p \quad (6)$$

$$\frac{d}{dt} \int \rho \left(e + \frac{1}{2} v^2 \right) dv = - \int p v \cdot n da + \int \rho f \cdot v da - \int q \cdot n da, \forall DC \mathfrak{B}$$

It is considered that the basic state of the environment in which the jet operates is undisturbed, so it can be considered that it is at rest, in uniform motion or with a given speed distribution. It is well known that the problem of determining perturbations can be solved only in cases where they are small, because only in these cases e the methods of classical analysis or the methods of distribution theory can be approached.

Taking into account that the order of magnitude of the disturbance is given by the basic movement and the shape of the body, for this case study the theory of thin bodies will be applied, with low incidence.

The validation conditions of the linear theory cannot be established before, this following to be established after determining the solution of the linearized equations, but making the condition that the result does not lead to physical impossibilities.

The systems of equations will be linear and with constant coefficients if the basis state is constant and will be linear with variable coefficients if the basis motion is uneven.

Taking into account the previously imposed conditions, for modelling the characteristics of nanofibers according to process parameters, the phenomenological model described in figure 1 was considered, where the liquid jet is replaced by rectilinear linear segments, subjected to a convective field, the jet being connected in a "Viscoelastic chain".

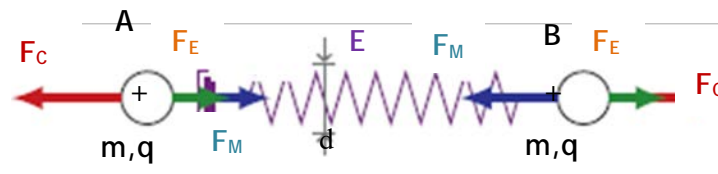


Figure 1. Force analysis for a rectilinear linear segment of the jet placed in the electrostatic field [4]: F_C - Coulomb repulsive force; F_E - electrostatic field strength; F_M - viscoelastic force; η - dynamic viscosity; E - modulus of elasticity; d - diameter; l - length; m - mass; q - loading

2.1 Mathematical modelling of the main descriptive parameters of the jet:

The mass loss of the solvent is calculated by equation 7:

$$\frac{dm_{si,i+1}}{dt} = h_m \pi d_{i,i+1} l_{i,i+1} \rho (c_{s,eq} - c_{s,\infty}) \quad (7)$$

where: $m_{si,i+1}$, $d_{i,i+1} l_{i,i+1}$ represents the instantaneous mass of the solvent, the instantaneous diameter and the instantaneous length relative to the rectilinear and linear segment (i, i + 1) of the electrically charged jet between the element i and i + 1 at time t, h_m is the mass transfer coefficient, ρ is the density of the polymer solution, $c_{s,\infty}$ represents the concentration of the solvent saturated vapor.

The mass transfer coefficient can be written according to the Sherwood criterion 8:

$$Sh = \frac{h_m d_{i,i+1}}{D_{S,a}} = \text{const. Re}^a \text{Sc}^b \quad (8)$$

where $D_{S,a}$ is binary diffusion coefficient, Re, Sc - Reynolds and Schmidt numbers, respectively, a, b - exponents, which can take 1/3 values, 1/2 respectively [5].

It's resulting that equation 9:

$$h_m = \frac{0.495 \text{Re}^{1/3} \text{Sc}^{1/2} D_{S,a}}{d_{i,i+1}} = \frac{0.495^3 \sqrt[3]{\frac{\rho_a l_{i,i+1} |v_{ni,i+1}^i|}{\eta_a}} \sqrt{\frac{\eta_a}{\rho_a D_{S,a}}} D_{S,a}}{d_{i,i+1}} \quad (9)$$

Using a few transformations, the equation governing the evaporation of the solvent becomes equation 10:

$$\frac{dm_{si,i+1}}{dt} = 0.496 v_a^{1/6} D_{S,a}^{1/2} \pi \rho (c_{s,eq} - c_{s,\infty}) l_{i,i+1}^{4/3} \sqrt[3]{|v_{ni,i+1}^i|} \quad (10)$$

Simple, it can also be determined the volume loss factor, using relationships 11:

$$\Lambda_{i-1,i} = \frac{V_{i-1,i}}{V_0} \quad \Lambda_{i,i+1} = \frac{V_{i,i+1}}{V_0} \quad (11)$$

Friction force - caused by the friction of the jet with the gaseous medium. Considering that the current lines depend on the shape of the body and the Reynolds number, it can be written successively in equations 12-17:

$$F_{Di-1,i}^i = C_f S_{fi-1,i} \frac{\rho_a (v_{ni-1,i}^i)^2}{2} + C_p A_{pi-1,i} \frac{\rho_a (v_{ti-1,i}^i)^2}{2} \quad (12)$$

$$F_{Di,i+1}^i = C_f S_{fi,i+1} \frac{\rho_a (v_{ni,i+1}^i)^2}{2} + C_p A_{pi,i+1} \frac{\rho_a (v_{ti,i+1}^i)^2}{2} \quad (13)$$

where C_f is friction coefficient and C_p - pressure coefficient.

$$S_{fi-1,i} = \frac{1}{2} \pi d_{i-1,i} l_{i-1,i} \quad S_{fi,i+1} = \frac{1}{2} \pi d_{i,i+1} l_{i,i+1} \quad (14)$$

$$A_{pi-1,i} = \frac{1}{2} \pi d_{i-1,i} l_{i-1,i} \quad A_{fi,i+1} = \frac{1}{2} \pi d_{i,i+1} l_{i,i+1} \quad (15)$$

$$v_{ni-1,i}^i = \frac{v_i \cdot n_{i,i-1}}{n_{i,i-1} \cdot n_{i,i-1}} \frac{r_{i-1} - r_i}{|r_{i-1} - r_i|} \quad v_{ni,i+1}^i = \frac{v_i \cdot n_{i+1,i}}{n_{i+1,i} \cdot n_{i+1,i}} \frac{r_i - r_{i+1}}{|r_i - r_{i+1}|} \quad (16)$$

$$v_{ti-1,i}^i = v_i - v_{ni-1,i}^i \quad v_{ti,i+1}^i = v_i - v_{ni,i+1}^i \quad (17)$$

where $n_{i,i-1} = r_{i-1} - r_i$ si $n_{i+1,i} = r_i - r_{i+1}$.

From $c_f = f(\text{Re}_l)$ and $c_p = f(\text{Re}_d)$ is resulting equations 18 and 19:

$$\text{Re}_l = \frac{\rho_a l_{i-1,i} |v_{ni-1,i}^i|}{\eta_a} \quad \text{Re}_l = \frac{\rho_a l_{i,i+1} |v_{ni,i+1}^i|}{\eta_a} \quad (18)$$

$$\text{Re}_d = \frac{\rho_a d_{i-1,i} |v_{ti-1,i}^i|}{\eta_a} \quad \text{Re}_d = \frac{\rho_a d_{i,i+1} |v_{ti,i+1}^i|}{\eta_a} \quad (19)$$

For laminar flow, take into account that $c_f = 24/\text{Re}_l$ and $c_p = 24/\text{Re}_d$.

It's resulting:

$$F_{Di} = 6\eta_a \pi d_0 l_0^2 \left[\left(\frac{\Lambda_{i-1,i}}{l_{i-1,i}} \right)^{\frac{1}{2}} \frac{(v_{ni-1,i}^i)^2}{|v_{ni-1,i}^i|} + \left(\frac{\Lambda_{i,i+1}}{l_{i,i+1}} \right)^{\frac{1}{2}} \frac{(v_{ni,i+1}^i)^2}{|v_{ni,i+1}^i|} \right] \quad (20)$$

$$+ 6\eta_a \left[l_{i-1,i} \frac{(v_{ti-1,i}^i)^2}{|v_{ti-1,i}^i|} + l_{i,i+1} \frac{(v_{ti,i+1}^i)^2}{|v_{ti,i+1}^i|} \right]$$

The viscoelastic behaviour of the jet (constitutive relation) is described by the equation 21:

$$\frac{d\sigma_{i,i+1}}{dt} = \frac{\eta_{i,i+1} (r_i - r_{i+1}) \cdot (v_i - v_{i+1})}{\tau_{i,i+1} l_{i,i+1}^2} - \frac{\sigma_{i,i+1}}{\tau_{i,i+1}} \quad (21)$$

where: $\sigma_{i,i+1}$, $\eta_{i,i+1}$ si $\tau_{i,i+1}$ represents the normal stress, the instantaneous dynamic viscosity and respectively the instantaneous relaxation time of the polymer solution.

The motion equation becomes equation 22:

$$\frac{dp_i}{dt} = m_i \frac{dv_i}{dt} - \left| \frac{dm_i}{dt} \right| v_i = F_{Ei} + F_{Ci} + F_{Mi} + F_{Si} - F_{Di} \quad (22)$$

It is easy to notice that the second order differential equation for the position of the mass point can be rewritten as a system of first order equations 23 and 24:

$$\begin{cases} \frac{dr_i}{dt} = v_i & (23) \\ m_i \frac{dv_i}{dt} = \left| \frac{dm_i}{dt} \right| v_i + F_{Ei} + F_{Ci} + F_{Mi} + F_{Si} - F_{Di} & (24) \end{cases}$$

The solvent evaporation equation 10, the constitutive relationship 21, the kinematic equation 23 and the motion equation 24 form the system of equations that describe the behaviour of an ideal linear jet segment moving in an electrostatic field.

The numerical solution for the equations determined above is based on the Euler method (for the predictor) and the Adams-Moulton method (for the corrector), respectively.

The group of dimensionless parameters were determined using scale factors as follows: (equations 25 - 31): normal tension:

$$\sigma_{i,i+1}^* = \frac{\sigma_{i,i+1}}{E_0} \quad (25)$$

- dynamic viscosity:

$$\eta_{i,i+1}^* = \frac{\eta_{i,i+1}}{\eta_0} \quad (26)$$

- diameter:

$$d_{i,i+1}^* = \frac{d_{i,i+1}}{d_0} \quad (27)$$

- vector components of the radius:

$$x_i^* = \frac{x_i}{L}, \quad y_i^* = \frac{y}{L}, \quad z_i^* = \frac{z}{L} \quad (28)$$

- mass:

$$m_{i,i+1}^* = \frac{m_i}{m_0} \quad (29)$$

- electrostatic charging:

$$q_{i,i+1}^* = \frac{q_i}{q_0} \quad (30)$$

- time:

$$t_{i,i+1}^* = \frac{t}{t_0} \quad (31)$$

where $E_0 = \eta_0 / \tau_0 =$ Young's modulus of the polymer solution
 $m_0, q_0 =$ initial mass and initial electrostatic charge

$$L = \sqrt{\frac{\tau_0 q_0^2}{\varepsilon_0^2 \varepsilon_r \pi^2 \eta_0 d_0^2}} = \text{characteristic length}$$

Dimensional equations 32 – 42:

$$\frac{dm_{si,i+1}^*}{dt^\#} = C_m^* (l_{i,i+1})^{\frac{4}{3}} |v_{ni,i+1}^i|^{\frac{1}{3}} \quad (32)$$

$$\frac{d\sigma_{i,i+1}^*}{dt^*} = \frac{\eta_{i,i+1}^* (r_i^* - r_{i+1}^*) \cdot (v_i^* - v_{i+1}^*)}{\tau_{i,i+1}^* (l_{i,i+1}^*)^2} - \frac{\sigma_{i,i+1}^*}{\tau_{i,i+1}^*} \quad (33)$$

$$\frac{dr_i^*}{dt^*} = v_i^* \quad (34)$$

$$\begin{aligned} m_i^* \frac{dv_i^*}{dt^*} = & \left| \frac{dm_i^*}{dt^*} \right| v_i^* + C_E^* q_i^* E^* + C_c^* q_i^* \sum_{j=1}^n \frac{q_i^*}{|r_i^* - r_j^*|^2} \frac{r_i^* - r_j^*}{|r_i^* - r_j^*|} + C_M^* \left(\sigma_{i-1}^* d_{i-1,i}^{*2} \frac{r_{i-1}^* - r_i^*}{|r_{i-1}^* - r_i^*|} + \right. \\ & \sigma_{i,i+1}^* d_{i,i+1}^{*2} \frac{r_{i-1}^* - r_i^*}{|r_{i-1}^* - r_i^*|} \left. \right) + C_S^* \left(d_{i-1,i}^* \frac{r_{i-1}^* - r_i^*}{|r_{i-1}^* - r_i^*|} + d_{i,i+1}^* \frac{r_{i-1}^* - r_i^*}{|r_{i-1}^* - r_i^*|} \right) + C_S^* \left(d_{i-1,i}^* \arcsin \frac{l_{i-1,i}^*}{2R_i^*} + \right. \\ & d_{i,i+1}^* \arcsin \frac{l_{i,i+1}^*}{2R_i^*} \left. \right) \frac{r_c^* - r_i^*}{|r_c^* - r_i^*|} + C_{Df}^* \left(d_{i-1,i}^* \frac{(v_{ni-1,i}^i)^2}{|v_{ni-1,i}^i|} + d_{i,i+1}^* \frac{(v_{ni,i+1}^i)^2}{|v_{ni,i+1}^i|} \right) + C_{Dp}^\# \left(l_{i-1,i}^* \frac{(v_{ti-1,i}^i)^2}{|v_{ti-1,i}^i|} + \right. \\ & \left. l_{i,i+1}^* \frac{(v_{ti,i+1}^i)^2}{|v_{ti,i+1}^i|} \right) \end{aligned} \quad (35)$$

where:

$$C_m^* = \frac{0.495 \pi v_a^{\frac{1}{6}} \tau_0^{\frac{2}{3}} D_{S,a}^{\frac{1}{2}} L^{\frac{5}{3}} (c_{s,eq} - c_{s,\infty})}{m_0} \quad (36)$$

$$C_E^* = \frac{\tau_0^2 q_0^2}{\varepsilon_0 m_0 L^3} \quad (37)$$

$$C_c^* = \frac{\tau_0^2 q_0^2}{4\pi\epsilon_0\epsilon_r m_0 L^3} \quad (38)$$

$$C_M^* = \frac{\pi\eta_0\tau_0^2 d_0^2}{4m_0 L} \quad (39)$$

$$C_S^* = \frac{\pi\gamma\tau_0^2 d_0^2}{m_0 L} \quad (40)$$

$$C_{Df}^* = -\frac{6\pi\eta_a\tau_0 d_0}{m_0} \quad (41)$$

$$C_{Dp}^* = -\frac{6\eta_a\tau_0 L}{m_0} \quad (42)$$

Based on these theoretical hypotheses, the established input data and the numerical discretization, the equations that describe the motion of the jet in the convective zone (the so-called whipping phenomenon) can be solved. These will highlight which of the process parameters decisively influences the characteristics of the obtained nanofibers.

The further development of the mathematical model could lead to the prediction of the breaking strength and elongation of the nanofiber.

3. RESULTS AND DISCUSSIONS

The mathematical modelling performed in this stage show the following:

- a particularly important parameter in the electrospinning process is the initial dynamic viscosity, η_0 ; the decrease of the values of this parameter determines the increase of the whipping area and the decrease of the linear part of the jet, which implies an elongation of the liquid jet and implicitly a decrease of the nanofiber diameter.

- the initial relaxation time τ_0 observed in the previous equations is another very important parameter of the process. As the relaxation time increases, the Young's modulus of the polymeric liquid decreases, the width of the whipping area increases and the length of the linear area decreases, in other words the normal surface tension is responsible for the length of the linear area of the jet.

4. CONCLUSIONS

Electrostatic spinning is a complex process that involves diffusion/evaporation/cooling, heat transfer, water condensation and polymer diffusion, all these stages of the process being accompanied by their associated variables, such as jet initiation, laminar and turbulent motion, solidification and deposition of nanofibers.

The control of the morphology and the mechanical behaviour of the nanofibers is still at the beginning, the mathematical models obtained so far predicting these parameters specifically for the field of use.

It is necessary to deepen the specific phenomenology of this process for future modelling routes, especially regarding the evolution of nanoscale structures and parameter control.

ACKNOWLEDGEMENTS

The authors would like to express appreciation for the support of the Project Number 496PED/2020.

REFERENCES

- [1] Yarin, A.L., Koombhongse, S., Reneker, D.H., *Bending instability in electrospinning of nanofibers*, In: J Appl Phys, 2011, 5, 89, 18-26
- [2] Casper, C.L., Yang, W., Farach-Carson, M.C., Rabolt, J.F., *Coating electrospun collagen and gelatin fibers with perlecan domain I for increased growth factor binding*, In: Biomacromolecules, 2007, 4, 8, 1116-23
- [3] Kenawy, R., Layman, J.M., Watkins, J.R., Bowlin, G.L., Matthews, J.A., Simpson, D.G., *Electrospinning of poly(ethylene-co-vinyl alcohol) fibers*, In: Biomaterials, 2013, 6, 24, 907-13
- [4] Zhong, S., Teo, W.E., Zhu, X., Beuerman, R.W., Ramakrishna, S., Yung, L.Y., *An aligned nanofibrous collagen scaffold by electrospinning and its effects on in vitro fibroblast culture*, In: J Biomed Mater Resarch, 2016, 3, 79, 456-63
- [5] Yarin, A.L., Koombhongse, S., Reneker, D.H., *Bending instability in electrospinning of nanofibers*, In: J. Appl. Phys., 2011, 5, 89, 3018-3026
- [6] Fisher, A.C., De Cossart, L., How, T.V., Annis, D., *Long term in-vivo performance of an electrostatically-spun small bore arterial prosthesis: the contribution of mechanical compliance and anti-platelet therapy*, In: Life Support Syst, 1985, 1, 3 Suppl, 462-465
- [7] Doshi, J., Reneker, D.H., *Electrospinning process and applications of electrospun fibers*, In: J Electrostatics, 1995, 35, 2-3, 151-160
- [8] Song, J.H., Kim, H.E., Kim, H.W., *Production of electrospun gelatin nanofiber by water-based co-solvent approach*, In: J Mater Sci Mater Med, 2017, 19



FLOATING TANK FOR TRANSPORTING OIL AND HYDROCARBONS FOLLOWING A MARITIME DISASTER

DOI: 10.35530/TT.2021.06

M. Jomir^{1*}, D. Zamirache², A. Ene¹, C. Mihai¹

¹National Research Development Institute for Textiles and Leather, Romania
(E-mail: mihaela.jomir@incdtp.ro)

²Design & Research Department, SC CONDOR SA, Romania
(E-mail: dan.zamfirache@condor-sa.ro)

Abstract: Storage of recovered oil and oily water is an important issue when it comes to maritime disasters, being a significant factor of the overall operation. Using large storage vessels is not always an option especially when the vessel is close to the shore. Currently, floating or non-inflatable tanks made of composite textile materials are used worldwide for the storage of the water/hydrocarbon mixture, regardless of the area of action (maritime or fluvial). The research carried out so far by INCDTP specialists, which consists in modelling, simulation and numerical analysis of various constructive forms and devices, led to the conclusion that for the making of a floating tank for storing water/hydrocarbon/oil mixtures, the best solution for its construction is represented by textile materials woven from high-tech yarns (*p*-aramid and polyamide 6.6) covered with polyurethane. The experimental model of the floating tank for the transport of oils and hydrocarbons in case of disaster was designed by INCDTP specialists and consists of five experimental models of floating materials (made of five variants of covered textile structures) and assembled in collaboration with specialists from SC CONDOR SA, in the form of a floating storage tank. The storage tank that has been created will be tested on the ground first, in order to perform all gravimetric and quality measurements.

Keywords: CAD, high-tech yarns, innovative textile technology, mobile tank, skimmer

1. INTRODUCTION

The consequences of marine disasters are multiple and affect particularly:

- the environment: oil slicks have triggered big destruction to coastal fauna and flora, to sea bottom and to the habitat of numerous species,
- health: marine transport is a carrier of microbes and contagious diseases; in past history, it had caused the spread of serious epidemics, hence the practice of ship quarantine;
- the economy: in the specific case of hydrocarbon transport, the claim generates a chain economic consequence, such as the devaluation of the shores, the high costs incurred in beach clean-up operations, the contamination of fisheries, the technical unemployment of fishing flotilla and related jobs on shore etc.

Disasters resulting from natural hazards can cause severe environmental and infrastructural disruption and significant economic losses [1-3]. When the release is a result of a technological accident, events can exacerbate the impact of a natural disaster on the environment, because of hazardous materials, fires and explosions (figure 1) [4,5]. In this

respect, one of the most conspicuous forms of damage to the aquatic environment is oil pollution [5-7].



Figure 1. Sheep disasters [5]

Oil represents a broad range of hydrocarbon-based substances (crude oil and refined petroleum products, animal fats, vegetable and non-petroleum oils) with a complex physical and chemical properties [4-7]. Oil spills may be due to releases of crude oil from tankers, offshore platforms, drilling rigs and wells, as well as spills of refined petroleum products (ex. gasoline, diesel) and their by-products, heavier fuels used by large ships (bunker fuel), but it is very difficult to precisely estimate global oil inputs into marine environment. For example, around 35% comes from tanker traffic and other shipping operations. Together with inputs from industrial effluents and oil rigs, it accounts for 45% (figure 2) [7-9].

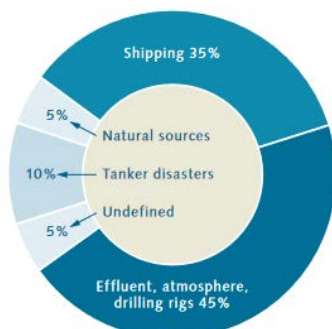


Figure 2. Various pathways of oil entering the sea [7]

Factors which affect the ability of an oil spill to spread are:

- surface tension – the higher oil’s surface tension, the more likely a spill remain in place [4,8,9]; if the surface tension of the oil is low, it will spread even without help from wind and water currents [4,9,10]; supplementary, oil is more likely to spread in warmer waters than in cold waters (increased temperature reduce a liquid’s surface tension);
- specific gravity - can increase if the lighter substances within the oil evaporate; heavier, vegetable oils and animal fats may sink and form tar balls or may interact with rocks or sediments on the bottom of the water body;
- viscosity – the higher the viscosity of oil, the greater the tendency for it to stay in one place [4,8,11].

Oil inputs include volatile constituents which are emitted into the atmosphere during various types of burning process and after enter the water (figure 3). The breakdown of the petroleum hydrocarbons depend on a variety of different environmental conditions: temperature, nutrient content in the water, wave actions etc. During the first few hours or even the first few weeks, the oil is modified by various physical, chemical and biological

processes: evaporation of volatile constituents spreading of the spilled oil in large oil slicks drifting on surface water; formation of dispersions and emulsions; photo-oxidation (molecular changes) and solution [4,12,13]. Other processes (sedimentation and breakdown by bacteria) may continue months or years [13,14]. The speed of breakdown depends on:

- the molecular structure of the oil constituents – the more complex the petroleum hydrocarbon molecules, the longer process for the oil breaking down by microorganisms;
- the cumulative action of the complex factors for promoting bacterial activity – high temperatures, large surface area, good oxygen and nutrient supply and low number of predator organisms.

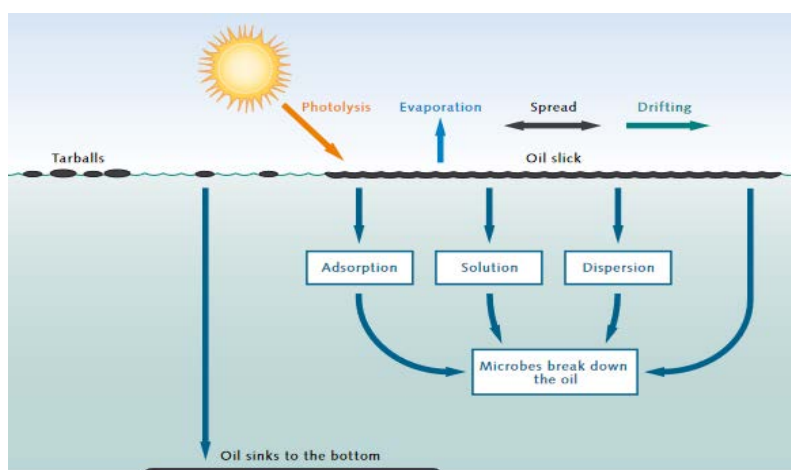


Figure 3. Modification of the crude oil in the sea [8]

There are a few solutions to respond to marine oil spills. Each of them is used according to the gravity of the situation, the surface polluted with oil and the weather conditions on the sea.

When oil (petroleum, crude oil) occurs on water, it is critical to constrain the spill as quickly as possible in order to minimize danger and potential damage to sea resources.

In this respect, [8-10] two major steps involved in controlling oil spills are:

1. containment – using floating barriers - booms to restrict the spread of oil and to allow for its recovery, removal, or dispersal (figure 44) and

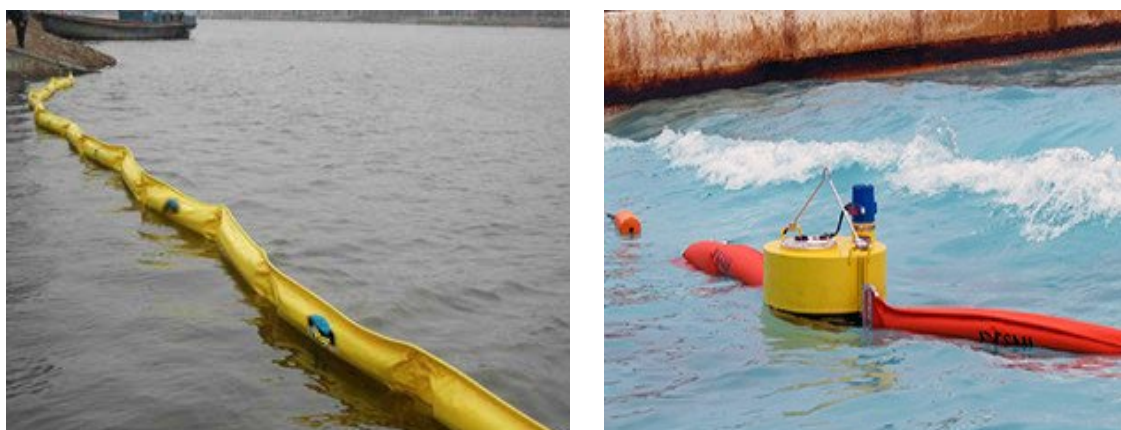


Figure 4. Anti-oil barrier [9]

2. recovery – with three different types of equipment – booms, skimmers and sorbents. Variation in the design and construction (typo-dimensional characteristics of booms for containment) are linked with four basic characteristics [10-13]:

- above-water freeboard to contain the oil and to help prevent waves from splashing oil over the top of the boom;
- flotation device;
- below-water skirt to contain the oil and help reduce the amount of oil lost under the boom;
- longitudinal support along the bottom of the skirt, that strengthens the boom against wind and wave action (figure 1).

When used in recovering oil, booms are often supported by a horizontal arm extending directly off one or both sides of a vessel, forming a “U”– or “J”–shaped pocket in which oil can collect; trapped oil can be pumped out to holding tanks (shuttles) for transporting to shore for proper disposal and recycling [9-11,13]. Skimmers (type weir, oleophilic and suction, depending on type of oil being cleaned up, condition of the aquatic environment, in presence of ice or debris in water) – figure 5 may be self-propelled or may be used from shore or operated from vessels.



Figure 5 – Skimmers [9]

Sorbents are materials used to recover oil through the mechanisms of absorption, adsorption or both.

For a modern unit (figure 6), the following functional characteristics are required: operational in strong sea currents oil spill recovery (min. 4bf), transport and storage (at min 2kt); rapid response in an emergency (possibility to be used in max. 1 h in conjunction with oil spill recovery equipment: vessel, booms, skimmers etc.); hydrodynamic configuration providing stable and secure storage solutions; added design features to aid clean up and separation; light, compact and highly portable.



Figure 6. Horizontal tanks

Furthermore, petroleum hydrocarbon fractions contain a wide range of individual hydrocarbon compounds and variations in physicochemical properties such as volatility and solubility need to be taken into consideration when considering the textile- reinforced composite materials for naval emergency shuttle.

2. MATERIALS AND METHODS

The research carried out so far by INCDTP specialists, which consists in modelling [14-18], simulation and numerical analysis of various constructive forms and devices by INCDTP specialists, made on the equipment from SC Majutex SA. The identification data of the 3 textile versions are presented below in table 1.

The experimental models in the composition of the tank are differentiated by: the geometric shapes, the dimensions of the realization and the types of variants of composite materials used for construction [19-24].

These aspects are presented centrally in table 1.

Table 1. Textile structures/versions

Characteristics	Structure 1 (V1)	Structure 2 (V2)	Structure 3 (V3)
Raw material Warp/Weft	100% Kevlar/ 100%Kevlar	100% Kevlar/ 50%Kevlar/50%PA6.6 $R_b = 2:2$	100% Kevlar/ 100%PA6.6
Weave type	Plain weave	Plain weave	Plain weave
Finishing type/colour	Covered with PU/orange	Covered with PU/orange	Covered with PU/orange

The experimental models in the composition of the tank are differentiated by: the geometric shapes, the dimensions of the realization and the types of variants of composite materials used for construction. These aspects are presented centrally in table 2.

Table 2. Experimental models of the composite modules

Characteristics	ME15	ME16	ME17	ME18	ME19
Composite material – variant	V1	V2	V2	V3	V3
Constructive form	Straight circular cylinder	Straight circular cylinder	Straight circular cylinder	Cone	Frustum of a cone

The experimental model of the floating tank for the transport of oils and hydrocarbons in case of disaster was designed by INCDTP specialists and consists of five experimental models of floating materials (made of five variants of covered textile structures) and assembled in collaboration with specialists from SC CONDOR SA, in the form of a floating storage tank (figure 7).

3. RESULTS AND DISCUSSIONS

The constructive dimensions of the experimental models from the floating storage tank component were the following (figure 4):

- ME15: bases 1200 mm, length 3600 mm;
- ME16 and ME17: bases 300 mm, length 2400 mm;
- ME18: base 1200 mm, height 1000 mm;
- ME19: large base 1200 mm, height 800 mm, small base 200 mm.

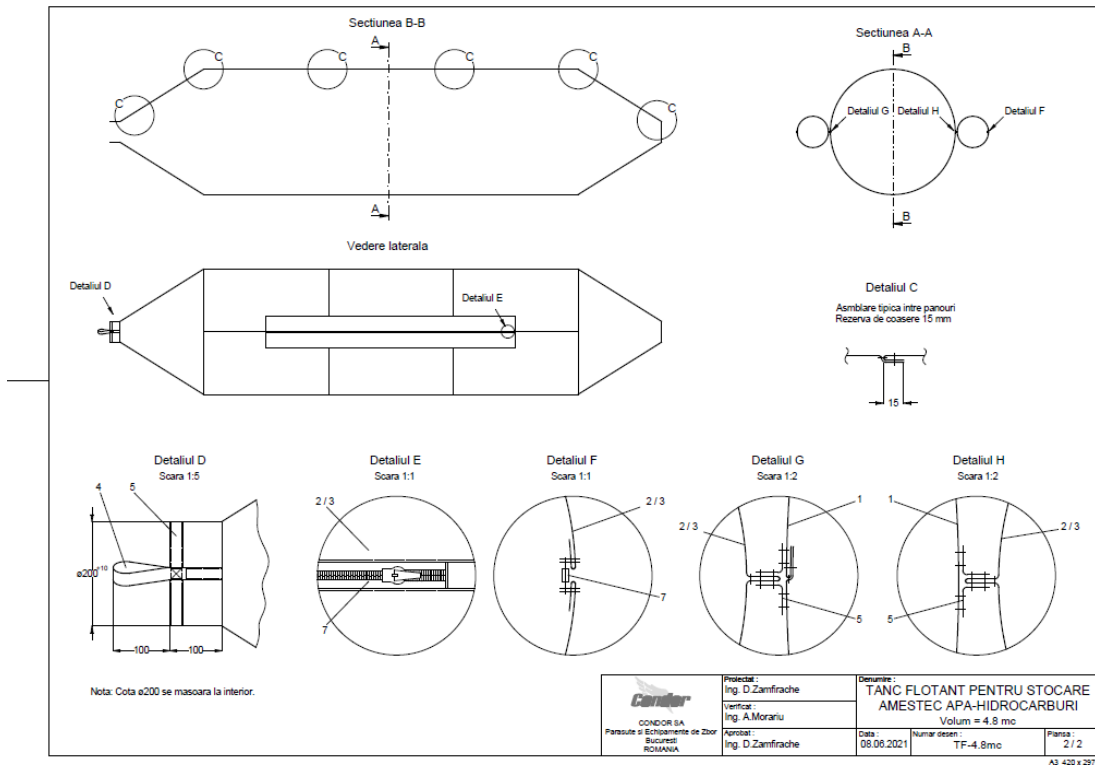


Figure 7. Sections and details for ME15 – ME19

The designed experimental models were assembled using sewing assembly technology, but using special equipment adapted for sewing para-aramid structures (figure 8).

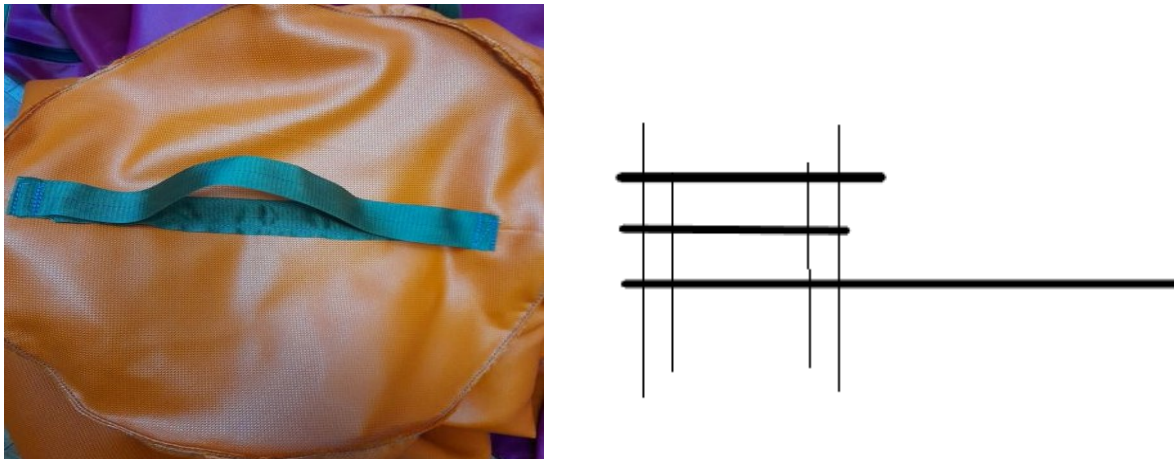


Figure 8. Sewing para-aramid structures

Particular attention was paid to the fact that there must be no bases between ME15, ME18 and ME19, in order to allow access to the mixture of water/hydrocarbons/oil recovered inside the tank to be transported to shore.

To assemble the Kevlar parts, the edge of the cut parts was stabilized by a 301 “safe stitch” using Nylon 135 Tex sewing thread, needle size 140/22 and Pfaff 2235 sewing machine with Ecodrive servomotor. A binding with scalloped edge Petersham type 30 mm was used to cover the edges, in order to eliminate the curling/wrinkling of the material during sewing (figure 9).

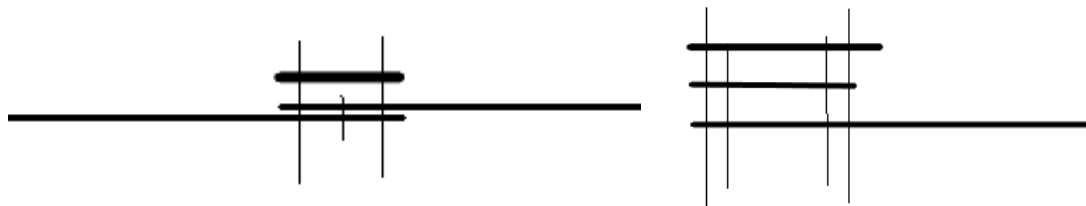


Figure 9. Elimination of the curling/wrinkling of the material during sewing

When assembling the rectangle with the circle on the straight circular cylinder, the sewing machine with two retractable needles and 25 mm wide grosgrain were used. Zippers with water-resistant tape and zipper strap reinforcement seams (ME16, ME17) were also used.

For ME18 and ME19, the assembly of the parts was done with reinforcing strips superimposed on each other - grosgrain 25 mm wide and binding with scalloped edge (Petersham), to cover and strengthen the edges of the cone and of the frustum of the cone.

The experimental model of floating tank will be tested on the ground, to verify the gravimetric measurements, as well as in real conditions of use, in the Port of Constanta.

4. CONCLUSIONS

The structural analysis that has been performed, on the basis of which the composite materials made of high-tech yarns were designed and made, forms the basis for the realization of the experimental models of modules from the floating tank component for storing water/hydrocarbon mixtures.

The experimental model of floating tank was made on the specific technology of assembling high-tech materials, which involves, on the one hand, the combination of large modules and, on the other hand, the use of special accessories for assembling composite textiles made of high tenacity polyamide or yarn of type p-aramid.

The storage tank that has been created will be tested on the ground first, in order to perform all gravimetric and quality measurements. It will then be tested in real experimental conditions in the Port of Constanta in order to establish the technical resource.

REFERENCES

- [1] Legea nr.310/28.06.2004 pentru modificarea și completarea Legii apelor nr.107/25.09.1996
- [2] IMP, International Maritime Organisation (IMO), *Guidelines for Sampling and Identification of Oil Spills – Manual on Oil Pollution*, 2012
- [3] TDGR, Transportation of Dangerous Goods Regulations, Available at: <https://www.tc.gc.ca/eng/tdg/clear-tofc-211.htm> [Accessed on June 2021]
- [4] Brown, L., *Probleme globale ale omenirii. Starea lumii*, Editura Tehnica, București, 2001, 78-93
- [5] BP America Inc, *Waste Management Handbook, Guidance for Pre-Planning, Preparedness and response to Emergency Response Events*, 2012
- [6] Angelescu, A., Ponoran, I., Ciobotaru, *Mediul ambiant și dezvoltarea durabila*, Editura A.S.E., București, 1999, 13-25
- [7] Scotian Basin Exploration Project - *Oil response plan, Annex E – Waste Management Tactical Response Plan*, 2020, 166-208

- [8] *** *Sendai framework for disaster risk reduction 2015– 2030*, Geneva: United Nations Office for Disaster Risk Reduction, 2015, Available at: http://www.preventionweb.net/files/43291-_sendaiframeworkfordrren.pdf [Accessed on June 2021]
- [9] *** *World Ocean Review, WOR 5 – Coasts. A Vital Habitat Under Pressure 2019*, Cap 1 – Coastal Dynamics, 93-102
- [10] *** *The cyanide spill at Baia Mare, Romania: before, during and after*. Geneva: United Nations Environment Programme/Office for the Coordination of Humanitarian Affairs, 2002, Available at: <http://archive.rec.org/REC/Publications/CyanideSpill/ENG/Cyanide.pdf> [Accessed on June 2021]
- [11] Leaning, J., Guha-Sapir, D., *Natural disasters, armed conflict, and public health*, New England Journal of Medicine, 2013, 369, 1836-1842, <https://doi.org/10.1056/NEJMra1109877>
- [12] *** *Chemical releases caused by natural hazard events and disasters*, Geneva: World Health Organization, 2018, 16-28
- [13] European Commission - *Best Available Techniques Guidance Document on up stream hydrocarbon exploration and production*, 25 February 2019, 124-193
- [14] Ravi, S., Iyengar, N.G.R., Kishore, N.N., Shukla, A., *Influence of Fiber Volume Fraction on Dynamic Damage in Woven Glass Fabric Composites: An Experimental Study*, In: Adv. Composite Mater., 2020, 9, 319-334
- [15] Ghionea, I.C., *Proiectare asistata in CATIA V5. Elemente teoretice si aplicatii*, Ed. Bren, 2015, 210-250
- [16] Wen, C., Yazdani, S., *Anisotropic damage model for woven fabric composites during tension-tension fatigue*, In: Composite Structures, 2008, 82, 127-131
- [17] Kuo, W.S., Ko, T.H., Chen, C.P., *Effect of Weaving Processes on Compressive Behavior of 3D Woven Composites*, In: Composites: Part A, 2007, 38, 555-565
- [18] Hallal, A., Younes, R., Fardoun, F., Nehme, S., *Improved analytical model to predict the effective elastic properties of 2.5D interlock woven fabrics composite*, In: Composite Structures, 2012, 94, 3009-3028
- [19] Colorado, H.A., Chaves Roldán, C., Vélez, J.M., *Internal Friction and Anelastic Behavior in Solids*, In: Dyna, 2006, 73, 39-49
- [20] Scardino, F., *An Introduction to Textile Structures and Their Behavior. Textile Structural Composites*, In: Composite Materials series, eds. Chou T.W. and Ko F.K, Elsevier, 1989, 3
- [21] Gibson, L.B., Cumiskey, S., Macosko, C.W., *Compaction of Fiber Reinforcements*, In: Polymer Composites, 2002, 23, 307-318
- [22] Gu, H., *Tensile behaviours of woven fabrics and laminates*, In: Materials and Design, 2007, 28, 704-707
- [23] Wan, Y.Z., Wang, Y.L., Dong, X.H., Cheng, G.X., *Comparison of Mechanical Performance and Fracture Behavior of Gelatin Composites Reinforced With Carbon Fibers of Different Fiber Architectures*, In: Polymer Composites, 2001, 22, 111-117
- [24] Mahadik, Y., Robson Brown, K.A., Hallett, S.R., *Characterisation of 3D woven composite internal architecture and effect of compaction*, In: Composites: Part A, 2010, 41, 872-880



TRAINING OF TEXTILE CREATIVES IN THE FIELD OF E-TEXTILES DESIGN SOFTWARE

DOI: 10.35530/TT.2021.40

I.R. Radulescu*, R.M. Aileni, A. Salistean, S. Olaru, M.C. Grosu, R. Scarlat,
I. Sandulache

National Research Development Institute for Textiles and Leather, Romania

(Email: razvan.radulescu@incdtp.ro, raluca.aileni@incdtp.ro, adrian.salistean@incdtp.ro,
sabina.olaru@incdtp.ro, catalin.grosu@incdtp.ro, razvan.scarlat@incdtp.ro,
irina.sandulache@incdtp.ro)

Abstract: *Textile technologies are rapidly developing and coping with the modern software applications of e-textile design means a substantial benefit for textile creatives. The target group of textile creatives is considered to include both young professionals in the textile industry as well as students of Higher Education in technical fields. A partnership of six prestigious research and educational providers in Europe, coordinated by INCDTP – Bucharest have joined their expertise to offer educational modules related to this need, within the Erasmus+ project “OptimTex- Software tools for textiles creatives”. The project has duration of two years (2020-2022) and has already implemented the educational modules in e-learning format on the project’s website (www.optimtex.eu). The five educational modules follow the main textile technologies and describe in a Problem-Based-Learning (PBL) approach software applications for: weaving, knitting, virtual prototyping of clothing, embroidery of e-textiles (electronic textiles) and experimental design. The PBL approach consists in learning by examples, followed by the theory, the corresponding software applications and a quiz for self-assessment. The e-learning instrument was programmed in HTML5 and JavaScript and offers quick access the educational modules. INCDTP has conceived the fifth module on experimental design, by tackling plasma treatments of textiles for various functionalities: hydrophobic, hydrophilic and electrical conductivity. Full factorial, Central Composite Design and Fractional factorial experimental design plans were described. This topic is of interest for the envisaged target group, for it represents alternative and useful knowledge to the official curricula of Higher Education engineering studies. Intensive Study Programs and Multiplier events will be organized in the second project’s year for students of Higher Education and textile professionals.*

Keywords: *design, e-textiles, e-learning, software, education*

1. INTRODUCTION

The world-of-work in textiles requires a well-skilled labour force with knowledge of the latest trends in textile technology [1]. Among these latest trends, a special role is represented by the computer software applications for design of e-textiles [2]. As such, a high value-added professional competence is given by the knowledge and skills in software for textiles. The skilled work force has improved chances to find a good work place and to benefit from the value-added competences.

The software applications in e-textiles are grouped on the various textile technologies, such as weaving, knitting, virtual prototyping of clothing, embroidery of e-textiles and experimental design. Since these types of software demand specialists with basic notions of textiles and computer, the process to upskill the competences in this domain is targeted

towards young professionals from the textile industry as well as by students of higher education. This target group was generically named “textile creatives”. The need of improving skills in design software for e-textiles (electronic textiles) was tackled by the Erasmus+ OptimTex project – “Software tools for textile creatives”.

2. THE ERASMUS+ OPTIMTEX PROJECT

The Erasmus+ project OptimTex – “Software tools for textile creatives” is a strategic partnership project in the field of Higher Education. It has an implementation period of two years (Dec. 2020 – Nov. 2022) and was funded by the Erasmus+ National Agency in Romania ANPCDEFP. INCDTP – Bucharest coordinates a prestigious partnership formed of research and educational providers in Europe: TecMinho / University of Minho from Portugal, Ghent University from Belgium, University of Maribor from Slovenia, Technical University “Gh. Asachi” from Iasi, Romania and University West Bohemia from Czech Republic. Basic info related to objectives, results and the partnership of OptimTex may be accessed on the project’s website www.optimtex.eu . Figure 1 presents the Erasmus+ logo and the project’s logo.



Figure 1. Images of: a - Erasmus+ logo; b - Project’s logo

The educational content was divided in several modules according to the main textile technology domains and the key expertise of the six partners, as follows:

- Design and modelling of woven structures – Ghent University
- Design and modelling of knitted structures – Technical University Iasi
- Design and modelling of garments by 3D scanning software and CAD/PDS software – University of Maribor
- Design and modelling of embroidered structures – University West Bohemia
- Software for research experimental design – INCDTP – Bucharest

The educational modules were conceived of about 40 pages including images and videos. These modules were already accomplished by the project’s partners in the first project’s year and they form the basic content for the three Intensive Study Programs with students of Higher Education, as well as the six Multiplier events with professionals from the industry. In order to organize these training / multiplier events, the educational modules are going to be implemented in e-learning format on the project’s Moodle platform at www.advan2tex.eu/portal/. The Moodle e-learning platform includes already the educational materials of the previous three Erasmus+ VET projects, with open access (figure 2).

3. THE E-LEARNING INSTRUMENT

The OptimTex educational modules were already implemented online, by means of an e-learning instrument. The instrument was conceived to enable quick access in a visual and structured manner to the educational modules [3,4]. All the provided modules described examples of software for textiles in a Problem-Based-Learning approach [5,6]. As such, each module included 4-5 examples, completed by the corresponding theory, the required software applications as well as the multiple-choice questions for self-assessment of the acquired

knowledge. In order to support the learning process, the e-learning instruments provide access to each of these four elements of the educational modules. Please consult figure 3 on the concept of the e-learning instrument with the four HTML buttons: Example, Theory, Application and Quiz.

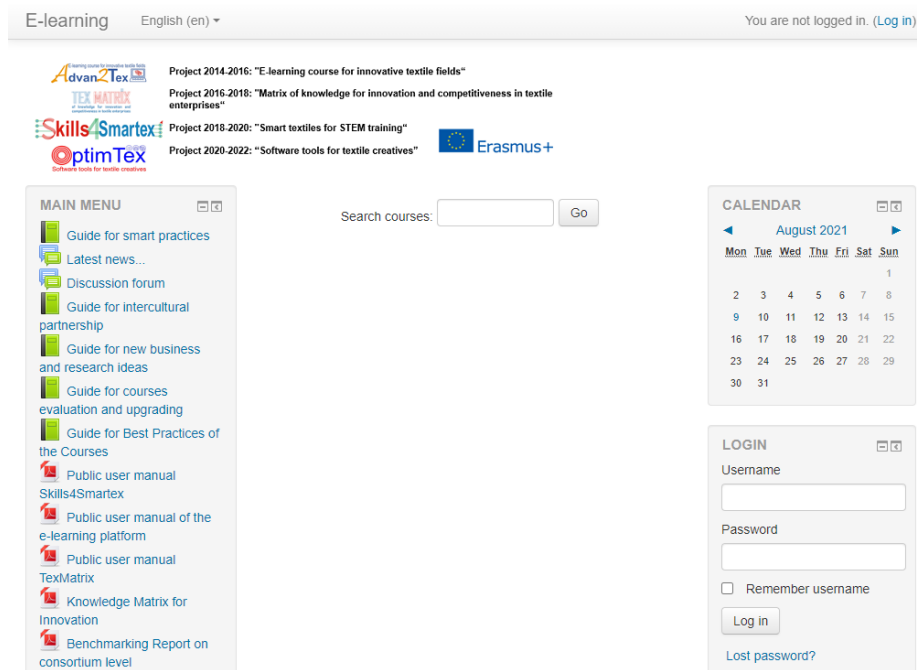
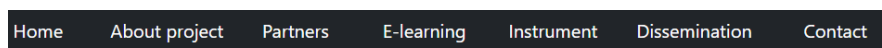


Figure 2. The Moodle e-learning platform



OptimTex e-learning instrument

The educational content of OptimTex is divided on 5 modules on software for design of e-textiles:

- Design and modelling of woven structures
- Design and modelling of knitted structures
- Design and modelling of garments by 3D scanning software and CAD/PDS software
- Design and modeling of embroidered structures
- Software for research experimental design

Each module is conceived in a Problem-Based-Learning approach and is structured with several practical examples, the corresponding theory, software for design and quiz for self-assessment. The e-learning instrument is meant to share quick access on the structured educational content of the Erasmus+ project.


Module	Design and modelling of woven structures	<p>Example</p> <p>Woven structures are all around you. A tablecloth, bedsheets, your jeans, they are all created from woven fabric. In this case we will learn you how you can create a digital representation of one, and how this representation contains the information needed to produce the woven structure on a weaving machine.</p> <p>We will use the TexGen software. TexGen is open source software licensed under the General Public License developed at the University of Nottingham for modelling the geometry of textile structures. TexGen has been used by the Nottingham team (http://texgen.sourceforge.net/index.php/Main_Page) as the basis of models for a variety of properties, including textile mechanics, permeability and composite mechanical behaviour [1][2]. Install it for windows with the instruction on the webpage.</p> 
Lesson	1	
	<input type="button" value="Increment"/> <input type="button" value="Decrement"/>	
Category	1	
	<input type="button" value="Example"/> <input type="button" value="Theory"/>	
	<input type="button" value="Application"/> <input type="button" value="Quiz"/>	

Figure 3. The HTML5 / JavaScript e-learning instrument

The e-learning instrument was programmed in HTML5 and JavaScript and was included as webpage on the online project's website (www.optimtex.eu). Each of the four elements of an example may be accessed by the corresponding HTML5 button. This modality to present the educational content of the project is in line with the open-access provisions of Erasmus+ EC program and is conceived as well in a Problem-Based-Learning approach.

4. THE MODULE ON EXPERIMENTAL DESIGN

INCDTP – Bucharest has prepared the fifth educational module, named “Software for research experimental design”. This module tackles by four examples the topic of experimental design and the related software solutions of regression computing. The examples belong to the plasma treatment of textile materials for various functionalities, such as hydrophobic, hydrophilic and electric conductive properties. The used experimental design plans were:

- Full factorial with two input parameters and three variation levels
- Box-Wilson – Central Composite Design with two input parameters and five variation levels
- Full factorial with four input parameters and two variation levels
- Fractional factorial with six input parameters and two variation levels

In order to optimize the plasma treatment on textile materials, several input parameters, such as the power of the generator, the process time, the gas flow and the process pressure have to be simultaneously varied, according to an experimental plan and the corresponding experimental matrix (design phase). A mathematical model, usually a polynomial equation second degree may be associated between the input parameters of the physical process and the result variable and its coefficients computed by regression (analysis phase). This mathematical model may be further used to compute intermediate values by interpolation and to perform the MINMAX analysis for optimizing the result and determine the corresponding input parameters (prediction phase) [7,8].

The first example tackles the hydrophobic plasma treatment by hexafluoro propane gas, on cotton fabrics, by the low-pressure plasma equipment of INCDTP. The power of the generator and the process time were considered as input parameters. The result variable to characterize the hydrophobic functionality was considered the Water Contact Angle (WCA) – (figure 5), measured by means of a goniometer equipment (figure 4).



Figure 4. The contact angle instrument



Figure 5. Photo of water droplet on the cotton fabric

The values of the three variation levels of the two input parameters Power and Time are presented in table 1.

Table 1. The variation levels of the input parameters

Level	Power (W) x	Time (min) Y
upper: +1	30	4
medium: 0	20	3
lower: -1	10	2
delta Δ	10	1

The input parameters were encoded by equations 1 and 2, while the mathematical model, the polynomial equation second degree is given by equation 3.

$$x = \frac{P - 20}{10} \quad (1)$$

$$y = \frac{t - 3}{1} \quad (2)$$

$$Z = a_0 + a_1x + a_2y + a_{12}xy + a_{11}x^2 + a_{22}y^2 \quad (3)$$

The experimental matrix of the physical process, with the result variable WCA is given by table 2.

Table 2. The experimental matrix with result variable WCA

Sample code		Power	Time	Variables			Result
		X	y	Xy	x ²	y ²	Z
P1	1	1	1	1	1	1	138.3
P2	1	1	0	0	1	0	133.6
P3	1	1	-1	-1	1	1	134.7
P4	1	0	1	0	0	1	135.8
P5	1	0	0	0	0	0	137.2
P6	1	0	-1	0	0	1	128.1
P7	1	-1	1	-1	1	1	135.6
P8	1	-1	0	0	1	0	131.6
P9	1	-1	-1	1	1	1	128.4

The regression computing in EXCEL was used, in order to compute the coefficients of the polynomial equation (figure 6).

This is an example of experimental design in the textile field to serve as educational content for Higher Education students. The software application, such as EXCEL, was applied to support the computational process of regression. The other examples of the course include more software applications with the practical modality to use: MATLAB, MODDE, NCSS, OpenOffice CALC. In this way, we aim to support the textile creatives to improve their knowledge and skills by practical applications. Please consult for the complete set of educational examples the e-learning instrument on the project's website www.optimtex.eu.

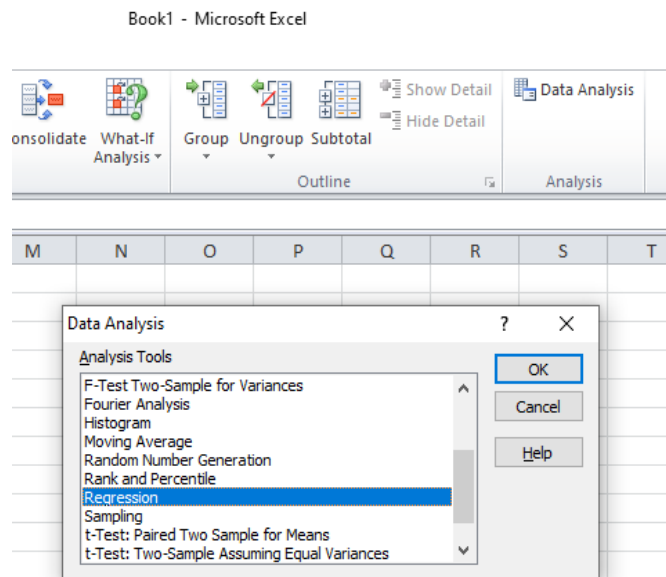


Figure 6. Regression computing in Excel

5. CONCLUSIONS

The knowledge of software applications is crucial for the textile creatives. The Erasmus+ OptimTex project was conceived, in order to support them with educational materials in software for e-textiles design of weaving, knitting, virtual prototyping of clothing, embroidery of e-textiles and experimental design. The educational modules are structured in a Problem-Based-Learning approach, with examples, theory, applications and quiz. An e-learning instrument was programmed in HTML5 and JavaScript, in order to enable quick access to the educational content. The fifth educational module “Software for research experimental design” was prepared by the team of INCDTP – Bucharest. It follows several examples of experimental design plans, based on the plasma treatment of textiles for various functionalities. The complete educational materials are already available on www.optimtex.eu. Intensive study programs with 60 students and multiplier events with 115 professionals will be organized in the second project’s year.

ACKNOWLEDGEMENTS

The authors would like to express appreciation for the support of the funding received by the Erasmus+ National Agency in Romania, ANPCDEF [Project Number = 2020-1-RO01-KA203-079823]. This project has been funded with support from the European Commission.

REFERENCES

- [1] Van Langenhove, L., *Smart textiles for protection: an overview*, In: Chapman R.A., Editor: Smart textiles for protection, Woodhead Publishing Limited, 2013. 3–33, ISBN 978–0–85709-762-0
- [2] Çelikel, D.C., *Smart E-Textile Materials*, In: *Advanced Functional Materials*, edited by Tasaltin, N., Nnamchi, P.S., Saud, S., In: IntechOpen, 2020, <https://doi.org/10.5772/intechopen.92439>
- [4] Malengier, B., Radulescu, I.R., Blaga, M., Stjepanovic, Z., *Design based learning in textiles for higher education*, At: MCCSIS E-learning Conference, 2021, ISBN: 978-989-8704-29-0
- [5] Radulescu, I.R., Ghituleasa, C., Visileanu, E., Almeida, L., Malengier, B., Stjepanovic, Z., Blaga, M., Dufkova, P., *E-learning instruments for design based learning in textiles*, At: The 17th eLearning and Software for Education Conference – eLSE, 2021
- [5] Markham, T., *Project Based Learning*. Teacher Librarian, 2011, 39, 2, 38-42

- [6] Dolmans, D., *How theory and design-based research can mature PBL practice and research*, In: *Advances in Health Sciences Education*, 2019, 24, 879–891, <https://doi.org/10.1007/s10459-019-09940-2>
- [7] Titu, M., Oprean, C., BoroIU, A., *Cercetarea experimentală aplicată în creșterea calității produselor și serviciilor (Experimental design applied to increasing quality of products and services)*, In: AGIR Publishing House, 2011
- [8] Sartorius Stedim Data Analytics, Version 12, *User Guide to MODDE*, Available at: <https://blog.umetrics.com/hubfs/Download%20Files/MODDE%2012.0.1%20User%20Guide.pdf>
[Accessed on June 2021]



A STUDY ON ENHANCING THE FLAME RETARDANCY OF POLYPROPYLENE YARN WITH BORON COMPOUNDS

DOI: 10.35530/TT.2021.22

E. Eskiyyapar^{1*}, H.K. Kaynak¹, H.İ. Çelik¹, E. Sarioglu²

¹Textile Engineering Department, Gaziantep University, Gaziantep, Turkey
(E-mail: edaeskiyyapar@gmail.com, tuluçe@gantep.edu.tr, hcelik@gantep.edu.tr)

²Textile and Fashion Design Department, Gaziantep University, Gaziantep, Turkey
(E-mail: sarioglu@gantep.edu.tr)

Abstract: Functional properties such as; water resistance, flame retardancy, antibacterial efficiency etc. are required from textile products. One of the most commonly demanded products among functional textile products is the flame-retardant textiles. In this study, it is aimed to produce polypropylene filament yarn with permanent flame retardancy functionality by adding boron compound, which is Anhydrous disodium tetraborate powder (particle size < 38 micron), to the fiber structure during melt spinning process. In this study two different yarn samples are produced with anhydrous disodium tetraborate content by mass ratios of 2% and 5%. A control polypropylene filament yarn sample is also produced with no additive. By this way, three samples are produced by a conventional BCF polypropylene melt spinning machine with the same production parameters. Then, three knitted fabric samples were produced flat knitting machine. Limiting Oxygen Index (LOI) and vertical flammability tests were applied to the samples. According to results an important level of increase for LOI value is obtained with the sample which has 2% boron compound additive. Nevertheless, there is not a consistent effect of increasing boron content in yarn structure for LOI value. The reason of this situation may be resulted due to the uneven distribution of the boron compound in the yarn structure because of the particle size.

Keywords: Anhydrous disodium tetraborate, Boron compound, filament yar, flame retardancy, polypropylene

1. INTRODUCTION

Today, functional properties such as; water resistance, flame retardancy, antibacterial efficiency etc. are required from textile products. Flame retardant applications are mainly applied to combustible textile materials used in carpets, curtains and children's wear for avoiding easily flammable fabrics. In principle, the best flame retardant process for textile materials have to char the fiber, prevent afterglow and release no toxic gas or smoke. The new regulations regarding environment, health and fire require halogenated flame retardant chemicals to be phased out. Today, researchers concentrate on creating halogen free flame retardants for different kinds of textile materials. The modern flame retardant chemistry uses silicone, phosphorus and nitrogen compounds. Researches focus on green chemistry such as enzymes and intumescent flame retardants like expandable graphite as well. Inorganic compounds and interactive combinations of conventional flame retardants are likewise in demand [1]. On the other hand, providing permanence of the functionality is as important as obtaining flame retardancy. Polypropylene is a widely

used synthetic polymer due to its high strength and low-price advantages. On the other hand, it has a disadvantage that the material burns very quickly and does not leave ash residue, but it is an advantage that it burns smokeless [2]. Flame retardancy for textile products can be achieved by different ways; as using commercially available flame retardant fibers, finishing of textile products by flame retardant chemicals or adding flame retardant additives to the structure during fiber production [3].

In the literature there are many studies which deal with the flame retardancy effect of boron compounds. In a previous study, various boron compounds were used to achieve flammability. The synergistic effect of four different boron containing substances, zinc borate, borophosphate, boron silicon containing preceramic oligomer and lanthanum borate were used to increase the flame retardancy of a polypropylene intumescent system composed of ammonium polyphosphate and pentaerythritol. LOI test results showed that boron compounds reach their highest synergistic effect at 1 % wt loading. Borophosphate containing composite showed the highest LOI value of 30, lowest maximum heat release rate and lowest total heat release rate value. Even though the char yield increases as the amount of boron compounds increases, the flame retarding effect decreases. Results of cone calorimeter test and thermogravimetric analysis showed that the boron compounds are likely to achieve their synergistic effect by reinforcing the integrity of char which improves its barrier effect rather than increasing the char yield [4]. In another research, effect of commercial flame retardant (CFR) on upholstery leathers treated with borax, boric acid and zinc borate was investigated. Chemical solutions were applied to the leathers by padding finishing technique, and after the flame retardant application the leathers were finished with traditional finishing methods. According to LOI results, CFR CFR+borax+boric acid and CFR+zinc borate+boric acid treated groups of leather had 28.5%, 29.2% and 29.9% oxygen concentration, while control sample had 27.0%. It is concluded that, flame retardant property of leathers was increased by the effect of boron derivatives [5]. In a study which deals with the flame retardancy of zinc borate, organic phosphinate (diethyl phosphinic acid) (DPA) and zinc borate/organic phosphinate combination doped polybutylene terephthalate (PBT) was investigated. LOI values of ZnB/PBT samples were found very low even with higher filling content. At higher loading of ZnB, the dripping of the sample strongly decreased and also char residue increased. It was concluded that organic phosphinate acid-based additives DPA was particularly effective with PBT. It was also seen that the combination of DPA and ZnB can be used to increase the char residue and decrease the melt dripping of PBT [6]. In another study, neutralized intumescent fire retardant (NIFR) was synthesized in “one step and one pot” using a protocol. Flame retardant properties of the intumescent polypropylene showed the efficiency of the new synthesized intumescent compound. It was also demonstrated that, under hydrolytic conditions, zinc borate allowed reducing the migration and keeping good flame retardant properties [7]. Ayar et al. aimed to produce, economically favourable, easy processed, strong coverageable, flame retardant, high temperature resistant, low temperature expansion and high corrosion resistance dye by means of anhydrous zinc borate pigment. According to test results, it is approved that thermal and fire resistance of metallic, wooden and woven textile materials were improved by means of anhydrous zinc borate based pigment dye. This dye can be used to increase the materials resistance against extreme temperature, corrosion and to provide dimensional stability in industrial applications [8].

In another study, two eco-friendly boron chemicals, boric acid, and borax decahydrate, were used as flame-retardant. The flame-retarding functions for polypropylene bulked continuous filament polypropylene (BCF PP) yarn were investigated through the applications of boron chemicals. Boric acid and borax decahydrate are added to BCF PP

yarns during the spin finish process. LOI values of samples were examined and the results of the study showed that application of boron compounds improves flame retardancy. Borax decahydrate shows better flame-retarding effect than boric acid [9]. Another study is about boron oxide and boric acid application to impart flame retardant property for comonomer containing polyacrylonitrile fabrics. In the study, boron compounds were applied to fabrics by using various combinations of the atmospheric plasma modification and sol-gel methods. After these treatments, ignition times of the atmospheric plasma and sol-gel treated fabrics were compared. Test results showed that, ignition times of all the samples treated with boron oxide and boric acid were increased, but the highest increase was obtained by the plasma+sol-gel method. SEM (Scanning Electron Microscopy) images and FT-IR (Fourier-transform infrared spectroscopy) spectrums of the treated samples demonstrated the presence of boron in all samples treated under various conditions. When TGA (Thermogravimetric analysis) thermograms were examined, it was determined that the decomposition temperature of PAN fabrics, treated with boron compounds increased. It is concluded that the flame retardancy of PAN (Polyacrylonitrile) fabrics was improved by environmentally friendly boron compound application [10]. In a study, flame retardancy effect of boron on two cotton fabrics was investigated. Different concentrations of boric acid nanoparticles were examined to optimize the flame-retardant functions. Results showed that; the flame spreading times of the coated fabrics and burning time were increased by increasing the concentration of boric acid nanoparticle content. In addition, tensile strength of the treated fabric decreased [11]. In a study which deals with the effects of zinc borate (ZB) and micro capsulated red phosphorus (MRP) with modified magnesium hydroxide (MH) on the flame-retardancy property of polypropylene (PP), it is seen that the MRP powders had a little effect on the mechanical properties of the PP composites. Test results showed that addition of ZB and MRP weakened the heterogeneous nucleation effect of MH on PP. The addition of ZB and MRP had a great effect on the flammability of the PP/MH/EG composites. The thermal stability of PP/MH/ZB and PP/MH/ZB/MRP composites was better than that of PP/MH composite [12]. Gültaş et al. studied the rheological properties of zinc borate reinforced polypropylene. In the study reinforced polypropylene granules were produced and the zinc borate was added to powder polypropylene material at different ratios. To prevent oxidation, maleic anhydride used as an antioxidant, it was added to PP during the production of zinc borate reinforced polypropylene granule. It was determined that viscosity value increased depending on zinc borate rate but viscosity decreased depending on increasing temperature and pressure. It was determined that MFI (melt flow index) values had been increased depending on increasing temperature and pressure whereas MFI values have been decreased according to increasing zinc borate ratio. Additionally, shear rate decreased depending on increasing proportion of additive but shear rate increased with the increasing of temperature and pressure [13].

In the present study, it is aimed to produce polypropylene filament yarn with permanent flame retardancy functionality by adding boron compounds to the fiber structure during melt spinning process. It is known that boron compounds are flame retardant, environmentally friendly when used, do not cause toxic gas emissions, have low volatility, and suppress combustion by covering the burning material in such a way that prevent the contact of burning material with oxygen [14].

2. MATERIALS AND METHOD

In this study, Anhydrous disodium tetraborate (Etibor 68) which is produced by ETİ Mining Operations General Directorate (Turkey) is used. The master batch is

produced via twin screw extruder by mixing Anhydrous disodium tetraborate powder (particle size < 38 micron) by polypropylene polymers. For production of masterbatch, polypropylene and anhydrous disodium tetraborate are mixed by a mass basis ratio of 50/50. Then, three different polypropylene filament yarn samples are produced by a conventional BCF polypropylene melt spinning machine with 3000 dtex/144f yarn linear density. Two samples are produced with 2% and 5 % (weight basis) anhydrous disodium tetraborate additive. The control sample is produced without additive. The production parameters of the sample yarns are given in table 1.

Table 1. The production parameters of yarn

Parameter	Value
Temperature of extruder	220°C-250°C
Cooling air velocity	0.7 m/s
Temperature of air chamber	20°C
Lubrication rate (spin finish)	0.7%
Tailstock	28 pcs/m-30 pcs/m
Spot pressure	4.5 bar
Output Speed	2800 m/min

The produced yarn samples are used to produce knitted fabrics by flat knitting machine. Then, Limiting Oxygen Index (LOI) of yarns is measured according to ASTM D2863 standard. Flammability behaviors of knitted fabrics are also measured by vertical flammability test according to ASTM D 6413 – 08 method.

3. RESULTS

In this study, surface views of produced yarns are examined by SEM images and given in figure 1.

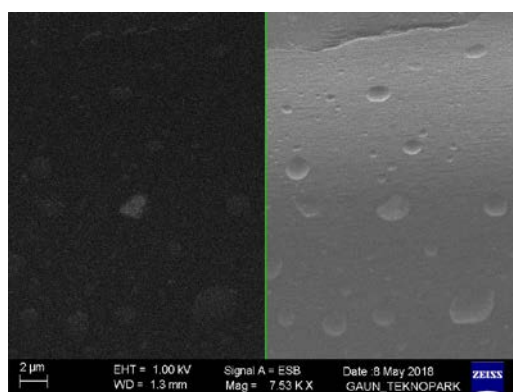


Figure 1. SEM images, with 2% (left side) and 5% (right side) anhydrous disodium tetraborate additives

It can be seen from SEM results that the boron compound is not evenly distributed on the surface of yarn. It is thought that, the particle size of boron compound (38 micron) is not suitable for yarn production; as a result the particle size of compound must be lowered.

LOI is the measure of the minimum percentage of oxygen in an oxygen/nitrogen mixture that is required to support the combustion of material. LOI values of samples are determined and are given in table 2.

Table 2. LOI (Limiting Oxygen Index) of yarns

Samples	LOI (%)
Without boron additive	19.0
%2 anhydrous disodium tetraborate	22.1
%5 anhydrous disodium tetraborate	20.6

It can be seen from LOI values that the yarn without boron additive has a very low value which can be regarded as easily flammable. It is also seen that better results are obtained with the sample which has 2% boron compound additive in comparison to control sample (without boron additive). However, the same trend is not seen in 5% boron additive yarn. Flammability behaviours of knitted fabrics were measured by vertical flammability test and the results are given in table 3.

Table 3. Vertical flammability test results

Parameter	Value			
	1	2	3	Mean
Control sample				
Self-extinguishing time, second	86	48	55	63
Combustion distance, cm	20	10	13	14.3
2% anhydrous disodium tetraborate				
Self-extinguishing time, second	40	75	12	42.3
Combustion distance, cm	8	20	6	11.3
5% anhydrous disodium tetraborate				
Self-extinguishing time, second	50	125	40	71.6
Combustion distance, cm	11	20	12	14.3

After vertical flammability tests the sample views are taken and the images are given in figure 2.

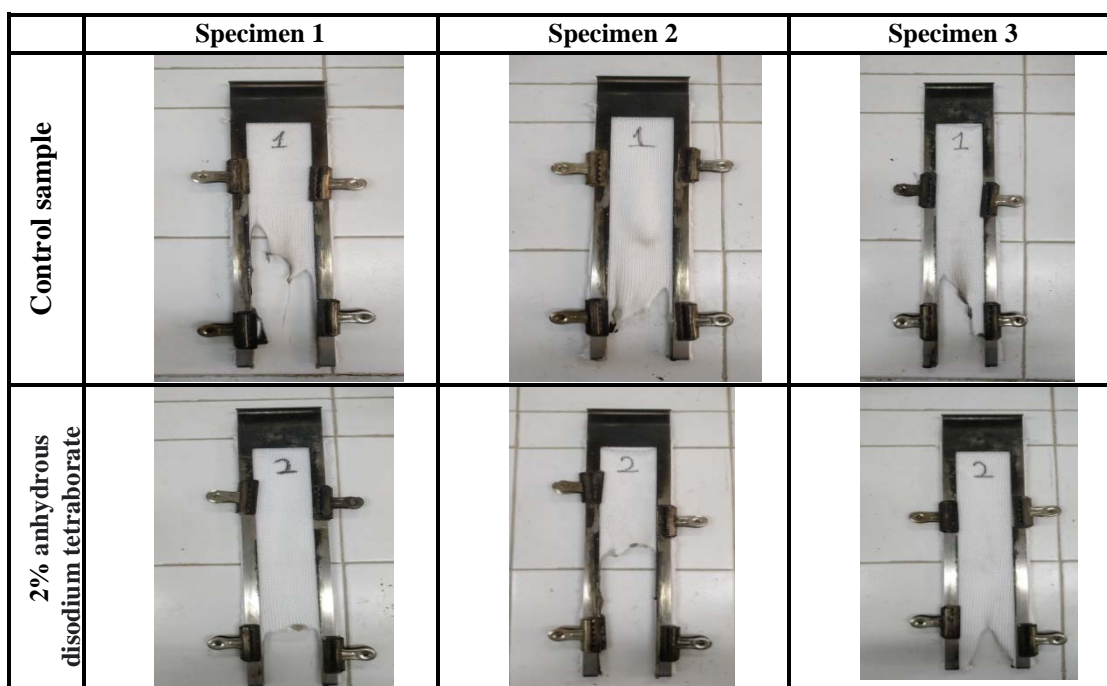




Figure 2. Vertical flammability sample views

It is seen from the sample images (figure 2) that the better results are obtained by the specimens, which have 2% boron compound additive in comparison to control sample. But the flame retardancy does not increase when the boron compound ratio increases. So, the flame retardancy of the boron compound is found to be inconsistent as a negative result.

4. CONCLUSIONS

The flame retardancy performance of the samples is investigated by LOI test and vertical flammability tests. An obvious level of increase for LOI value is obtained with the sample which has 2% boron compound additive. But there is not a consistent effect of increasing boron content in yarn structure for LOI value. This situation may be resulted due to the uneven distribution of the boron compound in the yarn structure. The probable reason is thought to be the inappropriate particle size of boron compound. Similar inconsistent results are also seen for vertical flammability test results. For this reason, for further study, the particle size of boron compounds will be reduced and also homogenization boron compound in the yarn structure will definitely be ensured. After the discussions with the synthetic yarn manufacturers, it was concluded that adding particles of approximately one-tenth of the yarn diameter to the yarn structure would be suitable for synthetic yarn production. It is concluded that the particle size of 5 microns and below would be more sufficient for the boron compounds to be used.

REFERENCES

- [1] Paul, R., *Functional finishes for textiles: An overview*, In: Performance and Protection, 2015, 1-14
- [2] Zhang, S., Horrocks, A.R., *A Review of Flame Retardant Polypropylene Fibres*, In: Progress in Polymer Science, 2003, 28, 1517-1538
- [3] Çerkez, İ., *Butekom Akademi Tekstilde Özel Konular Cilt 2: Tekstil Ürünlerinde Güç Tutuşurluk Eğitim Kitapçığı*, BUTEKOM, 2015, ISBN: 978-605-65630-2-7
- [4] Doğan, M., Yılmaz, A., Bayramlı, E., *Synergistic effect of boron containing substances on flame retardancy and thermal stability of intumescent polypropylene composites*, In: Polymer Degradation and Stability, 2010, 95, 2584-2588
- [5] Açıklık, S.M., *Development of Commercial Flame Retardant in Upholstery Leathers By Boron Derivatives*, In: Tekstil ve Konfeksiyon, 2018, 28, 4, 319-323
- [6] Üreyen, M.E., *The Combined Effect Of Organic Phosphinate Based Flame Retardant And Zinc Borate on The Fire Behaviour of Poly(Butylene Terephthalate)*, In: Anadolu University Journal of Science and Technology A- Applied Sciences and Engineering, 2016, 17, 5, 775-785
- [7] Fontaine, G., Bourbigot S., Duquesne S., *Neutralized flame retardant phosphorus agent: Facile synthesis, reaction to fire in PP and synergy with zinc borate*, In: Polymer Degradation and Stability 2008, 93, 68-76

- [8] Ayar, B., Gürü, M., Çakanyıldırım, Ç., *Solid Phase Synthesis of Anhydrous Zinc Borate from Zinc and Boron Oxide and Utilization as a Flame Retardant in Dye and Textile*, In: Gazi University Journal of Science, 2014, 27, 3, 987-991
- [9] Avcioğlu Kalebek, N., *Functionalized Polypropylene Filaments for Flammability*, In: INTECH, Textiles for Advanced Applications, 2017, 10, 275-291
- [10] Bozacı, E., *Borlu bileşiklerin çevre dostu yöntemlerle poliakrilnitril kumaşlara uygulanması*, In: Journal of BORON, 2018, 3, 1, 17-23
- [11] Akarslan, F., *Investigation on Fire Retardancy Properties of Boric Acid Doped Textile Materials*, In: Special issue of the International Conference on Computational and Experimental Science and Engineering (ICCESEN 2014), 2015, 128
- [12] Chen, X., Yu, J., He, M., Guo, S., Luo, Z., Lu, S., *Effects of zinc borate and microcapsulated red phosphorus on mechanical properties and flame retardancy of polypropylene/magnesium hydroxide composites*, In: J. Polym. Res., 2009, 16, 357-362
- [13] Güldaş, A., Çankaya, A., Güllü, A., Gürü, M., *Determination of Rheological Properties of Zinc Borate Reinforced Polypropylene*, In: Journal of the Faculty of Engineering and Architecture of Gazi University, 2014, 29, 2, 227-234
- [14] Yılmaz Aydın, D., Gürü, M., Ayar, B., Çakanyıldırım, Ç., *Bor bileşiklerinin alev geciktirici ve yüksek sıcaklığa dayanıklı pigment olarak uygulanabilirliği*, In: Journal of BORON, 2016, 1, 33-39



ANTIMICROBIAL PROPERTIES OF RABBIT COLLAGEN GLUE-CHITOSAN BIOMATERIAL LOADED WITH *CYMBOPOGON FLEXUOSUS* ESSENTIAL OIL

DOI: 10.35530/TT.2021.46

M. Râpă¹, M.D. Berechet^{2*}, C. Gaidău², R.R. Constantinescu², A. Moșuțiu³

¹Faculty of Material Science and Engineering, University POLITEHNICA of Bucharest, Romania
(E-mail: maria.rapa@upb.ro)

²National Research Development Institute for Textiles and Leather-Division, Romania
(E-mails: marianadanielaberechet@yahoo.co.uk, carmen_gaidau@hotmail.com,
rodica.roxana@yahoo.com)

³SPD STAR SRL, Romania
(E-mail: mosutiu.anamaria@gmail.com)

Abstract: One approach to develop innovative antimicrobial wound dressing materials is to use natural polymers loaded with antimicrobial agents. The valorisation of animal proteins as biomaterials with antimicrobial properties is a new concern for development of wound healing. Plant essential oils (EO) also indicate a potential approach for new wound dressing materials able to replace the synthetic antimicrobial agents. In this paper, plant-polymeric film was prepared by casting film-forming emulsion based on lemongrass (*Cymbopogon flexuosus*) essential oil/Tween 80 dispersed into rabbit collagen glue hydrolysate–chitosan biomaterial. The effect of biomaterial film composition on *Staphylococcus aureus* ATCC 6538 and *Escherichia coli* ATCC 10536 standard bacteria, and *Candida albicans* ATCC 10231 pathogenic fungus was studied according to European Pharmacopoeia 10/2020 as compared with biomaterial film without essential oil. The *in vitro* antibacterial tests against three bacterial strains showed that the rabbit collagen glue hydrolysate–chitosan biomaterial inhibited all the three microorganisms. The rabbit collagen hydrolysate glue-chitosan film loaded with lemongrass essential oil exhibits antimicrobial activity towards tested microorganisms but lower as compared with control. The explanation could be due to the short time of investigation, or maybe some active compounds constituents of EO, which favour the cellular proliferation. Preparation of rabbit collagen glue hydrolysate-chitosan biomaterial loaded with lemongrass essential oil is an environmentally friendly solution, which may contribute to the development of wound healing materials as an alternative to topical antimicrobial agents.

Keywords: antimicrobial activity, chitosan, lemongrass, rabbit collagen hydrolysate glue, wound dressing materials

1. INTRODUCTION

Currently, conventional wound medical dressing includes introduction of therapeutic agents into polymeric synthetic in order to increase the healing process [1,2]. Unfortunately, chronic wound infections resist to the antibiotics administration. One approach to develop innovative antimicrobial wound dressing materials is to use natural polymers loaded with antimicrobial agents like chitosan, ZnO nanoparticles and TiO₂ nanoparticles by electrospinning technology [3,4]. The valorisation of animal proteins as biomaterials with antimicrobial properties is a new concern for development of wound healing. Thus, collagen

derived from bovine tendons and rabbit skin and keratin extracted from sheep's wool represent a sustainable potential raw materials to be exploited in wound healing [5]. Animal proteins are biodegradable, show antimicrobial and antioxidant properties and biocompatibility with tissue and correspond to the circular economy strategy. The collagen hydrolysate valorized from rabbit skin contains alanine and arginine amino acids in structure and good biocompatibility and bioactive activity compared to synthetic polymers being a major issue to consider in the field of medical, cosmetic or tissue engineering products [4]. However, the properties of collagen to external factors need to be improved. Ferulic acid [6], waterborne polyurethane [7] or chitosan [4] are few agents used for stabilization of collagen.

Chitosan is a biomaterial derived from the chitin shells of shrimp and other crustaceans in alkaline solution and has been used in wound healing due to its biocompatibility [8]. Its structure is composed from glycosidic bonds, hydroxyl and amino groups with hydrogen bonds making chitosan to have a crystalline structure [9]. The introduction of collagen to chitosan led to form a polyelectrolyte complex by interactions between amino groups of chitosan with carboxylic groups of collagen. This stable structure will prove favourable physicochemical properties with maintaining of biological activity [10].

Plant essential oils also indicate a potential approach for new wound dressing materials able to replace the synthetic antimicrobial agents. These natural antimicrobial agents are widely available, with low degree of toxicity, and rich in bioactive compounds having anti-tumor, anti-diabetic, analgesic, and antiviral properties [11], which are beneficial in wound healing [12]. Among all, lemongrass (*Cymbopogon flexuosus*) is a plant cultivated as culinary and medicinal herbs because of their scent, resembling that of lemons. It is used in the pharmaceutical industry, being especially effective in treating of dermatological infections. Essential oil of lemongrass was proved as effectiveness in both animal and human cells [13]. It was established that lemongrass strongly reduced the proliferation of *Candida albicans* fungus of fibrous dressings wound care [14]. However, this essential oil is hydrophobic, unstable, volatile, which limits their use for new formulations for wound dressing management [15]. The encapsulating of essential oils in nanocarriers [15] or film-forming emulsion films into chitosan [16] are proposed as strategies to overcome these deficiencies.

Based on these considerations, the objective of this paper was to analyze the preparing of rabbit collagen hydrolysate glue-chitosan loaded with lemongrass (*Cymbopogon flexuosus*) essential oil by casting film-forming emulsion method. The film was investigated for its antimicrobial activity. The antimicrobial property of rabbit collagen glue-chitosan biomaterial loaded with lemongrass essential oils proved the potential use of this formulation for wound dressing.

2. MATERIALS AND METHODS

2.1. Materials

Rabbit collagen hydrolysate glue was extracted from pickled rabbit skin by Leather Research Department, Bucharest, Romania. The extraction process involved the hair removal with 4 w/w% CaO and delimed with 3 w/w% (NH₄)₂SO₄, crushed and boiled in a water bath at 90°C for four hours. Chitosan with high molecular mass was provided by Sigma, Riedst, Germany. Lemongrass (*Cymbopogon flexuosus*) essential oil was acquired from SOLARIS PLANT SRL, Bucharest, Romania. Other solvents used were of analytical grade.

2.2. Preparation of film-forming emulsion

Film-forming emulsion was prepared by solvent casting of lemongrass (*Cymbopogon flexuosus*) essential oil/Tween 80 dispersed into rabbit collagen hydrolysate glue-chitosan in glass Petri dishes. 2.66% (w/v) solution of rabbit collagen hydrolysate glue was prepared by gentle mixing of solid extract with a previously 1.5% (w/v) solution of chitosan prepared in acetic acid with a concentration of 80% (v/v) under magnetic stirring at 800 rpm, and 90°C for 3 hours. The use of low concentration of rabbit collagen hydrolysate glue will permit the partial helical structure of protein to be preserved. In order to obtain the rabbit collagen hydrolysate glue/chitosan/lemongrass essential oil emulsion, 2 mL of EO and 0.375 g Tween 80 were added to the 85 mL rabbit collagen hydrolysate glue/chitosan solution. The film without lemongrass was prepared as control.

2.3. Antimicrobial activity

Staphylococcus aureus ATCC 6538, *Escherichia coli* ATCC 10536, and *Candida albicans* ATCC 10231 were used from the ICPI collection. Determination of microbial contamination was assessed according to the European Pharmacopoeia 10/2020. The test consists of exposing the test sample to an inoculum prepared with a suitable microorganism, storing the inoculated preparation at 37°C±1°C for bacteria and 28°C±1°C for fungi, respectively, observing the test samples at 24 hours and counting the microorganisms grown on the samples. The culture media used were: TSA (Casein soya bean digest agar) in the case of bacteria and Sabouraud agar for fungi (Mediclim, Otopeni, Romania). The initial cell concentration of microorganism tests was previously determined by decimal dilutions from which 100 µl were taken and spread on nutrient agar. The counts on the plate were performed at 24 hours of incubation, these being kept as a reference for the cellular developments in the control sample from the sample set. 1.2×10^5 CFU/mL, 1.0×10^5 CFU/mL and 2.5×10^4 CFU/ml were the initial bacteria concentrations determined by decimal dilutions for *S. aureus*, *E. coli* and *Candida albicans*, respectively. To quantify the antimicrobial efficacy, the degree of microbial (R %) and logarithmic reduction (Log₁₀ red.) of each sample were calculated relative to the initial bacteria concentration.

3. RESULTS AND DISCUSSIONS

Figure 1, a-f shows the images of tested films in contact with microorganism tests. Table 1 shows the quantitative results of antimicrobial activity of test samples exposed to the inoculum at 24 hours.

Data from Table 1 shows clear inhibition growth against *E. coli* ATCC 10536, *S. aureus* ATCC 6538 and *Candida albicans* ATCC 10231 in the case of rabbit collagen hydrolysate glue&chitosan film (control sample). The rabbit collagen hydrolysate glue-chitosan film loaded with lemongrass essential oil exhibits antimicrobial activity towards tested microorganisms but lower as compared with control. The explanation could be due to the short time of investigation, or maybe some active compounds constituents of EO favour the cellular proliferation. Though the citral, a mixture of the two aldehydes geranial and neral, is considered the main bioactive compounds from lemongrass essential oil with strong antimicrobial properties, the accompanying natural components have instead contrary effects [17]. Another explanation could be associated with the concentration of lemongrass essential oil into film. The maximum effect against both negative and positive bacterial strains was reported at 30% concentration, while the minimum effect was found at 5% concentration of lemongrass essential oil [18]. It is possible that the low content of

lemongrass essential oil (2.35%) did not permit the interaction of bioactive compounds with cell membrane. The investigation will continue for observation at long period times.

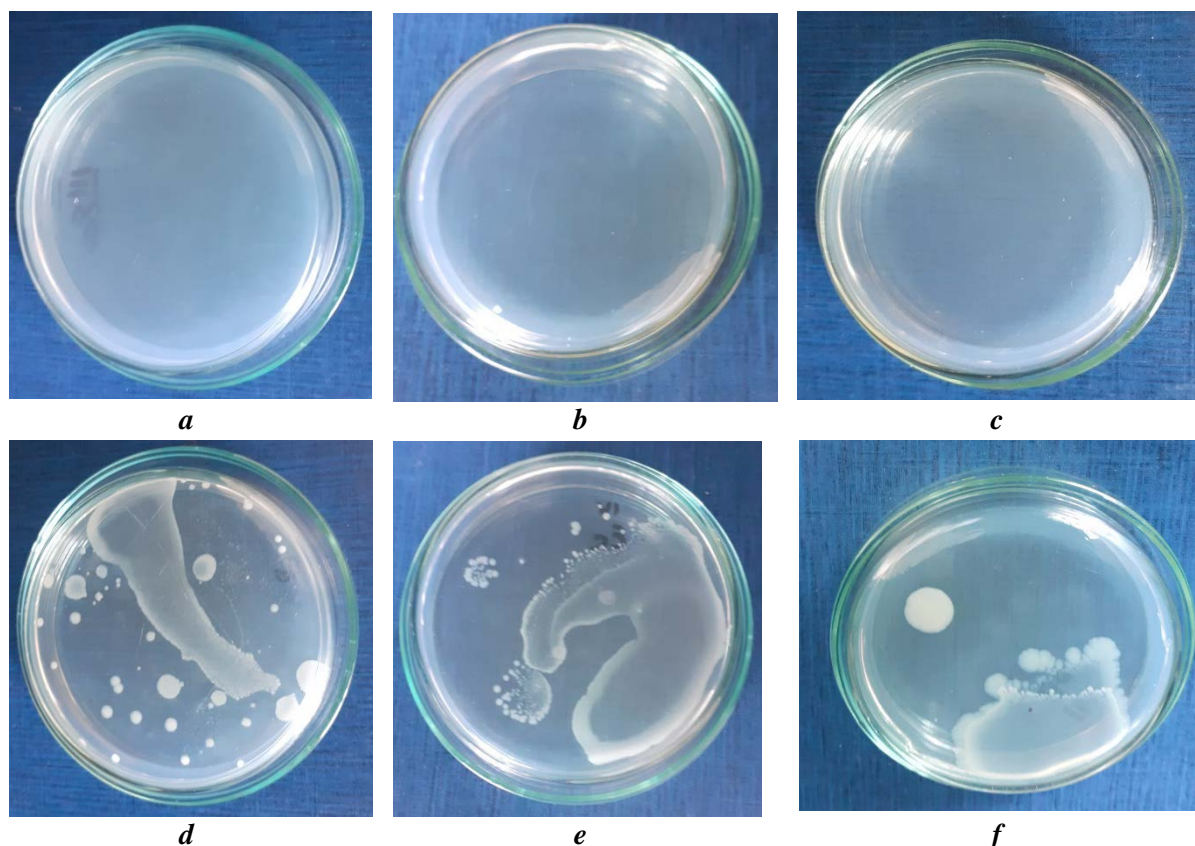


Figure 1. Photographs of Petri dishes for control sample against: a - *S. aureus* ATCC 6538; b - *E. coli* ATCC 6538; c - *C. albicans* ATCC 6538; and rabbit collagen hydrolysate glue/chitosan/lemongrass film against: d - *S. aureus* ATCC 6538; e - *E. coli* ATCC 6538; f - *C. albicans* ATCC 6538

Table 1. Antimicrobial activity of rabbit collagen glue-chitosan biomaterial loaded with *Cymbopogon flexuosus* essential oil

Sample	Results (CFU/ml)	R (%)	Log ₁₀ red.
Microorganism test: <i>Escherichia coli</i> ATCC 10536			
Rabbit collagen hydrolysate glue&Chitosan	0	100	5.00
Rabbit collagen hydrolysate glue &Chitosan&Lemongrass	1.5x10 ²	99.90	3.00
Microorganism test: <i>Candida albicans</i> ATCC 10231			
Rabbit collagen hydrolysate glue&Chitosan	0	100	5.00
Rabbitcollagen hydrolysate glue &Chitosan&Lemongrass	4.3x10 ¹	99.83	2.76
Microorganism test: <i>Saphylococcus aureus</i> ATCC 6538			
Rabbit collagen hydrolysate glue&Chitosan	3.4x10 ¹	99.97	3.55
Rabbitcollagen hydrolysate glue &Chitosan&Lemongrass	9.7x10 ¹	99.92	3.09

4. CONCLUSION

The use of collagen from rabbit skin glue as indigenous natural resource together with chitosan and lemongrass essential oil for production of the antimicrobial biomaterial with wound dressing potential application was reported in this research. Film-forming emulsion film was prepared using casting method. The replacement of synthesis antimicrobials with pathogen resistance potential with the natural polymers and plant derived essential oil, which are available at commercial level, open the way for new nonactive wound dressing development. Preparation of rabbit collagen-chitosan biomaterial loaded with lemongrass essential oil is an environmentally friendly solution, which may contribute to the development of wound healing materials as an alternative to topical antimicrobial agents.

ACKNOWLEDGMENT

The authors would like to express appreciation for the support of the Romanian Ministry of Education and Research, CCCDI - UEFISCDI, Project Number PN-III-P3-3.5-EUK-2019-0237, within PNCIDI III (NonActivPans), under the Contract No 219/2020.

REFERENCES

- [1] Akopian, G., Nunnery, S.P., Piangenti, J., et al., *Outcomes of Conventional Wound Treatment in a Comprehensive Wound Center*, In: The American Surgeon. 2006, 72, 4, 314-317, <https://doi.org/10.1177/000313480607200407>
- [2] Kadam, S., Shai, S., Shahane, A., et al., *Recent Advances in Non-Conventional Antimicrobial Approaches for Chronic Wound Biofilms: Have We Found the 'Chink in the Armor'?*, In: *Biomedicines*, 2019, 7, 2, 1-26, <https://doi.org/10.3390/biomedicines7020035>
- [3] Matei, E., Gaidau, C., Rapa, M., et al., *Sustainable Coated Nanostructures Based on Alginate and Electrospun Collagen Loaded with Antimicrobial Agents*, In: *Coatings* 2021, 11, 2, Article Number: 121, <https://doi.org/10.3390/coatings11020121>
- [4] Matei, E., Gaidau, C., Râpă, M., et al., *Sustainable Rabbit Skin Glue to Produce Bioactive Nanofibers for Nonactive Wound Dressings*, In: *Materials*, 2020, 13, 5388, <https://doi.org/10.3390/ma13235388>
- [5] Râpa, M., Gaidau, C., Stefan, L.M. et al., *New Nanofibers Based on Protein By-Products with Bioactive Potential for Tissue Engineering*, In: *Materials* 2020, 13, 14, 3149, <https://doi.org/10.3390/ma13143149>
- [6] Kaczmarek, B., Lewandowska, K., & Sionkowska, A., *Modification of Collagen Properties with Ferulic Acid*, In: *Materials* (Basel, Switzerland), 2020, 13, 15, 3419, <https://doi.org/10.3390/ma13153419>
- [7] Han, Y., Jiang, Y., Hu, J., *Collagen incorporation into waterborne polyurethane improves breathability, mechanical property, and self-healing ability*, In: *Compos. Part A: Appl. Sci. Manufa.*, 2020, 133, 105854, <https://doi.org/10.1016/j.compositesa.2020.105854>
- [8] Shikhi-Abadi, P.G., Irani, M., *A review on the applications of electrospun chitosan nanofibers for the cancer treatment*, In: *Intern. J. Biolog. Macromol.*, 2021, 183, 790–810
- [9] Dash, M., Chiellini, F., Ottenbrite, R.M., Chiellini, E., *Chitosan-a versatile semisynthetic polymer in biomedical applications*, In: *Prog. Polym. Sci.*, 2011, 36, 981–1014, <https://doi.org/10.1016/j.progpolymsci.2011.02.001>
- [10] Potaś, J., Szymańska, E., Winnicka, K., *Challenges in developing of chitosan – Based polyelectrolyte complexes as a platform for mucosal and skin drug delivery*, In: *Europ. Polym. J.*, 2020, 140, 110020, <https://doi.org/10.1016/j.eurpolymj.2020.110020>
- [11] Vivcharenko, V., Przekora, A., *Modifications of Wound Dressings with Bioactive Agents to Achieve Improved Pro-Healing Properties*, In: *Appl. Sci.* 2021, 11, 4114, <https://doi.org/10.3390/app11094114>

- [12] Woollard, A.C., Tatham, K.C., Barker, S., *The influence of essential oils on the process of wound healing: a review of the current evidence*, In: Journal of Wound Care, 2007, 16, 6, 255–257, <https://doi.org/10.12968/jowc.2007.16.6.27064>
- [13] Han, X, Parker, T.L., *Lemongrass (Cymbopogon flexuosus) essential oil demonstrated anti-inflammatory effect in pre-inflamed human dermal fibroblasts*, In: Biochim Open., 2017, 4, 107-111, <https://doi.org/10.1016/j.biopen.2017.03.004>
- [14] Liakos, I., Rizzello, L., Hajiali, H., et al., *Fibrous wound dressings encapsulating essential oils as natural antimicrobial agents*, In: J. Mater. Chem. B, 2015, 3, 8, 1583-1589, <https://doi.org/10.1039/C4TB01974A>
- [15] Dheebika, N., Sharmila, S., Sundar, K., et al., *Formulation of essential oil-loaded chitosan–alginate nanocapsules*, In: Journal of Food and Drug Analysis, 2015, 23, 3, 560-568, <https://doi.org/10.1016/j.jfda.2015.01.001>
- [16] Pereira Dos Santos, E., Nicácio, P.H.M., Coêlho Barbosa, F., et al., *Chitosan/Essential Oils Formulations for Potential Use as Wound Dressing: Physical and Antimicrobial Properties*, In: Materials (Basel), 2019, 12, 14, 2223, <https://doi.org/10.3390/ma12142223>
- [17] Viktorová, J., Stupák, M., Řehořová, K.T., et al., *Lemon Grass Essential Oil does not Modulate Cancer Cells Multidrug Resistance by Citral-Its Dominant and Strongly Antimicrobial Compound*, In: Foods. 2020, 9, 585, <https://doi.org/10.3390/foods9050585>
- [18] Naik, M.I., Fomda, B.A., Jaykumar, E., Bhat, J.A., *Antibacterial activity of lemongrass (Cymbopogon citratus) oil against some selected pathogenic bacteria*, In: Asian Pac. J. Trop. Med., 2010, 3, 7, 535-538, [https://doi.org/10.1016/S1995-7645\(10\)60129-0](https://doi.org/10.1016/S1995-7645(10)60129-0)



ANTIMICROBIAL ACTIVITY OF FIR FUNCTIONALIZED TEXTILE MATERIALS

DOI: 10.35530/TT.2021.57

O. Iordache, E.C. Tanasescu, I. Sandulache, C. Lite, L.O. Secareanu,
E. Perdum

National Research Development Institute for Textile and Leather, Romania
(E-mail: iordachevidiu.g@gmail.com)

Abstract: Far Infrared (FIR) functionalized textile materials are enjoying a special attention nowadays, as a viable and practical solution for treating a wide range of medical conditions (relief of acute or chronic inflammation and circulatory problems, prevention of microbial infections, improvement of nervous system functions, reduction of skin lipids, improvement of blood circulation, removal of accumulated toxins by improving lymphatic circulation etc.). At the molecular level, FIR compounds and functionalized materials exert strong rotational and vibrational effects, with beneficial biological potential. These materials are based on the principle of absorbing light energy and then irradiating this energy back into the body at specific wavelengths. FIR functionalized textile materials are a new category of functional textiles that have the potential to improve well-being and health. Present paper explored the antimicrobial potential of four textile materials, functionalized with FIR, UV protection and antimicrobial functionalization compounds, tested according to two methods for assessment of antimicrobial character: a testing method in dynamic conditions and a testing method in static conditions. The evaluation of the antimicrobial character showed very good rates of reduction of the microbial population, of the functionalized textile materials, following the testing on four strains of pathogenic fungi: *Candida albicans*, *Epydermophyton floccosum*, *Tricophyton interdigitale* and *Aspergillus niger*, with reduction rates between 76.16% and 96.06%.

Keywords: FIR, far infrared, textiles, antimicrobial

1. INTRODUCTION

Pyroelectric materials are functional materials that can generate an electrical response following a change in temperature. Modern solutions often include a combination of polypropylene and special lead-free bio-ceramics to create functional FI garments that are materialized in commercially available products such as socks, pillows, linens, knee pads, pants, bedspreads, bed linen, shoulder pads etc. [1]. Several studies have suggested improvement in patients' condition that suffered of atopic dermatitis in response to the use of special fabrics in the affected area.

Previous studies have also shown that the effects of infrared radiation can activate fibroblasts, increase collagen synthesis and the expression of growth factor-beta1 (TGF-beta1) in rat wounds. Thus, particles of germanium (Ge) and silicon dioxide (SiO₂) were incorporated at the nano scale into polyvinyl alcohol (PVA) nanofibers. The emission wavelength of these nanofiber membranes was between 5-20µm at 37°C and had an emissivity value of 0.891 (a perfect black body has a maximum emissivity of 1). The antimicrobial effects of infrared radiation may be effective in reducing the number of

Staphylococcus aureus and *Escherichia coli* bacteria by 99.9%, and have shown a reduction in the viability of *Klebsiella pneumoniae* by 34.8% [2-4].

2. MATERIALS AND METHODS

2.1 Functionalized textile materials

Four functionalized textile materials (FIR + UV protection + antimicrobial functionalization compounds), figure 1, and were subjected to antimicrobial analysis against three strains of pathogenic fungi.

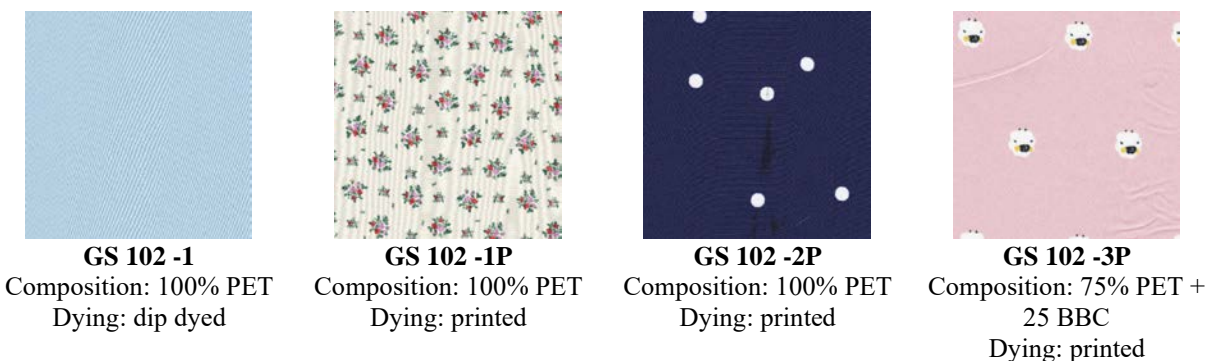


Figure 1. Functionalized textile materials

2.2 Fungal strains

The evaluation of the antimicrobial character was performed on the functionalized materials, compared with a control sample (single control, from each strain, taken as the microbial inoculum). The test was performed according to two methods, one in dynamic contact conditions (under agitation), and one in static contact conditions (inoculation on the material), and against four microbial strains of pathogenic fungi: *Candida albicans* (ATCC 90028), *Epidermophyton floccosum* (CCM 8339), *Trichophyton interdigitale* (ATCC 9533) and *Aspergillus niger* (IMI 45551).

At the end of the tests, the number of viable cells was quantified, and the degrees of microbial percentage reduction were calculated, based on the initial number of colony forming units (CFUs). In both methods, each material was tested in duplicate, and the final result was expressed as the average of the readings from two Petri plates.

Initial microbial concentrations, expressed as average of readings on two Petri plates:





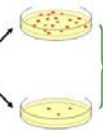
Candida albicans: 3.32×10^3 UFC/ml;
Epidermophyton floccosum: 3.2×10^2 UFC/ml;
Trichophyton interdigitale: 4.1×10^2 UFC/ml;
Aspergillus niger: 3.5×10^2 UFC/ml.

2.3 Evaluation of antimicrobial character in dynamic conditions

Testing of the antimicrobial character of functionalized textile materials, under dynamic conditions, was performed according to the ASTM E2149 standard, which describes a standardized method for testing the antimicrobial activity of antimicrobial agents immobilized on a solid substrate under dynamic contact conditions. This method was developed for routine quality control tests and antimicrobial screening tests being used to test the character and antimicrobial efficiency of immobilized functionalization treatments on various substrates. The samples were tested according to the scheme in table 1, in

duplicate, the results being reported by averaging the reading from two Petri plates. The quantification of the number of cells on the plates with a high number of colonies was performed with specialized software, OpenCFU, a free open-source colony counting software.

Table 1. Test scheme according to ASTM E2149

Step	Description	Representation
1. Sample preparation	Sampling, in duplicate, with a final mass of 1 g (+/- 0.1 g), and placement in sterile 100 ml PE flasks in 60 ml of sterile saline (0.875% NaCl) with Tween 80 anionic detergent (2 drops/l), in order to be able to confer a better dispersion of the microbial cells in the volume of liquid. Thus, the saline/Tween 80 mixture was previously sterilized for 15' at 121°C.	
2. Inoculation	Stock cultures were diluted with sterile saline and Tween 80 anionic detergent until final inoculation variants were obtained (inoculated into sample vessels).	
3. Incubation	The samples were incubated for 24 in an orbital shaking incubator (SIF6000R, Medline Scientific), according to the tested strain: 28°C for <i>Tricophyton interdigitale</i> , <i>Epidermophyton floccosum</i> and <i>Aspergillus niger</i> ; 36°C for <i>Candida albicans</i> . Plates inoculation was carried out in two sets, following 1 hour of incubation and 24 hours of incubation.	
4. Sampling and plates inoculation	After the incubation period, 100 µl of liquid were taken from each sample flask and pipetted onto the Petri plates with nutrient medium (Sabouraud-Agar).	
5. Incubation and plates counting	After plates inoculation (in duplicate) the plates were incubated at a temperature of 28°C for <i>Tricophyton interdigitale</i> , <i>Epidermophyton floccosum</i> and <i>Aspergillus niger</i> ; 36°C for <i>Candida albicans</i> , for 48 hours, timespan which allowed the counting of the formed colonies.	

2.4 Evaluation of antimicrobial character in static conditions

The testing of antimicrobial efficacy, in static conditions, was done according to ISO 20743:2007, a method applicable to all textile products, including canvas, cotton wool, yarns and materials for clothing, home furniture and various products, regardless of the type of antibacterial agent used (organic, inorganic, natural or synthetic) or method of application (incorporated, post-treatment or grafting). The absorption method was used, in which the microbial suspension is inoculated directly on samples (figure 2), these being sterilized beforehand, to avoid contamination of the plates from the last stage of the protocol (1.6- Plate counting). The tested materials were sampled in surfaces of 1cm², then sterilized at 121°C for 15', and inoculated with 50µL of the last dilution made for each strain tested during the stage (in sterile tubes) and incubated for 24 hours at a temperature of 28°C for each filamentous fungal strain, and at 37°C for the *Candida albicans* strain. After the incubation period, each sample was vortexed for approx. 20" in 1mL sterile distilled water and inoculated on specific nutrient medium (Czapek-Dox and Sabouraud-Agar), followed by an incubation period of 2-3 days. The tests were performed in duplicate, for each material, and in order to quantify the results, the technique of counting the CFUs (Colony Forming Units) on the incubated plates was used, reported to the initial cell concentration in the inoculum.

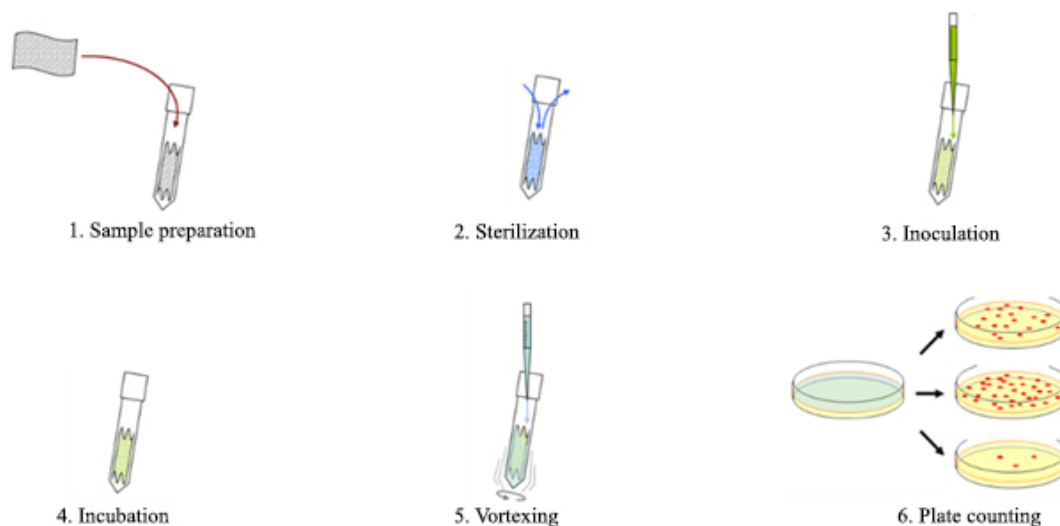


Figure 2. Test scheme according to ISO 20743:2007

3. RESULTS AND DISCUSSION

The results of the antimicrobial testing, on the four functionalized materials, compared to the four microbial strains, in dynamic contact conditions, are presented in table 2 and figure 3.

Table 2. Percentage microbial reductions in dynamic contact conditions

Sample	Plate 1	Plate 2	Average	% Red
<i>Candida albicans</i> (3.32×10^3 UFC/ml)				
GS 102-1	1.98×10^2	2.1×10^2	2.04×10^2	93.86
GS 102-1P	1.12×10^2	1.2×10^2	1.16×10^2	96.51
GS 102-2P	2.1×10^2	2.23×10^2	2.165×10^2	93.48
GS 102-3P	1.78×10^2	1.65×10^2	1.715×10^2	94.84
<i>Epidermophyton floccosum</i> (3.2×10^2 UFC/ml)				
GS 102-1	7.8×10^1	8.1×10^1	7.95×10^1	75.16
GS 102-1P	6.8×10^1	6.5×10^1	6.65×10^1	79.22
GS 102-2P	5.9×10^1	6.1×10^1	6.0×10^1	81.25
GS 102-3P	7.1×10^1	7.3×10^1	7.2×10^1	77.50
<i>Tricophyton interdigitale</i> (4.1×10^2 UFC/ml)				
GS 102-1	3.1×10^1	3.2×10^1	3.15×10^1	92.32
GS 102-1P	2.8×10^1	3.0×10^1	2.9×10^1	92.93
GS 102-2P	4.1×10^1	4.2×10^1	4.15×10^1	89.97
GS 102-3P	3.8×10^1	3.7×10^1	3.75×10^1	90.86
<i>Aspergillus niger</i> (3.5×10^2 UFC/ml)				
GS 102-1	5.1×10^1	5.4×10^1	5.25×10^1	85.00
GS 102-1P	4.8×10^1	4.3×10^1	4.55×10^1	87.00
GS 102-2P	3.9×10^1	4.2×10^1	4.05×10^1	88.43
GS 102-3P	3.7×10^1	4.1×10^1	3.9×10^1	88.86

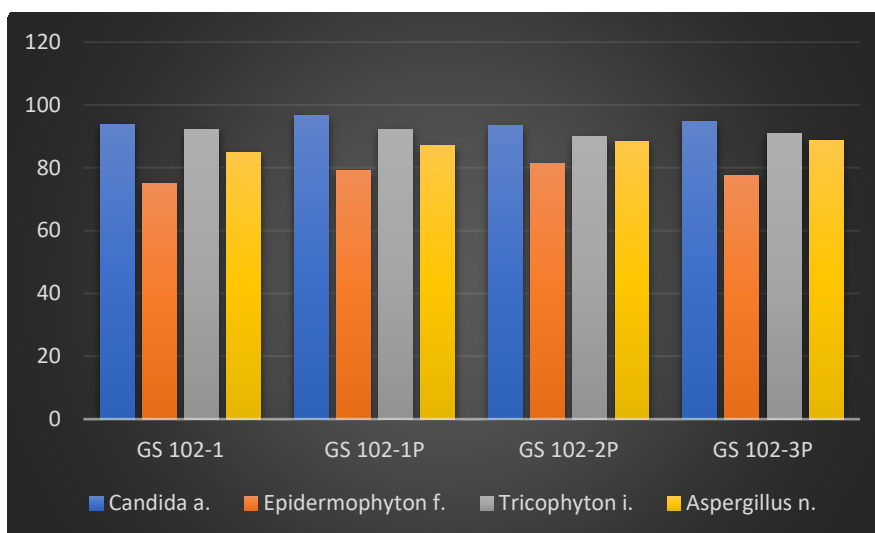


Figure 3. Comparative analysis of microbial reduction rates under dynamic conditions

The test results show very good degrees of microbial reduction, for all four materials, with values between 75.16%, for the GS GS-1 material, tested against the *Epidermophyton floccosum* strain, and 96.51%, for the GS 102-1P material, tested against *Candida albicans* strain. The materials showed the highest efficiency against *Candida albicans* strain, with an average microbial reduction rate of 94.67%, the most resistant strain being *Epidermophyton floccosum*, with an average microbial reduction rate of 78.28% (table 3).

Table 3. Percentage microbial reductions in static contact conditions

Sample	Plate 1	Plate 2	Average	% Red
<i>Candida albicans</i> (3.32x10³ UFC/ml)				
GS 102-1	2.21x10 ²	2.45x10 ²	2.33x10 ²	92.99
GS 102-1P	1.98x10 ²	1.81x10 ²	1.895x10 ²	94.30
GS 102-2P	2.45x10 ²	2.56x10 ²	2.505x10 ²	92.46
GS 102-3P	1.17x10 ²	1.45x10 ²	1.31x10 ²	96.06
<i>Epidermophyton floccosum</i> (3.2x10² UFC/ml)				
GS 102-1	5.1x10 ¹	4.9x10 ¹	5.0x10 ¹	84.38
GS 102-1P	3.4x10 ¹	3.8x10 ¹	3.6x10 ¹	88.75
GS 102-2P	2.5x10 ¹	2.4x10 ¹	2.45x10 ¹	92.35
GS 102-3P	1.9x10 ¹	2.1x10 ¹	2.0x10 ¹	93.75
<i>Tricophyton interdigitale</i> (4.1x10² UFC/ml)				
GS 102-1	2.1x10 ¹	2.5x10 ¹	2.3x10 ¹	94.40
GS 102-1P	4.1x10 ¹	3.9x10 ¹	4.0x10 ¹	90.25
GS 102-2P	2.5x10 ¹	2.6x10 ¹	2.55x10 ¹	93.79
GS 102-3P	2.3x10 ¹	2.1x10 ¹	2.2x10 ¹	94.94
<i>Aspergillus niger</i> (3.5x10² UFC/ml)				
GS 102-1	2.1x10 ¹	2.5x10 ¹	2.3x10 ¹	93.43
GS 102-1P	3.2x10 ¹	3.6x10 ¹	3.4x10 ¹	90.29
GS 102-2P	2.8x10 ¹	2.7x10 ¹	2.75x10 ¹	92.15
GS 102-3P	1.9x10 ¹	2.3x10 ¹	2.1x10 ¹	94.00

The test results show very good degrees of microbial reduction, slightly better than the test results in dynamic conditions. This may be due to the test method, which allowed a longer contact time between the microbial inoculum and the functionalized material. The values of the reduction rates were between 84.38%, for the GS GS-1 material, tested against *Epidermophyton floccosum* strain, and 96.06%, for the GS 102-3P material, tested against the *Candida albicans* strain. The materials showed the highest efficiency against the *Candida albicans* strain, with an average microbial reduction rate of 93.95%, the most resistant strain being *Epidermophyton floccosum*, with an average microbial reduction rate of 89.80% (figure 4).

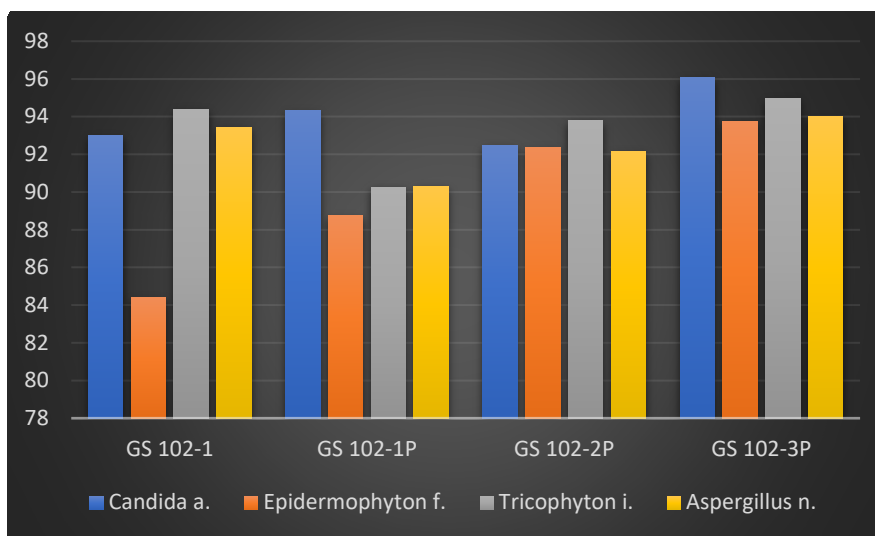


Figure 4. Comparative analysis of microbial reduction rates under static conditions

4. CONCLUSIONS

FIR functional textile may represent the future for alternative therapies, as they have great health benefits of FIR, ranging from regulating body heat, restoring physical function, muscle pain relieving, arthritis pain management, bronchitis etc. [7,8]. Infrared functionalized textile materials offer a unique way to apply various therapies for continuous use. These functional textile structures, existing in different forms (e.g., fibres, fabrics, composites, films etc.) have significant benefits for many types of diseases, symptoms and problems, as FIR functionality can be incorporated into textiles in a variety of ways.

The antimicrobial properties of four FIR functionalized textile materials were tested against four strains of pathogenic fungi: *Candida albicans*, *Epydermophyton floccosum*, *Tricophyton interdigitale* and *Aspergillus niger*. The evaluation of the antimicrobial character showed very good rates of reduction of the microbial population, of the functionalized textile materials, following the testing on four strains of pathogenic fungi: *Candida albicans*, *Epydermophyton floccosum*, *Tricophyton interdigitale* and *Aspergillus niger*, with reduction rates between 76.16% and 96.06%.

ACKNOWLEDGEMENTS

This paper was published under Eureka Traditional program, project “Far Infrared Rays and Anion Releasing Fabrics”, acronym FairTex, financed by The Executive Agency for Higher Education, Research, Development and Innovation Funding (UEFISCDI), national project ID 134E (PN-III-P3-3.5-EUK-2017-02-0044).

REFERENCES

- [1] Dyer, J., *Infrared functional textiles. Functional Textiles for Improved Performance*, In: Protection and Health, 2011, 184-197
- [2] Toyokawa, H., et al., *Promotive effects of far-infrared ray on full-thickness skin wound healing in rats*, In: Exp Biol Med (Maywood), 2003, 228, 6, 724-729
- [3] Chung, J., Lee, S., *Development of nanofibrous membranes with far-infrared radiation and their antimicrobial properties*, In: Fibers and Polymers, 2014, 15, 6, 1153-1159
- [4] Tsai, S.R., Hamblin, M.R., *Biological effects and medical applications of infrared radiation. Journal of photochemistry and photobiology*, In: B. Biology, 2017, 170, 197-207
- [5] *Development of fiber-based active thermal infrared camouflage textile*, In: Applied Materials Today, 2020, 20, 100624
- [6] Ying-Nan, S., Yue, L., Ding-Xiang, Y., Jun, L., Zhong-Ming, L., *Novel passive cooling composite textile for both outdoor and indoor personal thermal management*, In: Composites Part A: Applied Science and Manufacturing, 2020, 130, 105738

Organizers



**INCDTP The National R&D Institute for Textiles and
Leather - Bucharest, Romania**



ITA-Texconf Business Incubator

Co-Organizers



**HOGENT University of Applied Sciences and Arts,
Belgium**



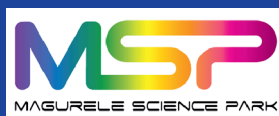
**University of Maribor, Faculty of Mechanical
Engineering, Slovenia**



University of Minho - TecMinho, Portugal



**Yazd University, The Textile Engineering Department,
Iran**



Magurele Science Park, Romania

ISSN 2068-9101, Vol. 10